CRANFIELD UNIVERSITY

CRANFIELD DEFENCE AND SECURITY

DEPARTMENT OF ENGINEERING & APPLIED SCIENCE

Vijarn Vachirawongsakorn

Environmental taphonomic processes and their effects on skeletal trauma analysis

Supervisor: Dr. Nicholas Marquez-Grant

Co-supervisor: Dr. Jonathan Painter

July 2019

Abstract

In recent years there has been extensive research focusing on skeletal trauma as a result of different types of weapons inflicted on bone. However, an important factor that has not been investigated in depth is the potential modification to the observed dimensions and morphology of trauma marks after environmental exposure. Detailed information derived from traumatic lesions to bone is highly valuable in forensic anthropological casework. It is important to understand how taphonomic variables, namely the outdoor environment or fire, may alter trauma morphology. Therefore, the aim of this study is to evaluate the influence of different environmental taphonomic agents on fresh and burned bone trauma that have been inflicted by either blunt or sharp instruments.

This research used blunt and sharp weapons to inflict trauma on manually macerated porcine ribs (n=364) and femurs (n=60). Subsequently each specimen was examined, analysed, and photographed. Qualitative and quantitative analyses were undertaken using macroscopic, microscopic and radiological techniques to investigate specific traumatic lesions, such as cut and chop marks, as well as blunt-inflicted fractures. The traumatised bones were subsequently deposited on the surface or in a buried environment for a pre-determined length of time (6, 12 and 18 months). In addition, sharp force trauma was inflicted on ribs which were then burned at 850°C in a furnace prior to being buried or placed on the surface for 1 month. The samples were then re-examined and the trauma evidence was compared between pre- and post-environmental exposure.

The results showed several trends. Surface colour and taphonomic alterations were linked to macro- and micro-environmental factors, and were also dependent on the duration of environmental exposure. Surface-deposited samples underwent higher degrees of degradation than buried samples. In addition, perimortem blunt and sharp force traumatic lesions on the ribs and femurs were still clearly identifiable after 18-month environmental exposure. This study also illustrated that taphonomic modifications of blunt and sharp injuries were different depending on the interaction between bone, the type of trauma and the surrounding environment. Fractures from different types of weapon showed dissimilar responses to environmental variables.

Pre-exposure bone and different types of depositional environment had an effect on the rate and pattern of taphonomic modifications on dimensions and morphology of the traumatic lesion.

The results of this study should enable an improved determination of skeletal trauma analysis after environmental exposure. Moreover, this study has emphasised the need for a combination of macroscopic, microscopic and radiological techniques to analyse taphonomic phenomena. As environmental factors have the potential to conceal perimortem skeletal trauma, this study advises that when carefully examining traumatic lesions on ribs and femurs as an alteration of their dimensions and morphology is likely to have occurred after prolonged environmental exposure.

Acknowledgements

I would like to truly and honestly express my sincere thankfulness to my supervisor Dr.Nicholas Marquez-Grant and Dr.Jonathan Painter for all of your continued help, support, encouragement and guidance starting with my time here until the completion of my thesis research.

There are several people who must receive recognition for their help in the completion of this thesis. My special thank you to Dr.Sophie Beckett and Dr.Charlene Greenwood whose valuable guidance has helped to make this thesis possible. Many thanks go to Adrian Mustey and Peter Andrew for all of your help through the project. I would also like to acknowledge Professor Ian Horsfall for his guidance in setting an impact testing machine and feedback of my traumatization event. I would particularly like to thank Dr.Trevor Ringrose for his support of the statistical tests.

I would like to sincerely thank you to my family whose support means the world for me, particularly my parents and my wife for supporting the whole way through. They were always there when I needed them.

Last but not least, and most importantly, I would like to say thank you to “Siriraj Foundation” in Thailand for providing me the scholarship to achieve my studies in my long education period.

Table of contents

List of Figures

List of Tables

Chapter 1: Introduction

1.1 Overview of forensic anthropology and trauma

Forensic anthropology, an applied subfield of physical anthropology, involves the application of physical anthropology to medico-legal contexts, particularly those relating to the recovery and analysis of skeletal remains (Byers, 2010; Christensen *et al.*, 2014; Tersigni-Tarrant and Langley, 2017). Crime scenes involving skeletonised human remains demand specific knowledge of osteology and anthropology, and most forensic pathologists may not have the necessary experience. In addition, forensic anthropologists can use their particular expertise drawn from the disciplines of physical anthropology and forensic sciences to search for and recover skeletonised human remains and fulfil their main objectives namely, the identification of a victim, the estimation of the time since death, the detection of traumatic lesions, and the determination of the cause and manner of death (Byers, 2010; Bristow *et al.,* 2011; Davidson *et al.*, 2011; Christensen *et al.*, 2014). In particular, establishing the cause and manner of death is essential for proceeding in a court of law. As to the forensic aspects, the cause of death is described as an injury or disease that initiated pathological alterations in the body leading directly to death, while the manner of death refers to its classification as natural death, suicide, homicide, disease, or undetermined death (DiMaio and DiMaio, 2001; Pinheiro, 2006; Saukko and Knight, 2015).

In suspicious death cases, the accurate recognition and interpretation of traumatic skeletal injuries may be the only imperative evidence for establishing the cause and manner of death (Berryman and Symes, 1998; Symes, *et al.*, 2012; Galloway *et al.*, 2014). A traumatic injury is defined as a deeply distressing or disturbing experience that overwhelms an individual's ability to response (DiMaio and DiMaio, 2001; Saukko and Knight, 2015). For a correct investigation of the cause and manner of traumatic death, the analysis of traumatic lesions is essential, especially those involving a fracture of skeletal materials, in which the traumatic lesions can be preserved for a long time (Kimmerle and Baraybar, 2008; Galloway *et al.*, 2014). A skeletal fracture is described as a disruption in the continuity of skeletal tissue (Kimmerle and Baraybar, 2008; Christensen *et al.*, 2014; Zephro and

Galloway, 2014), and fracture morphological analysis has become one of the fundamental components in the analysis of skeletal remains. The identification of perimortem traumatic lesions in skeletal remains is critical in forensic pathology and anthropology. To this end, forensic pathologists usually rely on the expertise of forensic anthropologists. Contrary to the concepts in forensic pathology, in which perimortem and postmortem are defined in terms of time periods correlated to the actual moment of death, these terms in forensic anthropology are based on the quality of the skeletal elements, namely whether the bones are fresh or dry (Ubelaker and Adams, 1995; Moraitis and Spiliopoulou, 2006; Wieberg and Wescott, 2008; Galloway *et al.*, 2014).

Perimortem skeletal trauma analysis assists in identifying the type of trauma, the number and location of the impacts to the body, the amount of force applied to the body, and the sequence of blows. Trauma analysis can also be used to determine the characteristics of the weapon used for trauma infliction by comparing these tool marks with experimental patterns created by the same class of suspected weapon (Bonte, 1975; Berryman and Symes, 1998; Zephro and Galloway, 2014; Pinheiro *et al.*, 2015), making studies examining the characteristics of trauma vital to forensic investigations. Sharp and blunt force injuries are extremely common causes of death in homicidal cases (Kominato *et al.*, 1997; Hunt and Cowling, 1991; Webb *et al.*, 1999; Cassidy and Curtis, 2005; Ambade and Godbole, 2006; Allen and Audickas, 2018; Park and Son, 2018). This is specifically true in the United Kingdom, which strictly controls the use of firearms (Webb *et al.*, 1999; Allen and Audickas, 2018). Consequently, a wide range of experimental studies with skeletal trauma analysis as their central theme has been conducted over recent years (Cappella *et al.*, 2014; Cerutti *et al.*, 2014; Boucherie *et al.*, 2017; Humphrey *et al.*, 2017; Macoveciuc *et al.*, 2017; Norman *et al.*, 2018; Vegh and Rando, 2019).

1.2 Taphonomy and taphonomic agents

The evaluation of skeletal remains can present considerable difficulty due to the many variables playing a role in its alteration, especially the effects derived from taphonomy (Symes *et al.*, 2002; Calce and Rogers, 2007; Poppa *et al.*, 2011; Macoveciuc *et al.*, 2017). Taphonomy is the study of the events that have happened

to an organism after death, which are assessed by gathering and analysing information between the organism's deposition and its recovery (Haglund and Sorg, 1997; Lyman, 2004; Lyman, 2010). This approach and analysis can be used to distinguish perimortem injuries from postmortem damage to the remains, to reconstruct the events during the depositional period, and to estimate the postmortem interval (Ubelaker, 1997; Dupras and Schultz, 2014; Simmons, 2017). The determination of an individual's postmortem alterations is an important component in medico-legal and forensic anthropological contexts (Ubelaker, 1997; Lyman, 2010; Cattaneo and Cappella, 2017). Human remains left in a depositional environment undergo several types of taphonomic modifications, such as decomposition, animal scavenging and bone weathering. A variety of physical and chemical processes can have an influence on an organism after its death. Recently, in-depth studies have been conducted of different types of common taphonomic alterations (Behrensmeyer, 1978; Bass, 1997; Haglund and Sorg, 1997; Reeves, 2009; Pokines and Symes, 2014; Pokines, 2016). The findings could be used in combination with crime scene investigations to investigate the original depositional environment of unknown skeletons, such as terrestrial surface-deposited or burial remains (Pokines and Baker, 2014; Pokines, 2016). The physical, chemical, and biological processes associated with different depositional environments leads to different taphonomic modifications to bones. In cases where the origin is unknown, these taphonomic findings can be analysed to establish from which original environmental setting the skeletal remains came (Pokines, 2018). Despite their ubiquity, few publications have been dedicated to comparing the overall postmortem profile of surface-deposited and buried skeletal remains (Pokines, 2016).

Few taphonomic variables to a bone can rapidly cause as much significant damage as thermal destruction (Fairgrieve, 2008; Ubelaker, 2009; Symes *et al.*, 2015). Within medico-legal contexts, burned human materials are frequently found in many circumstances such as after a natural disaster, transportation accident or house fire. Forensic investigators therefore have to investigate all deaths by burning in house and industrial fires as well as mass fatalities and disasters (Mayne Correira, 1997; Fairgrieve, 2008). Thompson (2003) argued that the burning incidence is increasing as a clandestine method of concealing homicide cases. Recently, several retrospective statistical analyses of fire-related deaths have been

performed. The incidences of fire-related deaths found in the studies varied from 1.5% to 6%, and depended upon the fire prevention and extinction capabilities in the respective areas (Escoffery and Shirley, 1992; Gerling *et al.,* 2001; Thompson 2003). Fire-related deaths can be the direct result of burn injuries, the inhalation of hot or toxic gas or direct trauma caused by surrounding objects, as well as subsequent complications such as wound infections and multi-organ failure.

The analysis of burned human remains is challenging as not only is it difficult to establish personal identity, but it is also particularly problematic to determine the time since death and the cause of death (Mayne Correira, 1997; Ubelaker, 2009; Symes *et al.*, 2015; Macoveciuc *et al.*, 2017). Body incineration is also a common method employed to obliterate a body or other evidence of criminal activity (Symes *et al.,* 2002; Pope and Smith, 2004). There is a widespread belief that fire can destroy all evidence of the cause and manner of death and make personal identification nearly impossible. In fact, the complete destruction of a body by fire is rare (Mayne Correira, 1990; Mayne Correira, 1997). It is frequently possible that personal identification and certain types of trauma can still be determined after a body's exposure to fire. However, the use of fire as an attempt to destroy a body is frequent (Herrmann and Bennett, 1999; de Gruchy and Rogers, 2002; Fairgrieve, 2008; Marciniak, 2009). Recognition of homicidal acts is more problematic when burning damages the soft and hard tissues that are routinely used for trauma analysis (Herrmann and Bennett, 1999; Symes *et al.*, 2015; Macoveciuc *et al.*, 2017). Heat exposure also results in bone fragility and susceptibility to damage or fracture (Thompson, 2003, 2004; Macoveciuc *et al.*, 2017). Forensic investigators should be sufficiently skilled and knowledgeable to recognise the evidence of trauma in burned remains.

The recovery of burned human remains from a fire scene is very challenging to forensic practitioners because of the fragmentary nature of the heat-exposed materials. A good scene recovery can enable a highly informative anthropological analysis to be performed. Thus, a comprehensive understanding of how burned remains become fragmentary is essential. This knowledge also permits the use of efficient search strategies and improves decisions on instruments. The effects of weather notably the freeze-thaw cycle and rainfall on burned bone fragments should

be taken into consideration (Waterhouse, 2013a, 2013c). However, the question arises as to how environmental factors affect burned bone trauma interpretation and the rate of fragmentation.

1.3 Taphonomic effects on skeletal trauma analysis

Recently, forensic literature have provided a better understanding of taphonomic modifications, especially postmortem skeletal modification (Symes *et al.*, 2002; Berryman and Saul, 2015; Hart, 2015; Cattaneo and Cappella, 2017). Taphonomic variables play a significant role in making the interpretation of skeletal trauma difficult by hiding or damaging a perimortem fracture and creating new postmortem damage that often alters pre-existing bone lesions. For example, evidence of criminal activity may be altered by bone weathering and misinterpreted by forensic investigators or scavenging carnivores can disguise a perimortem skeletal fracture (Fisher, 1995; Haglund, 1997a; Tsokos and Schulz, 1999; Calce and Rogers, 2007). Therefore, experiments focusing on differentiating between perimortem trauma and postmortem damage can assist forensic investigators to precisely interpret the cause and manner of a victim's death.

Tool mark identification and taphonomic information can clarify the circumstance of a death, explain alternative hypotheses, and postulate forensic assessment regarding the tools used for criminal activity and related illegal behaviour (Symes *et al.*, 2002; Symes *et al.*, 2014; Cattaneo and Cappella, 2017). Even though forensic anthropology has been developed substantially in recent decades, the more problematic topics like trauma interpretation, and taphonomic agents such as an outdoor environment and the burning process have not achieved the same success (Cappella *et al.*, 2014; Thompson, 2015). Major questions have emerged on the taphonomic effects on skeletal trauma analysis in forensic cases. Was the evidence of trauma preserved after exposure to the outdoors environment or heat? How can taphonomic factors be excluded when analysing the evidence of trauma? Conducting research focusing on taphonomically derived traumatic lesions can assist forensic practitioners to interpret accurately the damage inflicted to bone, particularly to differentiate perimortem trauma from postmortem damage, and to identify postmortem modifications that have the potential to damage evidence of

criminal activity (Calce and Rogers, 2007). These issues are critical given that legal personnel demand state-of-the-art techniques to support arguable justification in a court of law.

As identified by the literature review carried out in the next chapter, the anthropological investigations have focused on several aspects of skeletal trauma and taphonomy. Nevertheless, there are still many questions either in need of resolution or with unsatisfactory answers. Though the level of understanding of these topics has improved in the last few years, forensic anthropologists are still not aware of the influence of taphonomic changes on the reliability of skeletal trauma analytical methods traditionally used in forensic anthropology. Therefore, the present study has used a controlled, methodological approach to evaluate the effects of environmental taphonomic alterations on fracture sites inflicted by blunt and sharp instruments.

1.4 Aims and objectives of the research

The idea for this study arose out of the recognition of the limited knowledge of how skeletal traumatic lesions degrade and altered post-deposition. The main purpose of this research is to investigate the effects of environmental taphonomic factors on fresh and burned bone fractures that have been inflicted by either blunt or sharp instruments, and to consider the interpretation problems. Environmental taphonomic variables are significant as they may contribute to alterations in a perimortem fracture and create new postmortem damage. More specifically, the study focuses on how to recognise traumatic skeletal lesions during 18-months environmental exposure with taphonomic changes to traumatic skeletal lesions being explored at the specific time points of 6, 12 and 18 months. Furthermore, this study emphasises the investigation of taphonomic variables in the making of a difficult interpretation of a trauma by the destruction of significant perimortem features and the creation of a variety of taphonomic modifications. Different variables such as maceration methods, types of experimental animals used and types of trauma infliction impact the results to a greater or lesser degree. These variables will be discussed in ongoing and related chapters.

Another goal of this study is to investigate surface modifications of skeletal tissues in South-east England. There have been previous studies in a temperate climate (Andrews and Cook, 1985; Andrews, 1995; Fernández-Jalvo *et al.,* 2010), but the influences of the micro-environmental factors were not recorded and clarified. Although many weathering studies have been conducted in different parts of Central Africa (Behrensmeyer, 1978; Tappen, 1994), Canada (Marceau, 2007), and the United States (Haynes, 1981; Galloway *et al.*, 1989; Bass, 1997; Junod, 2013), only a few publications on this topics have concentrated on how environmental factors can conceal skeletal trauma (Symes *et al.*, 2002; Calce and Rogers, 2007). Moreover, the mechanisms of how environmental factors affect traumatic features in different depositional environments have undergone relatively little research. Given that, this study investigates the pattern of early bone diagenesis in South-east England and its effects on traumatic lesions. Although there have been previous studies of postmortem bone modification in the UK (Andrews and Cook 1985; Fernández-Jalvo *et al.* 2010), different microhabitat and taphonomic factors have a significant influence on bone diagenetic rate and pattern. Consequently, the bone deterioration in this study is established based on the seasonal context and variations in temperature and precipitation in Shrivenham, Oxfordshire, Great Britain.

The hypothesis being tested is that, by the end of this study, five expectations will be postulated:

(1) Blunt and sharp-inflicted skeletal trauma are damaged by environmental taphonomic factors such as sunlight exposure, fluctuation of temperature, precipitation, vegetation growth and soil erosion (Behrensmeyer, 1978; Galloway *et al.*, 1989; Tappen, 1994; Bass, 1997).

(2) Taphonomically-derived skeletal trauma can be identified and distinguished from other postmortem lesions by using macroscopic, microscopic and radiological examinations (Calce and Roger, 2007; Cappella *et al.,* 2014).

(3) The rate of weathering is expected to increase during spring and summer due to an increase in UV radiation (Behrensmeyer, 1978) in areas of bone that are exposed and unprotected.

(4) The bone weathering process that might be expected to be encountered after the experimental period includes cracking and flaking of the bone surface (Behrensmeyer, 1978) and soil erosion (Littleton, 2000).

(5) Environmental factors make burned bone trauma more fragmentary and challenging to interpret fracture sites, but it is still possible to evaluate their trauma morphology (Waterhouse, 2013c).

Analysis of all experiments would offer crucial evidence needed to substantiate or refute these postulations. The acceptance of the hypothesis provides valuable information for analysing traumatic lesions. Nevertheless, a negation of the hypothesis is also beneficial, as professionals can be aware of the taphonomic changes they may encounter. The results of this study enable forensic anthropologists to recognise a traumatic lesion exposed to the outdoors environment and heat and help them to identify signs of postmortem modifications during their examination.

1.5 Outline of chapters

It is now appropriate to demonstrate the structure of this thesis as a whole. The thesis explores two major topics related to skeletal trauma analysis: sharp force trauma and blunt force trauma. All issues addressed in this work have been investigated regarding outdoors environmental exposure, which can derive traumatic lesions and their related information. Hence, the thesis develops into different sections.

Before approaching the central issues of the present project, a comprehensive review of the studies and literature concerning the general knowledge of skeletal trauma and taphonomy is undertaken in chapter 2 to summarise the existing practices and methods. This chapter is divided into the detailed backgrounds of bone structure and property, the bone diagenetic process, skeletal trauma, and heat-induced skeletal changes. Chapter 3 focuses on a series of experimental protocol outlines based on the literature and anthropological study. This chapter also provides an overall context of the investigation, documentation, and analysis of bone samples in each experimental group.

It was decided to not use the traditional format of “Methodology-Results-Discussion” for this thesis. Therefore, the next five chapters present only the results and a discussion of the selected aspects. Chapter 4 focuses on the interpretation of surface modifications of skeletal materials after outdoor environmental exposure. Chapters 5 to 7 concentrate on the results of the environmental effects on blunt and sharp force injuries to femoral samples and sharp force injuries to rib samples. Chapter 8 deals with the effects of heat on sharp-inflicted bone morphology and the effects of the environment on burned bones and their trauma morphology. Chapter 9 discusses the combinations of the bone changes of the previous chapters and shifts the focus of the thesis from the effects of the outdoor environment to the consequences, and the implications of the experimental findings for forensic practice and study. Lastly, this chapter contains the conclusions of the outcomes of this thesis and notes the potential areas for future study.

Chapter 2: Literature Review

2.1 Bone structure and property

2.1.1 The structure of bone tissue

Bone is a complex connective tissue consisting principally of protein collagen impregnated with minerals and closely resembles carbonated hydroxyapatite and ground organic substances such as mucopolysaccharides and glycoproteins. It also contains water which is very important mechanically (Rho *et al.*, 1998; Currey, 2002; Olszta *et al.*, 2007). The percentage of skeletal components by weight differs depending on species and skeletal element. In human bone, the mineral phase makes up approximately 65% of bone weight, whereas approximately 25% of bone weight comes from organic component and there is contribution from water (10%) (Zioupos *et al.*, 2000; Olszta *et al.*, 2007).

In addition, bone is considered as a composite material consisting of two or more distinct components (Braidotti *et al.*, 1997; Currey, 2002). Two basic types of bone structural tissues are distinguished as cortical and cancellous. Cortical bone comprises the dense outer surface of the bone forming a protective layer around the porous and fragile cancellous bone. Cortical bone comprises around 80% skeletal tissue mass and its main role is to maintain bony structure and the rigidity required for weight-bearing (White *et al.*, 2012). Cancellous bone, also called trabecular bone, is characterised by a lattice of thin branching bony spicules known as trabeculae which form a network filled with marrow cells (Olszta *et al.*, 2007; White *et al.*, 2012).

Microscopically, the cortical bone comprises several concentric layers of lamellae, within which are a number of osteocyte lacunae. Haversian canals, containing blood vessels, align with the long axis of the bone and connect to one another by Volkmann's canals. Each unit of the Haversian canal surrounded by cylindrical layers of lamellae is known as osteon. The trabecular bone comprises only simple rows of lamellae without pattern of osteon. At the microstructural level, bone is laid down, maintained, and remodelled throughout life by three types of bone cells. Osteoblasts are bone-building cells. Their roles are to secrete osteoid,

which is the un-mineralized organic substance of bone matrix, and are responsible for laying down new bone material. Once osteoblasts are surrounded by bone matrix, they become mature bone cell (osteocytes) and their main function is bone tissue maintenance. Lastly, osteoclasts are bone-resorbing cell that remove bone tissues (Currey, 2002; Olszta *et al.*, 2007; White *et al.*, 2012).

Nanoscopically, bone material structure consists of hydroxyapatite crystals ($Ca_{10}(PO_4)_6(OH)$) embedded within a collagen matrix. Type I collagen is a triple polypeptides complex constituting most of the organic content in mature healthy bone (Currey, 2002; Viguet-Carrin *et al.*, 2006; Olszta *et al.*, 2007). Its main role is to act as a supportive structure for the hydroxyapatite crystals and provide strength and flexibility (Rho *et al.*, 1998; Olszta *et al.*, 2007). The polypeptide chains are linked together with hydrogen bonds in a characteristic left-handed triple helix (Currey, 2002; Olszta *et al.*, 2007). Impregnating and surrounding the collagen fibril is a crystalline calcium phosphate mineral called hydroxyapatite, which is very small plate-like or needle-shaped molecules resulting in very large surface area. This means that the hydroxyapatite crystal is very reactive, an important factor affecting bone diagenesis in any various environment (Currey, 2002; Smith, 2002). The intrinsic property of the bone matrix contributes to bone strength as the mineral components provide the stiffness, while the collagen fibres provide the ductility and the ability to absorb energy (Rho *et al.*, 1998; Currey, 2002; Sahar *et al.*, 2005; Viguet-Carrin *et al.*, 2006).

2.1.2 Mechanical properties of bone tissue

Biomechanics is the study of the physical science of force and energy acting to a living tissue. An understanding of biomechanical and physical properties of bone provide valuable information relating to fracture formation and propagation. The following details are after Berryman and Symes (1998), Brinckmann and colleagues (2002), Currey (2002), Freivalds (2011), Kroman (2007), Schmitt and colleagues (2014), Turner and Burr (1993), and Zephro and Galloway (2014).

The following definitions of important concepts are described. Force is expressed as a mechanical loading resulting in movement or deformation of an object. A direct force can simply push or pull an object as a description of Newton's

first law of motion or the law of inertia. This law states that an object remains at rest or in constant velocity until it is acted by an external force. While Newton's second law of motion or law of acceleration states that the resulting change in momentum of a body is proportional to the unbalanced force applied. Mathematically, this law is expressed as force (F) is proportional to the product of mass (m) and acceleration (a).

The applied force per unit area can be used as a common term of stress. A unit of stress is newton per square metre, Pascal or pound per square inch (psi). Force can be further divided into three subtypes: tension, compression, and shear. Tensile force is produced when a force is applied to stretch a material. Compressive force occurs when a force is applied to make a material shorter. Shear is produced when a force is applied parallel to the surface of a material. Daily scenarios usually occur in combination of multiple types of forces. In addition, bone material is stronger in compressive stress than tensile and shear stresses. These would be explained from adaptation of bones in order to resist compressive forces usually encountered in daily activity.

Strain is described as percentage change in length, or relative deformation. It can also be expressed as the ratio of the change in material dimension (deformation) to the original form. The relationship between stress and strain in the elastic region of a material is known as Young's modulus or the modulus of elasticity (Figure 2.1). This curve is often used to describe how brittle or stiffness a material is. In general, the elastic property of organic matter of bone allows it to return to its original size and shape if the stress is removed. However, when the bone is loaded to its yield point, the bone is still structurally integrated but it cannot return to its original state (plastic deformation). When application of force attains the ultimate strength, the material reaches the failure point and fracture occurs. In bone trauma, fracture is described as a discontinuity of a bone and is dependent upon the amount and direction, as well as rate and duration of force. Furthermore, fracture can also be the result of a congenital and acquired bone disease such as osteogenesis imperfect and osteoporosis.

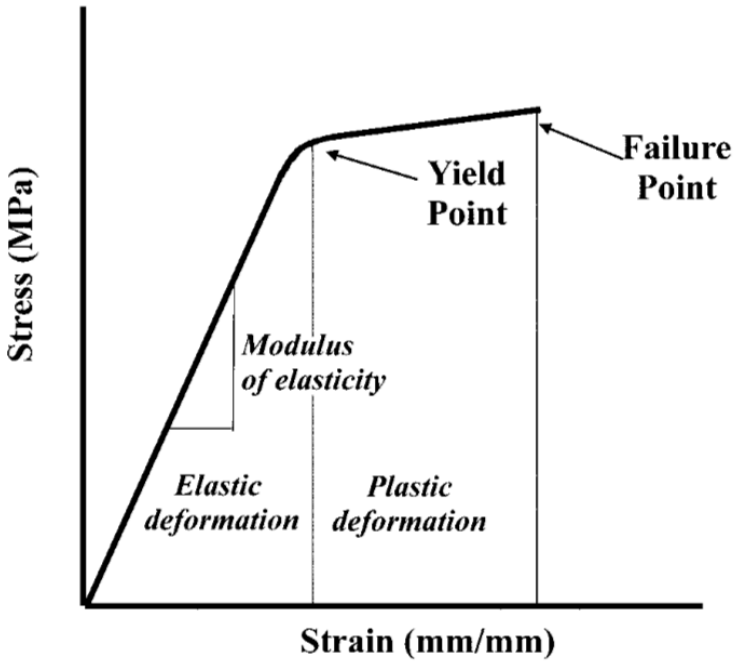

Figure 2.1: Stress-strain curve or Young's modulus or modulus of elasticity (from Wedel and Galloway, 2014: 35)

To completely understand bone fracture biomechanics, it is important to understand bone properties. Bone tissue is considered as an anisotropic and viscoelastic material. Typically, anisotropic material is better able to tolerate stress based on specific direction. For example, human long bone is stronger in the longitudinal dimension than transverse dimension (Figure 2.2). As a viscoelastic material, bone expresses to impacted force in a number of different ways depending upon the rate and length of loading. Then, bone can deform prior to fracture and this property differs markedly with the rate of applied force. For example, a bone reacts as an elastic material with plastic deformation before fracture in the case of low-velocity blunt instrument impact. While catastrophic fracture damage occur without plastic deformation when a bone is impacted with a high velocity projectile.

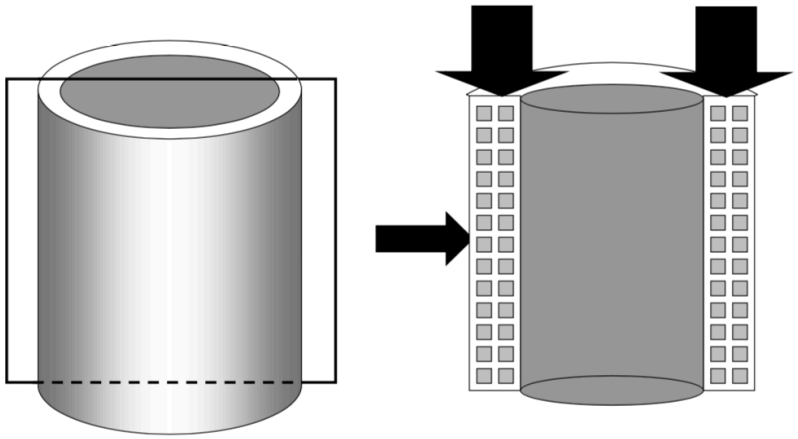

Figure 2.2: Anisotropic property of a material; in this case, the model of material is stronger in longitudinal direction (large arrows) than in transverse direction (small arrow) (from Kroman, 2007: 12)

Some unusual condition such as freezing has been theorized to affect biomechanical properties of skeletal materials. In fact, bone tissues under freezing condition less than five years or being exposed to eight freeze-thaw cycles have no a significant effect on bone structure or biomechanical properties (Borchers *et al.*, 1995; Jung *et al.*, 2011; Karr and Outram, 2012; Lee and Jasiuk, 2014).

2.1.3 Consideration of non-human bone experiment

The application of non-human skeletons as analogues of human bone in forensic anthropological research has a long history. Johnson (1985) firstly explored bone fracture study using mammalian bone, but she did not further discuss the possibility of interspecies variation. Mammalian bone microstructure can be divided into three categories: woven bone, lamellar bone, and plexiform bone (Martin *et al.*, 1998; Hillier and Bell, 2007).

1. Woven bone, or immature bone, comprises poorly organized, randomly oriented collagen fibrils. In human, this type of bone formed during periods of embryonic growth, healing bone, and certain pathological conditions such as bone tumours.
2. Lamellar bone is very consistent and highly organized bone structure with well-mineralized parallel sheets of bone tissue (lamellae).

3. Plexiform bone is a type of fibrolamellar that is characteristics of fast growing. Plexiform bone lies down rapidly, and has a more dense structure when compares with lamellar bone. This type of bone is found in large mammal bone such as bovine, pig, artiodactyls as well as carnivore, and less frequently in the bone of primates.

Structurally, there are vast differences between human and porcine bone. The typical human cortical bone is the lamellar bone consists of secondary osteon or Haversian systems (Martin *et al.*, 1998). Blood vessels and nerves inside a central canal are encircled by concentric layers of lamellar bone structure resulting from the resorption of existing bone with the outer border of the cement line. By contrast, mature pig (*Sus scrofa*) skeletons consist of plexiform bone with a dense Haversian system. This plexiform bone may also exist throughout an immature femoral shaft without any Haversian tissue (Hillier and Bell, 2007). Patterns of distinctive rows of five or more primary or secondary osteons, known as osteonal banding, are also found near the endosteal layer along with the lamellar bone and these can be used to distinguish between human and nonhuman bone (Mulhern and Ubelaker, 2001; Hillier and Bell, 2007).

The benefit of using animal models stems from their availability, capability for control of variables and fewer regulations compared to using human subjects (Aerssens *et al.*, 1998; Neyt *et al.*, 1998; Liebschner, 2004). Nowadays, many biomechanical researchers use animal models (table 2.1), but no standards exist for bone biomechanical experiments in animal models. Selection of animal bones for biomechanical research should be based on their availability and composition (Liebschner, 2004). It is currently unclear how data from research using nonhuman animal models can be used for human skeletal trauma reconstruction. The suitability of non-human bone as a proxy for human skeletal fracture has been discussed. However, fracture properties of non-human models have yet to be satisfactorily explored and results may not be acceptable in a court of law. The ethical consideration of using specimens as human bones is controversial and non-human bones are now primary specimens of fracture research. Perhaps the best way to adapt non-human experimental actuality to forensic practices is to “proceed with caution” when interpreting results on the witness stand (Zephro *et al.*, 2014).

Table 2.1: Demonstration of sample species and skeletal material type used in previous literature about skeletal trauma

Authors	Sample species	Type of skeletal materials
Houck (1998)	Bovine	Tibia
Bartelink *et al*. (2001)	Human	Humerus
Alunni-Perret *et al*. (2005)	Human	Femur
Saville *et al*. (2007)	Porcine	Femur
Lewis (2008)	Bovine	Tibia
Bello and Soligo (2008)	Porcine	Rib
Bello *et al.* (2009)	Deer	Scapula, femur, tibia
Thompson and Inglis (2009)	Porcine	Rib, radius, scapula, vertebra, carpal bone
de Juana *et al*. (2010)	Deer	Humerus, femur, radius, tibia
Boschin and Crezzini (2012)	Bovine	Metapodials and phalanges
Shaw *et al.* (2011)	Porcine	Skull
Moretti *et al*. (2015)	Bovine, deer	Scapula, innominate

2.2 Skeletal trauma

According to international classification of World Health Organization, trauma is defined as “a physical wound or injury caused by acute exposure to physical agents such as mechanical energy, heat, electricity, chemicals, and ionizing radiation in amounts that exceed the threshold of physiological tolerance” (DiMaio and DiMaio, 2001; Kimmerle and Baraybar, 2008; Zephro and Galloway, 2014; Saukko and Knight, 2015). Skeletal trauma is described as a modification of bone from a slow- or rapid-load impact with an object (Berryman and Symes, 1998; Kimmerle and Baraybar, 2008; Symes *et al.*, 2012). Skeletal trauma can express as incomplete or complete bone discontinuity and fracture as well as joint displacement or dislocation. With advances in the field of forensic anthropology,

trauma analysis has become a valuable component for examination of osteological remains.

Skeletal trauma is considered as the interaction between intrinsic factors of the bone and external applied forces (Ritchie *et al.*, 2005; Symes *et al.*, 2012; Schmitt *et al.*, 2014). The three key extrinsic variables are force, interacted surface area, and the rate of impact (acceleration/ deceleration). An object acted by external force can be deformed, change its state of motion, or both. Main categories of directional force, such as tension, compression, shearing, and torsion are responsible for certain types of bone trauma (Berryman and Symes, 1998; Zephro and Galloway, 2014). However, in real-life situation, a combination of these types of force often involve in a single fracture event. All of these are drawn by relying on biomechanics, the science of physics and material properties to understand the failure and fracture, as discussed earlier. Forensic anthropologists work together with forensic pathologists in increasing numbers and are called on to examine skeletal trauma for evidence of cause and manner of death. As such, recent studies have focused on examination techniques (Bartelink *et al.,* 2001; Alunni-Perret *et al.,* 2005; Bai *et al.,* 2007), interpreting bone injury with other natural taphonomic processes such as tooth marks, weathering process (Maples *et al.*, 1989; Fisher, 1995; Walsh-Haney, 1999; Symes *et al.*, 2002), and those made by human weapons or implements (such as an edged weapon, a metal tool, or a gun) and weapon identification (Calce and Rogers, 2007; Dominguez-Rodrigo *et al.*, 2009; de Juana *et al.*, 2010). Skeletal trauma researches have been also utilized as a mean of investigating into archaeology. Some of these studies have focused on comparing fracture between fresh and dry bones (Outram, 2001; Wheatley, 2008; Wieberg and Wescott, 2008; Bradley *et al.*, 2014; Scheirs *et al.*, 2017). Distinguishing the timing of trauma is another aspect of a forensic examination of skeletal remains. Forensic anthropologists and forensic pathologists have a different idea in their use of perimortem and postmortem terminology. From the pathological and medico-legal perspective, antemortem injuries occur prior to death, and give background information about the individual during life; perimortem trauma occurs around time of death, or shortly before or after; postmortem damage is clearly defined as being after death of the individual. However, from the anthropological definition, the perimortem period can extend as long as a bone

retains its moisture and viscoelastic property (Wieberg and Wescott, 2008; Galloway *et al.*, 2014).

Extrinsic traumatic mechanism can be classified into three major categories: blunt force trauma, sharp force trauma, and gunshot trauma (Kimmerle and Baraybar, 2008; Symes *et al.*, 2012; Spatola, 2015). Blunt force trauma can be described as a relatively slow-loaded impact to a bone over a relatively large surface area. Whereas sharp force trauma involves an impact applied by a tool with a narrow-edged surface area such as an instrument with a point or bevelled edge. However, there is no definite impact size for blunt and sharp force separation (Kimmerle and Baraybar, 2008; Symes *et al.*, 2012). Gunshot injury is defined as an injury from a fast-loaded force by a bullet fired from a gun or the explosion (Berryman and Symes, 1998; Kimmerle and Baraybar, 2008; Spatola, 2015).

2.2.1 Injury database

Within countries adopting stringent laws upon firearms such as the United Kingdom, the most commonly used weapons in violent crimes and homicides is sharp force trauma (Hunt and Cowling, 1991; Webb *et al.,* 1999; Henderson *et al.,* 2005; Allen and Audickas, 2018), with 37% of total violent death in 2016/17 compared with 36% in 2015/16 (Allen and Audickas 2018). Blunt trauma and hitting are the second most frequent cause of homicidal deaths, accounting for 20% of the total. In addition, Henderson *et al.* (2005) considered 62 non-firearm homicide cases in London between 1992-2001 and found that the majority of their cases (58.1%) involved stabbing homicides. Blunt injury was declared as cause of death in 25.8% of the homicidal cases.

Conversely, an obvious difference in the most common weapon using in homicide cases among any countries is recognised. Ambade and Godbole (2006), who reported autopsy cases performed in their university in India during the period 1998-2000, found that the total 241 homicidal cases in their study, 99 cases (41.1%) were inflicted by blunt instruments, whereas 91 cases (37.8%) were resulted from sharp weapons (Ambade and Godbole 2006). These findings are similar to the work reported by Kominato et al. (1997) demonstrating homicide cases occurring in the Toyama prefecture, Japan. Of the 63 homicides studied,

38.1% were killed by blunt instrument, whereas only 17.5% of cases died from knife crimes. On the other hand, criminal statistics in the U.S. demonstrated that firearms were used in most of homicides (66.5%), followed by sharp weapons (12.9%) and blunt instruments (7%) (Karch *et al*. 2014). From these views, it can conclude that which weapon using in violent crime is dependent upon socioeconomic and cultural characteristics, as well as how easy for accessibility.

Specifically, the distribution of trauma over the body by blunt and sharp weapons is different. All previous literature (Hunt and Cowling, 1991; Rogde *et al.*, 2000; Banasr *et al.*, 2003; Cassidy and Curtis, 2005; Henderson *et al.*, 2005; Ambade and Godbole, 2006; Karch *et al.,* 2014; Vassalini *et al.*, 2014; Park and Son, 2018) reported that thorax is the most common region followed by head and neck in the victims inflicted by sharp instrument. Webb et al. (1999) studied 120 fatal and non-fatal knife injuries in Edinburgh, Scotland between 1992 and 1996. During that period, there were 20 dead persons (17%) and 16 of them had the most severely injured body area at chest (80%). 3 for head and neck injury (15%) and only one person involved abdominal region (5%). Knives have been reported to be the most frequently used weapons (64.9%) of homicides in South Korea, and injuries to the torso was significantly higher (78.4% of all cases) when compared with other regions (Park and Son 2018). In addition, Schmidt and Pollak (2006) explored 158 victims of sharp force injuries in Freiburg from 1992 to 2004. The result indicated that the most common injury location was thoracic area (45.9%) and the lower extremities were less often affected (6.1%). Banasr *et al*. (2003) also reported that the highest incidence of bone and cartilage injuries in fatal stab cases was reported on the ribs and sternum. A stab wound to the thorax affects the bony structure in two ways: a puncture and a cut. The cut mark is a result of the knife blade passing through the intercostal space and leaving a mark on the superficial surface of the rib (Kooi and Fairgrieve 2013). Despite the fact that the thorax is the most common area for stabbing, few forensic literature pay attention to tool mark analysis and how taphonomic factors influence on its examination.

The leading cause of blunt force trauma in the U.K. is the kicking or hitting without a weapon, accounting for 20-25% of all homicide cases (Hunt and Cowling, 1991; Rogde *et al.*, 2000; Henderson *et al.*, 2005). Blunt force injury from motor

vehicle accidents results in road fatalities totally around 1775 victims and 22807 serious injured persons in 2014 (Office for National Statistics, 2015). Likewise, the distribution of trauma over body by blunt and sharp weapons is different. Blunt injuries are usually encountered at head followed by upper and lower extremity (Department of transport, 2017).

2.2.2 Sharp force trauma

Sharp force trauma refers to an injury created by a narrow edge or point of any tool with the combination of compressive and shearing forces, resulting in alterations such as straight line incisions, punctures, gouges, and chopping (Kimmerle and Baraybar, 2008; Symes *et al.*, 2012). This type of injury occurs under loading force similar to mechanism of blunt force trauma, but using an instrument with a very small surface area. While sharp force injury can be generated by a wide variety of instruments, the most commonly utilized and extensively researched weapon is a knife. Stabbing and cutting are complicated sequences of different movements, which produce axial and non-axial forces and torques. Therefore, it is difficult to reproduce in an experimental methodology (Jones *et al.,* 1994; Chadwick *et al.* 1999; O'Callaghan *et al.*, 1999; Hainsworth *et al.*, 2008). Moreover, the knife characteristics including shape, geometry, and sharpness of the knife blade as well as resistance factors such as skin tension, clothing and bone strength have an important role on the severity of trauma.

Tool mark interpretation from a knife wound made on bone surface is one of the well-established topics in forensic practices. Forensic anthropologists are usually the ones to realize the appearance of trauma on skeletal remains, and focus on defining general description, type and timing of these physical alterations. Attention to knife and saw marks on human bones is firstly demonstrated by Bonte (1975), who indicated that sharp weapons could leave recognisable marks on bone. Injuries caused by sharp instruments is of major importance for crime investigations and well analysed in previous forensic literature (Walsh-Haney, 1999; Bartelink *et al.*, 2001; Tucker *et al.*, 2001; Humphrey and Hutchinson, 2001; Symes *et al.*, 2002; Thali *et al.*, 2003; Alunni-Perret *et al.*, 2005; Thompson and Inglis, 2009; Lynn and Fairgrieve, 2009a; Lynn and Fairgrieve, 2009b; Symes *et al.*, 2010; Pounder and Reeder, 2011; Pounder and Sim, 2011; Boschin and Crezzini, 2012; Tennick, 2012;

Cerutti *et al.*, 2014; Moretti *et al.*, 2015; Waltenberger and Schutkowski, 2017; Vegh and Rando, 2019). These aspects were also associated with the reconstruction of human behaviour in archaeological contexts such as act of violence, sacrifice, mortuary behaviour, cannibalism and butchery (Shipman and Rose 1983; Olsen 1988; Bello and Soligo 2008; Lewis, 2008; Bello *et al*. 2009; Dominguez-Rodrigo *et al*. 2009; de Juana *et al*. 2010; Moretti *et al*. 2015).

When a tool is used, it often leaves more or less specific marks on the surface it was applied to. These tool marks manifest themselves as a notch, an impression, or striations (Kimmerle and Baraybar, 2008; Symes *et al.,* 2012). This negative impression and cast replication can usually be examined by microscopic methods (Houck 1998; Olsen 1998; Saville *et al.* 2006; Tucker *et al*. 2001). Recent investigations of tool mark analysis include identification of weapons from bone and cartilage injuries (Symes *et al.*, 2010) and specific tool such as saw mark analysis (Symes, 1992; Saville *et al.,* 2007; Freas 2010).

2.2.2.1 Tool marks and their inference of weapon

Inferring the origin of an unknown mark is important for forensic case interpretation. The current literature identifies various options to establish the cause of marks or distinguish between different sources of origin. As an edge weapon progresses though a bone, the plastic response of the organic components of skeletal tissues plays an important role in imprint of weapon characteristics on the cut surface (Tucker *et al.*, 2001; Waltenberger and Schutkowski, 2017; Norman *et al.*, 2018). Thereby, this creates a kerf, or groove that can be analysed for determining the class of the knife used. To date, previous literature has focused on the morphological traits of sharp-inflicted marks to reconstruct the type of weapon used (Bonte, 1975; Symes, 1992; Saville *et al.*, 2007; Marciniak, 2009; Symes *et al.*, 2010; Tennick, 2012); however, the metric analysis of the sharp-inflicted mark and its relationship to the type of weapon used has been neglected, with a few exceptions (Symes, 1992; Symes *et al.*, 2012; Cerutti *et al.*, 2014).

Methods used for interpretation of levels of inference recognise different diagnostic criteria. Many literature on sharp force weapon identification focused on certain investigations, mainly macroscopic (Frayer and Bridgens, 1985; Walsh-

Haney, 1999; Humphrey and Hutchinson, 2001; Lynn and Fairgrieve, 2009a) and microscopic (Bello *et al.*, 2009; Lynn and Fairgrieve, 2009b; Shaw *et al.*, 2011; Boschin and Crezzini, 2012; Tennick, 2012; Kooi and Fairgrieve, 2013; Moretti *et al.*, 2015; Boucherie *et al.*, 2017; Waltenberger and Schutkowski, 2017; Vegh and Rando, 2019) examinations. Scanning electron microscopic analyses providing high resolution images have been also used for identification of specific features on the cut surfaces of the inflicted bone (Tucker *et al.*, 2001; Thompson, 2005; Lynn and Fairgrieve, 2009b; de Juana *et al.*, 2010). Recently, more sophisticated three-dimensional methods such as micro-computed tomography have been employed (Thali *et al.*, 2003; Chappard *et al.*, 2005; Bello *et al.*, 2009; Thali *et al.*, 2009; Rutty *et al.*, 2013; Waltenberger and Schutkowski, 2017; Komo and Grassberger, 2018; Norman *et al.*, 2018).

Table 2.2 illustrates levels of inference in forensic contexts. Ideally, individual level of inference is the ultimate aim of forensic investigation. This level can lead to specify the most potential weapon for criminal activity, whereas class level of inference only allows a number of suspect weapons. Compared objects are established to be individuations if they used to be parts of a whole; for example, a broken knife blade recovered from the victim that can fit into the suspect knife. However, most of forensic cases only establish criteria of class characteristics (Houck, 1998; Tennick, 2012; Cerutti *et al.,* 2014; Moretti *et al.,* 2015).

Table 2.2: Inference of forensic evidence in mark examination (Houck 1998; Tennick 2012)

Level of inference	Definition	Examples
Identification	Basic characteristics without using a specific reference criteria	Blunt force or sharp force trauma
Classification	Particular type of object or weapon	A knife or a saw
Sub-classification	Specific feature of object or weapon	A serrated or fine blade knife
Individualization	Specific object or weapon and no other weapon can made this mark	The knife found with a suspect

The class characteristics of an incised mark can become more precise depending on the number and combination of features considered in the examination. The greater the number of specific traits used to describe class characteristics, the more precise the classification can become (Houck 1998). The same type of knife blade shares the same class features especially for items from the same manufacturer. Many characteristics can be used to identify class characteristics of a cut mark such as kerf width, kerf depth to width ratio, cross-sectional shape, striation pattern, and shoulder effect (Kimmerle and Baraybar, 2008; Byers, 2010; Tennick, 2012). However, only a few studies of cut marks in contemporary bone evidence concern taphonomic changes of class characteristics (Symes *et al.,* 2002; Cappella *et al.,* 2014; Fernández-Jalvo and Andrews, 2016).

2.2.2.2 Knife and chop mark characteristics

A knife cut wound acting on a bone results in a relatively superficial and linear V-shaped groove, penetrating the skeletal surface with smooth sides. Occasionally, a slight ridge is orientated parallel to the incision (Bartelink *et al.*, 2001; Kimmerle and Baraybar, 2008; Andrews and Fernández-Jalvo, 2012; Langley, 2017). The word “kerf” is widely used as a groove made by a cutting tool, and the kerf floor is defined as the termination point of the tool cut (Symes *et al.*, 2010; Tennick, 2012). This type of wound is typically made by a short-light instrument. Most relevant outcomes of cut mark examinations still remain controversial and caution should be observed when predicting blade characteristics from the shape of a knife cut marks on bone. A blade may cut through the bone surface and leave a linear cut mark with a kerf. As the sharp instrument penetrates the bone at an angle, a kerf margin is lifted and peeled away from the bone (Kimmerle and Baraybar, 2008; Langley, 2017). These patterns of defect are more common in a rib when the knife enters at a considerable angle of the rib surface (Tennick, 2012; Langley, 2017).

The type of weapon identification and sometimes the specific individual weapon can be analysed from macroscopic and microscopic examination of knife cut wounds. Previous literature interpreted sharp force injury of bone to make statements about the context of death in both forensic and archaeological cases. Such work involves the definition of kerf dimensions and properties (Bartelink *et al.*, 2001; Bello and Soligo, 2008), the differentiation of cut mark origin (Alunni-Perret *et*

al., 2005; Saville *et al.*, 2007; Bello and Soligo, 2008). For example, Tennick (2012) examined microscopic striation analysis, Bartelink *et al.* (2001) explored cut mark width with micro-CT to create weapon identification, and Thompson and Inglis (2009) looked for morphologically macroscopic difference between serrated and non-serrated blades in order to establish classification criteria. The dimensions and shapes of sharp force trauma to bone are well maintained because of the rigidity of bone tissues (Humphrey and Hutchinson, 2001). Straightforwardly, the dimension of the linear marks vary depending upon the size and shape of the causing weapon; for example, being narrow V-shaped defect with a sharp blade such as a kitchen knife, and broader defect with a tool such as an axe. Directionality of the cut marks can be indicated by direction of Hertzian fracture cones of the kerf edges, pseudo-steps of the kerf surfaces, and supination at the end of the mark (Bromage and Boyde 1984). Striation analysis was also conducted in order to identify a specific knife from the marks made on bone.

In addition to a cut mark, a linear defect on bone can be the result of other edged tool with either long or thick blade edges such as a cleaver, a machete or an axe. The first study trying to distinguish different types of chop marks (sword and axe) on bone was conducted by Wenham (1989). Then, a number of researcher (Humphrey and Hutchinson, 2001; Tucker *et al.*, 2001; de Gruchy and Rogers, 2002; Alunni-Perret *et al.*, 2005; Lynn and Fairgrieve, 2009a; de Juana *et al.,* 2010) conducted extensive research on overall morphology of hacking trauma that could allow to explore several noticeable characteristics of wounds caused by specific types of weapon. They provided a comprehensive analysis of hacking injury. Their works can be summarised as following statements:

(1) Similar to knife wounds, a hacking weapon produces a smooth, flat cut surface when the angle of entry is 90°.

(2) If the blade enters bone tissue at an angle greater 90°, the obtuse-angled side shows a smooth border, while the acute-angled side is rough and sometimes has small bone detachment to form thin flakes.

(3) Chop marks made with a cleaver do not produce radiating fractures around the entry site, while machete wounds have less clear fragmented

appearance. Striations are distinctly oriented perpendicular to kerf floor.

A cleaver and a machete are mainly used in multiple trials on human and non-human long bones with or without control of the direction and force of the blow. The bone defects were then investigated for several features using for differentiating the weapons. Originally, the summary reviewed in Table 2.3 indicate three defined classes of hacking trauma.

Table 2.3: Summary of entry and exit characteristics of bone marks from cleavers, machetes, and axes (from Humphrey and Hutchinson 2001)

Features	Cleaver	Machete	Axe
Entry site recognition	Clearly recognisable	Less clearly recognisable	Sometimes clearly recognisable
Entry site appearance	Clean	Clean and chattering	Clean, chattering, crushing, fracture
Entry site width	Narrow (approx. 1.5 mm)	Medium (approx. 3.5 mm)	Medium to large (approx. 4-5 mm)
Entry site fracture	Never	Originate from past-entry site at kerf floor; several fragment	Originate at entry site and extend outward; large pieces of bone pushed into entry
Depth of penetration	Never penetrate whole bone	Rarely penetrate whole bone	Rarely penetrate whole bone
Exit site recognition	No exit site	Clearly recognisable	Clearly recognisable
Exit site appearance and fractures	No exit site	Fracture with small to medium bone fragments	Fracture with large triangular bone fragments (often only one)

Humphrey and Hutchinson (2001) suggested that it is possible to use macroscopic examination to make a reasonable assessment of particular chopping weapon type. However, some characteristics such as the depth of the chop mark varied due to an individual strength. In addition, no information concerning fracturing associated with hacking trauma was discussed. In addition to gross examination, the microscopic analysis of hacking trauma was thoroughly investigated by Tucker *et al*. (2001). Twenty-eight semi-fleshed porcine long bones were chopped with a cleaver, a machete, and an axe with uncontrolled force but regulated direction. The bones were then macerated and cut surfaces were casted before investigation with SEM. Tucker *et al*. (2001) advised that comparisons of cut bone surface and striations could be used for identifying the class and possibly the individual weapon. Cleaver-induced trauma is identified by fine, thin and distinctive parallel striations, while all bones inflicted with machetes showed coarse, thick and ill-defined striations. No striation is shown in axe-inflicted trauma due to complete bone breakage. Therefore, the absence of traumatic characteristics assists in class identification of an axe as the causative weapon.

2.2.2.3 Cut marks and other bone surface modifications

Linear defects can also result from organic processes such as animal, plant and microorganism (Fernández-Jalvo *et al.* 2016: 25). The researchers can distinguish different causes of marks from their cross-sectional characteristics, especially the shape, width and degree of rounding of the marks. Recently, archaeological study of cut mark has developed diagnostic criteria to differentiate between bone defects made by natural taphonomic processes and those made by human-made implements. An unknown mark can be explored to identify a cut mark as opposed to other marks created by natural agents including scavenger tooth marks, rodent gnawing marks, burning, plant root etching, weathering, animal digestion, sedimentary particles, and trampling (Behrensmeyer, 1978; Shipman and Rose, 1983; Olsen, 1988; Fisher, 1995; Dominguez-Rodrigo *et al.* 2009; Andrews and Fernández-Jalvo, 2012; Fernández-Jalvo and Andrews, 2016). Percussion marks and modern excavation marks can also mimic cut mark morphology (Olsen, 1988; Fisher, 1995; Dominguez-Rodrigo *et al.*, 2009).

Carnivore tooth marks can produce striations, furrows, pits and punctures, and bone flakes (Olsen, 1988; Fisher, 1995; Tsokos and Schulz, 1999). The shape and size of carnivore tooth marks vary depending upon tooth type and animal species (Haglund, 1997a; Young, 2017). Tooth marks tend to have a uniform depth, while cut marks usually are shallower at the ends than in the middle. It is observed that the width and cross-sectional shape of bone marks can be used as differentiating characteristics between tooth marks and cut marks. Microscopically, cross-sectional shape of cut marks is narrow V-shaped feature, in contrast to that is broad and shallow U-shaped in tooth marks and chopping marks (Haynes, 1981; Shipman and Rose, 1983). Cut mark width can also be used as a reliable criterion for distinguishing between weapon types, but it still has variation from the angle at which the tool is impacted, the amount of soft tissue around impact area, and the load applied to the tool (Shipman 1983).

A plant root can etch into a bone surface through acids associated with plant roots or by fungi associated with decomposing roots (Walker and Long, 1977; Bunn, 1981; Potts and Shipman, 1981; Fisher, 1995). Typically, patterns of root etching involve multiple lines imparted as a distinctive branching network that is macroscopically visible with U-shaped cross-sections to the individual surface scores (Behrensmeyer, 1978; Andrews and Cook, 1985). These features, as well as very fine vascular grooves on bone surface, can be confused with cut marks (Lyman, 1994; Fisher, 1995; Fernández-Jalvo and Andrews, 2016).

Trampling can press the bones lying on the ground into rocky surfaces or sediment and create multiple fine and superficial scratch marks as the bones were rubbed against the stones. Although there is a little chance to interpret trampling marks as cut marks, Olsen (1988) advised to evaluate this feature on archaeological bone with cautions. A trampling mark usually has fine and shallow with smooth walls and internal parallel striations. The highly variable width and orientation of a trampling mark is also considerable. However, it may mimic cut mark when the bone rubs against sharp-pointed stones (Fisher, 1995). They differ, nevertheless, in being commonly less deep and much more abundant with no proximity to origin or insertion of muscle and tendon (Andrews and Cook, 1985; Olsen, 1988).

Classification criteria in different contexts were developed. According to Fernández-Jalvo and Andrews (2016), the main characteristic which distinguishes different forms of linear marks is their cross-sectional feature. Based on their shape, width and degree of rounding of the mark, linear marks can be categorised into those with V or U shaped cross-sections. Caution must be observed when relying on only one feature for identification and the most reliable analysis should be based on consideration of all data (Eickhoff and Herrmann, 1985).

2.2.3 Blunt force trauma

Blunt force trauma is defined as the relatively slow-loaded and non-penetrating physical injury from a blunt instrument over a relatively large area of contact with the bone, resulting in a fracture and a dislocation (Berryman and Symes, 1998; Byers, 2010; Wedel and Galloway, 2014; Langley, 2017). Common causes of this traumatic lesion include homicidal assaults, traffic accidents, and fall from heights. The morphology of blunt force trauma is regulated by various factors including the nature of impact, the affected area, the angle, duration, and magnitude of the load (Berryman and Symes, 1998; Symes, *et al.*, 2012; Zephro and Galloway, 2014). A number of studies have drastically conducted to understanding blunt force trauma in contexts of forensic anthropology; for example, how difference between antemortem, perimortem, and postmortem contexts (Berryman and Symes, 1998; Moraitis and Spiliopoulou, 2006; Moraitis *et al.*, 2008; Wheatley, 2008; Wieberg and Wescott, 2008; Wright, 2009; Cappella *et al.*, 2014; Cappella *et al.*, 2014; Scheirs *et al.*, 2017); how about mechanism of fractures and their classification (Kroman, 2007; Kimmerle and Baraybar, 2008; Zephro and Galloway, 2014); how difference between blunt and ballistic injury (Berryman and Symes, 1998; Ritchie *et al.*, 2005; Symes *et al.*, 2012). These allow forensic anthropologists to attempt to assess biomechanics reconstruction and manner of death.

2.2.3.1 Biomechanical consideration

To understand the basic principles of skeletal fractures, biomechanical properties should be thorough understood. As mentioned earlier, the skeletal response to a force is described by Young's modulus of elasticity (Figure 2.1).

Generally, bone is weakest in area of tension and strongest in area of compression. Thus, bone fracture should start at the side of the bone in tension with the fracture propagating under shear stresses and finally under the area of compression on the opposite side (Berryman and Symes, 1998; Moraitis and Spiliopoulou, 2006). Specifically, some types of fracture are created through a combination of tensile, shear, and compressive forces. The classification of complete fracture type is dependent on the type, amount and location of the force applied, as well as the type of bone. Therefore, complete fractures are divided based on the shape and location of fracture. Transverse fractures are fractures that run at approximately perpendicular to the long axis of the long bone, and these may be caused by a three-point loading mechanism, when a blunt instrument imparts severe angulation (Gozna, 1982; Moraitis *et al.*, 2008; Galloway *et al.*, 2014). Oblique fractures run at a 45-degree angle across the diaphysis, resulting from the combination of angulation and compressive forces. Comminuted fractures occur when more than two fragments are generated, which usually involves relatively high levels of force (Gozna, 1982; Moraitis *et al.*, 2008; Byers, 2010; Galloway *et al.*, 2014).

For this study, it is essential to understand the bone fracture with angulation or bending mechanism. The proximal and distal ends of a long bone are stabilized and a force is applied to a diaphyseal part, resulting in bending around the point of impact. Bending mechanism applies tensile forces along one side of a bone while each other side experiences compressive forces as well as shear forces are produced within the middle (Berryman and Symes, 1998; Moraitis and Spiliopoulou, 2006; Zephro and Galloway, 2014). Because bone materials have a greater resistance to compressive force, the fracture initially occur from tensile forces at a convex side opposite of the point of impact. Then fracture will propagate back to a concave side, where the compressive site accumulates (Ubelaker and Adams, 1995; Symes *et al.*, 2012; Kroman and Symes, 2013; Zephro and Galloway, 2014). As a result, bending fractures are generally oblique or transverse; sometimes they may also have butterfly fragments. Fracture propagations along the shearing plane in combination with oblique transverse fractures, result in a triangular wedge-shaped bone on the concave side. This specific type of fracture is defined as consisting of two segments of bone and a small butterfly fragment (Ubelaker and Adams, 1995; Galloway *et al.*, 2014; Reber and Simmons, 2015). Sometimes, full

formation of the butterfly fragment does not occur, leading to an incomplete butterfly fracture (Reber and Simmons, 2015).

2.2.3.2 Microscopic fracture surface analysis

The character of fracture caused by different mechanical processes of blunt force trauma has been approached through morphological analysis. Microscopic imaging, or also called fractography, can be used for qualitative analysis of fracture surfaces. Fractography is the microscopic exploration of fracture surface features in an effort to investigate underlying mechanisms of fracture and mechanical properties (Corondan and Haworth, 1986; Wise *et al.*, 2007; Christensen *et al.*, 2018). This term is firstly used by Carl A. Zapffe in 1944 in order to analyse the fracture features in metallurgical research (Möser, 1987). This examination can be conducted by optical or electron microscopy. The variation of microscopic features of fracture surfaces depends upon the mechanism of failure (Zephro and Galloway, 2014; Christensen *et al.*, 2018). As a consequence, fractography can be used in supplementing the interpretation of failure behaviour and the manner occurring underneath the topography of the fracture surface (Mills *et al.*, 1987). Moreover, previous literature have linked fractographic features to biomechanical characteristics between perimortem fractures and postmortem damages using fractographic features (Wynnyckyj *et al.*, 2011; Scheirs *et al.*, 2017). As noted that the differentiation between perimortem fractures and postmortem damages is largely regulated by the nature of the bone materials instead of the timing of injury (Ubelaker and Adams, 1995; Moraitis and Spiliopoulou, 2006; Wieberg and Wescott, 2008; Galloway *et al.*, 2014).

Several authors found that the microscopic fracture surface is variable depending on which type of force is applied (Ubelaker and Adams, 1995; Moraitis and Spiliopoulou, 2006; Wieberg and Wescott, 2008; Galloway *et al.*, 2014). In term of investigating failure mechanism, the most common microscopic characteristics on the perimortem fracture surface is inter-lamellar delamination and layered morphology, protruded fibre bundles, and osteon pullout (Braidotti *et al.*, 2000; Wise *et al.*, 2007; Scheirs *et al.*, 2017; Wynnyckyj *et al.*, 2011). Compressive force causes inter-lamellar delamination and layered morphology, relating to the inter-lamellar micro-cracks. For a preliminary investigation of perimortem fracture and

postmortem damage, Scheirs *et al.* (2017) determined the time of injury by means of macroscopic comparing fractured bones from autopsy cases with both fresh and dry experimental bone fractures. Scheirs *et al.* (2017) found a relationship between five distinctive characteristics and perimortem fracture. Layered morphology in compressive side was the most common macroscopic trait occurring 82% of all perimortem samples. While bone scales, flaking, crushed margins, and wave lines were insignificantly visualized using microscopic examination.

In contrast, osteon pullout occurs at the tensile area when tensile strength exceed the shear strength at its cement line, causing inter-laminar interfaces crack across intact osteon embedded in the interstitial matrix. As a result, osteons debond from the interstitial matrix and pull out to reduce the strain, resulting in the irregular projection of osteon pullout on tensile fracture surface (Nalla *et al.*, 2003). Concomitantly, Braidotti and his colleagues (1997) carried out a research about dry and wet human femoral shaft fracture surface examined with SEM. The hydrated and dry samples were broken by a three-point bending machine, and then the features of both tensile and compressive regions of fracture surfaces were studied. It was demonstrated that there were different characteristics between wet and dry fracture bone samples due to difference in the collagen behaviour. The fracture surfaces were photographed and then taken for percent measurement of the osteonal pullout area. Hiller and his co-workers (2003) found that the amount of osteon pullout is dependent upon the mode of mechanical loading (fatigue vs. monotonic) and cortical region. Osteonal pullout appeared in the area that collagen fibres were more transversely oriented, smaller osteon, and longer fatigue lives.

Wynnyckyj and colleagues (2011) investigated bone failure mechanism and compared between fresh and collagen-degraded bone. KOH has an effect on bone collagen matrix by accelerated collagen degradation, but there is no any change to the bone mineral. Area of tension and compression were identified from fracture surface images and they are divided into rough and smooth areas (Figure 2.3). The average smooth and roughness area was determined and calculated using software computer, and then the ratios of rough to smooth areas was used for distinguishing between each fracture area. From their view, KOH-treated collagen degraded samples showed a significant higher rough region compared to untreated

bones, and this phenomenon reflect a change of biomechanical properties of degraded bone (Wynnyckyj *et al*. 2011).

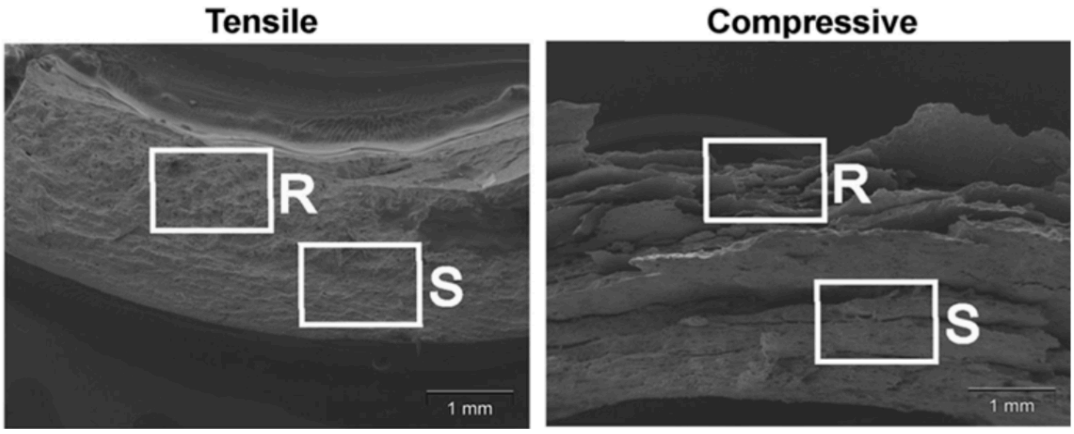

Figure 2.3: tensile (left) and compressive (right) fracture surface of KOH-treated degraded bones, demonstrating smooth (S) and rough(R) regions (from Wynnyckyj *et al.*, 2011)

Christensen *et al.* (2018) also advised to use fractographic technique in conjunction with other fracture characteristics such as morphological patterns, metric technique, and discoloration. Fractography can help clarify the trauma event and can be used to help in our understanding of blunt force trauma and its related topics (Scheirs *et al.*, 2017; Christensen *et al.,* 2018).

2.3 Taphonomic processes of skeletal remains

2.3.1 Overview of taphonomy

Taphonomy, originally a branch of paleontology and zooarchaeology, is concerned with understanding decomposition processes of dead organisms and factors affecting them. This term, derived from the Greek meaning the laws of burial, is described as the study of what happens to plants and animals after they die, and all aspects of the transition process of organisms from the biosphere to the lithosphere (Haynes, 1981; Lyman, 1994; Haglund and Sorg, 1997; Lyman, 2010; Bristow *et al.,* 2011). Traditionally, Brett and Baird (1986) stated taphonomy as the systematic study of fossilization and how fossils preserved in the geological record, includes aspects of biogenic processes occurring from the death of an organism

until its final emplacement within the sediment, namely transportation, skeletal dissolution, sediment filling, and mineralization (Haynes, 1981; Brett and Baird, 1986). In essence, the study of taphonomy is developed to understand the ecology of a decomposition location, how change of ecosystem when the plant or animal remains are introduced to it, and how site ecosystem have affected the decomposition process of these remains (Lyman, 2004; Carter and Tibbett 2008; Lyman, 2010; Bristow *et al.,* 2011). The scope of taphonomy is broadened and involves a number of different academic experts such as archaeology, entomology, botany, chemistry, and forensic science (Nawrocki, 2016).

Forensic taphonomy, a subfield of forensic anthropology, is defined as the study of taphonomy as relevant in a medico-legal investigation (Haglund and Sorg, 1997; Rogers, 2010; Pokines and Symes, 2014). This knowledge is incorporated by forensic scientists to focus on the decomposition process of human remains (Bass, 1997; Carter *et al.*, 2007; Damann, 2010; Ross and Cunningham, 2011; Pankowská *et al.*, 2017; Fernández-Jalvo *et al.*, 2018), to estimate postmortem or post-burial interval (Galloway *et al.*, 1989; Megyesi *et al.*, 2005; Bristow *et al.,* 2011; Kontopoulos *et al.*, 2016; Pollock *et al.*, 2018), to assist in the investigation of cause and manner of death (Ubelaker and Adams, 1995; Symes *et al.*, 2002; Calce and Rogers, 2007; Cappella *et al.*, 2014; Macoveciuc *et al.*, 2017), and to reconstruct circumstances surrounding death scene (Crist *et al.*, 1997; Galloway *et al.*, 2001; Dupras and Schultz, 2014; Pokines, 2016; Pankowská *et al.*, 2017). Forensic taphonomy can be divisible into two broad branches; biotaphonomy, directly concerned with the remains; and geotaphonomy, concerned with the burials and how a buried body affects surrounding environment (Nawrocki, 1996). The variables within each topic were demonstrated in Table 2.4.

The research concerning taphonomic modified skeletal remains has been profited from the cooperation between archaeological and forensic research (Lyman, 2010). Even though their chronology and specific aims are different in some degree, both focus on the same objective- the skeletal remains. Experimentation relating to bone modification is a common utilized method for creating analogies to taphonomy occurring in both buried and unburied bodies. The research in surface decomposition is one of critical developments in the field of

forensic taphonomy (Galloway *et al.*, 1989; Bass, 1997; Carter *et al.*, 2007; Pokines, 2016). Whereas the discussion of decomposition in a buried environment has been largely untreated in detail (Nicholson, 1996; Littleton, 2000; Neher *et al.*, 2003; Dent *et al.*, 2004; Jaggers and Rogers, 2009). It is widely accepted that burial often shows decomposition rate slowing down because of lower temperature and limitations of insects and scavengers (Rodriguez, 1997; Dent *et al.*, 2004). Recent studies have been carried out on various factors affecting decomposition process such as temperature (Archer, 2004; Megyesi *et al.*, 2005), microbiological activity (Catts and Goff, 1992; Tibbett *et al.*, 2004; Bristow *et al.,* 2011), soil pH and moisture (Dent *et al.*, 2004; Forbes *et al.*, 2005; Carter *et al.*, 2008; Carter *et al.*, 2010).

Table 2.4: The sub-disciplines of forensic taphonomy
(adapted from Nawrocki 1996)

Branches of forensic taphonomy	Categories (and subsequent examples)
Biotaphonomy	Environmental factors (animals and climate)
	Individual factors (body size, age at death)
	Cultural (or behavioural) factors (embalming, trauma)
Geotaphonomy	Disturbance of the soil (change of soil compaction, aeration and layer mixing)
	The production of tool marks and footprints in the grave formation
	Disruption of plant growth in the grave vicinity
	Alterations of water drainage, erosion patterns, and surrounding soil pH

2.3.2 Diagenesis of skeletal material

Bone diagenesis is defined as a process referring to preservation or destruction of organic and mineral components of bone (Nicholson, 1996; Hedges,

2002; Fernández-Jalvo *et al.*, 2010; Fernández-Jalvo *et al.*, 2016; Kendall *et al.*, 2018). When soft tissues have undergone decomposition process and skeletal materials are exposed, a bone goes through different destructive processes leading to its deterioration. These include physical breakage, decalcification, and mineral dissolution (Nielsen-Marsh and Hedges, 2000; Hedges, 2002; Dent *et al.*, 2004; Fernández-Jalvo *et al.*, 2016; Kendall *et al.*, 2018).

Several researchers from archaeological and anthropological communities put great emphasis on studies of early bone diagenesis to understand its process and pattern. Similar to soft tissue decomposition, skeletal deterioration occurs in recognisably sequential stages. The timing of each stage is mainly dependent on depositional environmental factors (Behrensmeyer, 1978; Andrews and Cook, 1985; Andrews, 1995; Bell *et al.*, 1996; Andrews and Whybrow, 2005; Janjua and Rogers, 2008). The organic and inorganic components of skeletal remains are also degraded by the action of microorganisms, plants, soil and underground water (Nielsen-Marsh *et al.*, 2000; Collins *et al.*, 2002; Turner-Walker and Syversen, 2002; Stodder, 2008; Janaway *et al.*, 2009; Rogers, 2010; Sidrim *et al.*, 2010). The organic portion of bone is mainly degraded by the action of bacterial products especially collagenase enzymes, which can break down the protein-mineral bond to shorter peptide chains and finally reduce to amino acids (Gill-King, 1997; Rogers, 2010; Boaks *et al.*, 2014). Concomitantly, the inorganic phase of bone is degraded through the loss of hydroxyapatite (Nielsen-Marsh *et al.*, 2000; Kendall *et al.*, 2018).

Diagenetic factors can be divided into two different categories: extrinsic and intrinsic factors. Intrinsic factors are those that take place within the bone (Von Endt and Ortner, 1984; Hedges, 2002; Kendall *et al.*, 2018). Lyman (1994) expressed diagenetic factors by the equation:

$$D = f (M, C, D, S, T)$$

In which D is the sum of the diagenetic factors affecting a hard tissue; M is the original physical and chemical structures of the hard tissue of concern; C is the climate of depositional environment; D is the mode of deposition; S is the nature of soil and sediment in which the hard tissue is buried; and T is the time span of

deposition (Lyman 1994). Depending upon various factors of the depositional environment, survivability of a bone over time is predicted.

Survival of skeletal materials is dependent on several intrinsic variables including bone type, size, shape, maturity and density (Lyman, 1994; Stodder, 2008; Lininger, 2015; Nawrocki, 2016). Differences of structural properties of skeletal tissues affect the prevalence and severity of bone diagenesis. The influence of bone density on diagenetic process is very well attested (Lyman, 1994; Willey *et al.*, 1997; Collins *et al.*, 2002; Kendall *et al.*, 2018). Skeletal elements with a high proportion of cancellous bone such as vertebrae and ribs are susceptible to decay. In contrast, bones with high amount of cortical bone such as skull, mandible and long bones are less damaged (Waldron, 1987). A small bone with low bone density may not survive (Willey *et al.*, 1997; Bello *et al.*, 2006). Bones of children are both smaller and less dense than adult bones; as a consequence, juvenile bones tend to disperse, lose and destroy comparing to adult bones (Guy *et al.*, 1997; Cunningham *et al.*, 2011; Manifold, 2012). Nevertheless, there is a lack of studies on the chemical makeup of the juvenile skeleton to reach a conclusion (Manifold, 2012).

Surface porosity is also a crucial indicator for bone diagenesis, as more porosity means more rapid decay of skeletal tissues (Von Endt and Ortner, 1984; Manifold, 2012). Therefore, the porous nature of infant and subadult skeleton tends to diagenetic deterioration. This porous structure can accelerate mineral dissolution. Particularly a large pore permits groundwater to fill in, and then increases the bone-water interaction. However, Lyman (1994) and Nicholson (1996) indicated that bone density is more important factor, as the process through porosity affects archaeological bone, but do not disturb contemporary bone. Skeletal pathology is known to accelerate skeletal diagenesis (Waldron, 1987; Manifold, 2012). When bones are damaged by a disease, it is easier for soil and environmental organism to invade bone materials. For example, Rickets and scurvy increase number of surface porosity especially the skull and the growth plates, leading to mineral dissolution (Lewis, 2010).

When skeletal remains are discovered outside, extrinsic factors are of considerable importance, and a comprehensive analysis of environmental factors is

imperative. During taphonomic modifications, extrinsic biotic and abiotic agents can modify bone surface, structure and histology (Andrews and Cook, 1985; Nielsen-Marsh *et al.*, 2000; Hedges, 2002; Boaks *et al.*, 2014). Taphonomic phenomena on remains are not limited to single cause, but comprise a variety of sources, including both human interference and environmental variables. These can be divided into those caused by a living organism and those not (Ubelaker, 1997; Junkins and Carter, 2017). Living taphonomic agents include animal and human effects (Andrews and Cook, 1985; Haglund and Sorg, 1997; Tsokos and Schulz, 1999; Reeves, 2009; Pokines, 2016), plants (Willey and Heilman, 1987; Lyman, 1994; Coyle, 2004; Miller, 2017) and microorganism (Tibbett *et al.*, 2004; Hyde *et al.*, 2013; Pechal *et al.*, 2013). Abiotic environmental taphonomic agents include temperature and humidity (Behrensmeyer, 1978; Galloway *et al.*, 1989; Archer, 2004; Carter *et al.*, 2010), weathering (Behrensmeyer, 1978; Lyman, 1994; Potmesil, 2005; Junod and Pokines, 2014) and depositional contexts (Ubelaker, 1997; Huculak and Rogers, 2009; Junkins and Carter, 2017). These variables can deteriorate and modify skeletal tissues, thus decrease their chances of survival (White and Hannus, 1983; Andrews and Cook, 1985; Galloway *et al.*, 1989; Vass *et al.*, 1992; Bass, 1997; Littleton, 2000; Archer, 2004; Potmesil, 2005; Rogers, 2010). The action of bacterial collagenases proceeds to degrade bone collagen, whereas hydroxyapatite crystal is eliminated mainly by chemical weathering.

The general consensus in the literature suggests that temperature and moisture are the most substantial factors affecting the decomposition process (Galloway *et al.*, 1989; Mann *et al.*, 1990; Gill-King, 1997; Megyesi *et al.*, 2005). Megyesi *et al.* (2005) suggested that temperature could be used to predict the progression of decomposition compared to postmortem interval. The effect of temperature on decomposition also varies with latitude, season and depth of burial (Janaway *et al.*, 2009). Temperature is considered as the principal determinant of decomposition process. Indeed, an increase in temperature can accelerate biological and chemical activity resulting in an increase speed of decomposition rates and decomposer microbial activity (Vass *et al.*, 1992; Sauer, 1998; Carter *et al.*, 2007). According to an original work by Von Endt and Ortner (1984), they used three different temperatures (100°C, 120°C and 130°C) to accelerate the loss of nitrogen in bovine bones. Their results showed that as the temperature rises, the

lost of bone nitrogen and protein increase as well (Von Endt and Ortner, 1984). Moreover, temperature has an effect on taxa of microbes during decomposition. As Carter *et al.* (2015) investigated an increase in a cold-tolerant bacterial genus *Psychrobacter* in soils related to decomposition of swine carcasses in winter, so temperature can select for certain microbial decomposers. Therefore, the effects of soil microbial communities on decomposition process are different in hot and cold weather (Carter *et al.*, 2015).

Environmental fluctuations are the most destructive to skeletal tissues (Collins *et al.*, 2002; Hedges, 2002; Calce and Rogers, 2007; Fernández-Jalvo *et al.*, 2010). Cyclical freezing and thawing as well as wetting and drying events trigger bones to swell and shrink repeatedly resulting in radial cracking, flaking and spalling (Fernández-Jalvo *et al.*, 2010; Pokines, 2016). An expansion of freezing water within pore spaces of a bone has a high potential to cause micro-crack. After the thawing process, water molecule penetrates the newly opened cracks and subsequently leads to further expansion of cracks (Lee and Jasiuk, 2014; Pokines *et al.*, 2016). Subaerial weathering is the good example of this damage (Behrensmeyer, 1978; Fernández-Jalvo *et al.*, 2010). Temperate environment with recurrent freeze-thaw cycles may be more damaging to skeletal remains than tropical, desert, or tundra zones that have fewer annual periods of ambient temperature change above and below freezing point (Junod and Pokines, 2014; Pokines *et al.*, 2016).

2.3.3 Weathering processes

Recently, the term “weathering” has been used by palaeontologists, zoo-archaeologists and forensic anthropologists to define postmortem processes which alter the chemical and physical properties of skeletal elements and teeth (Behrensmeyer, 1978; Hedges, 2002; Blau, 2017). The weathering phenomenon is unquestionably a highly complex process, causing bleaching, cracking, and flaking as a result of exposure to solar radiation, fluctuation of temperature and precipitation, and chemical exposure. These micro-fissures and cracks deepen over time and develop further bone tissue disintegration and loss of organic component. The end result of weathering is fragmented bone and eventually loss of bone structure, becoming part of the lithosphere and completing the taphonomic pathway

(Behrensmeyer, 1978; White and Hannus, 1983; Gill-King, 1997; Lyman and Fox, 1997; Junod and Pokines, 2014).

Forensic anthropologists often observe processes of bone weathering as a general indicator of postmortem modification. It was the palaeobiologist Anna Kay Behrensmeyer who defined six stages of bone weathering as the deterioration of bones by physical and chemical agents operating on the bone *in situ* (Table 2.5). Bone samples were classified ranging from weathering stage 0 (bone displays no surface cracking or flaking) through stage 5 (bone is falling apart). Behrensmeyer (1978) also considered that the main cause of an increase in weathering rate was mainly from temperature and precipitation fluctuation. Differential stages on the same bone were also detected between the exposed area (more progressive) and ground-contact side. Conversely, the lower surface of bones may show more advanced weathering stage in some situation due to contact with vastly acidic soil (Behrensmeyer, 1978; Marceau, 2007; Junod and Pokines, 2014). Despite the fact that the original intention of this study is for use in zooarchaeology and paleoanthropology, Behrensmeyer's staging (1978) is included in *Standards for Data Collection from Human Skeletal Remains* (Buikstra and Ubelaker 1994), a standard textbook used as a means for recording bone taphonomic changes found in archaeological and forensic contexts, and her stages have been cited in numerous studies relating to bone weathering and skeletal decomposition (Buikstra and Ubelaker, 1994).

Weathering can occur even in subterranean and sub-aerial conditions (Lyman, 1994). However, most of previous research agreed that skeletal materials promptly deposited in burial context rarely display evidence of weathering (Behrensmeyer, 1978; Cunningham *et al.*, 2011; Junod, 2013), as burial deposition potentially shuts out most weathering agent. The original work by Behrensmeyer (1978) also stated that no sign of weathering in buried elements even if surface bones showed weathering stage 4 or 5.

Table 2.5: stage of weathering (modified from Behrensmeyer (1978))

Stage	Description	Year since death
0	- Bone is greasy, marrow cavities contain tissue - Fat, muscle, and ligament may cover the bone surface - No cracking or flaking on bone surface	0-1
1	- Bone show cracking parallel to the fibre structure - Articular surface show mosaic cracking of the bone - Soft tissue may be present	0-3
2	- Outermost bone surface show flaking, usually associated with cracking - Deeper and more extensive flaking follows, until most of the outermost bone is gone - Remnants of soft tissue and cartilage may be present	2-6
3	- Bone surface is characterised by patches of rough, homogenously weathered compact bone - In these patch, all the external, concentrically layered bone has been removed, resulting in a fibrous texture. - Weathering does not penetrate deeper than 1-1.5 mm - Soft tissue rarely present	4-15+
4	- The bone surface is coarse fibrous and rough in texture - Large and small splinter occur and may fall away from the bone when it is moved - Weathering penetrates into inner cavities	6-15+
5	- Bone is fragmenting apart into pieces - Original bone morphology is difficult to identify	6-15+

The exact mechanisms of bone deterioration from weathering are poorly understood but the main physical processes involve loss of organic and inorganic components as caused by exposure to sunlight, saturation, temperature fluctuation and desiccation (Behrensmeyer 1978; Junod and Pokines 2014; Ubelaker 1997). Bone weathering cracks prefer to follow the orientation of collagen fibres of bone tissue. Dead bones no longer have the capacity to maintain collagen fibres and water in their tissue from environmental stresses. As a result, collagen breakdown results in reduced bone matrix ability to bear cracking. Soluble mineral dissolution and organic component breakdown by microbes can also weaken bone structures (Nielsen-Marsh *et al*. 2000; Fernández-Jalvo *et al*. 2010). A number of variables influencing bone weathering can be divided into two groups: intrinsic and extrinsic factors. Intrinsic conditions include animal species, size, age, as well as skeletal density and micromorphology. Extrinsic and micro-environmental aspects involve vegetation coverage, soil property, water proximity and scavenger activity (Nielsen-Marsh *et al.*, 2000; Fernández-Jalvo *et al.*, 2010). Freezing and thawing cycles can also cause cortical cracking and flaking in bone surfaces (Behrensmeyer, 1978; Junod and Pokines, 2014). These variations within microenvironment are realized by the fact that a single bone usually presents more than one stage of weathering (Pokines *et al.*, 2016).

Influences of different environments and microhabitats on rates of bone weathering have received scant attention and been sparsely investigated in geographical regions (Behrensmeyer, 1978; Andrews, 1995; Ubelaker, 1997). Bone weathering rate alters considerably from region to region, based on fundamental differences in temperature, precipitation, and flora and fauna in that area. These factors are also important considerations when a forensic anthropologist uses bone weathering stage for postmortem interval estimation (Tappen and Peske, 1970; Behrensmeyer, 1978; Tappen, 1994; Littleton, 2000). For example, skeletal elements placing on temperate or rainforest environments have longer survival when compare with those depositing in arid climate (Bell *et al.*, 1996; Ubelaker, 1997; Calce and Rogers, 2007; Ross and Cunningham, 2011; Junod, 2013). These mean colder and sunlight-protective environments tend to decelerate weathering rate, whereas the rate of weathering is faster in the warmer, high temperature fluctuation, and strong sunlight (Behrensmeyer, 1978; Andrews and Cook, 1985;

Tappen, 1994). Colder climates can depress microbial activity and its degrading effects on bone (Marceau, 2007; Junod and Pokines, 2014). Previous literature showed that skeletal materials deposited in temperate environment have a slower rate of skeletal deterioration than skeletal remains placed in an arid environment (Andrews and Cook, 1985; Andrews, 1995; Fernández-Jalvo *et al.*, 2010; Junod, 2013; Junod and Pokines, 2014). In addition, weathering rate can be slower in tropical rainforest climate condition because of constant precipitation, lack of freeze-thaw cycles, and dense vegetation protecting bone materials from solar radiation. Bones kept moist and protected by vegetation and other cover undergo slower weathering (Tappen, 1994; Pokines, 2009; Ross and Cunningham, 2011).

In addition, skeletal remains deposited in the same place can have a different weathering rate and pattern due to various micro-environmental conditions. The fact that each bone of a carcass has different stages of weathering is encountered (Behrensmeyer, 1978; Gifford, 1981; Haynes, 1981). Behrensmeyer (1978) suggested that microenvironment such as temperature, moisture, and sunlight shade is more important in dictating the weathering rate and pattern than the overall habitual factors. Therefore, localized conditions such as patches of vegetation, soil composition, burial potential, snow cover, and scavenger activity can affect rate of osseous weathering (Behrensmeyer, 1978; Tappen, 1994; Pokines, 2009); thus, exposure duration can vary within a carcass as well as between carcasses (Behrensmeyer, 1978; Andrews and Cook, 1985; Tappen, 1994; Fernández-Jalvo *et al.*, 2010; Junod, 2013). Tables 2.6 and 2.7 demonstrate conclusion of research information from previous bone weathering studies.

The main problem concerns the time needed to observe bone weathering changes or the necessity to deal with bones with known depositional age (Andrews and Cook, 1985; Tappen, 1994; Lyman and Fox, 1997; Littleton, 2000; Ross and Cunningham, 2011; Junod, 2013). The study by Ross and Cunningham (2011) focused on short-term surface alterations (within a year) of juvenile domestic pig bones in the warm temperate climate of the central Piedmont region of North Carolina. All recovered skeletal materials showed no sign of any advanced weathering signs and were determined to be at stage 0 of the Behrensmeyer (1978) stage. Nevertheless, short-term changes were observed in all sample subjects.

Erosion of outer layer of articular facets and epiphyseal articulations was the most frequently prevalent and affecting the ribs and vertebrae. A term of circular pockmark pattern was used in case of an erosion of cortical bone layer exposing the underlying trabecular bone. Lastly, the fine marble-like pattern on the outermost cortical layer of a diaphysis was defined as flaking (Cunningham *et al.*, 2011).

Table 2.6: Comparison of bone weathering appearance in different environment

Literature	Location	Environment	Samples	Weathering rate*
Brain (1967)	Southwest Africa	Desert	Goat	More rapid
Haynes (1981)	North-central US and Canada	Subarctic/ sub-humid plains	Deer, moose, and bison	More rapid
Andrews and Cook (1985)	Somerset, UK	Temperate	Cow	Slower
Galloway *et al.* (1989)	Arizona, US	Desert	Human	More rapid
Tappen (1994)	Zaira, Africa	Savanna and rainforest	Buffalo, duiker, elephant, and monkey	Slower
Andrews (1995)	Somerset, UK	Temperate	Sheep	Slower
Bass (1997)	Tennessee	Hot and humid	Human	More rapid
Marceau (2007)	Alberta, Canada	Subarctic	Pig, and deer	Slower
Janjua and Rogers (2008)	Southern Ontario	Temperate	Pig	Slower
Junod (2013)	New England, US	Temperate	Moose, and deer	Slower

* Compare with Behrensmeyer (1978) study

Table 2.7: Summary of bone weathering according to four types of macro-environment

Site	Year-since-death	Weathering stage
Savanna (Behrensmeyer 1978; Tappen 1994)	2-4	1-2
	4-6	3-5
	7-9	3-4
	10-12	5
Tropical (Tappen 1994)	<10	0
	10-15	1
	15-20	2
	20-30	3
	30+	4
Temperate (Ross and Cunningham, 2011)	8	0
	10-12	1
	19	2
Arid (Andrews and Whybrow 2005)	2-4	0-1
	4-8	1
	10-15	2-3

Many of previous weathering studies have used retrospective in nature (Lyman and Fox, 1997; Junod and Pokines, 2014). However, this type of study cannot provide an accurate time frame for understanding when bone surface modifications occur. Janjua and Rogers (2008), and Pyle (2016) stated the need of more weathering research to understanding of bone weathering, as well as other correlated characteristics (e.g. bone staining, scavenging, and trauma). These have a beneficial effect on providing the best practice of skeletal decomposition and ultimately the ability to better forensic investigation. Direct study of the breakdown of a skeleton is the best method to understand taphonomic processes acting on skeletal remains in archaeological and forensic practices (Lyman and Fox, 1997).

Warm temperate climate is defined as a climate with a temperature of the coldest month above -3°C, while a temperature of the hottest month below 18°C (Kottek *et al.*, 2006). A lot of recent research has focused on weathering rate and pattern in warm temperate climate (Andrews and Cook, 1985; Fernández-Jalvo *et al.*, 2010; Madgwick and Mulville, 2012; Junod, 2013). In the UK, Andrews and Cook (1985) studied bone weathering of a juvenile cow carcass resting on a slight shelf covered by limestone and occasional used as a cattle track way. This site was visited annually to observe taphonomic alterations for eight years. Superficial surface modifications, almost striations and scrapes from trampling, scavenging and plant root marks, were observed. However, the skeletal materials did not show any signs of weathering due to sunlight protection from vegetation (Andrews and Cook 1985). Another long-term taphonomic study with a large number of 150 large and small animal bones was conducted in a variety of environment in Wales (Andrews, 1995). This study showed that surface-deposited bones had reached weathering stage 1 and 2 if they were uncovered and exposed for 10-12 years and 19 years respectively. Andrews (1995) suggested developing a system of weathering stages for warm temperate climate based on a long-term observation.

2.3.4 Burial environment

Burial is one of the most common methods for disposal of human remains. Human remains buried in soil can either be the result of illegal activity or correlated to non-criminal anthropology as funerals. The burial process is important because not only hard tissues would experience different diagenetic factors, but they may also be reoriented, broken, and abraded during burial by various taphonomic agents (Lyman, 1994; Littleton, 2000; Galloway *et al.*, 2001). In underground environments, skeletal remains undergo specific changes which influence their degradation. Wide-ranging environmental factors including soil type, moisture, acidity, temperature, humidity, and microbiological activity play important roles in decomposition processes (Mann *et al*., 1990; Carter and Tibbett 2008; Carter *et al*. 2010; Tumer *et al*. 2013) which involve uptake and exchange of materials from soils and breakdown and leaching of collagen fibres and mineral ions (Hedges, 2002).

Unfavourable soil conditions are one cause of poor skeletal preservation dependent on burial sites. The geology of Great Britain is complex, with varying

types of soil in each region. For example, the soil type in the area of Wiltshire and Oxfordshire is pelocalcaric brown or pelocalcaric gley soil with associated brown and gley soils. This soil type is usually neutral concentration (pH 5.5-7.0) (European Commission, 2005). The burial process may be also affected by how deeply remains are buried and the texture and environment of soil and sediment in which they are buried. Some taphonomic processes are dependent upon the depth of burial. For example, the scavenger activity of insects and vertebrates are not possible in deep burial remains. However, there is little study pertaining to decomposition and degradation in a buried body. The first study focusing on underground decomposition of human cadavers was reported in 1985 by Rodriguez and Bass (1985). They buried six human cadavers at various depths for a time period (months to a year). Analysis of the data showed that underground decomposition process is similar to a surface-deposited case, but at a slower rate and is highly dependent upon the depth of burial, soil type and surrounding temperature (Mann *et al.* 1990; Rodriguez and Bass 1985). Bone preservation is dependent upon the burial environment. It has been proposed that decomposition rate of a buried body is eight times slower than a surface-deposited body because of a decrease in insect and vertebrate scavenging, and a decrease in temperature (Rodriguez and Bass, 1985; Mann *et al.*, 1990), yet the exact rate is arguable depend on soil environment (Rodriguez, 1997).

Soil texture have a direct effect on bone diagenetic process (Nicholson, 1996; Haglund and Sorg, 1997; Dent *et al.*, 2004). Soils have different textures and biochemical compositions varying from one place to others. According to size of constitutional particles, soils are generally determined as clay (<0.002 mm), silt (0.02-0.002 mm), and sand (2-0.02 mm) (Carter *et al.*, 2010). Sand soils are loose and not aggregated together. Whereas fine-textured clayey soils always form extremely hard lumps when dry and are particularly sticky when wet. Clayey soils have lower rate of gas diffusion and can hold water much more than sand soil (Brown, 2003), hence sufficiency of gas exchange is not enough for aerobic microbiological activity. As a result, this condition causes domination of anaerobic microorganisms which are less efficient decomposer (Soil Science Society of America, 1997). In addition, the anaerobic environment and presence of moisture observed in clayey soils promote the formation of adipocere (Rodriguez and Bass,

1985; Littleton, 2000; Rogers, 2010). While the high rate of gas diffusion and the absence of moisture in sandy soils stimulate desiccation of soft tissues (Forbes *et al.*, 2005). Therefore, type of soil is one of the most substantial factors influencing on decomposition rate of organic carcasses.

Generally, bone surface erosion occurs from burial in acidic or alkaline soil as well as surface abrasion from exposure, repeated deposition and rubbing on the surface. Soil acidity plays an important role in bone diagenesis. According to Carter *et al.* (2010), acidic (pH 3.5-4.5) soil environment is more destructive to mammal bones than alkaline (pH 7.5-8.0) soil environment; this result is similar to the result observed in human bones for both the adult and children's bones (Gordon and Buikstra 1981; Nielsen-Marsh *et al*. 2007). In the acidic environment, mineralized contents start to lose their bio-apatite because of increased bioavailability of hydrogen ions (Nielsen-Marsh *et al*. 2000). Calcium ions within the hydroxyapatite near the bone surface can be soluble and replaced by hydrogen ions if this bone is in an acidic environment (Nielsen-Marsh *et al.*, 2000). Bone materials tend to survive better in alkaline environment because bone apatite is less likely to dissolve. Along with the degradation of hydroxyapatite, extreme acidity can also result in the hydrolysis of collagen bundles (White and Hannus, 1983). Nevertheless, between these two sets of figures there are many variables affecting bone preservation. Gordon and Buikstra (1981) and Nielsen-marsh *et al.* (2007) concluded that skeletal materials are stable as it is exposed to a pH level higher than 8.1.

Environmental factors include the availability of water in and around the bones. Water is an excellent chemical buffer and temperature stabilizer (Collins *et al.*, 2002). Water, as rainfall or well-drained sandy soil, flows diffusely through bones. Groundwater is also a factor to be considered in bone deterioration through burial. More porous bones, such as archaeological bone, are prone to absorb and desorb more water. The presence of water in the immediate environment surrounding the bones causes dissolution of minerals from bone materials via ion exchange between water and bone, thus weakening protein-mineral relationships and enhancing degradation (Gill-King, 1997). More significantly, porosity results in the demineralization of collagen to microbial collagenase which eventually leads to

complete destruction of the skeletal tissue (Von Endt and Ortner, 1984; Nielsen-Marsh *et al.*, 2000). Moreover, It is generally accepted that soil moisture has an influential effect on decomposition rate because the soil moisture can affect decomposer microorganism activity. Therefore, buried bones in free-draining soil are more likely to bio-erosion and dissolution due to the rapid loss of soluble materials. In contrast, in the opposite environment such as waterlogged environment, the persistent presence of water produces a buffered local setting, therefore slowing down diagenetic processes (Von Endt and Ortner, 1984; Nielsen-Marsh *et al.*, 2000; Kendall *et al.*, 2018).

The oxygen content of the burial environment has an effect on decomposition process. Wet, fine-textured clayey soil has been associated with a decrease in skeletal breakdown because of a low rate of gas diffusivity. Therefore, anaerobic microorganisms, being less effective decomposers than aerobic organisms, dominantly play a role in decomposition process. In other words, dry, coarse-textured soil generally promotes desiccation (Nielsen-Marsh *et al.*, 2000; Tutken and Vennemann, 2011; Fernández-Jalvo *et al.*, 2016).

To summarise, soil environment greatly affects the rate of decomposition as well as the composition of soil decomposer communities (Carter *et al.*, 2008). Changes to buried bones occur as a result of ion and material exchanges, collagen breakdown, microbiological attack, and mineral content alterations (Neher *et al.*, 2003; Tibbett *et al.*, 2004). The decay rate is dependent upon many characteristics and processes including mineralization process and nutrient cycle in ecosystems. Therefore, burial practices tend to either hasten or retard the decomposition of the body.

2.3.5 Colour staining of bone

Naturally, the colouration of normal bone surface is a yellowish-white or ivory colour from the existence of lipids and other biological fluids (Dupras and Schultz, 2014; Pollock *et al.*, 2018). Because of their porous surface and pale colour, bones are likely to take on the colour of the medium that they are deposited. The normal bone colour can transform into a variety of colouration based on exposure to decomposition fluids, sunlight, organic and mineral content of soil, water, plant,

moss and algae, fire, or metallic materials (Owsley *et al.*, 1995; Mayne Correira, 1997; Andrews and Whybrow, 2005; Dupras and Schultz, 2014; Pokines, 2016; Pollock *et al.*, 2018). Five main colour differences were observed (Table 2.8). In fact, it is imperative to recognise that similar colour change can result from different taphonomic factors; for instance, sun bleaching, fire exposure, chemical whitening, and adipocere formation can cause white discolouration to bone.

Table 2.8: Summary of surface colour analysis

Colour change	The most possible cause
Yellowish-white	Normal fresh bone
White	Sun bleaching
Dark reddish brown	Haemolysis
Light yellowish brown	Soil staining
Dark reddish grey	Decomposition fluid staining
Greenish	Algae or fungi

Skeletal remains exposing to soil environment tend to display dark-brown colour resulting from tannins and humic substances, which form by degradation of plant materials. These acidic groups are consistent of phenolic and carboxylic acids and provide humic matters that are able to form compounds with ions such as Ca^{2+}, Fe^{2+} and Fe^{3+}. Uptake of humic substances in the soil can form non-specific cross-links with bone collagen (van Klinken and Hedges, 1995; Pollock *et al.*, 2018). As a result, outer surface of a buried bone usually has displayed darker brown discolouration. In acidic soil, skeletal materials become discoloured because of the staining of soluble metal ions and humic acids. In contrast, bone deposited in alkali soils become lighter and cream in colour because of the locking up of insoluble carbonate and oxy-hydroxides (Nielsen-Marsh *et al.*, 2000; Turner-Walker, 2008).

Skeletal remains on a surface environment for extended periods of time are exposed to solar radiation, and these remains then display signs of subaerial weathering including sun bleaching, cortical surface cracking and flaking (Galloway *et al.*, 1989; Calce and Rogers, 2007; Huculak and Rogers, 2009; Pokines, 2016;

Pyle, 2016). Sun bleaching is one of the earliest taphonomic changes that occur (Beary and Lyman, 2012; Dupras and Schultz, 2014). UV exposure from sunlight degrades and accelerates the decomposition processes of many organic compounds and also breaks chemical bonds during photolytic and photo-oxidative reactions (Pokines and Symes, 2014). The colour of bleached bones is from the mineral hydroxyapatite, which is naturally white in colour. It is currently unknown how long a bone must be exposes to sunlight for natural bleaching and weathering to occur (Ross and Cunningham, 2011; Pokines, 2016). Pyle (2016) carried out research about effects of solar radiation on human remains at Texas State University. He reported the median value for the appearance of sun bleaching was 51366.4 W/m^2, 997 ADD, and 47 calendar days. However, the results found in this study can only apply to areas that its weather is similar to Central Texas and the Southwest U.S. (Pyle, 2016).

The main problem with observation of bone surface colour is that the definition of a given colour is entirely subjective. As a result, inter-experiment comparison is remarkably problematic. In order to standardise bone colour documentation, Munsell® colour chart should be used (Dupras and Schultz, 2014). To interpret colour of a sample, the researcher can compare it to 251 colours of this chart and make some quasi-quantitative examination by assigning a level of the hue, value and chroma of each colour (Munsell, 1992). The use of Munsell® colour chart would be the most appropriate method for standardization and comparison between each research, thereby reducing intra- and inter-observer error (Thompson, 2003; Dupras and Schultz, 2014).

2.4 Taphonomic modifications and skeletal trauma analysis

Identification of perimortem trauma is associated with the cause and manner of death (Sauer 1998). The distinction between traumatic lesions occurring around death and those after death is not always easy to perform. Forensic pathologists usually assign clear differentiation between perimortem and postmortem settings on the basis of the presence of vital reaction in soft tissues (Sauer, 1998; DiMaio and DiMaio, 2001; Saukko and Knight, 2015). With a fresh cadaver, a forensic

pathologist can consider several characteristics of soft tissue (e.g. tissue reaction and haemorrhage), but for a forensic anthropologist, this task is more complicated.

Confusion concerning perimortem trauma and postmortem damage usually occurs when the forensic anthropologist is consulted in a medical examiner office. Morphological characteristics used to differentiate perimortem fracture and postmortem bone damage are problematic because the period following death until bone significantly loses its organic and moisture content is variable, dependent upon the postmortem depositional environment (Sauer, 1998; Wieberg and Wescott, 2008; Cappella *et al.*, 2014; Scheirs *et al.*, 2017). As soon as the organic matrix begins to degrade and bone moisture begins to decrease, bone materials exhibit dissimilar response to environmental stresses. Therefore, the differences in skeletal trauma morphology in conjunction with death may be significant particularly if the bone exposes to different taphonomic factors.

Multiple criteria used by forensic anthropologists to discriminate blunt force fracture between wet and dry bones include fracture morphology, colour staining of fracture surface, fracture line around lesion, and pattern recognition (such as carnivore scavenging and weathering) (Sauer, 1998; Calce and Rogers, 2007; Wieberg and Wescott, 2008; Cappella *et al.*, 2014) (Table 2.9). In practice, the criteria used for distinguishing perimortem fracture from postmortem damage are still uncertain, as forensic anthropologist should rely on all obtainable features to make a decision (Outram, 1998; Sauer, 1998; Coelho and Cardoso, 2013; Galloway *et al.*, 2014; Symes *et al.*, 2014; Scheirs *et al.*, 2017).

In addition, taphonomic variables can make this task even tougher because they can modify morphological characteristics of bone lesions. Bones degradation has been experienced as a result of different environmental conditions. Several researchers have been afforded the chance to deal with morphological changes resulting from the decomposition process, taphonomic events and environmental factors occurring over time (Ubelaker and Adams, 1995; Sauer, 1998). A variety of taphonomic variables can produce skeletal modifications confusing with perimortem trauma (Sauer, 1998; Calce and Rogers, 2007; Wieberg and Wescott, 2008; Cappella *et al.*, 2014). Freezing and thawing, rain and snow exposure, displacement of the skull and soil erosion have a considerable influence on the

morphology of pre-existing fractures. However, it is unclear how different between interdependent variables such as freeze-thaw cycles and presence of rain and snow. Calce and Rogers (2007) encouraged expansion of this topic to all environmental patterns to detail specific procedures used for examining different inflicted trauma on remains affected by taphonomic processes.

Table 2.9: Summary of blunt-inflicted fracture characteristics of perimortem and postmortem period

Fracture features	Perimortem	Postmortem
General appearance	Curved	Transverse
Anatomical location	Susceptible to injury	Every area
Completeness of fracture	Incomplete or complete	Complete
Surface of the cross-sectional edge	Sharp and smooth	Jagged or stepped
Slope between external and internal cross-sectional surface	Angled surface	Perpendicular surface
Surface colour comparing with surrounding bone	Same colour	Different colour
Layered morphology (breakage) of compressive surface area	Present	Absent
Radiating fracture	Present	Absent
Concentric fracture	Present	Absent
Hinging	Present	Absent
Fracture edges morphology	Sharp	Rough, likely to small shatter
Fracture freshness score	Less	More
Finding of scavenging pattern	Absent	Present

The analysis of effects of taphonomic factors on sharp-inflicted injury is also important. Elimination of cut marks can be an outcome from bone surface modifications such as weathering, exfoliation, gnawing, or other degradation processes. Microscopic surface exfoliation from weathering can significant affect marks (Sauer, 1998; de Juana *et al.*, 2010; Junod and Pokines, 2014). In the early period, weathering processes have an influence on bone surface that exposes to the environment. The inner structure of cut mark is not mostly affected by this stage of weathering (Dominguez-Rodrigo *et al.*, 2009; de Juana *et al.*, 2010). In addition, bone surface abrasion from sedimentary particles can substantially modify the shape of pre-existing cut mark. These alterations can make the characteristics of cut mark ambiguous or unrecognisable (Fisher, 1995; Madgwick and Mulville, 2012; Cappella *et al.*, 2014). Also, dimensional changes in the cut marks after environmental exposure have so far been addressed by few studies. Houck (1998) noted the presence of post-dimensional shrinkage of the periosteum surrounding cut marks. He placed the bone with cut marks in an air-dried condition over a period of 72-80 hours at room temperature. By SEM examination, the location of cut marks was separated from the line where the periosteum was first cut (Houck 1998). However, the morphological changes of traumatic lesions produced after death remains an unsolved issue.

In sum, previous literature suggested that there is no justification for determining perimortem fracture from postmortem damage. Forensic anthropologists have to rely on the whole set of available indicators to make the decision. Diagnosis of a suspected surface lesion is frequently based on macroscopic and microscopic examinations as explained in detail in previous literature (Fisher, 1995; Katterwe, 1996; Littleton, 2000). In this instance, both biomechanical and environmental factors are important to distinguish postmortem from perimortem trauma (Ubelaker and Adams, 1995; Bartelink, 2015; Cattaneo and Cappella, 2017).

2.5 Burned skeletal remains

Burning is an oxidative reaction in which a fuel, an oxidizer (often the oxygen) is consumed and converted into organic gases, light and heat (Symes *et al.*, 2012;

DeHaan, 2015). Heat-induced alterations in bone are divided into primary and secondary level changes (Ubelaker, 2015; Thompson *et al.*, 2017). Primary level changes are more fundamental process occurring during the burning process such as the elimination of the organic component and the recrystallization of the inorganic component. While secondary level changes are the manifestation of heat-induced change such as colour change, heat-induced fracture and fragmentation (Herrmann and Bennett, 1999; Gonçalves *et al.*, 2011; Thompson *et al.*, 2017). Though knowledge of thermally induced changes on bone has been improved in the last few decades, it is still not completely understood how the effects of heat-induced changes affect the reliability of macroscopic examination used in forensic anthropology.

When burned, bone is influenced by a range of variables including intrinsic (bone structure, soft tissue coverage and thickness) and extrinsic factors (temperature of heat, exposure duration, oxygen levels, humidity, presence of accelerants) that induced skeletal changes such as fracture, shrinkage, deformation, and colour change (Symes *et al.*, 2015; Thompson *et al.,* 2017). These aforementioned variables affect the degree of destruction for evidence from skeletal remains. Burned remains are less informative for forensic analysis due to the tremendous modifications that the hard tissues have suffered. Interpretation pattern of injury in skeletal tissue of fire deaths rises to challenges for forensic pathologists and anthropologists. While most fire-related deaths are accidental, some are deliberately set to demolish homicidal acts (Fanton *et al.,* 2006; Symes *et al.*, 2015). The use of fire to obscure a body is commonly used to potentially destroy evidence concerning the cause and manner of death as well as inhibit the possibility of personal identification. Nevertheless, fire does not necessarily destroy the evidence of skeletal trauma in all circumstances (Herrmann and Bennett, 1999; Thompson, 2004; Thompson, 2015).

For many years, the studies of the effect of heat and fire, or any means of combustion, on skeletal remains have been emphasized (Thompson *et al.*, 2017). It is imperative to characterise and comprehend skeletal material changes, which occur at high temperature conditions as this can provide a foundation for evidence of foul play. In addition, interaction between archaeological and forensic research

focusing on burned remains has improved mechanisms of bone modification from heat exposure and their implication for forensic analysis (Reinhard and Fink, 1994; Herrmann and Bennett, 1999; de Gruchy and Rogers, 2002; Pope and Smith, 2004; Fairgrieve, 2008; Poppa *et al.*, 2011; Symes *et al.*, 2015; Macoveciuc *et al.*, 2017).

2.5.1 Effects of burning on hard tissues

Extensive literature provides key information on fire damage to a bone material (Bradtmiller and Buikstra, 1984; Bohnert *et al.*, 1998; Hiller *et al.*, 2003; Thompson, 2003, 2005; Pope, 2007; Gonçalves *et al.*, 2013). Calcination is complete when temperature exceeds 800-890°C for a duration of at least 10 minutes (Shipman *et al.*, 1984; Holden *et al.*, 1995; Quatrehomme *et al.*, 1998). Once the soft tissue is removed, the remaining hard tissue is directly exposed to heat and undergoes changes. Heat tends to alter the chemical composition and subsequently modify the overall structure. A burned bone is fragile and exhibits deformation, shrinkage, fracturing and colour change (Thompson, 2004).

It was recognised that fire can be used to potentially obliterate forensic evidence, especially the issues of recovery of human remains and reconstruction of the scene, trauma interpretation, as well as the possibility of victim identification (Cattaneo *et al.*, 1999; Macoveciuc *et al.*, 2017). Generally, heat exposure leads to an elimination of organic materials and a reorganization of inorganic components. Previous studies reviewed a series of predictable stages of heat-induced transformation in bone include dehydration, decomposition, inversion, and fusion (Mayne Correira, 1997; Cattaneo *et al.*, 1999; Thompson, 2003; Macoveciuc *et al.*, 2017). Though the above mentioned authors described the same four stages, they disagreed about the temperature range to which each stage progresses (Table 2.10). With extreme heat, dehydration occurs from the breakdown of hydroxyl bonds and loss of water. This leads to the alteration of the bone's structural integrity and reduction of its weight (Cattaneo *et al.*, 1999; Thompson, 2003). Drying of burned bone continues with the degradation of organic elements (such as collagen, mucopolysaccharides, amino acid, etc.), leading to loss of mechanical strength and increased fragmentation. Stages of inversion and fusion of the crystal matrix concern the ultrastructural change of hydroxyapatite to β-tricalcium phosphate, resulting in the bone dimensional shrinkage, distortion, discolouration and

crumbling (Gruppe and Hummel, 1991; Mayne Correira, 1997; Thompson, 2003; Thompson, 2005). Trauma in burned skeletal remains is always difficult to interpret due to heat-induced fracturing and fragmentation (Mayne Correira, 1997; Herrmann and Bennett, 1999; Thompson, 2003; Macoveciuc *et al.*, 2017). In addition, heat-induced dimensional changes of bone can affect any anthropological techniques (Thompson, 2005; Thompson *et al.*, 2017).

Table 2.10: The four stages of heat-induced transformation in bone (Mayne Correira, 1997; Thompson, 2003)

Stage of transformation	Findings	Temperature range (Mayne Correira 1997)	Temperature range (Thompson 2004)
Dehydration	Fracture formation; weight loss	100-600°C	100-600°C
Decomposition	Colour change; weight loss; reduction in strength; porosity change	500-800°C	300-800°C
Inversion	Recrystallization; increase in crystal size	700-1100°C	500-1100°C
Fusion	Increase in strength; dimensional change; recrystallization; porosity change	1000+°C	700+°C

2.5.2 Dimensional, mass, and colour changes

Heat-induced bone shrinkage and expansion have been noted to affect anthropological analysis. Temperature-related bone shrinkage is significantly observed in the fusion stage, starting at 700°C and augmented at 1000-1200°C, although a minor degree of shrinkage does occur during lower intensity burning

event (Thompson, 2005; Ubelaker, 2009). A comparison of a burned bone with an unburned piece yields variably, between a 3.9% expansion and a 37.7% shrinkage (Ubelaker, 2009). Study results have suggested that shrinkage variation is not only temperature dependent but also correlates with bone type, the coverage of soft tissue or other protective materials, exposure duration, and oxygen supply (Bradtmiller and Buikstra, 1984; Thompson, 2005). In addition, analytical techniques for burned bones are significantly obstructed and accuracy is greatly reduced. Weight references can be applied to use for estimating the completeness of skeletal remains, the minimum number of individuals, or the sex of an unknown individual (Thompson, 2004; Gonçalves *et al.*, 2013). Changes in burned bone mass occur because of elimination of water and organic matters (Bradtmiller and Buikstra, 1984; Thompson, 2005). Loss of burned bone mass differs considerably and ranges between 30% and 60% (Thompson, 2004).

Heat-induced discolouration of hard tissue is often seen as the most obvious consequence of the burning event, and this phenomenon has been supported by a number of publications (Thompson, 2004; Ubelaker, 2009; Gonçalves *et al.*, 2011; Dupras and Schultz, 2014; Thompson *et al.*, 2017). These heat-induced colour changes are influenced by the intensity of combustion and several independent variables (such as temperature, duration of exposure, oxygen level, clothing, presence of accelerants). However, it is a very poor predictor of the temperature of burning (Bennett, 1999; Devlin and Herrmann, 2015; Ellingham *et al.,* 2015; Thompson, 2015). In addition, inter-personal variation in the ability to distinguish colour can affect the assessment (Bennett, 1999; Devlin and Herrmann, 2015; Thompson, 2015). Traditionally, anthropologists have interpreted bone surface colours using the Munsell® Soil Colour Chart, which relies on human perceived assessment of three aspects of colour: hue, chroma, and value (Devlin and Herrmann 2015).

Anthropologists have incorporated the use of bone colour change into their descriptions of bone material affected by heat. Importantly, degree of oxidation of organic matter is revealed by the colour of burned bones ranging from the natural colour of creamy white through dark greys and black, light greys and finally transforming into white bones with occasional light blue patches (Mayne Correira,

1997; Thompson, 2003; Gonçalves *et al.*, 2011; Ellingham *et al.,* 2015; Thompson *et al.*, 2017). This trend has been associated with alteration of organic bone components with loss of carbon from bone matrix during exposure to various temperature transitions. The osteological tissues become black as a consequence of the combustion of the carbon and its compound within the bone. Subsequently, grey and white colours occur when the carbon is completely lost from the bone (Stiner *et al.*, 1995; Mayne Correira, 1997; Quatrehomme *et al.*, 1998; Thompson, 2015). A variety of colours can be found in a single bone fragment, especially in cases of fleshed remains (Stiner *et al.*, 1995; Mayne Correira, 1997; Quatrehomme *et al.*, 1998; Ellingham *et al.,* 2015; Thompson, 2015).

By the way, not all colours found on burned bones are related to degradation of carbon compounds. Minor colour groups such as greens, yellows and pinks have been attributed to the presence of various trace metals and contaminants from surrounding burned objects in funerary contexts (Stiner *et al.*, 1995; Thompson, 2003). Mayne Correira (1990) and Symes *et al.* (2015) reported an archaeological case of excavated bones with the black colour, and more detailed analysis was found to be the result of environmental staining. Stiner *et al.* (1995) also pointed out that examination of the internal surface of the bone have an important role in differentiating between burning process and normal diagenesis, as this medullary surface was affected by diagenetic process but not by burning.

2.5.3 Heat-related fracture and perimortem trauma

Apart from colour change, the formation of heat-related fractures is the most common alteration in hard tissues (Thompson *et al.,* 2017). This postmortem alteration is particularly problematic because fractures also represent the principal evidence of trauma. Thermal exposure complicates trauma interpretation and may create misleading artefacts. As noted above, burned skeletal remains generally demonstrate bone fragmentation and heat-induced fracture imposing limits of perimortem fracture analysis. Furthermore, thermal fragmentation complicates fracture interpretation by making the bone more difficult to recover and interpret (Herrmann and Bennett, 1999; Symes *et al.*, 2015; Thompson, 2015). Also, warping and deformation of burned bones directly affect the visual interpretation.

An understanding of heat-induced fracture formation is clearly important. With heat exposure, dehydration of collagen reduces bone elasticity and considerably changes the skeletal integrity, causing distortion and deformation (Shipman *et al.*, 1984; Herrmann and Bennett, 1999). Changes in crystal size and shape also affect the formation of cracks as burning breaks the hydroxy-bonds of the apatite minerals and causes a decrease in crystal size with reduced tensile strength. The disruption of bone crystal structure may take responsibility to make the bone material more vulnerable to breakage (Shipman *et al.*, 1984; Herrmann and Bennett, 1999).

Heat-induced fracture, defined by location and direction of fracture propagation, can be classified into five different features, including longitudinal, curved transverse, straight transverse, patina and delamination (Shipman *et al.*, 1984; Herrmann and Bennett, 1999; Symes *et al.*, 2015; Thompson *et al.*, 2017). The longitudinal fractures characteristically extend down the axial length or grain of the bone and usually propagate with the orientation of collagen fibres along the cylindrically oriented osteon. Curved transverse, or thumbnail fractures, extend in a stacked arch formation from one side of the bone to the other. Straight transverse fractures occur horizontally across the grain and shaft and perpendicularly propagate from the margin of longitudinal fracture, forming a step. Patina fractures affect only the surface of the cortical bone and look like “patina of an old painting”. Finally, delamination fractures are the peeling or flaking away of bone layers, mostly the separation of cortical bone from cancellous bone.

Obviously, recent caseworks and experimental studies have shown that evidence of perimortem skeletal trauma is still survival after incineration (de Gruchy and Rogers, 2002; Pope and Smith, 2004; Waltenberger and Schutkowski, 2017; Vegh and Rando, 2019). Recent literature has focused on diagnostic evidence of perimortem trauma of burned remains. Knife wounds could retain their typical features when exposed to fire (Kooi and Fairgrieve, 2013; Waltenberger and Schutkowski, 2017; Vegh and Rando, 2019). In a homicidal case committed by a gunshot to the head, Herrmann and Bennett (1999) could distinguish between base of skull fracture caused by the gunshot and heat-exposure change. Pope and Smith (2004) tried to evaluate survivability of traumatic injury in burned cranial bones. Forty cadaveric human heads were inflicted by ballistic, blunt, and sharp trauma,

and then burned to simulate forensic fire environment. After reconstructed burned bone examination, they found that identification of ballistic, blunt force, and sharp force injury was still possible with gross and radiological examinations. The researchers could recognise sharp force trauma in the bones after fire-exposure. Sharp force trauma remained present but fracture morphology and pattern need to be carefully inspected. Nevertheless, blunt force trauma proved more difficult to differentiate from heat-related fracture, and larger fragments were related to traumatic events while smaller pieces appeared to be associated with heat-induced fracture. In addition, analysis of gunshot and blunt injuries was further obscured due to postmortem burn modification such as delamination and fragmentation of primary trauma sites (de Gruchy and Rogers, 2002; Marciniak, 2009; Kooi and Fairgrieve, 2013; Collini *et al.*, 2015).

Even though increasing research has focused on the effects of heat exposure on sharp-inflicted marks (Owsley *et al.*, 1995; Herrmann and Bennett, 1999; de Gruchy and Rogers, 2002; Pope and Smith, 2004; Collini *et al.*, 2015; Schmidt and Symes, 2015; Thompson, 2015), few studies have quantitatively analysed the dimensional changes of kerf marks (Mayne Correira, 1990; de Gruchy and Rogers, 2002; Vegh and Rando, 2019). In these studies, burned bone samples showed no significant difference in the kerf dimensions at 500°C and 700°C, but the samples showed more significant when these were burned at 1000°C (Bohnert *et al.*, 1997; Pope and Smith, 2004). Nevertheless, it was not answer whether these kerf dimensions change under different temperatures of heat exposure in controlled conditions. Some studies (Bohnert *et al.*, 2002; de Gruchy and Rogers, 2002; Pope and Smith, 2004; Marciniak, 2009; Kooi and Fairgrieve, 2013; Collini *et al.*, 2015; Robbins *et al.*, 2015; Macoveciuc *et al.*, 2017) displayed a significantly dimensional change. However, no significant differences were found in other literature (Symes *et al.*, 2002; Vegh and Rando, 2019). Bohnert *et al.* (2002) reported a suicidal case who fired a captive-bolt shot to his forehead before burning himself. They found a minor difference between the diameter of the skull defect and the diameter of the bolt found at the crime scene. The outer table defect was approximately 15% smaller than the bolt, and Bohnert *et al.* (2002) suggested that were attributed to the heat-exposure shrinkage.

Differentiation between heat-induced fractures and those of traumatic origin can be problematic. Where possible, macroscopic examination of fracture patterns and microscopic examination of all fracture margins provide useful information (Herrmann and Bennett, 1999; Pope and Smith, 2004; Thompson, 2004; Schmidt and Symes, 2015). Herrmann and Bennett (1999), and Schmidt and Symes (2015) recommended that suspected features should be obviously examined and compared with known surrounding areas of postmortem heat or traumatic fractures. Differentiating perimortem trauma from postmortem heat damage can be resolved by careful analysis of the fracture patterns. However, this topic still needs further experimental studies to find the best criteria for forensic anthropological contexts (Herrmann and Bennett, 1999; Pope and Smith, 2004; Thompson, 2004; Schmidt and Symes, 2015).

2.5.4 Heat-induced fragmentation and warping

When skeletal elements are burned, these materials transform from a natural state to calcined bones. Heat-induced changes such as loss of water and organic matter, and recrystallization lead to bone fragility and fragmentation (Herrmann and Bennett, 1999; Pope and Smith, 2004; Thompson, 2004; Schmidt and Symes, 2015). Prolonged exposure of the skeleton to extreme fire usually leads to severe fragmentation. Fragmentation from heat exposure can occur either directly, causing bone fracture and splitting, or from impacts such as falling debris or the recovery method (Fairgrieve, 2008; Symes *et al.*, 2015; Thompson *et al.*, 2017). These result in a much-reduced ability of perimortem trauma analysis. Such fragmentation not only complicates analysis but also challenges recovery efforts. Small burned bone fragments are difficult to locate and identify. Gonçalves *et al.* (2011) advised any archaeologists working with burned bone recovery to record post-excavation burned fragment size in order to illustrate exact amount of burned bone fragmentation. Burned remains associated with severe fragmentation often challenge to forensic investigators, and the role of the forensic anthropologists in such cases is therefore very important. Careful reconstruction following fragmentation is usually possible even with burned remains, and this process can facilitate not only trauma detection, but also other aspects of analysis such as personal identification.

Few studies have focused on how environmental factors affect burned bone fragmentation. To investigate how weather conditions affect burned bone fragmentation, Waterhouse (2013c) studied burned porcine limbs placed in different months of year to observe bone fragment size and characteristics. She categorised fragmented burned bones into 12 groups depending on their overall size and shape. By comparing samples recovered at 0, 24, 56, and 168 hours after burning process, Waterhouse (2013c) described more fragmented bones over time and different weather conditions have great effects on rate and size of fragmentation. Freeze-thaw cycles have a larger impact in the longer term, and wet weather conditions increase levels of fragmentation (Fairgrieve, 2008). Further research into the influence of other environmental conditions such as snowfall, hailstorm, and high wind can provide further information on the effect of weather conditions on burned bone fragmentation.

Warping, or deformed contour of a skeletal material, is purposed as an indicator of the pre-burned condition of the burned skeletal remains; however, this statement is arguable (Fairgrieve, 2008). Several statements were discussed for the occurrence of warping. Baby (1954, in Fairgrieve (2008), Waterhouse (2013a), and Thompson (2015)) explained that warping features present only on flesh bone due to the contraction of muscle fibres. By contrast, defleshed and dry bones demonstrate warping from contraction of the periosteum and collagen fibres. Preservation of collagen and collagen-apatite bonds play an important role in warping formation (Fairgrieve, 2008; Waterhouse, 2013a; Schmidt and Symes, 2015).

2.6 Related topics of skeletal tissue investigation

A forensic investigator is frequently confronted with the problem of the forensic analysis of skeletal trauma. Therefore, various analytical methods such as SEM and micro-CT are expected to investigate fully the forensic issues and provide the best quality evidence to a criminal court (Wakely, 1993; Bartelink *et al.,* 2001; Thali *et al.,* 2003; Alunni-Perret *et al.,* 2005; Bai *et al.,* 2007; Pounder and Sim, 2011; Pechnikova *et al.,* 2012). This review provides the basic knowledge and the

potential roles in which SEM and micro-CT can potentially be applied to enhance skeletal trauma analysis.

2.6.1 Scanning electron microscope (SEM)

SEM is an important tool used by scientists in many fields. Microscopic examination has been undertaken by several researchers to elucidate archaeological and anthropological inquiries (Wakely, 1993; Krüsemann, 2001). In particular, SEM can provide valuable information in the forensic context e.g. analysis of fibres, cartridge cases, gunshot residue particles, and bone surface modification (Bartelink *et al.*, 2001; Turner-Walker and Syversen, 2002; Alunni-Perret *et al.*, 2005; Boaks *et al.*, 2014; Kontopoulos *et al.*, 2016). It has been successfully applied to examine a variety of taphonomic modifications on bone and teeth as well as discover the processes producing such events (Fernández-Jalvo and Andrews, 2016). In general, it is misappropriate to review all theory of operation of SEM here. Thus, a brief summary of the process is explained here.

SEM components consist of source of electrons, electron column, sample chamber, and electron detector with computerized monitoring (Goodhew *et al.*, 2001). SEM functions by firing an electron beam from an electron gun at the top of the machine. This beam is condensed by a condenser lens to focus on the sample. The electrons then strike the surface of the sample and produce secondary electrons, which are collected by an electron detector. Different signals characteristics are then used to delineate the surface topography. The main aim of using SEM is that topographic surfaces of a sample can be investigated in fantastic detail. The advantage of using SEM to investigate bone morphology is that SEM offers higher magnification, better resolution, and greater depth of field. However, SEM has a number of disadvantages, including its prohibitive and financial costs, an over-reliance on microscopic feature of the mark rather than consideration of the overall mark morphology, and high-experienced examiner preference.

In recent decades, SEM has been used extensively to study the fracture surface of bone because of its great depth of field and the capacity of greater magnifications (Möser, 1987; Braidotti *et al.*, 2000; Wise *et al.*, 2007; Wynnyckyj *et al.*, 2011). Fracture surface observations appear to reflect real fracture growth

conditions and simplifies calculation. The use of SEM to explore tool marks on bone was conducted by a number of authors (Bartelink *et al.*, 2001; Alunni-Perret *et al.*, 2005; Ferllini, 2012; Kooi and Fairgrieve, 2013; Norman *et al.*, 2018). The utilization of a SEM to interpret traumatic lesions on bone and provide not only information on the tools used, but also about the postmortem fate and the treatment of bodies within specific contexts. Many researches used SEM for skeletal biomechanical behaviour studying (Wakely, 1993; Krüsemann, 2001; Sahar *et al.,* 2005). The light microscopy can also be used, but it has limit for examination of uneven rough fracture surface due to its particularly low depth of field.

Mouldings of specimens, instead of original specimens, are normally used to produce high resolution replica for SEM study (Krüsemann, 2001; Camaros *et al.*, 2016). This process has several advantages over the direct study. It allows (1) easy transport from the storage to an analytical laboratory; (2) sampling of a small area from a larger sample in order to permit examine in a small SEM chamber; and (3) casting offers a wide spectrum of specimen types, e.g. bone, skin, hair, and teeth (Krüsemann, 2001). Previous studies demonstrated that moulding can produce highly reliable replicas of specimen surfaces, even for inspection at high magnification of SEM (Krüsemann, 2001; Camaros *et al.*, 2016).

2.6.2 Micro-computed tomography (Micro-CT)

Forensic experts have embraced the potential advantages of radiological applications for forensic practices. In recent years, histo-morphometric techniques have been the standard method for investigating cortical and trabecular bone architectures. However, these destructive practices have limitations of bone micro-architecture evaluation because their structural analysis is derived from stereological model of a few two-dimensional sections. Differently, computed tomography (CT) has established bone microstructure measurements without relying on stereological methods (Turner-Walker and Syversen, 2002; Bouxsein *et al.*, 2010; Boaks *et al.*, 2014) . Clinical CT has also been proven as an effective instrument for detecting the presence of toolmarks in-situ (Schnider *et al.*, 2009; Gaudio *et al.*, 2014). However, one major drawback is its poor spatial resolutions (> 300 μm), which is inappropriate for characterising the microstructure within small, very detailed samples (Thali *et al.*, 2003; Bouxsein *et al.*, 2010). Nevertheless, micro-CT is now gaining acceptance as

more suitable for examination of incredibly fine detail such as small toolmarks and offers higher spatial resolutions (0.5-100 μm) (Pelletti *et al.*, 2017; Komo and Grassberger, 2018; Norman *et al.*, 2018).

Fundamentally, micro-CT is very similar in principle to clinical CT. X-ray beams project toward a sample, and those are captured by a charge-coupled device (CCD) sensor. Then 2D images are reconstructed to generate a high resolution 3D image of the sample (Stock, 2008; Thali *et al.*, 2009). These 3D models can be manipulated using the specific software to obtain an image of all aspect of the scanned object. Therefore, this technique can provide a wealth of novel information on the non-destructively and directly three-dimensional observations of bones from experimental animals or skeletal tissue biopsies of human, with faster procedure comparing with histological method (Muller *et al.*, 1998; Bello *et al.*, 2009; Rutty *et al.*, 2013; Kontopoulos *et al.*, 2016).

Nowadays, the use of imaging of micro-CT has been employed by a rapidly increasing number of laboratories for medico-legal investigation and research (Bouxsein *et al.*, 2010; Rutty *et al.*, 2013; Kontopoulos *et al.*, 2016). Also many areas of micro-CT technique can potentially be applied to enhance forensic investigations such as gunshot wounds (Cecchetto *et al.*, 2011, 2012), tool mark examination (Thali *et al.*, 2003; Pelletti *et al.*, 2017; Komo and Grassberger, 2018; Norman *et al.*, 2018), personal identification (Chappard *et al.*, 2005; Telmon *et al.*, 2005), and postmortem interval estimation (Richards *et al.*, 2012; Kontopoulos *et al.*, 2016; Garff *et al.*, 2017). In addition, the results of the surfaces and volumes of interest analysis of the bone by micro-CT are highly correlated with outcomes from 2D histo-morphometry (Bouxsein *et al.*, 2010; Rutty *et al.*, 2013). Consequently, this correlation between two procedures postulates the rationale for application of micro-CT for skeletal morphometric investigation.

The application of micro-CT in skeletal trauma investigations has been pioneered by Thali *et al.* (2003). They used micro-CT for taking 2D slicing images of stab marks in pork bones and visually matching them with the inflicted knife blade tip. Gaudio *et al.* (2014) used cone beam CT to measure the dimension of stab marks on bone with ±0.6 mm error in measuring. However, Rutty *et al.* (2013) suggested that this value can be much better with up-to-date technology. Pelletti *et*

al. (2017) analysed false starts of saw mark with micro-CT, and they qualified traumatic lesions successfully with high agreement across different rate. The potential of using micro-CT to facilitate quantitative approaches in knife mark analysis, especially toolmark properties, allows the possibility of increased statistical determination of class characteristics (Pounder and Reeder, 2011; Komo and Grassberger, 2018; Norman *et al.*, 2018). Micro-CT offers enormous potential in medico-legal investigation. This technique has the potential to answer investigative forensic questions and provide practitioners with high quality evidence that will be acceptable in courts of law.

The advantages and disadvantages of each technique are summarised in Table 2.11.

Table 2.11: Advantages and disadvantages of three techniques used in this study (adapted from (Vandervoorte, 2004; Telmon *et al.*, 2005))

Factors	Stereomicroscope	SEM	Micro-CT
Invasive preparation	Yes	Yes	No
Limitation of size	No	Yes	Yes
Perspective	Limited	Device-dependent	Unlimited
Depth of field	Very low	Moderate	Very high
Cost	Very low	Moderate	Very high

Chapter 3: Materials and methods

The outdoor project began on September 1, 2016 and finished on August 31, 2018 at the F3 taphonomic facility. Analytical procedures were performed at the Stephenson laboratory on the Shrivenham campus of Cranfield University. Although some methodological aspects have been modified from published skeletal trauma studies, the combination of factors analysed is novel and new terminology is introduced.

Different methods of examination and imaging were used to conduct an in-depth analysis of changes due to environmental exposure. The ideal conditions to test these ideas were to examine each bone lesion before and after exposure to the environment. Easily applied techniques with a simple stereomicroscope and more advanced equipment such as micro-CT and SEM were applied to investigate the changes of traumatic lesions as a consequence of environmental factors. An understanding of these alterations in outdoor environments is clearly vital to medico-legal and archaeological implications. Hence, experimental data such as the one used here can help to clarify these issues.

3.1 Sample preparation and trauma infliction

3.1.1 Bone for modification

Fresh juvenile domestic pig (*Sus scrofa domestica*) rib and femoral bones were used in this experiment. Pig bones have a long history of use in trauma and taphonomic researches (Humphrey and Hutchinson, 2001; de Gruchy and Rogers, 2002; Alunni-Perret *et al.*, 2005; Saville *et al.*, 2007; Lynn and Fairgrieve, 2009a). Though there are small differences in the characteristics between pig and human bone, more readily available pig bone specimens remain the best analogue for human bones on the basis of compositional similarity that shows the same type of fracture patterns (Catts and Goff, 1992; Aerssens *et al.*, 1998; Wang *et al.*, 1998; Saville *et al.*, 2007) and microstructural similarities (Hillier and Bell, 2007). Furthermore, the body mass of an adult pig is greater than five kilograms, which is relevant with taphonomic research (Behrensmeyer, 1978). Lastly, ethical restrictions on the use of human bones in England and Wales (Human Tissue Authorities, 2004)

mean that animal bones are the most feasible options for forensic experimental studies.

The exact weight and age of pigs used in this study were unknown, but their close size and patterns of unfused epiphyses indicate that they were still juvenile and all of a similar age. None of the sample exhibited completely fused epiphyses. Therefore their bone mineral density is much less than adult human bone mineral density, as a 40 kg pig has the same bone mineral density as an 8-10 year old human (Kalkwarf *et al.*, 2007). Longitudinal research data were collected on a total of 364 fresh ribs and 60 femurs (Table 3.1) obtained from local butcher shops. Only femoral and rib bones were chosen because these bones are larger and are often recovered at forensic crime scenes. Injury databases also indicate that these bones are more often exposed to traumatic injury. The samples included the 2nd to the 10th ribs separated from rib cages into individual pieces. They were cut off close to the sternal rib end and did not contain any costal cartilage. Burned samples consisted of only typical (5th – 8th) ribs because they had nearly the same size and morphology and were suitable for fragmented size comparison. The rib samples measured approximately 25 cm in length and 7 cm in width.

Table 3.1: Sample size and categories for rib and femur experimental group; BFT: blunt force trauma; SFT: sharp force trauma

	Month 6th	**Month 12nd**	**Month 18th**
Surface	BFT: 6 femurs SFT: 10 ribs, 3 femurs	BFT: 6 femurs SFT: 10 ribs, 3 femurs	BFT: 6 femurs SFT: 10 ribs, 3 femurs
Burial	BFT: 6 femurs SFT: 10 ribs, 3 femurs	BFT: 6 femurs SFT: 10 ribs, 3 femurs	BFT: 6 femurs SFT: 10 ribs, 3 femurs
Control	Pre-exposure BFT: 6 femurs; Non-traumatic ribs for cremation: 64 ribs		

	Spring	Summer	Autumn	Winter
Surface burned	SFT: 40 ribs	SFT: 40 ribs	SFT: 40 ribs	SFT: 40 ribs
Burial burned	SFT: 20 ribs	SFT: 20 ribs	SFT: 20 ribs	SFT: 20 ribs
Total: 364 ribs, 60 femurs				

All bone samples were collected from butchered animals that had been raised and slaughtered for human consumption. The majority of overlying tendon, muscle, and periosteum around all injury sites were removed prior to

experimentation by scalpel, scissor and forceps without any cut or damage to bone surfaces so that the locations of the bone surfaces would be suitable to observe fracture characteristics during the experiment (Humphrey and Hutchinson, 2001; Calce and Rogers, 2007; Lynn and Fairgrieve, 2009a). Any bones with antemortem bone lesion such as a healed fracture or bone disease were excluded. Each specimen was labelled with a unique number using a metal tag fastened by a wire. These numbers were used to guarantee that experimental information could later be linked to individual samples.

Bone samples were kept frozen in shrink-wrap to prevent decomposition, since freezing has no significant effect on the biomechanical nature of bones (Borchers *et al.*, 1995; Jung *et al.*, 2011; Karr and Outram, 2012; Lee and Jasiuk, 2014). Selected bone samples were defrosted at room temperature one day prior to trauma testing. Literature review (Ambade and Godbole 2006; Henderson *et al.* 2005; Hunt and Cowling 1991) suggests that ribs and thoracic areas are most frequently targeted when using sharp instruments, while extremities are the most common area for defensive wounds (Ambade and Godbole, 2006). Therefore, the proper bones used in this experiment corresponded with these data.

A total of 60 rib samples and 60 femoral samples were subjected to sharp and blunt force. In addition, 240 additional rib samples were subjected to heat exposure after sharp-inflicted trauma resulting in burned bones, with 64 rib samples included in a non-trauma group for cremation research. All specimens were allocated to either sharp or blunt force groups depending on their trauma characteristics.

3.1.2 Trauma infliction

3.1.2.1 Sharp force infliction for rib samples

Common household knives are the most common weapons used in sharp force trauma (Hunt and Cowling, 1991; Webb *et al.*, 1999; Henderson *et al.*, 2005; Ambade and Godbole, 2006) and were divided into non-serrated, coarse-serrated, and fine-serrated blade groups. New three different blade types with varying teeth per inch and serration styles were evaluated to increase the variety of cut mark characteristics in this research (Figure 3.1). These knives were purchased from the

same manufacturers (Richardson-Sheffield®). This study used new knives because it was thought that used instruments could contain damage that could mimic striations. Each knife was selected so as to represent many variables such as blade length and width as well as tooth set morphology. Each knife was labelled with numerals from 1 to 3 and photographed. Three variables were measured and documented in a spreadsheet to complete the documentation (Table 3.2).

Figure 3.1: The three knives used for the rib infliction in this study; A. non-serrated knife; B. fine-serrated knife; C. coarse-serrated knife

Table 3.2: General measurements of sharp instruments used in this study; NS: non-serrated knife; CS: coarse-serrated knife; FS: fine-serrated knife

Parameter (mm)	Definition	NS	CS	FS	Cleaver	Machete
Blade length	Distance from the point to beginning of the handle	199	201	207	-	-
Sharp edge width	Maximum width of the blade at the knife edge	1.78	2.45	2.31	2.05	3.13
Blunt edge width	Maximum width of the blade at the back of the knife	2.43	2.89	2.8	2.87	4.98

The ribs were used as a focal point for this experiment because it is the most commonly affected anatomical area for knife-related crime (Hunt and Cowling, 1991; Banasr *et al.*, 2003; Ambade and Godbole, 2006; Allen and Audickas, 2018). Targeted ribs (burned and unburned groups) were attached to a standard clamp-on-vice in order to stabilize them during a cut. The head end of the rib was placed into the vice, and each knife was used to make three incision marks at the outer surface of each rib. Manual sharp instrument application by the same researcher was used for incision at a right angle to the bone surface. The cutting motion was perpendicular to the long axis of the bones and was made by moving the blade back-and-forth and down in a repetitive, reciprocating motion across the surface of the ribs. Previous research relating to knife marks on bone preferred to control the force and angle of the cut (Houck, 1998; Alunni-Perret *et al.*, 2005). However, the force utilized was not measured because this research was conducted with the premise of a random attack. This study is novel to investigate the possibility of cut mark modifications from environmental exposure rather than mechanical means, and using knives as the sole weapon type.

Next, the blade was carefully withdrawn, and each defect was individually coded according to the type of knife used, photographed, analysed and documented in a data spreadsheet. The same procedure was repeated across all rib samples. The sequence in which the cuts were done was randomized to reduce potential bias based upon the sequence of cutting. In sum, a total of 60 ribs were inflicted, resulting in a total of 180 cut marks (three cuts per bone). After this process, the rib samples were prepared for analysis or to be placed in an outdoor environment.

3.1.2.2 Sharp force infliction for femoral samples

Eighteen domesticated pig femurs collected from commercial butcher shops were used for the purposes of this experiment. These bones were conventionally prepared by manual dissecting away periosteum and soft tissues, especially in the diaphyseal area. A new cleaver and machete were used in this experiment (Figure 3.2). The weapon types were chosen for their differences in size, thickness, and length (Table 3.2). Chopped weapon blade was cut to the appropriately smaller length around 15 mm and attached to a part of impact equipment. A drop-tower was used and the weapon blade were set up on a central piston to precisely control

kinetic energy. Eight hacking traumas, four from the cleaver and four from the machete, were made perpendicular to the long axis of anterior and posterior surfaces of femoral sample.

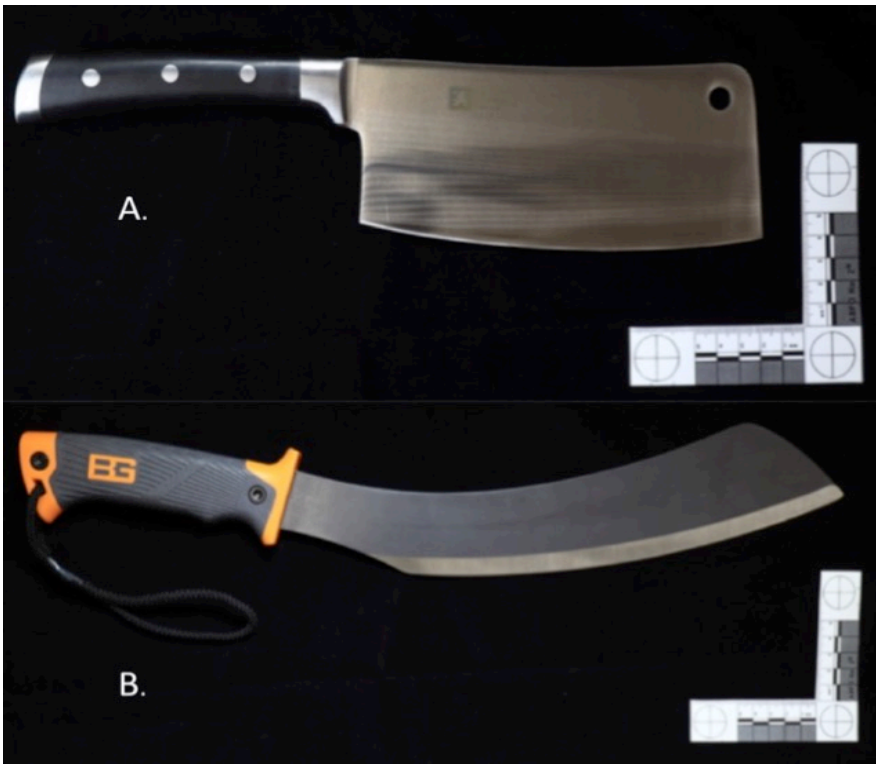

Figure 3.2: The cleaver (A.) and the machete (B.) used in this experiment

All femoral bone injuries targeted the femoral diaphysis using an IMATEK impact-testing machine with computerized impact control (Figure 3.3). A sample was firmly fixed inside the sample chamber on a metal plate to assure that the sample did not move during an impact event (Figure 3.4). A piece of the cleaver or the machete was attached to a knife handle located inside the carriage and striker chamber, so it was allowed to move upward to the wench chamber by electrical adjustment through a computerized control panel. Pilot tests were performed in order to ascertain optimal parameters that could prevent sample amputation. A velocity of 4 m/s and a total impact mass of 2.5-3.0 kg (striker mass 0.1 kg) depending on the type of attached weapon blade were chosen because the amount of force from these parameters was sufficient to break a femoral cortex while not penetrating the bone. This provided a maximum force ranging from 2.5-3.4 kN and was illustrative of an attack produced by a chopped weapon. The forces applied by

the machete blade were often more than those by the cleaver blade due to their larger and thicker blade mass.

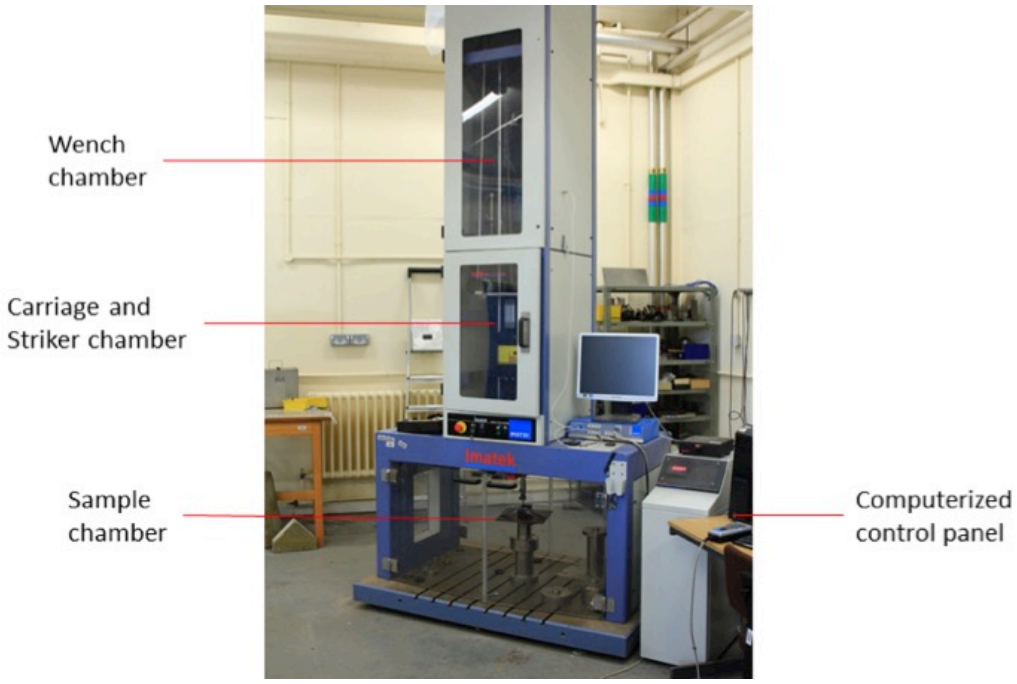

Figure 3.3: IMATEK Impact Testing Equipment

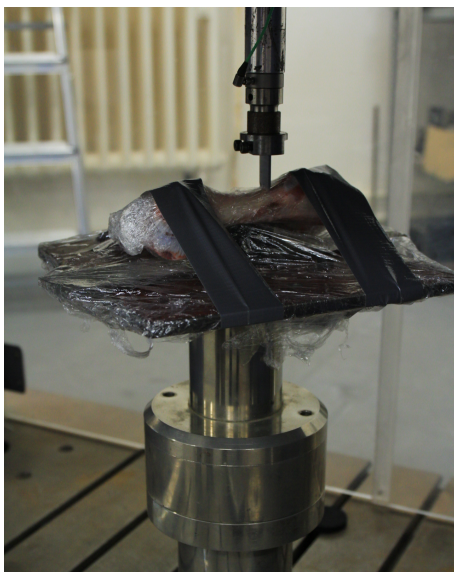

Figure 3.4: Sample placing and its correlation with the sharp striker

After parameter determination and instrument calibration, each femoral sample was supported with rigid, non-deformable sponges and placed in the sample

chamber to prevent a bounce effect from impact (Macoveciuc *et al.*, 2017). A reproducible series of eight lesions were inflicted perpendicular to the long axis with both types of the sharp blade for each femoral sample. The blows were randomly inflicted with the same parameter in order to produce different features and directions of trauma. This single impact was an incomplete cut and no particular attention was paid to the direction of the blow so that side of an uneven marginal edge of chop marks could be expected.

3.1.2.3 Blunt force infliction

Forty-two frozen porcine femurs were obtained from a local butcher shop and allowed to thaw to room temperature before processing. Briefly, femoral samples were separated from adjacent long bones with a scalpel and soft tissues were macerated without any injury to the bone surface. Then, the excised porcine femurs were broken using three-point bending to evaluate the fracture morphology.

All mechanical tests were performed using the Hounsfield Universal Testing Machine. Three-point bending was conducted to experimentally reproduce perimortem trauma characteristics. Theoretically, the bone breaks differently when it is loaded with different rates of energy (Symes, *et al.*, 2012; Wedel and Galloway, 2014). High fragmentation occurs when the bone is broken very rapidly and involving a great deal of kinetic energy. Therefore, the bone samples in this study were designed to break with a slow rate of loading in order to preserve enough fracture surface morphology for analysis. Furthermore, the researcher can clearly identify the area of tensile and compressive loads from less fragmented bone samples.

A femoral sample was placed posterior side down on the lower support at femoral head, greater trochanter, and femoral condyles so that the diaphysis was not in contact with the supporting object. A blunt striker was applied to establish contact with the anterior surface of the femur at mid-shaft. Then, the 42 fresh porcine bones were loaded in the antero-posterior direction to failure at a displacement rate of 100 mm/min during the test.

3.2 Photography and image processing

After trauma infliction, all bones were photographed. Standard digital photography was chosen as it allows for two-dimensional image review and comparison between pre and post-exposure. Digital photography forensic evidence (e.g. of bite marks (Golden, 2011)) is considered as an exacting standard of forensic practice, particularly because of its easy control and low acquisition costs. At the forensic anthropology laboratory of the Cranfield Forensic Institute, all samples were cleaned, labelled, photographed, and then prepared for analysis. To document the sample morphology and surface colour alterations, photography with a Canon EOS80D digital single-lens reflex (D-SLR) camera was used with a range of lenses (Canon EF 24-70mm f4 IS USM; Canon EF-S 10-22mm f/3.5-4.5 USM). The samples were photographed with a neutral colour and normal white balance setting in sRGB colour space and saved as JPEG image files at high resolution (2976 x 1984 pixels) resulting in clearer images. Some pictures needed to be rotated 90° to 180° to ensure that all photos were orientated in the same direction.

Oblique lighting was set up using two 40W desk lamps. Shutter speed and aperture were adjusted to achieve appropriate light. Low aperture (f11- f16) was usually used in order to ensure that the pictures have enough depth of field. The samples were placed on a black tablecloth with a forensic ruler scale to standardise their size. A standard distance was used for every photo to ensure that all pictures represented the same lighting conditions. Close-up images using the micro-mode of Canon EF 24-70mm f4 IS USM at a distance of one foot were taken. It was deemed not necessary to photograph every bone sample, while particular specimens were photographed as they were either the representative of the specific group or possessed a particular morphology of interest.

Images were taken of each sample to show the traumatic and taphonomic pattern, morphology and tool mark characteristics. Once completed, photo galleries were downloaded onto a MacBook Pro laptop and organized into individual folders. These images were later used to compare each bone lesion before and after environmental exposure.

3.3 Analytical methods

To undertake a detailed morphological analysis of injured rib and femoral samples, all measurement and pertinent observations for each sample were entered into Excel® spreadsheets. Digital imaging and stereomicroscope were used to analyse macroscopic and microscopic features created by sharp-edged weapons and blunt instrument. Furthermore, micro-CT was applied to the sharp-inflicted femoral group in order to investigate three-dimensional changes of chopping marks and SEM was specific to the blunt-inflicted femoral group. Comparisons between pre- and post-environmental exposure were conducted. After the first series of analytical methods, the bone samples were divided by their depositional environment into buried or placed on the ground surface for a specific time and then collected back to the anthropological laboratory for the second series of analysis.

Selected examinations for each group of the bone sample were summarised in Table 3.3. The analytical methods were chosen to investigate specific topics of selected trauma. SEM is used mainly to inspect the sample surface with a high magnification, particularly when a researcher has to magnify microstructural surface topography that could not be inspect using an optical stereomicroscope. Thus, this method was suitable to investigate blunt-inflicted fracture surface modification, which should be approached at a very high magnification (x1,200- x1,600) (Wynnyckyj *et al.*, 2011). Whereas the microscopic structures of sharp-inflicted trauma can be thoroughly investigated using an optical stereomicroscope, the researcher faced problems to measure the internal structure and kerf wall angle of chop marks. To solve this problem, Micro-CT was applied to image in three dimensions on a small scale with very high resolution.

Table 3.3: Methods for examining each group of the bone samples

Group	Examination methods			
	Visual	Microscope	SEM	Micro-CT
Sharp-inflicted rib samples	✓	✓		
Sharp-inflicted femoral sample	✓	✓		✓
Blunt-inflicted femoral sample	✓	✓	✓	
Burned rib sample	✓	✓		

Traditional microscopic examination has been the primary technique for tool mark analysis (Bello *et al.*, 2009; Boschin and Crezzini, 2012; Tegtmeyer, 2012). Recently, it has been demonstrated that microscopic examination can provide detailed information, which cannot be detected macroscopically or in radiographs. A light optical stereomicroscope is one of the most common instruments in the forensic analysis of topographical structure, including the examination of general features, tool marks and fracture surface characteristics produced by sharp and blunt instruments, as well as firearms (Katterwe, 1996; Tennick, 2012; Kooi and Fairgrieve, 2013). Stereomicroscopy was used because it can permit the researcher to demonstrate all of the surface lesions at once. This method is also non-destructive and permits repeated examination. The prevalence of each characteristic was noted.

The microscopic morphology of cut marks and fracture surfaces were examined using an Olympus® SZX10 stereomicroscope and Olympus® U-CMAD3 Microscope Camera Optics System with a magnification range between 0.63x – 6.3x. During the examination, the bone samples were placed on a supportive sponge in order to prevent trauma sites from lying on a hard surface. This also permitted easy manipulation to view different aspects of the cut marks or fracture surfaces. Superficial and anterior photographs of each mark were taken through the stereomicroscope. All specimens were then divided into two groups depending on their trauma characteristics and data were recorded in the data collection sheet.

3.3.1 Bone surface modification

Each bone was initially examined macroscopically, by evaluating the general and specific features of the overall bone surface and trauma site such as bone colour and taphonomic changes. Pre-environmental exposure samples contained considerable soft tissue remaining on the bone surface, while post-environmental exposure samples usually showed little or no soft tissue. Therefore, information regarding bone surface conditions and staining were recorded. Various techniques were available for magnifying to enhance surface modification to enable detailed information. A hand lens is more easily transported; an optical stereomicroscope offers greater magnification and the capability for taking photography that can transmit images to a high-resolution monitor. Before and after environmental exposure, bone surface changes were recorded and photographed in selected categories.

Fresh bone has an ivory colour. A variety of depositional circumstances, such as burial and grave, may cause bone surface discolouration. Evidence of stains and abnormal surface colour was recorded with the Munsell® soil colour chart system that consists of three independent properties of colour namely hue, value or lightness, and chroma. The value assigned for each of the 251 colours including those appropriate for bones altered by heat and sunlight was noted. Other surface colour or those modified by contact with soil require the acquisition of specific colour such as light brown or red-brown. It is important to keep in mind that bone samples usually express a range of colour within an individual sample.

Bone surface texture may be altered by heat exposure, weathering, depositional environment (e.g. insect, plant, micro-organism, soil and sediment), animal scavenging and human activity. Bone surface changes can be investigated by a magnifying lens or optical stereomicroscope (Buikstra and Ubelaker, 1994). Each bone sample would have a record of bone surface abrasion for exposed and buried bone in order to specify different grades. McKinley (2004) proposed a standardised system of grading bone surface abrasion and erosion using a 0-5 scale (from normal surface to complete obscuring of the bone surface) (Table 3.4).

Table 3.4: Surface abrasion and erosion grading system (McKinley, 2004)

Grade	Definition of surface morphology
0	Clearly visible with fresh appearance
1	Slight and patchy erosion
2	More extensive erosion than grade 1 with deeper surface penetration
3	Most of the surface is affected; general morphology maintained but the detail of parts of surface masked by erosion action
4	All of the bone surface is affected; general profile maintained; non-uniformity of the depth of modifications
5	Heavy erosion across the whole surface, completely masking normal surface morphology, with some modification of the profile
5+	As grade 5 but with extensive penetrating erosion resulting in modification of the profile

3.3.2 Sharp-inflicted trauma

Before moving onto a microscopic inspection for intensive examination. Some trauma feature could be also observed by visual examination, and then confirmed with microscopic examination, such as kerf margin characteristics of chopping marks (Figure 3.5). Chop marks close to the proximal or distal end of the bone samples would revealed little information and were discarded from this study. A list of variables was compiled based on macroscopic and microscopic mark features analysed through a stereomicroscope (Table 3.5).

Table 3.5: Definition of the variables and analytical methods; G: Gross examination; M: Microscopic examination

Variables	Methods		Definition
	G	M	
Kerf length	X		A maximum distance between the start and end of the kerf mark
Kerf width		X	A maximum distance between the edge of the kerf mark
Kerf shape	X	X	Overall shape of the kerf mark; observed from top view
Kerf margin	X	X	The margin of the kerf mark; classified both margins
Cross-sectional view		X	Overall cross-sectional view of the kerf mark
Striation		X	The microscopic parallel striations on the kerf wall
Chattering		X	Small fragments along the kerf margin

Figure 3.5: Image showing chopping marks on a femur: the white arrow indicates raised border of kerf margin

After reviewing the published literature (Bromage and Boyde, 1984; Bartelink, Wiersema and Demaree, 2001; Humphrey and Hutchinson, 2001; Alunni-Perret *et al.*, 2005; Tennick, 2012), general characteristics such as kerf dimension and morphology were selected because these aspects could contribute to the morphology observed with sharp-inflicted trauma. Maximum length was measured three times using a sliding digital calliper by the same person and instrument. The average value was calculated and used for analysis. Width could not be determined using the macroscopic method due to the minuscule scales. After kerf lengths were recorded, sharp-inflicted marks were inspected from the top view for macroscopic kerf shape (linear, elliptical, rectangular, or irregular shape) (Table 3.6).

3.3.2.1 Stereomicroscopic examination

The analysis of sharp-inflicted injury in skeletal remains necessitates an analytical technique to clarify distinguishing characteristics. Morphological and metric examinations can be applied (Houck, 1998; Bartelink *et al.*, 2001; Lyman, 2005; Lewis, 2008; Tennick, 2012). In general, most of the studies focus on the morphological examination of the cut marks, while metric study is less frequently

observed. Due to the unreliable metric evaluation of the size of the weapons, the metric measurements should be assessed with caution (Cerutti *et al.*, 2014).

Table 3.6: Descriptions of kerf shapes morphology

Kerf shape features	Description
Linear kerf	Two parallel kerf walls, close to each other with an extremely narrow distance between the kerf walls.
Elliptical kerf	Two inwardly angled kerf margins ending at the tip with a widest distance at the midpoint of the cut
Rectangular kerf	Two parallel kerf margins ending at the tips with a small U-shaped at the termination
Irregular kerf	Irregular kerf shape that cannot classify into any features

Cut and chop marks from experimental inflictions were viewed under a stereomicroscope. The main aim of this research is to investigate environmental effects on cut and chop mark analysis instead of weapon identification. Thus, different types of weapon edge were used to make a variety of characteristics so that different environmental effects could be observed and better understood their consequences. These examinations relied on morphological observations and recording the presence or absence of specific traits. There is actually no standard morphological classification system specific to skeletal cut marks in the forensic context. Therefore, it was necessary to adapt a classification system based upon parameters compiled from published studies in archaeology, and a few from forensic works (Alunni-Perret *et al.*, 2005; Dominguez-Rodrigo *et al.*, 2009; Thompson and Inglis, 2009; Tegtmeyer, 2012; Tennick, 2012; Cerutti *et al.*, 2014; Mccardle and Stojanovski, 2018). The prevalence of each characteristic was noted. These variables were following a number of authors as described:

1.) Kerf shape characteristics: Overall feature was identified and classified into linear, elliptical and rectangular. (Table 3.6 and Figure 3.6). When a kerf did not match one of these, it was classified as an irregular shape.

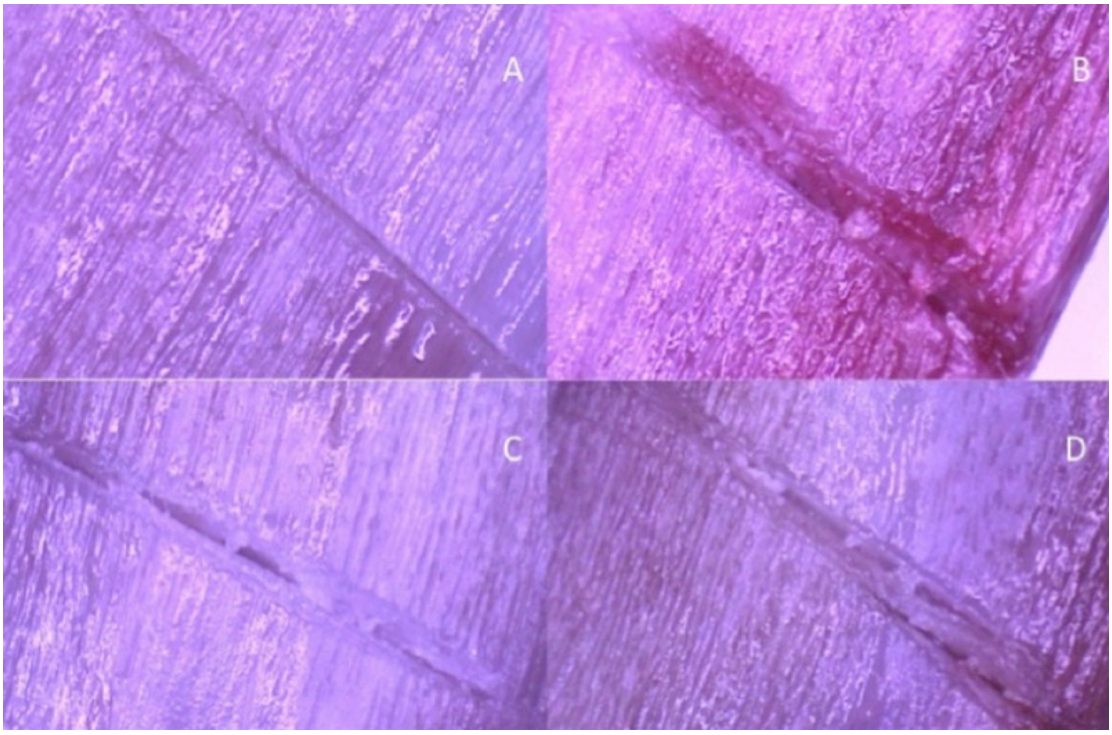

Figure 3.6: Illustrating kerf shape morphology; A: Linear kerf; B: Rectangular shape; C: Elliptical shape; D: Irregular shape

2.) Kerf margin characteristics: Kerf margin features were divided into the smooth margin that means the margins show regular and flat nature and the lateral raising that is the uneven ridge forming along the kerf margin and is still attached to the bone (Figure 3.7). Each margin was categorised and recorded as raised margin if one side showed the raised edge.

3.) Cross-section profile: The defect analysis was done by qualifying kerf shape in the cross-section view of the reconstructed picture to display possibly the cutting plane of the knife blade. Narrow, V-shaped and U-shaped cross-sectioned shapes were described (Table 3.7) (Figure 3.8).

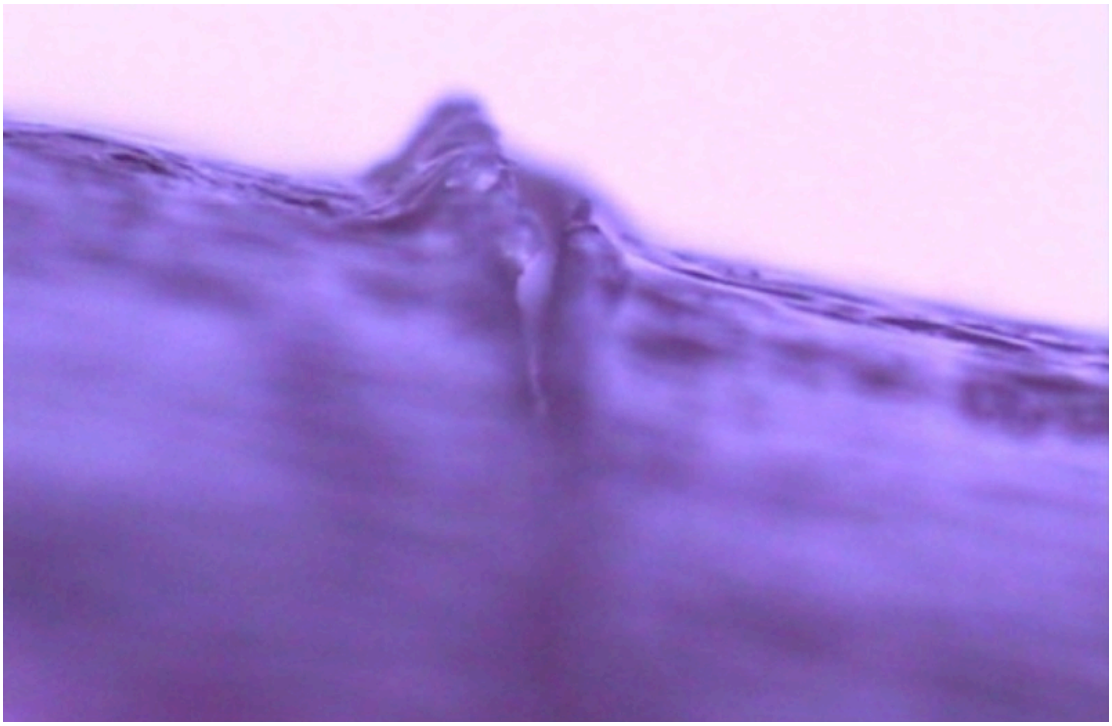

Figure 3.7: The raised kerf margin

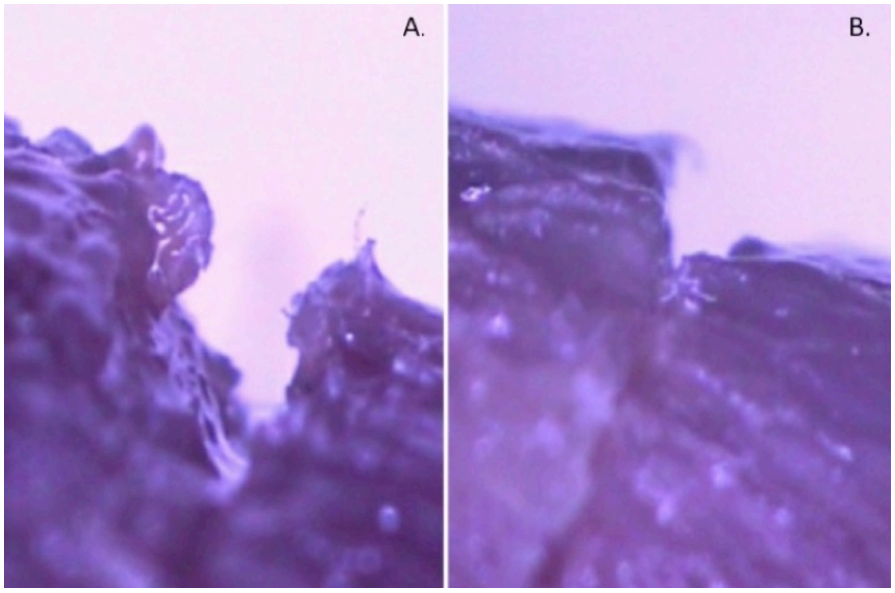

Figure 3.8: Cross-sectioned kerf shape; A: U-shaped feature; B: V-shaped feature

Table 3.7: Descriptions of cross-sectional kerf shapes

Kerf features	Description
Narrow kerf	Two parallel kerf walls, close to each other with an extremely narrow distance between the kerf walls.
V-shaped kerf	Two inwardly angled kerf walls ending at the kerf floor with a wide distance at the top of the cut and narrower when the walls descend to the kerf floor.
U-shaped kerf	Two parallel walls connected by a curved kerf floor, with a wide distance between the walls

4.) The presence or absence of striations was observed and recorded (Figure 3.9). Striations are presented as microscopic grooves along the kerf wall when the serrated edge of a knife incises through bone tissues. Both cut walls were examined and the presence of striations was recorded if any side of striations was identified.

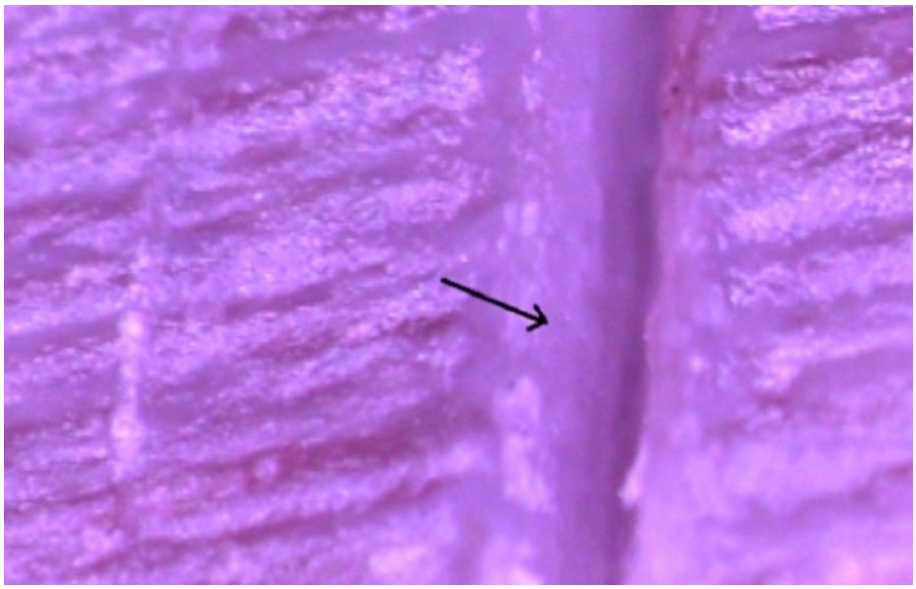

Figure 3.9: Kerf wall striation is presented as a groove along the kerf wall; a black arrow points at striation area

5.) Presence or absence of the chattering effects: Chattering is defined as pieces of small fragments of the shoulder margin caused by the vibrations of the

weapon (Figure 3.10). This feature can be related to a thicker and less straight sharp-edged morphology of the weapon (Humphrey and Hutchinson, 2001).

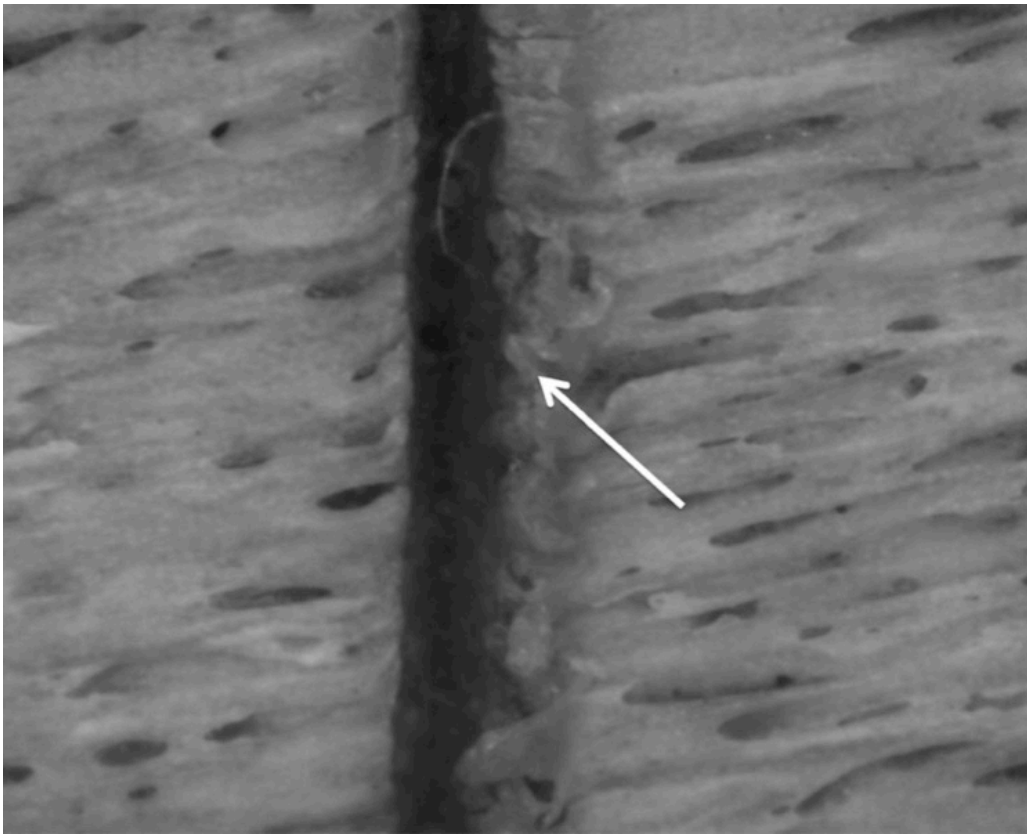

Figure 3.10: Cut mark showing chattering on the kerf margin (indicated by arrow)

6.) Width of the kerf mark (in mm): Kerf mark images were taken during microscopic examination and kerf widths were then measured in units of a millimetre from their pictures by ImageJ computer program, which could be used for very small-scale measurement. The image file was opened in ImageJ software and a measurement scale was calibrated based on the millimetre scale included in each image. After that, the kerf width was measured perpendicularly. Overall measurement method was concluded in APPENDIX 3.A. Three width measurements were performed at the widest point from the edge of cut marks and the average value was calculated.

3.3.2.2 Micro-computed tomographic examination

All 144 chop marks from femoral samples were scanned before and after environmental exposure. Three-dimensional images of the bone microstructure with

a spatial resolution were obtained by Micro-CT. The non-destructive nature of this method is one of its crucial advantages. This study was performed using a Nikon® XT H225 CT scanning. All bone specimens with chop marks were scanned vertically in a cylindrical sample holder placed on a moveable stage. The X-ray projection images were acquired at a voltage of 200 kV, intensity of 40 μA and magnification of 510 mm with total scanning time around 60-70 minutes. A tungsten source was used without a filter. The volume of interest was located in the centre of the bone and included all chopping wounds. Then, cross-section images were processed and stored in TIFF file format in order to evaluate with ImageJ program.

The size and shape of chop marks were rearranged to obtain the maximum dimensional information. Three-dimensional images were processed and reconstructed by VGStudio MAX 2.1 software so that the structural parameter could be ready to interpret (see APPENDIX 3.B). Because of the lack of standard tool mark terminology, some specific definitions were developed (Table 3.8 and Figure 3.11). Using the same process documented in Norman et al. (2018) and Waltenberger and Schutkowski (2017), the metric analyses were achieved by measuring dimension and angles in different views of the chop mark images. Therefore, these parameters could represent optimally the cutting plane of the weapons.

Table 3.8: Quantitative parameter for chopping mark micro-morphological analysis (adapted from Bello and Soligo (2008), and Waltenberger and Schutkowski (2017))

Parameters	Definition
Maximum length (mm)	The maximum length of a mark between both lateral tips on the bone surface level
Maximum width (mm)	The perpendicularly maximum width between both kerf margins on the bone surface level
Maximum depth (mm)	The perpendicular length between the deepest point of a mark to the natural bone surface level
Maximum shoulder height (mm)	The maximum length measured from deepest point of a mark to the tip of raised margin; measured on the proximal and distal sides
Opening angle	The angle between the proximal and distal kerf wall
Slope angles	The angle between the natural bone surface and the slopes of kerf wall; measured on the proximal and distal sides

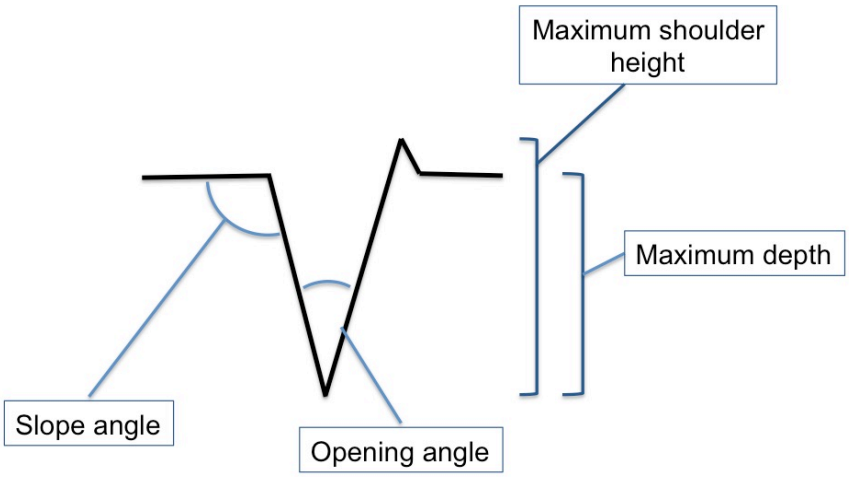

Figure 3.11: Cross-section of a chop mark demonstrating measured variables

In applying these methods, the appropriate images were arranged to the best plane to measure their maximum chop mark dimensions. Dimensional analyses of the maximum length, width, and depth of the chop marks were conducted (Figure 3.12). In addition, the three different angles (opening angle, proximal and distal slope angles) were detected and measured in cross-sectional views to characterise the form of the kerf marks (Figure 3.13). Measurements were conducted three times and the mean was calculated. The dimension, angle, and depth of the defect were investigated to compare between pre and post-environmental exposure data.

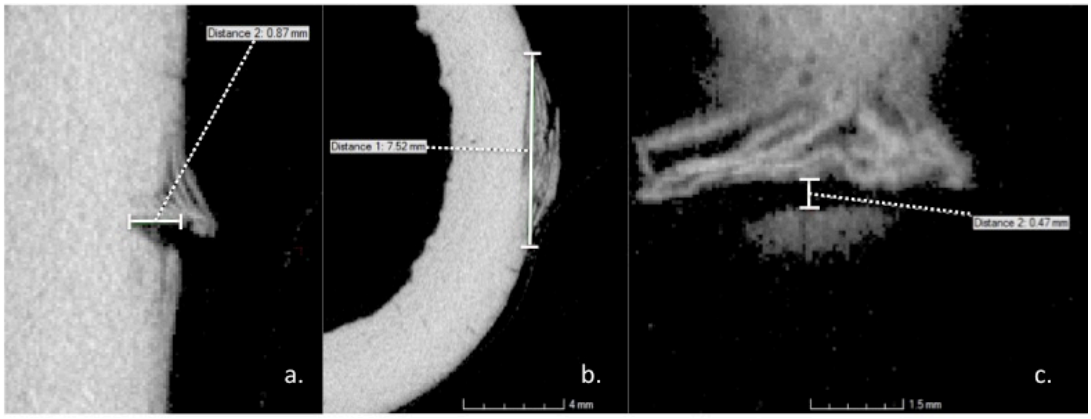

Figure 3.12: Dimensional characteristics: (a.) maximum depth; (b.) maximum length; (c.) maximum width

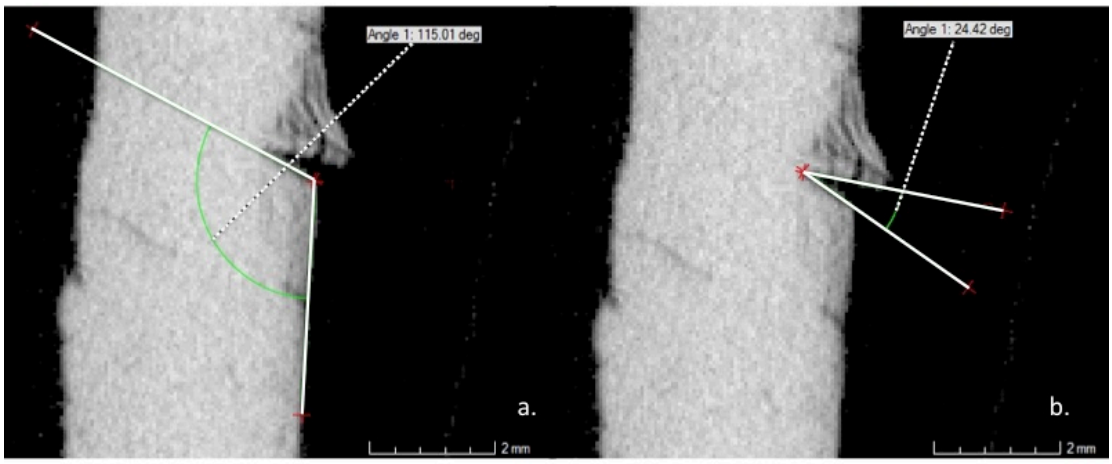

Figure 3.13: Kerf angle characteristics: (a.) slope angle; (b.) opening angle

3.3.3 Blunt-inflicted trauma

3.3.3.1 Macroscopic examination

Each fracture area was evaluated macroscopically by recording the general characteristics of the lesion, and any information visible to the naked eye (Table 3.9). A digital sliding calliper, an osteometric board and a measurement tape were used for general bone measurements. The observation was done by the naked eye to review and record the characteristics of fracture such as fracture type and outline, fracture angle, surface morphology (Wheatley, 2008; Wieberg and Wescott, 2008) as well as general measurements of sample bones.

Particular attention was given to the bone fracture surface. Bone is known to be weaker in tension than in compression. Hence, the tensile side should be the first part of mechanical failure in three-point bending (Berryman and Symes, 1998; Currey, 2002; Symes *et al.,* 2012; Zephro and Galloway, 2014). Fracture surfaces were photographed with a Canon EOS80D with 24-70 mm 4L IS lens in order to identify areas of tension and compression. However, these terms were used with the understanding that areas of pure tension and compression are uncommon in the three-point bending test of bone (Turner and Burr, 1993; Currey, 2002). For example, the compressive regions may have features of tensile failure, while the tensile regions may have a portion of shearing. Therefore, the term “tension” and “compression” in this experiment were used with this point in mind.

Table 3.9: Blunt force fracture characteristics

Parameters	Definition
Fracture outline	Recorded as transverse fracture, oblique fracture, butterfly fracture (complete and partial) (Reber and Simmons, 2015), and greenstick fracture
Colour variation	Colour difference between the fracture surface and bone surface; recorded as uniform or non-uniform
Fracture angle	The angle formed by the fracture surface and the bone surface; recorded as obtuse/ acute or right angle
Fracture surface morphology	Recorded as rough, smooth or intermediate
Fracture line	How many samples to identify a fracture line
Length of slope (mm)	The maximum distance between the tip of fracture surface and the hypothetical line of the origin of fracture surface
Length of fracture surface (mm)	The maximum length of the diameter of fracture surface
Cortical thickness (mm)	Maximum and minimum thickness of shaft edge of fracture sites
Maximum length (mm)	The maximum length of the sample
Maximum circumference (mm)	Mid-shaft bone circumference

Tensile areas were characterised by their relatively flat and smooth surface, while compressive areas were distinguished by areas of longitudinal splitting and inter-lamellar cleavage (Figure 3.14) (Wise *et al.*, 2007; Wynnyckyj *et al.*, 2011). The area that did not match with tensile or compressive characteristics was therefore defined as the transition area. ImageJ (Image 1.51g, National Institute of Health, USA) was used to manually trace the appropriate areas and calculate the relative area (see the method in APPENDIX 3.A). Following the macroscopic observation of the fracture surface, areas of tension and compression were categorised again with a stereomicroscopic zoom at 6.3x – 63 x magnifications to classify the lesion clearly. The tensile and compressive areas were investigated microscopically before selected regions were prepared for further SEM analysis.

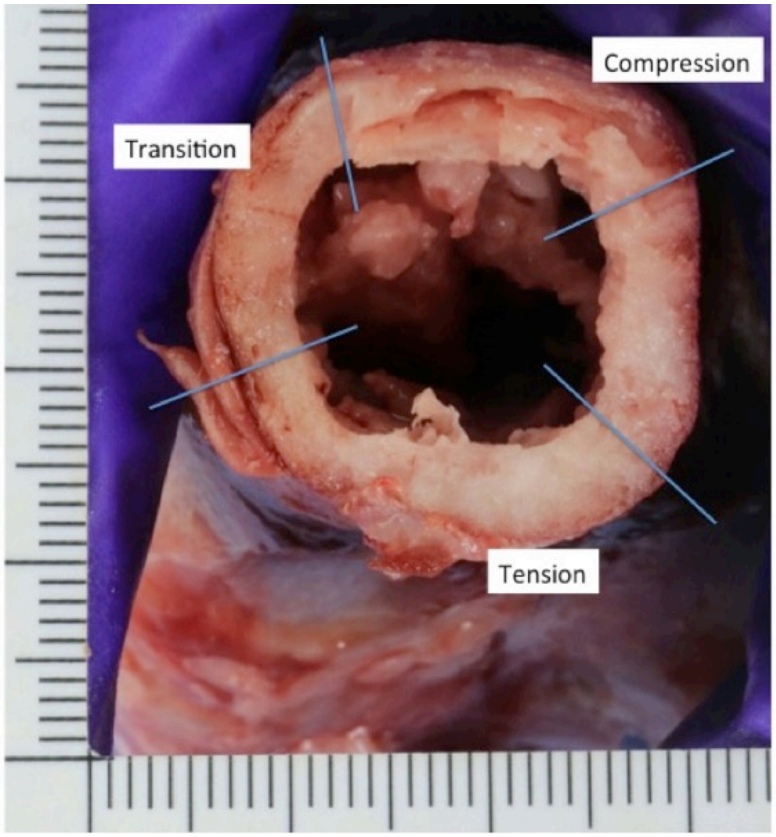

Figure 3.14: Representative fracture surface showing categorised areas

3.3.3.2 Replicating mould production

The selected areas of blunt-inflicted fracture surface were prepared for SEM examination. SEM was selected as it allows for high magnification and in-depth microscopic investigation of the bone fracture surface. After direct investigation, a negative impression was made following established guidelines using Isomark® forensic casting material, a high-resolution silicone, in order to view at higher magnification with the SEM. Isomark® forensic casting material was used in this study because it is highly accurate in copying the fine details of bone surface modifications; can be easily separated from the replicated surface, and lasts long enough for replication to be made. The material is characterised by a high level of accuracy of up to 0.1 μm and high contrast characteristics that allow details to be identified more easily when magnified.

To remove such contaminants, the bone surface was cleaned using a mild detergent solution and a soft, clean toothbrush. Next, the specimen was swiped with cotton swabs moistened with acetone and wait allowed to dry. The specimen was

then cleaned using ethanol and a cotton swab to eliminate any residue of acetone, and allowed to dry before applying high-resolution silicone.

An Isomark® cartridge was attached with a dispensing gun and a mixing nozzle. Before starting the replication process, the first amount of mixed fluid should be discarded because the silicone and catalyst were sometimes not well mixed. The compound was directly applied through the mixing nozzle, which must be as close as possible to the bone surface in order to prevent air bubbles forming on the mould surface. The time to set or harden was dependent on working and curing time indicated on the cartridge. Once the Isomark® compound was fully set, it could be removed from the bone surface. Lastly, the replicated mould was stored in a small, zip-lock plastic bag to prevent static electricity and avoid getting dust on the mould. An identified code was noted on the plastic bag and its container.

3.3.3.3 Fracture surface analysis

For a deeper investigation of fracture surface analysis on a microstructural level, changes in fracture surface micro-morphology were examined with SEM. Areas of interest were replicated using Isomark® forensic casting material. These moulds were first examined using a stereomicroscope, and representative sample areas from the middle of the tensile and compressive areas (approximately 5 mm long) were used for SEM examination. The moulds were then taken to the Microscopy unit, Cranfield Forensic Institute, Cranfield University where they were mounted onto specimen stub and locked with a specimen holder. A Hitachi® Scanning Electron Microscope SU3500 was used to visualize the sample, as it can provide a high-resolution magnified image and is commonly used in trauma studies (Alunni-Perret *et al.*, 2005; Saville *et al.*, 2007; Bello and Soligo, 2008; Thompson and Inglis, 2009). The SEM settings of 10-15 kV beam and 70Pa were used to visualise fracture surfaces as other studies have used these setting successfully in skeletal trauma studies (Thompson and Inglis, 2009; Wynnyckyj *et al.*, 2011; Ferllini, 2012). Resulting images were captured with a range of magnifications.

At higher magnification, fracture surface areas were then qualitatively classified according to their scanning electron microscopic morphology, attempting to quantify regions of interest. All regions within the tensile and compressive area

were qualitatively described as “smooth”, “indeterminate” or “rough” depending upon specific features (Table 3.10). The proportion of each categorised area was subsequently calculated with ImageJ program to evaluate the degree of smoothness and roughness (see the method in APPENDIX 3.A). Indeterminate areas were not included in this calculating process. The ratios of rough to smooth areas were independently compared within each fracture surface area.

Table 3.10: SEM characteristics of fracture surface (Wise *et al.*, 2007)

Macroscopic features	SEM category	Findings
Tension	Smooth	A relative clean, flat and undisturbed morphology (Figure 3.15)
	Rough	An irregular, uneven and coarse surface (Figure 3.16)
Compression	Smooth	Sharp, blunted layers of lamellae
	Rough	Fragmented and flaky appearance
Indeterminate		Area that cannot be categorised into either smooth or rough

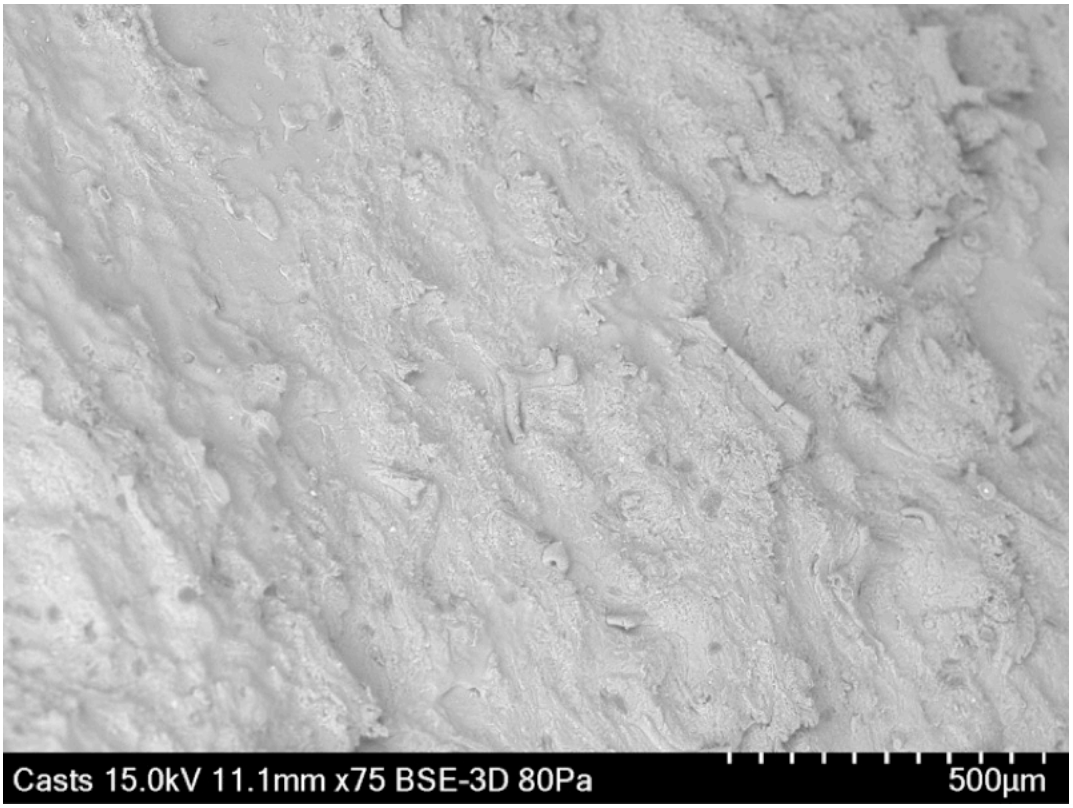

Figure 3.15: Smooth region of tensile fracture surface

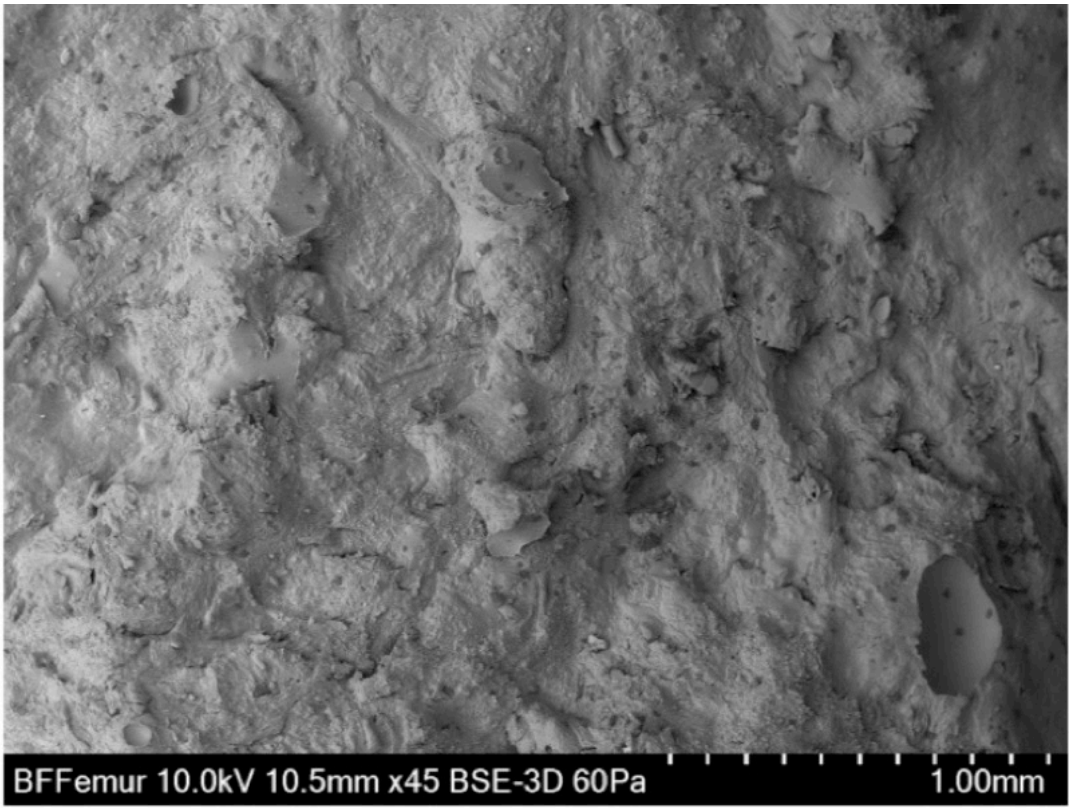

Figure 3.16: Rough area of tensile fracture surface

Replications of high-resolution casts for SEM observations of blunt trauma fracture surfaces can damage delicate lesions and cause pre-exposure artefact. Therefore, the same traumatic methodology was applied to a new set of femurs and new casts of the traumatic lesions were made for SEM examination. Data collections were made as pre-exposure records. Afterwards, these femurs would be excluded from this study.

3.4 Thermal alteration experiment and analysis

As described in the published literature (Mayne-Correira, 1990; Herrmann and Bennett, 1999), differentiation between a traumatic fracture and thermal damage has been problematic. This study was not only conducted to investigate the degree of fire modification to the cut mark characteristics of bone, but also attempted to discern the effects of weathering on burned bones and their traumatic lesions.

3.4.1 Thermal treatment

Previous studies involving experimental burning have applied different methods to control heat temperature. Some researchers have used a blower furnace, a crematorium, or an electric oven (Bradtmiller and Buikstra, 1984; Shipman *et al.*, 1984; Mayne Correira, 1990; Collini *et al.*, 2015; Macoveciuc *et al.*, 2017; Waltenberger and Schutkowski, 2017), whereas others chose to use outdoor fires to replicate a forensic context (Herrmann and Bennett, 1999; de Gruchy and Rogers, 2002; Marciniak, 2009; Kooi and Fairgrieve, 2013; Robbins *et al.*, 2015). Because it is more suitable to control the duration and temperature condition of the cremation process, a laboratory Carbolite CWF 110 electrical furnace (Carbolite® Gero Ltd., Parsons Lane, Hope Valley, S33 6RB, the UK) was used for cremation events in this study. It also has a peephole for visualization of samples during cremation. This furnace enabled greater temperature control, standardised the methodology and achieved uniformity of post-burn samples.

Three hundred and four pieces of 5^{th}-8^{th} adult domestic porcine ribs with minimal soft tissue were used. Specifically, specimens were equally divided into four groups of 76 ribs representing each season. Trauma inflictions were done on 60 rib samples using the same method as with the unburned sharp-inflicted sample group. Three marks were made with the non-serrated blade, coarse-serrated blade, and fine-serrated blade knives on each bone. Prior to the burning event, the macroscopic and microscopic examinations of all elements were carried out to demonstrate kerf features. Sixteen ribs were used as control samples without traumatic lesions to study how cut mark affect burned bone morphology and fragmentation after cremation and environmental exposure.

Every burning process followed the same methodology. All experimental burning processes started in the morning and burned samples were left to cool down overnight before the recovery process began the day after. A limestone slab was placed at the centre of the furnace chamber in order to raise the samples to a level that maximal temperature could be achieved. Ten samples inside separated metal cages were distributed and placed on top to minimize the chance of sample commingling (Figure 3.17). This study selected the temperatures of the cremation process of 850°C as the upper limit, which is considered as the average

temperature in a house fire (Shipman *et al.,* 1984; Ellingham *et al.* 2015) and sufficient to burn all organic materials and to incur greatest changes (Mayne Correira, 1997; Bohnert *et al.*, 1998; Cattaneo *et al.*, 1999; Thompson, 2005; Macoveciuc *et al.*, 2017). It was decided to gradually increase the temperature to this maximum of 850°C for at least 30 minutes. Next, the furnace was turned off and the samples were allowed to cool for 24 hours with the chamber door closed to prevent sudden cooling-induced fracturing of the specimens. The samples were not fully calcined because recrystallization and fusion processes occur at higher temperatures and up to 1000°C (Grupe and Hummel, 1991).

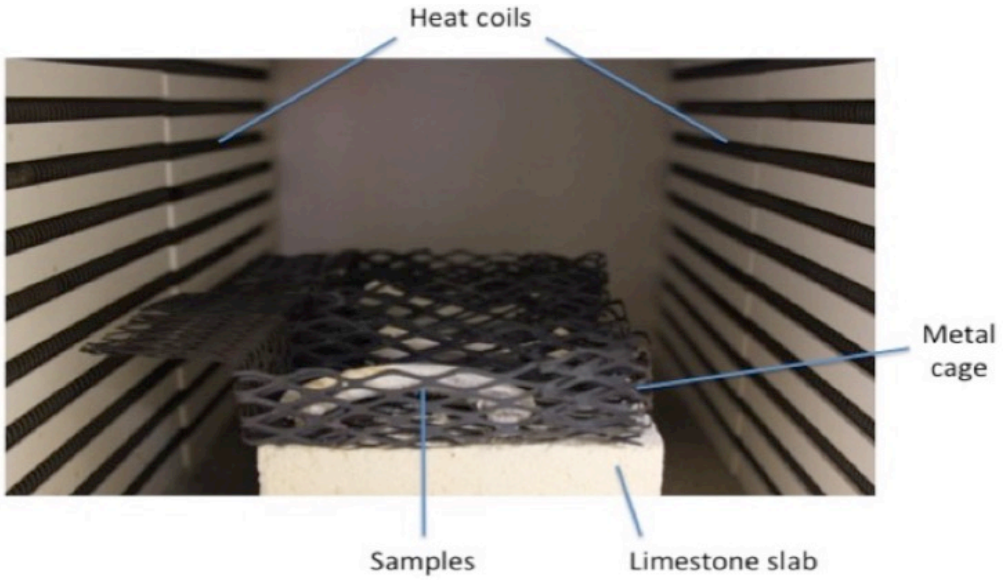

Figure 3.17: Sample position inside furnace chamber

Subsequently, each burned rib and its fragment was separately collected and packaged in a paper towel inside a plastic ziplock bag. Then, all bags were placed in a plastic box to prevent any transportation damage.

3.4.2 Burned sample analysis

All samples were examined macroscopically and microscopically before and after environmental exposure. The analysis of burned samples is entirely dependent upon their condition at the time of analysis. A process of sorting and cataloguing bone fragments must be completed prior to reconstruction. The reconstruction of heat-induced fractures is essential to the analysis of burned samples so as to

investigate perimortem fracture, the pattern of heat-induced fracture, and associated colour changes (Pope and Smith, 2004; Fairgrieve, 2008). These processes were not as complicated as there was no comminuted fracture.

Each burned bone was photographed, documented and analysed as the same method as un-burned samples again with careful manner. Cut marks and heat-induced fractures were also viewed under an optical stereomicroscope. Heat-related damage was identified and recorded according to type, length and alignment compared with the long axis of the sample. Any fragments were measured in millimetre and collected with their original bone. Each sample was also weighed before and after the burning process with an Ohaus Adventurer® analytical electronic balance. Variables describing the morphology and pattern of heat-induced damage and the degree of fragmentation were defined (table 3.11) and scored (Quatrehomme *et al.*, 1998; Herrmann and Bennett, 1999; Thompson, 2004, 2005; Gonçalves *et al.*, 2011). The fragmented sizes were appropriately adjusted from literature in order to investigate small flat bone used in this study (Grevin *et al.*, 1998; Herrmann and Bennett, 1999; Waterhouse, 2013a, 2013b).

Table 3.11: Macroscopic and microscopic features related to heat-induced damage

Variables	Descriptions
Type of heat-induced damage	Longitudinal, curved transverse, straight transverse, patina, delamination
Damage surface texture	Rough or smooth
Is the damage related based on pre-burn sharp trauma?	Yes or no
Number of fragments	Number of fragments collected
Size of fragments	Small series: smallest dimension <1mm Medium series: smallest dimension 1-5 mm Large series: smallest dimension >5 mm
Warping	Present (deformed contours) or absent (normal contours)
Bone shrinkage	Cut mark size (length and width)

3.4.2.1 Heat-induced fractures

As they burn, bones dehydrate, shrink, and their collagen is degrade, causing a loss of elasticity and tensile strength. As a result, fractures occur and travel along the line of greatest stress. Herrmann and Bennett (1999) summarised five typical patterns of heat-induced fracture in burned bone: longitudinal fracture, curved transverse fracture, straight transverse fracture, patina fracture, and delamination. Heat-induced fracture was also identified their morphology, fracture surface, and their correlation with pre-existing cut marks.

3.4.2.2 Colouration

Bone goes through distinctive colour changes depending upon the duration of heat exposure, the temperature of the fire, and the presence of soft tissue (Schmidt and Symes, 2015). The colour of each cortical bone surface was scored as “unburned” (no colour change), “charred” (brown or black), and “calcined” (light grey or white). If more than one type of discolouration was present, then the more prominent type was selected. The use of Munsell® Colour chart is another appropriate method to standardise the allocation of heat-induced colour change, but it has few analytical uses (Shipman et al. 1984).

3.4.2.3 Warping

Warping is defined as unusual bone alignment or deformity to any degree (Gonçalves *et al.*, 2011; Whyte, 2001). This finding was evaluated by carefully visual examination of the contours of each fragment especially looking for unusual bending of the shaft of burned ribs and of the heat-induced fracture ends of ribs. The score “present” was used if the burned bone contours appeared to be twisted or deformed to any abnormal degree (Bontrager and Nawrocki, 2015).

3.4.2.4 Burned bone fragmentation

Bone fragments were sorted and categorised into three groups based on size and shape using a digital sliding calliper. The first one, the small category, consists of a bone with the smallest dimension, not more than 1 mm. The medium category consists of bone fragments with the shortest fragment dimension is between 1 to 5

mm. The large category fragment has the shortest dimension of at least 5 mm. Each category was weighted and percentage of proportion was calculated in order to determine a comparison between each category within each group and each collection event.

3.4.2.5 Cut marks examination

Cut marks made with the edge of a knife are characterised by their V-shaped, narrow cross-sectional appearance with no area of penetration. As mentioned earlier, all cut marks were examined using a magnifying lens or a standard light stereomicroscope. For kerf wall observations, evaluation methods were done as the same method as the unburned sharp-inflicted sample group.

The degree of heat-induced dimensional change in burned samples could be expected to vary accordingly. The percentage of bone shrinkage and expansion has a greater effect on any metric analyses conducted rather than morphological methods (Thompson, 2005; Vegh and Rando, 2017). The current study aim to verify the influence of heat-induced dimensional change on the dimensions of cut marks inflicted by different sharp force tools. Changes to the kerf dimension were recorded with the same methods used in the non-burned experiment in order to examine the length and width of the cut marks before and after the burning process. The mean of three measurements was calculated giving a more representative dimensional change of the marks before and after burning events.

3.5 Experimental sites for deposition of bone samples

3.5.1 F3 taphonomic facility field site

The outdoor research was conducted in F3 taphonomic facility, an open grassland field used for studies of taphonomy. This facility locates at Shrivenham campus of Cranfield University, Oxfordshire, United Kingdom. In fact, the entire area of F3 taphonomic facility is a rural area and surrounded by a combination of grassland, livestock and forest areas (Figure 3.18-3.19).

Figure 3.18: F3 taphonomic facility before the sample deposition, August 2016

Figure 3.19: Aerial map of F3 taphonomic facility (from: https://www.google.co.uk/maps/@51.6048504,-1.6316365,244m/data=!3m1!1e3)

The climate in this area is variable depending on the season. The spring and summer seasons are normally warm during the day, with a maximum temperature of

16.7°C and 22.2°C respectively. Autumn and winter seasons are cooler with the maximum temperature of 18.7°C and 7.7°C respectively. Seasonal rainfall was recorded between 43.6-70.7 mm with the highest precipitation in October and November (Met Office 2017). It is imperative to note the climate in Southeast England where this study was taking place. According to the Köppen-Geiger Climate classification system, Southeast England is classified as Cfc climate. This classification means Southeast England has a warm temperate minimum temperature between -3°C to 18°C, fully humid with cool summer and cold winter (Kottek *et al.*, 2006). Certainly, this climate is different comparing to original work of Behrensmeyer.

To minimize access of animal scavengers, the experimental field was surrounded by chain-link wire and wooden plank fences. These barriers prevent scavenging activity while exposing the bones to environmental conditions. A 3.2 × 2.4 m area of roof house enclosed by net was used for surface-deposited specimens, which were separated from each other and placed in their 0.25 x 0.25 cm area of a metal frame. While buried samples were covered by approximately 2 feet of soil using backfill from the pits where the bones were deposited. Large rocks were removed from the burial site in order to ensure complete soil coverage of the sample. This depth was selected because the thermal stabilisation of soil temperature as the ambient temperature occurs in the soil at a depth of 0.6 m (2 ft.) (Rodriguez and Bass, 1985).

The sharp-inflicted group of ribs was placed in the taphonomic facility beginning in September 2016, while all of the traumatised femurs were placed in March 2017. The surface of every specimen was observed monthly for 18 months to record the onset and progression of morphological change. Bone samples were recovered from the depositional site at the specified time points (table 3.1) and brought back to the Stephenson anthropological laboratory to evaluate their morphological and structural changes. All macroscopic surface modifications developing from environmental exposure were compiled.

A total of 304 pork ribs were used in the burned experiment. Burned samples were placed in the F3 area in different fashions to investigate the effects of different seasonal and environmental exposure on burned sharp-inflicted ribs. Two sample

groups were set up in the F3 taphonomic facility. Forty traumatic samples and eight controlled samples were exposed to the surface environment, while another twenty traumatic samples and eight controlled samples were buried at a depth of two feet. In order to identify their detached fragments, each sample was separated from each other by placing on the centre of 1 x 1 metre rope grid (Figure 3.20). Each surface sample was examined for their change of general morphology, trauma characteristics, and number of fragmentation every week. Prior to examination, the experimental area was observed in order to search for any evidence of animal disturbance.

All burned samples were collected from the taphonomic field after one month of exposure. More precisely, every first and third week, 10 samples from the surface group were removed from the field for fragmentation index investigation. These samples were disturbed by intentional movement so they could not use again for a reflection of how change from environmental exposure. Additionally, 10 traumatic samples and 4 controlled samples from each group were recovered every second and fourth week. This experiment was conducted every season to allow for comparisons of the impact of different weather.

Figure 3.20: Sample placing in the F3 taphonomic facility; white arrows identify burned bone samples

3.5.2 Soil analysis

A fundamental understanding of the role of soil can contribute to taphonomic assessment by designating biological and chemical markers that aid in the location and dating of clandestine graves (Carter and Tibbett 2008). Possibly the most destructive factor of long-term burial is soil acidity (Pokines and Symes, 2014). Acidic soil can deplete calcium ions from hydroxyapatite crystal, resulting in bone corrosion. Studies have shown that acid soils can promote long-term bone degradation (Haglund and Sorg, 1997; Hedges, 2002).

Soil chemical analysis was performed including soil moisture and pH. Soil samples were taken within a 10 cm radius of bone samples from each burial pit immediately prior to the initial deposition of the samples and repeat at the recovery period. The international standard is applicable to the referenced document (British Standards ISO10390, 2005) . Samples were processed for soil pH according to the following procedure.

1. A soil sample of approximately 5 g was taken from soil deposition around burial samples.
2. The sample was air dried in room temperature for at least 72 hours.
3. The dried sample was passed through a 2 mm mesh sieve and bottled.
4. This test portion was diluted in five times its volume of distilled water.
5. The suspension was mechanical shaken for one hour.
6. Calibration of the pH-meter was done with buffer solutions per manufacture specification.
7. Measurement of the suspension pH at 20 ± 2 degree Celsius was done immediately after being shaken.
8. The researcher read the pH after stabilization of the value.
9. Second separately prepared suspension was prepared and measured.
10. If there was a difference between the pH measurements of two suspensions from the same soil samples, the test was repeated in order to satisfy the requirements (Table 3.12).

Table 3.12: Acceptable repeatability of pH measurement (ISO10390, 2005)

pH range	Acceptable difference
pH ≤ 7.00	0.15
7.00 < pH < 7.50	0.20
7.50 ≤ pH ≤ 8.00	0.30
pH > 8.00	0.40

Soil moisture indicates the amount of water present in the soil and is one of the major factors contributing to microbial, biological, chemical and physic-chemical activity (Jaggers and Rogers, 2009). The amount of water in the soil can facilitate bone mineral solubility and increase the ion exchange between bone and soil (Hedges, 2002). Soil moisture is evaluated by weighing 5 grams (± 1 mg) of field moist soil into a glass container and placed into an oven at 70 degree Celsius for 24 hours to vaporize the water. The sample is then allowed to cool down in room temperature environment before re-weighing. The difference between wet and dry weigh is used to calculate the moisture content percentage:

% Moisture content = [(Moisture loss)/(wet weigh soil)] x 100

This experiment was designed to establish whether environmental taphonomic factors can alter the morphology of blunt and sharp inflicted bone fractures, and if these characteristics can be identified and distinguished. Although some aspects of the following procedures were adapted from the literature, the combination of macroscopic and microscopic analyses was used for differentiation of perimortem injuries from postmortem damages.

3.5.3 Taphonomic monitoring

Monthly observations were conducted during the first twelve months to record environmental parameters, assess bone surface modifications, and to photograph using a Canon EOS80D. Observations were made every two months for the last six months of the study. Emphasis focused on physical surface alterations related to environmental exposure concerning bone weathering stage, a sign of soft tissue

decomposition, bleaching and abnormal colour staining, animal activity, and bone surface erosion. Data was recorded on every visit.

The extent of bone weathering was determined based on stages described by Behrensmeyer (1978). Observation of bone weathering includes bleaching, cortical cracking and flaking (Behrensmeyer 1978: 151). However, previous studies in warm temperate climates usually report no sign of changes due to exposure for longer than two years (Andrews and Cook, 1985; Andrews and Whybrow, 2005). Therefore, techniques advised by Cunningham et al. (2011) to observe minute changes were applied. All samples were recorded as presence or absence for following features demonstrated in Table 3.13. Bone surface erosion was scored using a scale of 0-5 ranging from the absence of any change to complete obliteration of normal cortical surface (Table 3.4). Different stages of any parts of the bone were recorded with the most advanced area of bone samples.

Table 3.13: Types of weathering changes from Cunningham *et al.* (2011)

Types of change	Definitions
Cortical bone flaking	Marbling pattern on the diaphysis of the elements and a series of fine cracks; only the outermost layer is affected
Erosion of the articular facets and diaphysis	Erosion of the outer layer of cortical bone, defined stage as McKinley (2004) (Table 3.4)
Pockmark pattern	A circular pattern due to wearing away of the cortical bone layer, exposing the underlying trabecular bone

Sun bleaching was indicated as one of the first effects of weathering to be displayed. Although Behrensmeyer did not include bleaching as a feature associated with bone weathering, bleaching was later included in a revision by Haglund and Sorg (1997). Moreover, fracture morphology, including fracture outlines, appearance of a new fracture site, and colour change of existing fractures were also noted. Because soft tissues cannot be totally removed during defleshing, some parts of muscle and tendon were present on periosteum of the sample. Therefore, soft tissue presentation was observed and related insect activity was

briefly recorded as adult present, egg present, larva present, and larva no longer present. Animal scavenging resulting in soft and hard tissue modification and consumption was also recorded. Taphonomic bone staining and bone erosion were observed and recorded. To establish whether environmental conditions have an effect on bone surface colour, five main colour differences were observed (Table 3.14). Upon final recovery, the surface colour was photographed and documented using a Munsell® colour chart under a natural daylight 18 W bulb.

Table 3.14: Summary of surface colour analysis

Colour change	The most possible cause
Yellowish-white	Normal fresh bone
White	Sun bleaching
Dark reddish brown	Haemolysis
Light yellowish brown	Soil staining
Dark reddish grey	Decomposition fluid staining
Greenish	Algae or fungi

3.5.4 Environmental monitoring

Several environmental variables, including temperature, precipitation, solar radiation, soil pH and moisture are believed to increase bone diagenesis (Haglund and Sorg, 1997). Qualitative evaluations such as exposure to sunlight or covered by vegetation were used. Daily air temperature, precipitation, wind speed, and hours of sunlight were recorded. Hours of sunshine per day was obtained from the nearest weather-observing station in Brize Norton, meteorological office of the United Kingdom (NGR 4292E 2067N, Altitude 82 m, Latitude 51:76N, Longitude 01:58W) and the other meteorological data were obtained from the F3-weather station of the Cranfield forensic institute. Average monthly values of these variables were calculated from an average of each day (see data in APPENDIX 4.A). The amount of sunlight exposure was also based on an assessment of the amount of shade from vegetation growth detected by photographs taken monthly from the facility. Observations were recorded from the early of September 2016 until the end of August 2018.

Temperature data and the number of calendar days were analysed in the form of accumulated degree day (ADD) in order to have a more holistic aspect of the decomposition process. ADD can be calculated by adding maximum and minimum values of temperature in degree Celsius for a day and then dividing to take the average value. This calculation was made to standardise temperature data in most of the taphonomic studies including soft and hard tissue decomposition.

3.5.5 Sample recovery, packaging and storage

Each bone sample represents unique circumstances that require the use of specific methods to carefully recover, package and transport fragile specimens in order to maintain the physical integrity of the samples. The aim is to minimize loss of information before laboratory analysis and transport the samples safely for subsequent examination.

Bone samples were left in the field as long as until they reach their recovery time. Forensic archaeological methods were applied to recover surface-deposited and buried bones to prevent man-made artefact during excavation (Hunter *et al.*, 2013). Because of exposure of metal identification tags, the search for the location of samples is therefore not difficult. The first step in the recovery process is careful removal of any overburden such as leaf litter or loose topsoil (Christensen *et al.*, 2014), then the samples and nearby environment were photographed. The recovery process of surface-deposited bones is often as simple as retrieving the samples from the ground. With buried samples, excavation of the samples is done by slow and careful digging using a shovel, trowel, brush, and bucket (Figure 3.21). Exposing of the samples allowed for surrounding materials relating to the buried bones such as plant roots. The samples were carefully exposed, photographed, and then removed. Burned bones; however, are more complex recoveries because the bones are very fragile. The recovery of pieces of bone must be conducted in a more careful manner. Each careless handling step can put fragile burned bones at risk of further physical damage (Fairgrieve, 2008).

All samples were recovered by hand or using a non-toothed forceps for smaller burned bone fragments with care. Fragments too small to be collected in this manner were excluded from this research. Care was taken in order to recover as

many bone sample as possible. Recovered bones and bone fragments were wrapped with soft toilet tissue, stored in sealable plastic bags, and kept in plastic containers during transportation to the laboratory. At the laboratory, they were evaluated for any possible damage during transport and stored on an aluminium tray to dry at room temperature.

Figure 3.21: Exhumation of the burial site and samples in situ

In the anthropological laboratory, the bones were unpackaged and washed with running water and cleaned with a soft, clean toothbrush to dislodge the soil sticking to the surface. Traumatised lesions were identified and rinsed with running water for 15-20 minutes. Burned samples were cleaned softly with a toothbrush to remove adherent soil. The bones were then allowed to dry at room temperature for one week prior to packaging. An identification label was maintained with all bone samples and fragments. Once a sample was dry, identification numbers with the date of the recovery were written on each bag. Bones were placed in a plastic bag and then kept in a properly labelled paper cupboard box at room temperature for long-term storage.

3.6 Statistical analysis

Once data collection was completed, statistical analysis was carried out. The obtained data were entered into the statistical program RStudio version 1.0.153. First of all, quantitative data were tested for normality using a Shapiro-Wilk's test in order to make sure that statistically analytical tests were appropriately used. For the comparative analysis, a general linear model was applied through a classical two sample t-test analysis. However, if normality tests revealed that data were not the normal distribution, then the median values were used for the report and statistical tests such as Mann-Whitney test, Kruskal-Wallis test, and logistic regressions along with linear regressions were applied. The Mann-Whitney test was selected in place of t-test to determine if there was a statistical significance in a skewed distribution dataset. The chi-square goodness of fit test was applied, given the original categorical nature of some of the variables. This would run on both the macroscopic and microscopic traumatic morphological data.

Intra-observer error analysis was performed in order to calculate the reproducibility of the study. This process was conducted by one researcher only and was considered successfully when the repeated measured values matched the original measurements to the closet millimetre. In this study, two measurements of the same traumatic lesion were regulated to not deviate from each other by more than 10%. This percentage was used instead of the conventional 5% due to the small sample size and the difficulty of measuring traumatic lesions precisely.

3.7 Summary

Because of the complexity of the methodology i.e. various samples and methods, a schematic diagram of the methodology is presented (Figure 3.22). Data were collected from two events: 1.) Data source 1; traumatised bone samples subjected to blunt or sharp force injury under experimental conditions, aimed at the study as an analysis of baseline traumatic lesions before environmental exposure; 2.) Data source 2; samples of bone from data source 1 and subjected to outdoors environmental exposure. Both groups received the same examination to compare the effects of environmental exposure on perimortem blunt and sharp force trauma. Specifically, in the burned study, Data source 1 sample were burned under

controlled conditions in the laboratory after receiving the examination, and additional examinations for data of burned sample were conducted. In addition, the samples in this study were deposited in outdoor environment at different times in 2016-2018 (Figure 3.23).

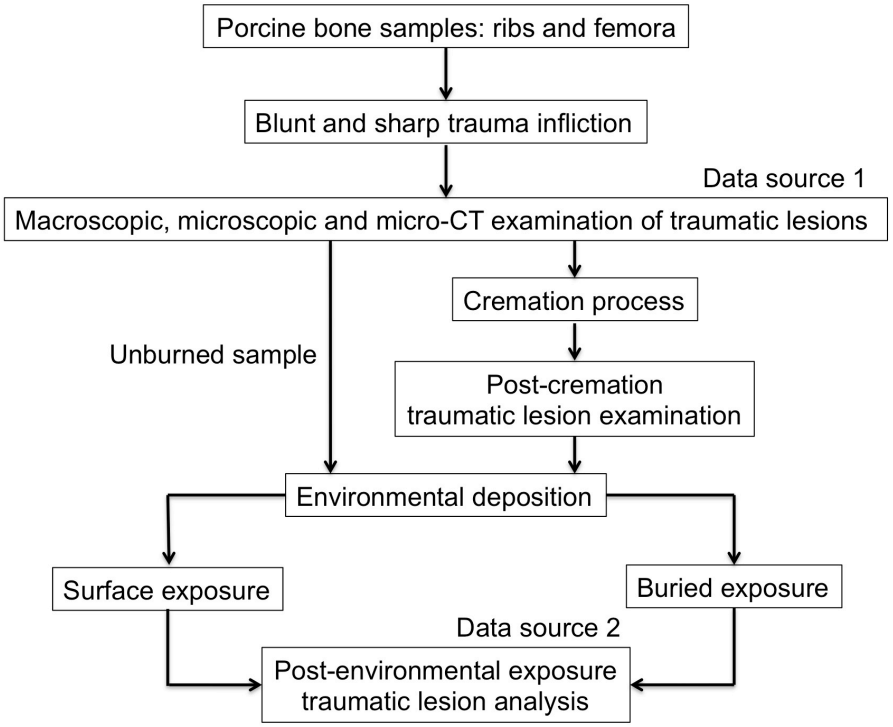

Figure 3.22: Diagrammatic summary of this study

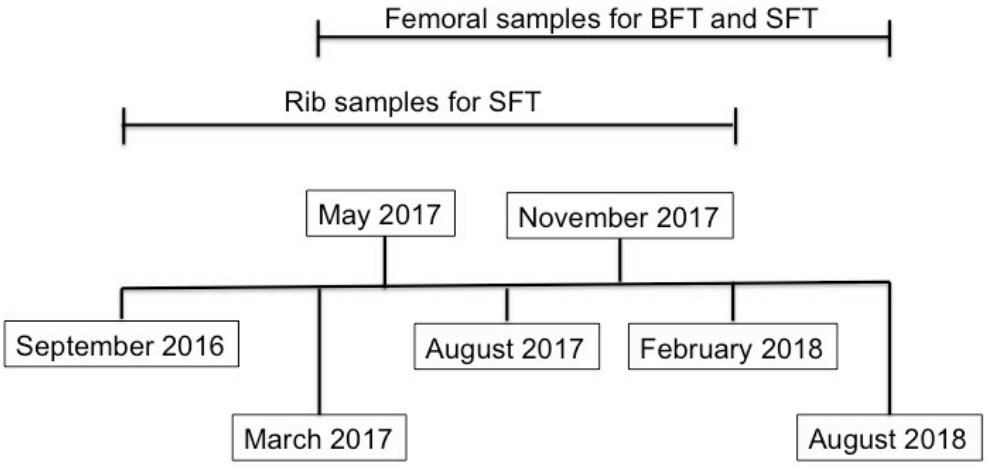

Figure 3.23: Diagrammatic summary of exposure period of each sample group in this study; the patterned boxes indicate selected months for environmental depositions of burned bone samples

Chapter 4: Depositional environment and surface modification to skeletal materials in a South-east England environment

4.1 Results

4.1.1 Weather and soil data

During two years of field research, spanning all seasons, average temperature ranged from 3°C to 20.5°C with the lowest occurring during wintertime (December to February) and the highest in the summer months (June to August). Precipitation levels fluctuated ranging from 0.1 mm to 3.72 mm, with the highest level of rainfall occurring in November and December (Figure 4.1). The longest days during summertime showed the highest hours of sunshine with the lowest occurring during winter. Wind speed patterns were unpredictable during the observation period ranging from 5-8 kn (Figure 4.2). Persistent low rainfall with relatively warm temperatures and long hours of sunshine were observed during the summer months of 2018. Soil pH and soil moisture are illustrated in Figure 4.3 (and raw data in Table 4.B in APPENDIX). The soil pH measurements at the F3 taphonomic research facility ranged from 5.9 to 6.4 and were considered to be mildly acidic soil content according to Soil Survey Division Staff (2017). Soil moisture ranged between 10% and 26% consistent with previous results of soil water analysis in Southern England (Evans *et al.*, 2016).

There is an obvious difference in field environment during experimental periods. Cold winter weather induces vegetation to die as a result of frost. Then, surface-deposited bones become totally exposed to environmental stresses, even though low levels of sunlight still persist (Figure 4.4). On the contrary, warmer spring and summer seasons are suitable for plant growth, which covers all surface-deposited bone (Figure 4.5) resulting in different taphonomic changes compared with colder periods.

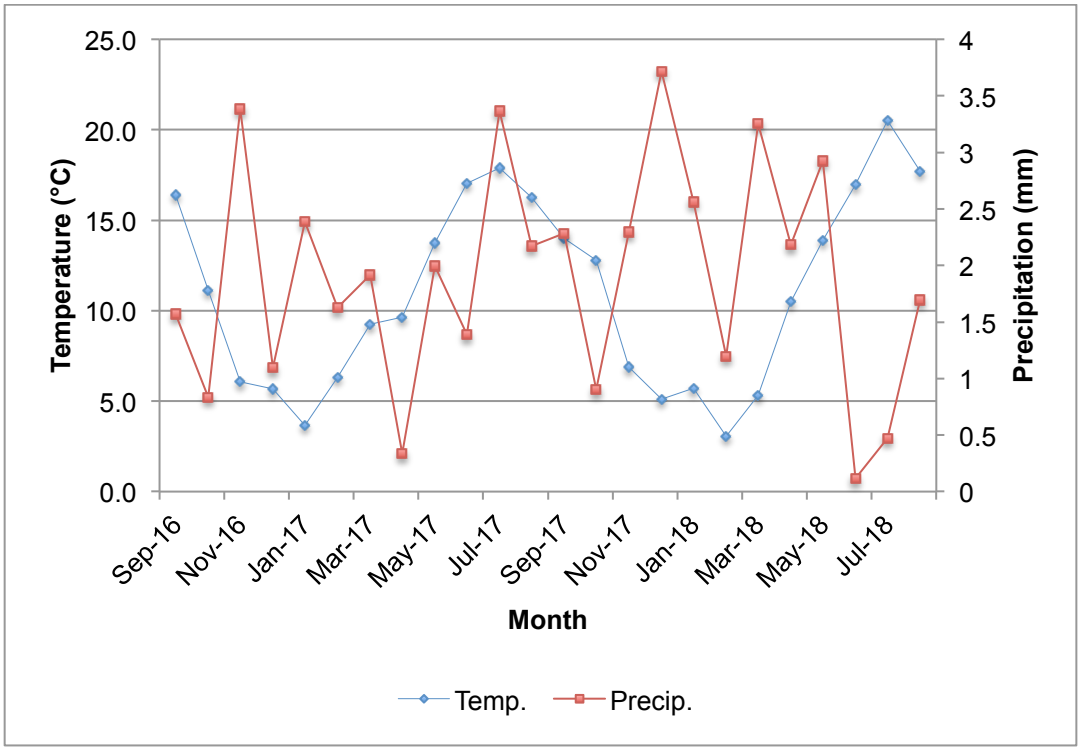

Figure 4.1: Line charts of temperature and precipitation in this study

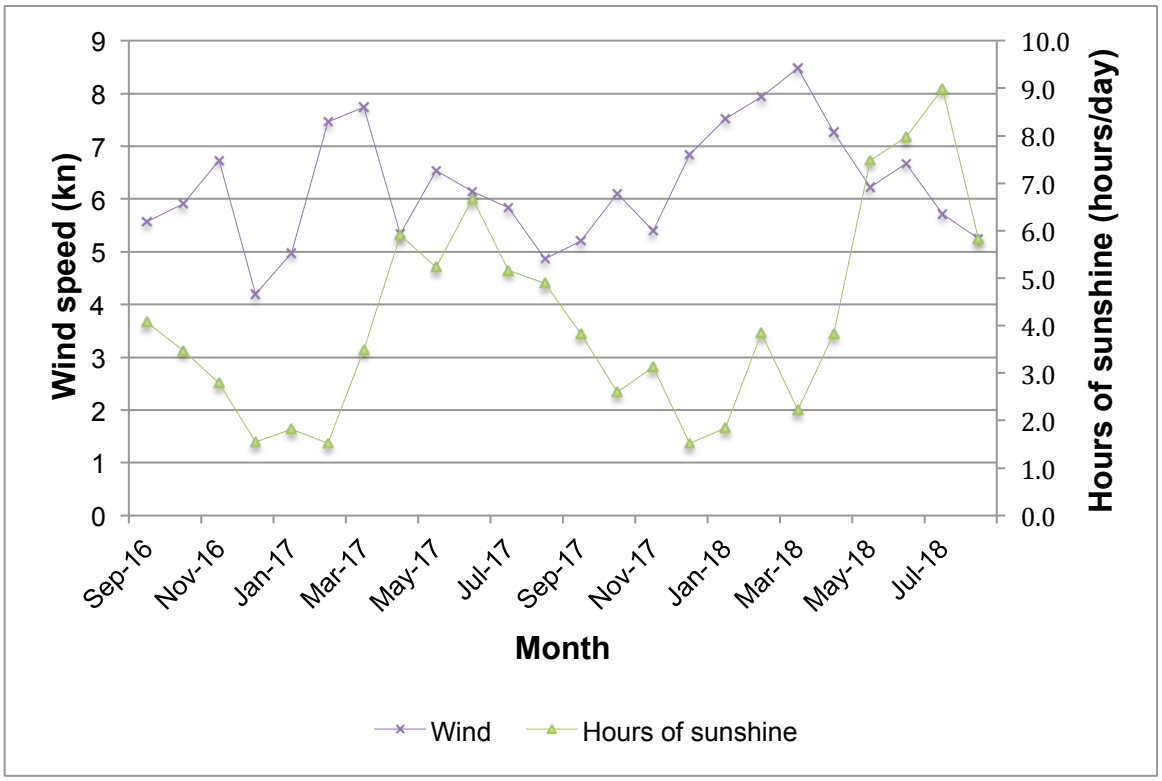

Figure 4.2: Line charts of wind speed and hours of sunshine in this study

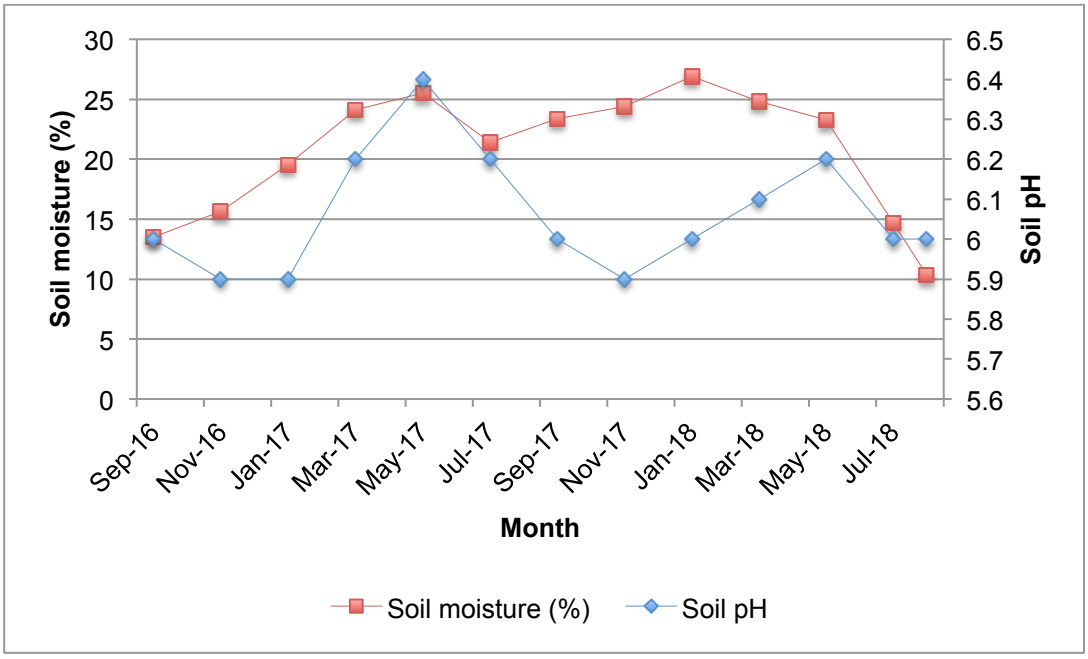

Figure 4.3: Line chart of soil characteristics in this study

Figure 4.4: Area of sample placing, December 2016

Figure 4.5: (A.) Same area as Figure 4.4, July 2017; (B.) A rib sample (the white arrow) totally covered by vegetation

4.1.2 Bone surface modification

All macroscopic taphonomic findings of bone samples resulting from physical and biological factors of environmental exposure were identified. The surface modifications are summarised in Table 4.1 for both surface-deposited and buried samples. Each depositional group has undergone similar patterns of taphonomic patterns. Seasonal weather conditions affect patterns and levels of bone surface modifications. In general, rib samples were placed in the outdoor environment during the early autumn (September 2016), whereas for femoral samples it was at the beginning of spring (March 2017). Because of limited access to the F3 taphonomic facility, it was difficult to conclude the exact day when surface modifications and weathering first appeared on each bone sample, and only approximate timings were established in this study.

Table 4.1: Summary of taphonomic modifications to ribs (total n = 72) and femurs (total n = 48) from surface and burial environment

Exposure time	Taphonomic characteristics	Surface group				Burial group			
		Rib (n=36)		Femur (n=24)		Rib (n=36)		Femur (n=24)	
		n**	%	n**	%	n**	%	n**	%
6 months	Organic staining	4/12	33	1/8	13	6/12	50	3/8	38
	Algae staining	9/12	75	0	0	0	0	0	0
	Weathering stage								
	0	12/12	100	8/8	100	12/12	100	8/8	100
	1	0	0	0	0	0	0	0	0
	Sun bleaching	5/12	42	3/8	38	0	0	0	0
	Soft tissue	3/12	25	6/8	75	7/12	58	8/8	100
	Adipocere	0	0	0	0	0	0	2/8	25
	Carnivore activity	0	0	0	0	0	0	0	0
	Rodent gnawing	0	0	3/8	38	0	0	0	0
	Mould	0	0	4/8	50	0	0	2/8	25
	Plant etch	0	0	0	0	0	0	0	0
12 months	Organic staining	12/12	100	3/8	38	12/12	100	6/8	75
	Algae staining	12/12	100	2/8	25	0	0	0	0
	Weathering stage								
	0	12/12	100	8/8	100	12/12	100	8/8	100
	1	0	0	0	0	0	0	0	0
	Sun bleaching	12/12	100	6/8	75	0	0	0	0
	Soft tissue	0	0	3/8	38	4/36	11	5/8	63
	Adipocere	0	0	0	0	0	0	3/8	38
	Carnivore activity	0	0	0	0	0	0	0	0
	Rodent gnawing	0	0	0	0	0	0	0	0
	Mould	0	0	0	0	0	0	0	0
	Plant etch	2/12	17	2/8	25	3/12	25	2/8	25
18 months	Organic staining	12/12	100	8/8	100	12/12	100	8/8	100
	Algae staining	12/12	100	8/8	100	0	0	0	0
	Weathering stage								
	0	12/12	100	8/8	100	12/12	100	8/8	100
	1	0	0	0	0	0	0	0	0
	Sun bleaching	12/12	100	6/6	100	0	0	0	0
	Soft tissue	0	0	2/8	25	0	0	0	0
	Adipocere	0	0	0	0	0	0	4/8	50
	Carnivore activity	0	0	0	0	0	0	0	0
	Rodent gnawing	0	0	0	0	0	0	0	0
	Mould	0	0	0	0	0	0	0	0
	Plant etch	6/12	50	5/8	63	7/12	58	6/8	75

n** = ratio of amount of the affected sample and total number of sample observed

4.1.2.1 Bone staining

Visual observation of level and pattern of bone staining were conducted on surface-deposited and buried femoral and rib samples. Prior to deposition, the bone sample exhibited either pale red or reddish brown colour from blood staining (Figure

4.7a-4.10a). This staining started to fade away after exposure to the outdoor environment (Table 4.2). All surface-deposited samples showed no blood staining at 6-months exposure. However, blood staining was still visible in the minority (24%) of 6-months exposure of buried samples, and faded away completely at twelve months after deposition.

Table 4.2: Percentage of the presence of bone surface with blood staining

Sample group		Pre-exposure	Second month exposure	Fourth month exposure	Sixth month exposure
Rib	Surface (n=36)	85%	48%	20%	0%
	Buried (n=36)	89%	-	-	24%
Femur	Surface (n=24)	92%	26%	0%	0%
	Buried (n=24)	90%	-	-	16%

As the study progressed, surface-deposited bone samples continued to show various staining resulting from soil, algae as well as sun bleaching. Alternatively, an area of staining might undergo various colours ranging from reddish-brown to dark as a consequence of recent decomposition of nearby soft tissues. In some cases, the bones were slowly buried as decomposed leaf builds up on them, forming more organic soil components. Surface-deposited bone samples usually express two different sets of surface colour change (Figure 4.6). It was seen that the lower surface in direct contact with the topsoil undergoes some of the same taphonomic colour alterations as buried bone such as medium brown colour (10YR 4/3; 10YR 5/3) from humus and soil staining, while the more exposed upper surface undergoes a different colour change or retains its natural colour. These taphonomic changes often characterise surface-deposited samples (Pokines, 2016).

4.1.2.1.1 Surface-deposited rib sample

Thirty-six porcine ribs were placed at F3 taphonomic facility during September 2016 – February 2018. Firstly, 85% of bones in the pre-exposure group exhibited dark-red blood staining. This was visible in only 20% of the samples by the fourth month of exposure and had totally disappeared by the sixth month (Table 4.2).

Figure 4.6: A surface-deposited femoral sample displays different colour sets (a.) exposed side; (b.) soil-contacting side

Sporadic green staining from green algae was first seen in surface-deposited samples around three months after deposition. Bone surface discolouration tended to be lighter during the earlier exposure months and became darker colouration as exposure time increase. At six months of exposure, 72% of the exposed area of rib samples displayed pale green (5GY 9/8) colouration from algae staining with limited areas of dark green (5GY 7/4; 5GY 5/12) and pale brown (10YR 7/3; 10YR 6/3). Patchy brown staining (10YR 4/3; 10YR 5/3) from humus and topsoil was found only along the surface in contact with topsoil or decaying layer of organic materials.

After sixth month of exposure, the weather got warmer as the season changed to the springtime. The staining was lighter, which consisted of pale green (5GY 9/8) and some spotted area of yellow brown (10YR 6/4; 10YR 5/4) on the exposed side and grey brown (10YR 5/2) on the groundside. This staining remained stable until the end of the summer by twelve months of exposure, when the staining of the exposed side started to brown (10YR 5/3; 10YR 4/3) with patches of grey brown (10YR 5/2; 10YR 4/2) and pale green (5GY 9/8) until the end of eighteenth months exposure (Figure 4.7).

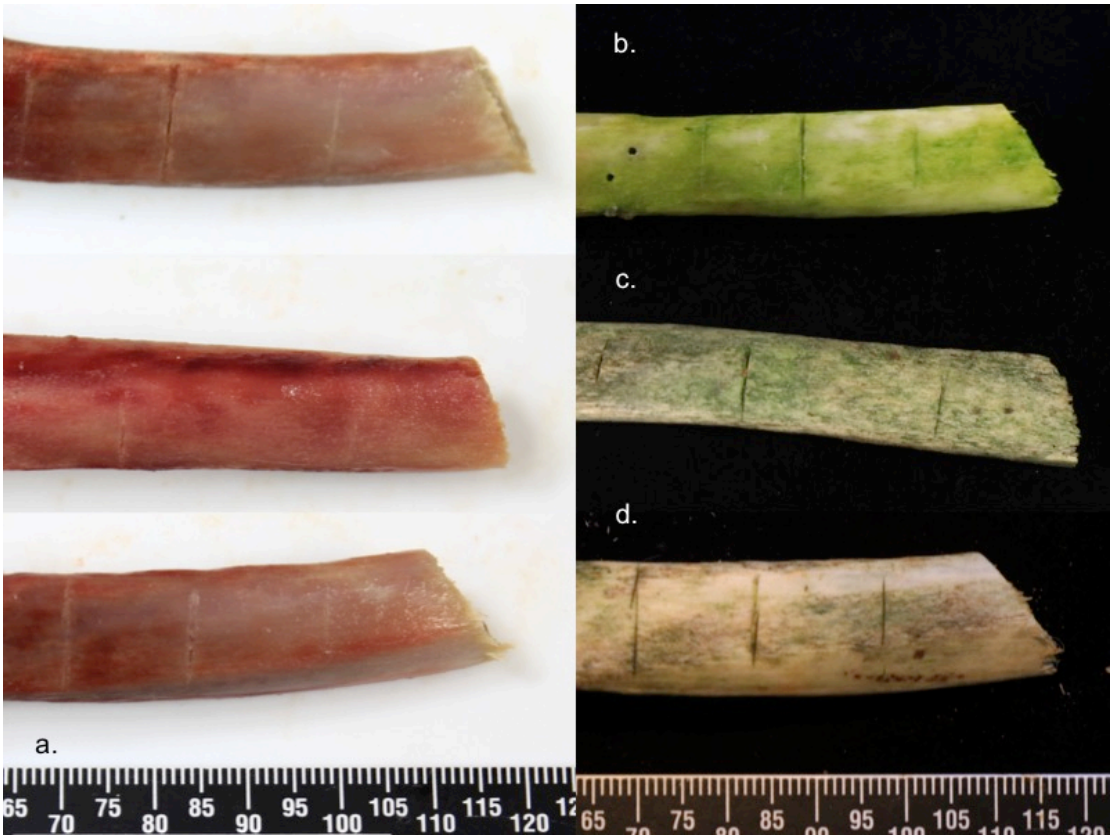

Figure 4.7: Surface-deposited rib samples showing different patterns of staining (a.) pre-exposure; (b.) 6-months exposure; (c.) 12-months exposure; (d.) 18-months exposure

4.1.2.1.2 Surface-deposited femoral sample

Twenty-four porcine femurs were placed in the F3 facility starting from March 2017 until the end of August 2018. The dark-red staining on the bone surface (92%) was presented after defleshing in the laboratory. This stain was detectable on 26% of femurs in the second months and totally disappeared by the fourth month (Table 4.2). After six months, pale brown (10YR 7/3; 10YR 6/3) and grey (10YR 4/2) discolouration were observed on the bone surfaces. After twelve month of exposure, the bone displayed light brown (7.5YR 6/3) and yellowish brown (10YR 5/6; 10YR 4/4) with pale green patches on the exposed side (5GY 9/8). By eighteen months of exposure, the majority of femurs exhibited very pale brown, brown, and greyish brown (10YR 5/1) with very pale green staining (5GY 9/14) along the exposed side (Figure 4.8).

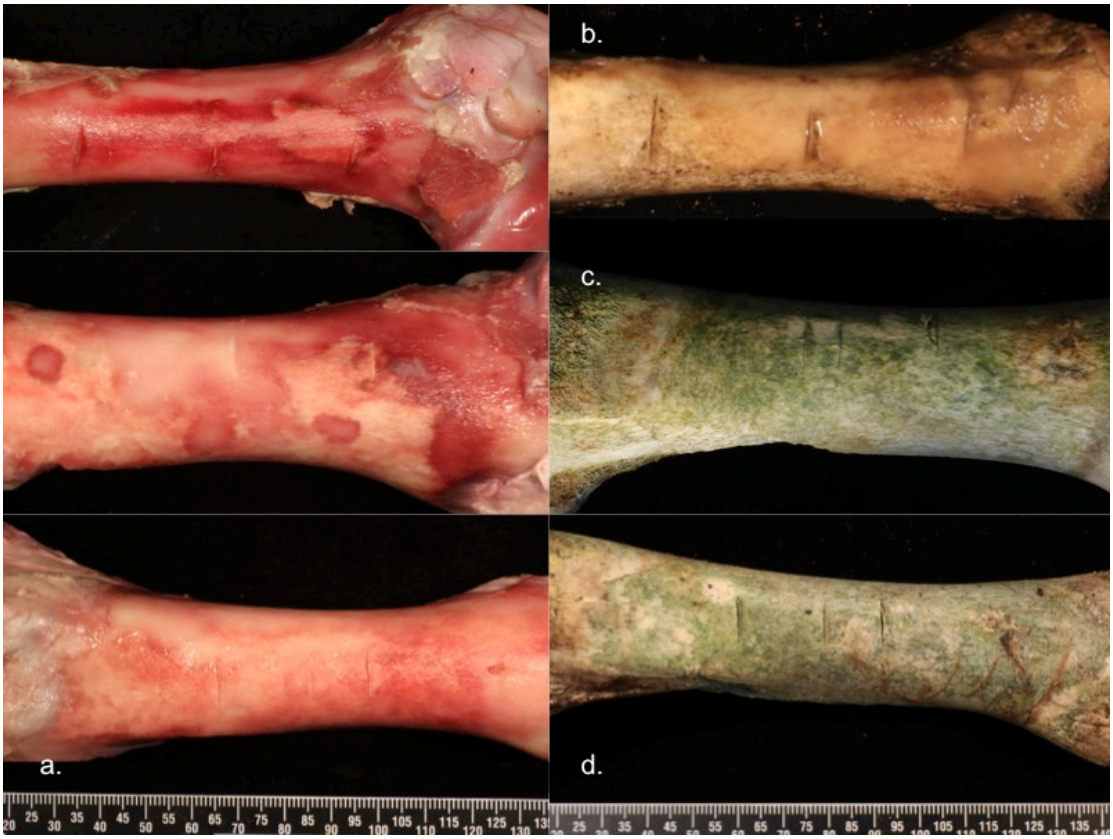

Figure 4.8: Surface-deposited femoral samples showing different patterns of staining (a.) pre-exposure; (b.) 6-months exposure; (c.) 12-months exposure; (d.) 18-months exposure

4.1.2.1.3 Buried sample

Colour staining of buried bones depends on local soil conditions, with darker topsoil staining bone closer to the colour of the soil (Pokines, 2018). The same pattern of colouration was observed in femoral and rib samples in the buried group. Samples deposited within the A soil horizon for six months displayed less uniform staining on the whole surface. The main colour appeared on these samples included brown (10YR 5/3) with spotted areas of greyish brown (10 YR 4/2; 10YR 3/2) and light brown grey (10YR 6/2). After twelve months of burial, bone samples were more uniform in appearance with brown, greyish brown, yellow brown and dark grey (10YR 4/1) colouration. Buried bone samples after eighteenth months were the same colour as the 12-months group with larger areas of dark grey colouration (Figure 4.9-4.10).

Figure 4.9: Buried ribs showing different patterns of staining (a.) pre-exposure; (b.) 6-months exposure; (c.) 12-months exposure; (d.) 18-months exposure

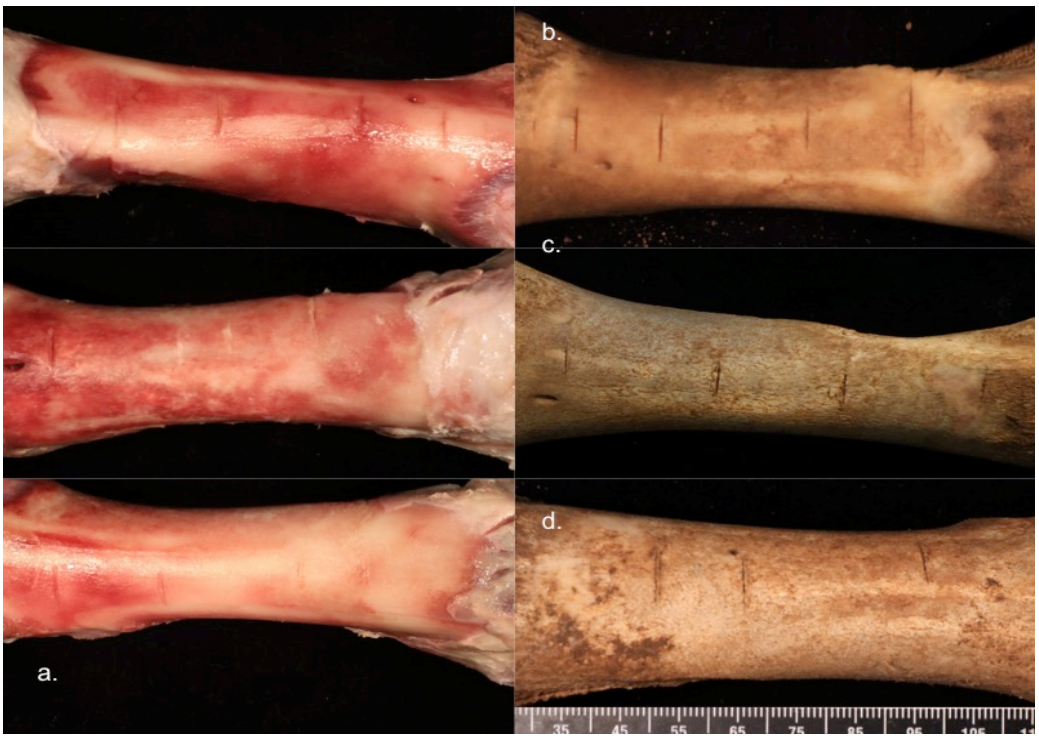

Figure 4.10: Buried femurs showing different patterns of staining (a.) pre-exposure; (b.) 6-months exposure; (c.) 12-months exposure; (d.) 18-months exposure

4.1.2.2 Sun bleaching

Solar ultraviolet light bleaching was characterised as areas of uneven brilliant white colour. Surface modifications are often associated with sunlight exposure on the upper more exposed areas of bone. Bleaching in rib samples was initially observed after four months of surface deposition, while femoral samples showed bleaching at around three months of surface-deposition. Colour of bleached bones depended on the length of sunlight exposure, with longer hours of daily sunshine producing greater bleaching (Figure 4.11). There is no statistical difference of bleaching rate between two types of bone samples in this study (X^2 = 2.627, p=0.2688).

It is crucial to remember that bones may also appear white because of other circumstances. For instance, the presence of adipocere, a pale waxy substance, on the external and internal surface of a bone (Figure 4.12) was detected in 25% of buried femoral samples in the first sixth months.

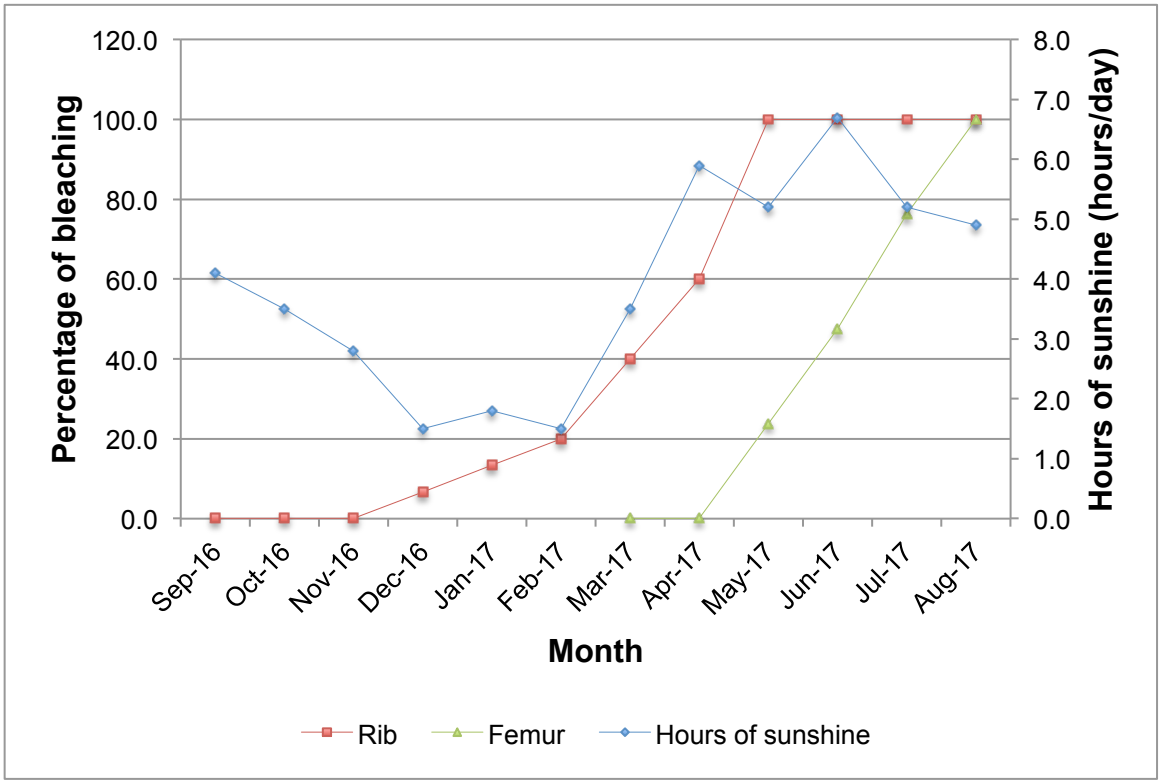

Figure 4.11: Line charts demonstrating correlation between hours of daily sunshine and rate of sun bleaching

Figure 4.12: A 6-months buried femoral sample demonstrating whitish patches from adipocere formation on the distal end of epiphysis

4.1.2.3 Plant root etching

In the present study, plant roots and stems adhering to buried bones were first found after 6 months of burial. For surface-deposited samples, slow plant growth during autumn and winter resulted in the first observed incidence of plant adherence and attachment to rib surfaces later than during the spring and summer samples of femurs at 7 and 4 months after exposure respectively. After plant removal, some of the exposed surfaces may display a fine, branching network of brown staining (Figure 4.13). This modification is frequently associated with buried bones, as it is likely to form over the entire surface of the bone. Bone surfaces surrounding plant root attachments displayed more erosion than other surface areas (Figure 4.14).

Significant growth of vegetation and environmental changes were observed throughout the study period in the warmer seasons (e.g. spring and summer). These vegetative growths affected the amount of sunlight exposure and moisture content of the bone samples and may affect the progression of weathering process. From May to September, surface bone samples deposited in the F3 grassland site were protected from exposure to direct sunlight by tall strands of grasses growing up over one metre high. The experimental ground area was covered by other

smaller plants. Bone samples remained partially shaded until early winter. Also, different rates of plant growth affected the rate of plant etching in both surface-deposited and buried samples.

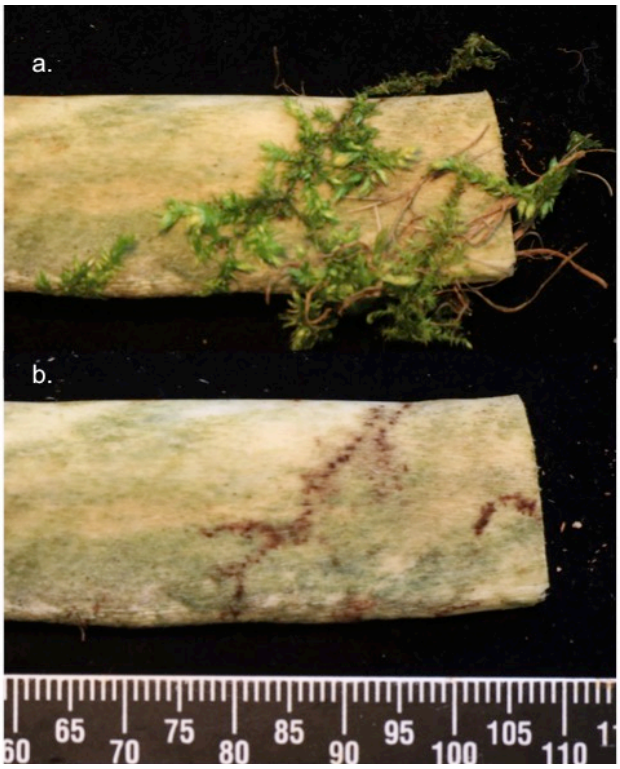

Figure 4.13: Interaction of plant roots with the bone surface: a.) Plant adhering; b.) Etching mark

Figure 4.14: Plant root attachment and erosion of surrounding bone surface

4.1.2.4 Bone weathering

Figures 4.15-4.16 demonstrate the percentage of the visual observations of weathering pattern on bone surfaces.

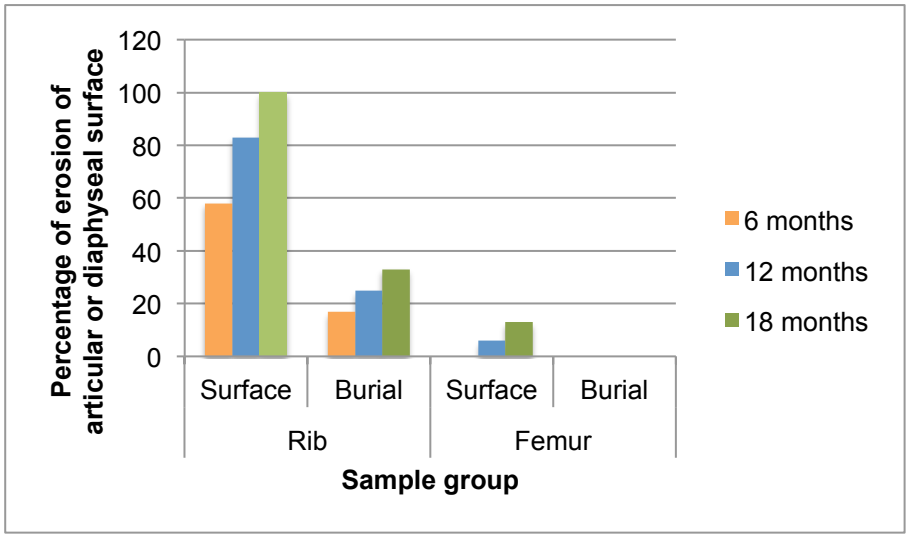

Figure 4.15: Percentage of erosion of articular or diaphyseal surface of surface-deposited group and buried group

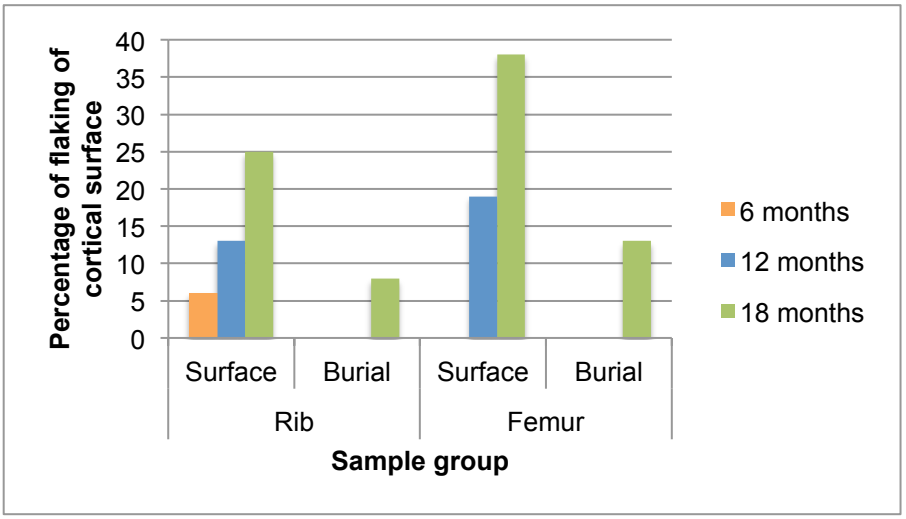

Figure 4.16: Percentage of flaking of cortical surface of surface-deposited group and buried group

All bones showed no sign of longitudinal cracking or other sign of advanced weathering, despite more than one-year exposure on the surface environment. They were still categorised into stage 0 on the Behrensmeyer (1978) staging of

weathering. Nevertheless, minute changes from short-term exposure mentioned by Cunningham *et al.* (2011) were analysed for early detection of bone weathering pattern in this study. Surface erosion was more specific on rib samples, which all displayed deterioration after 18 months of surface exposure. Nonetheless, femoral samples were more prone to cortical flaking. A slower rate of weathering of buried samples was observed in this study. A preliminary post-depositional interval can be demonstrated (Table 4.3). Evidence for surface weathering was first observed after surface exposure of four months when erosion on the outermost layer was identified in surface-deposited rib samples. Amongst surface-deposited bone samples present, this feature was most often seen in the form of erosion of the diaphyseal area of rib and femoral samples (Figure 4.17), especially on the exposed surface of surface-deposited rib sample (Figure 4.18).

Table 4.3: Post-depositional interval of surface samples based on weathering

Weathering pattern	First detection	Definition
Erosion of diaphyseal surface	4-7 months	Erosive lesion at diaphyseal bone surface
Pockmark pattern	7-9 months	Erosion of circular sections of bone
Cortical flaking	5-8 months	Flaking of outer layer of bone cortex

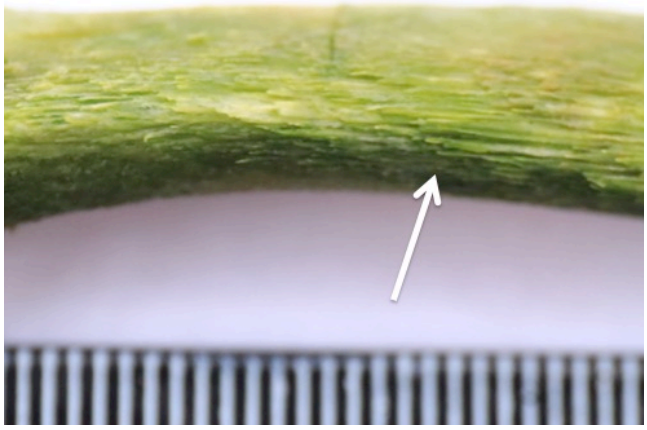

Figure 4.17: A four-month exposure rib sample demonstrating cortical bone erosion (white arrow) on the outermost layer; defined as erosive grade 1 (McKinley, 2004)

Figure 4.18: Erosion of surface-deposited rib sample after 12-months exposure; (a.) exposed surface; (b.) soil-contact surface

Cortical flaking was firstly detected in the rib samples during five-months surface exposure (Figure 4.19) and in the femoral samples after eight-months surface exposure (Figure 4.20).

Figure 4.19: A five-month exposure rib sample demonstrating a flaking surface (the white arrow)

Figure 4.20: An eighteen-month exposure femoral sample demonstrating flaking of the cortical bone (the white arrow)

Circular wearing away of the cortical bone layer, or circular pockmark pattern, affected only the surface-deposited femoral samples, and could be found in only 6% of bones after 12-months exposure and 13% after eighteen-month exposure (Figure 4.21). The weathering pattern was notably absent in all buried samples.

Figure 4.21: Pockmark pattern of 12-months exposure (the white arrow)

The system proposed by McKinley (2004) was used for recording bone surface erosion in a scale of 0-5 (Table 3.4) (Figure 4.22-4.23). Observations showed that the erosion of bone surface mostly occurred at the exposed surfaces of surface-deposited rib and femoral samples. After 6-months surface exposure, 58% of the rib samples altered to erosive grade 1 (Figure 4.24), whereas there was no erosive change in the femoral samples. After twelve months of surface exposure, bone erosion was more evident but the femurs weathered at a slower rate than the ribs. However, after eighteen months, all rib samples showed significant weathering with 25% at erosive grade 2 (Figure 4.25), while 13% of the femurs reached erosive grade 1. Despite extensive erosion, traumatic lesions were still identifiable on the bone samples.

Buried samples had only a minor degree of surface erosion. After eighteen-month burial exposure, only 33.3% of rib samples altered to erosive stage 1, while all femoral surfaces still remained a smooth surface appearance.

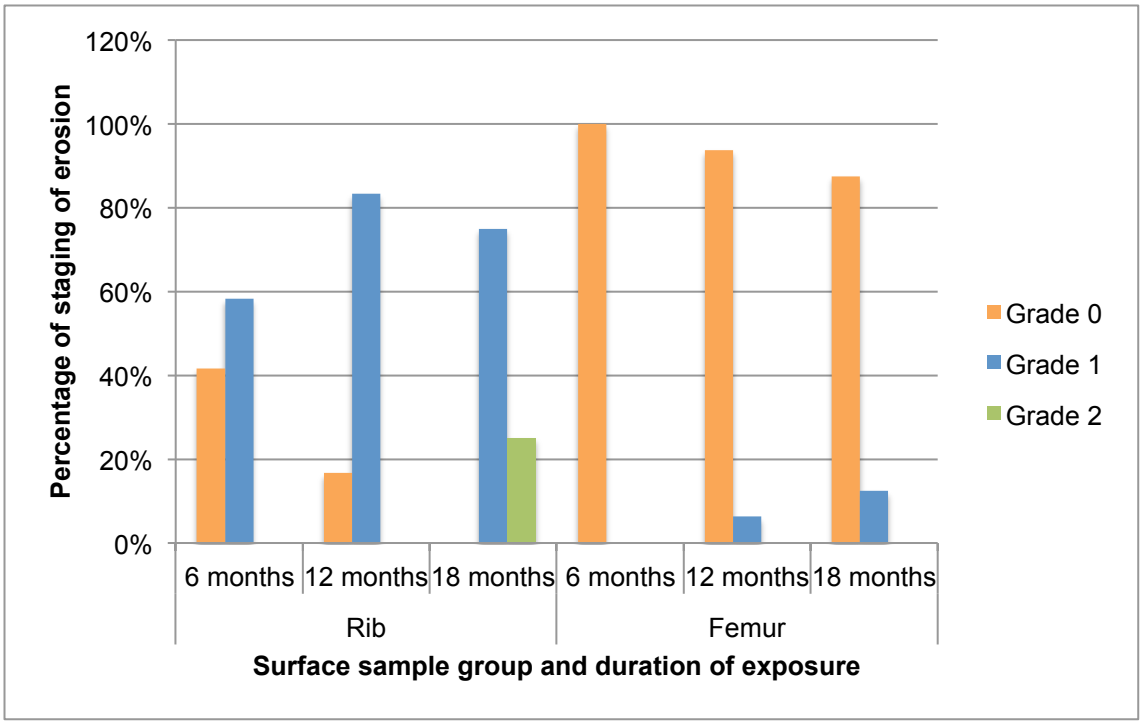

Figure 4.22: Percentage of McKinley (2004) grade of bone surface erosion of surface-deposited bone samples

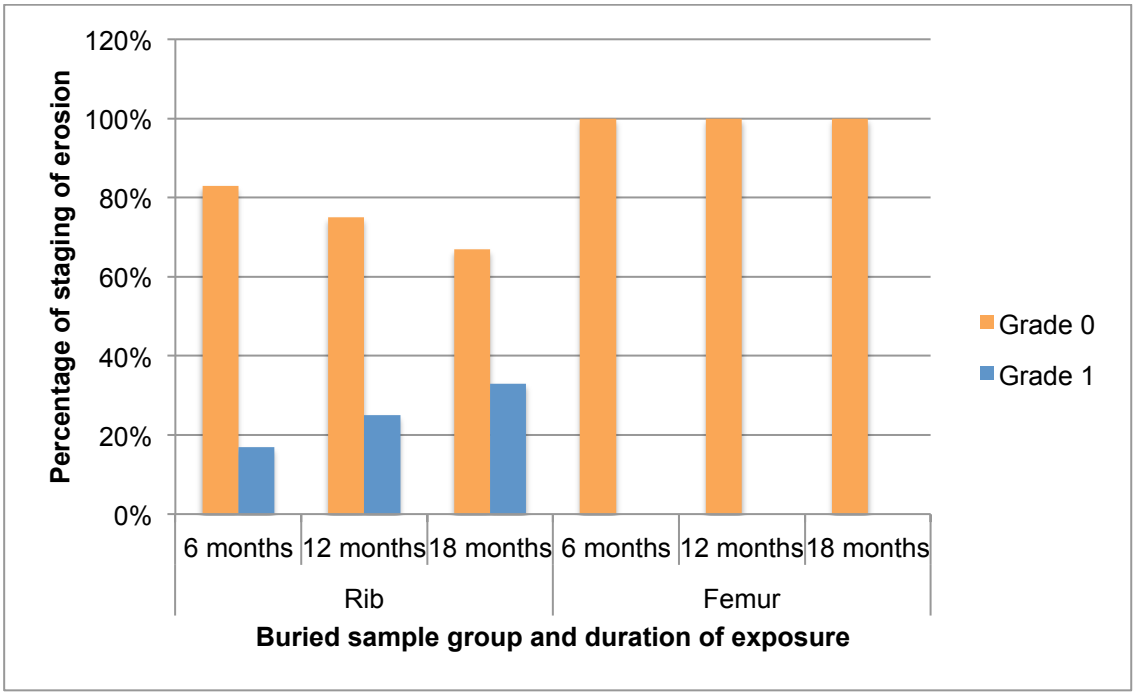

Figure 4.23: Percentage of McKinley (2004) grade of bone surface erosion of buried bone samples

Figure 4.24: A rib with slight and patchy surface erosion (the white arrow), corresponding to McKinley (2004)'s grade 1 of surface erosion

Figure 4.25: A rib with more extensive surface erosion, corresponding to McKinley (2004)'s grade 2 of surface erosion

The highest percentage increase in weathering patterns occurred during the winter season (December to February), with 58% of surface-deposited ribs observed with erosion of diaphyseal and articular areas, while percentage of surface-deposited femurs with flaking also increased from 22% to 38%. This may be due to fluctuation of temperature above and below freezing point combined with wetter weather that usually occurs during this period.

4.1.2.5 Soft tissue preservation

Although all bones were macerated by the researcher, some remnants of soft tissues such as periosteum, cartilage, ligament and tendon still remained. The majority (75%) of surface-deposited femoral samples maintained some decomposed and desiccated soft tissues in the first six months, while all buried femoral samples were observed with soft tissues. Gradual loss of remaining soft tissues was observed. By the end of this study, desiccated connective tissues were still identified in 25% of surface-deposited femoral sample (Figure 4.26). While soft tissues changed to a pale waxy substance of adipocere, which was firstly detected on bone surface in the five-months exposure. Adipocere was observed in 50% of 18-months buried femoral samples (Figure 4.12), and this entire sample group still retained greasiness.

Figure 4.26: An eighteen-month femoral sample with a remnant of desiccated soft tissues (the white arrow)

4.1.2.6 Mould and algae

The presence of mould was firstly observed within the first two months of surface deposition. Mould growth was presented in conjunction with soft tissues on 46% of the femoral surface at 6-months exposure, with substantial decrease in incidence toward zero at 12-months exposure (Table 4.1). Consequently, neither moss nor lichen growth was detectable on any of the bone surface at the end of this study.

The presence of algae was first noted on 20% of surface-deposited rib samples two months after deposition (Figure 4.27) and continued to rise throughout this study. By the end of the eighteen-months study, this alteration was presented in all rib and femoral samples. In contrast, algae were not seen on any of the buried bone samples.

Figure 4.27: Greenish colouration from algae growth; two months deposition

4.1.2.7 Animal scavenging and gnawing

Even though there was protection with chain-link wires and wooden plank fences, a number of bone samples were scavenged by some mammal species. The first evidence of scavenging occurred during the first month after deposition, when a rodent was seen gnawing on a femoral sample (Figure 4.28).

Figure 4.28: Rodent gnawing observed on the metaphysis of a femur

Thirty-eight percent of metaphyseal area of surface-deposited femoral samples presented sign of rodent gnawing. A badger's footprints were observed at the side but there was no sign of scavenging on existent samples. Loss of three buried femoral samples by an unidentified scavenger occurred during the first month of deposition.

4.2 Discussion

The present study aimed to investigate weathering and surface modifications for a field experiment in South-eastern England. Therefore, taphonomic modifications discussed here are specific to the southeastern England and other similar environmental conditions, and these are obviously different from findings encountered from other areas of the UK. For instance, extensive surface erosion may be typical in Welsh areas, where soil acidity is high and have constant high humidity (Andrews, 1995; Fernández-Jalvo *et al.,* 2010). Other taphonomic alterations; however, are described to be common throughout the UK, even though it is necessary to observe these on a regional basis. For example, most of the UK has temperate environments and low level of sunlight with high humidity, thus possibly causing lowered overall features of bone weathering (Andrews and Cook, 1985; Andrews, 1995; Fernández-Jalvo *et al.,* 2010). In the UK, skeletal remains develop a much slower rate of decomposition and bone diagenesis when compared with equatorial and arid climate (Andrews and Cook, 1985; Andrews, 1995; Andrews and Whybrow, 2005). These are expected to occur in warm temperate climate regions as previous research was demonstrated (Behrensmeyer, 1978; Andrews and Cook, 1985; Tappen, 1994; Andrews and Whybrow, 2005; Cunningham *et al.,* 2011; Pokines, 2016).

4.2.1 Bone staining

Normally, a fresh bone has been described as having a yellowish-white or yellowish-brown colour because of the retention of lipids and organic fluids (Byers, 2010; Dupras and Schultz, 2014). This normal colour may alter during the decomposition process, with colour change ranging from reddish brown to dark reddish grey from decomposition fluid staining and haemolysis of red blood cells (Dupras and Schultz, 2014; Huculak and Rogers, 2009). The bones buried solely

within the soil environment tended to display this blood staining longer than surface-deposited bones (Table 4.2). The bones deposited on surface environment would be exposed to ultraviolet radiation from sunlight, which can degrade many organic compounds contributing to the blood staining. Consistently, other results of this study show that femoral samples exposed to prolong sunlight during spring and summer exhibited a clearance of blood staining faster than rib samples exposed to shorter period of sunlight during autumn and winter.

Surface modification can be present on bone surfaces as staining from organic and inorganic substances. Different staining allows a distinction between the bone samples exposed to differently depositional environments. Those buried in a soil environment tended to stain more uniformly and into shades of brown staining for 6-months burial. The uniform staining suggested that the samples were deposited in an environment in direct contact with the surrounding soil to all surface of the bones (Pollock *et al.*, 2018). Sometimes a combination of colour staining can affect skeletal materials. The bone samples exposed to surface environment displayed sporadic staining across the majority of the bone surface. Bones expressed darker staining on the underside from contact with soil materials or decomposing organic materials underneath, while exhibiting a large range of colouration on the uppermost surface such as lighter colouration from exposure to sunlight (Owsley *et al.*, 1995; Pokines, 2016).

Determining staining pattern and colouration is useful for a forensic investigation to reconstruct an original crime scene in which skeletal remains have been deposited and may link the bone to a certain circumstance surrounding the death of an individual (Ubelaker, 1997; Pollock *et al.,* 2018). For example, reposition of the bone displaying darker soil staining surface away from the ground would be clearly indication that the bone has been disturbed, or white stains of sun bleaching can make the bone more visible against its background (Dupras and Schultz, 2014; Junod and Pokines, 2014). In addition, and of most importance in forensic cases, is the information that bone surface modification such as weathering may be used for postmortem interval estimation (Beary and Lyman, 2012; Junod and Pokines, 2014).

All surface-deposited bone samples displayed greenish discolouration from diffused green algae growth after 12-months exposure. It is common to find algae growth on surface-deposited bone from various environments, especially in a moist and shady environment (Bass, 1997; Ubelaker, 1997; Janjua and Rogers, 2008). Rainfall during the study period caused larger part of the bone samples to become stained with green algae, which faded back slowly to a bleached white or grey colour during the drier summer season. Algae can provide important information in a forensic setting; for instance, algae can link a suspect to a specific crime scene or a specific time of year (Dupras and Schultz, 2014). Algae were never observed in buried bone samples.

It is common to find ground staining on buried bones and bone surfaces in contact with the ground. Bone surface discolouration from soil staining is related to the soil particles and their coatings (Gordon and Buikstra, 1981; Dupras and Schultz, 2014). A buried bone generally displays brownish colouration resulting from the interaction between the bone surface and the soil solution. However, soil staining on skeletal materials can also be represented by the various colours of the organic and mineral components in the ground. For instance, the darker staining is also related to darker-coloured organic matter and minerals in the soil solution such as tannins and iron oxides (Pollock *et al.*, 2018).

4.2.2 Bone weathering

Simultaneously, subaerial bone weathering gradually developed in the exposed surface of skeletal materials deposited on the surface environment. Bone weathering stages have been described by Behrensmeyer (1978) as a process developing from stage 0 (unweathered bone) through stage 5 (unrecognisable bone with splintering apart). Not surprisingly, none of Behrensmeyer's weathering changes were observed during eighteen months of this study. This result is consistent with previous work in Wales by Fernández-Jalvo *et al.* (2010) where the maximum weathering stage of 100 carcasses exposed to unprotected areas was only stage 1-2 after 30 years of exposure, while bone samples buried or covered by vegetation were still unweathered after the same period of time (Fernández-Jalvo *et al.,* 2010). Andrews and Cook (1985) showed the same results of their study in

Somerset, England. After an eight-year exposure, the surface-deposited bones could be defined as weathering stage 0 with no apparent cracking and flaking.

This study discovered that, while all skeletal materials remained almost completely intact, specific surface areas were more influenced by different types of weather conditions. Overall, results showed that early signs of bone weathering often occur in certain types and areas of skeletal materials. The erosive lesion of articular facets and diaphyseal surface was the most commonly encountered weathering pattern in rib and femoral samples, followed by flaking of cortical bone, which occurred more commonly in long bones. Because of the vegetation cover and limited access to the experimental field, it is difficult to define the exact day when weathering patterns first appeared on each sample. Monthly observation; however, might make it possible to determine the approximate timing in relation to each weathering type.

Normally, bone weathering proceeds along structural lines of weakness influenced by the bone type and shape (Behrensmeyer, 1978; Lyman and Fox, 1997). Findings showed that femoral samples tended to exhibit flaking of outer layers of cortical bone, whereas rib samples were prone to erosion of their articular facets with exposure of the inner trabecular bones due to their fragile and less dense cortical structure. These findings are consistent with previous work by Cunningham *et al.* (2011), which showed that long tubular bones, including long bones, metacarpals, metatarsals, and phalanges were likely to show flaking of their outer cortex, while vertebrae, and ribs were more prone to have erosion of their outermost layer at the articular facet, leading to exposure of interior trabecular bone (Cunningham *et al.*, 2011).

As expected, sunlight exposure in a surface environment and temperature fluctuation appeared to accelerate bone weathering rates. The most significant weathering change observed in this study occurred in surface-deposited bones during the winter period. Wet and dry cycles as well as freeze and thaw cycles cause bones to swell and shrink setting up physical strains resulting in flaking, cracking and spalling of the bone (Fernández-Jalvo *et al.,* 2010; Pokines *et al.,* 2016; Kendall *et al*., 2018; Pokines *et al.*, 2018). Surface exposure causes loss of

bone moisture, leading to various degrees of dehydrated and brittle skeletal materials.

Femoral samples were likely to weathered at a slower rate than rib samples, even though they were exposed to warmer temperature and more sunlight. This finding is supported by other literature, which have shown that larger and denser skeletal materials have better preservation due to their greater bone density (Andrews, 1995; Lyman and Fox, 1997; Willey *et al.*, 1997; Stodder, 2008). Lyman and Fox (1997) indicated that the exact reason why different bones from the same skeleton undergo weathering at different rate is exactly unknown. While the general composition of mammal bone is constant, structural variability occurs in different skeletal elements reflecting the various assortment of their function. This variable has a profound effect on resistance of skeletal tissues to possible taphonomic forces. The fundamental factor determining the durability of skeletal materials is the amount of skeletal tissue per unit volume (Gifford, 1981). Therefore, thick compact bones can resist environmental stresses better than thinner cortical bones, and different bone materials from the same skeletal elements or different areas of the same can present diverse postmortem modifications (Brain, 1967; Gifford, 1981; Crist *et al.,* 1997).

It is important to realize that weathering rates vary depending on different species (Lyman and Fox, 1997). Gifford (1981) suggested that constructional difference is the reason why mammal bones of different taxa undergo weathering at fairly different rates. While Behrensmeyer (1978) noted that her weathering stages could only apply to mammals that have body weight more than 5 kilograms; variability of skeletal materials such as bone density and composition (Aerssens *et al.*, 1998) and bone microstructure and porosity (Hillier and Bell, 1997) have an important role. More heavily constructed bones tend to weather at a somewhat slower rate than smaller mammal bones (Lyman and Fox, 1997).

In addition, it is imperative to recognise that bone samples are actively growing and remodelling prior to death. Therefore the area of active growth can be commonly misclassified as pathological lesion due to its coarse and porous morphology (Buikstra and Ubelaker 1994). Moreover, this problem occurs in bone weathering investigation because this growth area looks like patterns of skeletal

decay. When dealing with juvenile skeletal remains as experimental subjects, Cunningham *et al*., (2011) advised to use location of a questionable lesion as an indicator of taphonomic modifications. If the area of exposed trabecular bone is located at the common area of growing activity such as proximal and posterior side of the long bones or posterior side of sternal end of the ribs, then it is more likely to be a sign of growth and not weathering. The timing of appearance of the suspected lesion can be also applied for solving this problem. If lesions were identified before the remains became early skeletonised, then they probably represent growth activity.

To conclude, the results of this study show that, compared to other types of climate (Brain, 1967; Behrensmeyer, 1978; Galloway *et al.*, 1989; Tappen, 1994; Marceau, 2007), there is less bleaching and flaking of bone surface because of less intense exposure to sunlight. The development of weathering cracks is noticeably slower than other environments, as no longitudinal crack was observed until 18 months of exposure. Weathering rate is slower and shallow penetration in temperate and high humidity climate than tropical and arid environment. Although it is argued that the time span from death until discovery of remains in a forensic setting is quite short and not enough to develop weathering stage as present in Behrensmeyer (1978), early signs of weathering process observed in this study can be used in contemporary contexts where environmental variables are more accessible. This study; however, reveals that weathering patterns are more variable than they are now understood to be. Conducting taphonomic research can aid in understanding the rate and pattern of weathering process and considerably assist in resolving forensic cases.

4.2.3 Burial environment

In general, soil properties including depth of soil, soil acidity, soil temperature, soil texture, and soil moisture have a considerable influence on the preservation of skeletal materials (Dent *et al*., 2004; Jaggers and Rogers, 2009; Nicholson, 1996; Surabian, 2012). The decay process is slower in buried bones (Andrews and Whybrow, 2005). Indeed, Rodriguez and Bass (1985) stated that decay rate of soft tissues in a buried environment is eight times slower than surface decomposition.

A small number of soil surface erosion was observed on rib samples resting on the mild acidic soil in this study (pH 5.9-6.4). Though surface erosion in bone is dependent upon time of exposure, with the severity of destruction rising with longer exposure (Fernández-Jalvo *et al.,* 2010). Soil acidity has a great effect on bone preservation, with skeletal decay normally advantageous in strong acidic (pH 3.5-4.5) soil (Gordon and Buikstra, 1981; Nicholson, 1996; Nielsen-Marsh *et al*., 2007; Surabian, 2012). High acidic soil can break down bone with an increase availability of hydrogen ions of bone mineral leading to dissolution of bioapatite crystal and the inorganic mineral components (Nielsen-Marsh *et al.*, 2000).

Also soil acidity has an influence on adipocere formation. Mild alkaline soil is the most favourable environment for adipocere development (Nielsen-Marsh *et al.*, 2000) and this postmortem formation is usually not apparent before three months after burial (Rodriguez and Bass, 1985; Ubelaker and Zarenko, 2011). Burial in clayey soils that retain moisture can also promote adipocere formation (Rodriguez, 1997; Forbes *et al.*, 2005). Ubelaker and Zarenko (2011) suggested that fundamental factors in adipocere formation comprise mild alkaline soil, warm temperature, anaerobic condition and adequate moisture. There is no adipocere formation in surface-deposited formation in this study, even though it can happen if appropriate (Ubelaker and Zarenko, 2011). These would be due to the high degree of decomposition in surface depositions.

At a depth of two feet in this study, temperature is presumably close to those above ground and to fluctuate by season (Rodriguez and Bass, 1985). Galloway *et al.* (2001) showed that thermal stabilization could be expected at a burial depth of more than 90 cm. Soil temperature has a significant effect on biological and chemical process (Carter and Tibbett, 2008). An increase in soil temperature can increase biological and chemical activity of soil microorganisms, resulting in a substantial increase in the rate of decomposition (Tibbett *et al.*, 2004; Carter and Tibbett, 2008). In addition, buried remains at shallow depths undergo increased degradation by plant and scavengers. Soil environment can protect a bone from animal activity when remains are buried at a depth of 90 cm or more (Rodriguez and Bass, 1985; Rodriguez, 1997). In a shallow burial, decompositional odours easily penetrate the soil to above ground and attract insect and other scavengers,

leading to sample scavenging in this study. Many shallow buried remains exhibit obvious plant root damage due to the enriched upper soil (Rodriguez and Bass, 1985; Nicholson, 1996; Rodriguez, 1997).

Soil texture affects the water content and availability of oxygen. Fine texture such as clayey soil can decrease decomposition rate due to the low rate of gas diffusivity and water content. As a result, anaerobic microorganisms, which are less effective decomposers than aerobic microorganisms, are a dominating group for promoting decomposition process (Tibbett *et al.,* 2004; Janaway *et al.,* 2009). Once excavated, removed soils cannot be put back into their original depth level as they never have the same soil horizons (Surabian, 2012). Predictably, disturbed soil contents are less compact than surrounding undisturbed soil, resulting in better permeability of gas and water (Dent *et al.,* 2004).

4.2.4 Other taphonomic alterations on bone samples

Generally, it is known that bone surfaces exposed to sunlight for long periods of time display less greasiness and a lighter colour. Sun bleaching process can be used as a part of the initial weathering process, although fine surface cracking of weathering stage 1 has not been detected (Pokines, 2018). A number of femoral bones in this study started to bleach by three months of sunlight exposure, while sun bleaching manifested on rib samples by four months during autumn and winter exposure. Statistical analysis revealed that the bleaching rate is not significantly different between flat bones and long bones. This finding implies that sun bleaching occurs in a relatively uniform manner regardless of the type of bone or area of bone being affected. Thus, the use of flat or long bones should be satisfactory to analyse weathering patterns in either an experiment or forensic evaluation (Pyle, 2016).

Exposure to plants on the ground surface results in plant growth on the bone surface, or staining of the bone surface from decomposing plant materials (Hall, 1997; Dupras and Schultz, 2014; Pokines, 2016). These plants can also etch on bone surface after prolong contact with the bone. Plant root etching is one of the most common surface modifications. It is recognised as a dendritic pattern of shallow groove or tract (Buikstra and Ubelaker, 1994; Dupras and Schultz, 2014). Plant and vegetation have an important role in micro-environment, or the

environmental conditions of the location where a bone is deposited (Behrensmeyer, 1978; Lyman and Fox, 1997). For example, vegetation can grow actively especially during the spring and summer periods, and bone materials were almost obscured for a long period. As a result, sunlight shading over a bone from plant cover is expected in that time. That is the depositional microenvironment of a bone may accelerate or decelerate weathering process.

Theoretically, carnivore scavenging appears as tooth scores, pits, and puncture as well as ragged margins. Rodent gnawing with their narrow incisors can leave distinctive bone lesions such as shallow and parallel striations (Haglund and Sorg, 1997; Tsokos and Schulz, 1999). The purpose of this may be to access mineral and nutrients or to wear out their ever-growing incisors. As expected, rodent gnawing in this study was at the epiphysis and surrounding areas of long bones, and that is the most common area of damage (Haglund and Sorg, 1997).

In conclusion, other taphonomic modifications commonly observed in addition to weathering included bone surface staining, sun bleaching, plant root etching and animal scavenging activity. All of these can have an effect on the interpretation of weathering. Algae staining and sun bleaching were more prominently observed on surface-deposited bone samples in a grassland area. Brown soil staining was observed on buried bone samples and also on soil-contact sites of surface-deposited samples. These taphonomic variations are largely influenced by climate and the depositional environment and require regional study. Therefore forensic practitioners should carefully consider these aspects when applying it in forensic cases.

Chapter 5: An analysis of environmental effects on knife cut marks to rib samples

As explained in Chapter 3, an overview of the materials and methods of this study are summarised in Figure 5.1. A student t-test, a chi-square test and Fisher's exact test were then run on the data to detect a significant difference between the two intervals of pre-exposure and post-environmental exposure.

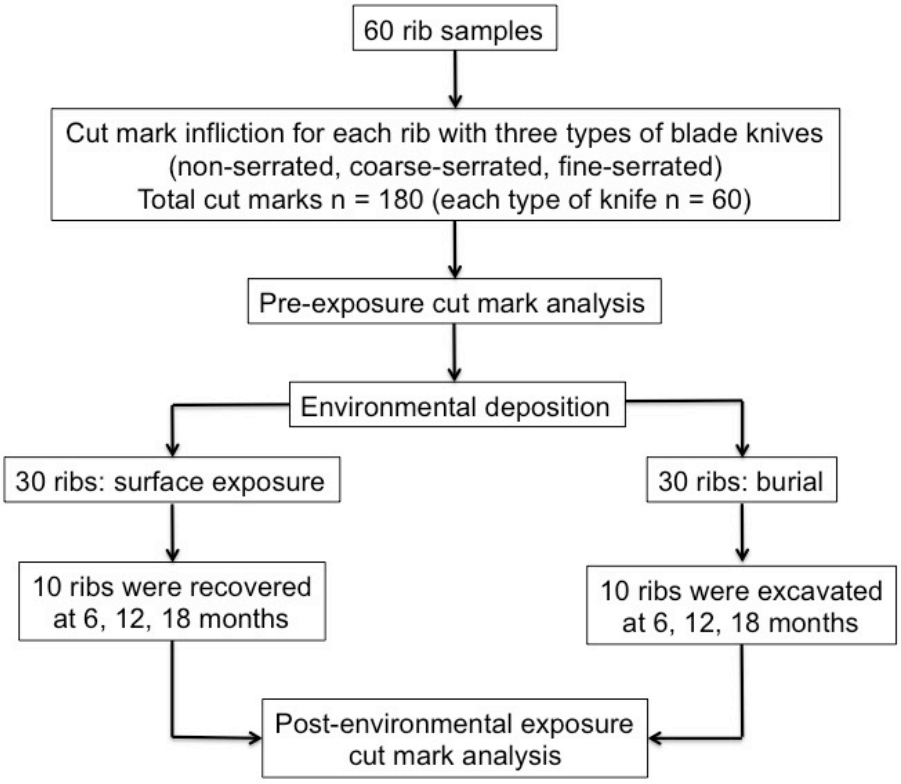

Figure 5.1: A diagram demonstrating the materials and methods in this study

5.1 Results

5.1.1 Pre-exposure comparison between different types of knife

Cut mark (n=180) characteristics were observed macroscopically and microscopically in six different areas of the kerf: maximum length, maximum width, kerf shape, cross-sectional shape, kerf margin, and kerf striations. Among three different types of knife, there was some consistency in the macroscopic and microscopic characteristics of cut mark patterns. Specifically, cut mark

characteristics appear to be correlated with knife blade type, as summarised in Table 5.1. Linear kerf shape and a narrow cross-sectional shape were specific to the non-serrated blade, whereas the serrated blade produced more open grooves with poor definition of the margins and irregular borders. An example of each type of cut mark is displayed in Figure 5.2-5.4.

Table 5.1: Diagnostic cut mark characteristics for each knife class

Kerf feature	Non-serrated blade	Coarse-serrated blade	Fine-serrated blade
Kerf shape	Linear	Mainly elliptical	Mainly elliptical
Cross-section	Narrow	V or U-shaped	V-shaped
Kerf margin	Smooth edge	Mainly raised edge	Mainly smooth edge
Kerf striations	Absence	Mainly striations	Mainly striations

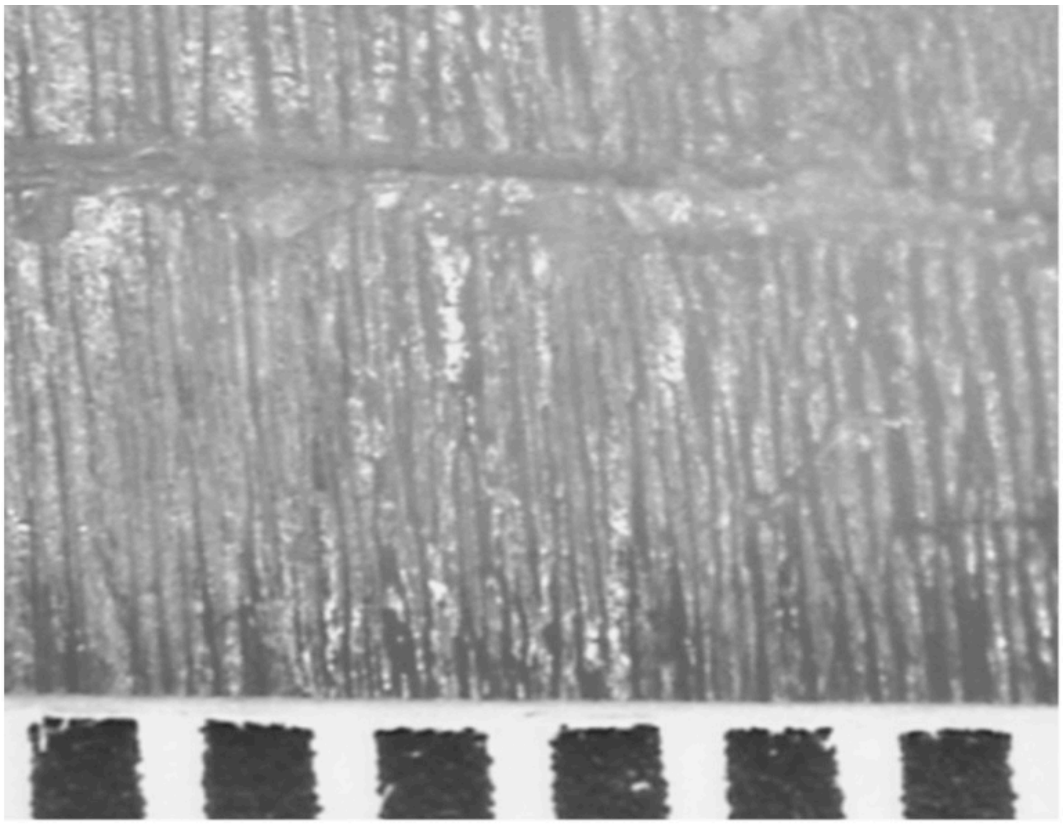

Figure 5.2: View of a cut mark inflicted by a non-serrated blade; scale in mm

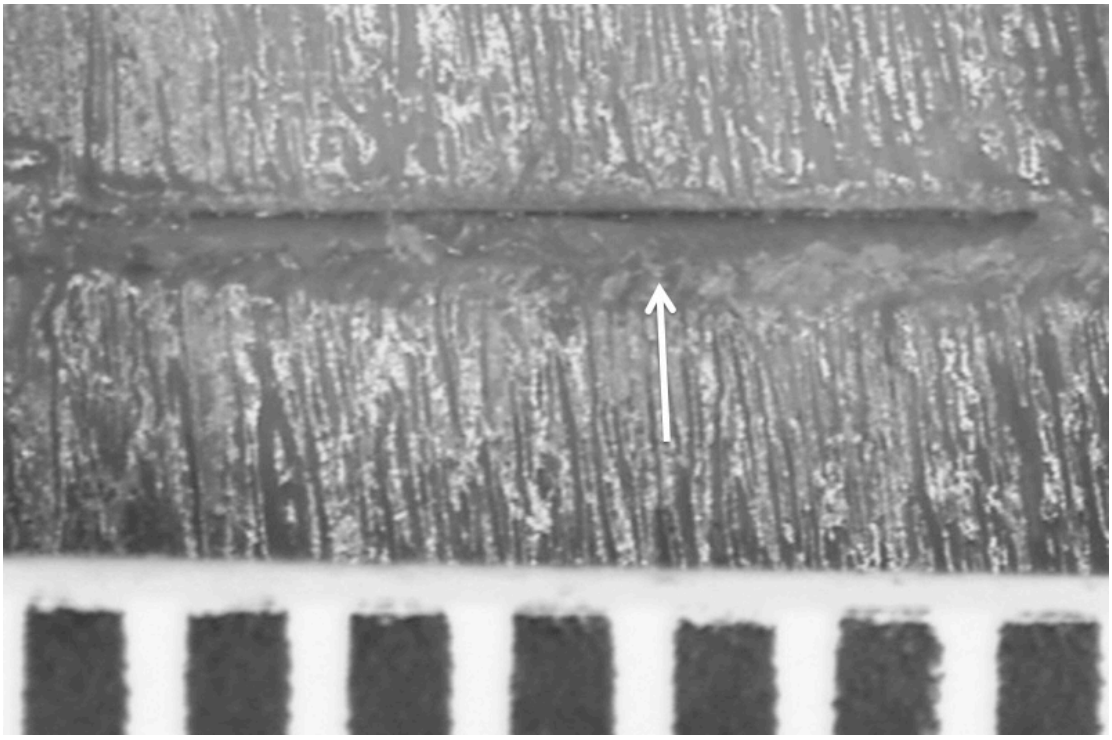

Figure 5.3: View of a cut mark inflicted by a coarse-serrated blade; the white arrow indicates a raised edge; scale in mm

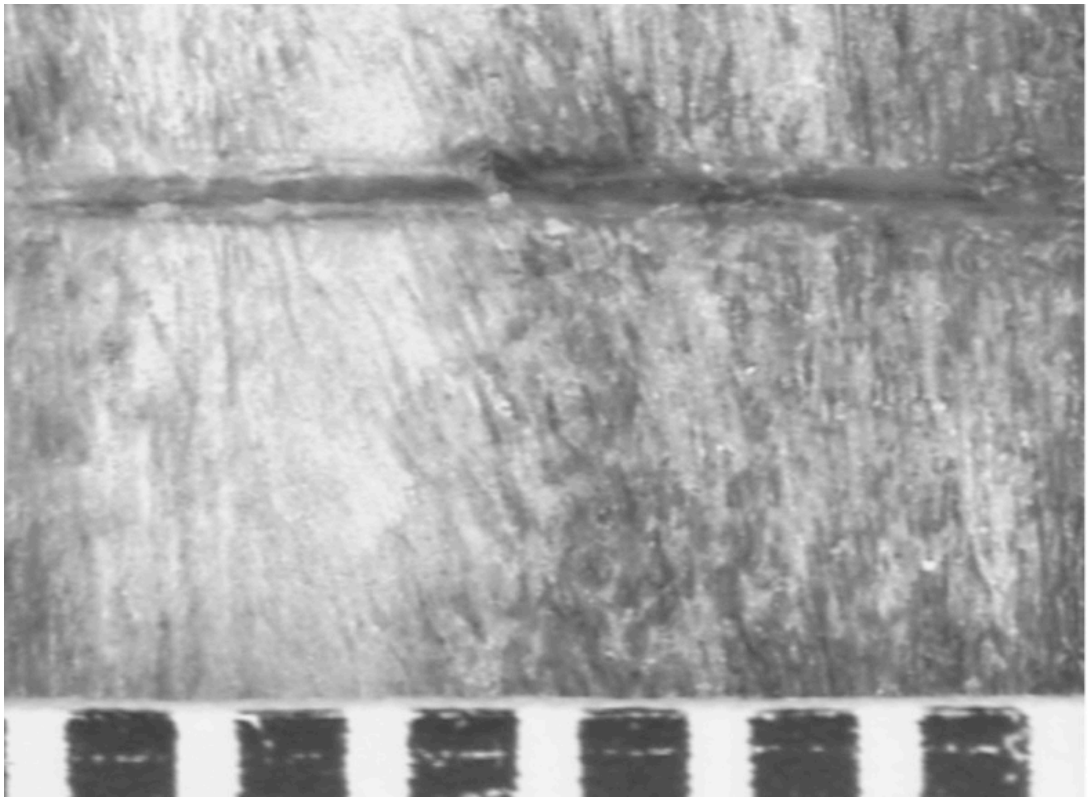

Figure 5.4: View of a cut mark inflicted by a fine-serrated blade; scale in mm

This study showed that kerf widths may be used to differentiate weapon types, but they were not correlated with the widths of sharp and blunt edge of inflicted weapons (Table 3.2 in chapter 3). A non-serrated blade 1.78 mm wide produced cut marks between 0.11-0.2 mm wide. The coarse-serrated 2.45 mm blade produced cut marks ranging from 0.3-0.48 mm wide; while the fine-serrated 2.31 mm blade produced cut marks of between 0.28-0.4 mm. Figures 5.5 demonstrates the boxplots of dimensional comparison between each type of the knife blade. A wide overlap of kerf length between different blade types was observed. However, the width of cut marks produced by different types of serrated blade varied considerably from those due to a non-serrated blade.

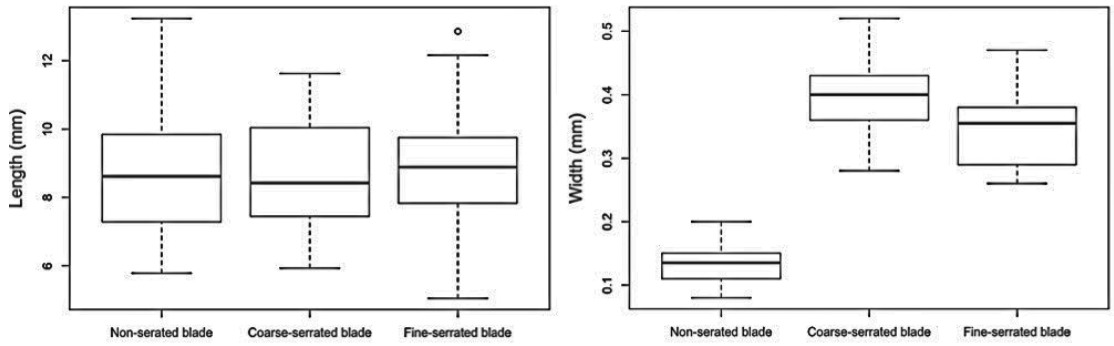

Figure 5.5: Observed length and width difference between the non-serrated knife, the coarse-serrated knife and the fine-serrated knife; each n=60

Some specific features were observed in each group. X-shaped cut marks, or fork-shaped marks, were recorded in 36 of 60 cut marks inflicted by the non-serrated blade (Figure 5.6). As the angle of the knife changes during a single cutting motion, multiple intersecting marks are created with retouched flakes. Dimension and morphology data were recorded from the largest and deepest mark. Multiple marks from only one action were recorded in 46 of 60 cut marks made from the coarse-serrated blade and in 28 of 60 cut marks made from the fine-serrated blade (Figure 5.7). These marks may be made by a sawing motion, in which a bone is contacted several times in a single stroke, resulting in multiple non-intersecting marks that accompany the main groove (Dominguez-Rodrigo *et al.*, 2009; Andrews and Fernández-Jalvo, 2012).

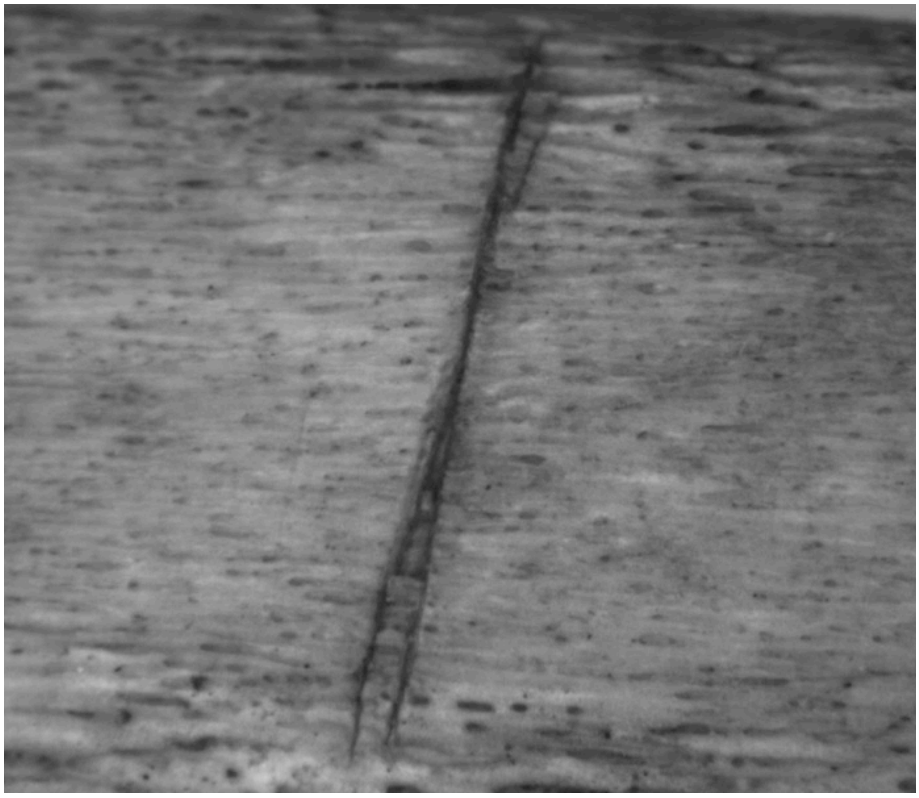

Figure 5.6: The typical X-shaped cut mark made from the non-serrated blade

Figure 5.7: Multiple marks made from the coarse-serrated blade

The independent observations of cut mark dimension and morphology were recorded. The student t-test, the chi-square test and the Fisher's exact test were

conducted to determine whether the profiles in different dimension and morphology were significantly different between each type of knife blade. Table 5.2 shows statistical tests between each pair of different knife blades. Significantly statistical differences were observed in the maximum width of all three types of knife blade. There was no statistical difference with respect to maximum blade length. Cut marks inflicted by a non-serrated blade were morphologically distinguishable from coarse-serrated and fine-serrated blades owing to their distinctive morphology. Cut marks inflicted by the coarse and fine-serrated blades exhibited the same patterns of cross-sectional shape, kerf margin and kerf striations.

Table 5.2: Student t-tests and frequency tests of pre-exposure kerf dimension and morphology between cut marks inflicted by non-serrated blade (NS), coarse-serrated blade (CS) and fine-serrated blade (FS) (*** significantly statistical difference)

Kerf dimension or morphology	**Statistical values**		
	NS and CS	NS and FS	CS and FS
Kerf length	t=-0.124, df=118, p=0.9015	t=0.012, df=118, p=0.9901	t=0.135, df=118, p=0.893
Kerf width	t=21.57, df=118, p<0.001***	t=17.82, df=118, p<0.001***	t=-3.512, df=118, p=0.0008679***
Kerf shape	Fisher's test: p<0.001***	Fisher's test: p<0.001***	Fisher's test: p=0.02372***
Cross-section shape	Fisher's test: p<0.001***	Fisher's test: p<0.001***	Fisher's test: p=0.6707
Kerf margin	Fisher's test: p=0.0003188***	Fisher's test: p=0.004575***	Fisher's test: p=0.5796
Striation	Fisher's test: p=0.0001236***	Fisher's test: p=0.000797***	X^2 = 0.0718, df=1, p=0.7888

5.1.2 Post-environmental exposure

Macroscopically, all cut marks remain recognisable after surface and buried exposure for 18 months. Several characteristics were used in order to identify the

effects of environmental factors on traumatic features. Table 5.3 demonstrates overall morphological changes of cut marks on rib samples in this study. Overall, there was no change of kerf margin or striations in surface-deposited and buried cut marks inflicted by a non-serrated blade knife. In contrast, all kerf morphologies of cut marks inflicted by a coarse-serrated blade knife and a fine-serrated blade knife underwent some degree of alteration after environmental exposure. Therefore, the following statements demonstrate the results according to their types of weapon and depositional environment.

Table 5.3: Summary of morphological changes after environmental exposure (X: present changes; O: no change; NS: non-serrated blade; CS: coarse-serrated blade; FS: fine-serrated blade)

Exposure and weapon type		Kerf shape	Cross-section	Kerf margin	Striations
Surface	NS	X	X	O	O
	CS	X	X	X	X
	FS	X	X	X	X
Burial	NS	X	X	O	O
	CS	X	X	X	X
	FS	X	X	X	X

5.1.2.1 Non-serrated knife blade group

5.1.2.1.1 Surface-deposited rib samples

5.1.2.1.1.1 Dimensional change

Figures 5.8 and Table 5.A in APPENDIX 5 demonstrates changes in kerf length and width of the non-serrated blade cut marks after surface environmental exposure. The overall average length differences compared to pre-exposure values were 0.326 mm at 6 months, 0.9344 mm after 12 months, and 1.0865 mm following 18 months of exposure. The overall width differences compared with the pre-exposure value were 0.003 mm at 6 months, 0.022 mm after 12 months, and 0.035 mm following 18 months of exposure. Remarkably, there was no statistical

significance (p>0.05) in either length or width comparing between pre and post environmental-exposure data after 6, 12, and 18 months (Table 5.B in APPENDIX 5).

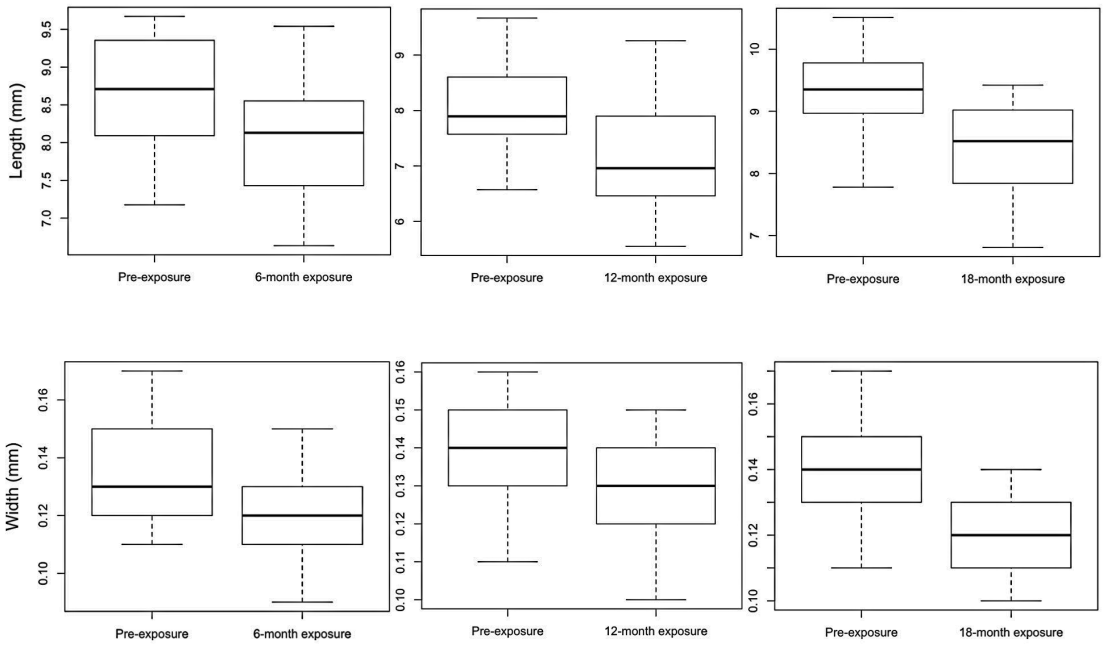

Figure 5.8: Observed length and width difference of surface-deposited non-serrated blade cut marks; each group n=10

A sequential decrease in dimension was observed in each post-exposure group, and a percentage of dimensional alterations was explored in-depth to compare between each group (Table 5.4). Additionally, Figure 5.9 demonstrates more intensive profiles of correlation of kerf length and width changes comparing between pre-exposure and three ranges of environmental exposure.

Table 5.4: Dimensional changes of the same non-serrated blade cut marks after exposure to surface environment for six, twelve, and eighteen months

Dimension	Alterations	Number of samples (%) (each group: n=10)		
		6-months	12-months	18-months
Length	Increase	4 (40)	-	-
	Decrease	6 (60)	10 (100)	10 (100)
Width	Increase	3 (30)	2 (20)	-
	Decrease	7 (70)	7 (70)	10 (100)
	No change	-	1 (10)	-

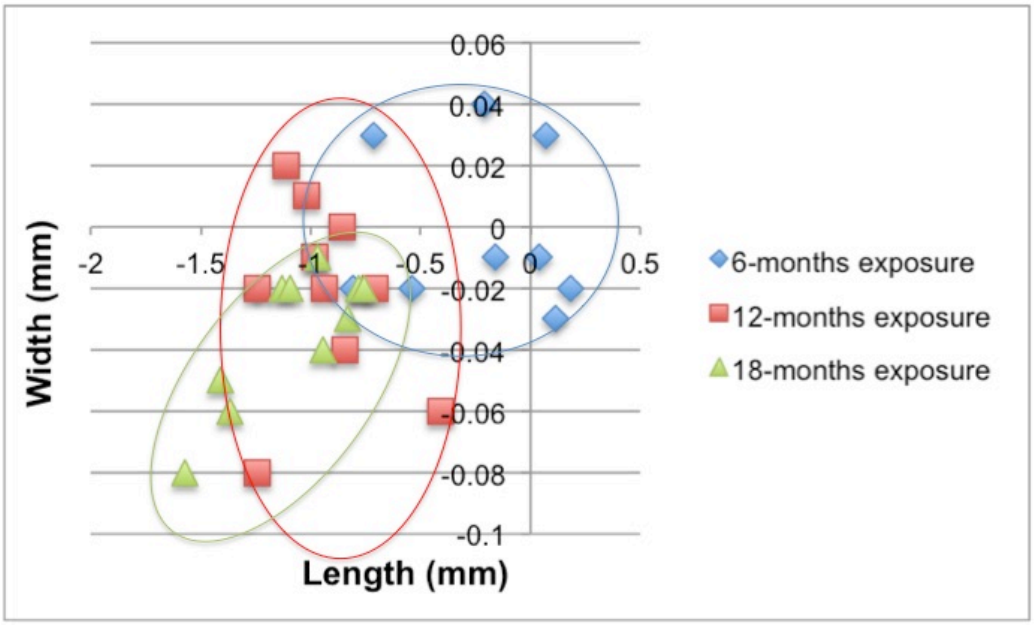

Figure 5.9: Demonstrating dimensional change comparing of kerf length and width of surface-deposited non-serrated blade cut marks; each group n=10

Three clusters were observed in the data. The 12-months exposure exhibited the widest range, which accumulated in the area between 6-months and 18-months exposure. Also, there was a decreasing range of maximum length of all cut marks at 12-months exposure, and variability in the maximum width was observed. All marks showed a decrease in their maximum length and width after 18-months of surface exposure, with the maximum decrease of 1.571 mm in length and 0.08 mm in width. These changes were not statistically significant. Linear regressions were conducted to study the relationship between exposed in the data (Figure 5.10-5.11). Predictive changes of the kerf dimension could be expected from the equation.

5.1.2.1.1.2 Morphological change

The morphology of cut marks inflicted by a non-serrated knife blade underwent alterations after environmental deposition. However, smooth kerf margin and the absence of kerf striations were not altered after 18 months of surface exposure (Table 5.2). Table 5.5 summarises percentage of kerf morphological changes of each surface exposure time of cut marks inflicted by a non-serrated blade knife, and Figures 5.12-5.13 give more information about how the change of each morphology after surface exposure.

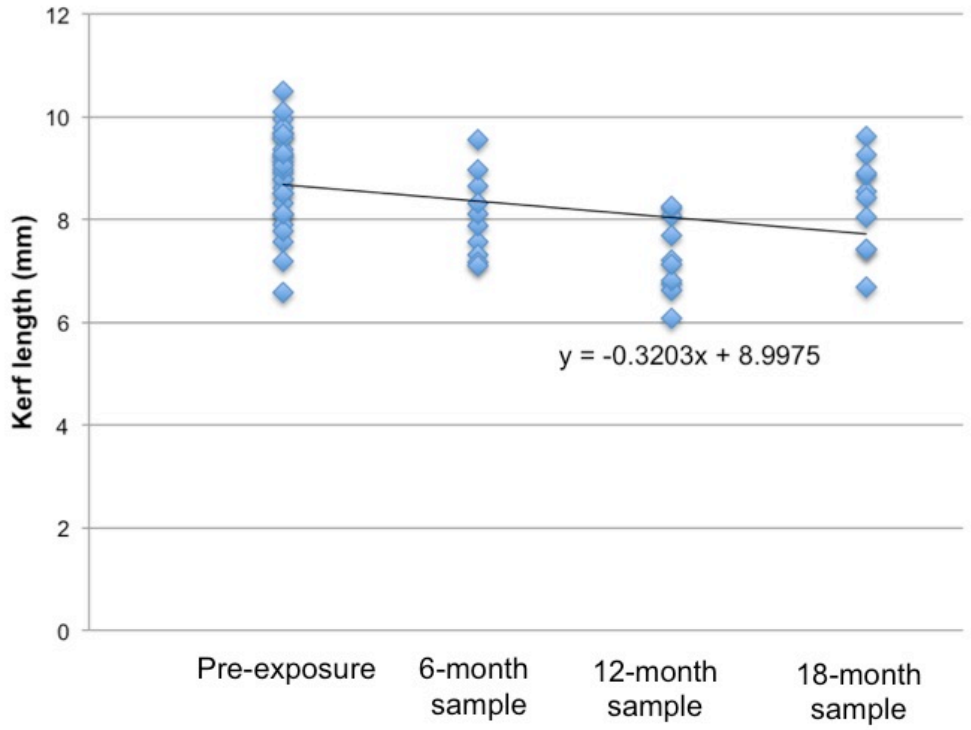

Figure 5.10: The scatter plot with a simple regression equation of kerf length of surface-deposited non-serrated blade cut marks

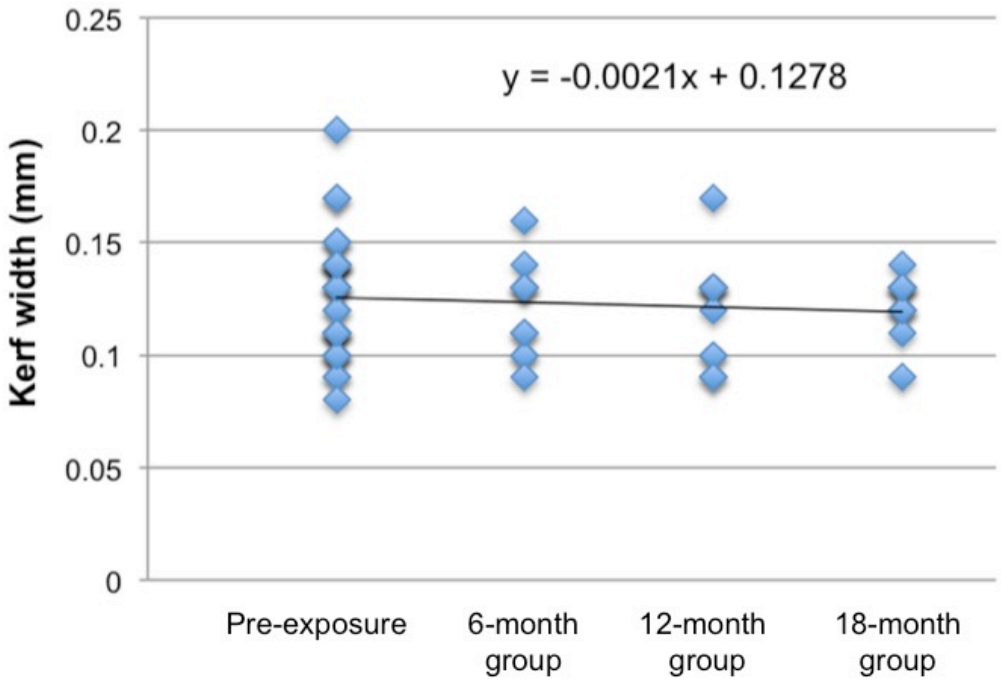

Figure 5.11: The scatter plot with a simple regression equation of kerf width of surface-deposited non-serrated blade cut marks

Table 5.5: Summary of frequency data of kerf mor phology changes between pre-exposure (Pre-E) and post-surface exposure (Post-E) cut marks from a non-serrated knife

Kerf morphology		6-months exposure (n=10) (%)		12-months exposure (n=10) (%)		18-months exposure (n=10) (%)	
		Pre-E	Post-E	Pre-E	Post-E	Pre-E	Post-E
Kerf shape	Linear	10(100)	10(100)	10(100)	8 (80)	10(100)	7 (70)
	Ellipse	0 (0)	0 (0)	0 (0)	2 (20)	0 (0)	1 (10)
	Rectangle	0 (0)	0 (0)	0 (0)	0 (0)	0 (0)	1 (10)
	Irregular	0 (0)	0 (0)	0 (0)	1 (10)	0 (0)	1 (10)
Cross-section	Narrow	8 (80)	8 (80)	8 (80)	6 (60)	8 (80)	5 (50)
	V-shaped	2 (20)	2 (20)	2 (20)	4 (40)	2 (20)	5 (50)
Kerf margin	Smooth	10(100)	10(100)	10(100)	10(100)	10(100)	10(100)
	Raising	0 (0)	0 (0)	0 (0)	0 (0)	0 (0)	0 (0)
Striations	Presence	0 (0)	0 (0)	0 (0)	0 (0)	0 (0)	0 (0)
	Absence	10(100)	10(100)	10(100)	10(100)	10(100)	10(100)

Non-serrated blades produced linear-shaped cut marks, and 80% of marks had a narrow cross-sectional shape. No cut marks inflicted by non-serrated blades had a raised kerf margin or kerf striations (Table 5.5). After environmental exposure, 20% of linear-shaped cut marks changed to ellipse-shaped with irregular morphology after 12 months of surface exposure (Figure 5.14). At the completion of the observation period, 30% of all linear marks changed equally to elliptical, rectangular and irregular shape (Figure 5.10). In addition, 25% of the narrow-shaped cross-section cut marks transformed into V-shaped after 12 months and 37.5% did so after 18 months (Figure 5.13).

Changes in kerf morphology between pre and post-environmental surface exposure were compared. There was no statistical significance observed in non-serrated blade cut marks from following 18 months of environmental exposure (Table 5.C in APPENDIX 5). In sum, the effect of surface taphonomic alterations

showed no potential to modify evidence of non-serrated blade-inflicted cut mark dimension and morphology within 18 months.

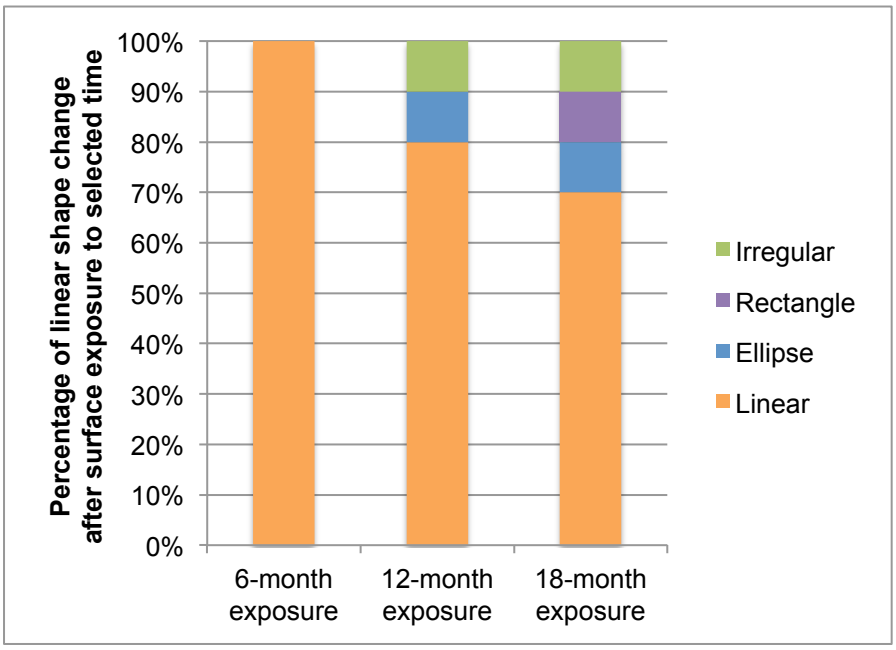

Figure 5.12: Percentage of linear shape alterations for each surface exposure group of cut marks inflicted by a non-serrated knife

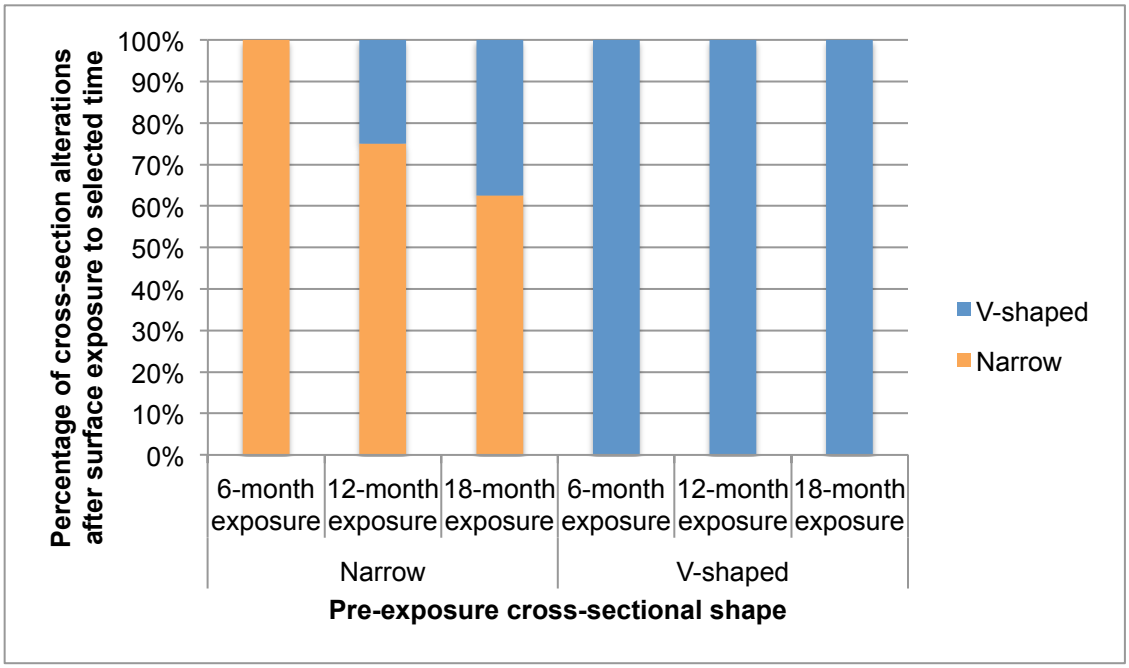

Figure 5.13: Percentage of cross-section shape alterations for each surface exposure group of cut marks inflicted by a non-serrated knife

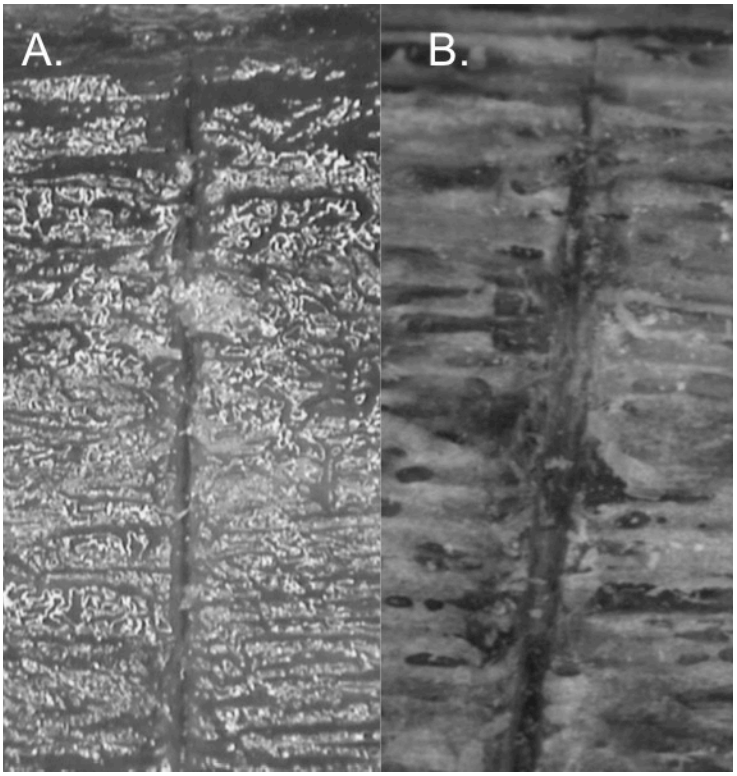

Figure 5.14: The morphological change of the same cut mark after environmental exposure; A. linear shape of the pre-exposure mark; B. elliptical shape of the 12-months exposure mark

5.1.2.1.2 Buried rib samples

5.1.2.1.2.1 Dimensional change

Figures 5.15 and Table 5.A in APPENDIX 5 demonstrates changes in kerf length and width of non-serrated blade cut marks after burial. Average length differences between pre and post-environmental exposure were 0.2106 mm at 6 months, 0.2853 mm at 12 months, and 0.67 mm at 18 months. The overall width differences were 0.0026 mm at 6 months, 0.011 mm at 12 months, and 0.0215 mm at 18 months. Thus, a progressive decrease in kerf dimension was observed. These differences were not statistically significant (Table 5.B in APPENDIX 5).

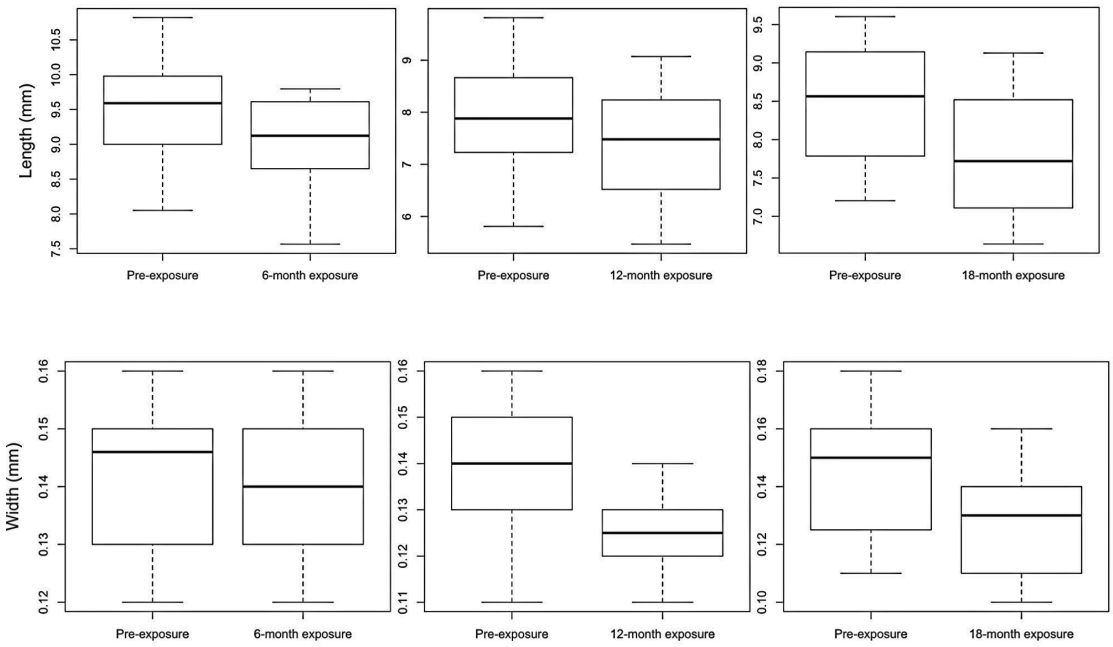

Figure 5.15: Observed length and width difference of buried non-serrated blade cut marks; each group n=10

A sequential decrease in dimension was observed in each post-exposure group, and a percentage of dimensional alterations was explored in-depth to compare between each group (Table 5.6). Additionally, Figure 5.16 demonstrates more intensive profiles of correlation of kerf length and width changes comparing between pre-exposure and three ranges of environmental exposure.

Table 5.6: Dimensional changes of the same non-serrated blade cut marks after exposure to buried environment for six, twelve, and eighteen months

Dimension	Alterations	Number of samples (%); (each group: n=10)		
		6-months	12-months	18-months
Length	Increase	4 (40)	2 (20)	-
	Decrease	6 (60)	8 (80)	10 (100)
Width	Increase	4 (40)	2 (20)	-
	Decrease	4 (40)	6 (60)	8 (80)
	No change	2 (20)	2 (20)	2 (20)

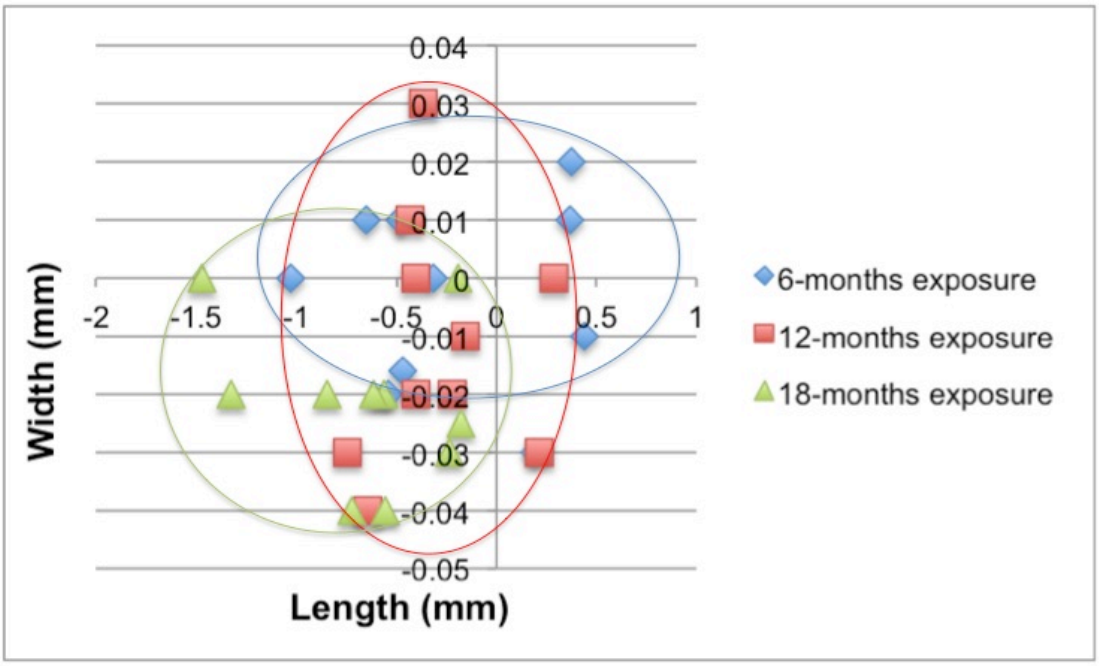

Figure 5.16: Demonstrating dimensional change comparing kerf length and width of buried non-serrated blade cut marks; each group n=10

A wide distribution was observed in maximum length and width at 12-months buried exposure, but the values were in a more narrow range compared to the surface exposure group. Almost all samples showed decreases in length and width after 18 months buried exposure, with only two cut marks showing no change in their width dimension (Table 5.6). Most of the cut marks in the buried group displayed a smaller reduction in the maximum length and width compared to the surface group, with a maximum decrease of 1.475 mm in length and 0.04 mm in width. Linear regressions were conducted to study the relationship between exposed in the data (Figure 5.17-5.18). Predictive changes of the kerf dimension could be expected from the equation.

5.1.2.1.2.2 Morphological change

Cut mark morphology by non-serrated blade underwent some alterations after burial. However, kerf margin and striations did not change throughout 18 months of surface exposure (Table 5.3). Table 5.7 summarises percentages of kerf morphological changes for each surface exposure time of cut marks inflicted by a

non-serrated blade knife, and Figures 5.19-5.20 gives more information about the change in morphology after buried exposure.

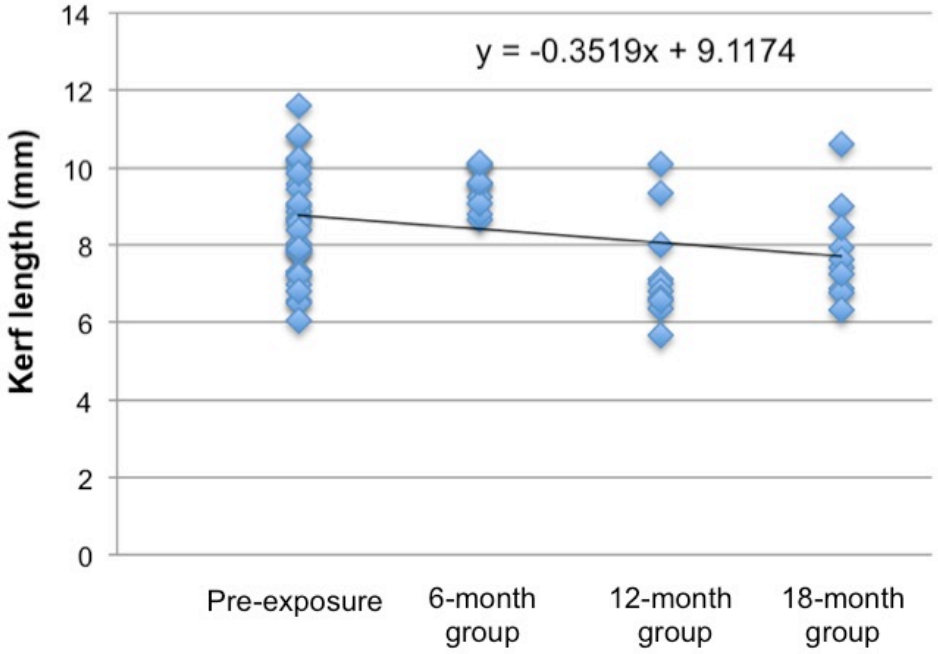

Figure 5.17: The scatter plot with a simple regression equation of kerf length of buried non-serrated blade cut marks

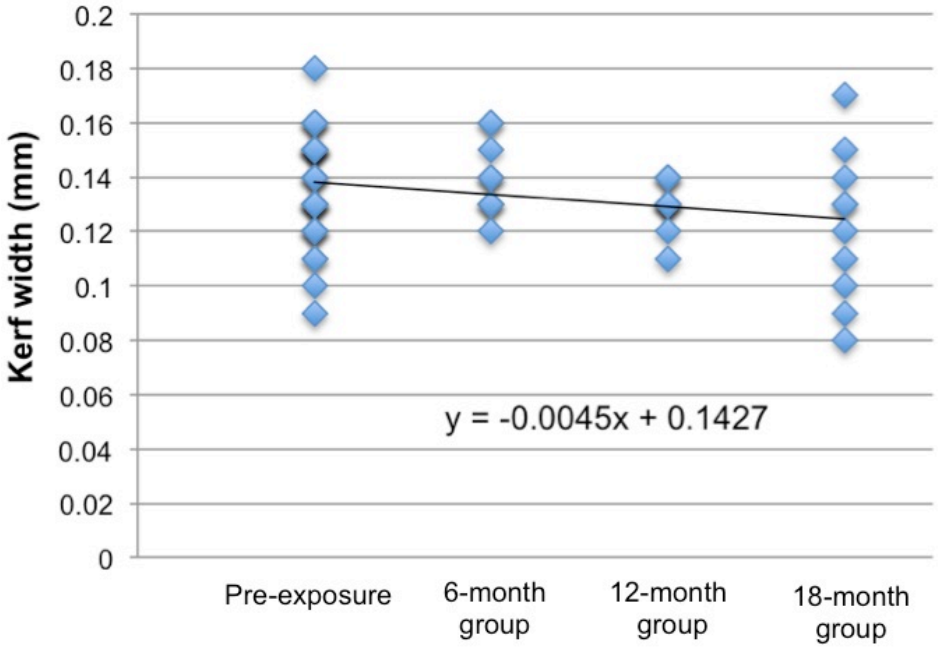

Figure 5.18: The scatter plot with a simple regression equation of kerf width of buried non-serrated blade cut marks

Table 5.7: Summary of frequency data of kerf morphology changes between pre-exposure (Pre-E) and post-burial exposure (Post-E) cut marks from a non-serrated knife

Kerf morphology		6-months exposure (n=10) (%)		12-months exposure (n=10) (%)		18-months exposure (n=10) (%)	
		Pre-E	Post-E	Pre-E	Post-E	Pre-E	Post-E
Kerf shape	Linear	10(100)	10(100)	10(100)	9 (90)	10(100)	8 (80)
	Ellipse	0 (0)	0 (0)	0 (0)	1 (10)	0 (0)	2 (20)
	Rectangle	0 (0)	0 (0)	0 (0)	0 (0)	0 (0)	0 (0)
	Irregular	0 (0)	0 (0)	0 (0)	0 (0)	0 (0)	0 (0)
Cross-section	Narrow	8 (80)	8 (80)	8 (80)	8 (80)	8 (80)	7 (70)
	V-shaped	2 (20)	2 (20)	2 (20)	2 (20)	2 (20)	3 (30)
Kerf margin	Smooth	10(100)	10(100)	10(100)	10(100)	10(100)	10(100)
	Raising	0 (0)	0 (0)	0 (0)	0 (0)	0 (0)	0 (0)
Striations	Presence	0 (0)	0 (0)	0 (0)	0 (0)	0 (0)	0 (0)
	Absence	10(100)	10(100)	10(100)	10(100)	10(100)	10(100)

As with the surface group, non-serrated blades produced linear-shaped cut marks, and 80% of marks had a narrow cross-sectional shape. No cut marks from non-serrated blades had raised kerf margin or kerf striations (Table 5.7). After 12 months of environmental buried exposure, only 10% of linear-shaped cut marks changed to ellipse-shaped, which increased to 20% after 18-months buried exposure (Figure 5.19). No change to rectangular and irregular shape was observed in the buried sample. In addition, 12.5% of originally narrow-shaped cross-sections transformed into V-shaped cross-sections after 18 months of exposure (Figure 5.20). Overall, buried samples showed more minor changes than surface exposed specimens.

Kerf morphology was compared between pre and post-environmental buried exposure (Table 5.C in APPENDIX 5). There was no statistical difference in the morphological change of cut marks inflicted by the non-serrated blade ($p>0.05$). In

sum, the buried environment exhibited no tendency to modify evidence of non-serrated blade cut mark morphology after 18 months.

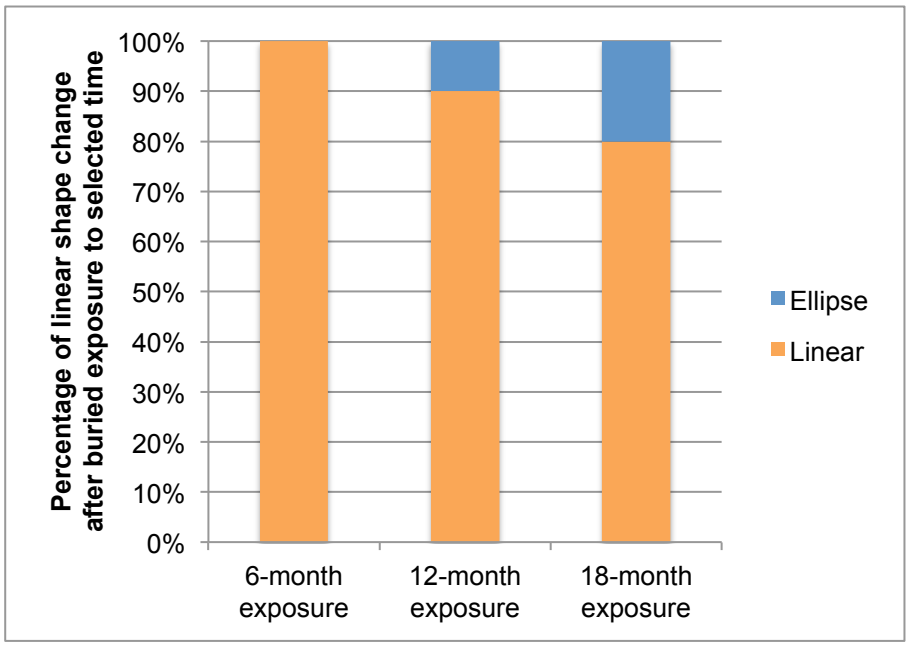

Figure 5.19: Percentage of linear shape alterations for each buried group of cut marks inflicted by a non-serrated knife

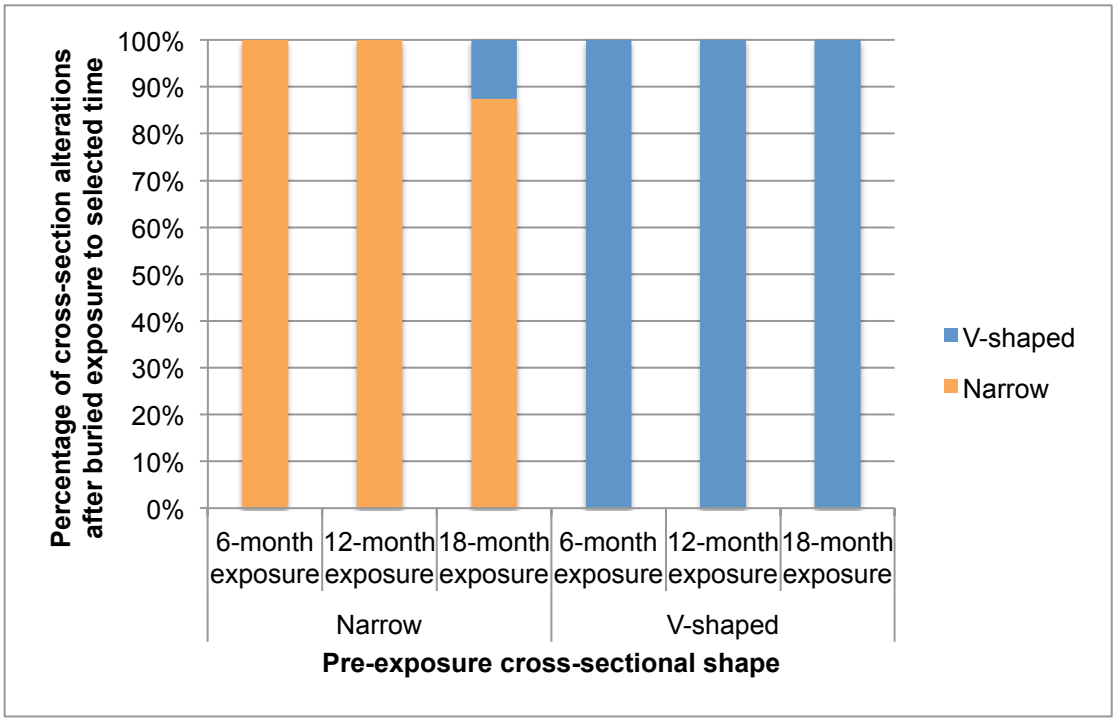

Figure 5.20: Percentage of cross-section shape alterations for each buried group of cut marks inflicted by a non-serrated knife

5.1.2.2 Coarse-serrated knife blade group

5.1.2.2.1 Surface-deposited rib samples

5.1.2.2.1.1 Dimensional change

Figures 5.21 and Table 5.D in APPENDIX 5 display changes in kerf length and width of the coarse-serrated blade cut marks in the surface group after environmental exposure. Compared to pre-exposure, overall average length decreased 0.3919 mm at 6 months, 0.6601 mm at 12 months, and 0.8099 mm at 18 months. Average width differences compared to pre-exposure values were 0.024 mm at 6 months, 0.027 mm at 12 months, and 0.045 mm at 18 months. These differences were not statistically significant (Table 5.E in APPENDIX 5).

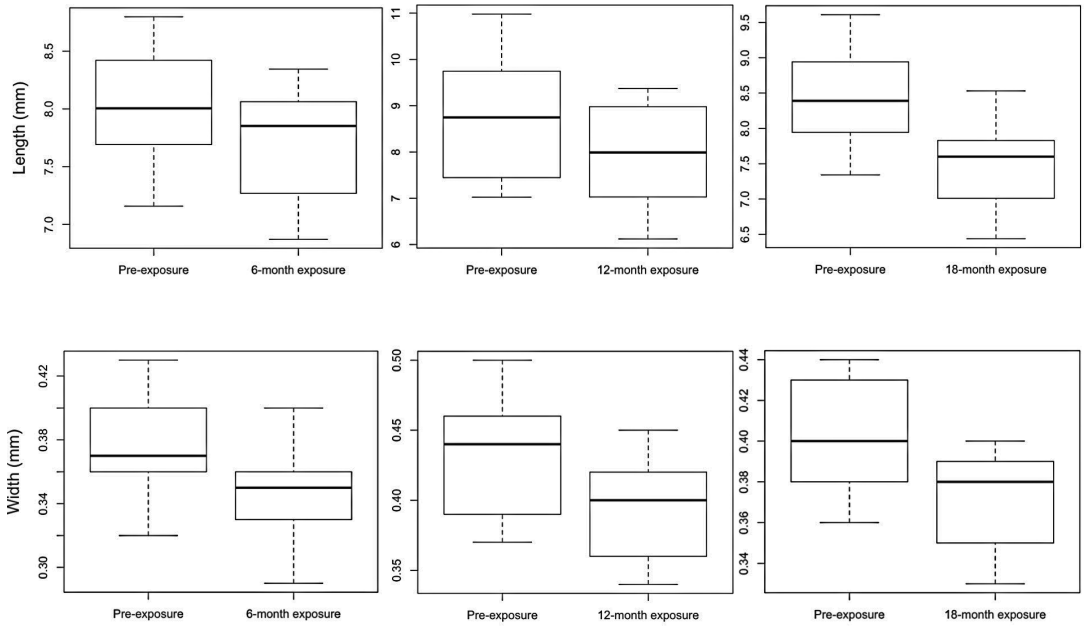

Figure 5.21: Observed length and width difference of surface-deposited coarse-serrated blade cut marks; each group n=10

A sequential decrease in dimension was observed in each post-exposure group, and the percentage of dimensional alterations was explored in-depth to compare between each group (Table 5.8). Additionally, Figure 5.22 demonstrates the correlation of kerf length and width changes comparing between pre-exposure and three ranges of environmental exposure. A wide range of the group-related pattern was observed in length and width changes in the surface exposure group.

Briefly, most marks exhibited a decrease in their maximum length and width following 12 and 18-month exposures, with a maximum decrease of 1.523 mm in length and 0.09 mm in width (Figure 5.22). These differences were not statistically significant. Linear regressions were conducted to study the relationship between exposed in the data (Figure 5.23-5.24). Predictive changes of the kerf dimension could be expected from the equation.

Table 5.8: Dimensional changes of the same coarse-serrated blade cut marks after exposure to surface environment for six, twelve, and eighteen months

Dimension	Alterations	Number of samples (%); (each group: n=10)		
		6-months	12-months	18-months
Length	Increase	3 (30)	-	-
	Decrease	7 (70)	10 (100)	10 (100)
Width	Increase	1 (10)	-	-
	Decrease	9 (90)	8 (80)	9 (90)
	No change	-	2 (20)	1 (10)

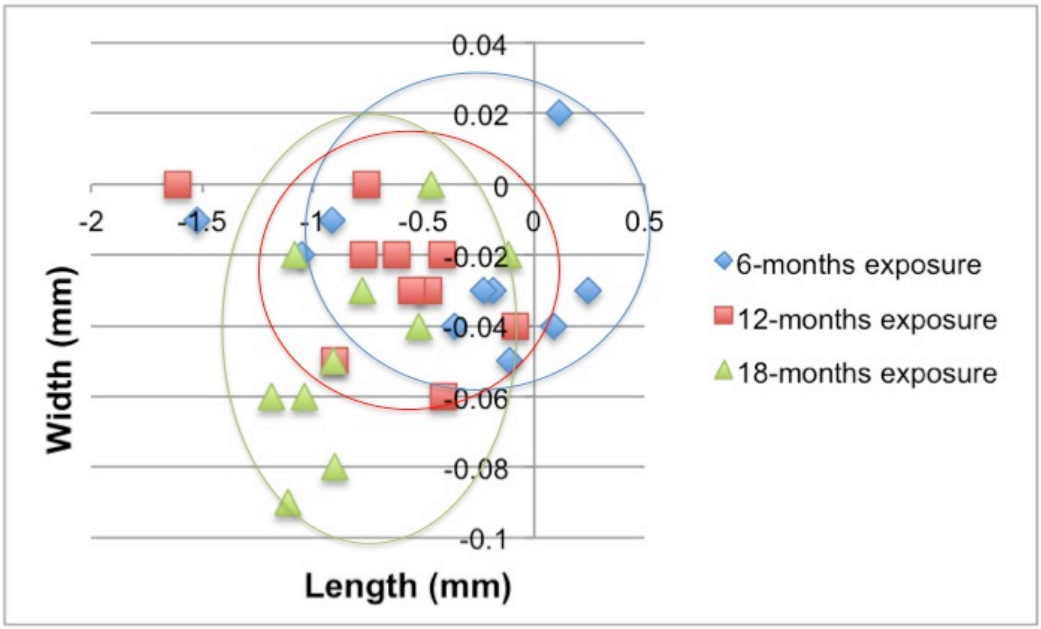

Figure 5.22: Demonstrating dimensional change comparing kerf length and width of surface-deposited coarse-serrated blade cut marks; each group n=10

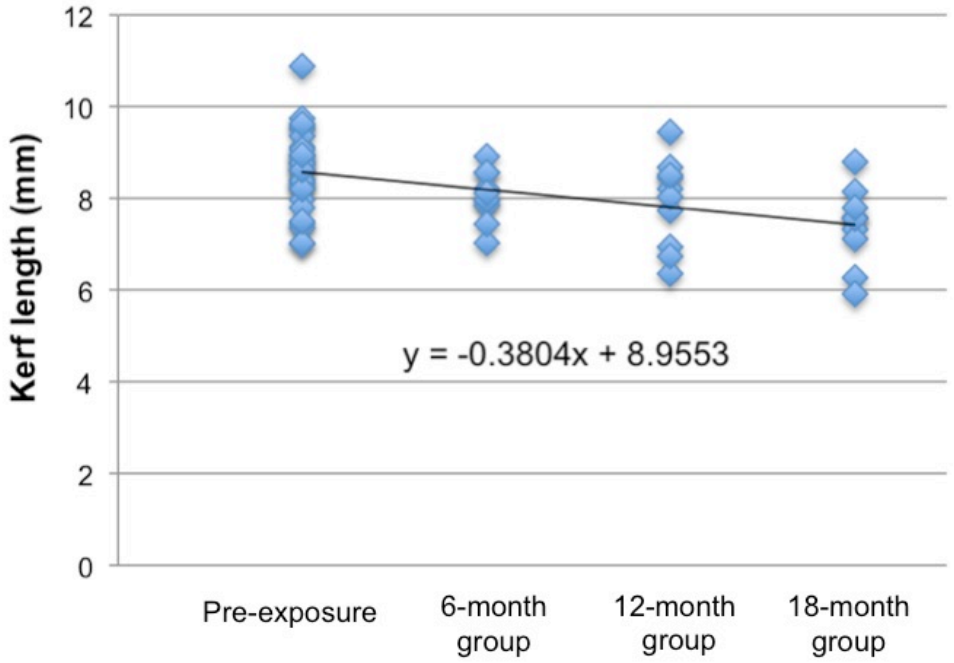

Figure 5.23: The scatter plot with a simple regression equation of kerf length of surface-deposited coarse-serrated blade cut marks

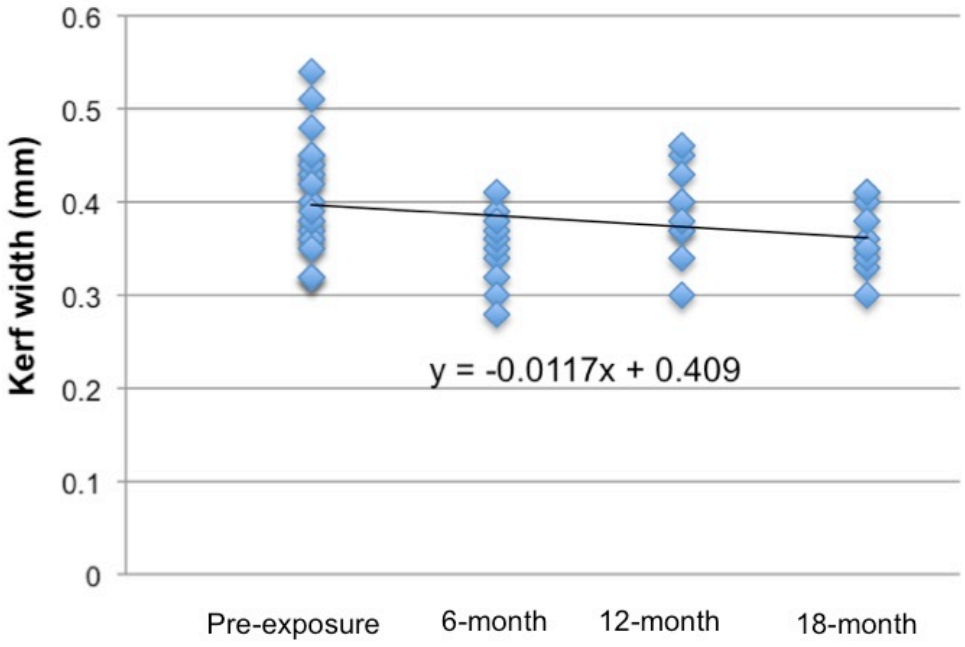

Figure 5.24: The scatter plot with a simple regression equation of kerf width of surface-deposited coarse-serrated blade cut marks

5.1.2.2.1.2 Morphological change

Cut mark morphology inflicted by a coarse-serrated blade underwent alterations after surface deposition. Table 5.9 summarises percentages of kerf morphological changes after surface exposure times of cut marks inflicted by a coarse-serrated blade knife, and Figures 5.25-5.28 gives more information about the change in morphology after surface exposure.

Table 5.9: Summary of frequency data of kerf morphology changes between pre-exposure and post-surface exposure marks from a coarse-serrated knife; Pre-E: pre-exposure; Post-E: post-exposure

Kerf morphology		6-months exposure (n=10) (%)		12-months exposure (n=10) (%)		18-months exposure (n=10) (%)	
		Pre-E	Post-E	Pre-E	Post-E	Pre-E	Post-E
Kerf shape	Ellipse	8 (80)	7 (70)	8 (80)	6 (60)	7 (70)	4 (40)
	Rectangle	2 (20)	2 (20)	2 (20)	2 (20)	2 (20)	2 (20)
	Irregular	0 (0)	1 (10)	0 (0)	2 (20)	1 (10)	4 (40)
Cross-section	V-shaped	5 (50)	5 (50)	5 (50)	4 (40)	6 (60)	4 (40)
	U-shaped	5 (50)	5 (50)	5 (50)	6 (60)	4 (40)	6 (60)
Kerf margin	Smooth	3 (30)	4 (40)	3 (30)	5 (50)	4 (40)	6 (60)
	Raising	7 (70)	6 (60)	7 (70)	5 (50)	6 (60)	4 (40)
Striations	Presence	5 (50)	5 (50)	7 (70)	5 (50)	6 (60)	4 (40)
	Absence	5 (50)	5 (50)	3 (30)	5 (50)	4 (40)	6 (60)

Initially, coarse-serrated blades produced 77% (23 of 30) of elliptical kerf shape and 53% (16 of 30) with a V-shaped cross-section. Coarse-serration produced the raised margin in 66.7% (20 of 30) samples. Sixty percent (18 of 30) of serrated blades made kerf striations (Table 5.9). After environmental exposure, 12.5% of elliptical kerf shape changed to an irregular shape at 6-months of surface exposure, increasing to 42.9% at 18-months of exposure. Nonetheless, there was no change of rectangular and irregular kerf shape after 18-months surface exposure (Figure 5.25). Thirty-three percent of V-shaped cut marks changed to U-shaped marks after 18-months surface exposure, while all U-shaped cross-sections exhibited no specific change at 18-months buried exposure (Figure 5.26). In

addition, raised kerf margin experienced morphological degradation. The raised edges of the kerf margins eroded and disappeared after surface environmental exposure (Figure 5.29), with an incidence of 14.3% at 6 months, 28.6% at 12 months, and 33.3% after 18 months (Figure 5.27). Lastly, around 28.6% of kerf striations started to fade away after 12-months of surface exposure and 33.3% after 18-months of surface exposure (Figure 5.28).

The statistical significance of kerf morphology was observed comparing between pre-exposure and post-environmental surface exposure (Table 5.F in APPENDIX 5). There was no statistical significance observed in the morphological change of kerf shape from coarse-serrated blade cut marks following environmental exposure ($p>0.05$). In sum, 18 months of surface environmental exposure showed a potential to modify evidence of coarse-serrated blade cut mark morphology.

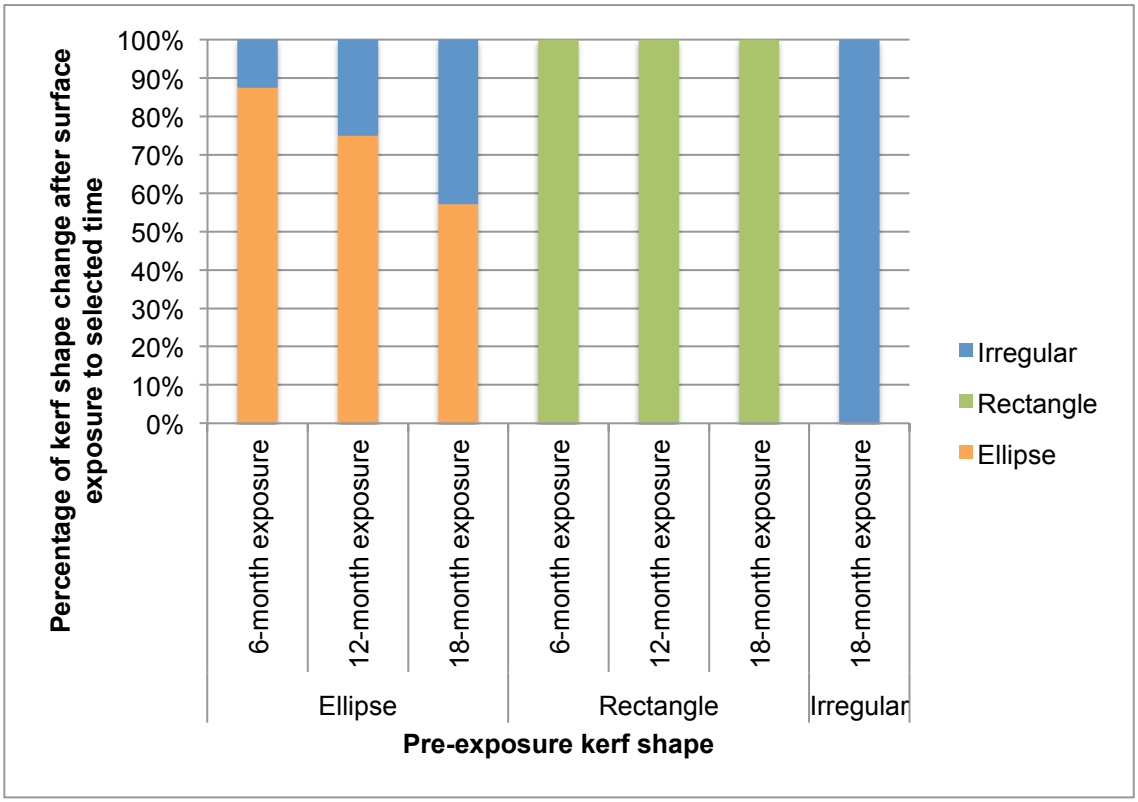

Figure 5.25: Percentage of kerf shape alterations for each surface exposure group of cut marks inflicted by a coarse-serrated knife

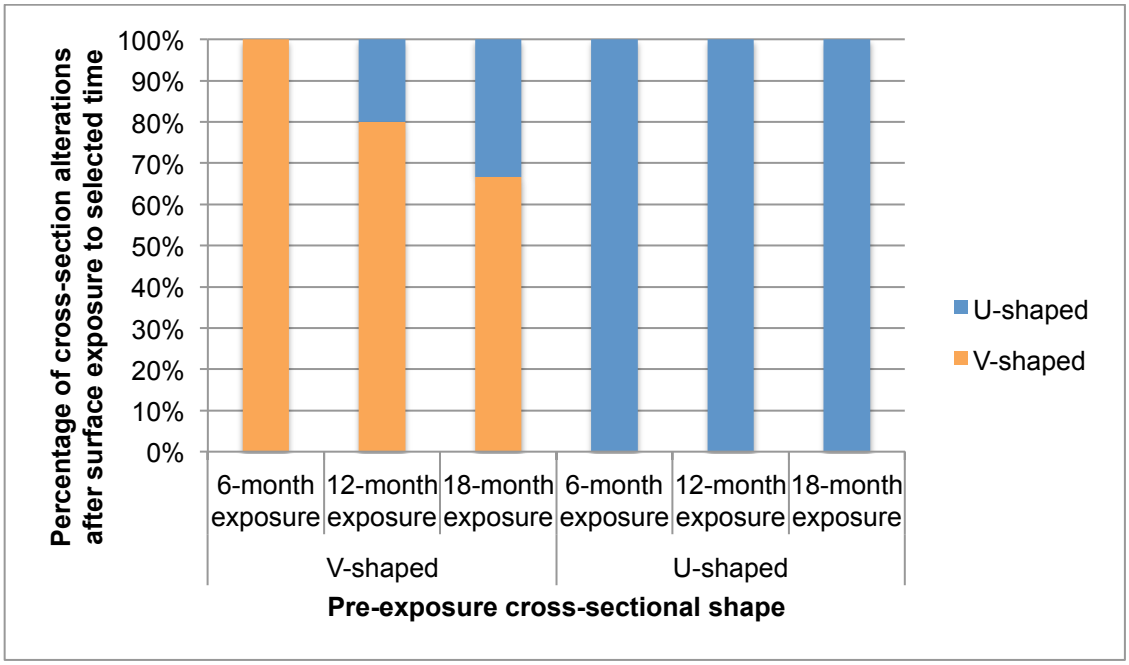

Figure 5.26: Percentage of cross-section shape alterations for each surface exposure group of cut marks inflicted by a coarse-serrated knife

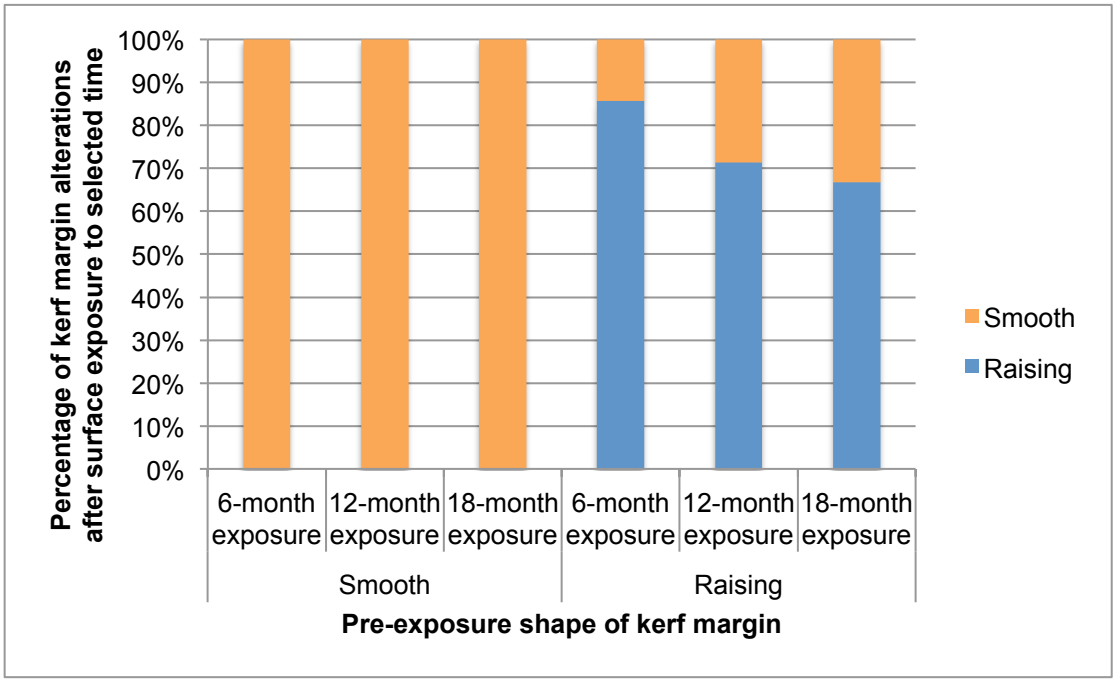

Figure 5.27: Percentage of kerf margin alterations for each surface exposure group of cut marks inflicted by a coarse-serrated knife

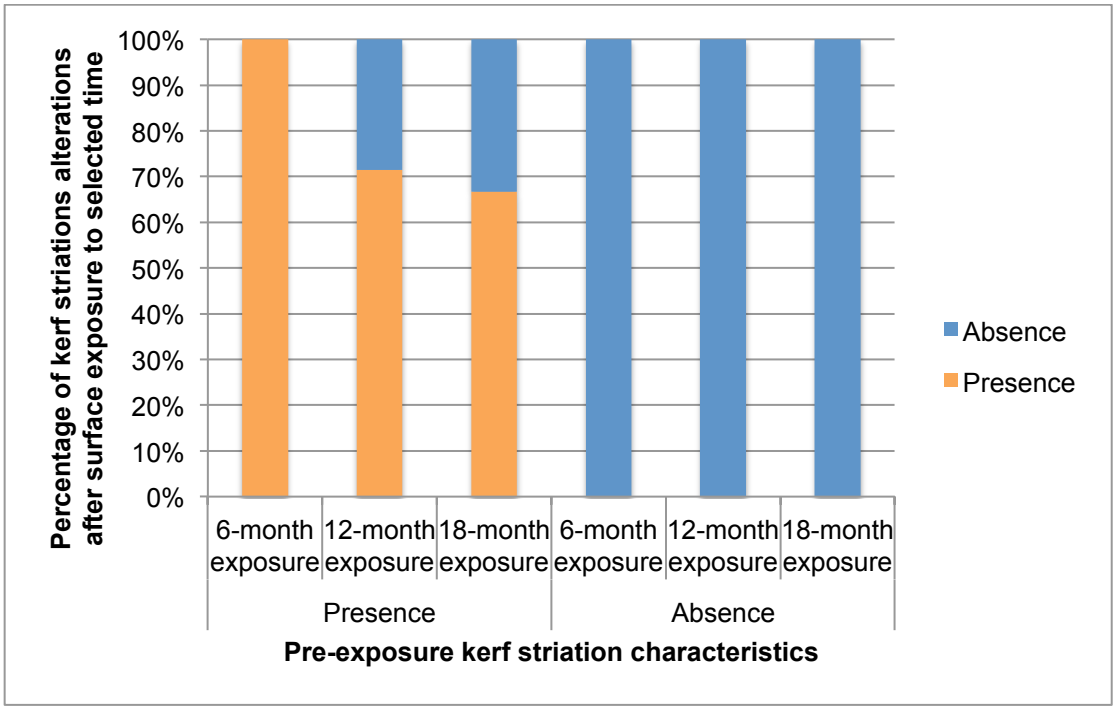

Figure 5.28: Percentage of change of striations for each surface exposure group of cut marks inflicted by a coarse-serrated knife

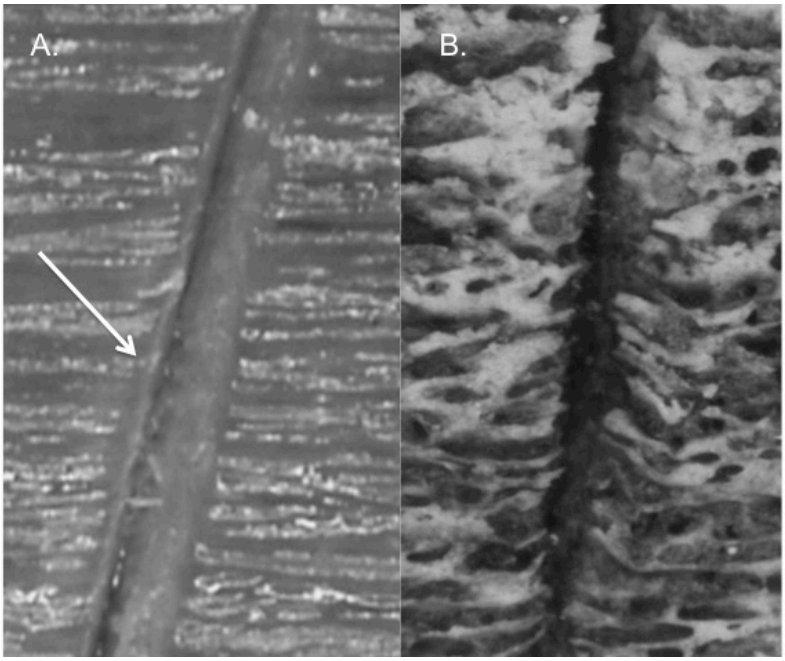

Figure 5.29: The kerf margin change of the same cut mark after environmental exposure; A. the pre-exposure mark; B. the 18-months exposure mark; the white arrow indicates raised kerf margin

5.1.2.2.2 Buried rib samples

5.1.2.2.2.1 Dimensional change

Figures 5.30 and Table 5.D in APPENDIX 5 demonstrate changes in kerf length and width of the coarse-serrated blade cut marks in the buried group. The average length difference between pre and post-exposure was 0.1636 mm at 6 months, 0.4314 mm at 12 months, and 0.6056 mm at 18 months. The overall width differences between pre and post-exposure values were 0.012 mm, 0.028 mm, and 0.029 mm for 6-months exposure, 12-months exposure, and 18-months exposure respectively. Nevertheless, there was no statistical significance change to both length and width comparing the same sample between pre-exposure and environmental-exposure data (Table 5.E in APPENDIX 5).

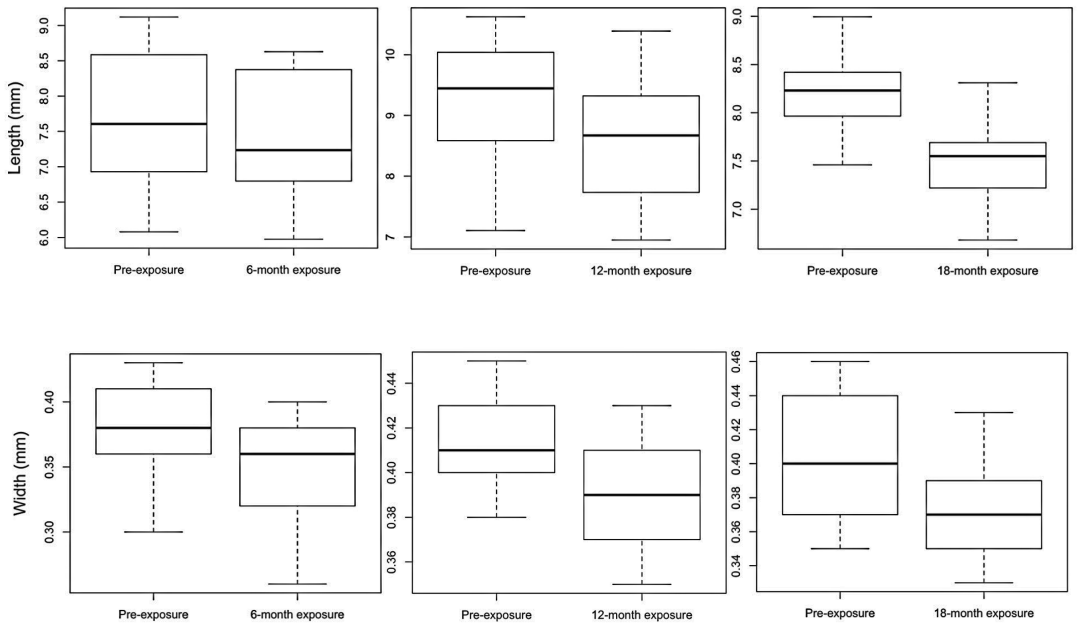

Figure 5.30: Observed length and width difference of buried coarse-serrated blade cut marks; each group n=10

A decrease in dimension was observed in each post-exposure group, and a percentage of dimensional alterations was explored in-depth to compare between each group (Table 5.10). Additionally, Figure 5.31 demonstrates the correlation of kerf length and width changes comparing between pre-exposure and three ranges

of the environmental exposure. Most of the samples showed a decrease in length and width at 18-months buried exposure.

Table 5.10: Dimensional changes of the same coarse-serrated blade cut marks after exposure to buried environment for six, twelve, and eighteen months

Dimension	Alterations	Number of samples (%); (each group: n=10)		
		6-months	12-months	18-months
Length	Increase	3 (30)	2 (20)	-
	Decrease	7 (70)	8 (80)	10 (100)
	No change	-	-	-
Width	Increase	3 (30)	1 (10)	-
	Decrease	6 (60)	7 (70)	9 (90)
	No change	1 (10)	2 (20)	1 (10)

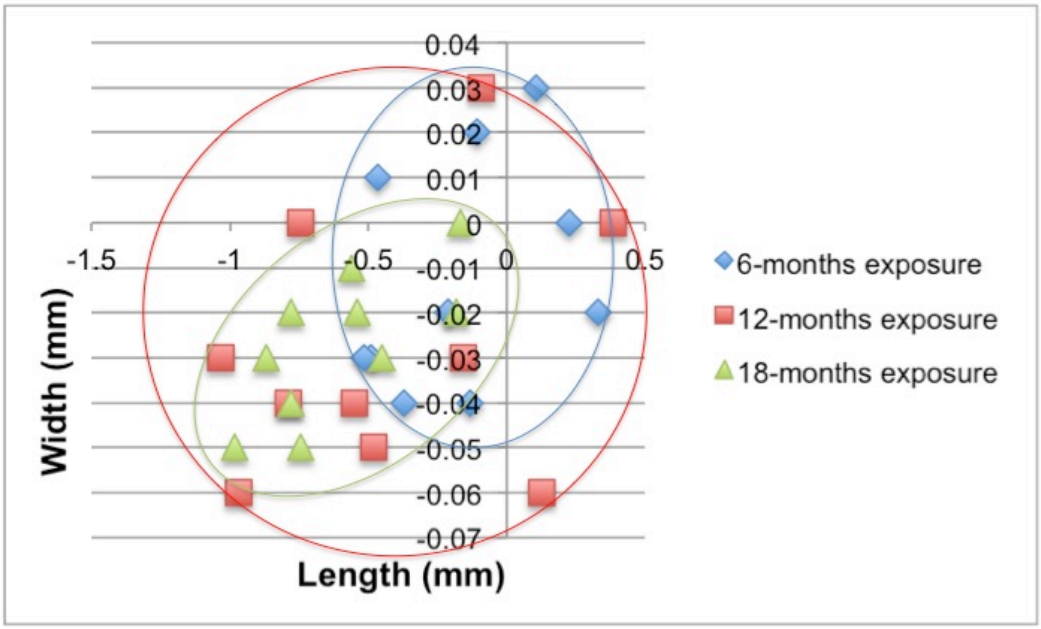

Figure 5.31: Demonstrating dimensional change comparing of kerf length and width of buried coarse-serrated blade cut marks; each group n=10

Intersection of scatter data was observed in Figure 5.31, particularly a wide distribution of values in the 12-months exposure group. Almost all buried samples showed decreases in length and width at 18-months with only one cut mark

showing no change in width. Most of the buried group cut marks displayed slower decreases in their dimensions and only a slight decrease in the maximum width compared to the surface group, with a maximum decrease of 1.035 mm in length and 0.06 mm in width. Linear regressions were conducted to study the relationship between exposed in the data (Figure 5.32-5.33). Predictive changes of the kerf dimension could be expected from the equation.

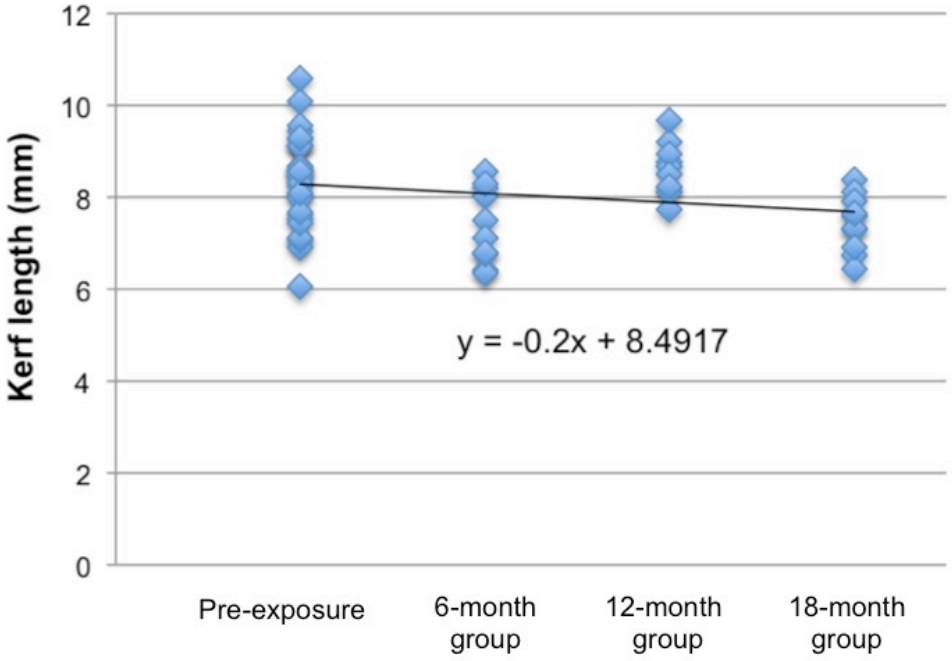

Figure 5.32: The scatter plot with a simple regression equation of kerf length of buried coarse-serrated blade cut marks

5.1.2.2.2.2 Morphological change

Cut mark morphology inflicted by a coarse-serrated blade knife underwent some alterations after burial. Table 5.11 summarises percentages of kerf morphological changes of each surface-exposure time of cut marks inflicted by a coarse-serrated blade knife, and Figure 5.34-5.37 gives more information about the change in morphology after surface exposure.

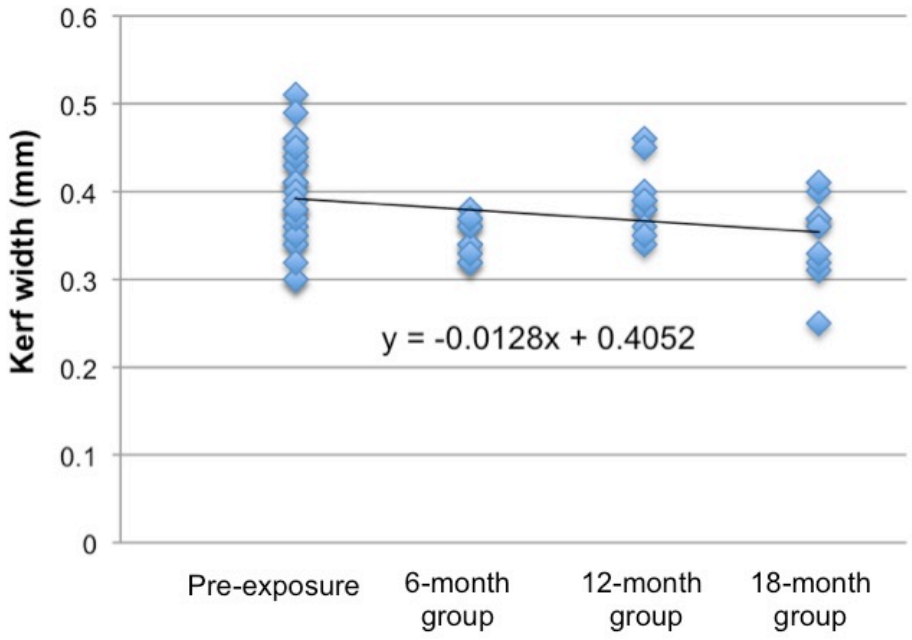

Figure 5.33: The scatter plot with a simple regression equation of kerf width of buried coarse-serrated blade cut marks

Table 5.11: Summary of frequency data of kerf morphology changes between pre-exposure (Pre-E) and post-burial exposure (Post-E) marks from a coarse-serrated knife

Kerf morphology		6-months exposure (n=10) (%)		12-months exposure (n=10) (%)		18-months exposure (n=10) (%)	
		Pre-E	Post-E	Pre-E	Post-E	Pre-E	Post-E
Kerf shape	Ellipse	8 (80)	8 (80)	7 (70)	7 (70)	7 (70)	6 (60)
	Rectangle	1 (10)	1 (10)	2 (20)	2 (20)	3 (30)	2 (20)
	Irregular	1 (10)	1 (10)	1 (10)	1 (10)	0 (0)	2 (20)
Cross-section	V-shaped	6 (60)	6 (60)	5 (50)	5 (50)	6 (60)	5 (50)
	U-shaped	4 (40)	4 (40)	5 (50)	5 (50)	4 (40)	5 (50)
Kerf margin	Smooth	2 (20)	2 (20)	3 (30)	3 (30)	3 (30)	4 (40)
	Raising	8 (80)	8 (80)	7 (70)	7 (70)	7 (70)	6 (60)
Striations	Presence	7 (70)	7 (70)	7 (70)	7 (70)	6 (60)	5 (5)
	Absence	3 (30)	3 (30)	3 (30)	3 (30)	4 (40)	5 (5)

Similar to the surface group, coarse-serrated blades produced 73.3% (22 of 30) ellipse-shaped cut marks in the pre-exposure burial group, and 56.7% (17 of 30) of marks had a V cross-sectional shape. Coarse-serration also produced a raised margin in 73.3% (22 of 30) of samples. Two-thirds (20 of 30) of serrated blades made kerf striations. Therefore, there was a large degree of overlap in cross-sectional shape (Table 5.11). Fourteen percent of ellipse-shaped cut marks changed to irregular marks after 18-months of surface exposure, while 33% of rectangle-shaped marks changed to irregular marks after 18-months of burial (Figure 5.34). Sixteen percent of V-shaped cut marks changed to U-shaped marks after 18-months of surface exposure, while all U-shaped cross-sections exhibited no specific changes after 18-months buried exposure (Figure 5.35). In addition, 14% of raised kerf margins were absent after 18-months of environmental exposure (Figure 5.36). Finally, 16.7% of kerf striations could not be detected after 18-months of buried exposure (Figure 5.37). Overall, buried specimens from coarse-serrated knives showed fewer changes in kerf morphology than the surface-exposure group.

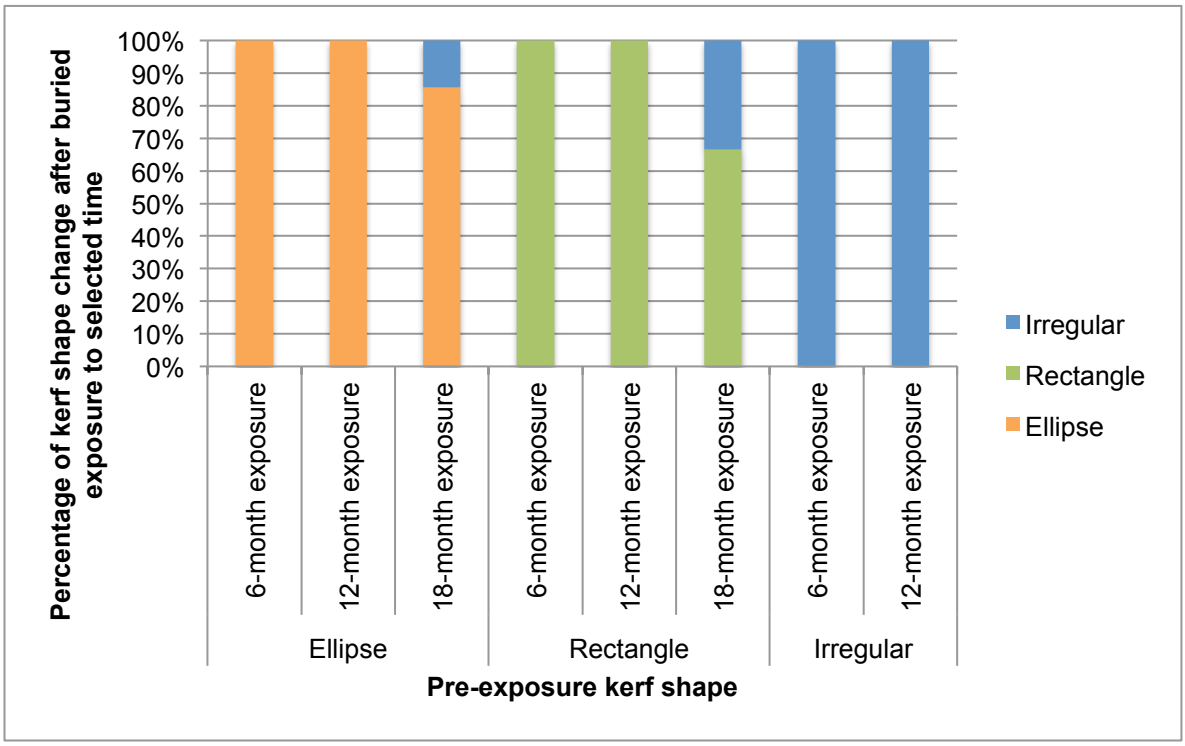

Figure 5.34: Percentage of kerf shape alterations for each buried group of cut marks inflicted by a coarse-serrated knife

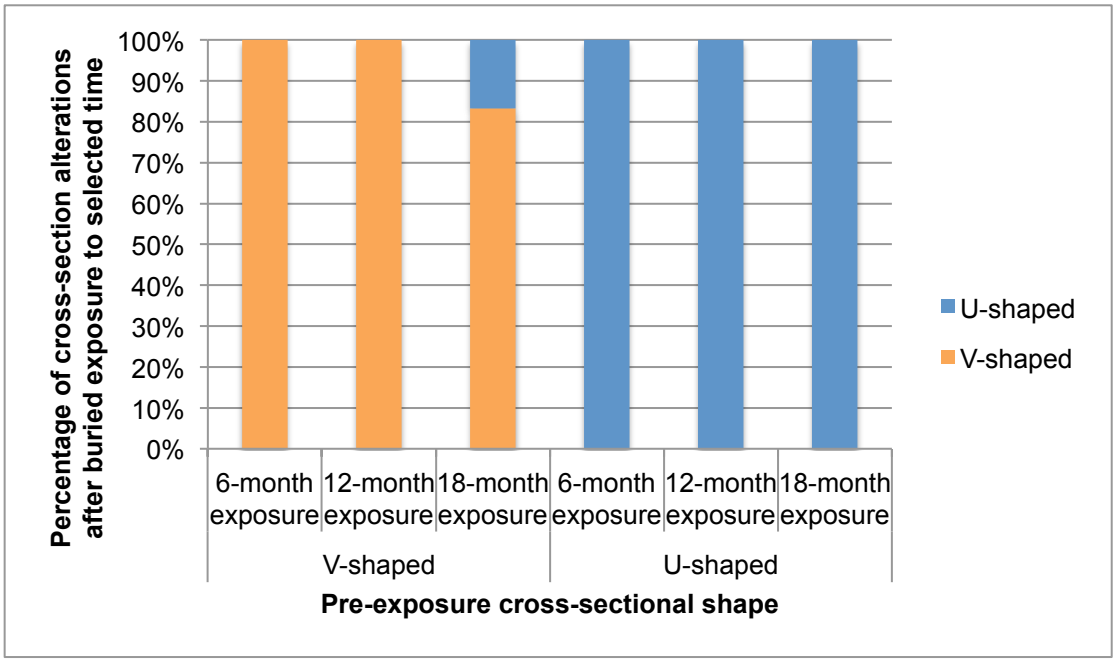

Figure 5.35: Percentage of cross-sectional shape alterations for each buried group of cut marks inflicted by a coarse-serrated knife

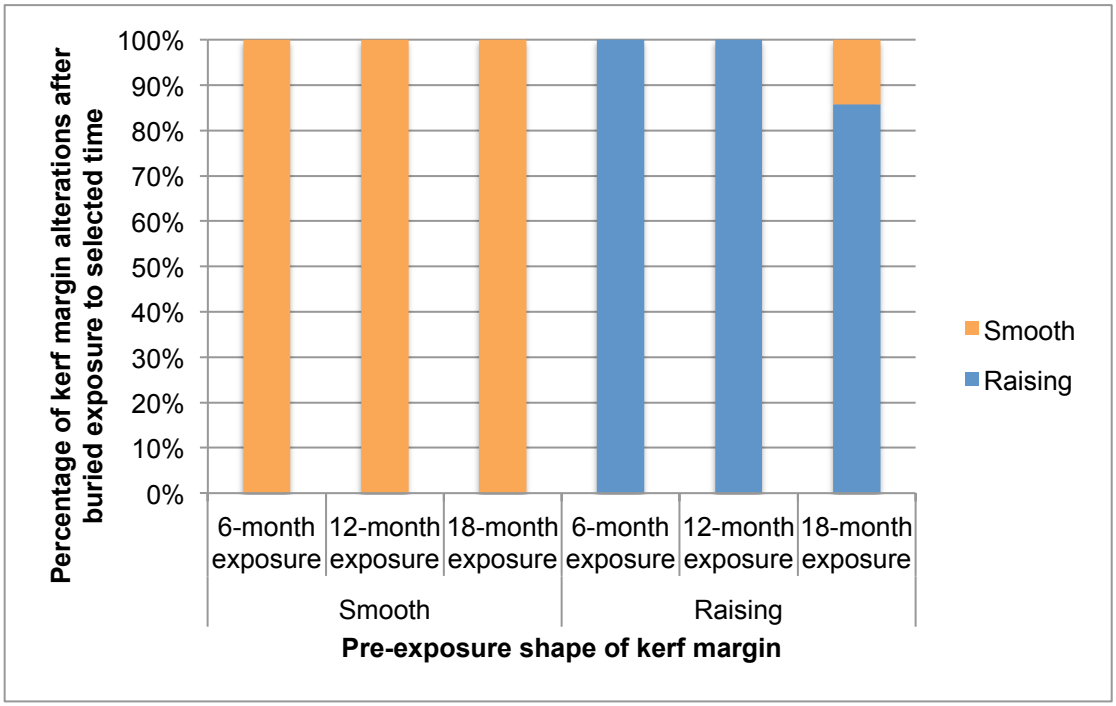

Figure 5.36: Percentage of kerf margin alterations for each buried group of cut marks inflicted by a coarse-serrated knife

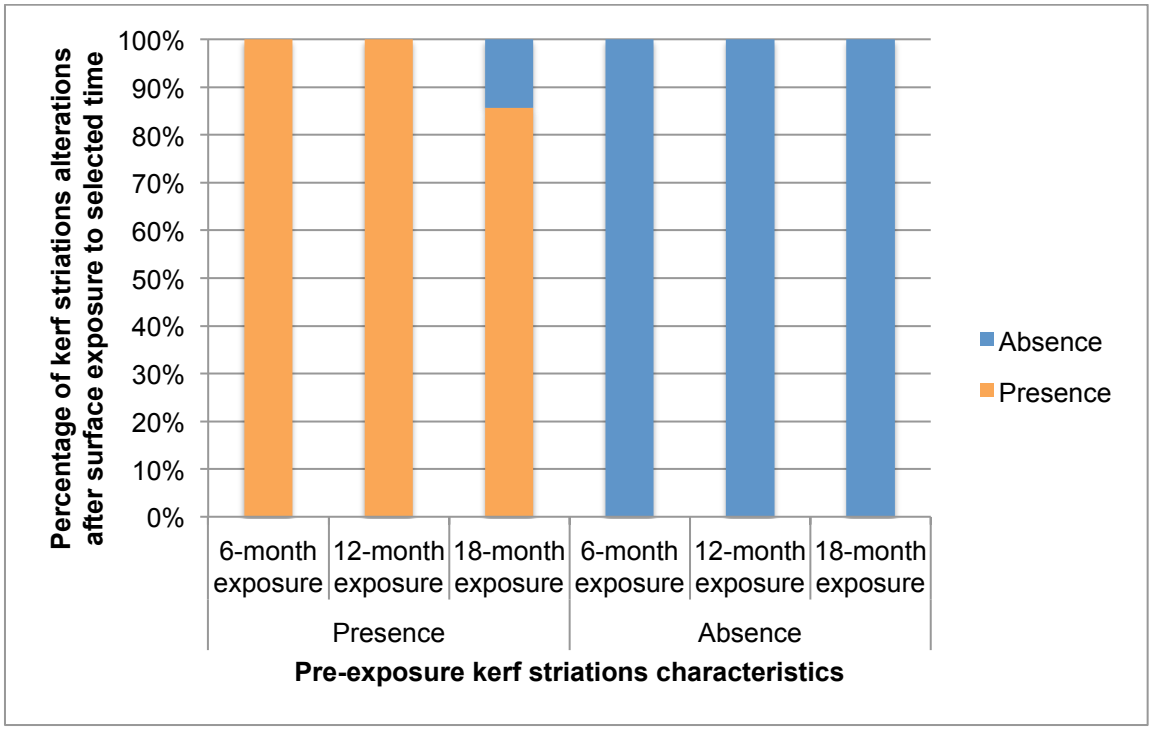

Figure 5.37: Percentage of change of striations for each buried group of cut marks inflicted by a coarse-serrated knife

The statistical significance of kerf morphology was observed comparing between pre- and post-environmental buried exposure (Table 5.F in APPENDIX 5). There was no statistical significance observed in the morphological change of kerf shape of coarse-serrated blade cut marks from buried environmental exposure ($p>0.05$). In sum, the effect of buried taphonomic alterations showed no potential to modify evidence of coarse-serrated blade cut mark morphology at 18 months.

5.1.2.3 Fine-serrated knife blade group

5.1.2.3.1 Surface-deposited rib samples

5.1.2.3.1.1 Dimensional change

Figures 5.38 and Table 5.G in APPENDIX 5 demonstrate changes in kerf length and width of the fine-serrated blade cut marks in the surface group after environmental exposure. The average length differences between pre and post-

exposure values are 0.1936 mm, 0.5872 mm, and 0.8629 mm for 6-months exposure, 12-months exposure, and 18-months exposure respectively. The overall width differences between pre and post-exposure value are 0.024 mm, 0.026 mm, and 0.037 mm for 6-months exposure, 12-months exposure, and 18-months exposure respectively. Remarkably, there was no statistical significance of length and width between the same sample between the pre-exposure and the environmental-exposure data (Table 5.H in APPENDIX 5).

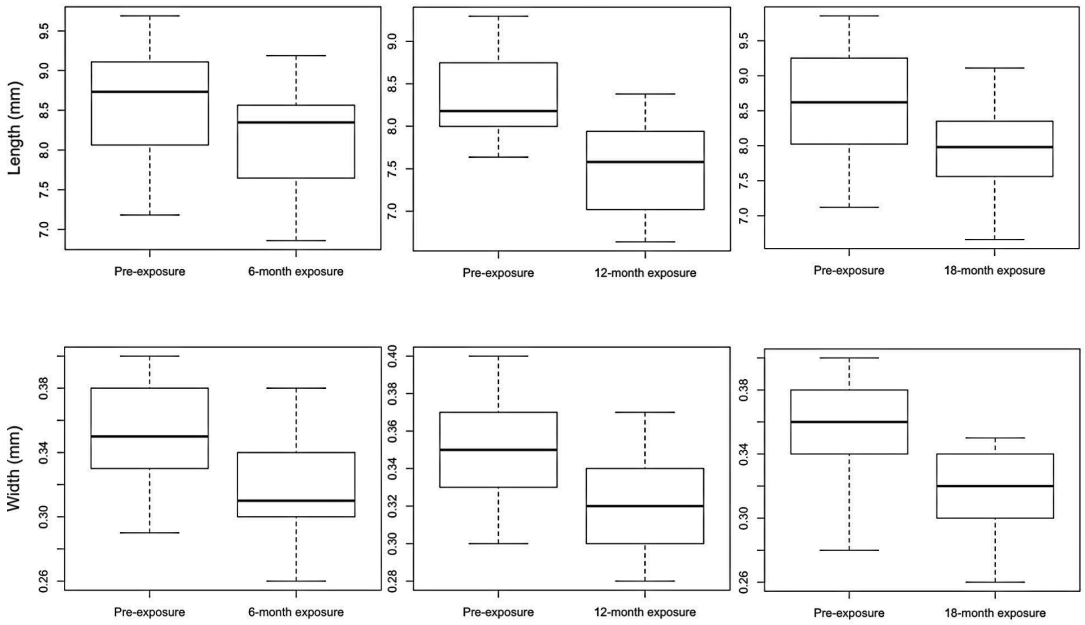

Figure 5.38: Observed length and width difference of surface-deposited fine-serrated blade cut marks; each group n=10

A sequential decrease in dimensions was observed in each post-exposure group, and so a subset of dimensional alterations was explored to compare between groups (Table 5.12). Additionally, Figure 5.39 demonstrates the correlation of kerf length and width changes comparing between pre-exposure and three ranges of environmental exposure.

Table 5.12: Dimensional changes of the same fine-serrated blade cut marks after exposure to surface environment for six, twelve, and eighteen months

Dimension	Alterations	Number of samples (%); (each group: n=10)		
		6-months	12-months	18-months
Length	Increase	3 (30)	-	-
	Decrease	7 (70)	10 (100)	10 (100)
Width	Increase	1 (10)	-	-
	Decrease	9 (90)	9 (90)	10 (100)
	No change	-	1 (10)	-

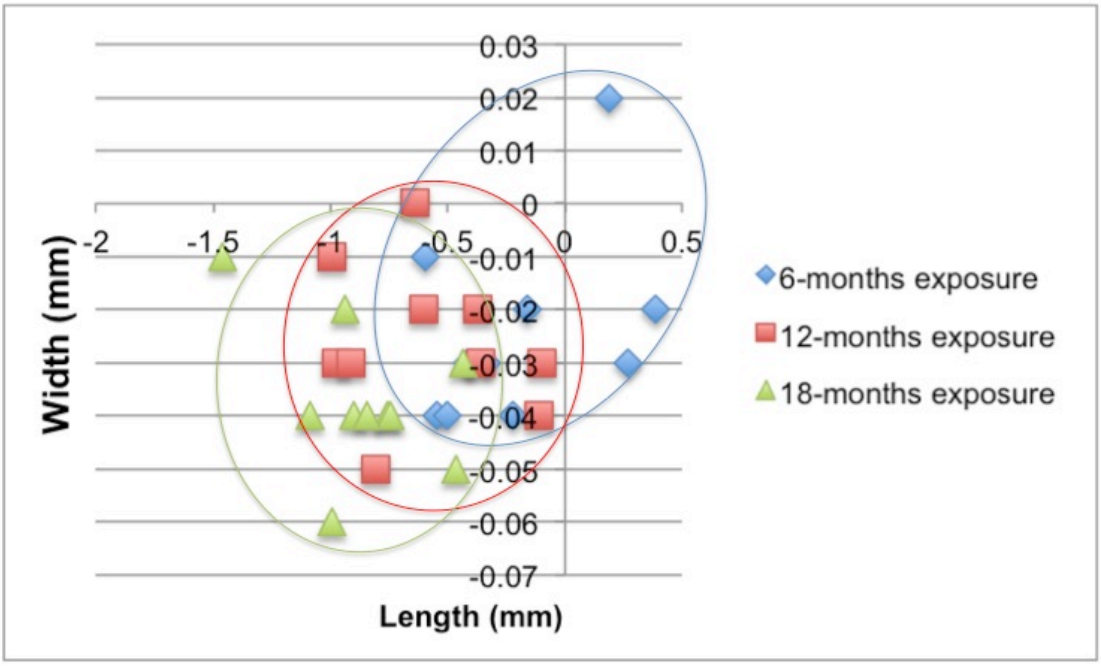

Figure 5.39: Demonstrating dimensional change comparing of kerf length and width of surface-deposited fine-serrated blade cut marks; each group n=10

Almost dimensional value gathered in a group. However, they can solely be discriminatory with their distributions. 12-months exposure accumulated in the area between 6-months and 18-months exposure (Figure 5.39). There was a decreasing range of maximum length of all cut marks at 12-months of exposure, yet a mixture of no change and decrease in maximum width was observed. As the extent of the exposure period increased, all marks showed a decrease in their maximum length

and width at 18-months surface exposure, with the maximum decrease of 1.461 mm length and 0.06 mm width. Linear regressions were conducted to study the relationship between exposed in the data (Figure 5.40-5.41). Predictive changes of the kerf dimension could be expected from the equation.

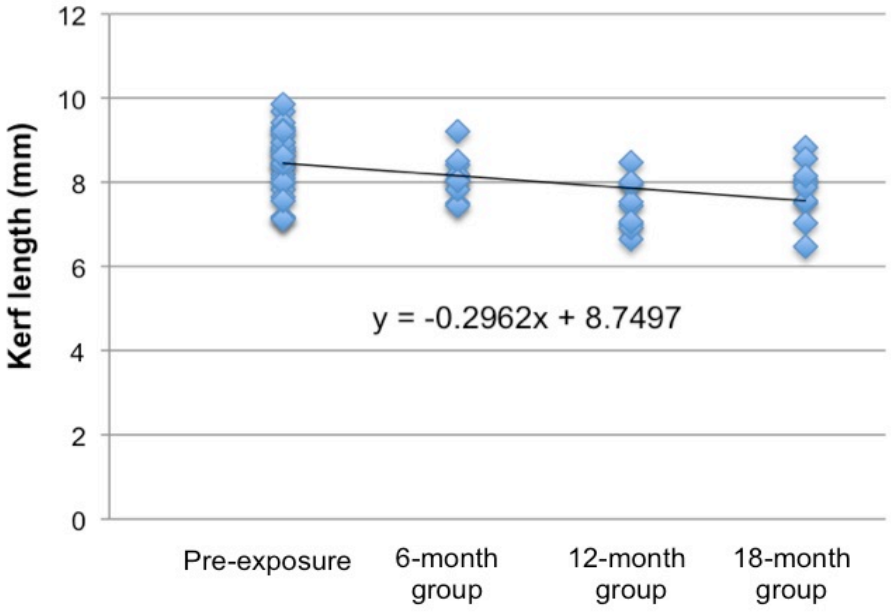

Figure 5.40: The scatter plot with a simple regression equation of kerf length of surface-deposited fine-serrated blade cut marks

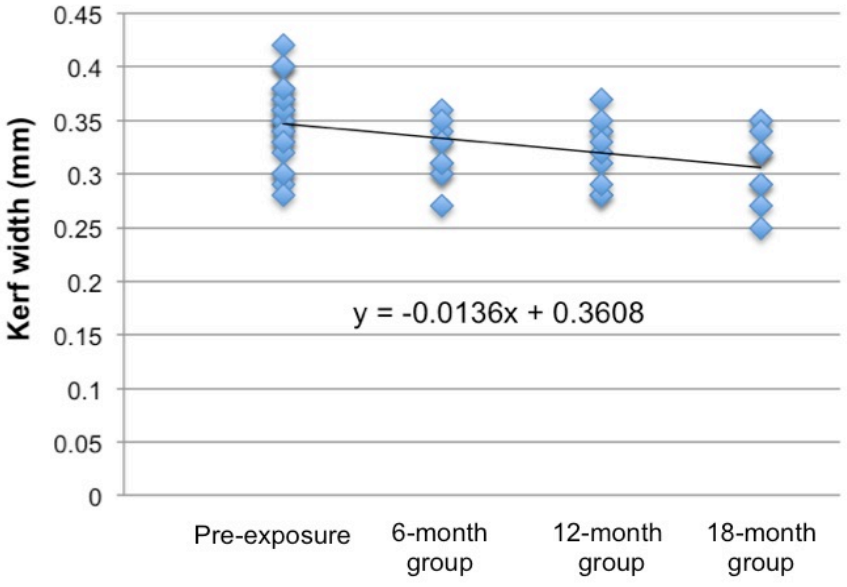

Figure 5.41: The scatter plot with a simple regression equation of kerf width of surface-deposited fine-serrated blade cut marks

5.1.2.3.1.2 Morphological change

Cut mark morphology inflicted by a fine-serrated knife underwent alterations after surface deposition. Table 5.13 shows percentages of kerf morphological changes of each surface-exposure time of cut marks inflicted by a fine-serrated knife, and Figures 5.42-5.45 give more information about how the change of each morphology after surface exposure.

Table 5.13: Summary of frequency data of kerf morphology changes between pre-exposure and post-surface exposure marks from a fine-serrated knife; Pre-E: pre-exposure; Post-E: post-exposure

Kerf morphology		6-months exposure (n=10) (%)		12-months exposure (n=10) (%)		18-months exposure (n=10) (%)	
		Pre-E	Post-E	Pre-E	Post-E	Pre-E	Post-E
Kerf shape	Ellipse	9 (90)	9 (90)	9 (90)	7 (70)	9 (90)	5 (50)
	Rectangle	0 (0)	0 (0)	0 (0)	2 (20)	0 (0)	2 (20)
	Irregular	1 (10)	1 (10)	1 (10)	1 (10)	1 (10)	3 (30)
Cross-section	V-shaped	9 (90)	9 (90)	9 (90)	8 (80)	10(100)	8 (80)
	U-shaped	1 (10)	1 (10)	1 (10)	2 (20)	0 (0)	2 (20)
Kerf margin	Smooth	7 (70)	7 (70)	7 (70)	7 (70)	6 (60)	7 (70)
	Raising	3 (30)	3 (30)	3 (30)	3 (30)	4 (40)	3 (30)
Striations	Presence	7 (70)	7 (70)	6 (60)	6 (60)	7 (70)	6 (60)
	Absence	3 (30)	3 (30)	4 (40)	4 (40)	3 (30)	4 (40)

Initially, 90% of the cut marks displayed an elliptical shape with V cross-sectional shape. Two-thirds (20 of 30) of cut marks showed smooth margins with the presence of kerf striations. After 12 months of environmental surface exposure, 22% of elliptical marks changed to rectangular marks, while another 22% of the elliptical marks transformed into rectangular and irregular cut marks at 18 months exposure (Figure 5.42). Twenty percent of V-shaped cut marks changed to U-shaped marks after 18-months of surface exposure, while all U-shaped cross-section marks exhibited no specific change after 18-months of surface exposure

(Figure 5.43). The raised edges of cut marks from a fine-serrated blade were more stable with degradation starting at 18-months of surface exposure, while cut marks from a coarse-serrated blade showed degraded margins after just 6 months of surface exposure (Figure 5.44). Kerf striations of cut marks inflicted by a fine-serrated blade were also more durable, with only 14% no longer visible after 18-months of surface exposure (Figure 5.45).

The statistical significance of kerf morphology was observed comparing between pre-exposure and post-environmental surface exposure (Table 5.I in APPENDIX 5). There was no statistical significance observed in the morphological change of kerf shape of fine-serrated blade cut marks from pre and post-buried environmental exposure ($p>0.05$). In sum, 18 months of buried environmental exposure showed no potential to modify evidence of fine-serrated blade cut mark morphology.

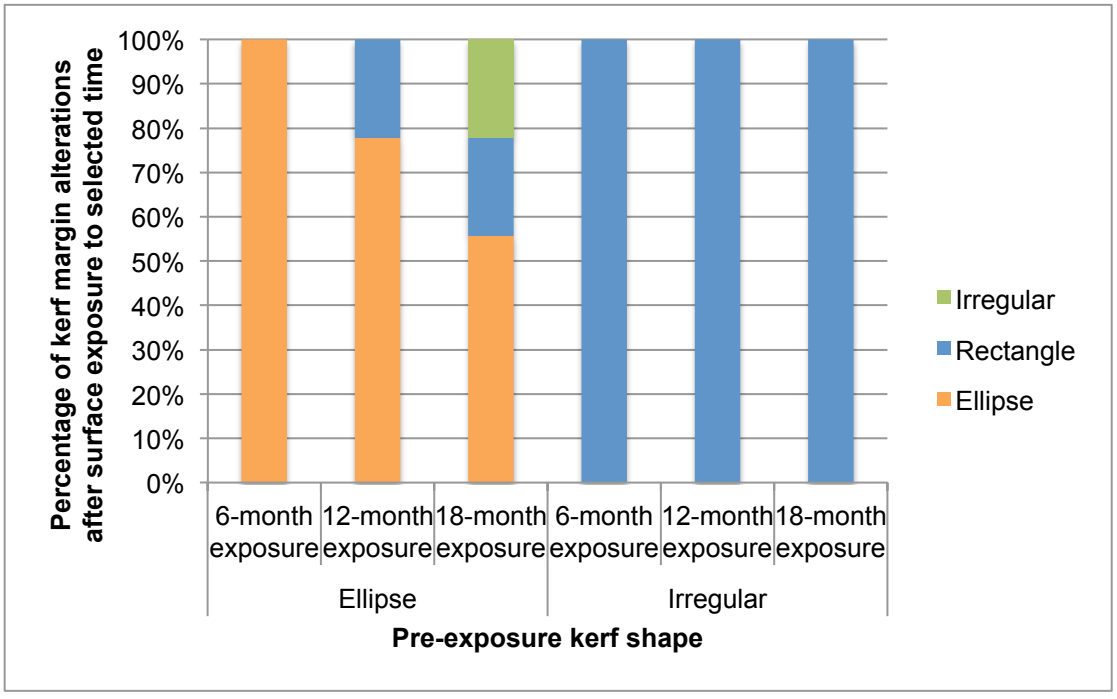

Figure 5.42: Percentage of kerf shape alterations for each surface exposure group of cut marks inflicted by a fine-serrated knife

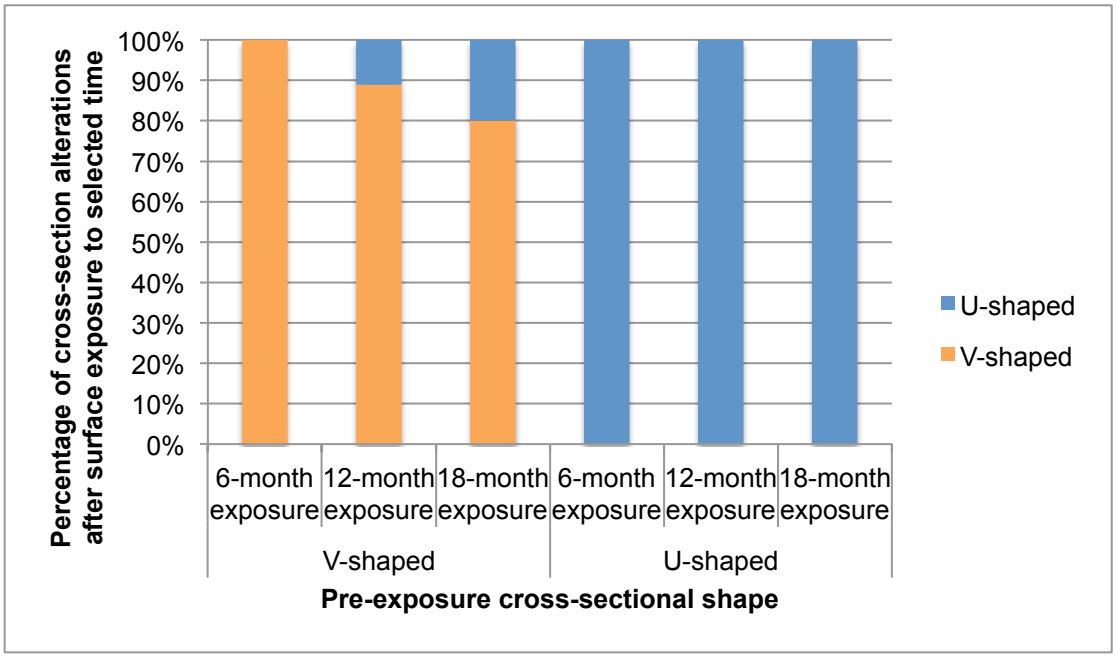

Figure 5.43: Percentage of cross-section shape alterations for each surface exposure group of cut marks inflicted by a fine-serrated knife

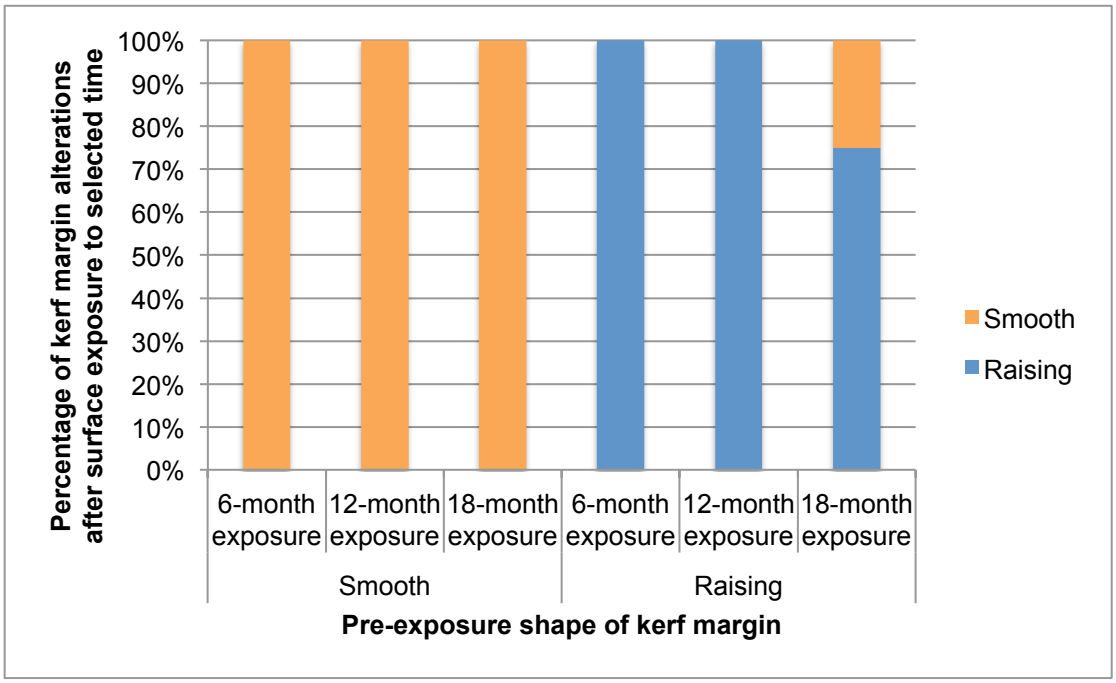

Figure 5.44: Percentage of kerf margin alterations for each surface exposure group of cut marks inflicted by a fine-serrated knife

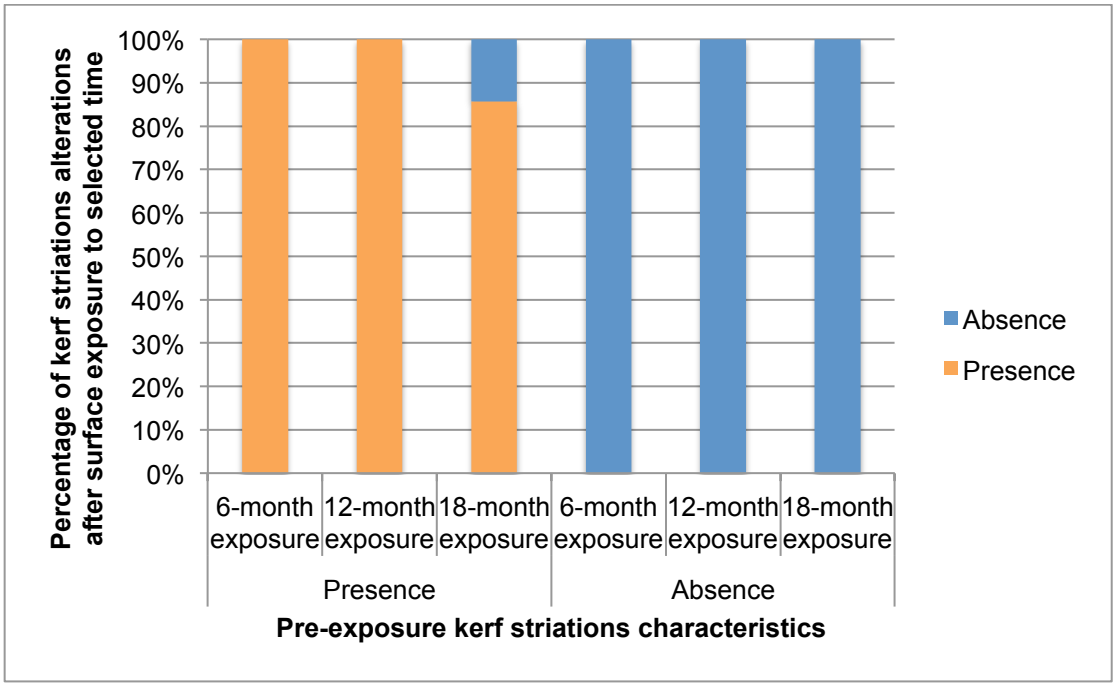

Figure 5.45: Percentage of change of striations for each surface exposure group of cut marks inflicted by a fine-serrated knife

5.1.2.3.2 Buried rib samples

5.1.2.3.2.1 Dimensional change

Figures 5.46 and Table 5.G in APPENDIX 5 demonstrate changes in kerf length and width of the fine-serrated blade cut marks in the buried group after environmental exposure. Average length differences comparing pre-exposure values of 0.1201 mm, 0.4442 mm, and 0.5666 mm for 6-months exposure, 12-months exposure, and 18-months exposure respectively were observed. The overall width differences comparing with pre-exposure value are 0.014 mm, 0.016 mm, and 0.032 mm for 6-months exposure, 12-months exposure, and 18-months exposure respectively. Remarkably, there was no statistical significance of both length and width comparing the same sample between the pre and post-environmental exposure data (Table 5.H in APPENDIX 5).

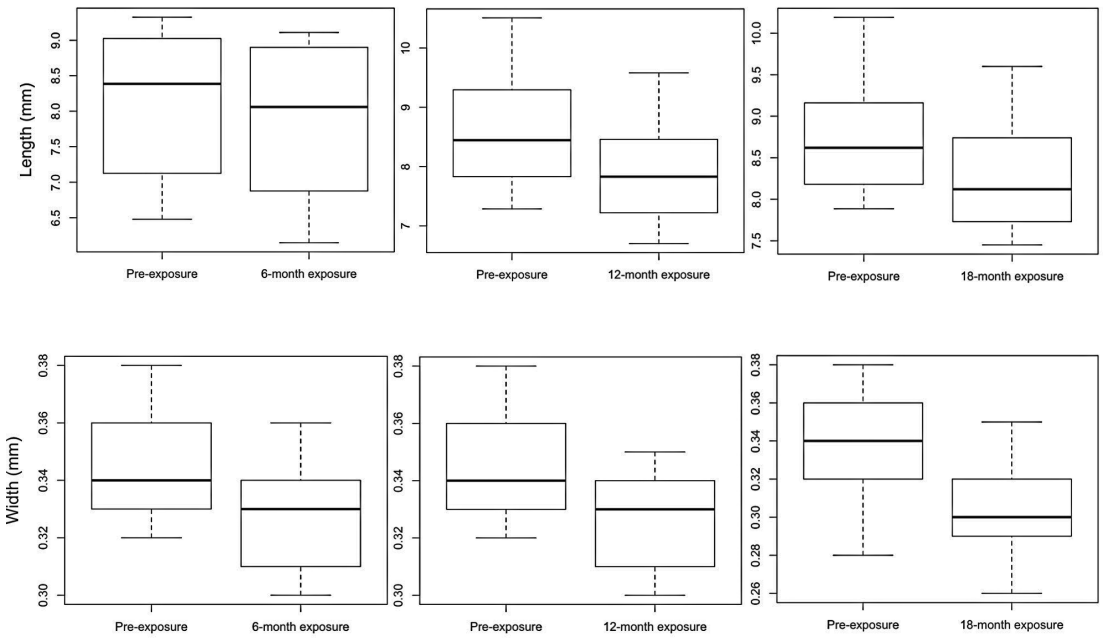

Figure 5.46: Observed width difference of buried fine-serrated blade cut marks; each group n=10

A sequential decrease in dimension was observed in each post-exposure group, and a subset of dimensional alterations was explored in-depth to compare between each group (Table 5.14). Additionally, Figure 5.47 demonstrates more intensive profiles of correlation of kerf length and width changes comparing between pre and post-environmental exposure. The widest distribution in values was observed in the maximum length and width at 12-months of buried exposure. All samples showed decreases in length and width at 18-months buried exposure. Most cut mark dimensions in the buried group displayed slower decreases and only a slight decrease in the maximum width compared to the surface group, with the maximum decrease of 1.146 mm in length and 0.05 mm in width. Linear regressions were conducted to study the relationship between exposed in the data (Figure 5.48-5.49). Predictive changes of the kerf dimension could be expected from the equation.

Table 5.14: Dimensional changes of the same fine-serrated blade cut marks after exposure to buried environment for six, twelve, and eighteen months

Dimension	Alterations	Number of samples (%); (each group: n=10)		
		6-months	12-months	18-months
Length	Increase	4 (40)	2 (20)	-
	Decrease	6 (60)	8 (80)	10 (100)
	No change	-	-	-
Width	Increase	2 (20)	1 (10)	-
	Decrease	8 (80)	8 (80)	10 (100)
	No change	-	1 (10)	-

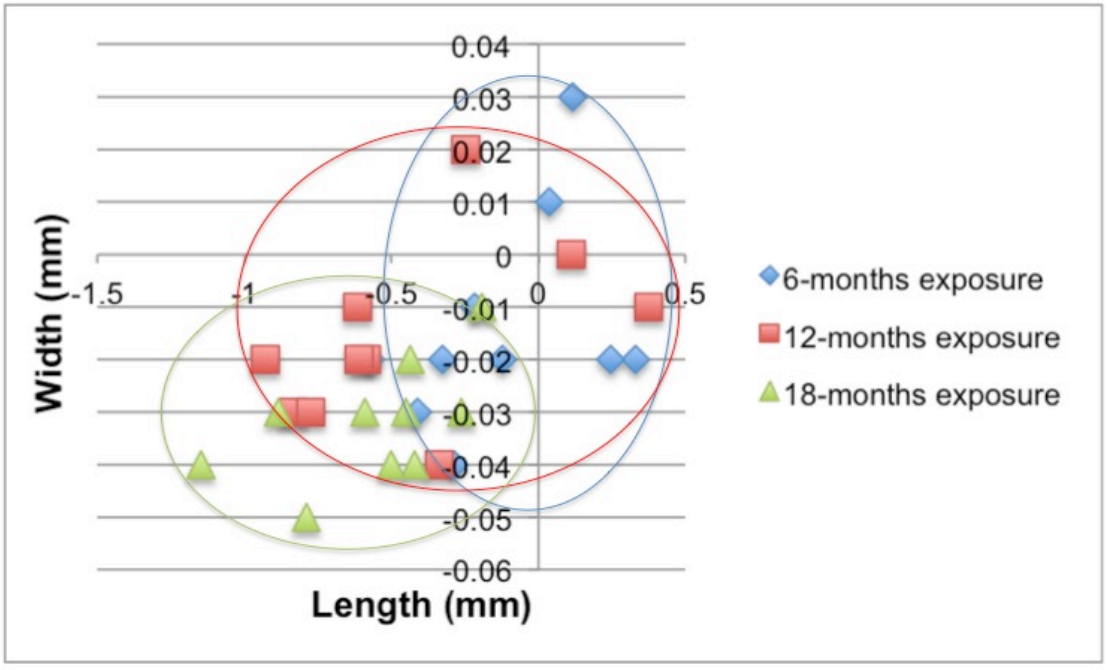

Figure 5.47: Demonstrating dimensional change comparing of kerf length and width of buried fine-serrated blade cut marks; each group n=10

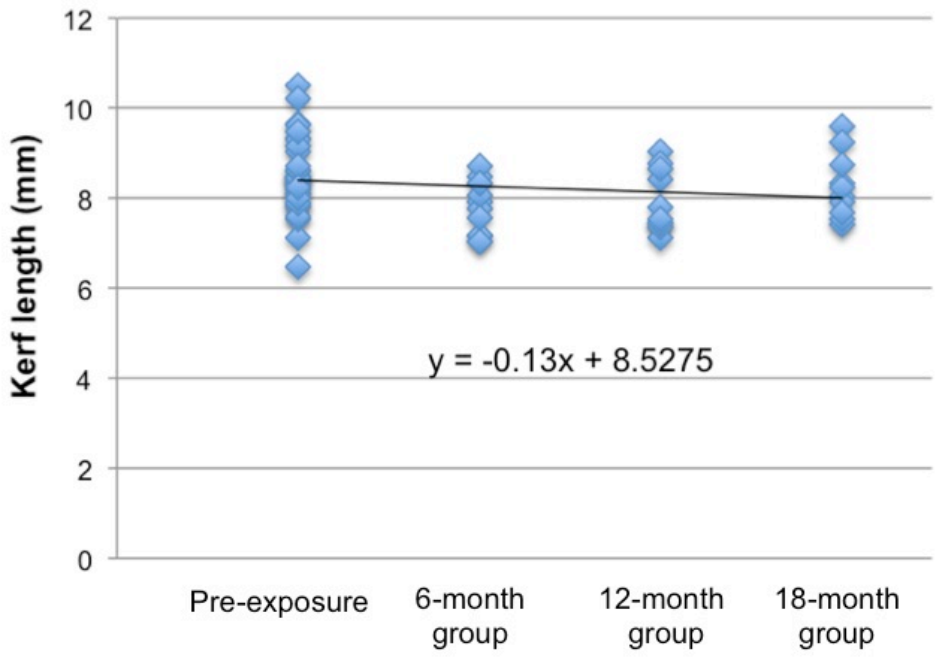

Figure 5.48: The scatter plot with a simple regression equation of kerf length of buried fine-serrated blade cut marks

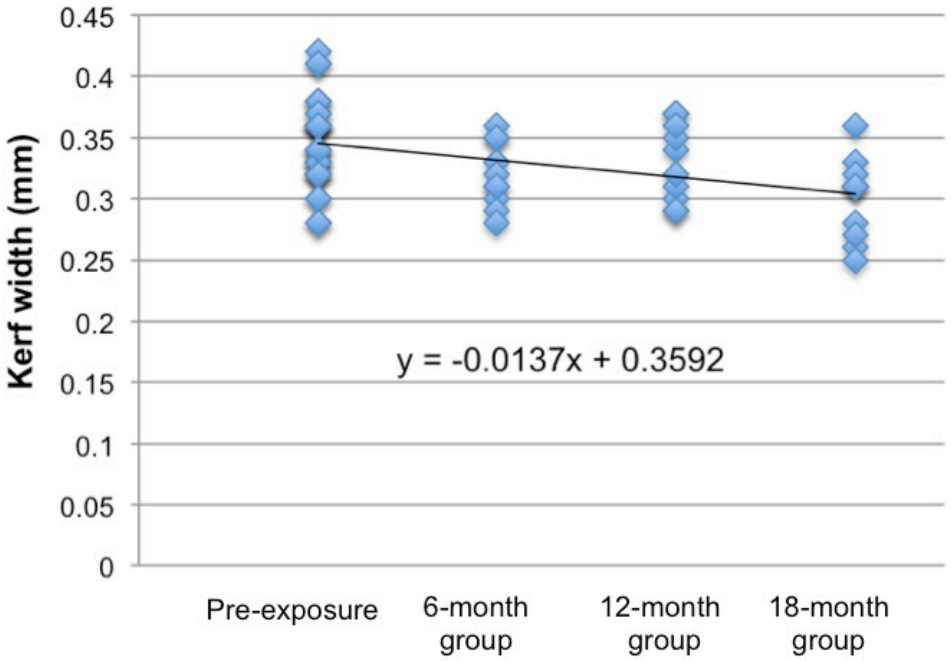

Figure 5.49: The scatter plot with a simple regression equation of kerf width of buried fine-serrated blade cut marks

5.1.2.3.2.2 Morphological change

Cut mark morphology inflicted by a fine-serrated knife underwent some alterations after buried deposition. Table 5.15 summarises percentages of kerf morphological changes of each burial time of cut marks inflicted by a fine-serrated knife, and Figures 5.50-5.53 gives more information about how the change of each morphology after surface exposure.

Table 5.15: Summary of frequency data of morphology changes between pre- (Pre-E) and post-burial exposure (Post-E) marks from a fine-serrated knife

Kerf morphology		6-months exposure (n=10) (%)		12-months exposure (n=10) (%)		18-months exposure (n=10) (%)	
		Pre-E	Post-E	Pre-E	Post-E	Pre-E	Post-E
Kerf shape	Ellipse	8 (80)	8 (80)	9 (90)	7 (70)	8 (80)	5 (50)
	Rectangle	0 (0)	0 (0)	0 (0)	2 (20)	0 (0)	2 (20)
	Irregular	2 (20)	2 (20)	1 (10)	1 (10)	2 (20)	3 (30)
Cross-section	V-shaped	8 (80)	8 (80)	9 (90)	8 (80)	9 (90)	8 (80)
	U-shaped	2 (20)	2 (20)	1 (10)	2 (20)	1 (10)	2 (20)
Kerf margin	Smooth	8 (80)	8 (80)	6 (60)	6 (60)	6 (60)	7 (70)
	Raising	2 (20)	2 (20)	4 (40)	4 (40)	4 (40)	3 (30)
Striations	Presence	6 (60)	6 (60)	6 (60)	6 (60)	8 (80)	6 (60)
	Absence	4 (40)	4 (40)	4 (40)	4 (40)	2 (20)	4 (40)

As with the surface-exposure group, 83.3% (25 of 30) of cut marks displayed an elliptical shape with V cross-sectional shape. Around 67% (20 of 30) showed smooth margins with the presence of kerf striations. After 12 months of buried environmental exposure, 22.2% of elliptical marks changed to rectangular marks, while some of the elliptical marks transformed into rectangular (12.5%) and irregular (25%) cut marks at 18 months of buried exposure. Nonetheless, there was no change of rectangular kerf shape in 18-months buried exposure group (Figure 5.50). Only 11.1% of V-shaped cross-section cut marks changed to a U-shaped cross-section in 12 and 18-months buried exposure (Figure 5.51). Additionally, 25%

of samples with raised margins became smooth margin after 18-months of buried exposure (Figure 5.52), while 25% of kerf striations disappeared in the same interval (Figure 5.53).

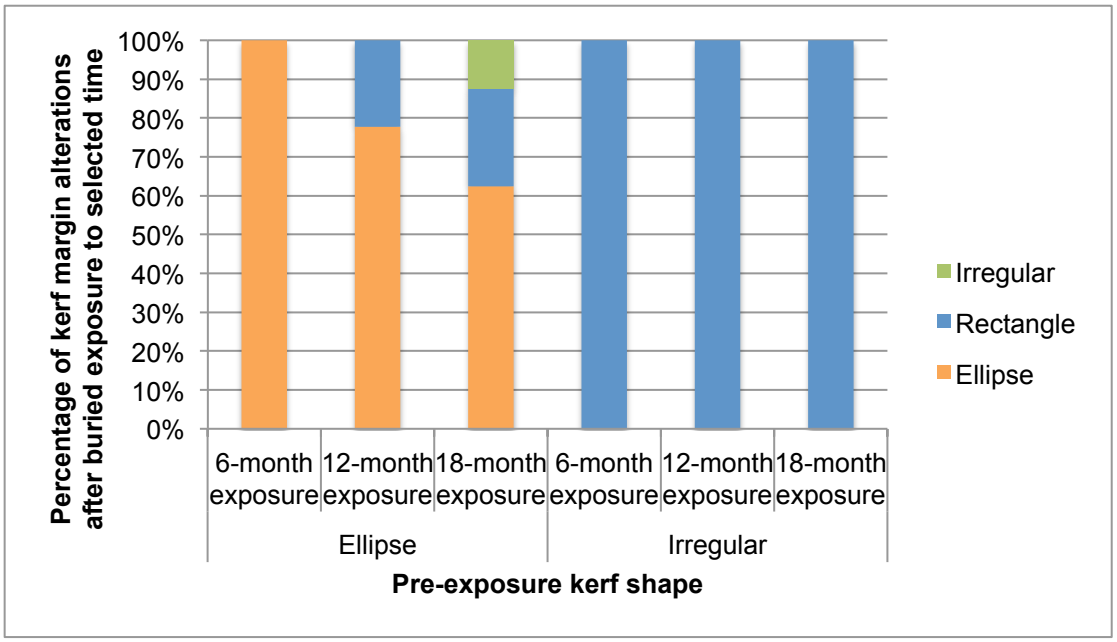

Figure 5.50: Percentage of kerf shape alterations for each buried group of cut marks inflicted by a fine-serrated knife

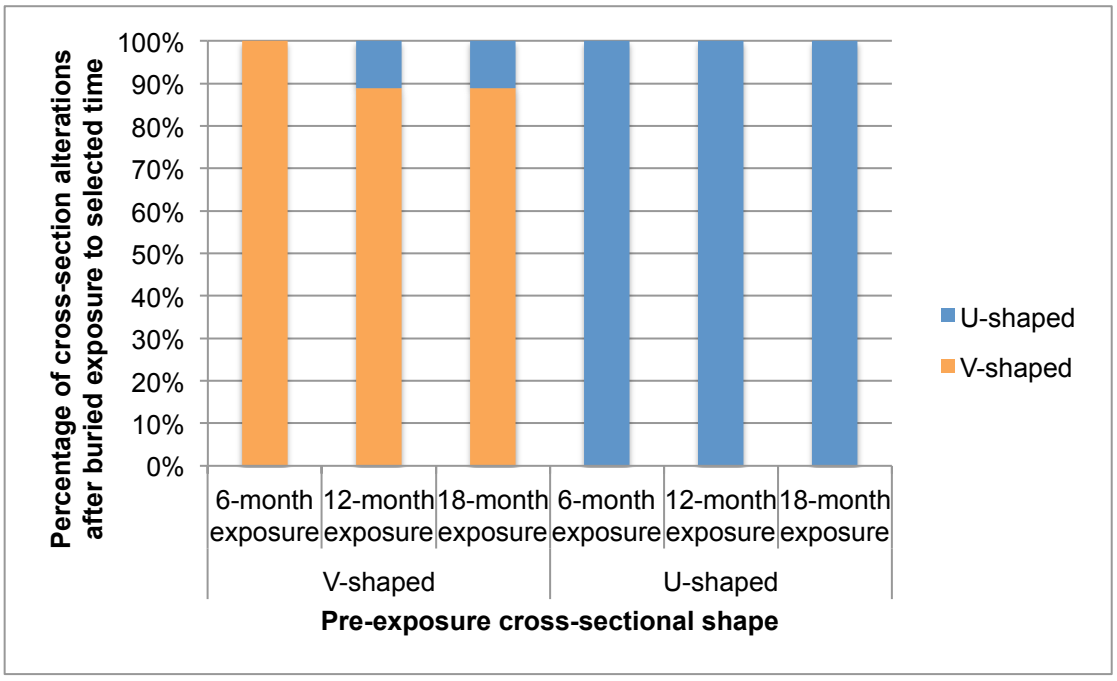

Figure 5.51: Percentage of cross-section shape alterations for each buried group of cut marks inflicted by a fine-serrated knife

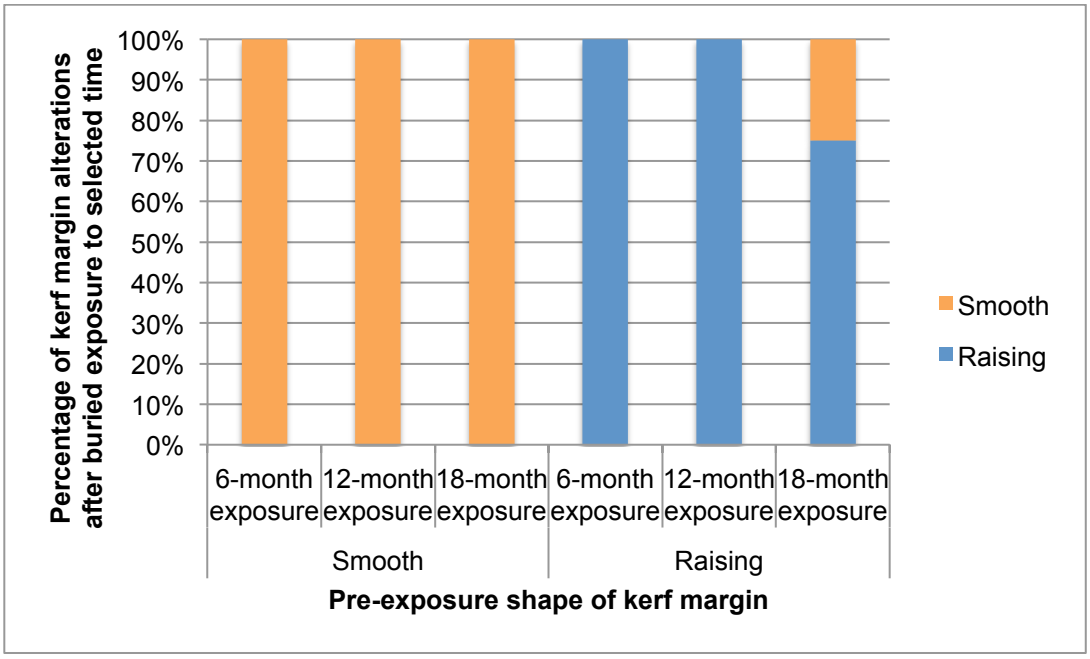

Figure 5.52: Percentage of kerf margin alterations for each buried group of cut marks inflicted by a fine-serrated knife

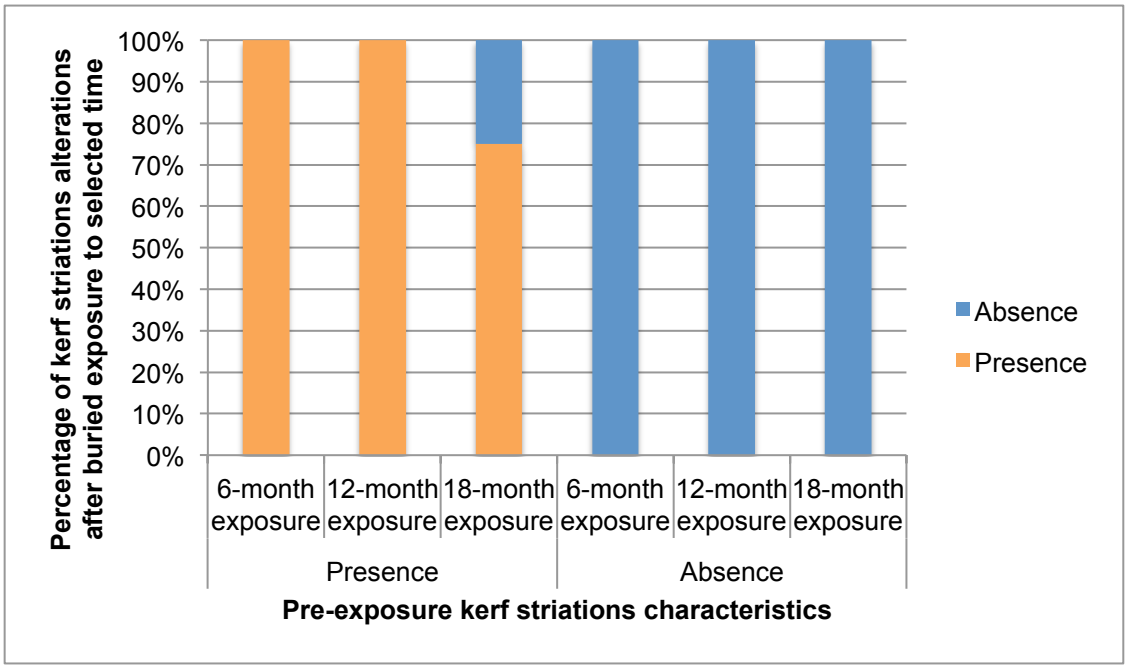

Figure 5.53: Percentage of change of striations for each buried group of cut marks inflicted by a fine-serrated knife

The statistical significance of kerf morphology was observed comparing between pre and post-environmental buried exposure (Table 5.I in APPENDIX 5).

There was no statistical significance observed in a morphological change of kerf shape of fine-serrated blade cut marks after buried environmental exposure ($p>0.05$). In sum, 18 months of burial exposure showed no potential to modify evidence of fine-serrated blade cut mark morphology.

5.1.3 Summary

Surface-deposited samples underwent higher rates of degradation, with the most significant changes in the coarse-serrated group. The pattern of alterations was manifested by dimensional changes in each group of cut marks. Repeated analysis after increased periods of environmental exposure revealed an average shrinkage of the kerf length and width, and a slower rate in buried samples.

Variance of cut mark morphology following environmental exposures was identified. Within each knife type group, a change of the kerf shape could be expected. The linear shape of cut marks made from non-serrated blades tended to change to an elliptical or rectangular shape. The elliptical shape of the cut marks inflicted by coarse-serrated blades tended to become irregular. Lastly, the elliptical shape of the cut marks from fine-serrated blades was likely to change to a rectangular or irregular shape. From a cross-sectional perspective, the shape usually changed to a larger space between the inner kerf walls, while the raised borders of the kerf margin typically eroded after environmental exposure. Kerf striations are likely to disappear after a longer durations of exposure. However, there were no statistical associations ($p>0.05$) identified between pre and post-exposure to the outdoor environment. Therefore, forensic anthropologists are able to confidently investigate cut marks in their practice, but they should keep in mind that dynamic variability of dimension and morphology may occur.

5.2 Discussion

In this study, 180 cut marks were generated under more real-world conditions using manual infliction by human forces. This made the cut marks variable in size and shape even though the same knife and person made them. This is in line with Ferllini (2012) and Norman *et al.* (2018) simulated real-world cases. This study attempted to simulate as many factors relevant to real-world injuries as possible.

For instance, the source of the knives used in this study was representative of the typical knife type used in cases of violence. Hunt and Cowling (1991) stated that a kitchen knife is the most common weapon used in fatal cut and stabbing incidents because it is easily purchased, pocketed, and disposed of. Other sharp force trauma studies usually created cut marks from newly purchased kitchen knives because of these have fewer blade defects (Bello and Soligo, 2008; Ferllini, 2012; Tegtmeyer, 2012; Norman *et al.*, 2018).

A variety of cut mark dimensions and morphologies may be encountered when using different knife blade types and manual operators. No knife type can repeatedly produce exactly the same cut mark dimension and morphology (Norman *et al.*, 2018). Real-world situations such as soft tissue coverage, bone properties, and knife structure make identification of the knife type difficult. Another consideration is the variation caused by human operators such as the uncontrolled force and angle of weapon infliction to the bone. The introduction of different researchers using the same weapon may result in different cut mark dimensions and morphologies. In addition, while the force with which the cut marks were made was held constant to the greatest degree possible, there was some variation from bone to bone. Even though this event is likely to be more realistic in mimicking true cutting actions, this variability may have influenced the expression of the trauma characteristics in this study. Future studies should take this into account when selecting either human forces or mechanical apparatus to inflict trauma.

The effects of the soft tissue removal process on cut marks should also be considered because the maceration process can damage fragile cut marks. Appropriate maceration techniques should not compromise the bone sample's integrity and morphology or result in the destruction of traumatic evidence (Fenton *et al.* 2003; King and Birch, 2015). The most suitable technique may be dependent on the specific case or situation. The current study aimed to investigate the effects of environmental exposure on cut marks, and so techniques that could impact bone structure and cut mark morphology were avoided. The most appropriate maceration technique should preserve fragile cut marks and not have any effect on bone structure. Although the most effective method in a 2015 study by King and Birch was the microwave oven, its effects on the bone structure and its taphonomic changes

are unclear, and the limitation of experimental resource in this study is also problematic. As a result, manual maceration, as the researcher removed almost soft tissues and periosteum before starting traumatic events, was chosen for this study because it has the least effect on cut marks and bone structure, despite requiring considerable time and the inevitable soft tissues that remain (King and Birch, 2015).

The investigation of the observed cut mark characteristics in juvenile bone samples in the current study should be carefully considered in a minimal fashion. Juvenile skeletal materials have different bone composition, with more inherently elastic and less mineralized mass than adult bone (Kalkwarf *et al.*, 2007). This pliable bone allows greater dimensional changes as a result of the loss of organic matter and moisture during environmental exposure (Cunningham *et al.* 2011). In addition, the ribs of juvenile pigs are less calcified and more flexible and less resistant to cutting than adult ribs (Kalkwarf *et al.*, 2007; Kooi and Fairgrieve, 2013). Therefore, the obtained results using pig bones may not be representative of adult human bones.

5.2.1 Comparison of cut marks between different types of knife

The knife cut mark morphology described here is in general agreement with other literature (Bromage and Boyde, 1984; Boschin and Crezzini, 2012; Cerutti *et al.*, 2016; Komo and Grassberger, 2018). Profiles of cut marks inflicted with a non-serrated knife exhibited linear, narrow cross-sections, smooth kerf margins, and an absence of striation. In contrast, the profiles of cut marks inflicted by a coarse-serrated knife typically had an elliptical shape with a V or U-shaped cross-section, raised or smooth margins, and were more often striated. Fine-serrated blade knives typically produced elliptical V-shaped cross-sections with smooth or raised margins and were more often striated.

5.2.1.1 Kerf dimension

A determination of blade type from a bone dimension has been challenged. Basically, Cut marks from serrated blades tend to be wider than those from non-serrated blades (Tegtmeyer, 2012; Capuani *et al.,* 2014; Komo and Grassberger, 2018). This study demonstrated a statistically significant difference ($p<0.001$) in the

kerf width between non-serrated and serrated cut marks (Table 5.2). This result showed that it might be possible to differentiate between non-serrated, coarse-serrated and fine-serrated blades. However, this study indicated there was a total overlap of width data between the coarse-serrated and fine-serrated blade groups, but this overlap was not found between non-serrated and serrated groups (Figure 5.5).

In principle, the width of a cut mark should correspond to the thickness of the blade edge. However, this study found that the cut mark width tends to be narrower than the knife blade that caused it. This finding may be due to elastic nature of skeletal bone. The sharp edge cuts into the skeletal material and the bone tissue adjacent to the cutting tract is compressed to the sides. When the knife blade is withdrawn, the fresh bone has a tendency to return to the nearest point of its original position. However, sometimes a blade can leave a wider cut mark according to the angle of impact (Cerutti *et al.,* 2014) and force applied (Humphrey *et al.*, 2017). Therefore, using the kerf width cannot be used to reliably identify the weapon type (Cerutti et al. 2014; Maples et al. 1989; McCardle and Lyons 2015). Furthermore, Bartelink *et al.* (2001) noted that the kerf measurements could not be used for weapon identification because there was too much overlap between each type of weapon. Further work should involve many more types of blade classes in order to determine if kerf width has the potential to help identify the weapon type.

Cut mark length made by different blade types tended to overlap. Therefore, it was not possible to determine the blade type according to the length of the cut mark. Theoretically, the kerf length is influenced by the direction of the blade. Cuts delivered from above have shorter lengths because only a small part of the blade actually penetrates the bones. Other factors that influence cut mark length including bone morphology and the force and speed of the cut were also described (Bello and Soligo, 2008; Humphrey, *et al.*, 2017). Therefore, no straight correlation between the kerf length and a weapon class has been illustrated.

5.2.1.2 Kerf morphology

Several different kerf shapes were observed including linear, elliptical, rectangular, and irregular shape. Significant associations between type of knife and

kerf shape were recorded in this study. All cut marks inflicted by non-serrated blades exhibited a linear kerf shape. Fine-serrated blades produced elliptical shape most frequently (90%), while coarse-serrated blades yielded an ellipse-shaped kerf in 75% of samples. Significant Fisher's exact tests ($p<0.01$) indicate that kerf shape is relatively specific to the knife class (Table 5.2). The shape of the cut marks is dependent on the size and morphology of the knife blade. While larger serrated blade can make a variety of kerf shapes, a non-serrated knife with a narrow blade can create only linear-shaped cut marks. The small teeth of a fine-serrated blade make good contact when cutting through the bone surface, resulting in consistently elliptical shaped cut marks. Coarse-serrated blades with larger teeth have greater penetrating power and typically produce elliptical and rectangular kerf shapes.

The size of the cross-sectional shape of a cut mark varies depending on the size and shape of the knife blade. In this study, the cross-sectional shape had a relationship with the class and blade type. All cut marks inflicted by non-serrated blades exhibited narrow shapes. In 55% of cases, coarse-serrated blades produced V-shaped cut marks, with the remaining 45% having a U shape. Around 90% of cut marks inflicted by fine-serrated blades showed V-shaped cross-sections. Therefore, the coarse-serrated blade produces more irregular cross-sectional shapes than the other blade types, and the non-serrated knife class produces a narrow cross-sectional shape. A V-shaped cross-sectional mark is the most common feature observed in a case of knife cut wound (Potts and Shipman, 1981; Shipman, 1983; Tennick, 2012), and Lewis (2008) recommended using this characteristic to differentiate between knife types. However, Cerutti *et al.* (2016) stated that this pattern cannot be used to distinguish different types of knife blade as any types of knife blade can express a V-shaped pattern. Nevertheless, this feature can be found more frequently in specific types of knife blades. For instance, fine-serrated blades can produce a narrow V-shaped cross-section (Potts and Shipman, 1981; Shipman, 1983; Alunni-Perret *et al.*, 2005; Symes *et al.*, 2010). Thus, the results of this study support these trends to a degree, but it is clear that a wide variety of V shape is still possible. The size of the V-shaped cross-section of cut marks varied depending on the size and shape of the blade (Potts and Shipman, 1981; Alunni-Perret *et al.*, 2005; Symes *et al.*, 2010; Boschin and Crezzini, 2012; Tegtmeyer,

2012; Capuani *et al.,* 2014; Cerutti *et al.,* 2014; Norman *et al.,* 2018). Depth and width of cut marks are also interrelated, with deeper cuts typically also being wider.

The wedge shape of a saw usually leaves a U-shaped cross-sectional mark, and this pattern may be also caused by other broad blade weapons such as stone tools (Potts and Shipman, 1981; Shipman, 1983; Bello *et al.,* 2009; Symes *et al.*, 2010). The coarse-serrated blades used in this study resulted in U-shaped cut marks in 45% of samples and V-shaped marks in the remaining 55%. This finding may be explained by the mechanical cutting motion of this blade. During cutting, the movement of the coarse-serrated blade is similar to a handsaw. As the blade moves freely over the bone surface, it is likely to change in cutting direction or surface skipping when it cuts through the bone tissue. This movement causes variations in the cross-sectional shape and multiple cut marks in only one thrust.

Several cut marks present raising kerf margin where a build-up of ragged and deformed bone appears along the kerf margin. The kerf margin morphology displayed a significant relationship to the cutting edge morphology of the knife blade. The cut marks inflicted by coarse-serrated blades had the highest frequency of raised kerf margins (around 70%), followed by fine-serrated blades (30%). In contrast, non-serrated blades produced only smooth margins. These results are consistent with previous studies demonstrating the prevalence of raised margins from serrated blades (Thompson and Inglis, 2009; Crowder *et al.*, 2011; Tennick, 2012). Raised and irregular kerf margins are likely to be the result of varying blade edge interactions with the bone surface, such as scraping, bouncing and chattering of bone surface that is common with serrated blade teeth (Tennick, 2012). The relative thickness of the blades as well as number and pattern of teeth at the blade edge may also play an important role. The fine-serrated blades are thinner and have many more teeth at their blade edge than the coarse-serrated blades. A much smaller and compact tooth pattern provides better grip on the bone surface, and thus the fine-serrated blades is likely to produce a smoother and more regular kerf margin. In contrast, the coarse-serrated blade with fewer and thicker teeth pattern have a poor grip, leading to produce skip or chatter pattern across the bone surface, resulting in irregular and raised kerf margin (Tennick, 2012).

The presence of blade teeth against the bone surface is likely to leave irregular striations on the kerf walls. The serrated blade was easily distinguishable from non-serrated blade because of their distinct, pattern kerf striations (Crowder *et al.*, 2011; Tennick, 2012). The overwhelming presence of kerf striations in the serrated cut marks and the absence of this feature in the non-serrated cut marks suggest that striations would be useful to identify knife class (Crowder *et al.*, 2011; Tegtmeyer, 2012). Two-thirds (67%) of coarse-serrated and fine-serrated blades showed this feature but there were no striations in any cut marks by non-serrated blades. Therefore, the presence or absence of kerf striations can be useful to determine if a serrated blade was used. Fine-serrated blade teeth interact closely with the bone surface. The fine-serrated blade creates smaller and more delicate striations than coarse-serrated blades. The relative thickness, size and indent of cutting teeth may also have an influence on striations morphology. Consistent with previous works (Tennick, 2012; Komo and Grassberger, 2018), not all cut marks resulting from a serrated blade showed kerf striations.

Identification of striations may be problematic. Bone debris or other artefacts (e.g. soil or plant materials) may lodge in the kerf walls and therefore make striations difficult to identify. Some cut marks inflicted by fine-serrated blades were relatively narrow, making kerf striations more difficult to observe with a light stereomicroscope. The depth of the kerf could also be challenging, as deep cut marks can prevent observations of their floor and make a reliable assessment of kerf striations using a stereomicroscope more difficult. A digital microscope could provide three-dimensional examination and possibly address this problem (Boschin and Crezzini, 2012; Moretti *et al.,* 2015; Boucherie *et al., 2017)*.

5.2.2 Effects of environmental exposure

Bone diagenesis refers to any natural modifications to skeletal remains, that can alter useful archaeological and forensic information, especially structural, chemical, and molecular evidence (Hedges, 2002; Smith, 2002; Boaks *et al.*, 2014; Kendall *et al.*, 2018). To date, research into an effect of taphonomic factors on skeletal cut marks has been limited. More studies are needed to investigate whether environmental conditions can make an important difference in cut mark

morphology. Therefore, this study focuses on the possible variability of sharp force lesions due to the gradual decay of skeletal materials with time.

After environmental exposure, all cut marks in this study remained recognisable and there were no macroscopic change to overall morphology following either surface or buried exposure. Cappella *et al.* (2014) noted that sharp force injuries were quickly and easily macroscopically identifiable even after almost 15 years of inhumation. There are many potential causes for bone surface and traumatic lesion modifications at a depositional site. Biological, chemical and physical agents are able to modify skeletal materials. These modifications can be also interpreted by investigations of observed processes produced by recognisable agents acting on previously unmodified traumatic lesions (Symes *et al.*, 2002; Cappella *et al.*, 2014). Bone surface alterations such as erosion, cracking and shrinkage have the most potential to affect cut marks due to the loss of water and organic matter from the bone materials. Microscopically, the cracked surface shows the appearance of being torn apart, with longitudinal and lateral displacement of surface tissue (Figure 5.54). Extensive erosion and cracking develop with time and temperature. Cracking can also be the result of other specific agents, such as animal digestion and chemical degradation (White and Hannus, 1983; Fisher, 1995; Nielsen-Marsh *et al.*, 2000; Turner-Walker, 2008).

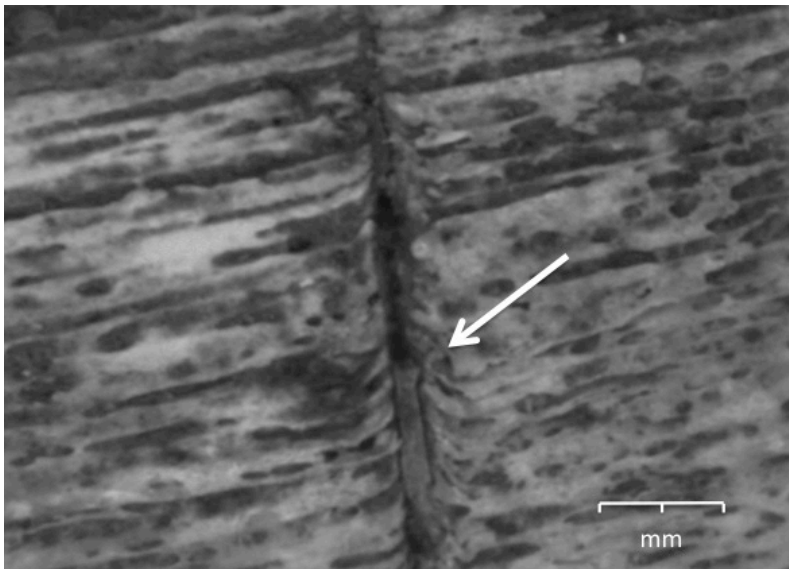

Figure 5.54: Cracking and the cut mark after 18-months surface exposure; the white arrow indicates an irregular kerf margin

The depositional environment has a great influence on the rate of bone degradation. Different environments have broad differences in temperature, precipitation, vegetation, and snow cover (Behrensmeyer, 1978; Junod and Pokines, 2014). The reduced rate of decomposition of buried remains is well recognised and could be attributed to the soil environment. Soil can provide an effective barrier to temperature fluctuation and solar radiation (Rodriguez, 1997). Soil pH also plays a key role in bone diagenesis, as bone cannot survive long term in highly corrosive soils (Gordon and Buikstra, 1981). However, the bone samples in this study were deposited in a more benign, mild acidic soil. Therefore, a slower rate of dimensional and morphological changes was observed in buried samples.

5.2.2.1 Dimensional changes of the cut marks

A number of reports in the taphonomic literature have concluded that multiple factors have an effect on the level of bone conservation, and that the fate of a bone sample is site-dependent (Collins *et al.*, 2002). The species, age at death, cause of death and form of depositional environment play an important role in diagenetic process (Boak *et al.,* 2014). Basically, the width of a cut mark is dependent on the size and shape of the blade edge, the depth to which the cut mark penetrates, and the raw material used, as discussed earlier. Repeatable methods were used to explore and interpret the effects of environmental exposure on cut marks. Subsequent reanalysis after environmental exposure revealed a mixture of enlargement and shrinkage of the maximum length and width. However, pre and post-environmental exposure dimensional changes of the cut marks were not statistically significant.

The difference between the maximum length and width of cut marks before and after environmental exposure could be explained by the contraction of collagen fibres in the lengthwise direction due to loss of bone moisture and collagen degradation over time. Several studies have been able to verify this phenomenon (van Klinken and Hedges, 1995; Bell *et al.*, 1996; Nielsen-Marsh and Hedges, 2000; Collins *et al.*, 2002; Hedges, 2002). Boaks *et al.* (2014) demonstrated that the significant loss of collagen started at the periosteal surface. This pattern of degradation is consistent with the process of bacterial attacks from depositional environment and decomposition process. Bone surfaces are also subject to

interaction with various extrinsic factors, including temperature, soil pH, and precipitation (Bell *et al.*, 1996; Nielsen-Marsh and Hedges, 2000; Collins *et al.*, 2002; Hedges, 2002).

During the first six months of exposure, a few cut marks exhibited an increase in their length and width. This phenomenon was most often encountered in the non-serrated blade group, especially with X-shaped cut marks. This suggests that differently shaped cut marks inflicted by the same knife may respond differently to environmental factors. This may be due to variations in the angle of impact or bone density at the impact site. Further comparative work is required to generate a comprehensive analysis specific to different morphologies of the cut mark using the same type of knife blade.

While the dimensional change took place over the course of the 18 months studied, the most significant changes in cut mark dimensions took place after the first 6 months of surface exposure (Figure 5.55-5.56). This pattern was inconsistent with the conclusions put forth by Bell *et al.* (1996), Boak *et al.* (2014) and Gutierrez (2001) who suggested that the highest level of bone protein degradation happened during the early postmortem phase. Bell *et al.* (1996) explained that decomposed soft tissues surround bone structure in this period and a bacteria-rich environment promotes surface bone protein degradation. Beyond this period, bone proteins continue to degrade but at a slower and more uneven rate. However, the manual maceration technique of this study might allow bone samples to skip processes of soft tissue decomposition, making skeletal tissues not significant change as expected in the first six months. In addition, during the first six months of this study was the time of near-freezing temperature of autumn and winter. This may have slowed bacterial growth and bone degradation over the time intervals as was expected. This environmental slowing effect was also observed during the 12-18 months period of this study (September 2017 – February 2018).

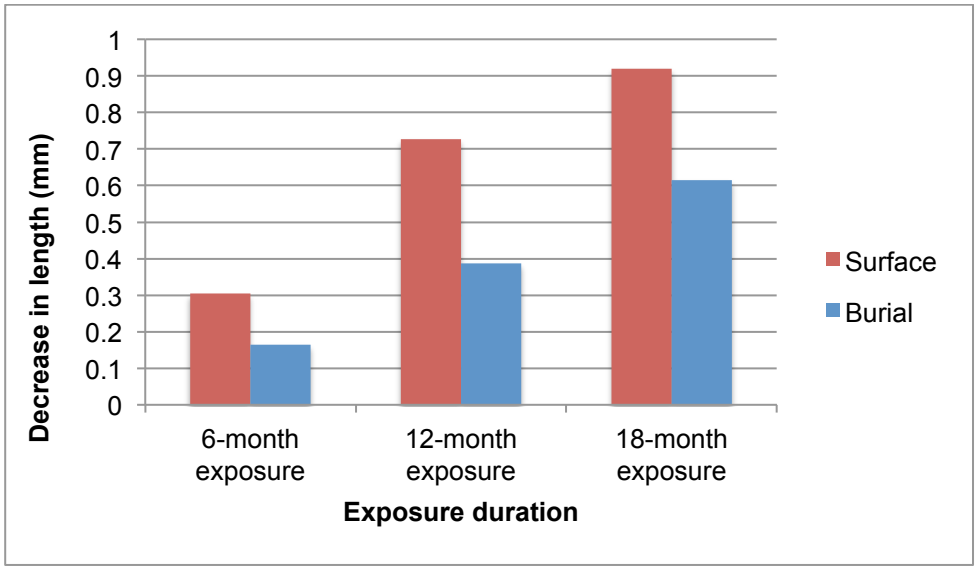

Figure 5.55: Reduction in the maximum length over time

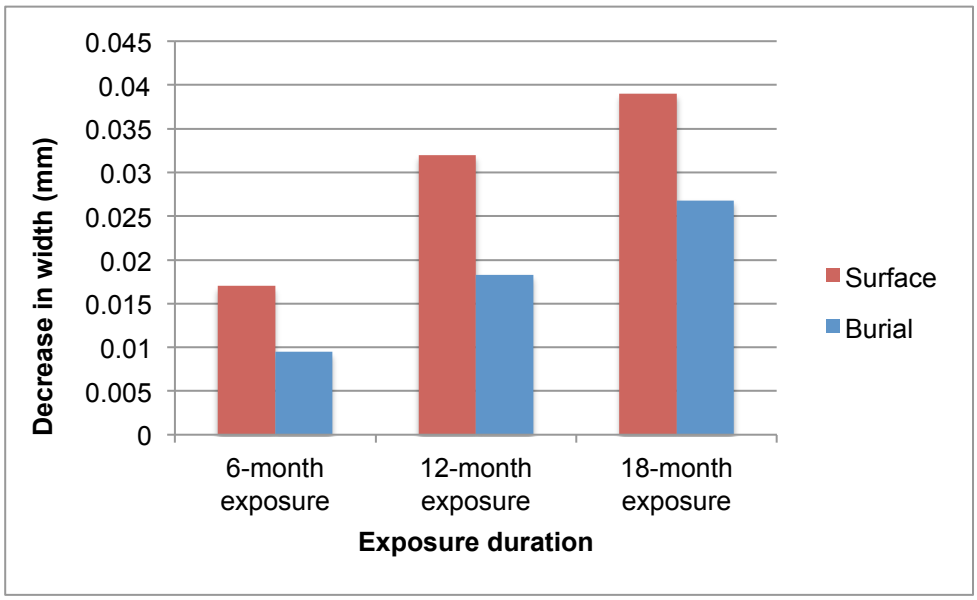

Figure 5.56: Reduction in the maximum width over time

The decomposition of organic matters in soil is influenced by several environmental factors, especially temperature and soil moisture (Carter and Tibbett, 2008). At a depth of two feet in this study, soil temperature shows no significant fluctuations other than by season (Rodriguez and Bass, 1985). In addition, soil moisture has the potential effect on tissue decomposition due to its effect on microbial activity. The availability of moisture influences microbial mobility, the diffusion of nutrients and waste, and the activity of biological enzymes (Jaggers and

Rogers, 2009; Carter *et al.,* 2010). Soil surrounding bone samples in this study was clayey soil, which usually retains moisture. Additionally, deep burial helped the bone samples reduce evaporation and retain moisture. The non-enteric bacteria can play an important role in the early stages of bone breakdown in soil, as mentioned by Carter *et al.* (2010), soil microorganisms are more prolific at shallow depths because of the more enriched environment. Thus, more rapid decomposition is expected in shallow burials. From these reasons, the deep burial allowed for a slower, more constant decrease in cut marks length and width over time. This means the soil environment is also appropriate to bacterial growths but at the slower rate than surface-deposited decomposition, as burial has been found to substantially slow the decay rate of skeletal materials (Rodriguez and Bass, 1985; Waldron, 1987; Dent *et al.,* 2004; Surabian, 2012).

5.2.2.2 Morphological changes of cut marks

The wide variability in cut mark morphology has made some archaeologists to study cut mark with sceptical idea (de Juana *et al.,* 2010). The results of the current study show the complexity of the allocation of an inflicted knife to the specific cut mark after environmental exposure. This study also found that there is more variation within the cut marks made from the same knife after longer environmental exposure. It is possible that the alterations in cut mark morphology after environmental exposure may be a result of specific ways in which the knife blades were manipulated such as different force and angle. Caution is advised when attempting to interpret morphological changes even though there is no statistical significance.

After environmental exposure, coarse-serrated blades produced more morphological changes than non-serrated and fine-serrated blades. The differences of morphological change are expected and can be associated with the bone structural changes occurring during the trauma event. The cut marks inflicted by coarse-serrated blades are likely to have more damage and rougher kerf wall and margins where the cuts are initially made, as opposed to non-serrated blade that make a cut with a smoother kerf wall and margin (Tegtmeyer, 2012). Non-serrated blade edges have the greatest level of contact with the bone, followed by fine-serrated and then coarse-serrated blades (Tennick, 2012). High levels of contact

allow the blade to move through the bone more consistently and with greater precision. Conversely, the teeth on the blade of a coarse-serrated knife might cause it to cut and chatter over the bone surface, thus potential damages are expected. These damaged, fragile kerf margins and walls were more vulnerable to physical changes from environmental effects. Therefore the absence of raised kerf margins and kerf wall changes after environmental exposure could be a result of the greater variety of environmental factors and the action of the blade edge. Although the difference was not statistically significant, the absence of raised margins and the presence of U-shaped cross-sections were more frequently observed in coarse-serrated blades than in non-serrated and fine-serrated blades.

Previous studies have suggested that serrated blades produce V-shaped cross-sectional profiles (Alunni-Perrat *et al.,* 2005; Lewis, 2008; Symes *et al.,* 2010; Tennick, 2012). Nonetheless, this study found that this is not always permanent. For example, 25% of narrow-shaped cut mark cross-section from non-serrated blades changed to V-shape after 12 months and 37.5% did so after 18-months of surface exposure. In addition, taphonomic changes were also found such as loss of kerf striations in cut marks made by serrated blades. Specifically, these variances were observed to occur only in cut marks, which also underwent a change in kerf shape. Some cut marks change from taphonomic factors much more quickly than others.

Some cut marks had fundamental differences in their structure and environment, resulting in different rates of taphonomic modifications. Variability in trauma infliction and bone structure, as well as different microenvironments could explain this. Different rates of taphonomic changes could occur even in samples deposited in the same environment. As Behrensmeyer (1978) and Potts and Shipman (1981) reported that different bone materials exposed at the same time commonly demonstrate varying weathering changes, and different parts of a single bone can weather at different rates. For example, bone samples in this study were deposited in grassland where they were covered by dense grass and vegetation, but some samples still developed sun bleaching while the other did not. The shade and moisture provided by long grass and fallen leaves did not protect some bones from sunlight.

It is apparent in this study that the degradation of buried bones occurs at a much slower rate than those placed on the ground. The cooler temperature and the effective insulation barrier to solar radiation would play an important role (Rodriguez and Bass, 1985; Dent *et al.*, 2004; Jaggers and Rogers, 2009). Finally, the degradation of cut marks showed a slower decrease in buried bone samples, with changes observed only after 18-months of exposure.

Other taphonomic modifications can resemble cut marks in morphology. For example, marks caused by trampling by large animals whereby the bone is rubbed against a rough surface or sediment. This action is able to create multiple, long and thin linear marks that may mimic cut marks (Behrensmeyer *et al.*, 1986; Olsen, 1988; Dominguez-Rodrigo *et al.*, 2009). However, these marks are distinctive from cut marks with their flat and less deep cross-sectional shape, as well as being more numerous and directional. Although none of the samples in this study showed this feature, a forensic anthropologist must be aware of this during an examination of surface-deposited skeletal remains.

5.2.3 Summary

This study illustrates the challenges in determining the knife blade type responsible for a particular sharp force lesion using cut mark analysis following long-term environmental exposure, as the results of this study show the complexity of the analysis of a cut mark. Caution is advised when using dimensional and morphological differences in cut marks to ascertain blade weapon type. Statistical analysis showed that cut mark width can be useful for knife type prediction even when these marks have been exposed to surface and buried environments for as long as 18 months. This study suggested that knife type could be also predicted from cut mark morphology.

The current study has limitations of physical variability such as applied force, angle of impact, and local geometrical characteristics of the bone that can affect kerf dimension and morphology. Nevertheless, the aim of this study was to investigate if outdoor environments have effects on cut marks, and therefore may be useful for detecting these taphonomic features. Furthermore, uncontrolled inflictions produce a wide variety of cut marks, providing more realistic variability. The different force and

angle at which the knives entered the bone also produced a large variety of kerf margin morphology. Caution is advised concerning dimension and morphology of the cut mark; not all cuts remain stable after environmental exposure. The morphological and dimensional assessment of a cut mark is dynamic and depends on environmental exposure time and the type of weapon used. The physical variables were also important, but they will be taken into account in further studies.

Some further limitations should take into consideration including the point that the interpretation of these microscopic characteristics is highly dependent on the experience of the observer (Crowder *et al.*, 2011; Boucherie *et al.*, 2017). The variety of taphonomic damages on cut marks are easily observed by a stereomicroscope; however, it is arguably better examined to more conventional observation with other types of microscope such as SEM or digital microscopy.

Chapter 6: Morphological and radiological analysis of environmental effects on hacking injuries to femurs

This study focuses on sharp force trauma data from femoral samples deposited in surface and buried environments. Investigations of the modifications to the bone damage were conducted by macroscopic, microscopic and radiological (micro-CT) examinations. As explained in Chapter 3, the materials and methods of this study are summarised in Figure 6.1.

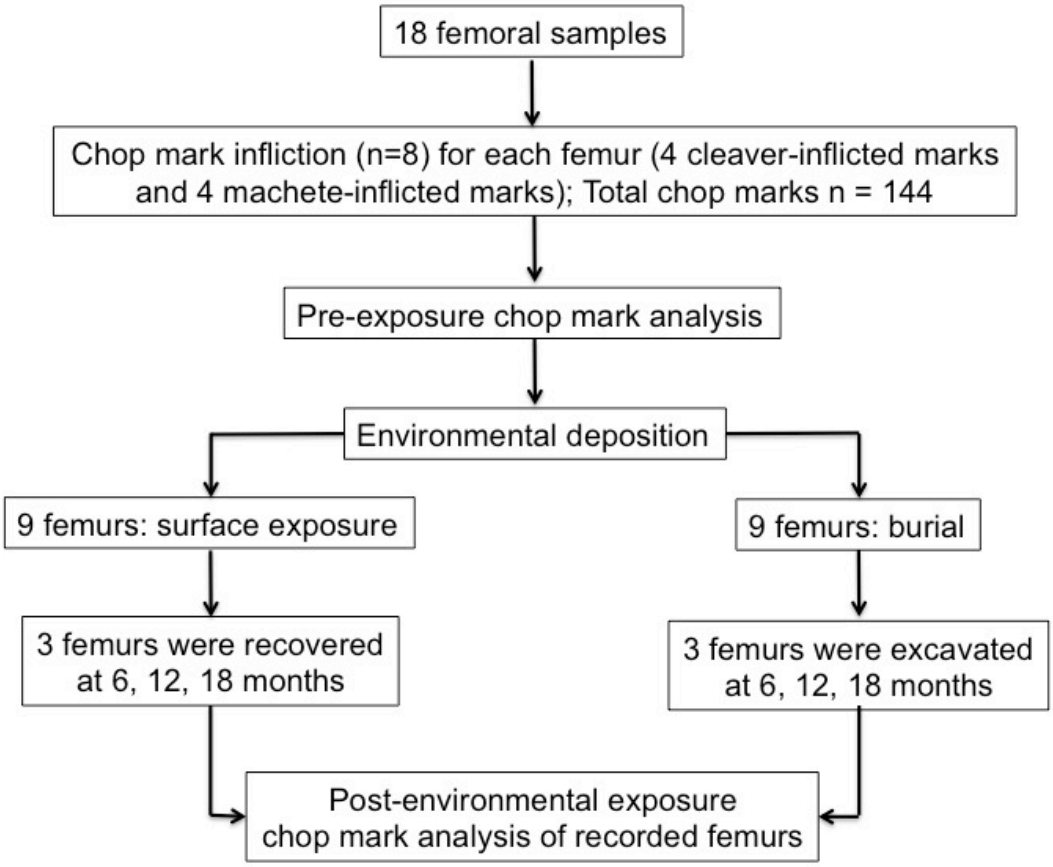

Figure 6.1: A diagram demonstrating the materials and methods in this chapter

6.1 Results

6.1.1 Pre-exposure comparison of cleaver and machete

6.1.1.1 Macroscopic and stereomicroscopic examination

Chop mark (n=144) characteristics were analysed macroscopically and microscopically for seven different areas of the kerf: maximum length, maximum width, kerf shape, cross-sectional shape, kerf margin, kerf striations, and chattering features. None of the femurs impacted by the cleaver and the machete were bisected upon impact. Briefly, the profiles of the chop marks produced with a cleaver exhibited mainly elliptical and V-shaped cross-sections. They also showed a smooth margin, the absence of a striation and chattering pattern, as well as a radiating fracture (Figure 6.2). In contrast, the profiles of the machete-inflicted marks showed a different pattern. Their morphology was elliptical or irregular in shape, with a V-shaped cross-section that had a more raised margin, more frequent striation chattering, and a radiating fracture on the kerf floor and margin (Figure 6.3). Variations among the chop mark characteristics appeared correlated with the weapon blade type, as summarised in Table 6.1. These differences in cleaver and machete chop marks indicate that the hacking weapon type can be distinguished in cases of recent trauma.

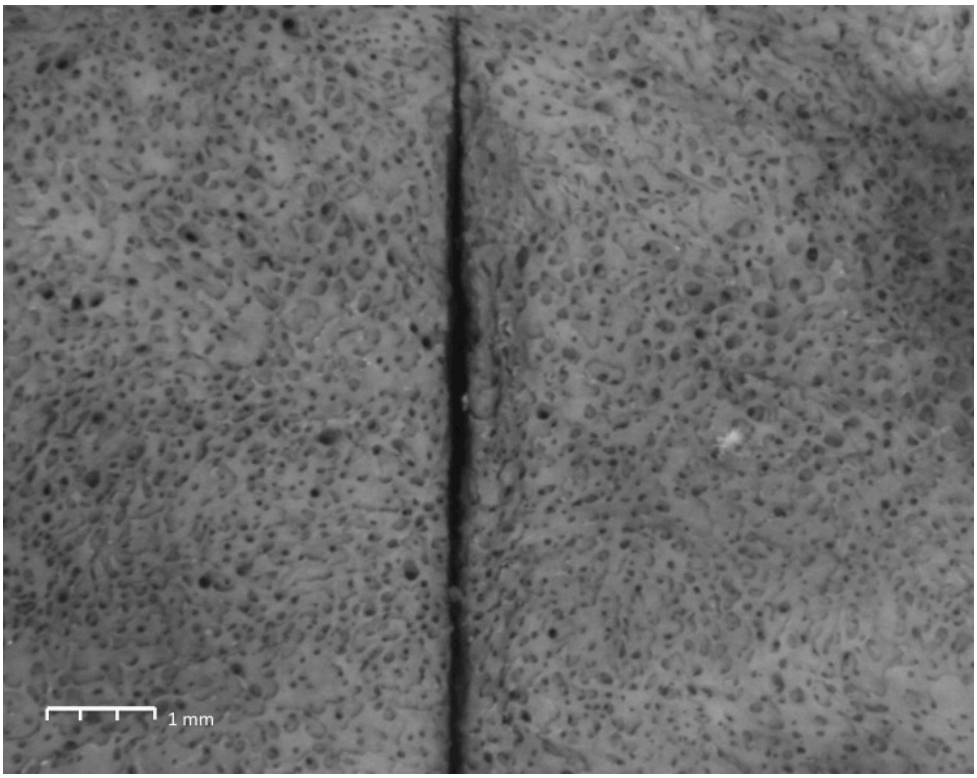

Figure 6.2: The feature of a cleaver-inflicted chop mark

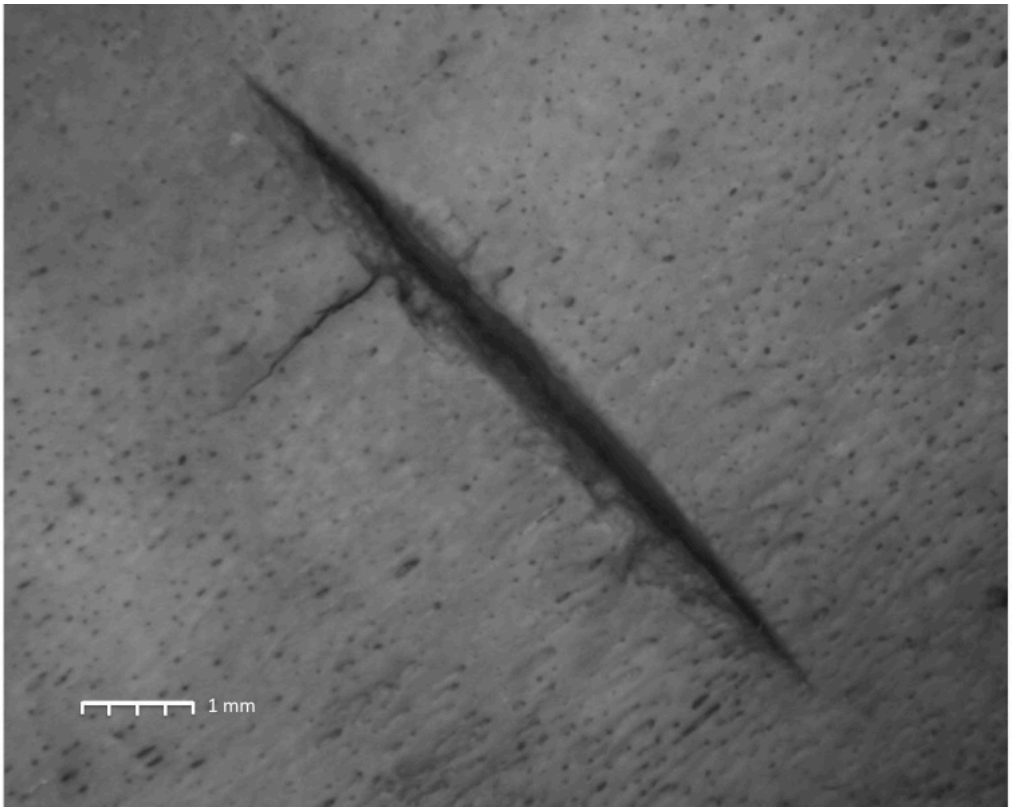

Figure 6.3: The feature of a machete-inflicted chop mark

Table 6.1: Diagnostic cut mark characteristics for each hacking weapon class

Kerf feature	Cleaver-inflicted chop mark	Machete-inflicted chop mark
Kerf shape	Elliptical	Mainly elliptical
Cross-section	V-shaped	V-shaped
Kerf margin	Smooth edged	Mainly raised-edge
Kerf striations	Absent	Mainly absent
Chattering	Absent	Present
Radiating fracture	Absent	Present

Figure 6.4 presents the boxplot of a dimensional comparison of the cleaver and the machete (Table 6.A and 6.F in APPENDIX 6). When examining the pre-exposure group, it is of interest to note that the cleaver-inflicted kerfs had significantly smaller widths (Mean=1.36 mm, S.D.=0.07) than those of the machete-inflicted kerfs (Mean=2.47 mm, S.D.=0.08), whereas no significant differences in kerf lengths were found for the two groups due to their having the same impacted surface area from the curvature of the bones.

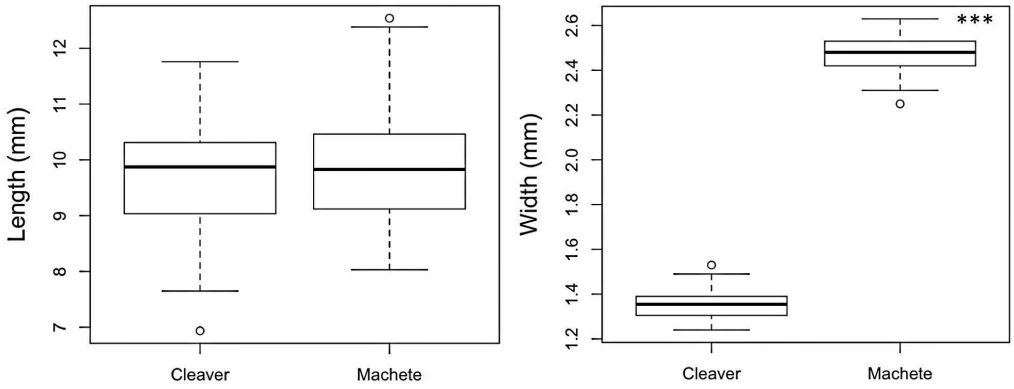

Figure 6.4: Observed length and width difference between the cleaver (n=72) and the machete (n=72) (*** statistically significant difference)

Independent observations of the chop mark dimension and morphology are provided in APPENDIX 6. Student t-tests, chi-square tests and Fisher's exact tests were conducted to statistically verify whether the profiles of the different dimensions and morphology were significantly different for the cleaver-inflicted and machete-inflicted chop marks. Within these main sample groups, a differentiation of the inflicting weapon types used in this experiment was observed. Statistically significant differences between the cleaver-induced and machete-induced trauma were found for kerf width, kerf shape, kerf margin, kerf striations and chattering morphology (Table 6.2).

Table 6.2: Statistical tests of pre-exposure kerf dimension and morphology between cleaver- and machete-inflicted marks (*** significantly difference)

Kerf dimension or morphology	Statistical values	df	P-value
Kerf length	t=1.134	142	0.259
Kerf width	t=79.63	142	<0.001***
Kerf shape	Fisher's test	-	<0.001***
Cross-section shape	X^2 =0.0443	1	0.8332
Kerf margin	X^2 =30.1238	1	<0.001***
Kerf striation	Fisher's test	-	<0.001***
Chattering	X^2 =15.7155	1	<0.001***

6.1.1.2 Micro-computed tomographic (micro-CT) examination

For this section, micro-CT data were used to compare the cleaver-inflicted and machete-inflicted samples (Figure 6.5). The following characteristics describing the proportions of the chop marks were measured, as demonstrated in Chapter 3: maximum length, maximum width, maximum depth, proximal and distal shoulder heights, proximal and distal slope angles, and opening angle (Table 6.D and 6.I in APPENDIX 6). The micro-CT data were also evaluated to assess the statistical differences between the cleaver-inflicted and machete-inflicted chop marks (Table 6.3), using a two-sample t-test.

Table 6.3: Statistical differences between cleaver- and machete-inflicted marks (*** statistical significance)

Parameter	t-test value	df	P-value
Length	-0.135	142	0.893
Width	44.37	142	<0.001***
Depth	28.95	142	<0.001***
Proximal shoulder height	1.09	142	0.2805
Distal shoulder height	1.181	142	0.14166
Proximal slope angle	3.993	142	0.0002019***
Distal slope angle	2.003	142	0.03522***
Opening angle	5.093	142	<0.001***

The kerf widths and depths, proximal and distal slope angles, and opening angles were observed to identify statistically significant differences (Table 6.3 and Figure 6.5). An interaction between the width, depth, the slope and opening angle created a framework for the chop marks to determine the class characteristics or the size and shape of the chop marks. It therefore seems that the inflicting weapon influenced the chop mark morphology, and micro-CT can be used to predict the weapon blade that had been used to injure a bone. The results highlighted that the thicker blade of the machete made a broader and deeper chop mark with a larger slope and opening angles than the cleaver.

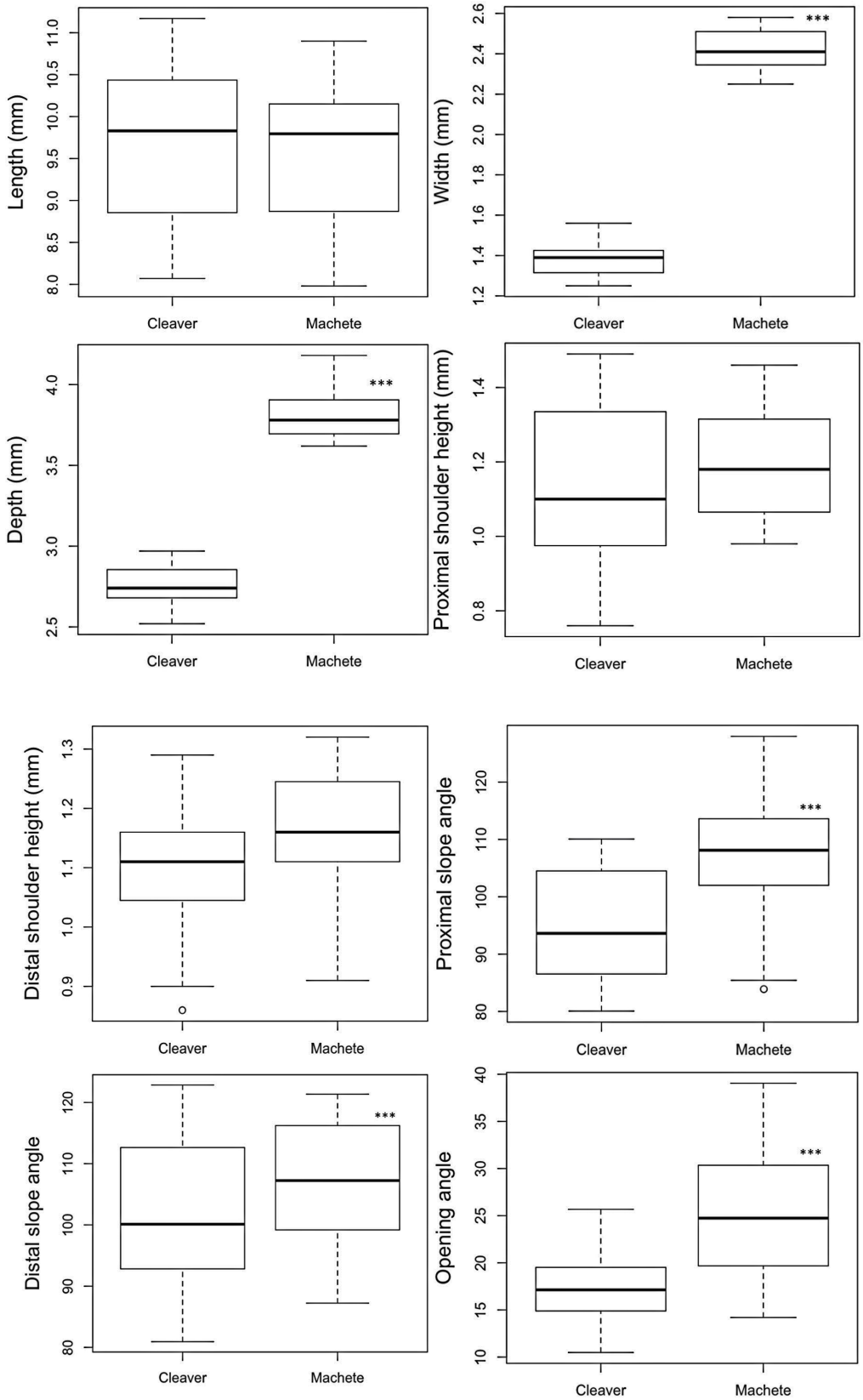

Figure 6.5: Measured micro-CT information difference between the cleaver (n=72) and the machete (n=72) (*** statistically significant difference)

6.1.2 Post-environmental exposure

6.1.2.1 Macroscopic and stereomicroscopic examination

Eighteen femurs were analysed; each bone had four cleaver-inflicted and four machete-inflicted chop marks. All samples were examined for their morphological and dimensional changes after 6-, 12- and 18-months environmental exposure. Table 6.4 summarises the overall morphological alterations of the femoral samples in this study. There were no changes in the kerf margin striations and chattering in the surface and buried cleaver-inflicted chop marks after 18-months environmental exposure. In comparison, all kerf morphologies of the machete-inflicted chop marks had some degree of change after environmental exposure. The following review depicts the results according to the type of depositional environment and weapon.

Table 6.4: Summary of morphological alterations after environmental exposure (X: presented changes; O: no changes)

Exposure and weapon type		Kerf shape	Cross-section	Kerf margin	Kerf striations	Chattering
Surface	Cleaver	X	X	X	O	O
	Machete	X	X	X	X	X
Burial	Cleaver	X	X	X	O	O
	Machete	X	X	X	X	X

6.1.2.1.1 Cleaver-inflicted group

6.1.2.1.1.1 Surface-deposited femoral samples

6.1.2.1.1.1.1 Dimensional change

Figures 6.6 and Table 6.A in APPENDIX 6 demonstrate changes in the kerf lengths and widths of the cleaver-inflicted chop marks for the surface-deposited group after environmental exposure. The descriptive analysis determined that, compared with pre-exposure values, the overall average length differences were 0.2327 mm, 0.2711 mm, and 0.5088 mm for 6-, 12- and 18-months exposure,

respectively. The overall width differences compared with pre-exposure values were 0.0011 mm, 0.0311 mm, and 0.0389 mm for 6-, 12- and 18-months exposure, respectively. Noticeably, there was no statistically significant difference in both the length and width of the same sample for the pre-exposure and the environmental-exposure data (Table 6.B in APPENDIX 6).

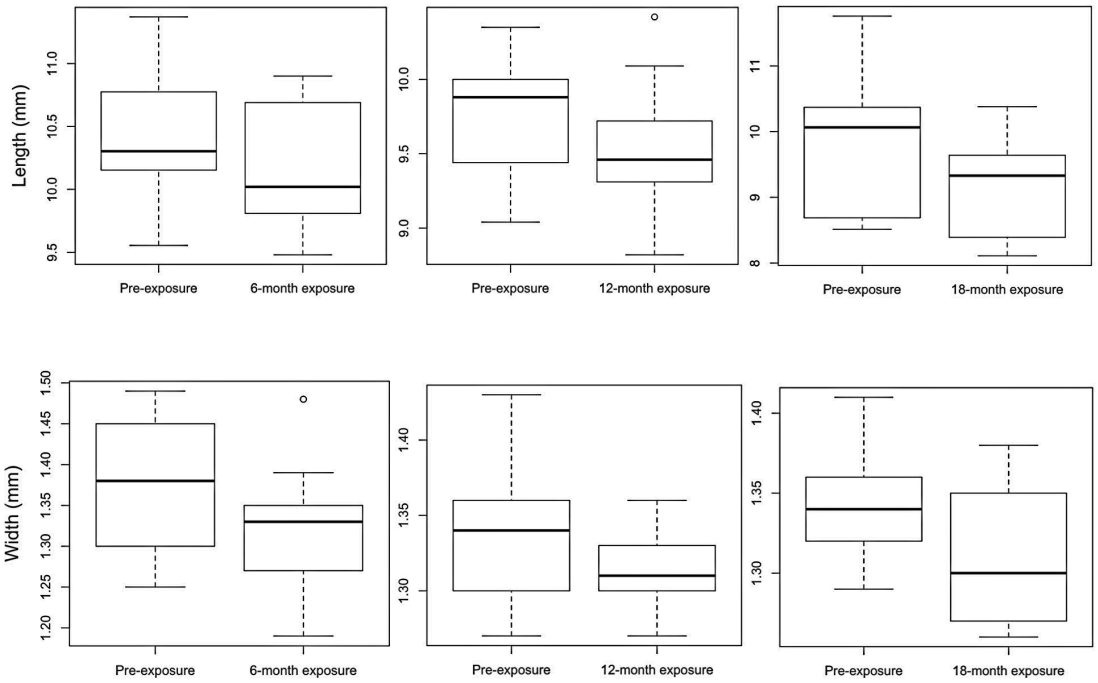

Figure 6.6: Observed length and width differences of surface-deposited cleaver-inflicted chop marks; each group n=12

A sequential change in dimension was observed for each post-exposure group, and the percentage of dimensional alterations was explored to compare each group (Table 6.5). In addition, Figure 6.7 shows profiles for the correlations of the kerf length and width changes compared between the pre-exposure group and the three environmental-exposure groups. All samples showed a decrease in length and width at 18-months exposure.

Three clusters were observed correlating with exposure time. Twelve-months exposure exhibited broad range of kerf lengths, which accumulated in the area between 6- and 18-months exposures. As to the extent of the exposure period, all marks showed a decrease in their maximum length and width at 18-months surface

exposure, with a maximum decrease of 0.79 mm in length and 0.09 mm in width. It is also noted that these changes had no statistically significant differences.

Table 6.5: Dimensional changes of the same cleaver-inflicted chop marks after exposure to the surface environment for 6, 12, and 18 months

Dimension	Alterations	Number of samples (%); each group: n=12		
		6-months	12-months	18-months
Length	Increased	3 (25)	1 (8.3)	-
	Decreased	9 (75)	11 (91.7)	12 (100)
	No change	-	-	-
Width	Increased	2 (16.7)	1 (8.3)	-
	Decreased	9 (75)	11 (91.7)	12 (100)
	No change	1 (8.3)	-	-

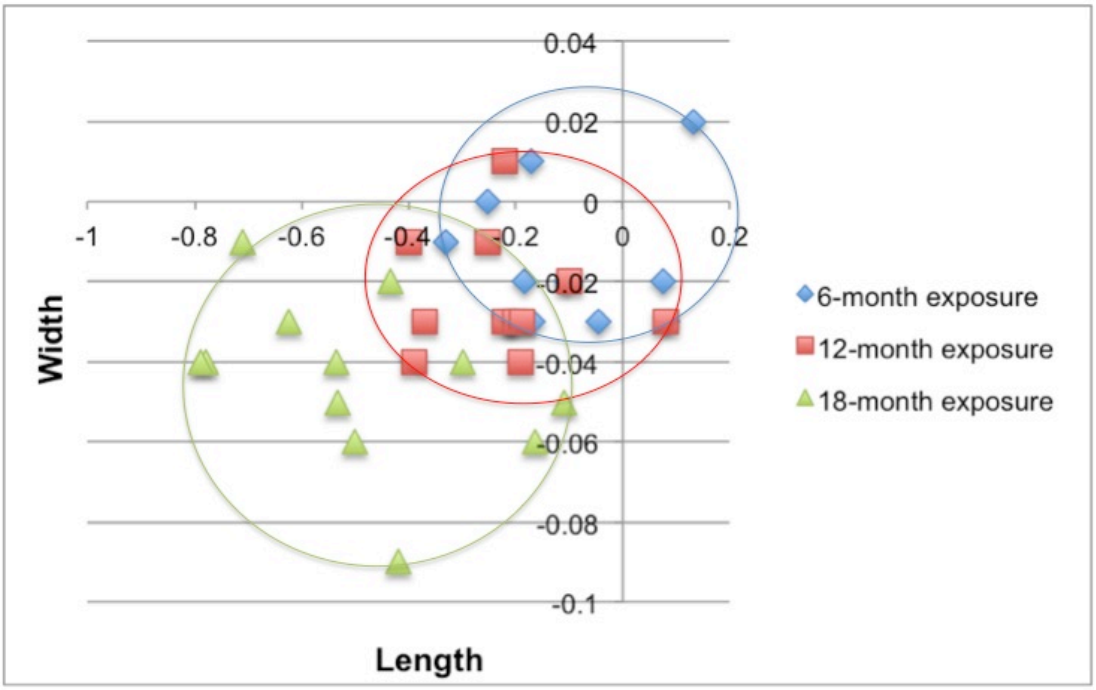

Figure 6.7: Dimensional changes for kerf lengths and widths of cleaver-inflicted surface chop marks

Linear regressions were conducted to study the relationship between exposed in the data (Figure 6.8-6.9). Predictive changes of the kerf dimension could be expected from the equation.

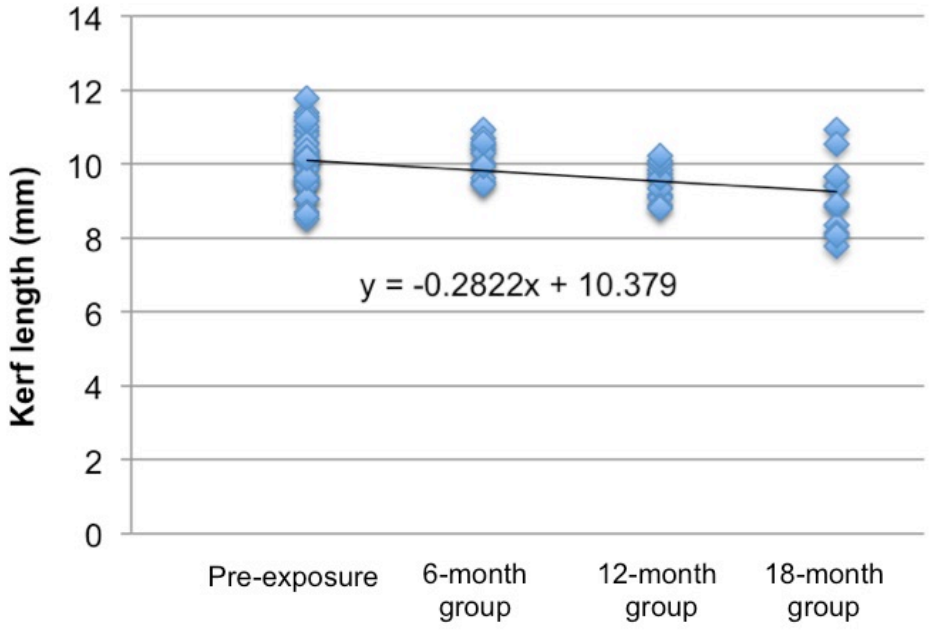

Figure 6.8: The scatter plot with a simple regression equation of kerf length of surface-deposited cleaver-inflicted chop marks

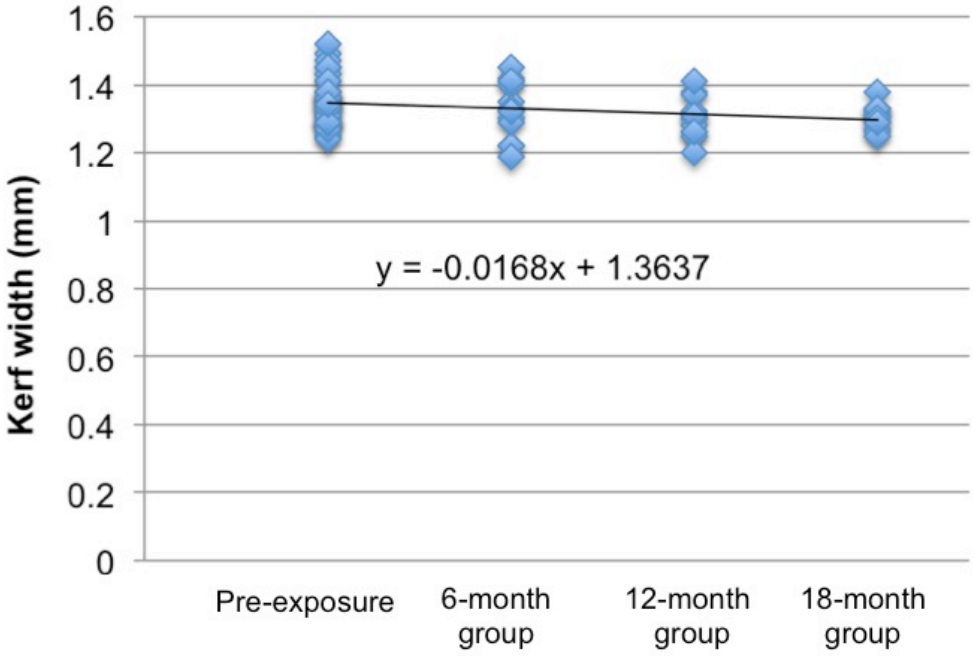

Figure 6.9: The scatter plot with a simple regression equation of kerf width of surface-deposited cleaver-inflicted chop marks

6.1.2.1.1.1.2 Morphological change

The cleaver-inflicted marks on the femoral samples that were exposed to the surface environment over the experimental period showed some alterations to their kerf features. Table 6.6 reviews the consistency of the pre-exposure characteristics and the percentages for the kerf feature changes for each surface exposure time of the cleaver-inflicted chop marks, and the results demonstrate a consistency in the pre-exposure morphological features. Figures 6.10 and 6.11 add more information about the changes in the kerf and cross-sectional shapes after environmental exposure. There were no changes in the kerf margins, kerf striations and chattering patterns throughout the 18 months of surface exposure.

Table 6.6: Summary of frequency data of kerf morphology changes for the pre-exposure and post-surface cleaver-inflicted surface samples; Pre-E: pre-exposure; Post-E: post-exposure

Kerf morphology		**6-months exposure (%; n=12)**		**12-months exposure (%; n=12)**		**18-months exposure (%; n=12)**	
		Pre-E	Post-E	Pre-E	Post-E	Pre-E	Post-E
Kerf shape	Elliptical	10 (83)	10 (83)	11 (92)	10 (84)	11 (92)	9 (75)
	Rectangular	2 (17)	2 (17)	1 (8)	2 (17)	1 (11)	3 (25)
Cross-section	V-shaped	9 (75)	9 (75)	9 (75)	8 (67)	10 (83)	8 (67)
	U-shaped	3 (25)	3 (25)	3 (25)	4 (34)	2 (17)	4 (33)
Kerf margin	Smooth	10 (83)	10 (83)	10 (83)	10 (83)	10 (83)	10 (83)
	Raised	2 (17)	2 (17)	2 (17)	2 (17)	2 (17)	2 (17)
Striations	Present	0 (0)	0 (0)	0 (0)	0 (0)	0 (0)	0 (0)
	Absent	12(100)	12(100)	12(100)	12(100)	12(100)	12(100)
Chattering	Present	0 (0)	0 (0)	0 (0)	0 (0)	0 (0)	0 (0)
	Absent	12(100)	12(100)	12(100)	12(100)	12(100)	12(100)

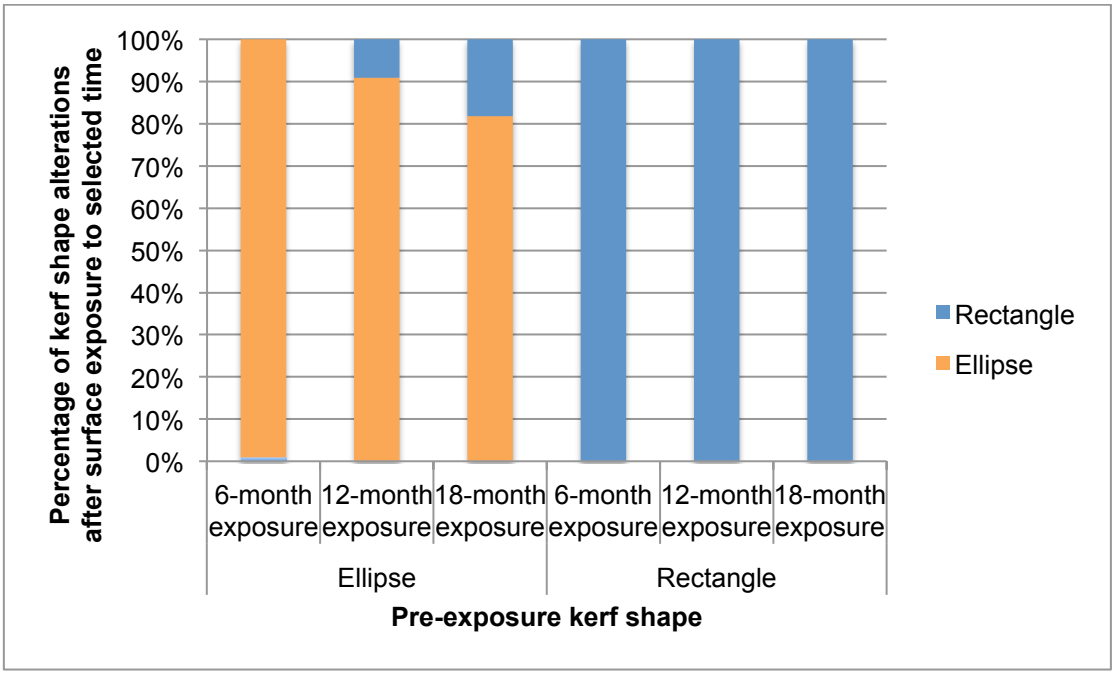

Figure 6.10: Percentage of kerf shape alterations for each surface exposure group of cleaver-inflicted chop marks

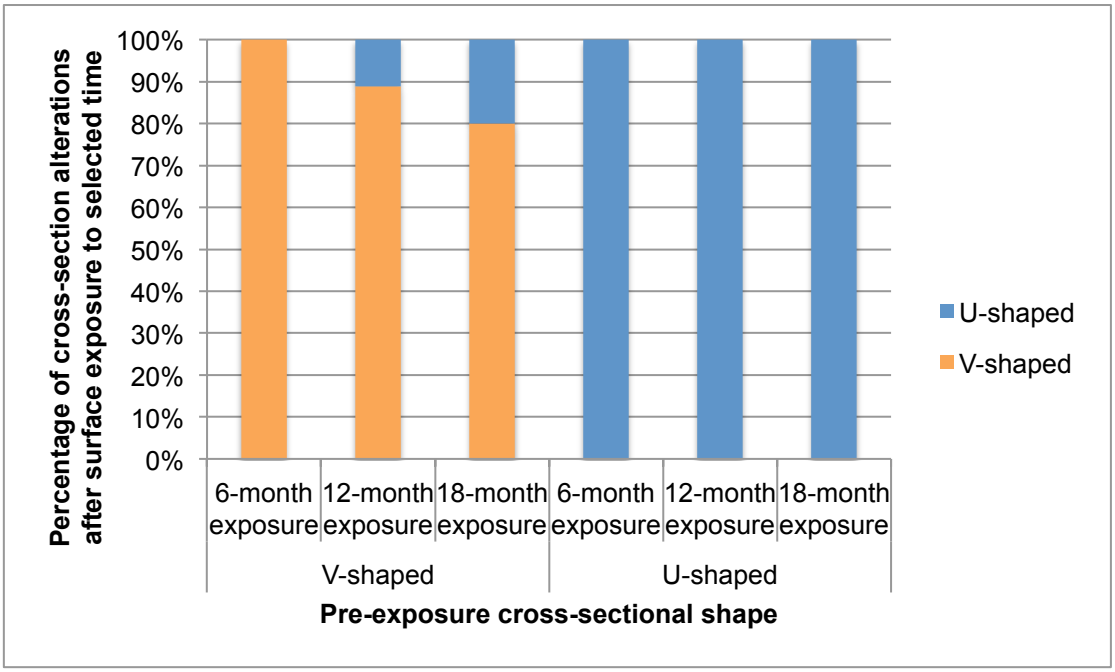

Figure 6.11: Percentage of cross-sectional shape alterations for each surface exposure group of cleaver-inflicted chop marks

The cleaver resulted in 88.8% of the samples having elliptically-shaped cut marks, and 77.8% of those marks had a V-shaped cross-section. By 12-months

surface exposure, 9.1% of the elliptically shaped marks had changed to a rectangular shape. In addition, 18.2% of the elliptical marks had changed to a rectangular shape by 18-months surface exposure, whereas the rectangular-shaped marks remained stable (Figure 6.10). Moreover, Figure 6.11 shows that some of the V-shaped cross-sections had transformed into a U-shaped cross-sectional shape by 12- and 18-months exposure (11.1% and 20%, respectively). Notably, a majority (75%) of the samples with a changed cross-sectional shape were located in the distal femur, which has a high percentage of trabecular bone. It thus seems that significant changes to chop marks depend on the bone composition.

The statistical significance of the kerf morphology was determined by comparing the pre-exposure and post-environmental surface exposure (Table 6.C in APPENDIX 6). No statistically significant differences were observed in the morphological changes of the cleaver-inflicted chop marks resulting from the environmental exposure. To summarise, there were no significant changes to cleaver-inflicted chop mark morphology during 18 months of surface exposure.

6.1.2.1.1.2 Buried femoral samples

6.1.2.1.1.2.1 Dimensional change

Figures 6.12 and Table 6.A in APPENDIX 6 demonstrate alterations in the kerf lengths and widths of the cleaver-inflicted chop marks in the buried group after environmental exposure. A gradual decrease in dimensions was observed in each post-exposure group. The overall average length differences rom the pre-exposure values were 0.1581 mm, 0.2107 mm and 0.4862 mm for 6-, 12- and 18-months exposure, respectively. Compared with the pre-exposure values, the overall width differences were 0.0012 mm, 0.0289 mm and 0.033 mm for 6-, 12- and 18-months exposure, respectively.

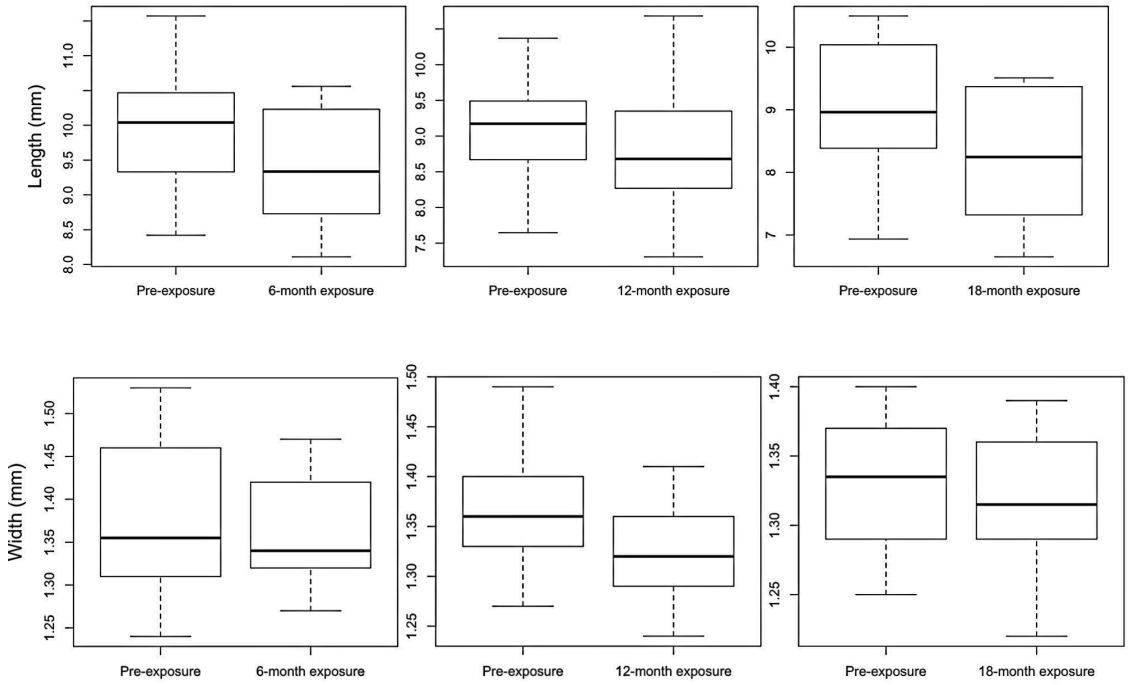

Figure 6.12: Observed length and width difference of buried cleaver-inflicted chop marks; each group n=12

The percentages of the dimensional alterations were explored in-depth to compare each group (Table 6.7). Additionally, Figure 6.13 illustrates more intensive profiles of the correlation between the kerf length and width alterations and the pre-exposure and three sets of environmental exposure. Almost all samples showed a decrease in their lengths and widths during the 18-months buried exposure.

Table 6.7: Dimensional changes of the same cleaver-inflicted chop marks after exposure to the burial environment for 6, 12, and 18 months

Dimension	Alterations	Number of samples (%; each group: n=12)		
		6-months	12-months	18-months
Length	Increased	2 (16.7)	1 (8.3)	-
	Decreased	10 (83.3)	11 (91.7)	12 (100)
	No change	-	-	-
Width	Increased	2 (16.7)	1 (8.3)	-
	Decreased	9 (75)	10 (83.4)	11 (91.7)
	No change	1 (8.3)	1 (8.3)	1 (8.3)

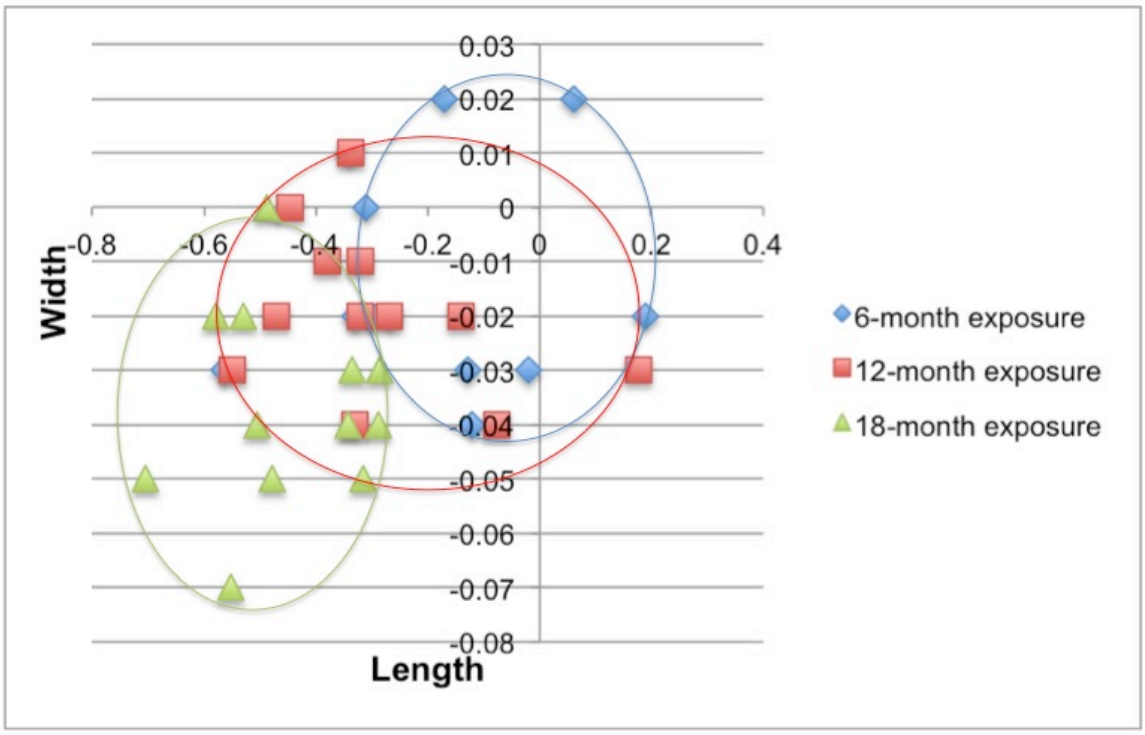

Figure 6.13: Dimensional changes of kerf lengths and widths of cleaver-inflicted buried chop marks

A wide distribution was observed in the lengths and widths for all exposures. Marked intersections of the data for the 12- and 18-months exposure were observed. Most samples showed both decrease in length and width at 18-months buried exposure, with only one chop mark showing no change in its width dimension. Most of the chop marks displayed slower decreases in their dimensions and only a slight decrease in the maximum width, compared with the surface group, with a maximum value of 0.705 mm in length and 0.07 mm in width. Remarkably, there were no statistically significant differences for both the lengths and widths between the pre- and the post-exposure data for the same samples (Table 6.B in APPENDIX 6). Linear regressions were conducted to study the relationship between exposed in the data (Figure 6.14-6.15). Predictive changes of the kerf dimension could be expected from the equation.

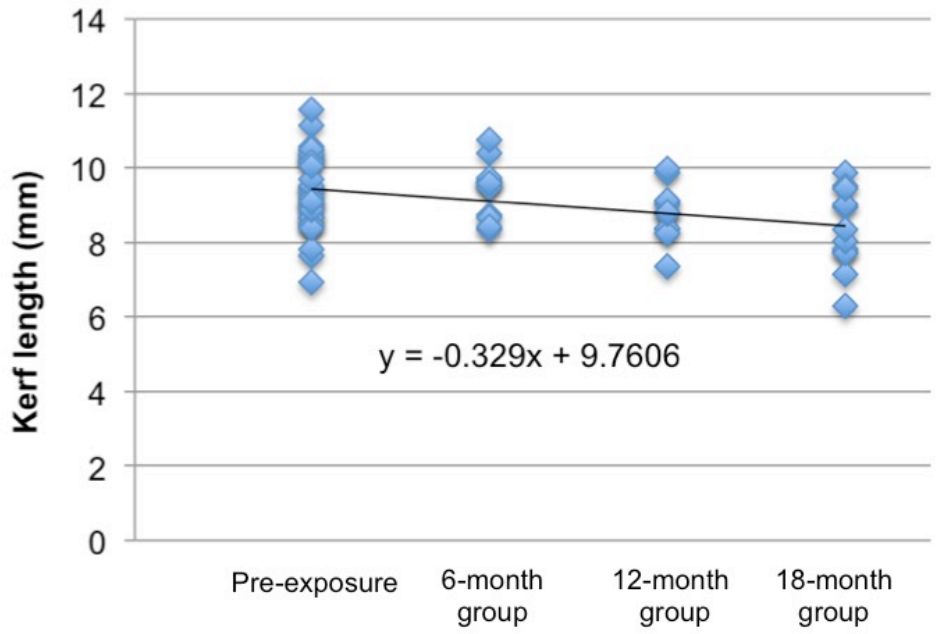

Figure 6.14: The scatter plot with a simple regression equation of kerf length of buried cleaver-inflicted chop marks

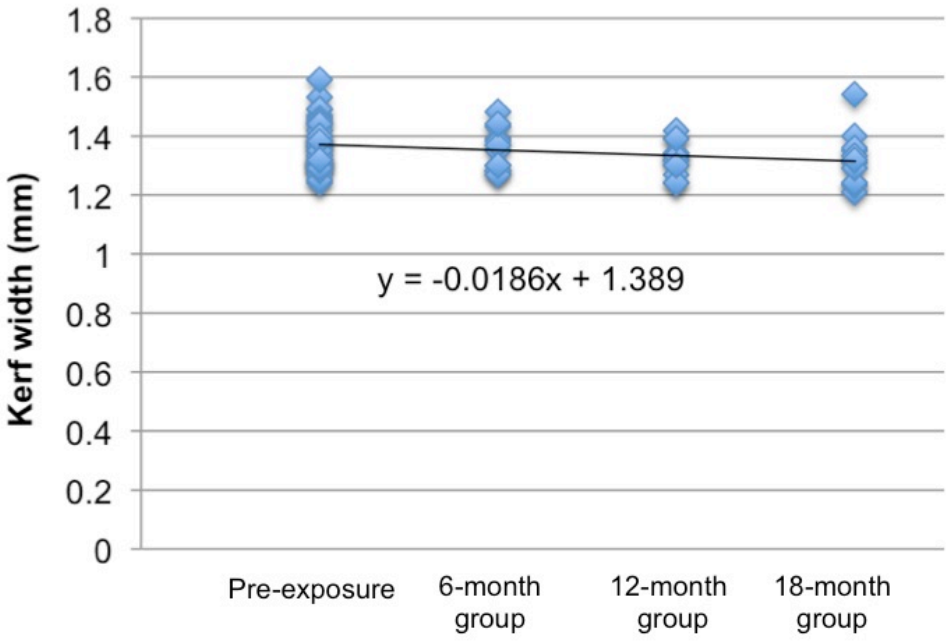

Figure 6.15: The scatter plot with a simple regression equation of kerf width of buried cleaver-inflicted chop marks

6.1.2.1.1.2.2 Morphological change

The cleaver-inflicted marks on the femurs exposed to the buried environment demonstrated some alterations to their kerf features over the three experimental periods. However, kerf margin striations and chattering morphology were not found to develop throughout the 18 months of exposure. Table 6.8 summarises the percentage of feature changes for each exposure time for the cleaver-inflicted marks, and Figures 6.16 to 6.17 add more information about the changes for each kerf morphology after burial.

Table 6.8: Summary of frequency data of the kerf morphology changes for the pre-exposure and post-burial cleaver-inflicted buried samples; Pre-E: pre-exposure; Post-E: post-exposure

Kerf morphology		6-months exposure (%; n=12)		12-months exposure (%; n=12)		18-months exposure (%; n=12)	
		Pre-E	Post-E	Pre-E	Post-E	Pre-E	Post-E
Kerf shape	Elliptical	10 (83)	10 (83)	10 (83)	10 (83)	10 (83)	9 (75)
	Rectangular	2 (17)	2 (17)	2 (17)	2 (17)	2 (17)	3 (25)
Cross-section	V-shaped	9 (75)	9 (75)	9 (75)	9 (75)	9 (75)	8 (67)
	U-shaped	3 (25)	3 (25)	3 (25)	3 (25)	3 (25)	4 (33)
Kerf margin	Smooth	11 (92)	11 (92)	10 (83)	10 (83)	10 (83)	10 (83)
	Raised	1 (8)	1 (8)	2 (17)	2 (17)	2 (17)	2 (17)
Striations	Present	0 (0)	0 (0)	0 (0)	0 (0)	0 (0)	0 (0)
	Absent	12(100)	12(100)	12(100)	12(100)	12(100)	12(100)
Chattering	Present	0 (0)	0 (0)	0 (0)	0 (0)	0 (0)	0 (0)
	Absent	12(100)	12(100)	12(100)	12(100)	12(100)	12(100)

Only 10% of the elliptically shaped marks changed to a rectangular shape after 18-months surface exposure, whereas the rectangular-shaped marks remained stable (Figure 6.16). Moreover, Figure 6.17 shows that only 11.1% of the V-shaped cross-sections had transformed into the U-shaped cross-sectional shape by 18 months of exposure. Nevertheless, there were no changes in the kerf margins during the 18-months surface exposure. To conclude, the results of the buried group showed minor changes unlike the surface group.

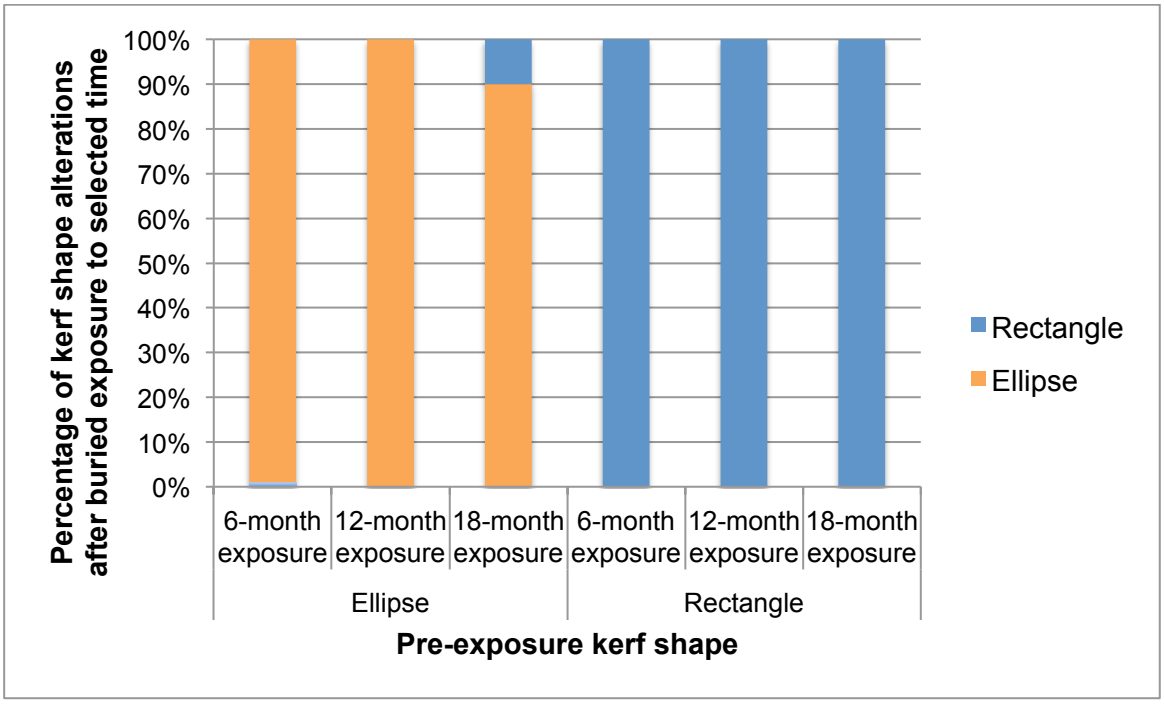

Figure 6.16: Percentage of kerf shape alterations for each buried exposure group of cleaver-inflicted chop marks

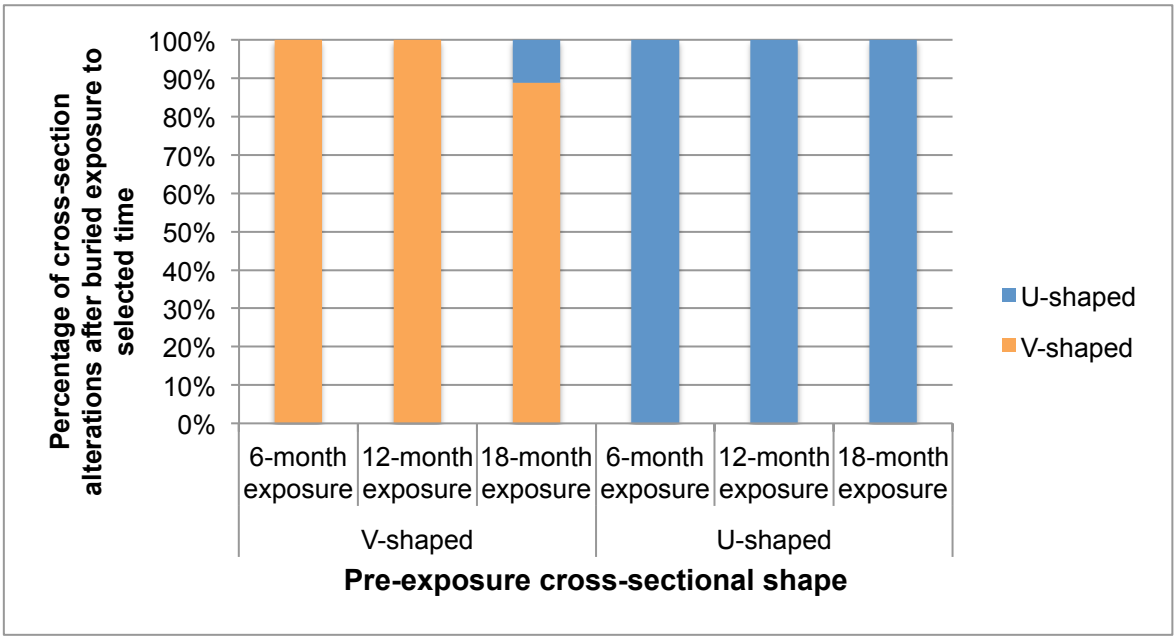

Figure 6.17: Percentage of cross-sectional shape alterations for each buried exposure group of cleaver-inflicted chop marks

The statistical significance of the kerf morphology was observed through comparisons between the pre-exposure and post-burial exposure data (Table 6.C in

APPENDIX 6). No statistically significant differences were found in the morphological changes of the cleaver-inflicted chop marks as a result of the environmental exposure. In sum, the buried taphonomic alterations showed no potential to modify the evidence of the cleaver-inflicted chop mark morphology over 18 months.

6.1.2.1.2 Machete-inflicted group

6.1.2.1.2.1 Surface-deposited femoral samples

6.1.2.1.2.1.1 Dimensional change

Figures 6.18 and Table 6.F in APPENDIX 6 illustrates the change in the kerf lengths and widths of the machete-inflicted chop marks for the surface-deposited group after deposition. The percentages of the dimensional alterations were explored in-depth to compare each group.

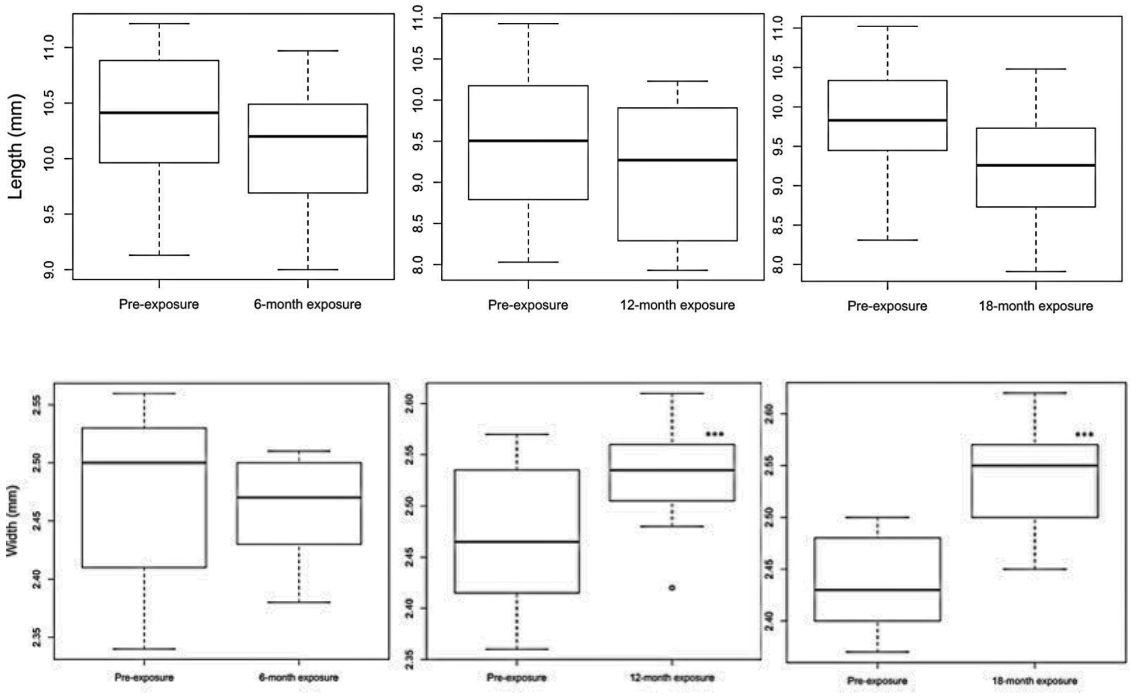

Figure 6.18: Observed width differences of surface-deposited machete-inflicted chop marks; each group n=12 (*** statistical significance of the same sample between pre-exposure and post-exposure values)

There were statistically significant differences between the pre-exposure data and the 12-months environmental-exposure data for the kerf width (t=2.394, df=22, p=0.0256), as well as the pre-exposure data and the 18-months environmental-exposure data (t=4.436, df=22, p=0.000415) (Table 6.G in APPENDIX 6). In addition, a sequential decrease in dimensions was observed in each post-exposure group (Table 6.9). Figure 6.19 demonstrates more intensive profiles of how the correlation of the kerf length and width changes compared between pre-exposure and the three ranges of environmental exposure. All of the 18-months surface exposure samples exhibited a decrease in their length; no sample showed an increase in both dimensional changes during the experimental periods (Figure 6.19). The kerf widths increased gradually during the first 6 months before rising substantially during the last 12 months of this study, with a maximum increase of 0.18 mm in width. Linear regressions were conducted to study the relationship between exposed in the data (Figure 6.20-6.21). Predictive changes of the kerf dimension could be expected from the equation. Diffuse plots were observed in kerf width of surface-deposited machete-inflicted chop marks (Figure 6.21).

Table 6.9: Dimensional changes of machete-inflicted chop marks after exposure to the surface environment for 6, 12, and 18 months

Dimension	Alterations	Number of samples (%; each group: n=12)		
		6-months	12-months	18-months
Length	Increased	4 (33.3)	1 (8.3)	-
	Decreased	8 (66.7)	11 (91.7)	12 (100)
Width	Increased	4 (33.3)	8 (66.7)	9 (75)
	Decreased	7 (58.4)	4 (33.3)	3 (25)
	No change	1 (8.3)	-	-

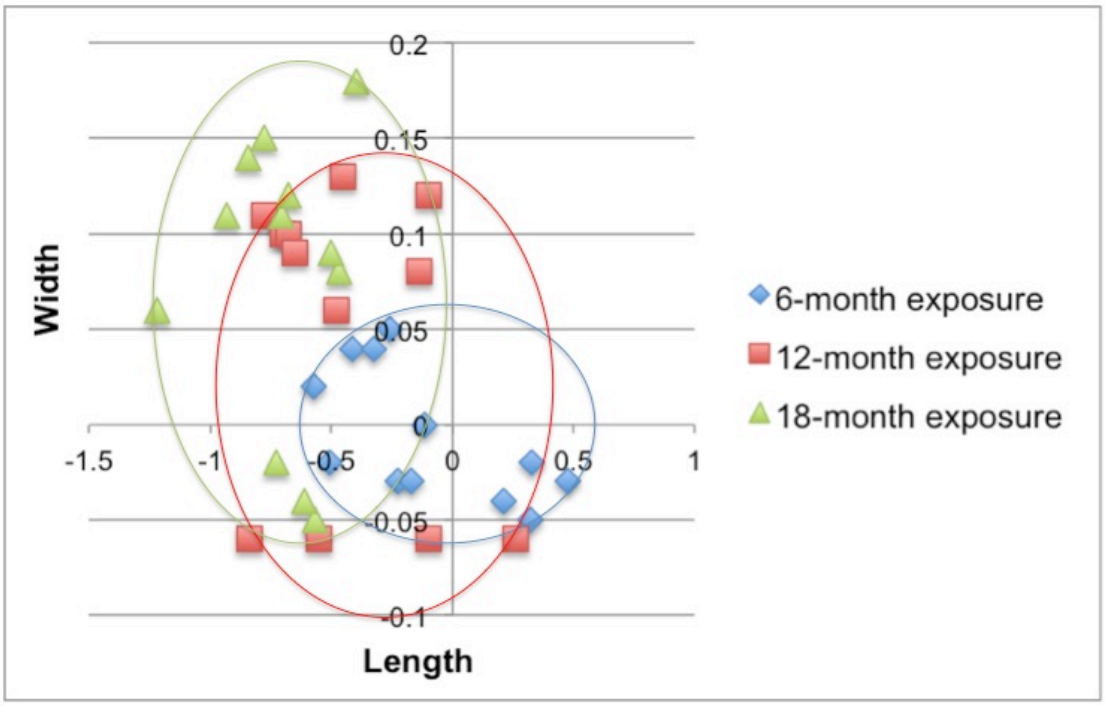

Figure 6.19: Dimensional changes in kerf lengths and widths of machete-inflicted chop marks.

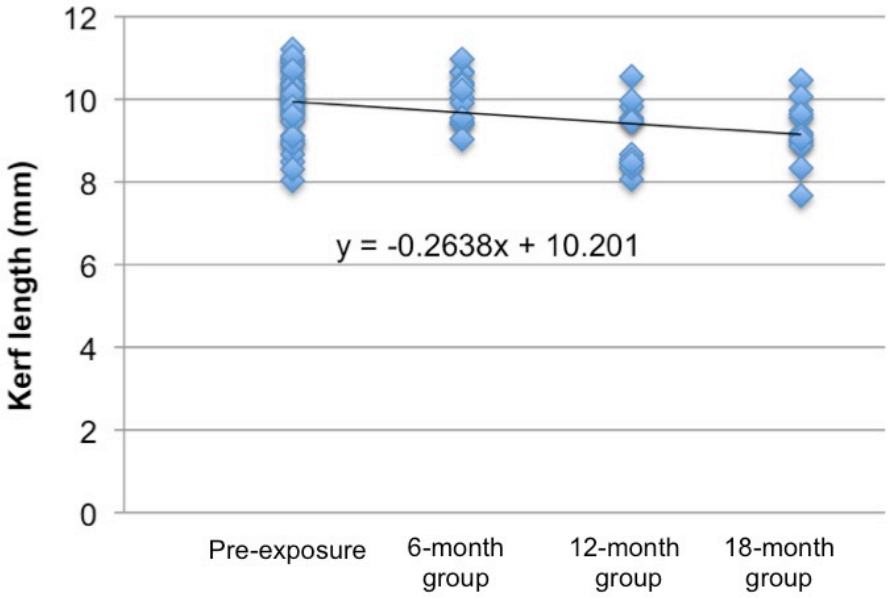

Figure 6.20: The scatter plot with a simple regression equation of kerf length of surface-deposited machete-inflicted chop marks

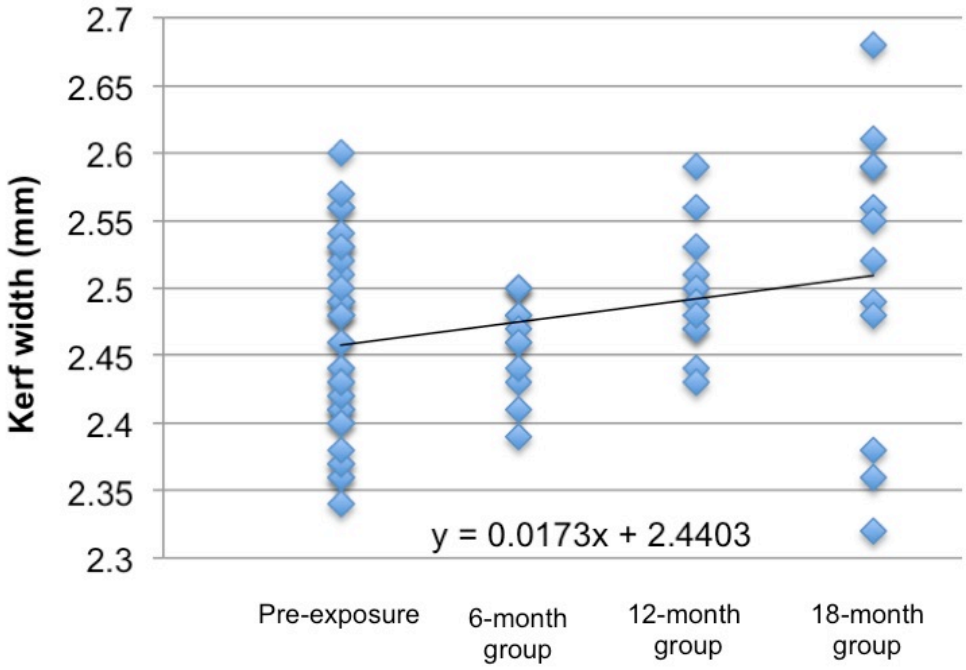

Figure 6.21: The scatter plot with a simple regression equation of kerf width of surface-deposited machete-inflicted chop marks

6.1.2.1.2.1.2 Kerf morphology

After environmental exposure, all chop marks remained recognisable, and there were no change in the overall morphological patterns after surface exposure for 6 months. Nevertheless, a significant change started to be detected at the 12-months surface exposure time point. Alterations to the machete-inflicted marks were observed, especially the loss of the raised border (Figures 6.22 to 6.23).

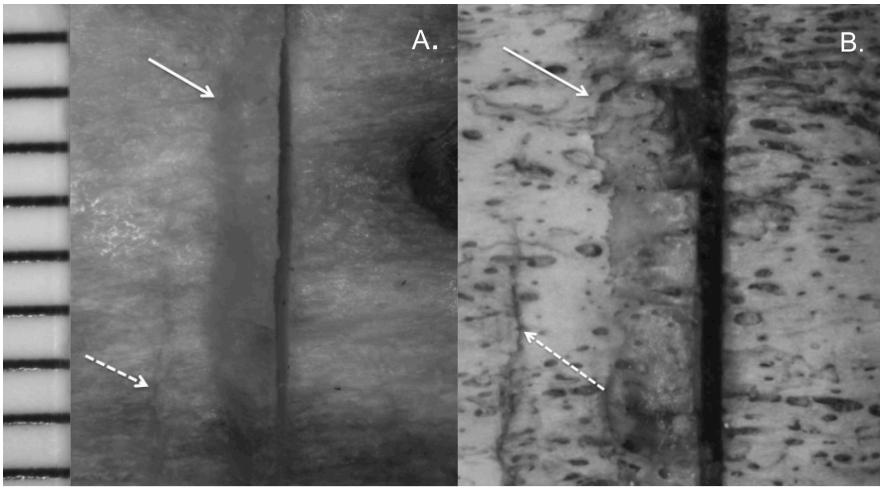

Figure 6.22: Two images of the same machete-inflicted mark: (A.) pre-exposure; (B.) 12-months surface exposure; the white arrow and the dotted arrow indicate the same landmark.

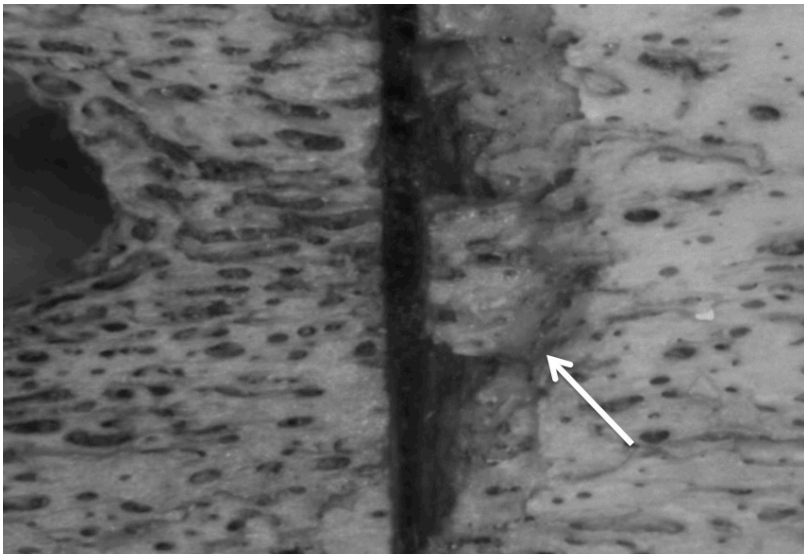

Figure 6.23: Loss of kerf margin (the white arrow) after environmental exposure for 12 months.

The machete-inflicted chop marks on the bones exposed to a depositional environment over the experimental periods exhibited some changes to their kerf features. Table 6.10 and Figures 6.24 to 6.28 summarise the percentages of the various aspects of the kerf feature changes to the machete-inflicted marks for each surface exposure time.

Table 6.10: Summary of frequency data of kerf morphology changes in pre-exposure and post-surface machete-inflicted samples; shaded area demonstrates statistical significance for the same sample between pre-exposure (Pre-E) and post-exposure (Post-E) values

Kerf morphology		6-months exposure (%; n=12)		12-months exposure (%; n=12)		18-months exposure (%; n=12)	
		Pre-E	Post-E	Pre-E	Post-E	Pre-E	Post-E
Kerf shape	Elliptical	8 (67)	8 (67)	8 (67)	7 (58)	8 (67)	5 (42)
	Rectangular	1 (8)	1 (8)	1 (8)	1 (8)	1 (8)	2 (17)
	Irregular	3 (25)	3 (25)	3 (25)	4 (33)	3 (25)	5 (42)
Cross-section	V-shaped	9 (75)	9 (75)	10 (83)	8 (67)	9 (75)	6 (50)
	U-shaped	3 (25)	3 (25)	2 (17)	4 (33)	3 (25)	6 (50)
Kerf margin	Smooth	5 (42)	6 (50)	4 (33)	7 (58)	4 (33)	10 (83)
	Raised	7 (58)	6 (50)	8 (67)	5 (42)	8 (67)	2 (17)
Striations	Present	9 (75)	9 (75)	10 (83)	8 (67)	10 (83)	6 (50)
	Absent	3 (25)	3 (25)	2 (17)	4 (33)	2 (17)	6 (50)
Chattering	Present	4 (33)	4 (33)	5 (42)	4 (33)	5 (42)	3 (25)
	Absent	8 (67)	8 (67)	7 (58)	8 (67)	7 (58)	9 (75)

Initially, the machete produced elliptical kerf shapes for 67% of the samples and V-shaped cross-sections for 78% of the samples. It also produced a raised margin for 64%, kerf striations for 80% and chattering for 39% of the samples (Table 6.10). By 12-months surface environmental exposure, 12.5% of the elliptical kerf shapes had changed to irregular shapes, and there was a subsequent substantial increase to 25% by 18-months surface exposure. Nonetheless, there was no change in the rectangular and irregular kerf shape after 18-months surface exposure (Figure 6.24). Thirty-three per cent of the V-shaped cut marks had changed to U-shaped marks by 18-months surface exposure; on the other hand, all U-shaped cross-sections exhibited no specific changes after 18-months buried exposure (Figure 6.25).

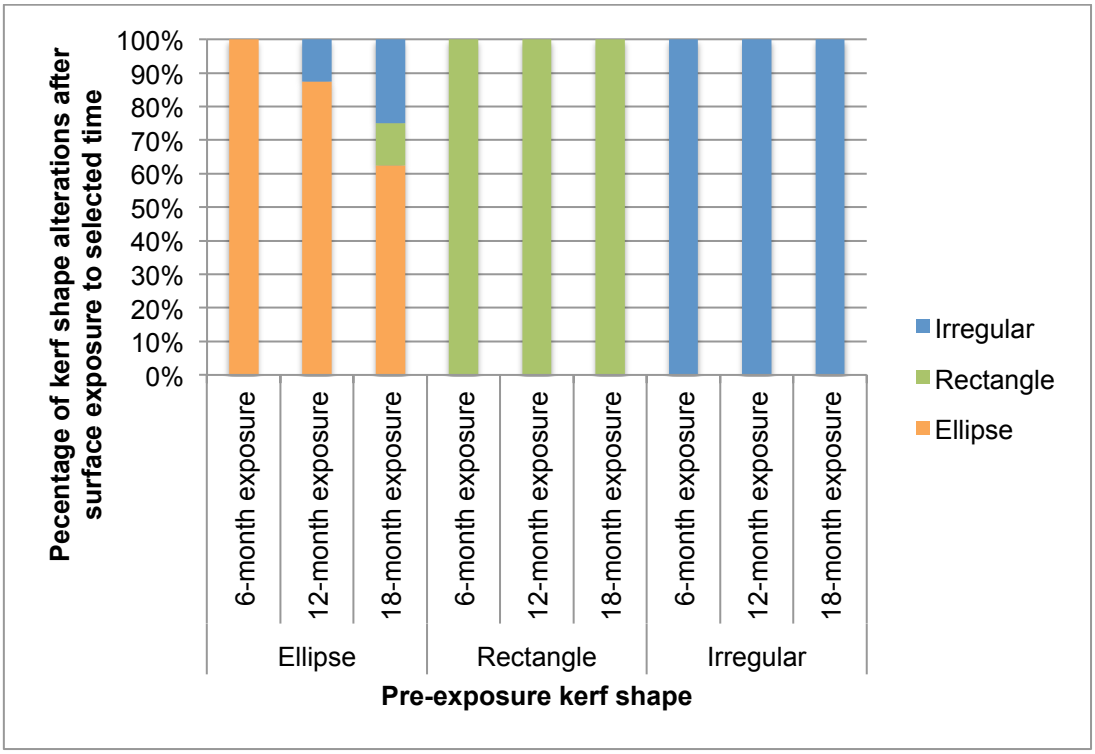

Figure 6.24: Percentage of kerf shape alterations for each surface exposure group of machete-inflicted chop marks

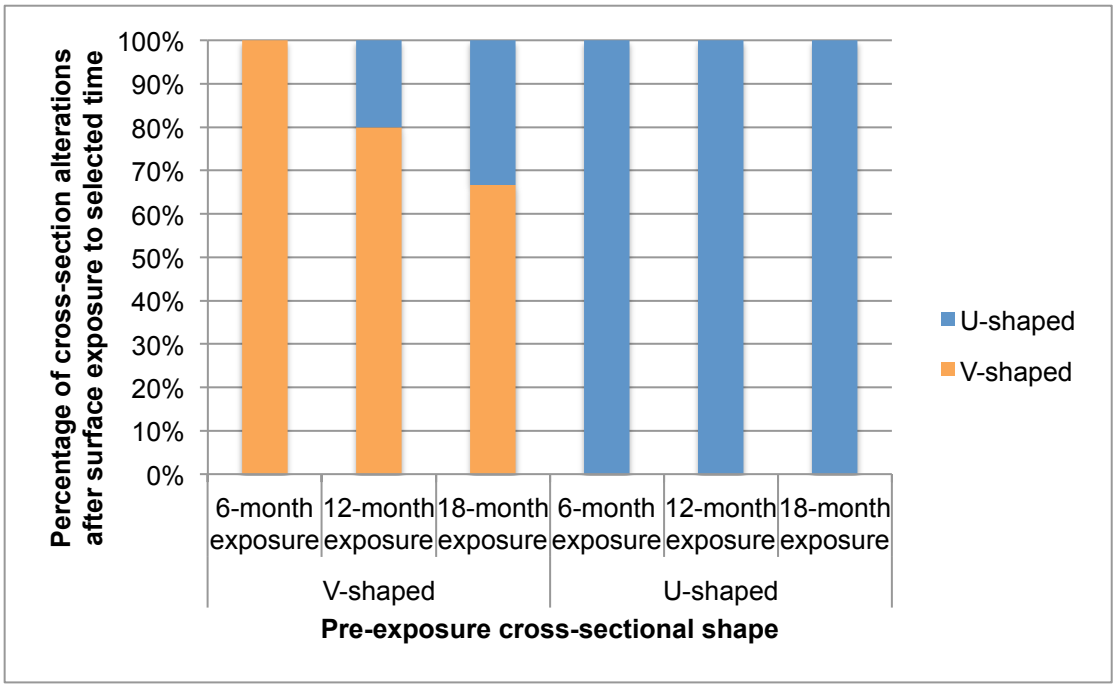

Figure 6.25: Percentage of cross-section shape alterations for each surface exposure group of machete-inflicted chop marks

In addition, the raised kerf margins experienced morphological degradation. The raised edges were eroded and disappeared after environmental exposure, with an incidence of 14.3%, 37.5%, and 75% after 6-, 12- and 18-months exposure, respectively (Figure 6.26). A high proportion (75%) of 18-months exposure raised machete-inflicted margins changed to smooth margins, which contrasted with no change to the cleaver-inflicted marks. Around 20% of the kerf striations had started to fade by 12-months surface exposure, with 40% having disappeared by 18-months exposure (Figure 6.27). Likewise, 40% of the chattering characteristics had been lost by 18-months surface exposure (Figure 6.28). As with the cleaver-inflicted mark changes, most of the changed machete chop marks (82%) were located at the distal part of the femurs, which has a high proportion of trabecular bone. In sum, the kerf morphology of machete-inflicted marks underwent more alteration than that of the cleaver-inflicted marks, which suggests that the morphological characteristics of the marks are affected by their positions on the bones.

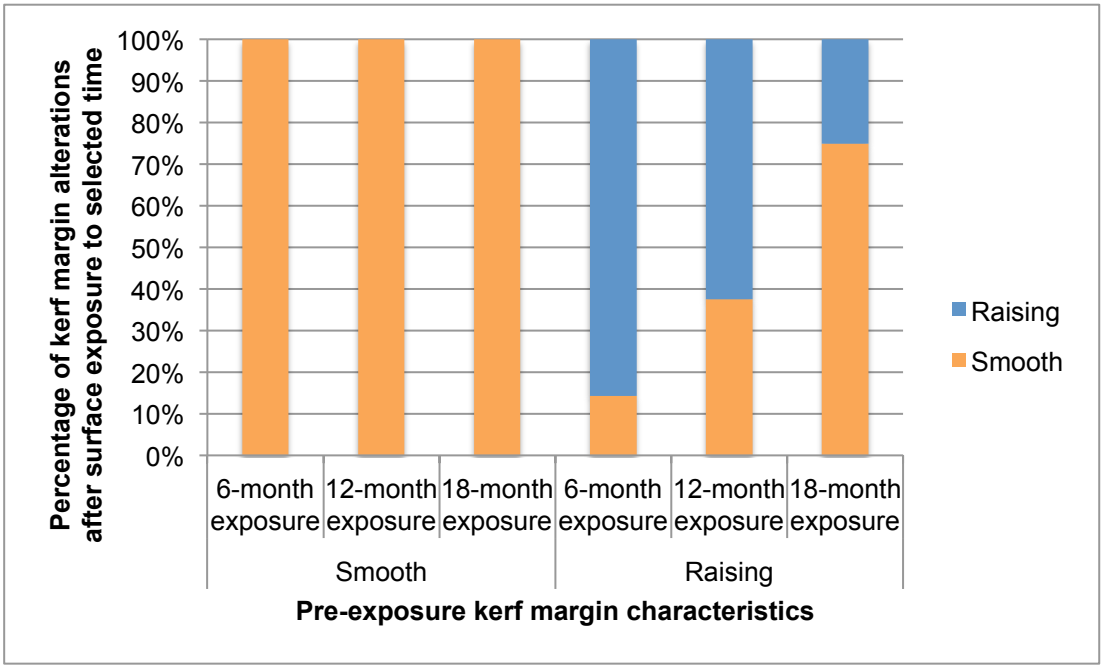

Figure 6.26: Percentage of kerf margin alterations for each surface exposure group of machete-inflicted chop marks

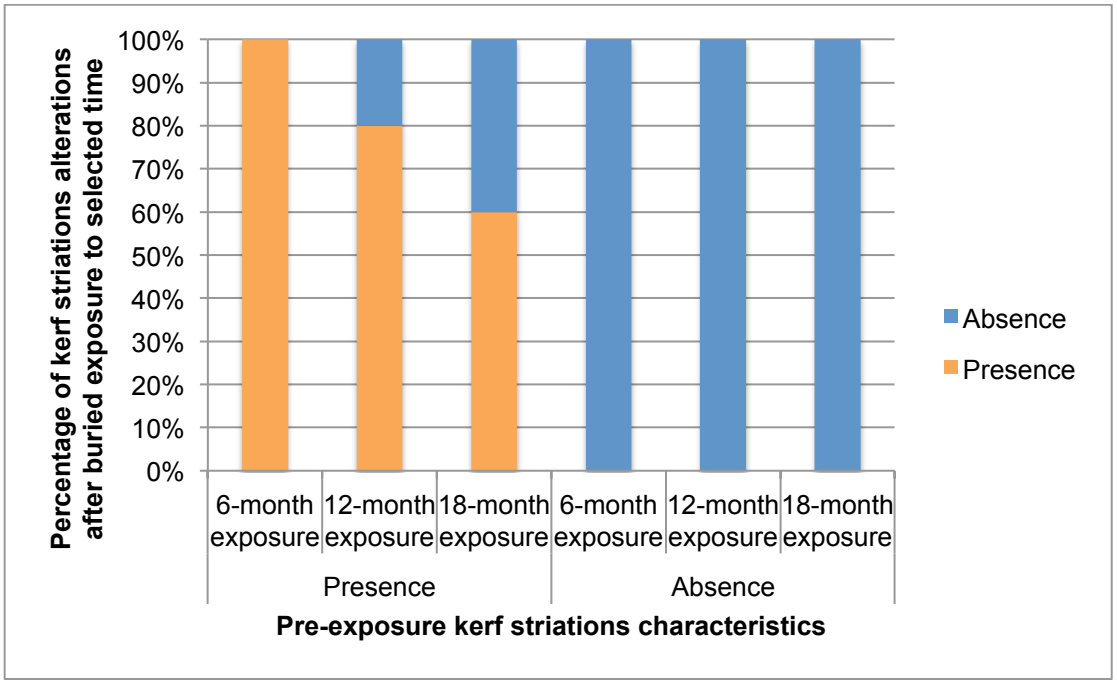

Figure 6.27: Percentage of kerf striation alterations for each surface exposure group of machete-inflicted chop marks

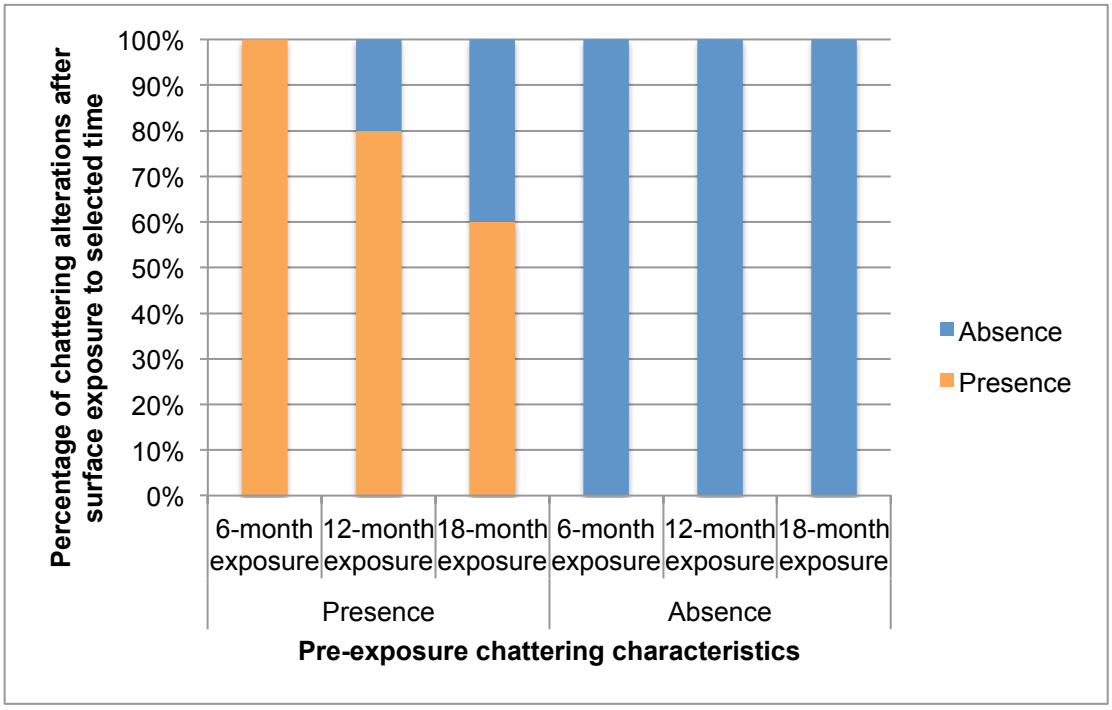

Figure 6.28: Percentage of chattering alterations for each surface exposure group of machete-inflicted chop marks

The statistical significance of the kerf morphology was observed by comparing the data relating to pre-exposure and post-environmental exposure (Table 6.H in APPENDIX 6). Fisher's exact test, which is more accurate with small sample sizes, was used to investigate the relationships between the pre-exposure and post-environmental exposure samples. The kerf margin was found to have undergone a significant change with 18-months surface exposure (p=0.03607), with an alteration from a raised to a smooth margin being detected.

6.1.2.1.2.2 Buried femoral samples

6.1.2.1.2.2.1 Dimensional change

Figures 6.29 and Table 6.F in APPENDIX 6 demonstrates the changes in the kerf lengths and widths of the machete-inflicted chop marks for the buried deposition. A gradual decrease in dimensions was observed for each post-exposure group, and the percentages of the dimensional alterations were explored in-depth to compare each group (Table 6.11). Figure 6.30 demonstrates more in-depth profiles of the correlation between changes in the kerf length and width by comparing the data for the pre-exposure and the three ranges of environmental exposure. All 18-months surface exposed samples exhibited a decrease in their lengths and widths. No sample presented an increase in both dimensional changes during experimental periods.

Table 6.11: Dimensional changes of machete-inflicted chop marks after exposure to the buried environment for 6, 12, and 18 months

Dimension	Alterations	Number of samples (%; each group: n=12)		
		6-months	12-months	18-months
Length	Increased	2 (16.7)	1 (8.3)	-
	Decreased	10 (83.3)	11 (91.7)	12 (100)
Width	Increased	2 (16.7)	4 (33.3)	7 (58.3)
	Decreased	9 (75)	8 (66.7)	5 (41.7)
	Same	1 (8.3)	-	-

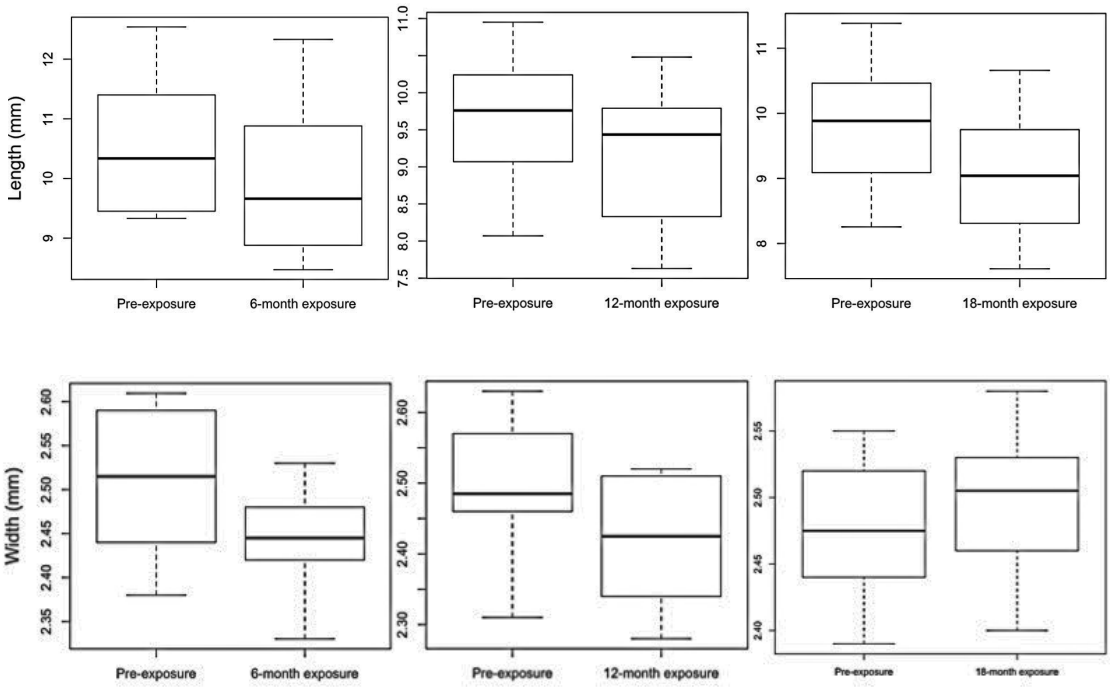

Figure 6.29: Observed width differences of the buried machete-inflicted chop marks; each group n=12

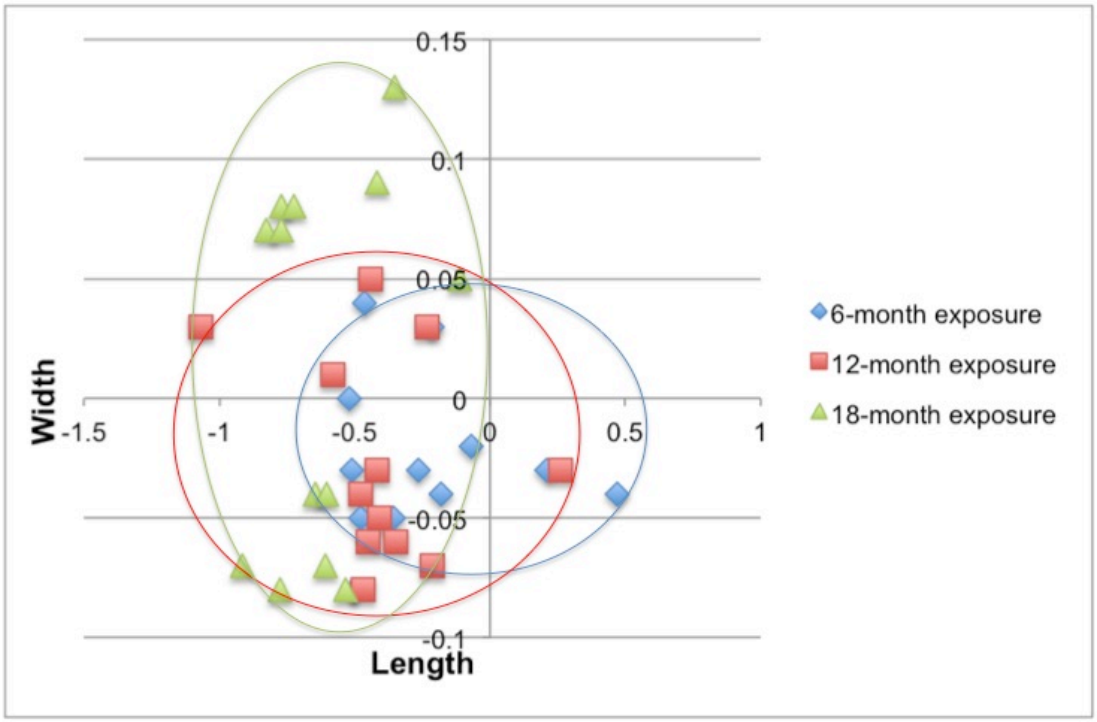

Figure 6.30: Comparison of the dimensional changes in the kerf lengths and widths of the machete-inflicted chop marks

Intersection of scatter data was observed, particularly a wide range in the distribution of the 6-months and 12-months exposure groups. The most extensive area of the group-related pattern was observed in the 18-months group. All 18-months samples showed a decrease in kerf length. The kerf widths increased substantially during the last 12 months of this study, with a maximum increase of 0.13 mm. However, there were no statistically significant differences between the pre-exposure and environmental-exposure values for both length and width of the same sample (Table 5.G in APPENDIX 5). Linear regressions were conducted to study the relationship between exposed in the data (Figure 6.31-6.32). Predictive changes of the kerf dimension could be expected from the equation.

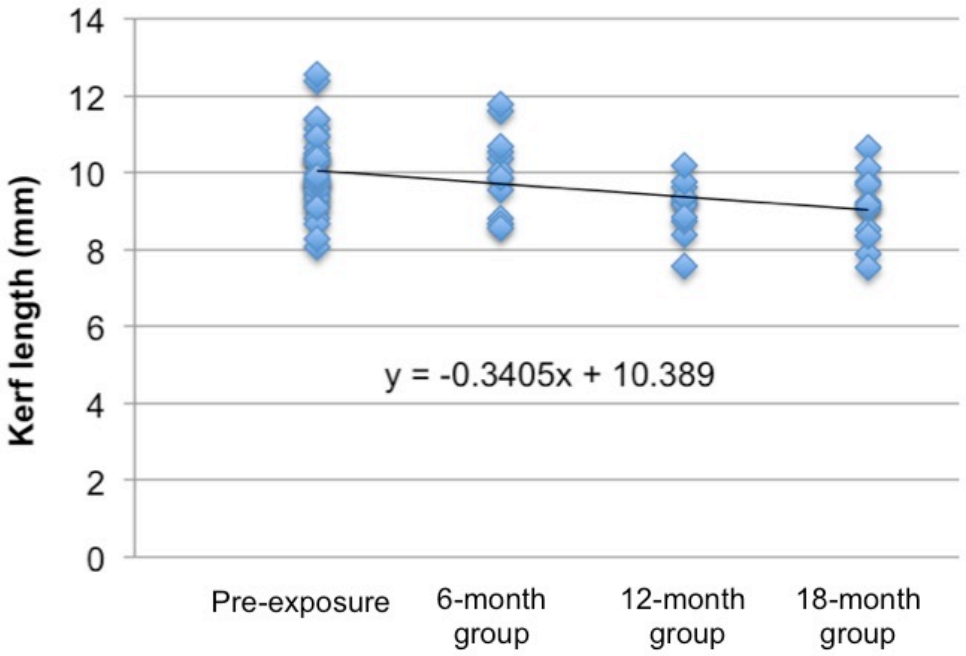

Figure 6.31: The scatter plot with a simple regression equation of kerf length of buried machete-inflicted chop marks

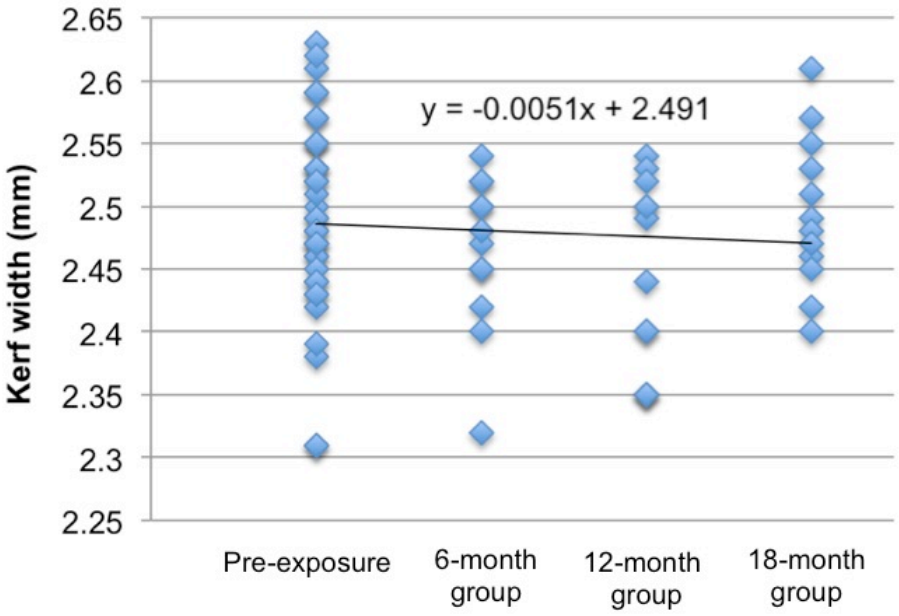

Figure 6.32: The scatter plot with a simple regression equation of kerf width of buried machete-inflicted chop marks

6.1.2.1.2.2.2 Kerf morphology

The machete-inflicted chop marks on the bones exposed to buried deposition over the experimental periods displayed some changes to their kerf features. Table 6.12 and Figures 6.33 to 6.37 summarised the percentages of the kerf feature changes for various aspects of the three surface exposure times of the machete-inflicted marks. According to Figure 6.33, only 14.3% of the elliptically-shaped marks adopted an irregular shape after 18-months surface exposure. In addition, 10% and 18% of the V-shaped cross-sections changed their morphology after 12- and 18-months buried exposure, respectively (Figure 6.34). Twenty-five per cent of the 18-months exposure raised machete-inflicted margins became smooth margins (Figure 6.35). Furthermore, 12.5% and 25% of the kerf striations characteristics had been gone by 12- and 18-months burial, respectively (Figure 6.36). Only 20% of the chattering disappeared after 18-months burial (Figure 6.37). These findings were different from the results for the surface-exposure group of machete-inflicted chop marks, which demonstrated faster and more significant changes of kerf morphology.

Table 6.12: Summary of frequency data of kerf morphology changes between pre-exposure (Pre-E) and post-burial (Post-E) machete-inflicted samples

Kerf morphology		6-months exposure (%; n=12)		12-months exposure (%; n=12)		18-months exposure (%; vn=12)	
		Pre-E	Post-E	Pre-E	Post-E	Pre-E	Post-E
Kerf shape	Elliptical	8 (67)	8 (67)	7 (58)	7 (58)	7 (58)	6 (50)
	Rectangular	1 (8)	1 (8)	1 (8)	1 (8)	2 (17)	2 (17)
	Irregular	3 (25)	3 (25)	4 (33)	4 (33)	3 (25)	4 (33)
Cross-section	V-shaped	10 (83)	10 (83)	10 (83)	9 (75)	11 (92)	9 (75)
	U-shaped	2 (17)	2 (17)	2 (17)	3 (25)	1 (8)	3 (25)
Kerf margin	Smooth	6 (50)	6 (50)	5 (42)	6 (50)	4 (33)	6 (50)
	Raised	6 (50)	6 (50)	7 (58)	6 (50)	8 (67)	6 (50)
Striations	Present	8 (67)	8 (67)	8 (67)	7 (58)	8 (67)	6 (50)
	Absent	4 (33)	4 (33)	4 (33)	5 (42)	4 (33)	6 (50)
Chattering	Present	5 (42)	5 (42)	5 (42)	5 (42)	5 (42)	4 (33)
	Absent	7 (58)	7 (58)	7 (58)	7 (58)	7 (58)	8 (67)

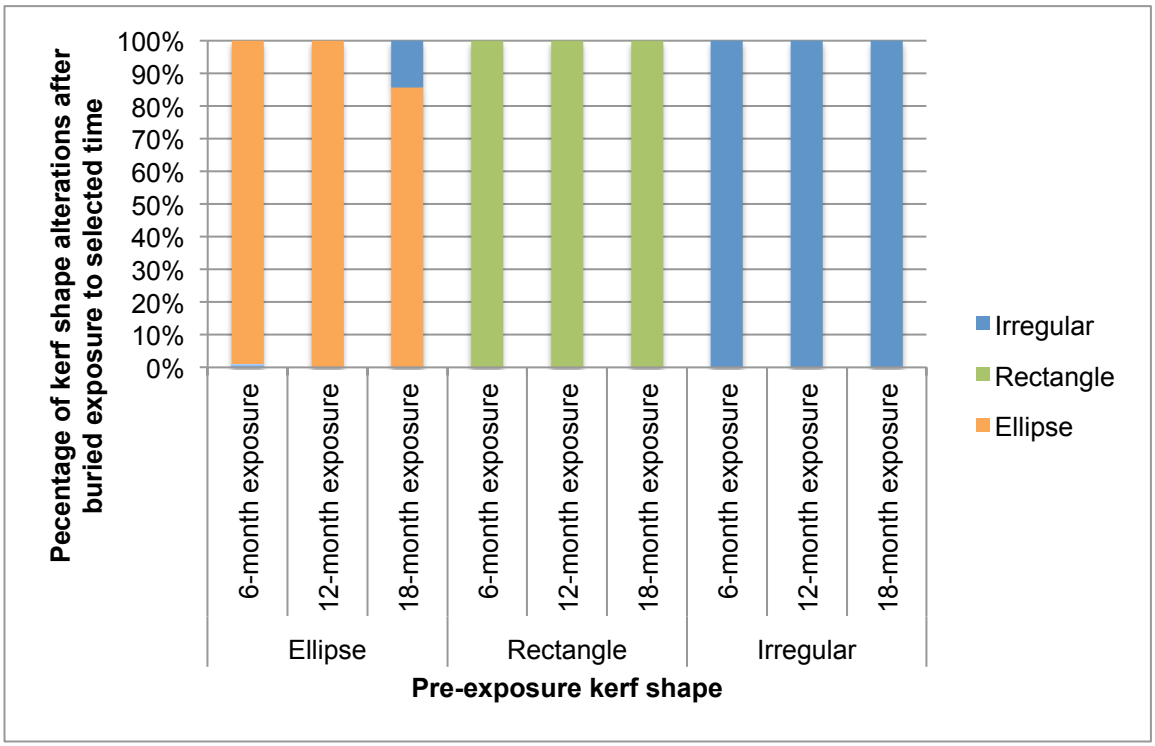

Figure 6.33: Percentage of kerf shape alterations for each buried exposure group of machete-inflicted chop marks

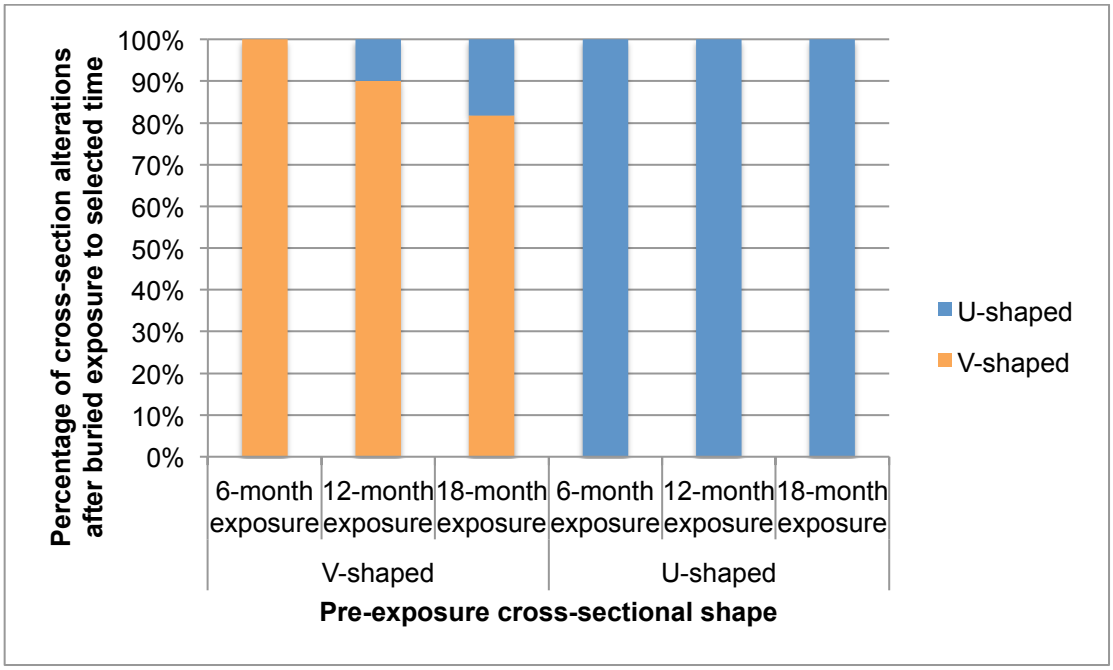

Figure 6.34: Percentage of cross-section shape alterations for each buried exposure group of machete-inflicted chop marks

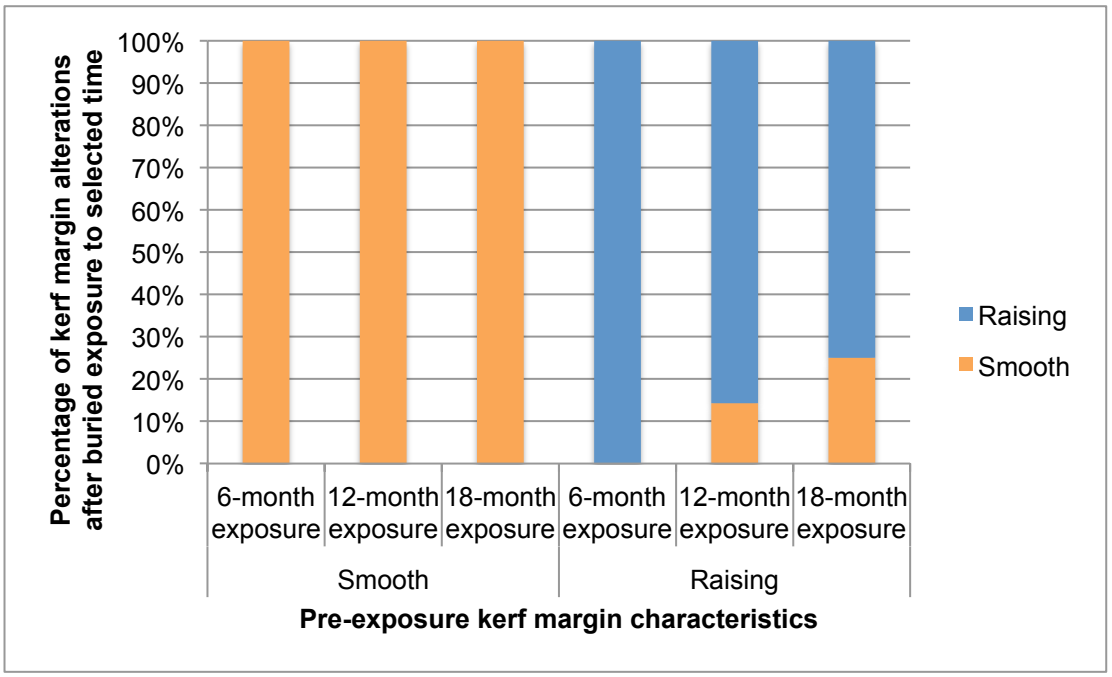

Figure 6.35: Percentage of kerf margin alterations for each buried exposure group of machete-inflicted chop marks

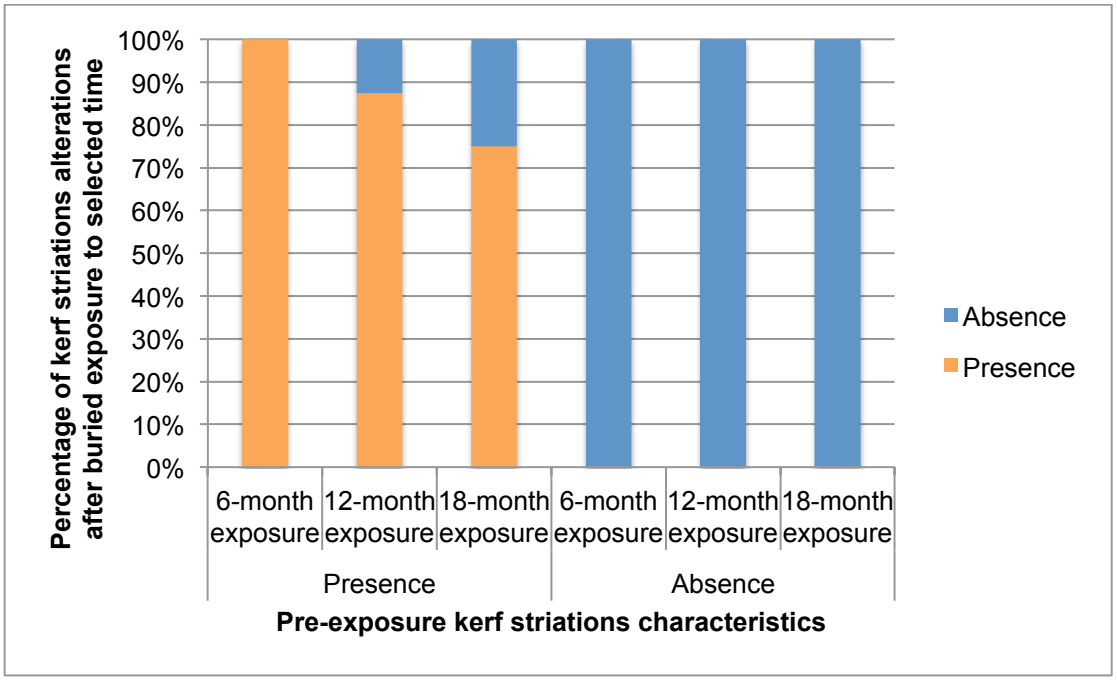

Figure 6.36: Percentage of kerf striations alterations for each buried exposure group of machete-inflicted chop marks

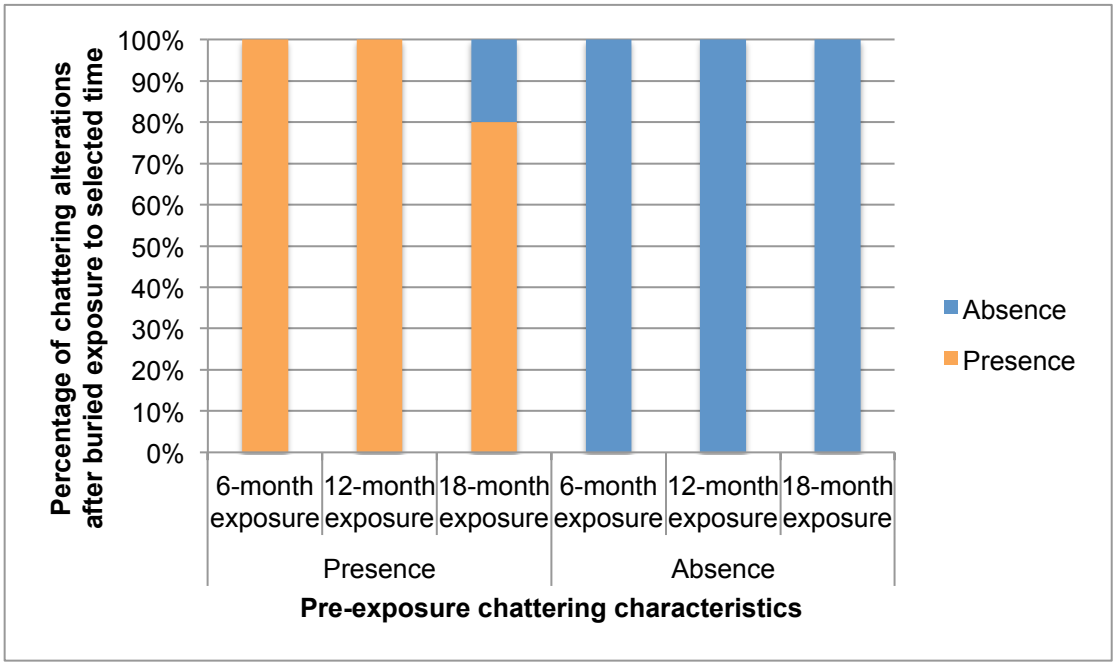

Figure 6.37: Percentage of chattering alterations for each buried exposure group of machete-inflicted chop marks

Statistical significance of the kerf morphology was observed by comparing the pre-exposure and post-environmental exposure data (Table 6.H in APPENDIX

6). Fisher's exact test, which is more accurate for a small sample size, was used to investigate the relationships between pre-exposure and post-environmental exposure samples. There were no significant changes in the data for the buried exposure group.

6.1.2.2 Micro-computed tomographic examination

The 3D micro-CT datasets relating to the sites of the chop marks were used to obtain two-dimensional slices that optimally showed the cross-sectional planes of the wound profiles (APPENDIX 3.B). Based on non-invasive techniques that can document bone structure and the associated fracture, the researcher was able to interactively section the suspected areas from the 3D datasets and analyse them.

A morphological variation within chop marks was observed. Every mark produced by the machete showed fracture lines at the base, with or without a raised margin. In contrast, relatively few cleaver-inflicted chop marks (20.8%) exhibited a fractured base. Figures 6.38 and 6.39 display two cross-sectional sets of the same machete-induced sample before and after environmental exposure. The proximal edge of the chop mark margin was clearly raised and fractured at its base. After environmental exposure, the same chop mark showed a loss of kerf margin and the site of the mark was enlarged (Figure 6.40). In contrast, cross-sectional profiles of cleaver-induced marks showed raised margins without cracking and fracture at their base; thus no flake becoming detached after 18-months exposure (Figure 6.41).

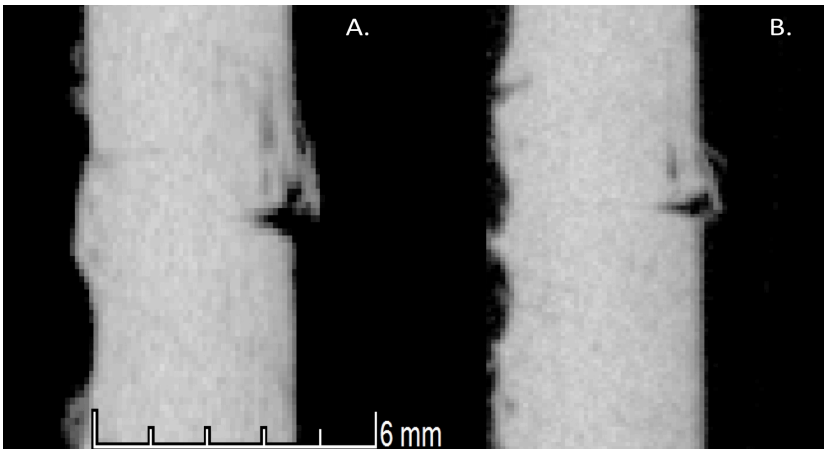

Figure 6.38: Images of the same machete-inflicted mark: (A.) pre-exposure; (B.) 12-month surface exposure; the loss of margin sharpness is observed

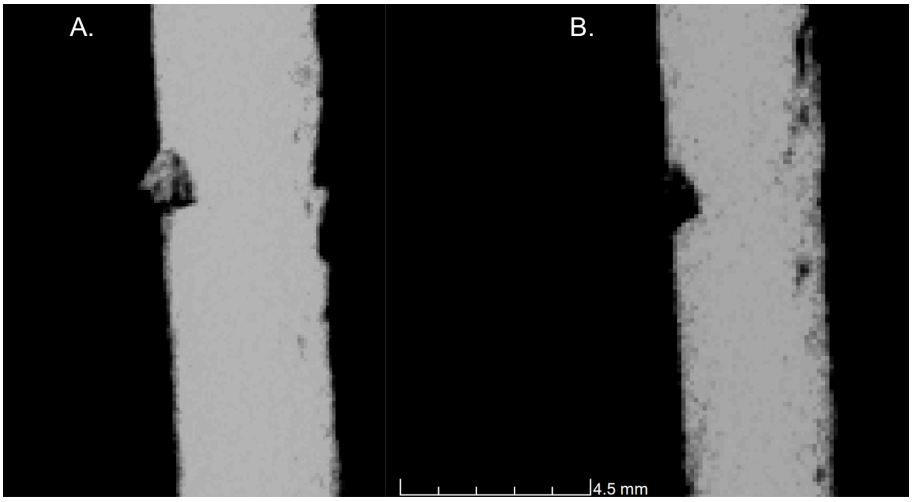

Figure 6.39: Morphological change of the machete-inflicted mark: A. pre-exposure; B. 18-months post-environmental exposure showing a loss of the chop mark margin

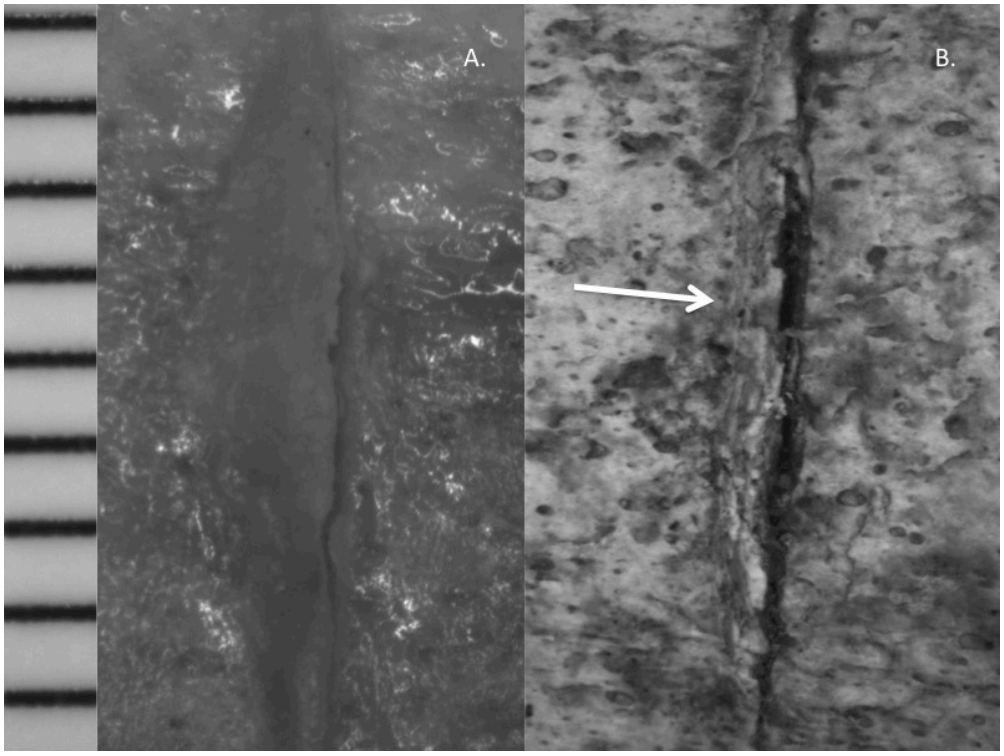

Figure 6.40: The same chop mark as Figure 6.31; A. pre-exposure; B. 18-months post-environmental exposure; the white arrow demonstrates the loss of kerf margin

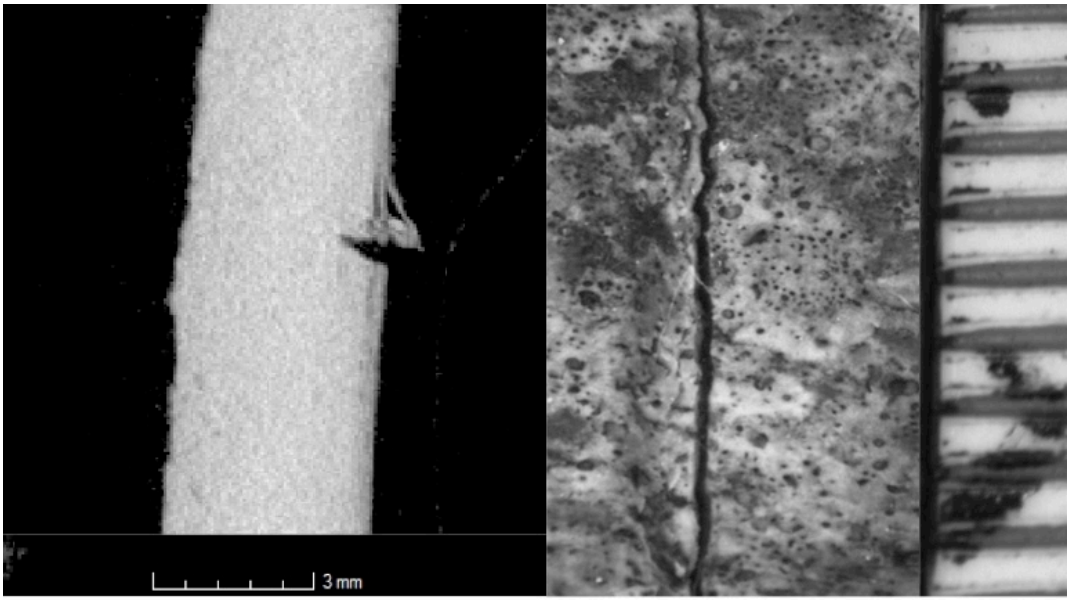

Figure 6.41: The 18-month surface-exposure chop mark inflicted by a cleaver; the scale on the right is in mm

A quantitative analysis of the micro-CT data was performed to compare the pre- and post-exposure samples. The following characteristics describing the proportions of the chop marks were measured: maximum length, maximum width, maximum depth, proximal and distal shoulder heights, proximal and distal slope angles, and opening angle. Most of the results of the dimensional changes for the cleaver-inflicted (n=72) and machete-inflicted (n=72) chop marks illustrated no statistically significant difference between pre-exposure and post-environmental exposure; however, the surface-deposited group of machete-inflicted marks demonstrated some modifications (Table 6.E, 6.J in APPENDIX 6). The kerf width and the proximal and distal shoulder heights were statistically significant different between pre-exposure and 12- and 18-months exposure (Figures 6.42 to 6.44).

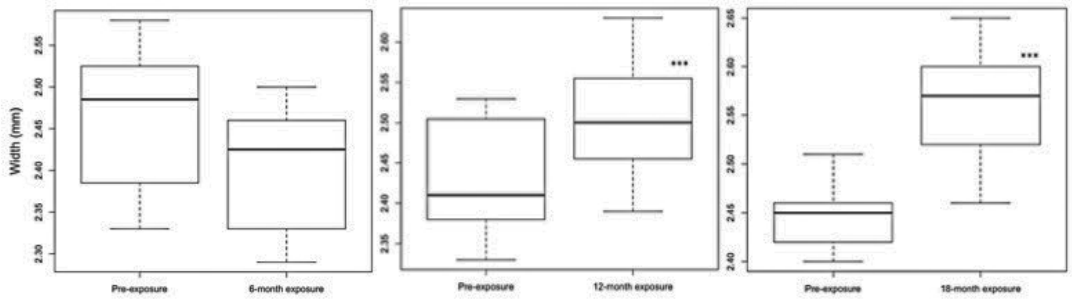

Figure 6.42: Observed width differences of surface-deposited machete-inflicted chop marks (*** statistical significance of the same sample between pre-exposure and post-exposure values)

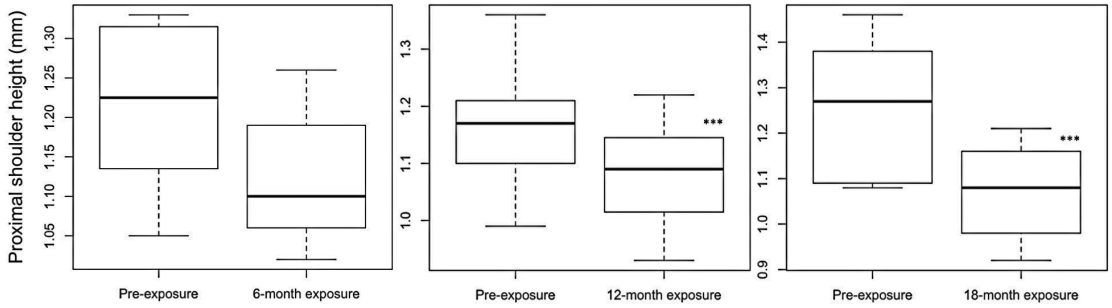

Figure 6.43: Observed proximal shoulder height differences of surface-deposited machete-inflicted chop marks (*** statistical significance of the same sample between pre-exposure and post-exposure values)

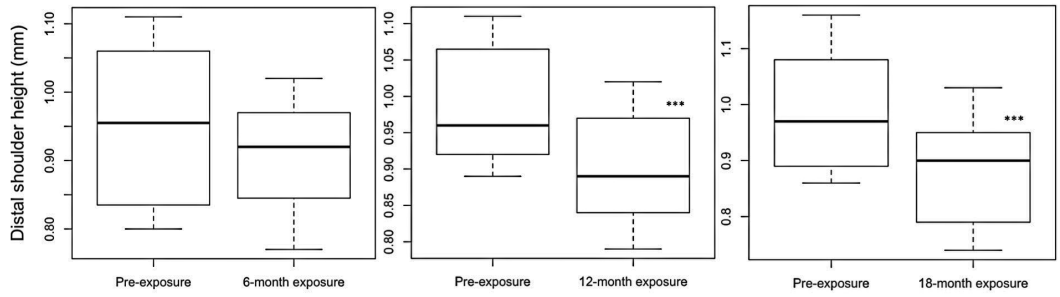

Figure 6.44: Observed distal shoulder height differences of surface-deposited machete-inflicted chop marks (*** statistical significance of the same sample between pre-exposure and post-exposure values)

6.1.3 Summary

Both types of weapon used in this study had a distinctive appearance. The cleaver-inflicted marks showed smaller, elliptical, V-shaped wounds without striations and chattering. The marks produced by the machetes had a crushed and fragmented appearance and exhibited V-shaped, raised margins. As observed in this study, although the kerf lengths and cross-sectional shapes could not be used for differentiation purposes, the other morphology and the kerf width had the potential to differentiate the marks inflicted by the cleaver and the machete.

The results of the current study showed an advanced degradation of the specific area of the surface-deposited samples, with the most significant alterations displayed by the machete-inflicted chop marks. These alterations could be recognised in the dimensional and morphological changes of the chop marks. Reanalysis of the traumatic lesions after surface environmental exposure exhibited significant changes, whereas a slower degradation was observed in the buried samples. Morphological analysis revealed that 14.3% of the raised kerf margins of the machete-inflicted chop marks started to be damaged after 6-months surface exposure, with 75% of the machete samples being damaged by 18-months surface exposure. Microscopically, fractured cortical margins were observed, and these features caused alterations to the kerf widths. However, no statistically significant differences were observed between the data for the pre-exposure and post-environmental exposure of the cleaver-inflicted chop marks.

6.2 Discussion

The overall objective of this study is to determine whether taphonomic factors can obscure or damage a traumatic lesion or, at least, change some characteristics of a sharp force injury. Despite the literature reporting results on the taphonomic identification of sharp force stigmata (Fisher, 1995; Symes *et al.*, 2002; de Juana *et al.*, 2010), very few forensic studies have focused on these topics to observe for real application (Symes *et al.*, 2002; Cappella *et al.*, 2014). Although this chapter deals with the specific area of sharp force trauma, especially hacking trauma, the concept of this chapter emphasises the effects of taphonomic modifications on hacking trauma analysis.

In the present study, 144 chop marks were produced on macerated femurs using a mechanical drop tower. The use of a mechanical apparatus for trauma infliction on a bone is common (Houck, 1998; Bartelink *et al.*, 2001; Alunni-Perret *et al.*, 2005; Shaw *et al.*, 2011; Macoveciuc *et al.,* 2017). This method permits the force and location of each weapon impact on the femoral samples to be controlled. As a result, it was apparent that the chop marks produced by this method were very consistent in size and shape. The chop marks inflicted by the two weapon types (cleaver and machete) were noticeable both qualitatively and quantitatively, appearing almost as literature examples of idealised chop marks. Therefore, the researcher endeavoured to control several extrinsic and intrinsic factors affecting traumatic lesion morphology, for example the implement used, the length of the impacted blade, and the force of the blow of each weapon type (Bartelink *et al.*, 2001; Alunni-Perret *et al.*, 2005). Nevertheless, there were some conditions in this study that could not be effectively controlled.

The appearance of morphological variability in the traumatic lesions inflicted by the same type of weapon is a sign that this experiment could not wholly control all the variables. Even though the blade was fixed firmly and was unable to move inside the carriage and striker chamber, rotation would have been produced by the sample itself. The bone material was flexible and could therefore have moved slightly as a result of the impact of the blade. In addition, although this study strove to control the trauma-inflicted event, the angle of impact was not totally controlled. Chop marks on most of the femoral samples were not made perpendicularly to the long axis of the femoral elements due to the slight curvature of the bone surface. As a result, glancing impacts at a slightly oblique angle produced an oblong shape with a raised edge at the acute-angled margin. This appearance confirms with that reported by previous studies (Wenham, 1989; Humphrey and Hutchinson, 2001; Lynn and Fairgrieve, 2009a). Because the impact angle is the only slight acute-angled impact, all raised borders found in this study were still attached to the underlying bone without any detached bone flakes.

Moreover, as explained in Chapter 3, the bone samples were placed on rigid, non-deformable sponges in the sample chamber during their blowing event. Therefore, this hacking trauma study is the most accurately used for scenarios

where an injury is inflicted on a bone that has been placed on a hard object (such as a person lying on the ground), rather than the usual situation in which a person is standing. The best experimental condition would be to have the bone samples held in the air and articulated with the rest of the body when it is struck with a weapon. This is able to offer the same resistance as found in the real scenario.

The bone properties have a substantial effect on a traumatic event and its analysis. Each bone used in this study was not equal in density at the impact site. Also, the juvenile bones used in this study had a different bone composition, with a more inherently elastic and less mineralised mass than adult skeletal material (Kalkwarf *et al.*, 2007; White *et al.*, 2012). These flexible bones consequently tended to have more significant changes in their dimensions as a result of the loss of organic and moisture components during environmental exposure (Cunningham *et al.*, 2011). Chop marks located in a lower bone density area tend to be affected by taphonomic factors (Haglund and Sorg, 1997).

A variety of sharp force traumas resulting from different types of hacking weapon were explored in this study. Sharp-inflicted fracture characteristics not only depend on the biomechanical property of the target bone but also the overall features of the inflicting weapon. The length and heaviness of cleavers and machetes, when compared to the shorter and more rigid structure of kitchen knives, may be a factor to consider. A knife used for a short stroke to cut or stab is defined as a short-light weapon, with most of the applied force coming from the attacker (Houck, 1998; Kimmerle and Baraybar, 2008). Conversely, a long-heavy weapon, such as a machete or an axe, has most of its force originating from the large stroke, and the weapon can build considerably more momentum and kinetic energy than a short-light weapon. In addition, the tapered edge of a long-heavy weapon tends to make a V-shaped cut that is much wider than that of a short-light weapons (Kimmerle and Baraybar, 2008). Although weapons such as cleavers fall in between short-light and long-heavy weapons because of their blade size and how their energy is acquired, the mark they leaves on target bone is more consistent with a hacking weapon (Kimmerle and Baraybar, 2008).

In comparison to previous literature, this study made a reasonable effort to control perimortem trauma by using a mechanically traumatic device. Although the

applied force was not standardised, each sample received a force as they could bear without breaking completely. Though it would be challenging to control all extrinsic and intrinsic variables, close observation suggested that the chop marks produced in this way were more realistic than in a controlled experiment and therefore were more meaningful for their application to real forensic cases.

6.2.1 Pre-exposure comparison between cleaver and machete

In this study, macroscopic, microscopic and micro-CT observations were used in order to distinguish the cleaver-inflicted marks from those inflicted by a machete (Humphrey and Hutchinson, 2001; Tucker *et al.,* 2001; McCardle and Lyons, 2015). Comparatively, this study utilised enough criteria to make a reasonable decision about which weapon was used. The morphological and dimensional differentiation between each type of hacking trauma is essential in order to establish predictable assessments in post-environmental exposure. As discussed earlier, the accurate identification of the taphonomic effects on sharp force trauma depends on traumatic pattern recognition as well as the extrinsic and intrinsic factors determining the mechanism of a fracture.

Normally, the elastic response of the organic component of bone enables chop marks to demonstrate evidence of the blade edge. Comparisons of the morphological appearance and its mechanism of hacking marks provide a basis for consideration and discussion of taphonomic effects on each characteristic. Hacking trauma tends to present with a combination of compressive and shearing forces applied dynamically with a narrow focus (Humphrey and Hutchinson, 2001; Alunni-Perret *et al.*, 2005; Lynn and Fairgrieve, 2009a; McCardle and Lyons, 2015; McCardle and Stojanovski, 2018). In other words, cleaver and machete-induced trauma is necessarily a blunt impact inflicted by a sharp object. This mechanism means that when a hacking weapon impacts on a bone, its sharp edge cuts into a bone material creating sharp force characteristics; meanwhile, the shearing force creates surrounding fractures representative of blunt force trauma (Humphrey and Hutchinson, 2001; Lewis, 2008). Therefore, the analysis of the nearby bone tissue is essential.

Injuries caused by hacking weapons tend to show significantly visually and microscopically more damage (Houck, 1998; Alunni-Perret *et al.,* 2005; Lewis, 2008; Thompson and Inglis, 2009). A lack of fracturing and crushing in cleaver-induced chop marks easily distinguished them from those by machete. Lewis (2008) and Humphrey and Hutchinson (2001) showed that the machete produced a deep V or U-shaped cross-section with severe damage on the kerf margins. These are consistent with the findings in this study. Fractures usually occurred at the kerf floor and then radiating to surrounding areas. Some fractures happened with small fragmented pieces of chattering at kerf margin. Although these features may be used to identify an inflicted weapon, it is necessitate to employing standard methods or protocols that can identify and provide additional unique characteristics of specific chop marks regarding cleaver and machete, as well as other hacking weapons. However, some less damaged chop marks created by the machete could potentially mimic those imparted by the cleaver. Thus, statistical tests were conducted to detect differences between a cleaver and a machete.

6.2.1.1 Kerf dimension

Quantification of chop mark dimension could have an enormous potential for distinguishing inflicting weapons. Even though the overlap of length and width between cleaver and machete of chop mark dimensions has been encountered in previous studies (Lyman, 2005; de Juana *et al.*, 2010). The current study demonstrated that a statistical significance ($p<0.001$) of the kerf width between each type of the chop mark was observed. This result showed that there is potential to differentiate between cleaver-inflicted and machete-inflicted chop marks with kerf width.

Macroscopic and microscopic examinations would allow the researcher to establish the general characteristics of each chop mark. Nevertheless, fundamental alterations were noted, such as differences in dimensional measurements within individual chop marks. As Humphrey and Hutchinson (2001) displayed that machete-inflicted marks showed mean kerf width of 2.46 mm, the current study's findings were consistent with their result, as mean kerf width of 2.477 mm. While the results of cleaver-inflicted marks exhibited different values, with 1.88 mm and 1.362 mm measuring in Humphrey and Hutchinson (2001) work and this study,

respectively. A larger weapon blade could produce longer and broader sharp-inflicted injuries (Humphrey *et al.*, 2017). This difference might be attributed to different weapon sizes and several extrinsic and intrinsic factors influence chop mark morphology rather than the weapon used, including the force and angle of the blow, and the bone density at the impact site (Bartelink *et al.*, 2001; Boucherie *et al.*, 2017).

The chop mark width is associated with the weapon edge thickness, and therefore this relationship may be used to matching a suspected weapon (Norman *et al.*, 2018). However, during the traumatic event, the fresh bone tissue adjacent to hacking trauma is compressed to the sides, and when the weapon is withdrawn, the elastic property of the bone tends to close (Humphrey and Hutchinson, 2001; Alunni-Perret *et al.,* 2005; Lynn and Fairgrieve, 2009a). As a result, the kerf width is usually smaller than the blade that caused it. These correspond with the findings in this study, as the maximum width of the cleaver blade and machete blade was 2.05 mm and 3.13 mm, respectively. Therefore, using the kerf width as a criterion to identify the unique hacking weapon, but not the type of weapon, is unreliable (Maples *et al.*, 1989; McCardle and Lyons, 2015).

The length of hacking marks in this study totally overlapped between cleaver and machete. Thus, it was not possible to distinguish the weapon blade type with the length of chop marks. Theoretically, the kerf length depends on the surface area of impact and amount of force (Bello and Soligo, 2008; Humphrey *et al.,* 2017). The increasing force from the different weight of the weapon blade could increase the length of the marks as the force acted primarily in the movement of the weapon blade. The force calculated in this study was dependent on the weight of the weapon blade mass, and it was intentionally controlled in this study. In addition, the surface area impacted by the weapon blade influenced the kerf length (Bello and Soligo, 2008; Humphrey *et al.*, 2017). This variable was also controlled by careful selection of the bone samples, to ensure consistency in size and surface area. Therefore, no significant association between the kerf length and a weapon type has been demonstrated in this study.

6.2.1.2 Kerf morphology

Kerf shape characteristics were another essential criterion to distinguish inflicting weapons. The current study sought to compare each morphological feature of chop marks made from cleaver and machete on femurs. Cleaver-induced trauma exhibited an elliptical V-shaped with a mostly smooth margin and absence of striations and chattering. In contrast, the profiles of machete-inflicted marks showed some different pattern. Their morphology exhibited an elliptical V-shaped cross-section with raised margin and more often striation and chattering on kerf margin. These appearances corresponded with the finding of previous literature (Humphrey and Hutchinson, 2001; Tucker *et al.*, 2001; de Gruchy and Rogers, 2002; Alunni-Perret *et al.*, 2005). It is essential to clarify that, while the presence of morphological features may help to identify a chop as inflicted from a cleaver or a machete, the absence of these features is unable to usefully assist to identify the other class. For example, the presence of irregular kerf shape can be used to identify chop marks inflicted by a machete; however, the absence of this feature does not necessarily support that a cleaver inflicted the chop mark. In sum, the characteristics described in this study should be used together with each other to reach the best conclusion.

The mechanism of blade impact in this study did not slide through the bone surface but struck above it, leading to more symmetrical kerf dimensions. Kerf shapes have a significant relationship with blade features of the hacking weapon. Machetes produced 65% of elliptical shape, followed by irregular shape (25%) and rectangular shape (10%), while cleavers produced a higher number of elliptical shape (around 85%) and rectangular shape (15%). Indeed, this difference might be due to different blade features, as the wider blade of machete could impact the larger surface area of the bone surface with its blunt edge, resulting in a more irregular shape. Therefore, it is reasonable that irregular shape and rectangular shape are more common for machete-inflicted marks. Location of the impact site also plays another critical role in kerf shape features. Chop marks at a lower bone density area, such as metaphyseal part of femurs, were often more irregular or rectangular shape because the pressure of the weapon blade could break the surrounding thinner cortical layer. Also, the variations in feature frequencies between each weapon group may indicate that the angle and the subsequent depth

may have effects on the kerf shape of the chop marks (Humphrey and Hutchinson, 2001; Lynn and Fairgrieve, 2009b; McCardle and Stojanovski, 2018).

This study revealed the same trend of V-shaped cross-section of cleaver and machete-inflicted marks, with fewer U-shaped chop marks (around 20%). Therefore, the cross-sectional shape was not suitable for weapon differentiation in this study. Not surprisingly, almost broader and deeper U-shaped kerfs were found in the area of lower bone density such as metaphyseal area. As discussed earlier, deeper sharp-inflicted marks are commonly broader and leave a U-shaped cross-sectional mark (Shipman and Rose, 1983; Symes *et al.*, 2010). The raised edge in 15% of the cleaver-inflicted marks was less frequent than 60% of machete-inflicted chop marks. The explanation of this phenomenon is probably a slight angle between the blade and the surface of the bone. As discussed earlier, the weapon blade in this study was not fully positioned at a 90-degree angle of the bone surface. Therefore, the pressure of the blade dissipates to the surrounding cortex at an angle other than 90° (Wenhan, 1989; Alunni-Perret *et al.,* 2005). Bone trauma by the wider and irregular edge of a hacking weapon such as the hatchet or machete is proven to give an impression of lateral destruction of the sample, which is significant compared with the use of knife or cleaver (Humphrey and Hutchinson, 2001; Tucker *et al.,* 2001; Alunni-Perret *et al.*, 2005; McCardle and Stojanovski, 2018).

It is possible to observe striations left by a specific tool on the floor and the walls of sharp force lesions. Bonte (1975) emphasised the crucial importance of the careful examination of striations found on bone or cartilage in order to identify the characteristics of the weapon as well as the direction of the inflicting blade. Capuani *et al.*, (2014) suggested that striations were more reliable variable than the feature of kerf wall. The plastic response of the organic components of skeletal tissues allows the kerf surfaces to show evidence of the blade edge. Kerf striations are oriented parallel to the direction of the blade, that is vertical to the kerf floor as noted by previous literature (Wakely, 1993; Humphrey and Hutchinson, 2001; Tucker *et al.*, 2001; Capuani *et al.*, 2014). In contrast, slicing striations in case of those left by saws or knife cut wound are oriented parallel to the kerf floor. In this study, kerf striations were found in the machete-inflicted marks, while this feature was not found in all cleaver-inflicted marks in the microscopic study. This is

inconsistent with the previous work by Tucker *et al.* (2001) revealing thin, fine and distinctive striations range from widely spaces to close spaces in their cleaver-induced marks. These may be due to the different condition of the cleavers. Tucker et al. (2001) used the cleavers that were previously used for several years, leading to several wear-and-tears along the blade surface. Therefore, it was apparent that striations observed on the kerf surface of the bone result directly from this wear-and-tear structure. However, the cleaver used in this study was a new purchase, that meant a few or none of the striations should be observed in this study. Additionally, it is important to note that Tucker *et al.* (2001) analysed chop surface with 20x to 160x magnification in a SEM. This technique showed more significant observations compared with the stereomicroscopic examination in this study.

There were by far more large flakes on the edge, wall and floor of the machete kerf in this study. As mentioned by McCardle and Stojanovski (2018), chattering has been identified as a characteristic of the machete in long bone injuries, and it is commonly present features (44%). Meanwhile, around 40% of machete-inflicted marks were found to exhibit chattering. However, this chattering was not found at kerf floor as observed in fully fleshed samples by Humphrey and Hutchinson (2001), this might provide further evidence to a shock-absorbing capacity of the flesh soft tissues around chop marks that can dissipate energy (Lynn and Fairgrieve, 2009a). It is well known that hacking trauma usually makes a great degree of bone damage. Radiating fractures starting from the impact sites are also predominant in machete-inflicted chop marks; these are likely due to the wedge action of the inflicting blade that can split the bone material in a greater degree than other types of the sharp weapon (Humphrey and Hutchinson, 2001; Lynn and Fairgrieve, 2009a).

6.2.1.3 Micro-computed tomographic examination

Recently, there has been an advanced instrument that enables high-resolution three-dimensional images such as micro-CT. These provide new insights into the interpretation of trauma dimension and morphology (Thali *et al.*, 2003; Bello *et al.*, 2009; Schnider *et al.*, 2009; Pounder and Sim, 2011; Rutty *et al.*, 2013; Komo and Grassberger, 2018; Norman *et al.*, 2018). This study indicated that the micro-CT showed a more effectively accurate technique comparing with microscopic

examination, particularly because micro-CT represented three-dimensional modality to document the injury in all aspects, which could provide a precisely defined measurement.

Micro-CT is an effective technique to visualise and investigate tool mark analysis (Bello *et al.*, 2009; Pounder and Sim, 2011; Komo and Grassberger, 2018; Norman *et al.*, 2018). This study displayed that micro-radiological methods, such as measurements from micro-CT data, were also imperative for analysing chop marks and provide a very useful tool to differentiate among different blade types. In order to discriminate between chop marks inflicted by cleaver and machete, the current study detected several variables, which statistically discriminated both types of marks. These variables were: kerf width, kerf depth, and kerf wall angle (proximal and distal slope angles, and opening angle). All variables were correlated with chop mark structural component and could be used to create a virtual cross-section of the inflicting weapon. However, kerf striations could not be reconstructed from micro-CT imaging.

From the micro-CT study, the depth of chop marks can be measured for dimensional analysis. Most of the machete impacts leave deeper chop marks than in cleaver impacts. In this study, the cleaver penetrated the samples for a mean distance of 2.754 mm, while the machete could chop into the bone for a mean distance of 3.814 mm. This fact can be explained by examining the amount of momentum of impact in this study (Humphrey *et al.*, 2017). Due to its heavier mass, the machete hits have more force, resulting in more in-depth than cleaver impacts. This mechanism may also explain many more findings of chattering and raised margin as discussed earlier. Depth and width of chop marks are related together, with deeper chops normally broader (Andrews and Fernández-Jalvo, 2012). In addition, this study showed that micro-CT could identify sub-surface fracturing in the machete-inflicted marks, which is useful in understanding future changes to chop marks with time.

The micro-CT findings demonstrated that both hacking weapons produced statistically different chop mark widths, depths, and wall angle. These findings correspond with previous work (Capuani *et al.,* 2014; Waltenberger and Schutkowski, 2017; Norman *et al.,* 2018). Micro-CT could be used to measure the

wall angle composing of slope and opening angle. These allow a virtual cross-sectional shape of the chop mark to be generated for overall outline examination. Wall angles were found to be useful variables to categorise weapon type and shape, particularly from the set of tool marks inflicted by the mechanical drop-tower (; (Norman *et al.*, 2018). Slope angles of chop marks were also investigated to test the angle of the weapon impact. If the blade hit the bone exactly vertical, both sides of slope angles should be symmetrical. Conversely, if the blade hit the bone obliquely from right to left, the slope angle should be larger on the right side and vice versa (Waltenberger and Schutkowski, 2017).

By using the micro-CT technique, the researcher could provide a new method for matching a possible weapon used for a pattern hacking injury on the bone materials. Micro-CT measurements of chop mark dimensions corresponded with the microscopic analysis in nearly all cases, therefore demonstrating that the morphological and radiological analysis could be a method for chop mark examination. This study also exhibited that the relationship of morphological changes from microscopic and micro-CT examinations was reliable enough for conclusive comparison.

Nevertheless, it should be noted that although weapon identification was high when judging chop mark shape, the results were never perfect. The amount of severe crushing damage varied considerably between chop marks, leading to making quantitative examinations more difficult. Despite micro-CT being qualified general chop mark morphology, it is a less effective method comparing with quantitative measures such as kerf width (Norman *et al.,* 2018). This specific case may need a further study to explore the implication for forensic cases to justify tool mark shape. In addition, micro-CT is expensive, time-consuming, and less accessible in comparison with microscopy and SEM. A lot of required storage space of micro-CT scans and its reconstructive processes is also a crucial issue in practice. One single TIFF file in this study had a size of more than one gigabyte. In addition, a smooth function of the processing software VGStudio MAX 2.1 requires a high-performance computer processor.

6.2.2 Effects of environmental exposure

To date, a forensic anthropologist is mostly unable to investigate taphonomic changes of traumatic lesions observed on skeletal remains (Capella *et al.,* 2014; Pokines and Symes, 2014). No literature prove how and how many signs of traumatic lesion show up on skeletal material after natural decomposition and taphonomic insults (Capella *et al.,* 2014; Fernández-Jalvo and Andrews, 2016; Schotsmans *et al.,* 2017). Consequently, this study was carried out to determine if macroscopic, microscopic and radiological examinations adequately and reliably detect alterations of chop marks on domestic pig femurs, as well as to determine whether these dimensional and morphological changes happen at a predictive rate with time in order that it might eventually be used to predict their original marks.

An important outcome of the present study was the characteristics of taphonomic modifications of chop marks itself in time. As previously stated in the result section, the most substantial alterations occurred during 6-18 months of surface exposure. At the earlier period kerf edges were clearly defined despite a progressive modification of texture of the bone material, yet after 6 months of exposure, these characteristics were statistically subverted. These findings, along with the progressive change in kerf width and disappearance of kerf striations and chattering, meant that after 18-months surface exposure, the original chop mark morphology cannot be identified. Thus, it is mandatory that forensic anthropologists should keep these results in mind when dealing with trauma analysis of skeletal remains with long-term outdoor exposure.

This study showed that the most significant change of traumatic lesion was noticed when evaluating chop marks near the distal area of femurs, where the most abundant trabecular bone is deposited. The vast majority (80%) of perimortem chop marks identified in this area changed in their dimension and morphology after 18-months environmental exposure. This area consists of thin cortical bone with a high percentage of trabecular bone, and therefore the fragile structure with the fine cortical portion is easily modified by environmental factors (Cappella *et al.*, 2014). These issues may cause an incorrect assessment of sharp force trauma on long bones. Previous work by Cappella *et al.* (2014) mentioned that the postmortem modifications usually happen in bone materials rich in spongy tissue such as ribs,

pelvic bones and vertebrae. This study has shown the results in the same way, in which the trauma interpretation was barely possible but no criterion existing for trabecular bone (Ubelaker and Adams, 1995; Ubelaker, 1997; Moraitis *et al.*, 2008; Wheatley, 2008; Wieberg and Wescott, 2008; Cappella *et al.*, 2014; Wedel and Galloway, 2014). Therefore, the lack of data regarding the bone fractures in trabecular-rich bones still poses a significant problem. Further study should be conducted in order to find more reliable criteria that can offer valuable help in the anthropological investigation of skeletal trauma.

6.2.2.1 Dimensional changes of the chop marks

The measurements reported here greatly extend the previous idea of diagenetic processes happening in contemporary skeletal remains. A marked difference in maximum length and width between before and after environmental exposure was observed. All cleaver-inflicted chop marks showed a decrease in all dimension after 18-months exposure to the surface and buried environment. However, a few cleaver-inflicted marks displayed an increase in their dimension during the first 6 months of exposure. These findings were consistent with dimensional alterations of cut marks in the previous chapter. Therefore, these results showed some similarity between cleaver-inflicted mark and knife cut mark, confirming cleaver was categorised between the short-light weapon and the long-heavy weapon because of their blade size and how the energy acquired (Kimmerle and Baraybar, 2008; Wedel and Galloway, 2014).

Compared with dimensional changes in a cut mark, cleaver-induced chop marks showed a different pattern of taphonomic modification. The most significant change of the dimension in this study is that which took place after 12 months of post-surface exposure (Figure 6.45-6.46).

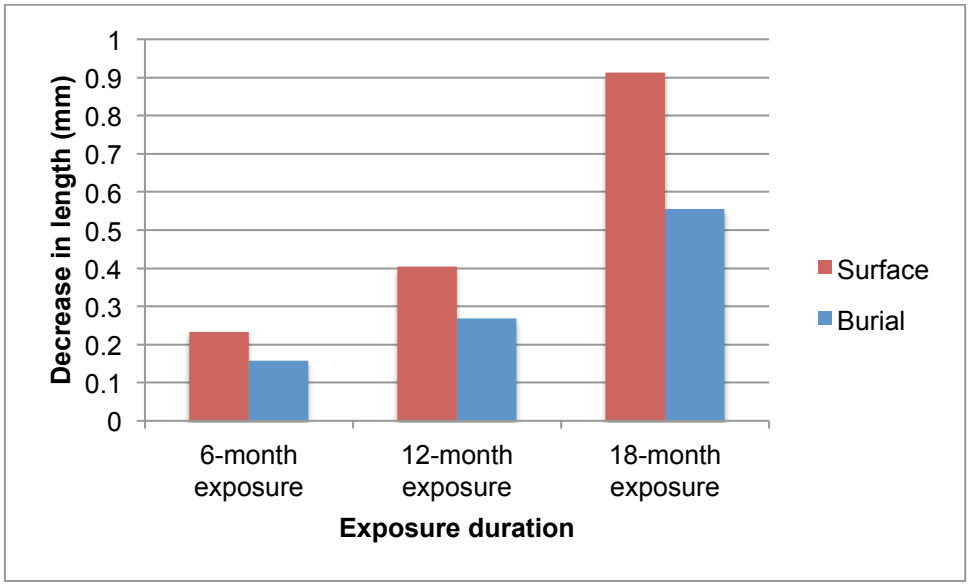

Figure 6.45: Reduction in maximum length over post-environmental exposure time in cleaver-inflicted marks

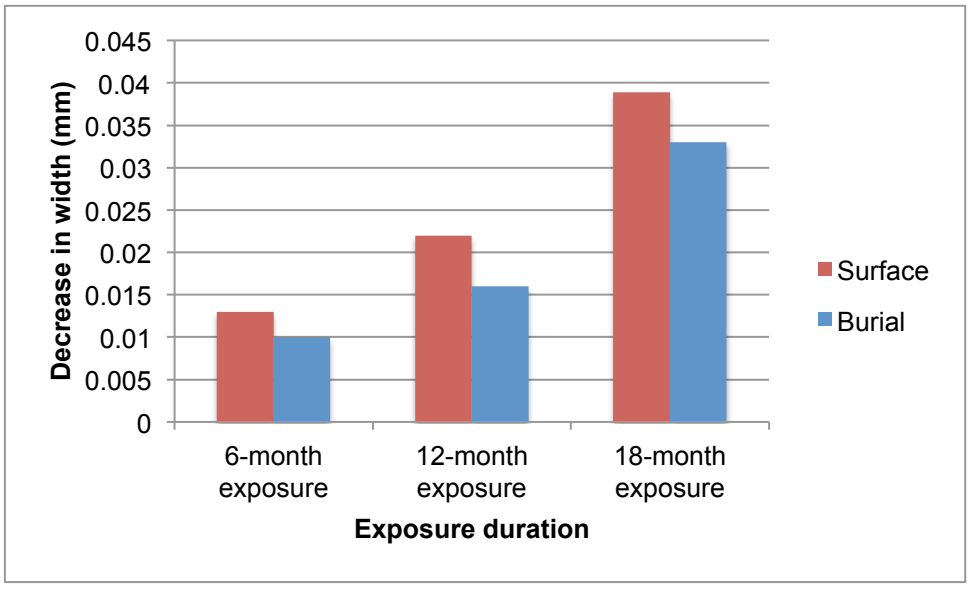

Figure 6.46: Reduction in maximum width over post-environmental exposure time in cleaver-inflicted marks

The early diagenetic process mentioned in previous literature was the contraction of collagen fibres due to collagen degradation and dehydration (van Klinken and Hedges, 1995; Bell *et al.,* 1996; Nielsen-Marsh and Hedges, 2000; Collins *et al.,* 2002; Hedges, 2002). As discussed in Chapter 5, the first 6 months of defleshed samples in this study did not show the highest rate of bone diagenesis,

possibly due to the missing bacteria-rich environment of soft tissue decomposition. The contribution of the depositional environment and weathering condition were shown to affect the rate of taphonomic alterations (Galloway *et al.*, 1989; Bell *et al.*, 1996; Fernández-Jalvo *et al.*, 2010). Bone diagenesis was not statistically significant during 6-12 months. These would be due to the near-freezing environment of autumn and winter season (September 2017 – February 2018). These results correspond with those in Chapter 5. Thus, this study showed that significant microbial community changed during the decomposition process, matching observations by previous literature (Sidrim *et al.*, 2010; Hyde *et al.*, 2013; Pechal *et al.*, 2013; Carter *et al.*, 2015). It is hypothesised that this might suggest periodic alterations in the environment particularly temperature that temporarily promote or hinder bacterial growth (Bell *et al.,* 1996; Collins *et al.,* 2002; Tibbett *et al.,* 2004; Turner-Walker, 2008; Damann, 2010; Fernández-Jalvo *et al.,* 2010; Karr and Outram, 2012). Therefore, the pattern of progressive kerf width change would be explained by this conclusion. A reduction in specific bacterial activity in the skeleton might be the primary cause of these findings. Unfortunately, this idea has not been tested in this study.

As expected in this study, the width of the machete blade does affect the surrounding bone tissues that the machete moved through, crush and fracture the bone, but the narrower-bladed cleaver usually injured only the bone tissue in its way without any fracture and crushing. Significant differences between pre-exposure and post-environmental exposure were found in 12- and 18-months surface machete-inflicted chop marks. These findings were consistent with morphological changes, as fracture and loss of formerly raised margin resulting in a larger area of kerf width that measures perpendicularly between the margins of the chop marks on the bone surface. Therefore, these topics would be discussed simultaneously with morphological changes of chop marks.

6.2.2.2 Morphological changes of the chop marks

Upon analysis of the dimensional changes of 144 chop marks on fresh juvenile porcine femurs, this study found that a statistical change ($p=0.036$) took place at 18-months surface exposures of machete-inflicted chop marks. The only morphological characteristic that significantly changes during the 18-months

experimental period was considerable damage to the machete-inflicted kerf margin. After environmental exposure, 75% of raised margins of machete-inflicted chop marks were likely to more damage, leaving only rough margin where the chops were initially made.

The differences in morphological change were expected and could be associated with the bone structural damages occurring during the traumatic events. The specific type of hacking weapon usually makes the bone materials more vulnerable to cracking and fragmentation near, or extending from, its kerf wall (Humphrey and Hutchinson, 2001; Symes *et al.*, 2002; Lynn and Fairgrieve, 2009b). As discussed earlier, the machete-inflicted trauma is a combination of compressive and shearing forces applied dynamically with a narrow focus (Humphrey and Hutchinson, 2001; Alunni-Perret *et al.*, 2005; Lynn and Fairgrieve, 2009a; McCardle and Lyons, 2015; McCardle and Stojanovski, 2018). This means that when a machete impacts on a bone, its sharp edge cuts into a bone material creating sharp force characteristics; meanwhile, the shearing force creates surrounding fractures representative of blunt force trauma (Humphrey and Hutchinson, 2001; Lewis, 2008). Lewis (2008) and Humphrey and Hutchinson (2001) showed that the machete produced a deep V or U-shaped cross-section with severe damage on the kerf margins. These are consistent with the findings in this study. Fractures usually occurred at the kerf floor and then radiating to surrounding areas. The overall fracturing and crushing ability of machete-inflicted chop marks make them easily distinguishable from cleaver-inflicted chop marks, and these make them more susceptible to bone weathering.

Weathering can produce a sequence of bone surface flaking, cracking and splitting related to time, while those buried bones are still unweathered after the same period (Behrensmeyer, 1978). These findings were corresponding with the previous chapter that the degradation of skeletal sharp-inflicted trauma occurred at a much slower rate than those placed on the ground. These might be due to the cooler temperature and the effective insulation from solar radiation (Behrensmeyer, 1978; Rodriguez and Bass, 1985; Jaggers and Rogers, 2009). Temperate climate in Southeast England would show reduced rates of bone weathering; however, a more fragile or damaged surface tends to be modified in the higher rate (Behrensmeyer *et*

al., 1986; Calce and Rogers, 2007). The raised margin described in this study was a weak zone. Hence, taphonomic modifications could easily occur in this zone. Marginal raisings and flakes are often lost and therefore they show only fractured cortical bone (Alunni-Perret *et al.*, 2005; Lewis, 2008). This finding confirms the nature of taphonomic modifications of more fragile and damaged margin, which are by nature potential to alter from environmental disturbance. Nevertheless, no exact time was indicative of the timing of first damage in this study.

To conclude, most of the morphological change from the outdoor environment was not significantly observed in cleaver and machete-inflicted chop marks. Only raised kerf margins of machete-inflicted marks were significantly alterative after 18-months surface exposure, with 75% changing to a smoother surface. The changeable morphologies of the chop mark pointed out by this study lead to conclude that more reliable criteria should be established in order to provide an accurate skeletal trauma assessment. Possibly, some more comprehensive research in this specific field should be conducted to verify the possibility to search for the best indicator. These could deal with the significant problem of traumatic skeletal lesions with ambiguous characteristics.

6.2.2.3 Micro-CT assessment for taphonomic modification

After environmental exposure, chop marks on femurs remained stable, and there was not much change in their overall morphology. Chop mark length and depth, slope angle, as well as opening angle, were not statistically significant. Therefore, an environmental effect did not substantially influence the overall structure of chop marks because these characteristics could be used for a straight interpretation of chop mark structure and framework, leading to an identification of weapon used (Lewis, 2008; Waltenberger and Schutkowski, 2017).

The only morphological observation that changed significantly was the proximal and distal shoulder heights. This result showed that the proximal and distal shoulder heights might not be useful for differentiating between both types of chop marks, because flaking and chattering fragments were very easily damaged and lost by the diagenetic process and environmental factors (Behrensmeyer *et al.*, 1986). In addition, cracks of the chop mark floor and in areas around chop marks

were also witnessed by micro-CT (Figure 6.47). Usually, these cracks start from the machete-inflicted kerf wall, possibly due to the great force of a chopping action with blunt force component. The mechanism of the chopping process was clearly determined that this action is not just a simple impact and it is not only damaging the bone tissue on its way. The high level of energy spreading through the bone makes multiple cracks in areas around a chop mark. This shoulder height might be the effects of bulged bone, which represents a slightly rotating movement of the weapon blade or the bone sample during the traumatic event. These areas are composed of bone fragments, which are attached to the bone material as the micro-CT scans revealed.

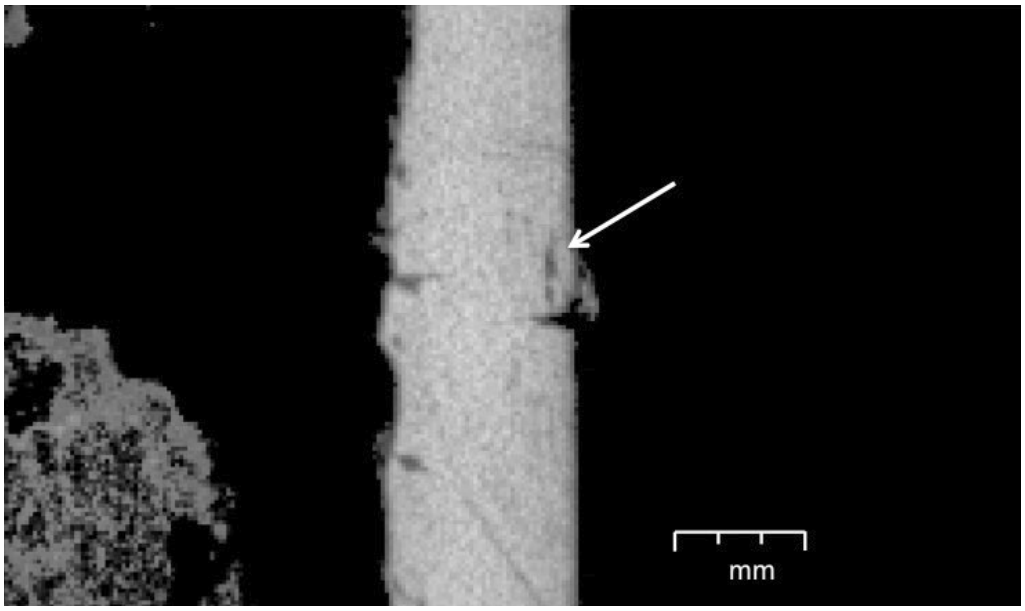

Figure 6.47: A micro-CT image demonstrates cracks of the bone tissue surrounding chop mark (the white arrow).

More importantly, one of the advantages of micro-CT is that it is the imaging technique in which a three-dimensional and cross-sectional view of chop marks can be examined and provided the possibility to observe bone tissue injury. This study showed the presence of small cracks of the bone material in the area next to the chop. These defects occurred from the energy absorption of the cleaver and machete impact. It is an acceptance that these cracks have weakened sharp force trauma structure (Waltenberger and Schutkowski, 2017), which would damage during environmental deposition. Nonetheless, more biomechanical research must

be carried out to prove this theory. Additionally, the combination of 3D diagnosis with the 2D technique can strengthen the ability to distinguish and identify chop marks when analysing forensic casework. Also, it is imperative to compare between chop marks and any other surface modifications resembling them, such as trampling marks and canine teeth marks (Andrews and Cook, 1985; Olsen, 1988; Dominguez-Rodrigo *et al.*, 2009). Maté-González *et al.* (2018) advised to use an additional examination with SEM for a higher degree of resolution of a questionable mark, while the micro-CT with 3D approach was used to find further information that was impossible to answer by the 2D approach.

6.2.3 Summary

In summary, this study of long bones (femurs) focuses on the general characteristics of chop marks inflicted by cleaver and machete and further investigating taphonomic modifications produced by surface and buried outdoor environmental exposure at 6, 12, and 18 months. This phenomenon generated evidence of specific features that can be detectable by the naked eye or with microscopic examination. Even though some traits described in this study change over time, it is often possible to distinguish chop marks on bones inflicted by different types of hacking weapon. While a large-bladed hacking weapon can produce a wide range of wound dimension and morphology, their traumatic stigmata are nevertheless distinguishable from other sharp weapon and within their class.

The identification of environmental artefact on chop marks in different weather conditions becomes even more varied, and thus, further study is required. Although none of the characteristics examined is specific to environmental changes. The presence of morphological alterations based on broad criteria for analysis is provided, and the potential for further investigation with criteria classification and feasibly the examination of more specific characteristics within each criterion is expected. The macroscopic and microscopic examinations combined with the micro-CT characteristics of chop marks have the potential to enable forensic anthropologists to detect diagenetic processes acting on hacking trauma. It appears that a stereomicroscope would be used as it allows investigating more particular aspects of the chop mark morphology (shape, cross-section, margin

and striations) and its fine details. In addition, the stereomicroscopic examination is cheap and more accessible in many laboratories.

Results of this study suggest caution in extrapolating indications regarding the chop mark analysis of skeletal remains depositing in the outdoors environment. This study; however, does not have the full potential to completely fulfil early postmortem alterations of sharp force trauma, especially on the question of the distinction between perimortem trauma and taphonomic modification. Nonetheless, the data suggest that biomechanical knowledge could be used to explain taphonomic changes in each type of traumatic lesion.

Chapter 7: Environmental effects on blunt-inflicted fracture characteristics in femoral samples

In this study, 42 femurs were fractured by a mechanical apparatus and exposed to depositional environment for a selected interval. As explained in Chapter 3, brief materials and methods of this study are summarised in Figure 7.1.

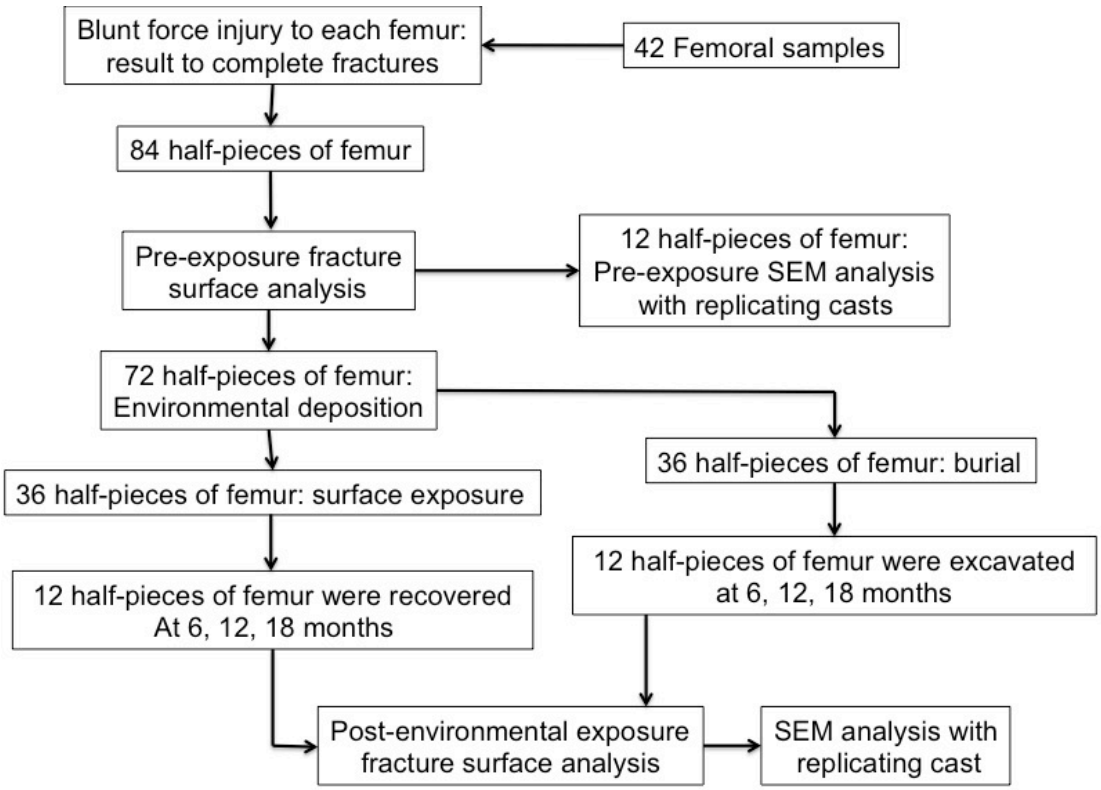

Figure 7.1: A diagram demonstrating the materials and methods in this study

Limitations and problems concerning the effect of environmental factors on interpretation of blunt-inflicted injury, particularly biomechanical assessment, were investigated by fracture surface analysis. Taphonomic modifications of the morphological patterns and fracture surfaces of blunt force injury were explored to further substantiate forensic expert opinion and decrease intrinsic variables.

7.1 Results

7.1.1 Pre-exposure traumatic findings

Bones were fractured by the application of a force perpendicularly to their long axes and then investigated for ten general variables. All 42 samples showed complete fractures with the bones broken into two halves. Most of the samples (66.7%) showed transverse fractures, with 10 out of 42 (23.8%) displaying oblique fractures, and 4 (9.5%) broken as partial butterfly fractures (Figure 7.2). All fracture surfaces had uniform colour similar to the bone surface. Fracture angles were investigated; 38 of 42 (90.5%) of cases displayed acute angles (Figure 7.3), while 4 (9.5%) had fracture surfaces showing right angle morphology. Rough and jagged edges (Figure 7.4) were presented in only 14 of 42 (33.3%), while smooth fracture edges were more frequently distributed (66.7%). Fracture lines were found radiating from the fracture sites in 80% of the fractures. All observations were conducted without a microscope and this methodology can be used and applied to bone samples in a forensic context.

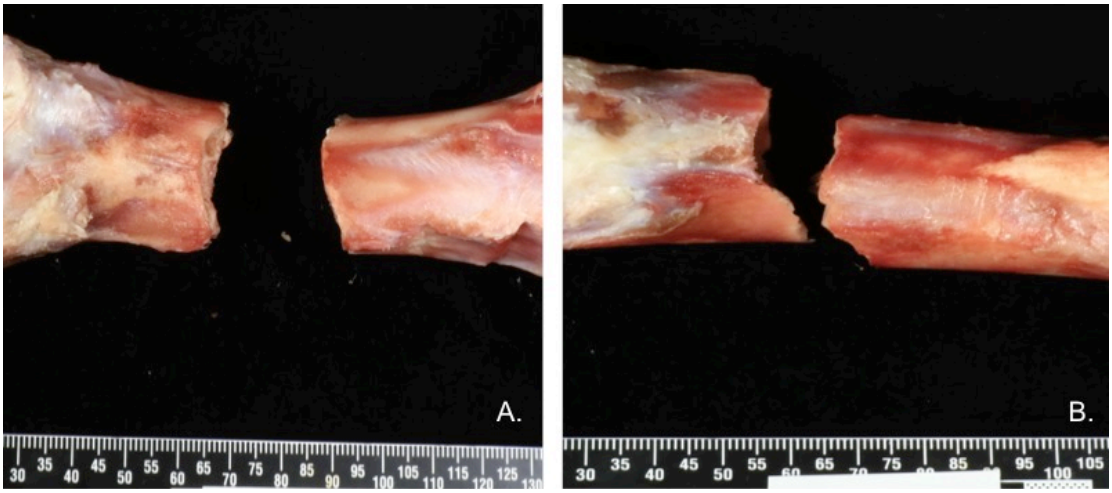

Figure 7.2: Overall fracture morphology; A. transverse fracture; B. partial butterfly fracture

Figure 7.3: Smooth, acute-angled fracture surface

Figure 7.4: Rough fracture surface

Table 7.1 contains information about the results for the common parameter and fracture surface characteristics of macroscopic structure of femurs used in this study. Fracture surface analysis of tensile and compressive surface areas was also conducted. Areas within sample images were defined as tension, compression, and transition. As explained in chapter 3, tensile areas are the relatively flat and smooth surfaces, while compressive areas are defined as area of layered breakage and interlamellar cleavage (Wise *et al.*, 2007; Wynnyckyj *et al.*, 2011). The pre-exposure group showed a significantly larger area of tensile surfaces compared to compressive surfaces, consistent with bending mechanisms. Fracture surface analysis showed 49% ± 2% tensile areas versus 38% ± 2% compressive areas with 13% ± 2% as transition areas. Statistical significance was observed between tensile and compressive areas ($p < 0.001$).

Table 7.1: General fractures of macroscopic surface characteristics

Parameters	Mean	S.D.	Max	Min
Maximum length (mm)	90.67	6.87	115	82
Maximum circumference (mm)	90.96	6.88	104	78
Maximum cortical thickness (mm)	6.71	0.71	8.87	5.71
Minimum cortical thickness (mm)	3.74	0.39	4.64	2.98
Tensile area (mm^2)	42.98	4.2	54.82	36.41
Compressive area (mm^2)	33.82	2.77	38.27	28.14
Length of slope (mm)	10.42	4.82	19.1	3.08
Length of fracture surface (mm)	26.06	3.08	32.26	21.33
Fracture surface angle	114.08	13.39	136	94
Maximum length of radiating fracture (mm)	4.65	1.18	9.44	1.06

Samples were then qualitatively categorised using stereomicroscope and SEM into either smooth or rough regions (Figure 7.5) by using the previously defined qualitative characteristics (Table 3.10). Percentages of the interesting areas were then calculated using ImageJ to estimate alterations to the degree of roughness. Fresh fracture surfaces showed similar trends of rough and smooth areas under both tensile and compressive areas (Figure 7.6). The tensile area displayed a 48:52 ratio of rough to smooth areas, whereas a 42:58 ratio was observed in the compressive area.

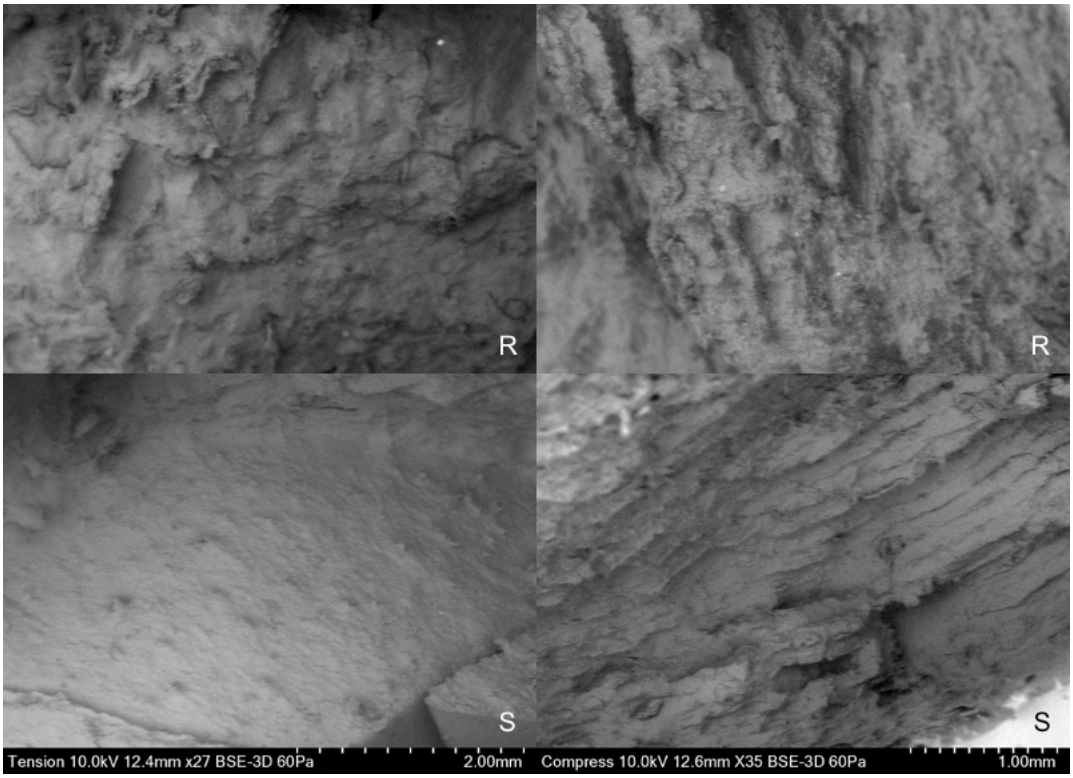

Figure 7.5: SEM examination demonstrating details of tensile (left) and compressive (right) fracture surface of pre-exposure femurs showing smooth (S) and rough (R) regions (Table 3.10)

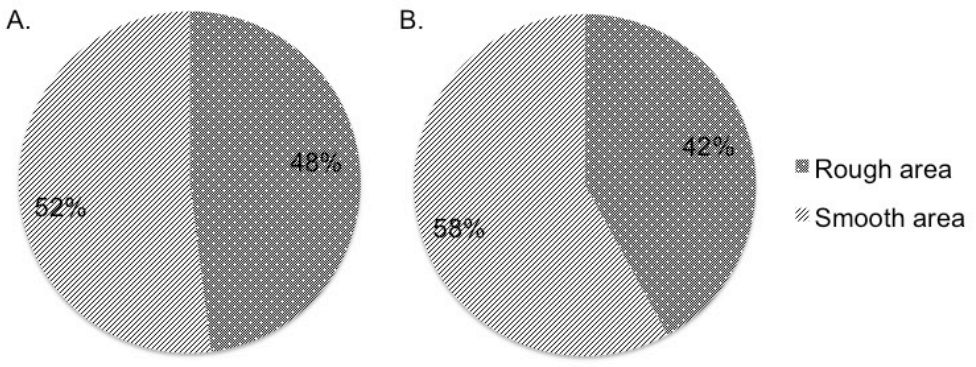

Figure 7.6: Pie charts demonstrating percentage of fracture surface roughness of tensile area (A.) and compressive area (B.)

7.1.2 Post-environmental exposure

Bone samples were exposed to surface and buried environmental stresses for 6, 12 and 18 months. Representative digital images of the fracture surfaces of pre-exposure and post-environmental exposure were compared to evaluate the effect of taphonomic factors. For clarity, each environmental group observed was recorded and discussed independently, though each was interdependent.

The outdoor environment displayed no potential to completely alter macroscopic evidence of blunt force injury to the femoral samples. As discussed in chapter 4, flaking occurred at the bone surface but this type of bone weathering did not affect the fracture surface. Pre-existing radiating fractures could still be identified in the individual samples, although a significant expanded width of the fracture line was observed (Figure 7.7).

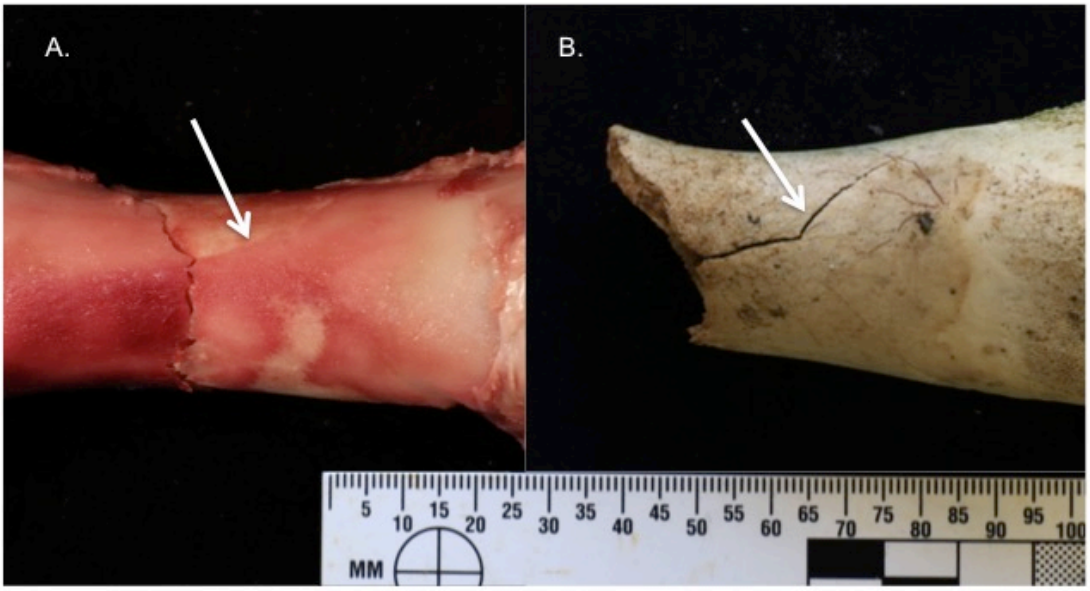

Figure 7.7: The radiating fracture from the fracture site before (A.) and after (B.) 12-months environmental exposure, noting the wider space was observed

All macroscopic assessments showed no statistical significance ($p>0.05$) (Table 7.A in APPENDIX 7). Assessment of fracture surfaces displayed similar overall morphology for both pre and post-exposure features (Figure 7.8). All samples showed similar colour of the fracture surface and cortical bone surface;

however, microscopic features elucidated some changes in the ratio between rough and smooth surface areas. These are discussed in the next section.

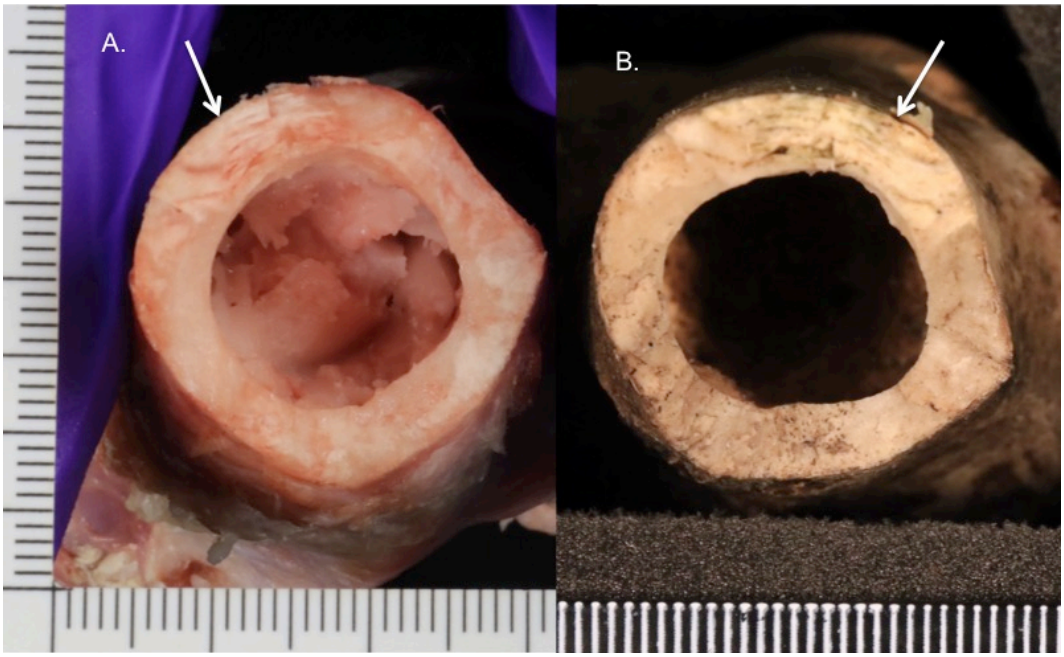

Figure 7.8: The same fracture surface before (A.) and after (B.) 18-month environmental exposure; the white arrows indicate the compressive area, scale in mm

7.1.2.1 Surface exposure

Rough to smooth area ratios were calculated from post-exposure samples and then compared with pre-exposure results. Fracture surface analysis displayed a progressive increase in rough areas over time (Table 7.2 and Figure 7.9). For example, for tensile areas, fracture surfaces of pre-exposure femurs exhibited a 47.5:52.5 ratio of rough to smooth areas, while fracture surfaces of 6-months post-exposure femurs showed a 54.3:45.7 ratio. In addition, percentage of roughness significantly increased ($p<0.05$) between pre-exposure and 18-months surface exposure groups for both tension and compression (Table 7.B in APPENDIX 7). A comparison between rough and smooth areas of each period was also conducted for both tensile and compressive sides (Table 7.2). Statistical significance ($p<0.05$) was observed in 18-months exposure of both tensile and compressive areas (Table 7.C in APPENDIX 7).

Table 7.2: Percentage of rough and smooth area of surface-exposure sample; Lowercase letters (a, b) show statistical significance ($p<0.05$) between two marked group; Uppercase letters (A, B) show statistical significance ($p<0.05$) versus pre-exposure group; data shown in mean ± S.D.

	Area	Pre-exposure	6-months exposure	12-months exposure	18-months exposure
Tensile area	Rough (%)	47.5 ± 5.2	54.3 ± 5.14	-	-
		48.3 ± 4.76	-	59.1 ± 4.76	-
		48.8 ± 4.48	-	-	66.6 ± 5.79 [a,A]
	Smooth (%)	52.5 ± 5.2	45.7 ± 5.14	-	-
		51.7 ± 4.76	-	40.9 ± 4.76	-
		51.2 ± 4.48	-	-	33.4 ± 5.79 [a,A]
Compressive area	Rough (%)	42.7 ± 5.11	47.9 ± 4.67	-	-
		41.3 ± 4.15	-	52.4 ± 4.83	-
		42.1 ± 4.94	-	-	57.1 ± 5.22 [b,B]
	Smooth (%)	57.3 ± 5.11	52.1 ± 4.67	-	-
		58.7 ± 4.15	-	47.6 ± 4.83	-
		57.9 ± 4.94	-	-	42.9 ± 5.22 [b,B]

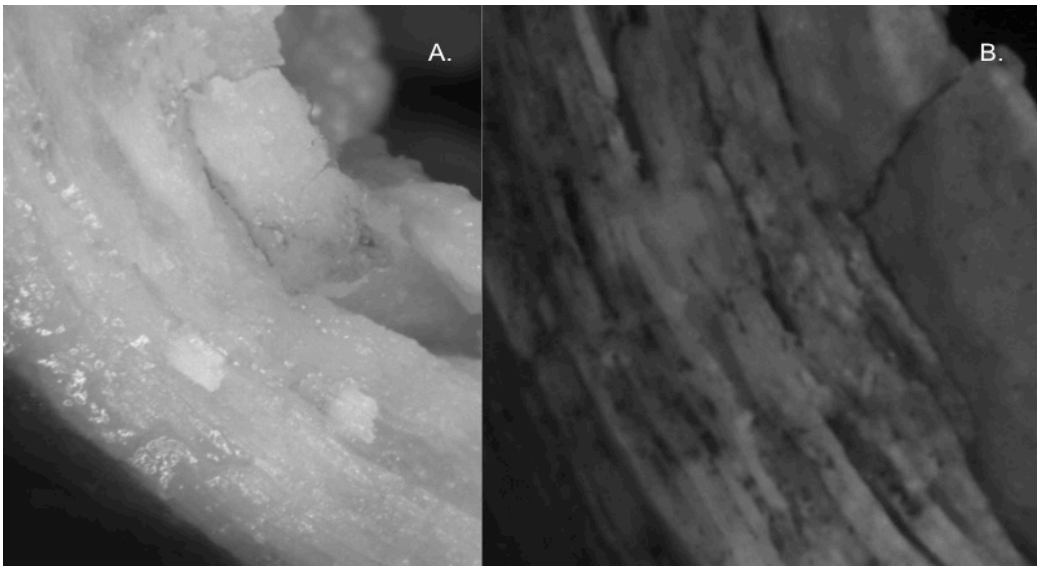

Figure 7.9: Stereomicroscopic examination demonstrates the compressive area before (A.) and after 18-months surface exposure (B.); noted that smooth surface changes to rougher surface

Areas of interest were also investigated in-depth at higher magnification (in μm) by SEM. Tensile areas of degraded smooth surfaces of 3 of 12 (25%) of 18-

months surface-exposure samples revealed a much rougher surface with the presence of micro-cracks (Figure 7.10). Conversely, this cracking was not found in rougher smooth surfaces of compressive areas (Figure 7.11). The layered structure of the compressive side displayed a rougher and coarser appearance after environmental exposure.

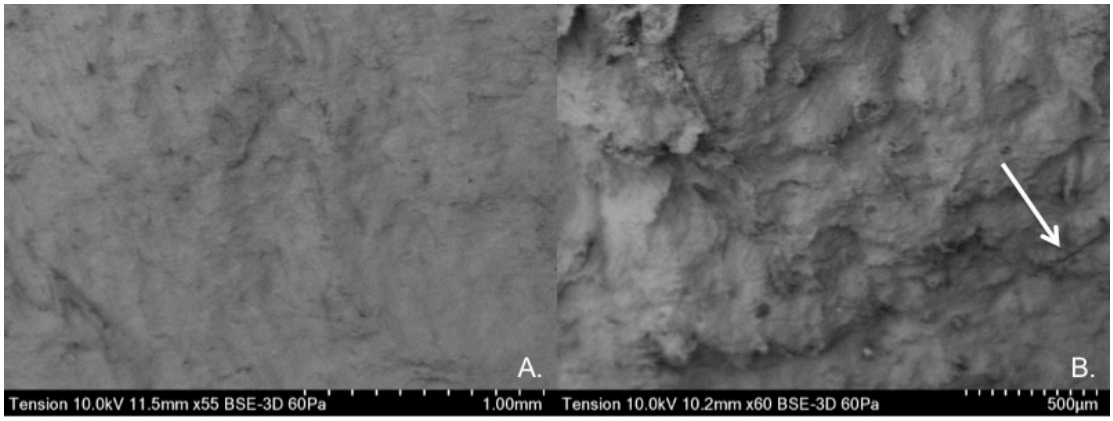

Figure 7.10: Tensile area comparing between the smooth area of pre-exposure (A.) and 18-months post-exposure (B.); the white arrow indicates a micro-crack on the degraded surface

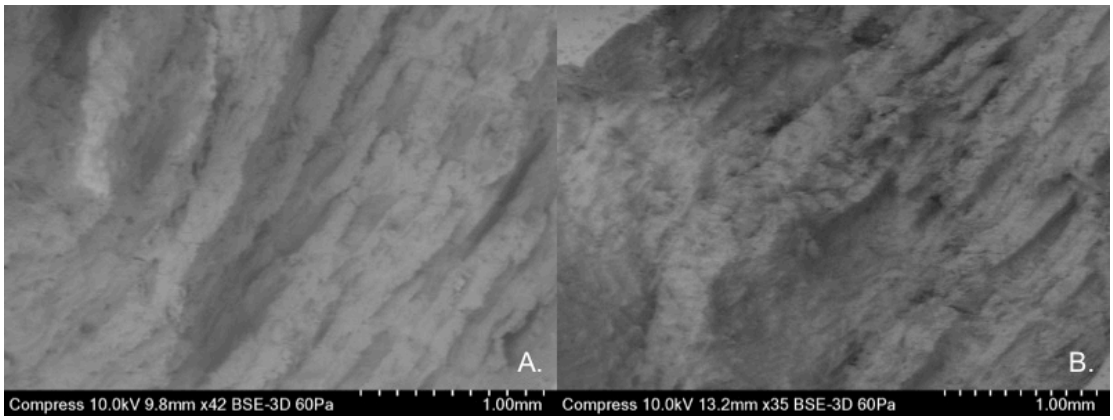

Figure 7.11: Compressive area comparing between the smooth area of pre-exposure (A.) and 18-months post-exposure (B.)

To sum up, these microscopic results implied that the smooth surfaces in tensile and compressive areas changed to rough surfaces as time passed. This change occurred gradually until reaching statistical significance ($p<0.05$) at 18-month exposure for both tensile and compressive areas. In addition, SEM examination confirmed rougher surfaces with micro-cracks in 25% of tensile areas.

7.1.2.2 Buried exposure

Post-environmental groups exhibited insignificant changes in all parameters compared to the pre-exposure group. Fracture surface analysis displayed a gradual increase in rough areas over time (Table 7.3). However, no statistical significance was shown by the 57:43 ratio of rough to smooth areas of tensile region for the 18-months exposure group, whereas an insignificant 51:49 ratio of compressive regions was also observed (Table 7.B in APPENDIX 7).

Table 7.3: Percentage of rough and smooth area of buried sample; data shown in mean ± S.D.

	Area	Pre-exposure	6-months exposure	12-months exposure	18-months exposure
Tensile area	Rough (%)	47.1 ± 4.94	50.5 ± 5.54	-	-
		48 ± 5.33	-	53.2 ± 4.58	-
		48.6 ± 4.65	-	-	57.1 ± 5.48
	Smooth (%)	52.9 ± 4.94	49.5 ± 5.54	-	-
		52 ± 5.33	-	46.8 ± 4.58	-
		51.4 ± 4.65	-	-	42.9 ± 5.48
Compressive area	Rough (%)	41.7 ± 5.64	44.2 ± 5.18	-	-
		42.7 ± 4.91	-	46.4 ± 5.48	-
		42.3 ± 5.91	-	-	50.8 ± 4.97
	Smooth (%)	58.3 ± 5.64	55.8 ± 5.18	-	-
		57.3 ± 4.91	-	53.6 ± 5.48	-
		57.7 ± 5.91	-	-	49.1 ± 4.97

Percentages of rough and smooth areas between the pre-exposure group and each post-environmental exposure group for each failure surface were compared. No statistical significance of increased percentage was recorded, even at 18-months exposure for both tensile and compressive areas (Table 7.C in APPENDIX 7). Taphonomic alterations of the fracture surfaces were detectable under SEM examination, with similar changes in rough areas of smooth surfaces of tensile and compressive areas.

7.1.3 Summary

The objective of this study was to investigate how environmental variables affected blunt-inflicted fracture morphology. Analysis of fracture surfaces can be used to investigate bone failure mechanisms; however, this feature may be damaged by environmental factors. Exposure caused some fracture surface alterations. No statistical differences were recorded in macroscopic examination but progressive microscopic changes were identified after environmental exposure. In addition, 18-months surface exposure revealed a significant increase in rough areas, which developed over time from the existing smooth areas.

7.2 Discussion

Forensic anthropologists use a variety of fracture morphologies to investigate important topics such as biomechanics (Symes *et al.*, 2014; Reber and Simmons, 2015) and taphonomic modifications (Moraitis *et al.,* 2008; Wheatley, 2008; Wieberg and Wescott, 2008; Pechníková *et al.,* 2011; Hentschel, 2014; Scheirs *et al.,* 2017). In tubular cortical bones, osteons are arranged next to each other in layers of concentric lamellae and aligned parallel to the long axis along the diaphyseal area of the long bone. This pattern enables the diaphysis to resist high compressive and tensile loads. Despite this, bone fractures still occur if the force applied directly to the lateral side of the diaphysis exceeds the tensile strength of skeletal material. Fracture surface analysis, or fractography, involves microscopic examinations to gain insights about the traumatic events implicated in bone failure (Corondan and Haworth, 1986; Braidotti *et al.*,1997; Braidotti *et al.*, 2000; Nalla *et al.*, 2003; Sahar *et al.*, 2005; Wynnyckyj *et al.*, 2011; Christensen *et al.*, 2018). This technique elucidates information regarding the magnitude and direction of fracture propagation (Christensen *et al.*, 2018). By investigating fracture surfaces, details of biomechanical bone failure can be examined. Tensile areas are normally regular and smooth, while compressive areas are more irregular. Therefore, fracture surface analysis is a very useful technique for biomechanical reconstruction to deduce the direction of force and interpret blunt force trauma to better understand bone failure mechanisms (Symes *et al.,* 2014; Scheirs *et al.,* 2017; Christensen *et al.*, 2018).

Fracture surfaces may also be related to perimortem events and used to differentiate between perimortem fractures and postmortem damages. Determining the time of injury is a challenging task in forensic anthropology. Generally, characteristics used for distinguishing between perimortem fractures and postmortem damages are a consequence of skeletal biomechanics and compositional characteristics (Moraitis and Spiliopoulou, 2006; Kimmerle and Baraybar, 2008; Symes *et al.*, 2012; Wedel and Galloway, 2014; Scheirs *et al.*, 2017). For fracture surfaces, interlamellar cleavage, or the layered breakage, on the compressive side is the most common perimortem trait and described in 82% of perimortem samples (Scheirs *et al.*, 2017). Hentschel (2014) used a 3D laser scanner to produce 3D images and determined that fracture surfaces change gradually as postmortem interval increases. Therefore, fractographic features can be applied as a more accurate criteria to describe the timing of skeletal trauma (Christensen *et al.*, 2018).

Because of the fragile nature of the fracture surfaces, careless contact can degrade this feature (Christensen *et al.*, 2018). Taphonomic variables of the outdoor environment may alter perimortem fractures and severely modify bone morphological characteristics, making analysis more difficult (Calce and Rogers, 2007; Capella *et al.,* 2014). Environmental variables such as temperature and precipitation influence the nature of decomposition and postmortem changes. The results of the current study show the importance of examining and documenting taphonomic changes at the microstructural level. While many results concur with previous literature, distinct findings of the effects of taphonomic alterations on fracture surface analysis were evident. Therefore, this study aimed to identify various morphological changes of fracture surfaces on long bones using readily available instruments and replicated casts to compare pre and post-exposure patterns with the outdoor environment. Both qualitative and quantitative methods were used to analyse variable features on fracture surface after environmental exposure. Morphological examination comprised visual, stereomicroscopic, and SEM techniques, while statistical analysis compared the results.

7.2.1 Morphological finding of pre-exposure blunt-inflicted fracture

The findings in this study supported previous literature illustrating that angulation of long bones produces a variety of complete fracture patterns (Reber and Simmons, 2015; Isa *et al.*, 2017). Fractures can be divided based on the shape and location of fracture material ((Moraitis *et al.*, 2008; Wedel and Galloway, 2014). None of the fracture patterns in the current study displayed complete butterfly fractures; this result neither supported nor contradicted the results of previous studies (Moraitis *et al.*, 2008; Wheatley, 2008; Reber and Simmons, 2015; Isa *et al.,* 2017). Here, 66.7% of samples showed transverse fracture. This finding corresponded with bones without compressive force from normal weight-bearing functions because loading force along the bone axis tends to change fracture propagation from the transverse pathway (Wedel and Galloway, 2014). Variations of fracture angle and surface were similar to those recorded in previous studies (Wheatley, 2008; Wieberg and wescott, 2008; Wright, 2009). Smooth fracture surfaces can be used to determine perimortem fractures; however, rough and jagged surfaces can occur in bones broken immediately after death. In addition, green bone fracture likely demonstrates acute or obtuse fracture angle surface, while dry bone fracture displays at a right angles. Nevertheless, results showed 9.5% of right angles for perimortem bone fractures.

This study explored some of the morphological variables that assist forensic anthropologists to categorise bone fracture morphology as perimortem or postmortem. Features of broken bone morphology depend to a large extent on the type of affected bone and on the amount and direction of force imposed on the bone by the weapon involved. Also, types of bone fracture relate to the skeletal material involved, skeletal age (adult or juvenile), and postmortem interval of the individual (Nalla *et al.,* 2003; Kimmerle and Baraybar, 2008; Andrews and Fernández-Jalvo, 2012; Wedel and Galloway, 2014). Therefore, no single morphological features of a bone fracture can be used to accurately estimate the timing of bone damages. Wieberg and Wescott (2008) suggested that multiple features provide more accuracy. Thus, a perimortem determination should be made with caution and this process should include many morphological traits to reach the

final decision (Wheatley, 2008; Wieberg and Wescott, 2008; Symes, *et al.*, 2012; Wedel and Galloway, 2014).

The results indicated that the tensile fracture surfaces (49%) are significantly larger than the compressive fracture surfaces (38%). This finding is explained by fracture behaviour as the three-point bending process of skeletal materials. At the starting point of the traumatic process, one half of the fracture surface undergoes compressive stresses, while the other half experiences tensile stresses. In general, bone materials are more susceptible to tensile stresses compared to compressive stresses (Gozna, 1982; Turner and Burr, 1993; Symes, *et al.*, 2012; Wedel and Galloway, 2014). Hence, the starting point of the break occurs on the tensile side. As the mechanical force progresses, the neutral axis correspondingly moves towards the areas of compression. Therefore, initial compressive area changes to tensile area and the majority of the fracture surfaces come under tensile stress (Turner and Burr, 1993; Wise *et al.*, 2007; Wynnyckyj *et al.*, 2011; Wedel and Galloway, 2014). Furthermore, fracture behaviour of the intact long bone under static bending can be estimated by observations of fracture surface morphology (Kimura *et al.*, 1977). For example, the break starts on the tensile ductile side is an indication of perimortem fracture, as Wieberg and Wescott (2008) found that fracture surface morphology displayed the greatest difference between a perimortem fracture and progressive postmortem damage.

All regions within each tensile and compressive area were categorised microscopically as being either rough or smooth. Results indicated that pre-exposure fracture surface exhibited larger smooth surface areas (Figure 7.6). Smooth surface morphology has been previously demonstrated to decrease due to lower toughness of a material (Sahar *et al.*, 2005; Wise *et al.*, 2007). Normally, the fracture surface is representative of resistance that a fracture propagation experiences in its way, therefore the smoother a surface exhibits, the less resistance a fracture has met, with the less energy required for fracture propagation (Wise *et al.*, 2007; Wynnyckyj *et al.*, 2011). The roughness of bone fracture surfaces can be used to qualify bone toughness and nature of bone itself during fracture such as fresh and dry bone (Wise *et al.*, 2007; Wynnyckyj *et al.*, 2011; Hentschel and Wescott, 2015).

Pattern differences between fracture surfaces were demonstrated in this study. Tensile fracture surfaces showed a small area of smoother surface while rough portions of tensile areas resulting from the mechanisms of collagen fibres were pulled out and acted as a bridge between adjacent lamellae (Braidotti *et al.*, 1997; Braidotti *et al.*, 2000). Low energy, commonly associated with slow propagating fractures, flowed through the interstitial matrix causing cracks across the osteons and producing smooth fracture surfaces (Herrmann and Bennett, 1999). The propagating cracks were bridged by the undamaged osteons as their tensile strengths exceeded the shear strength at each concentric lamella (Herrmann and Bennett, 1999). As a result, the osteonal structures eventually failed above or below the fracture interface, producing an irregular appearance as each fibre was pulled out of the matrix (Lynn and Fairgrieve, 2009b).

Macroscopic examination of pre-exposure femurs demonstrated unique characteristics as layered morphology on the compression side (Figure 7.12). Interlamellar cleavage or layered breakage pattern is very distinctive and can be observed in compression areas when a fracture occurs along the diaphysis of a long bone (Corondan and Haworth, 1986; Wise *et al.,* 2007; Scheirs *et al.,* 2017).

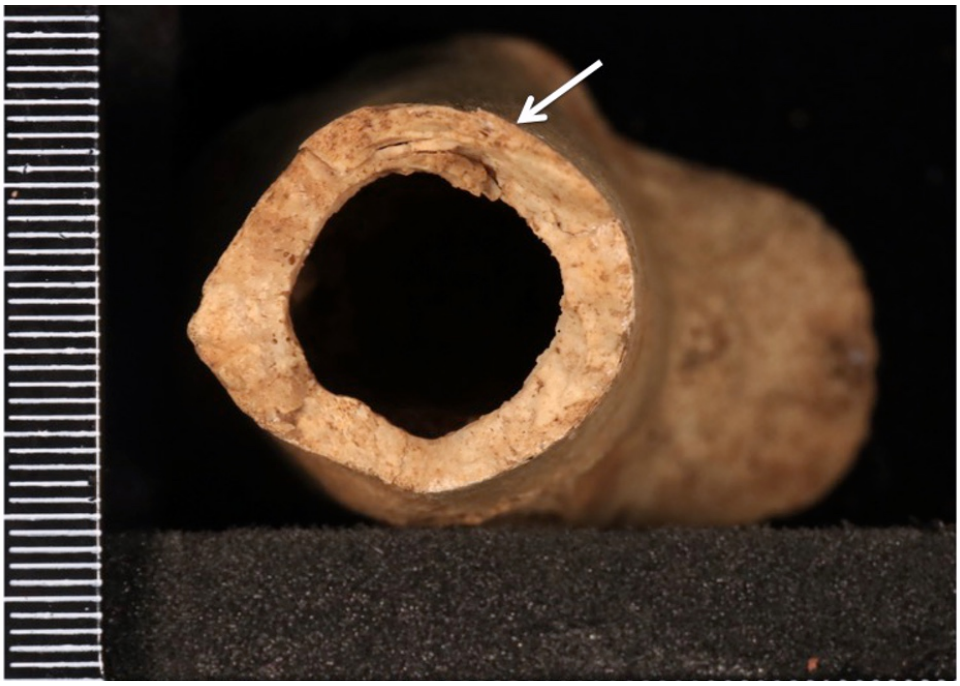

Figure 7.12: A fracture surface after 6-months exposure; the white arrow indicates the layered breakage; scale in mm

This unique breakage appeared in all cortical bone compressive areas in this study and was used as a characteristic for biomechanical reconstruction. In addition, this feature was not observed in dry bone fractures and can be useful for distinguishing fresh bone breakage (Scheirs *et al.*, 2017). Moreover, this morphology was not observed in spiral fractures and fractures at the epiphyses (Scheirs *et al.*, 2017). A fracture surface from a fresh bone is likely to exhibit fewer characteristics of fractographic irregularities because microstructural components such as osteons and pores can arrest micro-cracks (Braidotti *et al.,* 1997; Wynnyckyj *et al.,* 2011).

SEM examination offers researchers major advantages of improved resolution with a three-dimensional structure, increased magnification and depth of field not available using simple microscopic and stereomicroscopic examination (Wakely, 1993; Houck, 1998). Here, SEM was used to aid visualization of 3D features not visible to the naked eye or with optical microscopy (Krüsemann, 2001; Alunni-Perret *et al.,* 2005). Additionally, casting replication was a useful technique to remotely analyse traumatic lesions when skeletal samples were not available for microscopic observation at curating institutions (Camaros *et al.,* 2016). However, some limitations of SEM study as highly dependent on the experience of the examiner should be realised (Crowder *et al.*, 2011). SEM examinations were performed using replicated casts not directly on bone traumatic lesions. Therefore, some delicate and nano-structural finding could not be recognised and interpreted (Crowder *et al.*, 2011; Donnellan *et al.*, 2013). In addition, observation of narrow areas from replicated cast of the area of kerf walls may limit interpretation (Bello *et al.*, 2009; Boucherie *et al.*, 2017).

7.2.2 Environmental effects on blunt traumatic fracture

7.2.2.1 General appearance

Generally, environmental variables such as temperature, precipitation and ultraviolet exposure alter skeletal diagenesis and affect the nature of blunt skeletal trauma. Skeletal materials exposed to severe environmental stress over long time periods become discoloured, dry, grainy and fragile; they lose their moisture and organic substances, leading to various degrees of dehydration and weakness

(Hedges, 2002; Calce and Rogers, 2007; Wedel and Galloway, 2014; Kendall *et al.*, 2018). Perimortem blunt force traumas may undergo taphonomic modification rending them undetectable or imperceptible. Erosion from environmental changes can greatly modify perimortem characteristics of fracture margins and morphology which become similar in appearance to postmortem damages (Calce and Rogers, 2007; Cappella *et al.*,2014).

All bone samples in this study were found to be identical in colour of blunt fracture surface and cortical bone surface. In general, postmortem bone staining is caused by several causes including blood, soil, water, organic matter and fluids emitted from decomposition process (Ubelaker and Adams, 1995; Huculak and Rogers, 2009). However, a marked colour difference in fracture surfaces and cortical bone surfaces can be observed in postmortem damage (Wright, 2009; Honeycutt, 2012; Cappella *et al.,* 2014). This study highlighted that macroscopic fracture morphology did not seem to change significantly after 18-months of surface and buried environmental exposure. Therefore, fracture outline and angle were determined as helpful in identifying perimortem fractures and postmortem damages during the first 18-months exposure in Southeast England. Longer exposure may change this result. Cappella *et al.* (2014) mentioned that exhumations for re-examination of 15-years buried autopsy cases found that blunt injuries were greatly modified by time and environmental factors, making them almost impossible to identify (Cappella *et al.*, 2014; Cappella *et al.*, 2014b). Additionally, more extreme environmental factors showed potential to destroy perimortem injury. Calce and Rogers (2007) observed that sub-zero freeze-thaw cycles in Canada can create pseudo-trauma and conceal evidence of perimortem trauma after only 52-weeks exposure.

7.2.2.2 Taphonomic effects on fracture surface

Fracture surface analysis showed an obvious difference between pre and post-environmental exposure samples. Taphonomic modifications can alter fracture surfaces and result in dubious interpretation. The results in this study showed that smooth-edged fracture surfaces started to erode microscopically and acquired some features of postmortem damage. Fracture surface after 18-months surface exposure were significantly rougher compared with smooth areas in both tensile

and compressive regions. These findings concurred with stereomicroscope and SEM examinations, implying that taphonomic modifications to fracture surface morphology do not occur in discrete temporal intervals but rather undergo changes gradually. An extended experimental period may show final outcomes as the complete acquisition of postmortem morphology found in previous studies (Cappella *et al.*, 2014). Over time, total modifications of original morphology occurred and lesions could not be identified as perimortem since a multitude of environmental factors had eradicated important perimortem indicators. Buried samples were protected or at least buffered from the direct effects of environmental conditions; their fracture surfaces showed fewer changes compared with the surface exposure group. Nevertheless, the thorny issues of taphonomic modifications concerning blunt force injury were not completely investigated due to the limited experimental period.

Furthermore, the percentage of rough areas increased substantially with longer environmental exposure. Statistical significance was observed in samples that had been exposed for 18 months which exhibited a much rougher appearance. Statistical analysis exhibited that both tensile and compressive smooth areas significantly changed to rougher appearance. However, only a few changes were detectable by macroscopic examination. The “fresh” smooth surfaces were altered by taphonomic factors which in turn caused changes, making the perimortem fractures unrecognisable or imperceptible (Calce and Rogers, 2007; Cappella *et al.*, 2014). The final outcome suggested that a pre-existing perimortem fracture relating to criminal activity will become similar over time to a postmortem fracture and may lead to an incorrect interpretation as highlighted by results shown in the previous literature (Calce and Rogers, 2007; Cappella *et al.*, 2014).

Freeze-thaw cycle, rodent and carnivore activity, soil erosion as well as the presence of rain and snow have the potential to conceal perimortem skeletal fractures and decrease the possibility of identifying patterns, number of impacts, direction of blows and sites of injury (Ubelaker and Adams, 1995; Littleton, 2000; Calce and Rogers, 2007; Pokines *et al.*, 2016). Freeze-thaw cycles exhibit the most destructive effect on blunt injury evidence concerning skulls (Calce and Rogers, 2007). Fluctuating environments can create rough linear fractures from the

significant expansion of frozen water molecules, as well as cracking and flaking of bone surfaces. However, no significant differences in the rate of morphological fracture surface changes were observed during the winter period (post 12-months exposure) of this observation. Possible explanations for this may include: 1) the type of affected bone can influence the rate of bone diagenesis (Cunningham *et al.,* 2011; Pokines *et al.,* 2016); 2) fluctuating temperatures in this study were not sufficient to affect macroscopic features of blunt force trauma; therefore, results showed that thermal expansion-contraction of water within pore spaces had low potential to contribute to overall cracking in the early period of postmortem interval (Pokines *et al.*, 2016); and 3) the experimental time scale was not long enough. Pokines *et al.* (2016) demonstrated that bone samples did not reach weathering stage 1 even after 75 freeze-thaw cycles. However, significant changes of fracture surface were observed at 18-months surface exposure. Wet-dry cycles and sunlight during summer and spring periods might play an important role in these processes. Bones exposed to surface environments may undergo fluctuating cycles of wetting and drying (Pokines *et al.*, 2018), while buried bones remain protected.

Interpretation of perimortem fractures is usually dependent on its morphological patterns (Ubelaker, 1997; Calce and Rogers, 2007; Moraitis *et al.,* 2008; Wheatley, 2008; Wieberg and Wescott, 2008; Pokines and Symes, 2014; Wedel and Galloway, 2014). Nevertheless, results revealed limitations of macroscopic examination with lower sensitivity in identification of postmortem damage compared with microscopic investigation. The earliest sign of taphonomic modifications found here involved the particular aspect of diagnosing fractures inflicted by a blunt instrument as perimortem or postmortem.

7.2.3 Summary

The current study offers a multidisciplinary approach to investigate fracture morphology and taphonomic processes within an outdoor environment. The considerable difficulty in assessing perimortem blunt-inflicted injury has already been comprehensively emphasised and documented by a number of studies (Ubelaker, 1997; Calce and Rogers, 2007; Wheatley, 2008; Wieberg and Wescott, 2008; Cappella *et al.,*, 2014). Climatic conditions adversely impact on morphological characteristics of skeletal fracture such as breakage patterns or types of fracture

margins. Correct differentiation between a perimortem fracture and postmortem damage is, therefore, not always easy to achieve (Calce and Rogers, 2007; Passalacqua and Rainwater, 2015; Schotsmans *et al.*, 2017). Additionally, environmental variables render this task even more difficult since they can rigorously alter the morphological characteristics of skeletal materials and their traumatic lesions.

This study is one of only a few to investigate long-term effects of outdoor environmental exposure on the deterioration of blunt traumatic morphology. Effects of depositional environments on taphonomic changes were also found to be statistically significant. Erosion of microscopic fracture surfaces was most prevalent in terms of bone diagenesis. Microscopic examination performed on femoral samples produced some interesting results. Stereomicroscope and SEM are excellent complementary techniques to assess blunt trauma morphology. These techniques not only enable investigation of useful characteristics but also enhance the presence of other features. Specifically, perimortem long bones fractures can be more easily investigated and identified, possibly because the thick cortical bone results in better preservation of the fracture surface and fracture morphological features (Moraitis *et al.*, 2008).

Chapter 8: Survival of environment-exposure burned bone and sharp-inflicted injury identification

Every season, cut marks (n=180) were inflicted on porcine ribs (n=60) with the same three types of kitchen knives as stated in Chapter 5, and the ribs were then burned and exposed to depositional environment. General features and cut mark analysis was carried out using macroscopic and stereomicroscopic methods. This process was conducted every season in a year to compare how different environmental factors affect cut mark morphology and burned bone fragmentation (Figure 8.1).

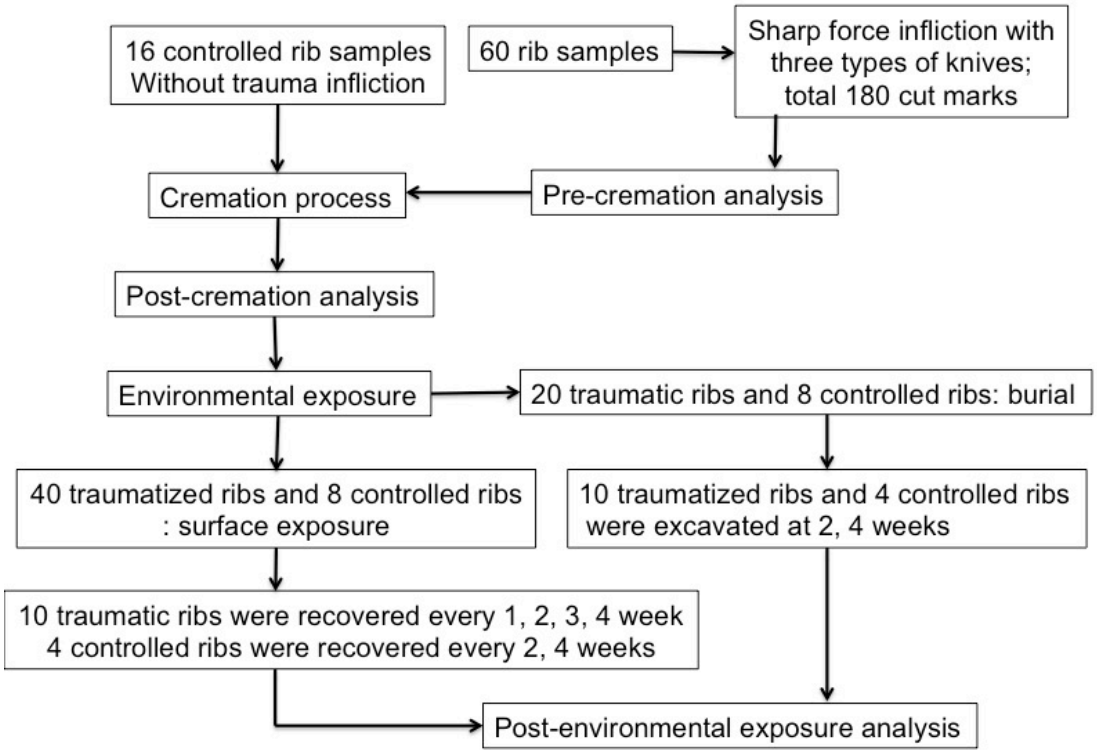

Figure 8.1: The sequence of the one-month event in this study; this diagram represents only one seasonal event

8.1 Results

8.1.1 Weather and soil data during burning experiments

To investigate the effect of weather conditions on cut marks and fragmentation of burned bones, weather data including ambient temperature, precipitation, wind speed, and hours of sunlight were collected from F3-weather station and Brize Norton weather station. As outlined in Figure 8.2 and table 8.A in APPENDIX 8, this experiment was carried out in a series at different times of the year in May 2017, August 2017, November 2017, and February 2018.

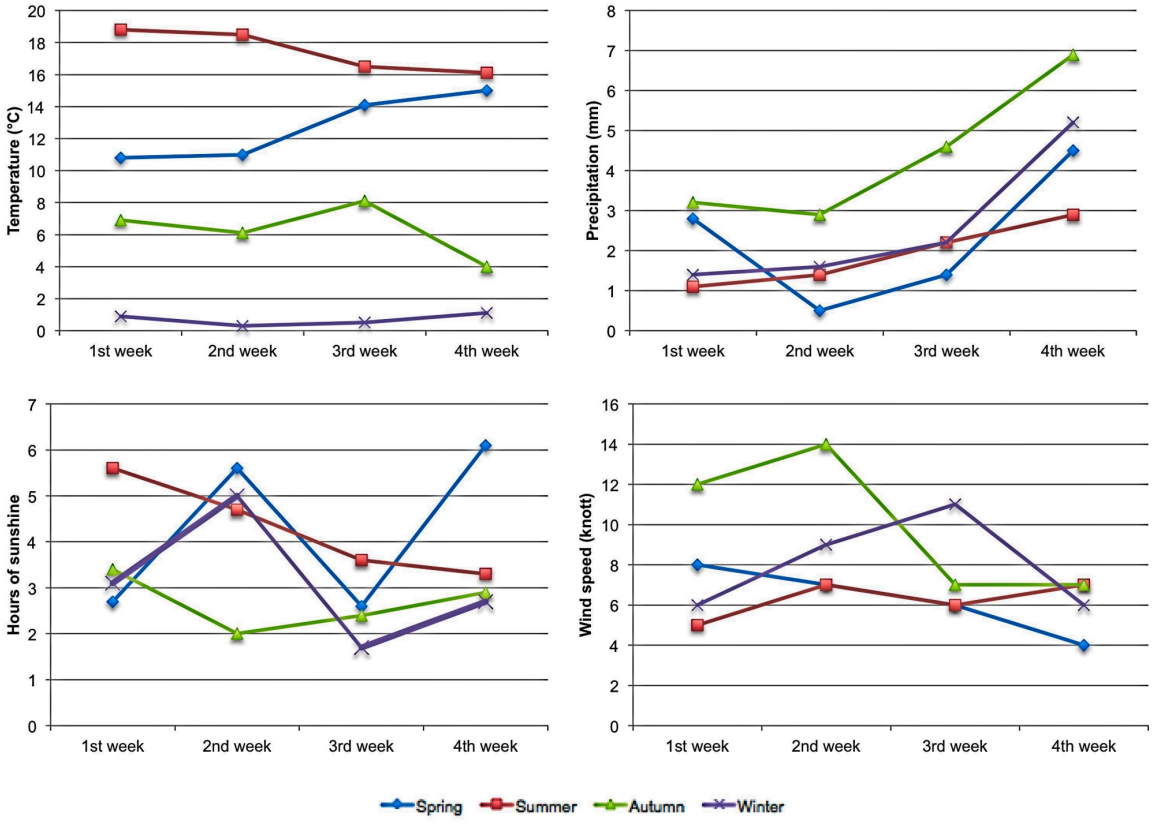

Figure 8.2: Summary of weekly weather condition during this study in the spring (May 2017), summer (August 2017), autumn (November 2017), and winter (February 2018)

Briefly, the springtime has a temperature averaging between 10-15°C with mild rainfall and wind. The summertime has the highest temperature with slight rainfall and wind. Significant rainfall is experienced during autumn with fluctuating temperature and strong wind. Lastly, the wintertime has a freezing temperature with

moderate wind speed. Throughout this experiment, a significant increase in rainfall level during the first week of spring and autumn, with strong wind speed in autumn was observed. During the second week, the autumn samples experienced the highest amount of rainfall and a decrease in ambient temperature when compared with spring and summer data. During the third week, an increase in the rainfall in the spring and summer groups was observed, but its level was not as much as the rainfall in the autumn groups. All groups faced a substantial increase in rainfall level during the fourth week. The autumn samples experienced a low level of temperature, but its level did not reach freezing temperature as the winter samples experienced. The freezing temperature of winter was observed during all weeks of this experiment.

Soil data consisting of soil pH and soil moisture was recorded at the starting and end point of each seasonal experiment (Table 8.1). Variability of mild acidic soil pH was observed ranging from 5.8 to 6.5. An increase in soil moisture was observed in the spring, autumn and winter, with the highest level occurring in the autumn. This information matched the rainfall data (Figure 8.1).

Table 8.1: Soil data in the burned bone experiment

Season	Soil pH		Soil moisture (%)	
	Start	End	Start	End
Spring	6.43	6.51	24.92	25.14
Summer	6.15	6.03	21.73	21.44
Autumn	5.89	5.93	24.94	25.22
Winter	6.08	6.11	24.65	24.71

8.1.2 General examinations

8.1.2.1 Pre-cremation

A cut mark inflicted with the non-serrated blade knife was characterised by a linear and narrow shape, smooth kerf margin and no kerf striations. The coarse-serrated knife blade created a cut mark with elliptical V- or U-shaped grooves,

irregular raised edge and kerf striations, whereas the fine-serrated blade produced a cut mark with mainly elliptical and smooth V-shaped with better identification of kerf striations (Table 5.1). More information is demonstrated in Chapter 5.

8.1.2.2 Post-cremation

The response of bone to heat follows a sequential progression as outlined by Mayne Correira (1997). After burning process, all rib samples were completely calcined (Figure 8.3). These bone samples were burned uniformly, but the range of colour alterations could be found from bluish-grey to white. A few bone fragments were observed in the furnace, although the burned samples presented very fragile and chalky appearance. There were heat-induced fractures due to thermal alteration at the bone surface, but all cut marks were still visible.

Figure 8.3: A post-burned rib sample; the white arrows indicate cut marks

Heat-induced fractures were identified in most of the samples, and their morphology can be clearly differentiated from sharp force traumatic lesion. The presence of six different heat-induced fracture types and warping on post-burned bones was noted and scored as either present or absent (Herrmann and Bennett, 1999). Figure 8.4 presents percentages of heat-induced damages observed in the

traumatic and controlled samples. Statistical significance ($p<0.05$) is not observed between traumatic and controlled samples. That means shallow cut marks inflicted by various types of knife have no effect on heat-induced fracture and warping, and heat-induced fractures did not propagate from cut marks.

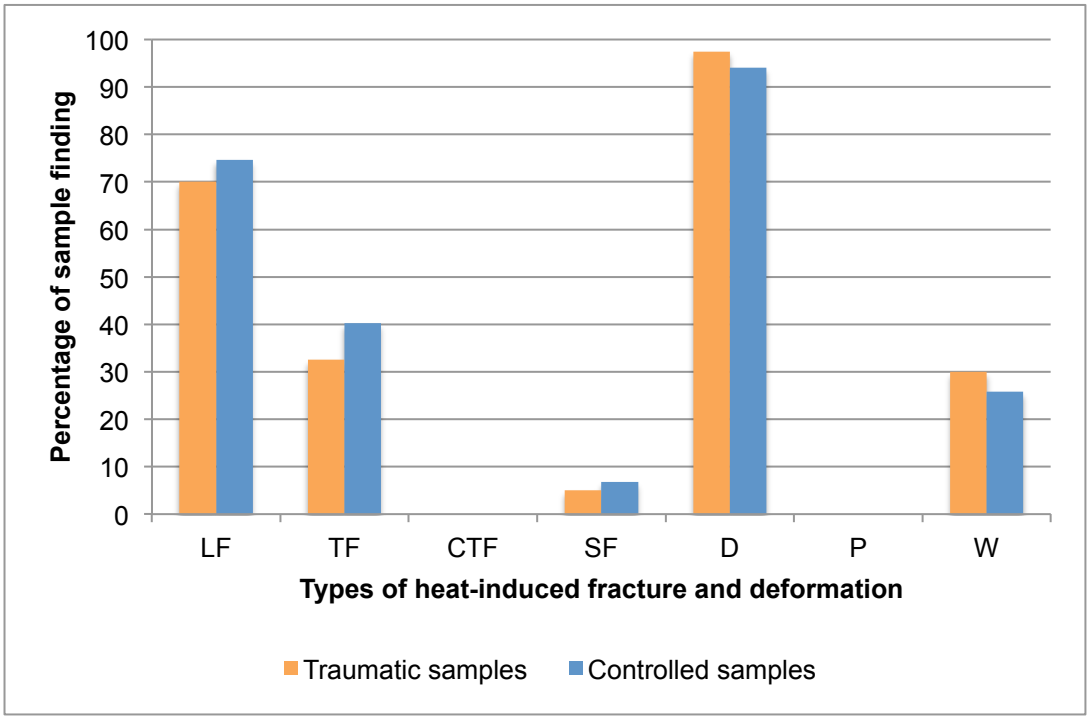

Figure 8.4: Incidence of heat-induced damages spotted in this study; LF: Longitudinal fracture; TF: Transverse fracture; CTF: Curved transverse fracture; SF: Step fracture; D: Delamination; P: Patina; W: Warping

Delamination, or peeling of bone layers (Figure 8.5), was the most common heat-induced fracture seen in this study. Longitudinal and transverse fractures appeared to be initiated at a distance from any previous defect, and extended to their end or intersected other fractures. After the burning process, burned samples were visually examined for heat-induced warping. Bones were checked for unusual bending or loss of their normal alignment. The overall data showed 30% of burned samples had warping, even though there was no soft tissue coverage in all samples.

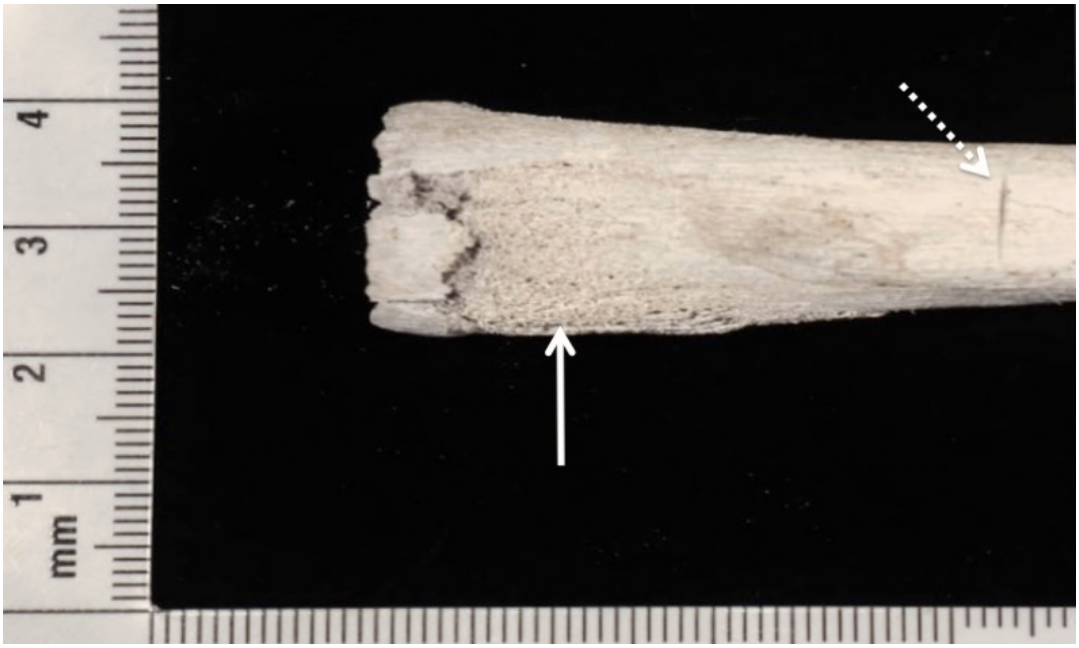

Figure 8.5: Delamination (the white arrow) of a burned rib; the dotted arrow identifies a cut mark

All cut marks made with non-serrated, coarse-serrated and fine-serrated blade knives were visible and easily identifiable, even in an area of heat-induced fracture intersection. Other cut mark characteristics such as a raised border could be seen on one or both margins of the kerf. In several instances, some cut mark morphological changes were observed. The reason for these being that heat-induced fractures terminated or traversed cut marks and expanded or distorted their width and length (Figure 8.6). The majority of longitudinal (82.1%) and transverse (84.6%) fractures traversed some of the cut marks but did not obliterate signatures of sharp-inflicted trauma. However, these cut marks were still identified from their macroscopic and microscopic characteristics.

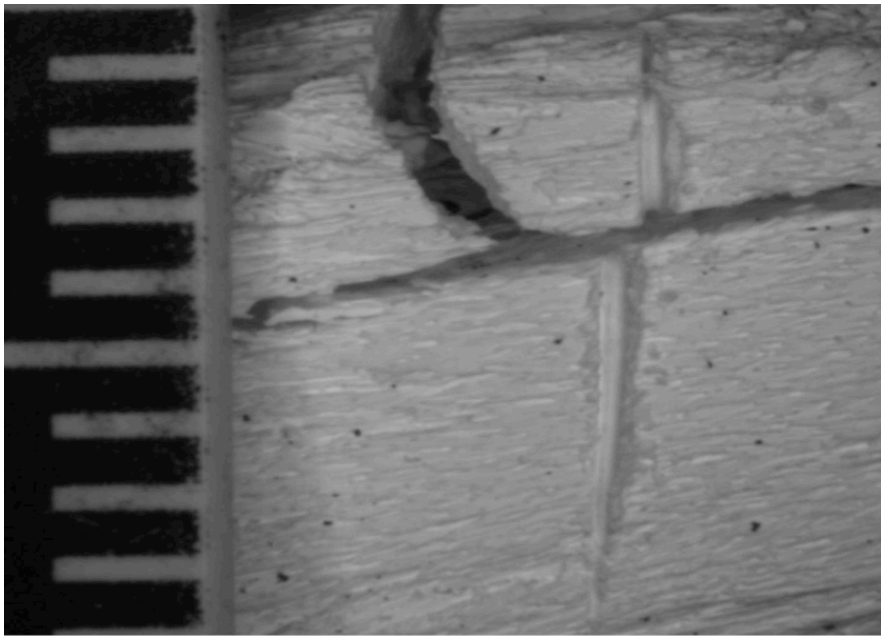

Figure 8.6: A cut mark transected by a heat-induced fracture; scale in mm

8.1.2.3 Post-environmental exposure

After recovery from the experimental site at the specified exposure period, burned bones and their fragments were dried and transported in sealed plastic bags. In the laboratory, general characteristics such as colour and cut mark damage were documented (Figure 8.7). All bone fragment dimensions were measured and recorded. Each sample was weighed pre and post-environmental exposure, enabling comparison of the effects of weathering conditions between the different bone elements. Cut marks and heat-induced damages were also identified and examined using a stereomicroscope with a magnification range to analyse microscopic characteristics of the marks, and then systemically recorded. The examination of cut mark morphology was not always possible because of dust and debris filling or different degree of exposure (angle, depth and width) preventing the observer from a full analysis of the kerf.

Figure 8.7: A post-burial exposure burned ribs; the white arrows identify cut marks

Overall, burned bones presented great fragmentation, cracking, and white and light grey colouration after exposure to the outdoor environment. When examining macroscopically, reconstruction of bone fragments might be required to view heat-induced fractures and cut marks (Figure 8.8). These enable the researcher to distinguish between cut marks from fractures that were heat-induced, or incidentally produced due to external forces acting on the bone. Some cut marks were obliterated or completely damaged and could not be identified. Some cracked cut marks could not be used for dimensional analysis due to their unreliable measurements. Therefore, cut marks with totally loss of macroscopic cut mark morphology were defined as non-survival cut mark.

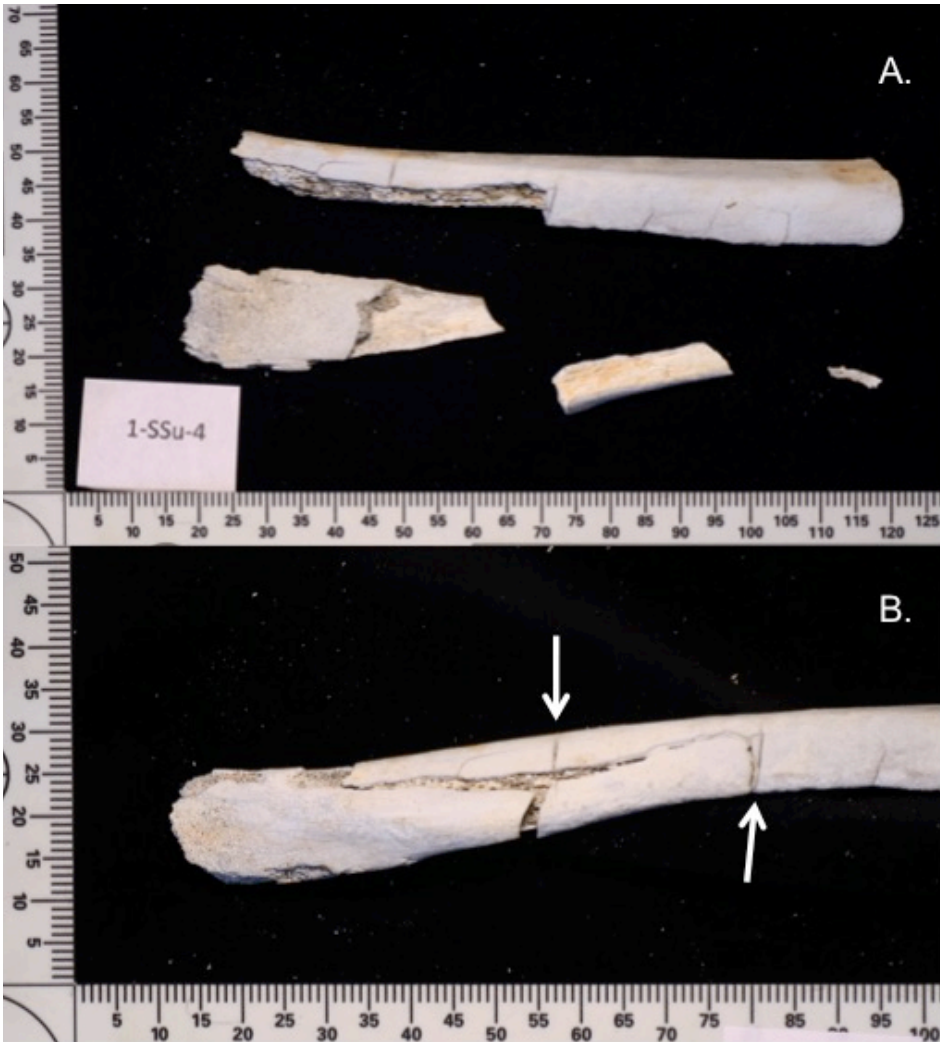

Figure 8.8: A surface-exposure burned rib before (A.) and after (B.) reconstruction; the white arrows indicate reconstructed cut marks

Figure 8.9 demonstrates the percentage of survival cut marks after two-weeks and four-weeks exposure to outdoor environment in each season. Obliteration of cut mark morphology differed considerably for burned bones exposed to a different season. The most destructive event occurred during autumn as only 26.7% could be identified after four-weeks surface exposure. The best survival rate was observed in spring and summer surface groups. Noticeably, the same damage pattern was observed in burial samples for all seasons.

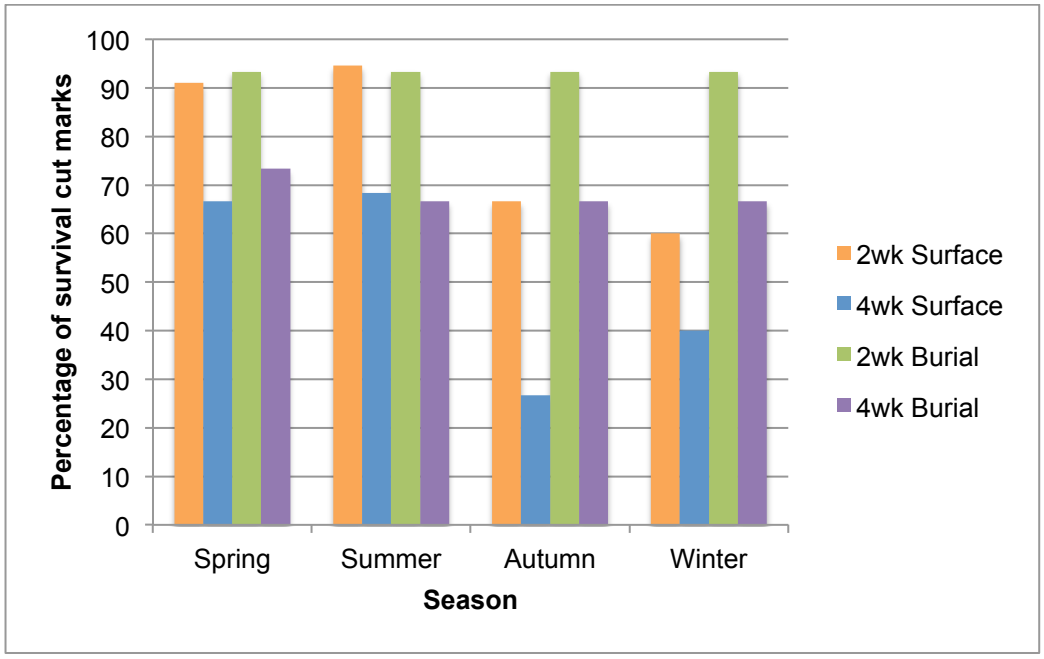

Figure 8.9: Percentage of survival cut marks in each seasonal group

8.1.3 Cut mark dimension and morphology

8.1.3.1 Post-cremation

All cut marks were not destroyed during the burning process. They still presented a V-shaped cross-sectional shape with a smooth or raised margin. The visibility of some cut marks was hindered by soot debris, heat-induced fractures, and residual and carbonized marrow protruding from the medullary cavity. A degree of heat-induced fracture and loss of cortical bone has been an important factor influencing the recovery of cut marks (Herrmann and Bennett, 1999; Kooi and Fairgrieve, 2013). The overall morphological and dimensional changes, as well as statistical analysis for burned bones, are summarised in Figure 8.10, Table 8.2-8.3 and Tables 8.B-8.E in APPENDIX 8. In total, 240 ribs were analysed. For the experimental subset, all samples were burned and reanalysed to compare with pre-burned data. Post-burned bone measurements showed a significantly statistical decrease in length and width ($p<0.05$) when compared with pre-burned samples of all blade types (Figure 8.10 and Table 8.3). Overall measurement showed that there was a decrease in the kerf length and width of 10.8-17.6%, and 28.5-34.9%, respectively. However, not all cut marks could be measured due to their heat damage or overlap with heat-induced fracture (Figure 8.11).

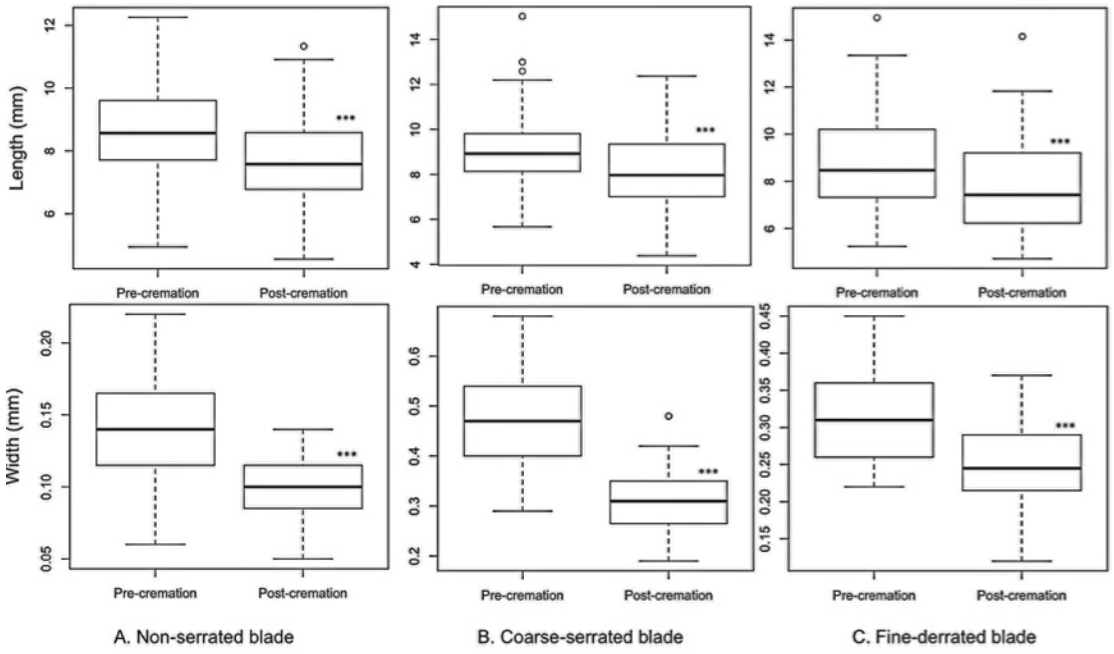

Figure 8.10: Boxplot illustrating a distribution of kerf length and width data; each n=240 (*** statistical significance of the same sample between pre-cremation and post-cremation data)

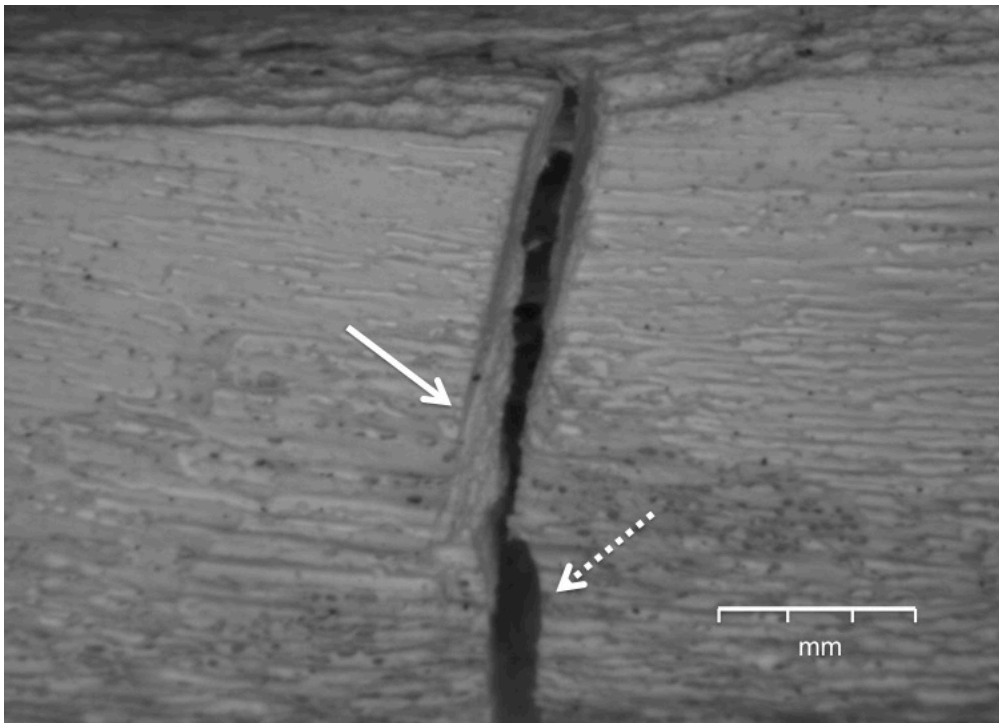

Figure 8.11: A cut mark (the white arrow) overlapped with a transverse heat fracture (the dotted arrow)

Table 8.2: Frequency data of kerf morphology between pre-burned and post-burned samples (shading demonstrating statistical significance)

Weapon type and trait			Pre-burned sample (%)	Post-burned sample (%)
Non-serrated blade (n=240)	Kerf shape	Linear	228 (95)	217 (90.42)
		Ellipse	12 (5)	23 (9.58)
		Rectangle	0 (0)	0 (0)
		Irregular	0 (0)	0 (0)
	Cross-sectional shape	Narrow	207 (86.25)	196 (81.67)
		V-shaped	33 (13.75)	44 (18.33)
		U-shaped	0 (0)	0 (0)
	Kerf margin	Smooth	236 (98.33)	240 (100)
		Raising	4 (1.67)	0 (0)
	Kerf striations	Presence	0 (0)	0 (0)
		Absence	240 (100)	240 (100)
Coarse-serrated blade (n=240)	Kerf shape	Linear	0 (0)	0 (0)
		Ellipse	192 (80)	141 (58.75)
		Rectangle	48 (20)	70 (29.17)
		Irregular	0 (0)	29 (12.08)
	Cross-sectional shape	Narrow	0 (0)	0 (0)
		V-shaped	133 (55.42)	119 (49.58)
		U-shaped	107 (44.58)	121 (50.42)
	Kerf margin	Smooth	100 (41.67)	137 (57.08)
		Raising	140 (58.33)	103 (42.92)
	Kerf striations	Presence	120 (50)	102 (42.5)
		Absence	120 (50)	138 (57.5)
Fine-serrated blade (n=240)	Kerf shape	Linear	0 (0)	0 (0)
		Ellipse	222 (92.5)	198 (82.5)
		Rectangle	18 (7.5)	26 (11.25)
		Irregular	0 (0)	15 (6.25)
	Cross-sectional shape	Narrow	0 (0)	0 (0)
		V-shaped	228 (95)	220 (91.67)
		U-shaped	12 (5)	20 (8.33)
	Kerf margin	Smooth	136 (56.67)	115 (47.92)
		Raising	104 (43.33)	125 (52.08)
	Kerf striations	Presence	168 (70)	151 (62.92)
		Absence	72 (30)	89 (37.08)

A significant association ($p<0.05$) was recorded in kerf shape morphology and kerf margin of incisions from coarse-serrated blade knives (Table 8.3). Elliptical shape presented in 80% of cases in the pre-burned group and 26.6% of this shape changed to rectangular and irregular shape after the burning process. In addition, 26.4% of raised kerf margin altered to smoother margins after cremation. In addition, a statistical significance was observed in kerf shape morphology of cut marks made from the fine-serrated blade (Table 8.3). Note the post-cremation change to linear shape was not observed. Additionally, the presence of kerf striations slightly decreases after the burning process.

Table 8.3: Summary of statistical significant p-value comparing between pre-burned and post-burned samples (*** statistical significance)

Kerf dimensions	**Blade type**		
	Non-serrated	Coarse-serrated	Fine-serrated
Length	t=-4.066, df=235, p<0.001***	t=-3.375, df=190, p=0.0009545***	t=-2.393, df=216, p=0.003828***
Width	t=-5.877, df=235, p<0.001***	t=-8.407, df=190, p<0.001***	t=-4.985, df=210, p<0.001***
Kerf shape	X^2 =3.0819, df=1, p=0.07917	X^2 =40.9125, df=2, p<0.001***	X^2 =17.824, df=2, p=0.0001348***
Cross-section	X^2 =1.5468, df=1, p=0.2136	X^2 =1.4119, df=1, p=0.2347	X^2 =1.6406, df=1, p=0.2002
Kerf margin	Fisher's test: 1.0	X^2 =10.8017, df=1, p=0.001014***	X^2 =3.3404, df=1, p=0.0676
Striations	Fisher's test: 1.0	X^2 =2.422, df=1, p=0.1196	X^2 =2.3926, df=1, p=0.1219

8.1.3.2 Post-environmental exposure

8.1.3.2.1 Dimensional changes

After environmental exposure, incisions had some different trends depending on types of knives inflicted. Figures 8.12-8.15 and Tables 8.B-8.E summarise dimensional changes of cut marks on ribs, while Tables 8.F-8.G in APPENDIX 8 show results of a statistical analysis comparing between individually burned samples before and after an outdoor environmental exposure.

When exposed to an outdoor environment, kerf length of all samples continued to decrease. The graphs given in Figures 8.12-8.15 show how the changes of kerf length and width from the cremation process and weather condition were positively or negatively correlated with increasing time. Most of the kerf dimension and post-environmental period displayed a low negative correlation as kerf length and width decreased when time passed. Because dependent variables (environmental factors) in this study were a categorical type, R-squared statistics was not possible to process, or it will typically give lower result than truly numeric data. Therefore, the results demonstrated and only compared between each season and weapon to discover some significant results.

The majority of four-weeks surface exposure of the cut marks inflicted by coarse-serrated blade were severely damaged and could not be used for cut mark analysis. Therefore they could not be displayed in these charts. With the exception of most of the cut marks inflicted by coarse-serrated blade or cut marks on the bones deposited in autumn, most of the cut marks could survive after one-month surface exposure. The buried samples showed better survival, with only the autumn group of cut marks made from coarse and fine-serrated blade damaged so that they could not be evaluated after one-month exposure.

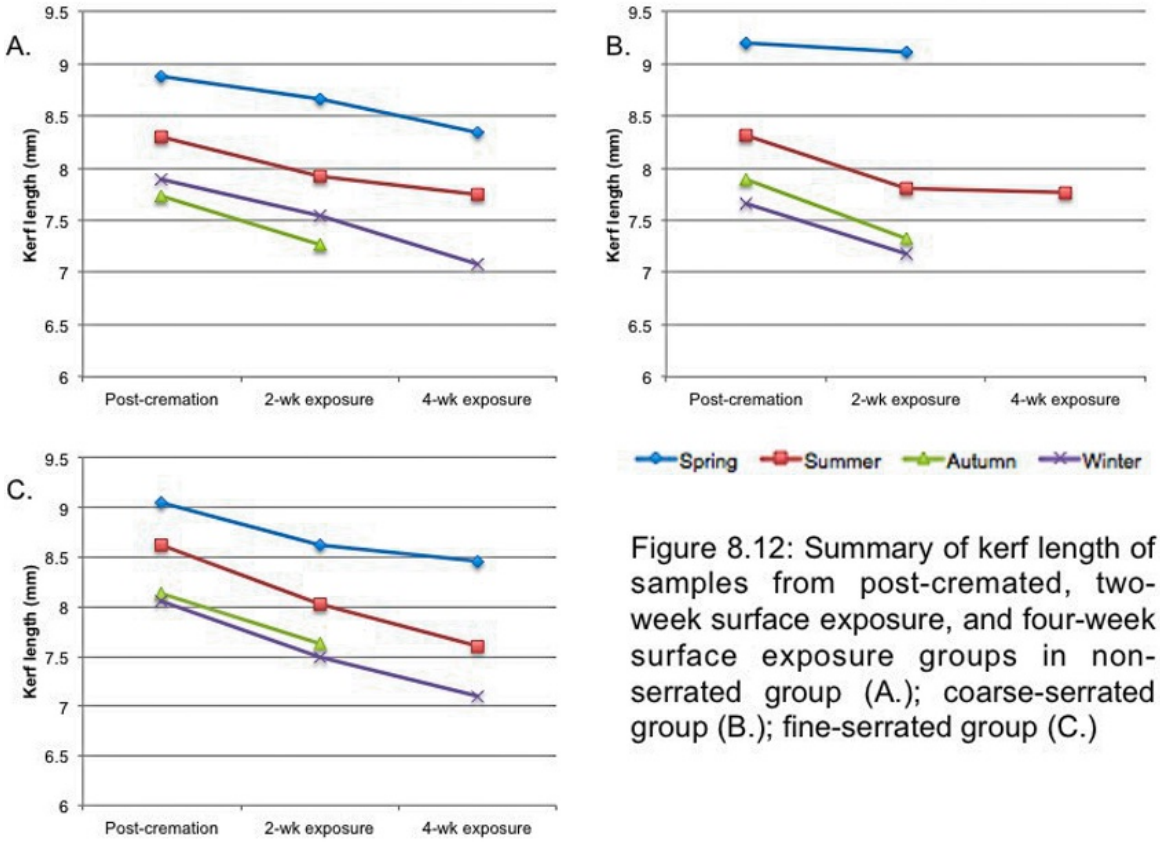

Figure 8.12: Summary of kerf length of samples from post-cremated, two-week surface exposure, and four-week surface exposure groups in non-serrated group (A.); coarse-serrated group (B.); fine-serrated group (C.)

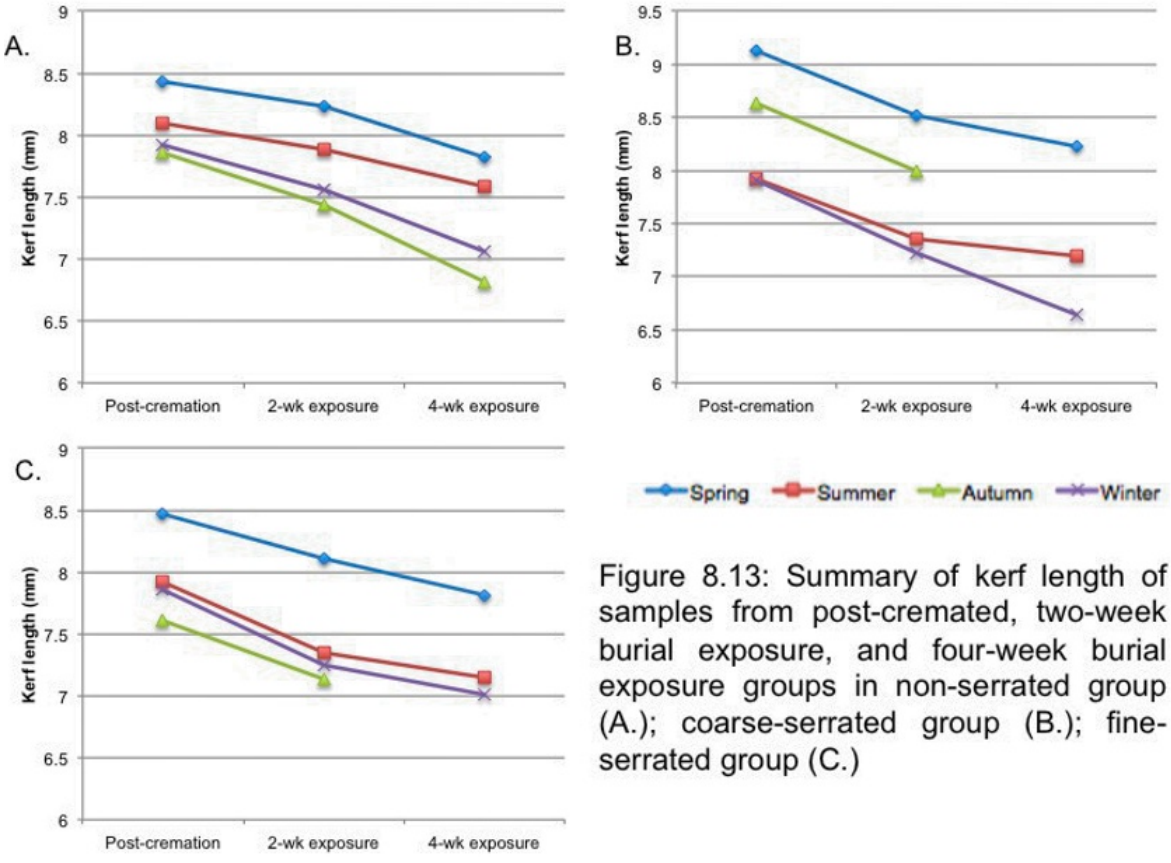

Figure 8.13: Summary of kerf length of samples from post-cremated, two-week burial exposure, and four-week burial exposure groups in non-serrated group (A.); coarse-serrated group (B.); fine-serrated group (C.)

The line charts in Figure 8.12 and 8.13 show how the kerf length changed during the four seasons for surface and burial exposure, respectively. In each of these cases, there was a negative correlation between kerf length and time. The slope patterns of all season were very similar in appearance for the surface and buried groups; their patterns showed summer group displayed milder negative correlations compared with the other groups. All results were not significant associations (Table 8.F in APPENDIX 8). Figures 8.14-8.15 demonstrate the kerf width results after surface and buried environmental exposure. Most of the cut marks exhibited negative correlations between kerf width and time. However, there was a different trend of dimensional change as an increase in kerf width of autumn samples at two-week surface exposure; while autumn buried samples of cut marks inflicted by coarse-serrated and fine-serrated blade knives showed slight decrease in their width size when compared with other season groups. Nevertheless, these results were all not a statistical significance ($p>0.05$) (Table 8.G in APPENDIX 8). An increase in kerf width in the winter group was also observed at four-week surface exposure.

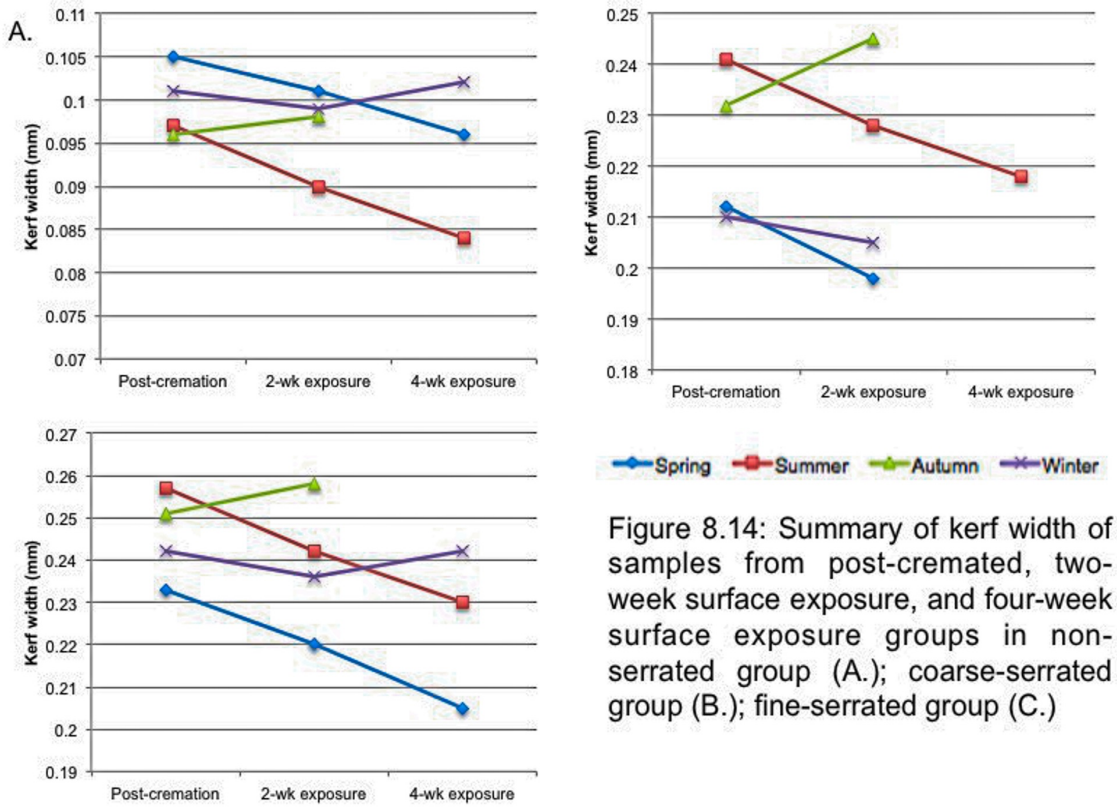

Figure 8.14: Summary of kerf width of samples from post-cremated, two-week surface exposure, and four-week surface exposure groups in non-serrated group (A.); coarse-serrated group (B.); fine-serrated group (C.)

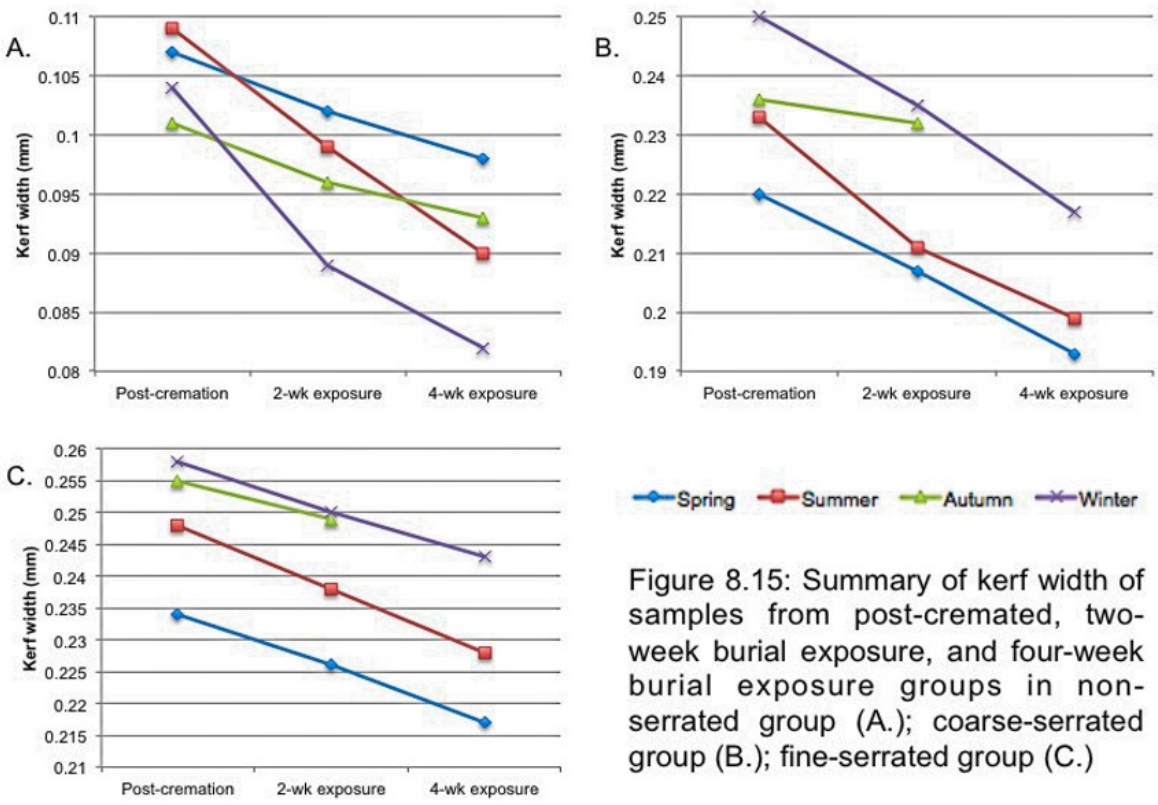

Figure 8.15: Summary of kerf width of samples from post-cremated, two-week burial exposure, and four-week burial exposure groups in non-serrated group (A.); coarse-serrated group (B.); fine-serrated group (C.)

8.1.3.2.2 Morphological changes

Burned cut mark inflicted by different blade types underwent some alterations after environmental exposure. Morphological changes were observed in four different aspects: kerf shape, cross-sectional shape, kerf margin, and kerf striations. These were tested against the three types of knife blade. The Chi-squared test and Fisher's exact test were used to examine the relationships between pre-exposure and post-exposure to the outdoor environment. The null hypothesis could be rejected if the p-value was less than 0.05. The classification of kerf morphology was not always possible, as a result of kerf damage, debris filling and fragmentation.

8.1.3.2.2.1 Non-serrated knife

Tables 8.4-8.5 summarise frequent data of morphological changes of the surface-exposure group, while Tables 8.6-8.7 demonstrate those of the buried group.

Table 8.4: Summary of frequency data of kerf morphology changes between pre-exposure (Pre-E) and two-week surface exposure (Post-E) cut marks from a non-serrated knife; KS: kerf shape; CS: cross-sectional shape; KM: kerf margin; KSt: kerf striations

Kerf morphology		Spring (n=10) (%)		Summer (n=10) (%)		Autumn (n=10) (%)		Winter (n=10) (%)	
		Pre-E	Post-E	Pre-E	Post-E	Pre-E	Post-E	Pre-E	Post-E
KS	Linear	8 (80)	8 (80)	8 (80)	8 (80)	8 (80)	8 (80)	8 (80)	8 (80)
	Ellipse	2 (20)	2 (20)	2 (20)	2 (20)	2 (20)	2 (20)	2 (20)	2 (20)
CS	Narrow	8 (80)	8 (80)	8 (80)	8 (20)	8 (80)	8 (80)	8 (80)	8 (80)
	V-shaped	2 (20)	2 (20)	2 (20)	2 (20)	2 (20)	2 (20)	2 (20)	2 (20)
KM	Smooth	10 (100)	10 (100)	10 (100)	10 (100)	10 (100)	10 (100)	10 (100)	10 (100)
	Raising	-	-	-	-	-	-	-	-
KSt	Presence	-	-	-	-	-	-	-	-
	Absence	10 (100)	10 (100)	10 (100)	10 (100)	10 (100)	10 (100)	10 (100)	10 (100)

Table 8.5: Summary of frequency data of kerf morphology changes between pre-exposure (Pre-E) and four-week surface exposure (Post-E) cut marks from a non-serrated knife; KS: kerf shape; CS: cross-sectional shape; KM: kerf margin; KSt: kerf striations

Kerf morphology		Spring (n=10) (%)		Summer (n=10) (%)		Autumn (n=10) (%)		Winter (n=10) (%)	
		Pre-E	Post-E	Pre-E	Post-E	Pre-E	Post-E	Pre-E	Post-E
KS	Linear	8 (80)	8 (80)	9 (90)	9 (90)	8 (80)	7 (70)	8 (80)	6 (60)
	Ellipse	2 (20)	2 (20)	1 (10)	1 (10)	2 (20)	3 (30)	2 (20)	4 (40)
CS	Narrow	8 (80)	8 (80)	8 (80)	8 (80)	8 (80)	8 (80)	8 (80)	8 (80)
	V-shaped	2 (20)	2 (20)	2 (20)	2 (20)	2 (20)	2 (20)	2 (20)	2 (20)
KM	Smooth	10 (100)	10 (100)	10 (100)	10 (100)	10 (100)	10 (100)	10 (100)	10 (100)
	Raising	-	-	-	-	-	-	-	-
KSt	Presence	-	-	-	-	-	-	-	-
	Absence	10 (100)	10 (100)	10 (100)	10 (100)	10 (100)	10 (100)	10 (100)	10 (100)

Table 8.6: Summary of frequency data of kerf morphology changes between pre-exposure (Pre-E) and two-week burial exposure (Post-E) cut marks from a non-serrated knife; KS: kerf shape; CS: cross-sectional shape; KM: kerf margin; KSt: kerf striations

Kerf morphology		Spring (n=10) (%)		Summer (n=10) (%)		Autumn (n=10) (%)		Winter (n=10) (%)	
		Pre-E	Post-E	Pre-E	Post-E	Pre-E	Post-E	Pre-E	Post-E
KS	Linear	9 (90)	9 (90)	8 (80)	8 (80)	7 (70)	7 (70)	7 (70)	7 (70)
	Ellipse	1 (10)	1 (10)	2 (20)	2 (20)	3 (30)	3 (30)	3 (30)	3 (30)
CS	Narrow	7 (70)	7 (70)	8 (80)	8 (80)	8 (80)	8 (80)	7 (70)	7 (70)
	V-shaped	3 (30)	3 (30)	2 (20)	2 (20)	2 (20)	2 (20)	3 (30)	3 (30)
KM	Smooth	10 (100)	10 (100)	10 (100)	10 (100)	10 (100)	10 (100)	10 (100)	10 (100)
	Raising	-	-	-	-	-	-	-	-
KSt	Presence	-	-	-	-	-	-	-	-
	Absence	10 (100)	10 (100)	10 (100)	10 (100)	10 (100)	10 (100)	10 (100)	10 (100)

Table 8.7: Summary of frequency data of kerf morphology changes between pre-exposure (Pre-E) and four-week burial exposure (Post-E) cut marks from a non-serrated knife; KS: kerf shape; CS: cross-sectional shape; KM: kerf margin; KSt: kerf striations

Kerf morphology		Spring (n=10) (%)		Summer (n=10) (%)		Autumn (n=10) (%)		Winter (n=10) (%)	
		Pre-E	Post-E	Pre-E	Post-E	Pre-E	Post-E	Pre-E	Post-E
KS	Linear	8 (80)	8 (80)	9 (90)	9 (90)	7 (70)	7 (70)	8 (80)	8 (80)
	Ellipse	2 (20)	2 (20)	1 (10)	1 (10)	3 (30)	3 (30)	2 (20)	2 (20)
CS	Narrow	7 (70)	7 (70)	9 (90)	9 (90)	8 (80)	8 (80)	7 (70)	7 (70)
	V-shaped	3 (30)	3 (30)	1 (10)	1 (10)	2 (20)	2 (20)	3 (30)	3 (30)
KM	Smooth	10 (100)	10 (100)	10 (100)	10 (100)	10 (100)	10 (100)	10 (100)	10 (100)
	Raising	-	-	-	-	-	-	-	-
KSt	Presence	-	-	-	-	-	-	-	-
	Absence	10 (100)	10 (100)	10 (100)	10 (100)	10 (100)	10 (100)	10 (100)	10 (100)

Apparently, most of the cut marks inflicted by non-serrated blade showed non-changing morphology after environmental exposure. Smooth margin and absence of kerf striations remained stable through four weeks of surface and burial exposure. After four-weeks surface exposure, 25% of linear kerf shape in the winter group and 12.5% of those in the autumn group changed to an elliptical shape (Figure 8.16). There was no significant association between post-burned and post-exposure in both surface and buried groups.

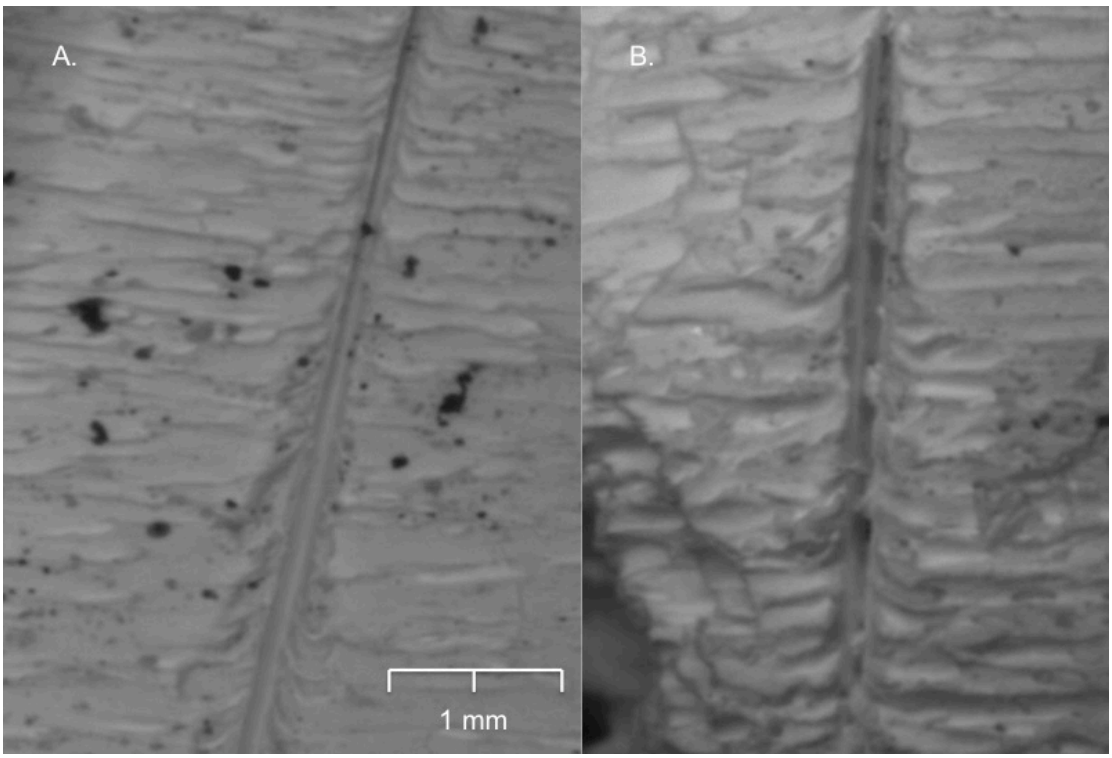

Figure 8.16: Kerf shape change from pre-exposure linear shape (A.) to elliptical shape after four-week environmental exposure (B.)

8.1.3.2.2.2 Coarse-serrated knife

Burned cut marks inflicted by coarse-serrated knife underwent some alterations to kerf feature. Tables 8.8-8.9 summarise frequent data of morphological changes of the surface-exposure group, while Tables 8.10-8.11 review those of buried group.

Table 8.8: Summary of frequency data of kerf morphology changes between pre-exposure (Pre-E) and two-week surface exposure (Post-E) cut marks from a coarse-serrated knife; KS: kerf shape; CS: cross-sectional shape; KM: kerf margin; KSt: kerf striations

Kerf morphology		Spring (n=10) (%)		Summer (n=10) (%)		Autumn (n=10) (%)		Winter (n=10) (%)	
		Pre-E	Post-E	Pre-E	Post-E	Pre-E	Post-E	Pre-E	Post-E
KS	Ellipse	7 (70)	6 (60)	7 (70)	6 (60)	7 (70)	4 (40)	8 (80)	6 (60)
	Rectangle	2 (20)	2 (20)	1 (10)	1 (10)	1 (10)	1 (10)	2 (20)	2 (20)
	Irregular	1 (10)	2 (20)	2 (20)	3 (30)	2 (20)	5 (50)	-	2 (20)
CS	V-shaped	6 (60)	5 (50)	5 (50)	5 (50)	5 (50)	5 (50)	5 (50)	5 (50)
	U-shaped	4 (40)	5 (50)	5 (50)	5 (50)	5 (50)	5 (50)	5 (50)	5 (50)
KM	Smooth	4 (40)	5 (50)	3 (30)	4 (40)	4 (40)	7 (70)	4 (40)	6 (60)
	Raising	6 (60)	5 (50)	7 (70)	6 (60)	6 (60)	3 (30)	6 (60)	4 (40)
KSt	Presence	7 (70)	6 (60)	6 (60)	6 (60)	7 (70)	5 (50)	7 (70)	6 (60)
	Absence	3 (30)	4 (40)	4 (40)	4 (40)	3 (30)	5 (50)	3 (30)	4 (40)

Table 8.9: Summary of frequency data of kerf morphology changes between pre-exposure (Pre-E) and four-week surface exposure (Post-E) cut marks from a coarse-serrated knife; KS: kerf shape; CS: cross-sectional shape; KM: kerf margin; KSt: kerf striations

Kerf morphology		Spring (n=10) (%)		Summer (n=10) (%)		Autumn (n=10) (%)		Winter (n=10) (%)	
		Pre-E	Post-E	Pre-E	Post-E	Pre-E	Post-E	Pre-E	Post-E
KS	Ellipse	8 (80)	6 (60)	6 (60)	4 (40)	8 (80)	2 (20)	7 (70)	3 (30)
	Rectangle	1 (10)	1 (10)	2 (20)	2 (20)	2 (20)	2 (20)	2 (20)	2 (20)
	Irregular	1 (10)	3 (30)	2 (20)	4 (40)	-	6 (60)	1 (10)	5 (50)
CS	V-shaped	5 (50)	5 (50)	6 (60)	5 (50)	6 (60)	4 (40)	6 (60)	4 (40)
	U-shaped	5 (50)	5 (50)	4 (40)	5 (50)	4 (40)	6 (60)	4 (40)	6 (60)
KM	Smooth	4 (40)	6 (60)	4 (40)	6 (60)	3 (30)	9 (90)	3 (30)	8 (80)
	Raising	6 (60)	4 (40)	6 (60)	4 (40)	7 (70)	1 (10)	7 (70)	2 (20)
KSt	Presence	6 (60)	5 (50)	7 (70)	5 (50)	7 (70)	4 (40)	6 (60)	4 (40)
	Absence	4 (40)	5 (50)	3 (30)	5 (50)	3 (30)	6 (60)	4 (40)	6 (60)

Table 8.10: Summary of frequency data of kerf morphology changes between pre-exposure (Pre-E) and two-week burial exposure (Post-E) cut marks from a coarse-serrated knife; KS: kerf shape; CS: cross-sectional shape; KM: kerf margin; KSt: kerf striations

Kerf morphology		Spring (n=10) (%)		Summer (n=10) (%)		Autumn (n=10) (%)		Winter (n=10) (%)	
		Pre-E	Post-E	Pre-E	Post-E	Pre-E	Post-E	Pre-E	Post-E
KS	Ellipse	7 (70)	7 (70)	8 (80)	8 (80)	8 (80)	7 (70)	6 (60)	5 (50)
	Rectangle	2 (20)	2 (20)	1 (10)	1 (10)	1 (10)	1 (10)	2 (20)	2 (20)
	Irregular	1 (10)	1 (10)	1 (10)	1 (10)	1 (10)	2 (20)	2 (20)	3 (30)
CS	V-shaped	5 (50)	5 (50)	5 (50)	5 (50)	5 (50)	5 (50)	6 (60)	5 (50)
	U-shaped	5 (50)	5 (50)	5 (50)	5 (50)	5 (50)	5 (50)	4 (40)	5 (50)
KM	Smooth	3 (30)	4 (40)	3 (30)	4 (40)	4 (40)	6 (60)	4 (40)	5 (50)
	Raising	7 (70)	6 (60)	7 (70)	6 (60)	6 (60)	4 (40)	6 (60)	5 (50)
KSt	Presence	6 (60)	6 (60)	6 (60)	6 (60)	6 (60)	5 (50)	7 (70)	6 (60)
	Absence	4 (40)	4 (40)	4 (40)	4 (40)	4 (40)	5 (50)	3 (30)	4 (40)

Table 8.11: Summary of frequency data of kerf morphology changes between pre-exposure (Pre-E) and four-week burial exposure (Post-E) cut marks from a coarse-serrated knife; KS: kerf shape; CS: cross-sectional shape; KM: kerf margin; KSt: kerf striations

Kerf morphology		Spring (n=10) (%)		Summer (n=10) (%)		Autumn (n=10) (%)		Winter (n=10) (%)	
		Pre-E	Post-E	Pre-E	Post-E	Pre-E	Post-E	Pre-E	Post-E
KS	Ellipse	7 (70)	5 (50)	7 (70)	5 (50)	7 (70)	4 (40)	9 (90)	7 (70)
	Rectangle	1 (10)	2 (20)	1 (10)	1 (10)	1 (10)	1 (10)	1 (10)	1 (10)
	Irregular	2 (20)	3 (30)	2 (20)	4 (40)	2 (20)	5 (50)	-	2 (20)
CS	V-shaped	5 (50)	5 (50)	5 (50)	5 (50)	6 (60)	5 (50)	6 (60)	5 (50)
	U-shaped	5 (50)	5 (50)	5 (50)	5 (50)	4 (40)	5 (50)	4 (40)	5 (50)
KM	Smooth	4 (40)	6 (60)	4 (40)	5 (50)	3 (30)	6 (60)	3 (30)	5 (50)
	Raising	6 (60)	4 (40)	6 (60)	5 (50)	7 (70)	4 (40)	7 (70)	5 (50)
KSt	Presence	7 (70)	7 (70)	7 (70)	7 (70)	6 (60)	4 (40)	6 (60)	4 (40)
	Absence	3 (30)	3 (30)	3 (30)	3 (30)	4 (40)	6 (60)	4 (40)	6 (60)

Cut marks made by coarse-serrated blade showed more variable kerf morphological change when compared with cut marks made by other types of knife blade. After environmental exposure, elliptical kerf shape was likely to change to irregular shape (Figure 8.17), while V-shaped cross-section altered to U shape. Raised kerf margin and kerf striations were found to erode after outdoor exposure (Figure 8.18). In addition, surface-exposure group exhibited more advanced changes compared with the burial group, particularly cut marks deposited in autumn and winter.

There was no significant association between post-burned and two-weeks post-exposure groups (Table 8.H), but some features of four-weeks exposure of cut marks from coarse-serrated knives exhibited significant association ($p<0.05$) (Table 8.I). Kerf shapes and kerf margins in the autumn group, and kerf margins in the winter group exhibited statistically significant changes after four-weeks surface exposure.

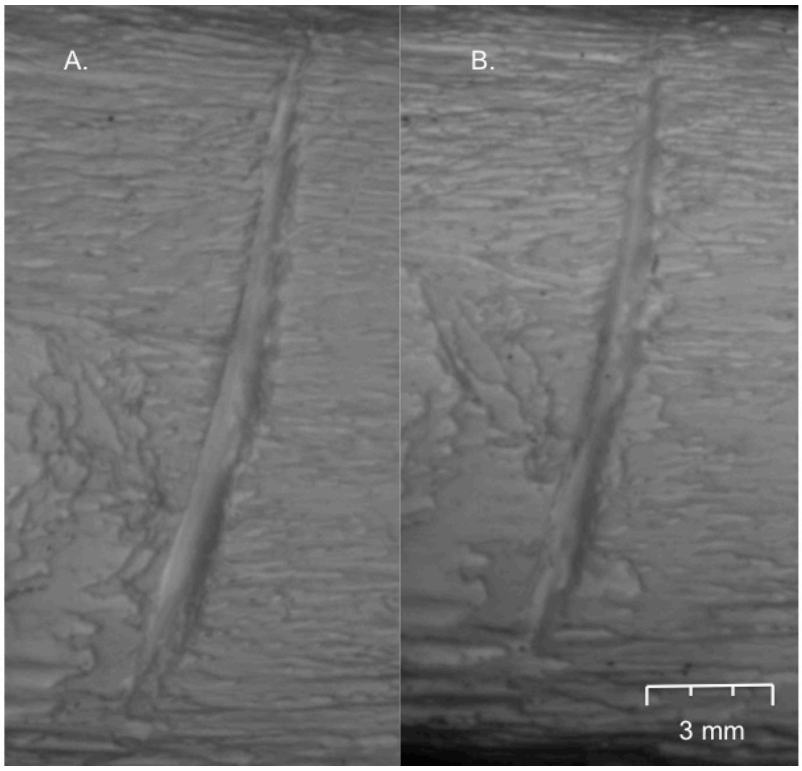

Figure 8.17: An alteration of coarse-serrated inflicted kerf shape; A. post-cremation; B. four-week surface exposure

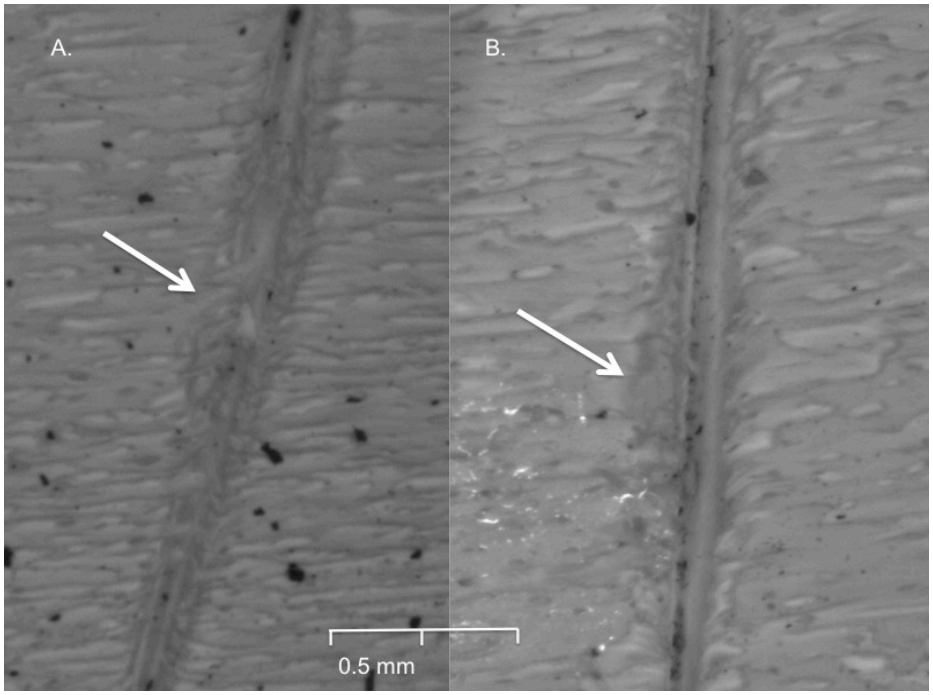

Figure 8.18: Kerf margin of a cut mark inflicted by coarse-serrated blade before (A.) and after one-month surface exposure (B.) with margin erosion in the winter; the white arrows indicate the same area of the kerf margin

8.1.3.2.2.3 Fine-serrated knife

Burned cut marks made by fine-serrated blade knife underwent morphological changes to kerf feature after surface and buried environmental exposure. Tables 8.12-8.13 summarise frequent data of morphological changes of the surface-exposure group, while Tables 8.14-8.15 reveal those of buried group. Overall, morphological post-exposure changes in burned cut marks made by fine-serrated blade knife had the same pattern as burned cut marks inflicted by coarse-serrated blade knife. Ellipse-shaped kerfs were likely to change their shape to irregular one. V-shaped cross-section changed to U shape, while some damages of raised margins and striations were observed. There was no significant association between post-burned and post-exposure groups (Table 8.H, 8.I in APPENDIX 8).

Table 8.12: Summary of frequency data of kerf morphology changes between pre-exposure (Pre-E) and two-week surface exposure (Post-E) cut marks from a fine-serrated knife; KS: kerf shape; CS: cross-sectional shape; KM: kerf margin; KSt: kerf striations

Kerf morphology		Spring (n=10) (%)		Summer (n=10) (%)		Autumn (n=10) (%)		Winter (n=10) (%)	
		Pre-E	Post-E	Pre-E	Post-E	Pre-E	Post-E	Pre-E	Post-E
KS	Ellipse	8 (80)	7 (70)	9 (90)	8 (80)	8 (80)	6 (60)	9 (90)	8 (80)
	Rectangle	1 (10)	1 (10)	-	-	1 (10)	1 (10)	-	-
	Irregular	1 (10)	2 (20)	1 (10)	2 (20)	1 (10)	3 (30)	1 (10)	2 (20)
CS	V-shaped	8 (80)	7 (70)	8 (80)	7 (70)	9 (90)	7 (70)	9 (90)	7 (70)
	U-shaped	2 (20)	3 (30)	2 (20)	3 (30)	1 (10)	3 (30)	1 (10)	3 (30)
KM	Smooth	6 (60)	7 (70)	7 (70)	7 (70)	7 (70)	8 (80)	6 (60)	8 (80)
	Raising	4 (40)	3 (30)	3 (30)	3 (30)	3 (30)	2 (20)	4 (40)	2 (20)
KSt	Presence	6 (60)	6 (60)	7 (70)	6 (60)	6 (60)	5 (50)	7 (70)	5 (50)
	Absence	4 (40)	4 (40)	3 (30)	4 (40)	4 (40)	5 (50)	3 (30)	5 (50)

Table 8.13: Summary of frequency data of kerf morphology changes between pre-exposure (Pre-E) and four-week surface exposure (Post-E) cut marks from a fine-serrated knife; KS: kerf shape; CS: cross-sectional shape; KM: kerf margin; KSt: kerf striations

Kerf morphology		Spring (n=10) (%)		Summer (n=10) (%)		Autumn (n=10) (%)		Winter (n=10) (%)	
		Pre-E	Post-E	Pre-E	Post-E	Pre-E	Post-E	Pre-E	Post-E
KS	Ellipse	8 (80)	6 (60)	9 (90)	7 (70)	9 (90)	6 (60)	8 (80)	5 (50)
	Rectangle	-	-	-	-	-	-	1 (10)	1 (10)
	Irregular	2 (20)	4 (40)	1 (10)	3 (30)	1 (10)	4 (40)	1 (10)	4 (40)
CS	V-shaped	9 (90)	8 (80)	8 (80)	8 (80)	8 (80)	6 (60)	8 (80)	5 (50)
	U-shaped	1 (10)	2 (20)	2 (20)	2 (20)	2 (20)	4 (40)	2 (20)	5 (50)
KM	Smooth	7 (70)	8 (80)	6 (60)	7 (70)	6 (60)	9 (90)	7 (70)	9 (90)
	Raising	3 (30)	2 (20)	4 (40)	3 (30)	4 (40)	1 (10)	3 (30)	1 (10)
KSt	Presence	6 (60)	5 (50)	7 (70)	5 (50)	6 (60)	3 (30)	6 (60)	4 (40)
	Absence	4 (40)	5 (50)	3 (30)	5 (50)	4 (40)	7 (70)	4 (40)	6 (60)

Table 8.14: Summary of frequency data of kerf morphology changes between pre-exposure (Pre-E) and two-week burial exposure (Post-E) cut marks from a fine-serrated knife; KS: kerf shape; CS: cross-sectional shape; KM: kerf margin; KSt: kerf striations

Kerf morphology		Spring (n=10) (%)		Summer (n=10) (%)		Autumn (n=10) (%)		Winter (n=10) (%)	
		Pre-E	Post-E	Pre-E	Post-E	Pre-E	Post-E	Pre-E	Post-E
KS	Ellipse	9 (90)	8 (80)	8 (80)	8 (80)	8 (80)	7 (70)	8 (80)	8 (80)
	Rectangle	1 (10)	1 (10)	-	-	1 (10)	1 (10)	1 (10)	1 (10)
	Irregular	-	1 (10)	2 (20)	2 (20)	1 (10)	2 (20)	1 (10)	1 (10)
CS	V-shaped	9 (90)	8 (80)	7 (70)	7 (70)	8 (80)	7 (70)	9 (90)	8 (80)
	U-shaped	1 (10)	2 (20)	3 (30)	3 (30)	2 (20)	3 (30)	1 (10)	2 (20)
KM	Smooth	7 (70)	7 (70)	7 (70)	7 (70)	7 (70)	7 (70)	6 (60)	7 (70)
	Raising	3 (30)	3 (30)	3 (30)	3 (30)	3 (30)	3 (30)	4 (40)	3 (30)
KSt	Presence	6 (60)	6 (60)	7 (70)	7 (70)	7 (70)	6 (60)	6 (60)	6 (60)
	Absence	4 (40)	4 (40)	3 (30)	3 (30)	3 (30)	4 (40)	4 (40)	4 (40)

Table 8.15: Summary of frequency data of kerf morphology changes between pre-exposure (Pre-E) and four-week burial exposure (Post-E) cut marks from a fine-serrated knife; KS: kerf shape; CS: cross-sectional shape; KM: kerf margin; KSt: kerf striations

Kerf morphology		Spring (n=10) (%)		Summer (n=10) (%)		Autumn (n=10) (%)		Winter (n=10) (%)	
		Pre-E	Post-E	Pre-E	Post-E	Pre-E	Post-E	Pre-E	Post-E
KS	Ellipse	8 (80)	6 (60)	9 (90)	8 (80)	8 (80)	5 (50)	9 (90)	6 (60)
	Rectangle	-	-	-	-	1 (10)	1 (10)	1 (10)	1 (10)
	Irregular	2 (20)	4 (40)	1 (10)	2 (20)	1 (10)	4 (40)	-	3 (30)
CS	V-shaped	8 (80)	6 (60)	8 (80)	6 (60)	8 (80)	5 (50)	9 (90)	6 (60)
	U-shaped	2 (20)	4 (40)	2 (20)	4 (40)	2 (20)	5 (50)	1 (10)	4 (40)
KM	Smooth	7 (70)	8 (80)	6 (60)	7 (70)	7 (70)	9 (90)	7 (70)	9 (90)
	Raising	3 (30)	2 (20)	4 (40)	3 (30)	3 (30)	1(10)	3 (30)	1(10)
KSt	Presence	6 (60)	5 (50)	7 (70)	6 (60)	7 (70)	5 (50)	6 (60)	4 (40)
	Absence	4 (40)	5 (50)	3 (30)	4 (40)	3 (30)	5 (50)	4 (40)	6 (60)

8.1.4 Burned bone fragmentation

To assess post-burning fragmentation of burned bone, fragmented size categories (Table 8.16) were used for sorting into one of the three defined categories based on overall size. Results showed considerable increases over time in fragmentation in all groups. Most of the separated fragmented cracks came from pre-existing heat-induced fractures, which normally happen during the burning process. Weather data in Table 8.A in APPENDIX 8 were used to investigate the effects of weather conditions on fragmentation level and size. There was no statistical significance between the controlled and traumatic burned samples.

Table 8.16: Definition of the fragmented size of a burned bone

Category	Definition
Small category	A bone fragment with the smallest dimension not more than 1 mm
Medium category	A bone fragment with the smallest dimension is between 1-5 mm
Large category	A bone fragment with the smallest dimension more than 5 mm

8.1.4.1 Post-burned fragmentation

When the bone samples were recovered, the effect of fragmentation was mixed, as seen in Figure 8.19-8.20. The vast majority of fragmentation was classified in the large category with around 80% found in all seasons.

8.1.4.2 Surface-deposited group

Proportional masses for each size category were demonstrated in Figure 8.19. When the recovery of fragmented bones was delayed by one week, the effect on fragmentation was mixed in each season. The results will be discussed separately into each week in order to compare with weather conditions.

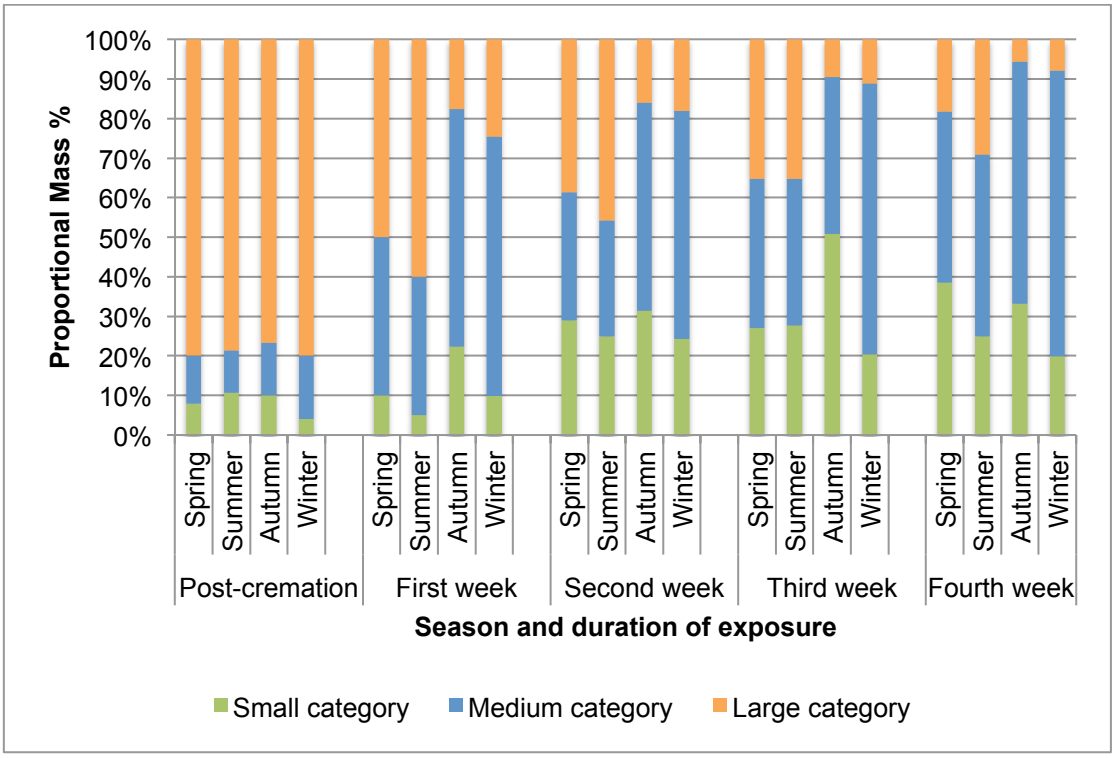

Figure 8.19: Percentage of proportional mass distribution of surface-deposited samples after the burning process and post-environmental exposure

8.1.4.2.1 First week

In the first week, the highest proportion mass of each group was different for each season. The spring and summer groups showed the highest for the large category suggesting low level of fragmentation, while lower proportion of the large category and the highest proportion mass of the medium category in the autumn and winter groups indicated increased fragmentation of large bone fragments.

The summer group exhibited the highest proportional mass (60%) of the large category, and the lowest proportional mass of the medium (35%) and small categories (5%) indicating the lowest level of fragmentation compared with other seasons. The autumn group showed the lowest level of the large category (18%) and the highest level of the small category (22.3%) indicating this group experienced the highest level of fragmentation. The highest level (65%) of fragmentation to the medium category of the winter group was also observed.

8.1.4.2.2 Second week

Proportional masses in all groups showed major differences indicating a vast difference in fragmentation. All groups exhibited an increase in the small category when compared with the first week, but a stable proportion of the medium category was observed in all groups. There were increases in fragmentation of the spring and summer groups but a better survival of the large category was found. The continuation of fragmentation was still found in the autumn and winter groups by considering from lower level of the large category and an increase in the proportion of the small category.

8.1.4.2.3 Third week

After three-weeks surface exposure, the effects of weather conditions on fragmentation pattern still increased but at a slower rate. As was seen in the medium category, an increase in fragmentation in the spring, summer and winter groups was observed. The markedly higher of the small category in the autumn groups was also witnessed. The autumn group still showed the highest rate of fragmentation based on the lowest level of the large category (9.6%) and the highest level of the small category (50.9%). The winter group had also an increase in fragmentation, with a decrease in the large category size (11.11%), but the lowest level of the small category was also observed (20.4%).

8.1.4.2.4 Fourth week

The highest fragmented rate was observed in the spring group as can be seen from a substantial decrease in the large category and a significant increase in the medium and small categories. By the autumn and winter, most of the large fragments were eliminated. The autumn group still showed more fragmentation than the winter group as evidence of a higher level of the small category. The summer group had a marked decrease in large category samples, but they were still the best preserved with the highest proportion of large series (29.2%) and the low number of the medium and small series. The majority of medium category level was observed in the winter group.

8.1.4.3 Burial group

Proportional masses for each size category were demonstrated in Figure 8.20. The excavation of burial samples was conducted every two weeks and fragmentation rate was analysed.

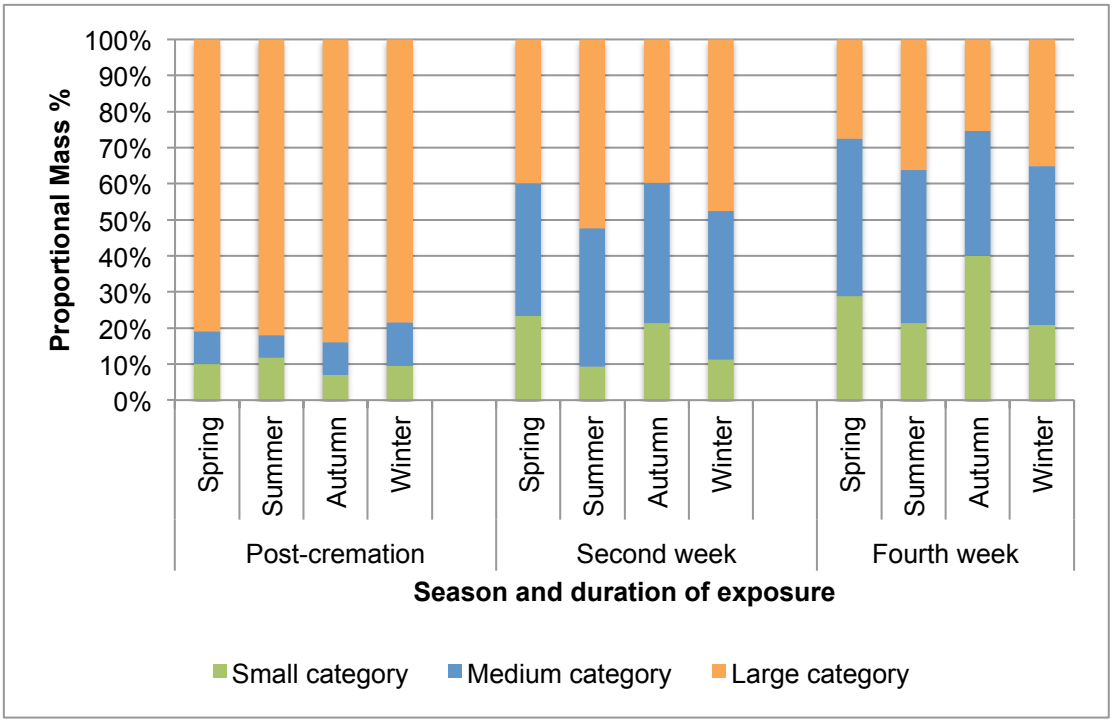

Figure 8.20: Percentage of proportional mass distribution of buried samples after he burning process and post-environmental exposure

8.1.4.3.1 Second week

The spring and autumn group had a higher fragmentation based on the low level of the large category and high level of the medium and small categories. The summer and winter group showed the same pattern of fragmentation change in proportional mass between each category where a high level of the large category corresponded with lower levels of the small and medium categories suggesting a proportional decrease in fragmentation in these groups. The lower level of the small category and high level of the medium category suggested that medium-sized bone fragments were less progressed to small-sized bone.

8.1.4.3.2 Fourth week

The same pattern of fragmentation as the second week was observed. The autumn group showed the highest level of burned bone breakdown. In contrast, the summer and winter group remained stable and a small proportion of small category was observed in these groups. Hence, delayed recovery had no effect on burned bone fragmentation during these seasons. Overall, greater survivability of large fragments in all groups was observed when compared with the surface-deposited group.

8.1.5 Loss of burned bone weight

The weight of bones and bone fragments was documented according to each bone, and the overall weight of exposed bones was determined as an indicator of survival of burned bones from environmental exposure. To fulfil this objective, the weight of each bone samples resulting from specific environmental deposition has been recorded and investigated separately.

8.1.5.1 Surface-deposited group

The results for bone weights are summarised in Table 8.17. Weight variations were observed due to different sizes of rib samples, but the same pattern of residual weight (approximate 22.4-28.9% of pre-burned sample weight) was detected. This variation may eventually be due to structural differences between each porcine individual. Percentage of bone fragment weight after surface exposure was calculated by dividing the post-exposure sample weight by the post-burned sample weight and multiply it by 100. Seasonal differences were indicated and demonstrated in Figure 8.21. The autumn samples showed the lowest survival of bone fragments in the first two weeks, whereas winter sample presented the lowest proportion after four-weeks exposure. The summer sample had the highest survival rate comparing with the other seasonal groups.

Table 8.17: Average sample weight and percentage of residual weight after exposure to heat and environment in the surface-deposited group

Season and exposure time		Pre-burn (gram)	Post-burn (gram)	%Residual weight after burn	Post-exposure (gram)	%Residual weight after exposure*
Spring	2wk	12.99±2.95	2.99±0.62	23.142	2.73±0.57	91.432
	4wk	13.33±2.1	3.25±0.57	24.356	2.44±0.55	75.08
Summer	2wk	13.11±2.62	3.48±0.63	26.618	3.38±0.63	97.182
	4wk	13.45±3.48	3.89±1.02	28.874	3.21±0.77	82.434
Autumn	2wk	12.39±1.67	3.22±0.48	26.01	2.36±0.48	73.244
	4wk	15.33±2.76	3.61±0.65	22.35	2.24±0.54	62.17
Winter	2wk	12.78±2.94	3.09±0.62	24.288	2.47±0.58	80.092
	4wk	14.12±2.39	3.37±0.76	23.74	1.56±0.47	46.4

* Compare between pre-exposure and post-exposure weight

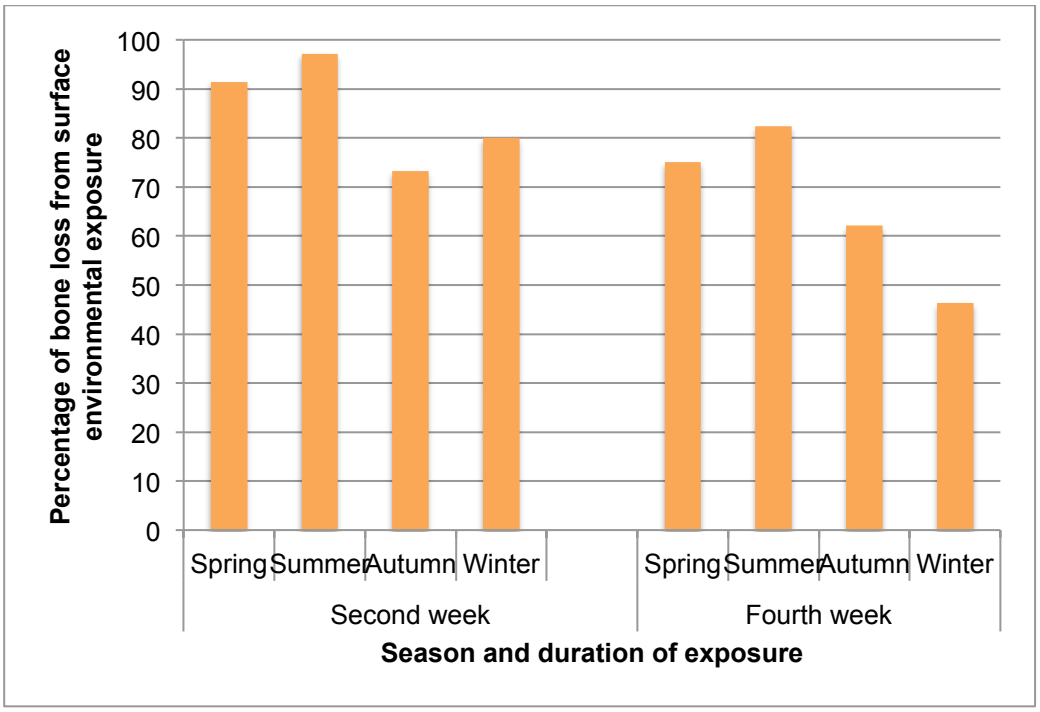

Figure 8.21: Percentage of fragmented weight loss of surface-deposited samples compared between each season

8.1.5.2 Buried group

The bone weight obtained for buried samples is demonstrated in Table 8.18 and Figure 8.22.

Table 8.18: Average sample weight and percentage of residual weight after exposure to heat and environment in the buried group

Season and exposure time		Pre-burn (gram)	Post-burn (gram)	%Residual weight after burn	Post-exposure (gram)	%Residual weight after exposure*
Spring	2wk	12.13±1.33	2.72±0.41	22.416	2.53±0.4	92.878
	4wk	14.18±2.32	3.35±0.56	23.666	2.86±0.57	85.348
Summer	2wk	13.9±3.6	3.8±1.05	27.226	3.61±0.91	95.118
	4wk	11.85±2.51	3.22±0.62	27.524	2.97±0.56	92.232
Autumn	2wk	12.45±3.58	2.83±0.87	22.686	2.55±0.82	90.174
	4wk	12.55±2.11	3.02±0.68	23.858	2.48±0.61	82
Winter	2wk	12.93±3.12	3.17±0.78	24.576	3±0.62	94.546
	4wk	13.43±2.73	3.32±0.67	24.776	3±0.74	90.416

* Compare between pre-exposure and post-exposure weight

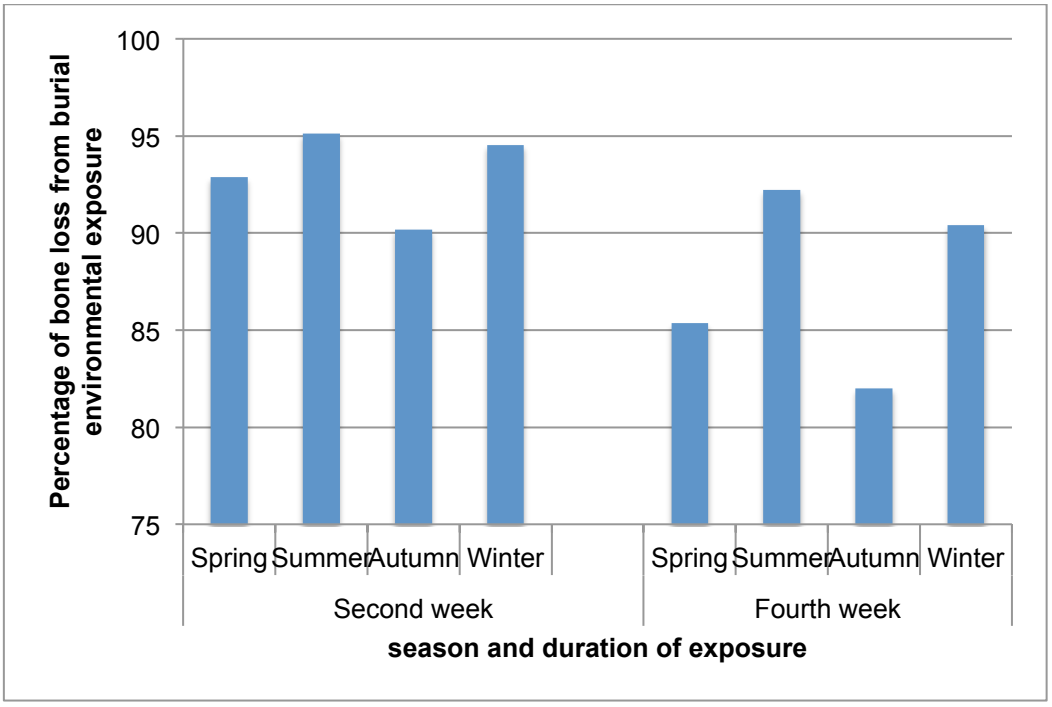

Figure 8.22: Percentage of fragmented weight loss of buried samples comparing between each season

Weight variations from different sizes of rib samples were observed, but the same pattern of residual weight (approximate 22.4-27.5%) was detected. As opposed to surface-deposited samples, burial samples showed a better survival

rate. The autumn samples showed the lowest survival of bone fragments, followed by the spring samples.

8.1.6 Summary

After the cremation process, cut marks on rib samples were well preserved, but they showed statistical changes in kerf dimension, kerf shape of cut marks made from coarse-serrated and fine-serrated knives, and kerf margin of cut marks inflicted by coarse-serrated knife. Heat-induced fractures could hinder interpretation of cut marks by traversing and fracturing some cut marks, but an examination of most of the cut marks could be conducted.

Additionally, the results highlighted the effects of an outdoor environment on cut mark dimension and morphology. The most destructive season for cut marks was observed during the autumn, with only 26.7% of surface exposure cut marks surviving. A decrease in kerf dimension was also observed, but these changes were not statistically significant. Furthermore, cut mark morphology showed some pattern alterations, showing a statistical difference between pre and post-exposure in kerf shape and kerf margin of cut marks inflicted by coarse-serrated knife in the autumn and winter.

Data presented here exhibited that fragmentation rate and pattern is affected by weather conditions and prolonged environmental exposure. High level of rainfall and wind speed might play an important role in post-exposure fragmentation. It was also observed that burned bone weight was corresponding with fragmentation rate.

8.2 Discussion

The objective of this study is to investigate a signature of the perimortem cut mark and heat-related damage, as well as environmental effects on burned cut marks through macroscopic and microscopic examination. Accurate analysis of traumatic lesions on a human bone is one of the pillars of forensic anthropology. Nevertheless, when a forensic anthropologist has to deal with burned remains, this task becomes more difficult. As a matter of fact, trauma morphology of burned bones becomes ambiguous because burned bone tissues are subjected to severe

alterations and distortions (Mayne Correira, 1997; Thompson, 2005; Ubelaker, 2009; Collini *et al.,* 2015). Moreover, a question remains as to whether specific criteria can be used to differentiate traumatic lesion morphology from taphonomic modifications. It is essential that when investigating a forensic cremation case, the ability to identify a cut mark on a fragment of burned bone can lead forensic investigators to the conclusion about cause and manner of death.

Even though *Sus scrofa domesticus* bone is a valid ethical alternative and quite similar in structure and composition to human bones (Aerssens *et al.*, 1998; Kalkwarf *et al.*, 2007; Symes *et al.*, 2010), there are some obvious differences which should be imperative to discuss in this context. Since domestic pigs are slaughtered as immature, the bones have more organic components and are less mineralised when compared with the bones of adult pigs (Kalkwarf *et al.*, 2007). Therefore, a larger proportion of the organic fraction of the juvenile bones are completely destroyed during the cremation process (Mayne Correira, 1997; Thompson, 2004, 2005; Ubelaker, 2009), which results in greater shrinkage and heat-induced bone fractures than is seen in adult pig bones, so these effects on the cut marks are to be expected (Waltenberger and Schutkowski, 2017). The results of the present study are therefore not necessarily representative of adult pig skeletons, and this application should be used with caution. Further research must be carefully conducted using adult human bones or bones from different animals that have a structural similarity to human bones.

Another important factor to take into consideration is the sample recovery protocol. An analytical process of burned bone becomes more difficult when it is damaged from poor recovery and handling. Therefore, careful recovery was performed when removing the burned ribs from the furnace and experimental taphonomic facility in this study. Separating burned bone fragments and packaging it in a layer of toilet paper, secured in a zip-lock plastic bag and then kept in a plastic box is clearly proven to be the most effective method for sample transportation to the laboratory (de Gruchy and Rogers, 2002; Schmidt and Symes, 2015). Burned bones should be handled and moved as little as possible to preserve their fragile structure. However, artificial situation fracture and fragmentation from the excavation process of buried samples might be inevitable. Particularly, fragmentation from

burial may be misinterpreted as being the result of the heat-induced fracture. To distinguish heat-induced fracture from burned bone fragmentation is easier if its original mechanisms were assessed. It is more likely that postmortem fractures produced by crime scene recovery should be distinguished from those produced from fragmentation due to the different mechanism of stress and force applied to the bone materials (Thompson, 2003).

A number of study limitations are recognised. For instance, the status of burned bones at the beginning is not identical. Although the researcher attempted to standardise the burning process and the juvenile pig bones used, it is not possible to control the amount of heat-induced changes in gross and microscopic appearance, colour, size and shape. Therefore, variability of the post-burned dimensions and morphology is expected.

8.2.1 Heat-induced alterations of bones

Generally, there is a wide range of heat-induced modifications to the skeletal tissues and these changes cause difficulties in forensic casework. Bone and teeth undergo four stages of transformation during the burning process: dehydration, decomposition, inversion and fusion (Mayne Correira, 1997; Thompson, 2004; Schmidt and Symes, 2015). Nevertheless, the two most significant events are the loss of the organic material in the decomposition phase, and the recrystallization of the mineral phase in the fusion stage (Thompson *et al.*, 2017). Therefore, these changes termed as primary-level heat-induced alterations would lead to all other findings that can be macroscopically observed, such as colour change and heat-induced fracture, are labelled as secondary-level heat-induced alterations (Thompson, 2005; Thompson *et al.*, 2017).

8.2.1.1 Burned bone colour alterations

The burning process can cause significant changes in the bone colour. In addition to structural and compositional alterations, heat-exposure to skeletal materials will result in colour changes that generally correlate with the temperature level and exposure duration. As the temperature increases, a burned bone proceeds from its normal colour to a dark-black (200-350°C), then to blue and grey (550-

600°C), and finally to a bright white calcined bone (more than 650°C) (Holden *et al.,* 1995; Stiner *et al.,* 1995; Mayne Correira, 1997; Quatrehomme *et al.,* 1998; Thompson, 2004; Fairgrieve, 2008; Ubelaker, 2009; Devlin and Herrmann, 2015). The present study used an electric furnace to control the temperature level to a maximum of 850°C for at least 30 minutes. This temperature level caused the loss of organic materials and impacted the crystalline structure (Thompson, 2003; Schmidt and Symes, 2015).

The heat-induced colour changes in this study exhibited the range of colour from bluish-grey to white. A full range of colour alterations are found within a single animal's remains or even in single bone, as Thompson (2003) mentioned that burned bones rarely transform into a single uniform colour. The remaining soft tissues and an unequal heat distribution during the burning process can be used to explain this phenomenon (Holden *et al.*, 1995; Glassman and Crow, 1996; Imaizumi, 2015; Schmidt and Symes, 2015). Subtle colour difference can be explained by positions of the bones in the furnace, that is, close proximity to the heat coils create "hot-spots" that result in hard tissues not burning uniformly. Some parts of the bone samples were burned more than other parts, resulting in differential loss of carbon and organic substance, and subsequently creating colour variations (Thompson, 2003). Additionally, colour variation can also occur as the heat travels from the outside to the inside of the skeletal material (Thompson, 2003). Furthermore, uneven soft tissue thickness may also affect this finding. Most soft tissues in all the samples were macerated, especially around the cut marks; although some areas still had soft tissue remaining. Consequently, varying degrees of burned bone colour occurred in the same sample.

Even though previous studies have highlighted that the colour of burned bones is an unreliable indicator of temperature and combustion duration due to high levels of variability (Shipman *et al.,* 1984; Devlin and Herrmann, 2015; Macoveciuc *et al.,* 2017), further studies should be conducted to determine other aspects of this phenomena, such as chemical alterations (Stiner *et al.*, 1995).

8.2.1.2 Heat-induced fracture and bone warping

Burning of skeletal materials can produce distinct fracture patterns. Theoretically, variable factors such as temperature of combustion, bone moisture content, remaining soft tissue coverage and cross-sectional diameter across the burning remains would have an influence on exacerbating heat-induced fracture (Bohnert *et al.*, 1997; Herrmann and Bennett, 1999; Pope and Smith, 2004; Ubelaker, 2009; Schmidt and Symes, 2015). Delamination, or peeling of bone layers, occurs when heat exposure causes the external cortical layer to shrink and separate from the deeper cortical layer and trabecular bones. This form is the most common heat-induced damage in this study, with 97.5% of burned ribs displaying this feature. This finding partially corresponds with the work by Pope and Smith (2004), who found delamination is the most common heat-induced fracture observed in the skull, so it is usual to find this type of heat-induced fracture in other flat bones such as ribs. As the outer cortical layer undergoes shrinkage from the dehydration process, there are tensile stresses proceeding in such a way to expose the underlying trabecular bone and inner table (Fairgrieve, 2008). Delamination can be also induced by an external force or handling of fragile burned bones during recovery, transport, and analysis (Pope and Smith, 2004; Fairgrieve, 2008; Schmidt and Symes, 2015).

After delamination, longitudinal fractures were the most common heat-induced fracture found in the present study. Pieces of rib samples responded differently to the cremation process, with 70% and 32.5% of the samples exhibiting longitudinal and transverse fractures, respectively. Longitudinal fracture propagates along the length of the bone. In fact, this fracture run along a line of weakness that is a result of the way the skeletal material is laid down during the bone formation and growth. Thompson (2003) explained that heat-induced fracture is caused by the difference of heat-induced expansion and shrinkage that result in tensile and compressive forces. When a bone is heated up, its dimension changes in an uneven fashion because heat is not evenly spread across to all part of the bone. As some areas of bone tissues may not expand or contract at the same rates as immediately adjacent areas, bone materials fail or fracture along the lines of greatest stress. This micro-variation leads to the formation of heat-induced fracture (Schmidt and Uhlig,

2012). Initially, heat-induced fractures propagated from pores in the bone surface, which are the weakest point, and then extend from pore to pore as burning continues (Thompson, 2003), resulting in smooth breaks that pass through the osteons and is similar to high-energy fracture (Herrmann and Bennett, 1999; Thompson, 2003). These lines of weakness are a direct consequence of the formation and growth of hard tissues. Longitudinal and straight transverse fractures originate from the external cortical surface where heat exposure is the longest and consequently reduce in width deeper into bone (Pope, 2007). The results show that it is not necessary to pass through the full thickness of the bone, but the heat-induced fractures in some control samples penetrated the entire cortical layer especially longitudinal fractures.

Fracture morphology and warping can be used for assessing some evidence concerning the condition of the individuals at the burning event. Traditionally, previous works (Gonçalves *et al.,* 2011) suggest that the condition of the individual before burning such as the presence of soft tissues has an impact on the nature of thermally induced fractures and warping. Thus the individual who is burned right after death should exhibit curved transverse fracture and bone warping, while burned dry bone should display very little variety of colour, shallow fracture, and little delamination and warping (Mayne Correira, 1997; Thompson, 2003; Gonçalves *et al.*, 2011). However, this study demonstrated that 30% of macerated ribs could develop warping and deeper cracks (i.e., those that puncture the medullary cavity). More recent research supports the findings in this study, as the collagen fibres within the bone structure play an important role instead of surrounding soft tissues (Spennemann and Colley, 1989; Whyte, 2001; Gonçalves *et al.*, 2011; Thompson, 2015). Alternatively, other causes may be due to the trapping air in the medullary cavity (Spennemann and Colley, 1989) and the contraction of the periosteum and collagen fibres (Thompson, 2005). Therefore, this study showed that thermally induced warping is not exclusively linked to the burning of bones with soft tissue coverage.

Similarly to heat-induced warping, the curved transverse fracture is related to collagen fibres and can be found in dry bones (Gonçalves *et al.,* 2011). Basically, the classic curved transverse fracture is the result of soft tissue and periosteum

shrinkage, pulling the brittle surface of burned bones (Schmidt and Symes, 2015). However, this study found the absence of curved transverse fracture after the burning of defleshed green bones. This type of heat-induced fracture usually occurs at the shaft of the femur, epiphyseal and metaphyseal area of the long bones. To date, there is no report of curved transverse fracture occurring on a rib. Further study of curved transverse fracture should be conducted, as Gonçalves *et al.* (2011) argued that its cause was uncertain and the clarification of the causes should be achieved.

In several instances, heat-related fractures were found to propagate along portions of deeper sharp-inflicted marks (i.e., chop marks that penetrate the medullary cavity), even though it does not appear that these sharp-inflicted traumas have an influence on the direction of fracture propagation during the cremation process (Herrmann and Bennett, 1999; de Gruchy and Rogers, 2002). However, this study showed that there was no significant difference in heat-induced fracture propagation between non-traumatic controlled samples and sharp-inflicted rib samples. Therefore, shallow cut marks that did not puncture the medullary cavity had no effect on heat-induced fracture propagations. These might be due to powerful traumatic lesion penetrating the medullary cavity such as hacking trauma can weaken the surrounding bone materials, and therefore these areas were more likely to fragment when burned (de Gruchy and Rogers, 2002; Kimmerle and Baraybar, 2008).

8.2.2 Heat-induced alterations of a cut mark

It is crucial to recognise the evidence of trauma on burned bone and attempt to identify the weapon used. Forensic casework and the previous study revealed that evidence of skeletal trauma can survive the burning process (Mayne Correira, 1997; Hermann and Bennett, 1999; Pope and Smith, 2004; Thompson 2004, 2005; Schmidt and Symes, 2015; Waltenberger and Schutkowski, 2017). However, thermal alterations can not only obscure morphological traits, but also influence measurements to such a degree that they are rendered useless. Burned bone materials lose water and organic components, which leads to bone shrinkage that affects metric traits and their diagnostic utility (Fairgrieve, 2008; Symes *et al.*, 2010). Furthermore, fragmentation and warping of the cortical bone may result in a

significant loss of evidence of a cut mark. The majority of sharp-inflicted trauma remains present, but careful analysis should be conducted on the burned bone surface morphology and the patterns of existing fractures (Herrmann and Bennett, 1999; de Gruchy and Rogers, 2002; Ubelaker, 2009; Kooi and Fairgrieve, 2013; Thompson, 2015; Macoveciuc *et al.,* 2017). Careful reconstruction following fragmentation can assist trauma analysis (Ubelaker, 2015).

All cut marks presented on the burned samples in this study were macroscopically visible, even when there was a degree of heat-induced fractures. All the cut marks were visually identifiable as uniform linear incisions on the bone surface. Correct identification and analysis of traumatic signs on skeletal remains are one of the pillars of forensic anthropology. Nevertheless, the cremation process can make trauma morphology distort significantly (Mayne Correira, 1997; Thompson, 2005; Ubelaker, 2009). Specific portions of the cut marks may alter due to the burning process. In fact, the statistical results could confirm how the burning process can alter the morphological and metric features of the injured site.

8.2.2.1 Kerf dimension

Bone tissue is subjected to intense water and organic material loss during heat exposure. These alterations can have profound effects on the size and shape of bone material, and even lesions as a result of disease and trauma (Thompson, 2005). Diagnostic tool marks on bone, such as those used for class characteristic identification of the inflicting tool can appear to be changeable from the burning process. These result in changes to the overall kerf mark morphology and all the metric parameters, and they also affect specific aspects of the analytical method and established standards based on normal bones, which has been previously explored by the literature (Mayne Correira, 1997; Hiller *et al.,* 2003; Thompson, 2004, 2005; Wheatley, 2008; Ubelaker, 2009; Collini *et al.,* 2015; Waltenberger and Schutkowski, 2017).

Burning also led to a statistically significant decrease of cut mark length and width. Significant differences between the cut mark dimensions prior to and after burning is explained as the consequence of the combination of collagen loss, bone moisture loss, and recrystallisation of the hydroxyapatite (Mayne Correira, 1997;

Fairgrieve, 2008), which resulted in the kerf wall being pulled together as shrinkage affected the bone. Bone shrinkage in a fire has been reported to affect all bone dimensions (Shipman *et al.*, 1984; Mayne Correira, 1990; Hiller *et al.*, 2003; Thompson, 2004, 2005; Ubelaker, 2009; Collini *et al.*, 2015). The results in this study were consistent with Vegh and Rando (2019), who found shrinkage of burned cut marks around high temperature at 1000°C. However, Waltenberger and Schutkowski (2017) and Symes *et al.* (2012) argued that cut marks on their rib samples remained stable after exposure to 500-700°C. All samples in this study were burned at 850°C. This temperature reaches inversion stage, resulting in recrystallization and an increase in crystal size, and therefore leading to more shrinkage (Mayne Correira 1990; Thompson, 2005). According to previous works (Reinhard and Fink, 1994; Thompson, 2005; Brouchoud, 2014), this phenomenon starts when the bone has been burned at 200°C, and temperature around 800°C (starting of fusion stage) is a critical temperature at which the degree of heat-induced shrinkage increases considerably. Indeed recrystallization process is the cause of much more shrinkage than the process of dehydration and organic degradation (McKinley, 2000; Thompson, 2005). In contrast, some samples displayed features of heat-induced expansion as mentioned in some literature (Thompson, 2004, 2005), although the results overall results showed a more substantial degree of heat-induced shrinkage.

In general, the metric traits of cut marks are useful in identifying the class characteristics of the inflicted weapon. Kerf mark width can be used to identify minimum blade width (Bartelink *et al.,* 2001; Symes *et al.,* 2010; Cerutti *et al.,* 2014; Norman *et al.,* 2018). During bone shrinkage, the dense bone on both sides of the kerf mark contract independently to pull the kerf edge and make the mark narrower. Uniform shrinkage of the burned bone may bring both edges of a kerf mark close to one another side. Depending upon how bone shrinkage affects its dimension, kerf mark width may lose all or some of its diagnostic value.

In this study the burning process resulted in a decrease in the kerf length of 10.79-17.6% and kerf width of 28.52-34.87% when compared with the original dimensions. Hence, the kerf dimension decreases are therefore more significant for certain dimensions, due to the alignment of the sharp-inflicted marks cutting through

a lengthwise direction the collagen fibres of samples that were along shaft of rib (Olszta *et al.*, 2007; White *et al.*, 2012). A function of bone is a factor regulating collagen orientation, and then becomes the main cause of different dimensional change in every bone. Therefore, degradation and shrinkage of collagen fibres from cremation process in this study does affect kerf width more than kerf length, and different parts of the burned bone respond differently to each other (Marciniak, 2009; Bailey *et al.*, 2011). Moreover, warping may affect the kerf dimensions by either pulling or pushing the kerf walls into other ones (Brouchoud, 2014).

If collagen components are indeed related to the dimensional changes of burned bone, age should also be a factor that affects this alteration as collagen fibres start to degrade during life (Rho *et al.,* 1998; Collins *et al.,* 2002). Using juvenile bone materials in this study has an effect on the cut mark dimension. Since juvenile bone cortex has higher organic and less mineralized compared to adult bones, there tends to be substantial decreases to the cut mark dimensions after the cremation process. The greater amount of dehydration and denatured collagen matrix by burning may play an important role in this finding. Therefore, the recovery and identification of cut marks on the burned juvenile remains may subsequently be negatively affected (Thompson, 2003; Kooi and Fairgrieve, 2013).

8.2.2.2 Kerf morphology

Generally, it is not possible to clearly distinguish between types of cut marks by considering only the metric assessments of the kerf dimensions (Tennick, 2012; Cerutti *et al.,* 2014; Norman *et al.,* 2018). Even though the measurements of the maximum widths of cut marks in this study could be used in this purpose, these values still overlap the partial range of measurements (Bartelink *et al.,* 2001; Cerutti *et al.,* 2014; Komo and Grassberger, 2018; Norman *et al.,* 2018). This suggested that the morphological characteristics of the cut marks need to be used in addition to the dimensional values to distinguish between the three types of cut marks.

A stereomicroscope was used for microscopic inspection. The results in the present study indicated that burned bones showed a degree of preservation of the cut mark characteristics, dependent on the type of knife used to inflict the cuts. Heat-induced fractures may traverse some cut marks, although there was no

evidence that these cut marks influenced the direction of fracture propagation during incineration. However, possible misdiagnosis might be encountered in terms of the biomechanical properties of the force, an angle of impact and characteristics of the inflicted weapon. A number of heat-induced morphological changes were statistically significant in this study. After the cremation process, the elliptical shape of cut marks inflicted by coarse-serrated and fine-serrated blades altered to become rectangular and irregular shapes, while the raised margins of marks inflicted by coarse-serrated blades changed to have smooth margins.

There was a great reduction in the selected kerf characteristics in the burned bone samples. A certain type of kerf shape such as the linear shape of the cut marks inflicted by a non-serrated knife blade was able to retain evidence for kerf shape analysis, whereas the elliptical shapes inflicted by coarse-serrated and fine-serrated knives were more prone to alterations due to burning. The rectangular and irregular shapes were significantly more pronounced and visible on the burned bones. The main idea to understand this phenomenon is based on understanding the basic nature of the cutting process. These are potentially due to greater mechanical trauma imparted by the coarse-serrated and fine-serrated knives on the surrounding bone tissue. As discussed in Chapter 5, the teeth of the serrated blades damage bone tissues using a cut and chatter mechanism, leading to areas with a fragile bone structure along the kerf margin. Therefore, these damaged and fragile structures were vulnerable to change during the burning process. Also, other fragile features, such as raised kerf margin and kerf striations, were exceptionally sensitive to the burning process and then could not be observed in many post-burned samples. Deformed, blackened and eroded kerf margins from the burning process were observed in the cut marks inflicted by the coarse-serrated blade knife. Nonetheless, the overall cut mark morphology remained identifiable.

Kerf striations were clearly visible using the stereomicroscopic examination (Figure 8.23). Even though some kerf striations damaged and disappeared, most of the kerf striations could be identified throughout the burning process. There was an enhancement of the visibility of post-burned kerf striations and these characteristics tend to be better expressed in kerf walls that have been heated. The prevalence of this characteristic was consistent with previous work (Marciniak, 2009; Brouchoud,

2014; Robbins *et al.,* 2015). The striations made by some instruments such as saws and knives were not entirely destroyed during the burning process, demonstrating that while fire can affect some traits generated through sharp weapons, it does not necessarily destroy them (Herrmann and Bennett, 1999; de Gruchy and Rogers, 2002; Fairgrieve, 2008; Marciniak, 2009; Robbins *et al.*, 2015). Burned cut marks still display clear and well-preserved morphology with some contaminants (ash and small combusted matter), V-shaped or U-shaped cross-section, as well as the presence of kerf wall striation.

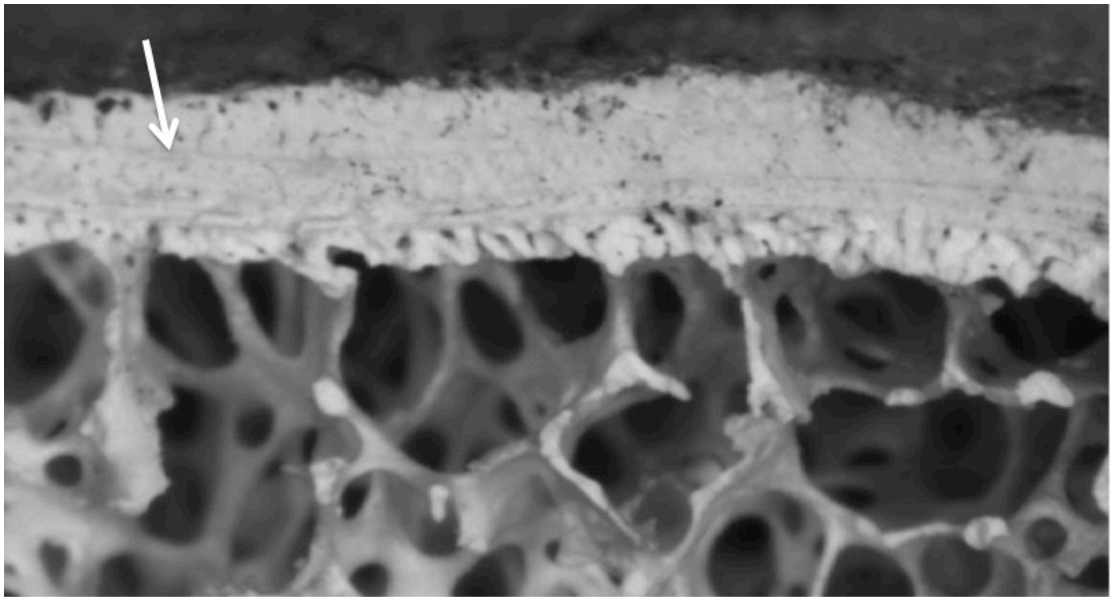

Figure 8.23: Microscopic examination of heat-exposure kerf wall of a cut mark; the white arrow indicates striation line

Distinguishing between bone damage from trauma infliction before heat exposure and that occurring as a result of burning is crucial to anthropological analysis. The differentiation between heat-induced fractures and cut marks was clearly distinguishable in this study. In general, the features of heat-induced fractures and traumatic fractures are the results of the type of loading stress and the nature of bone material involved (Herrmann and Bennett, 1999; Pope and Smith, 2004; Fairgrieve, 2008; Schmidt and Symes, 2015; Thompson *et al.*, 2017). Because of the different physical properties of fresh and burned bone, a heat-induced fracture produced in a brittle material should be different from traumatic fracture produced in a ductile material. Herrmann and Bennett (1999) concluded that

the mechanism of heat-induced fracture is similar to those resulting from high-energy stress such as ballistic injury because burned bone does not have energy-absorbing characteristics of normal bone.

Regardless of classic ballistic trauma, sharp force injury in bone is the easiest pattern to recognise during burned bone analysis (Herrmann and Bennett, 1999; Macoveciuc *et al.*, 2017; Waltenberger and Schutkowski, 2017). Macroscopically, all sharp force traumas were recognisable and identifiable after a heat exposure, and they are clearly distinguishable from heat-induced fracture. Cut marks exhibited linear and narrow lesions with smooth or light raising edges, whereas macroscopic features of heat-induced fractures usually show unpredictable alignment with sharp and well-defined margins. Erosions of the margins of traumatic fracture by the burning process were observed in this study (Figure 8.23), whereas heat-induced fractures had a very smooth and clean surface under microscopic examination (Figure 8.24).

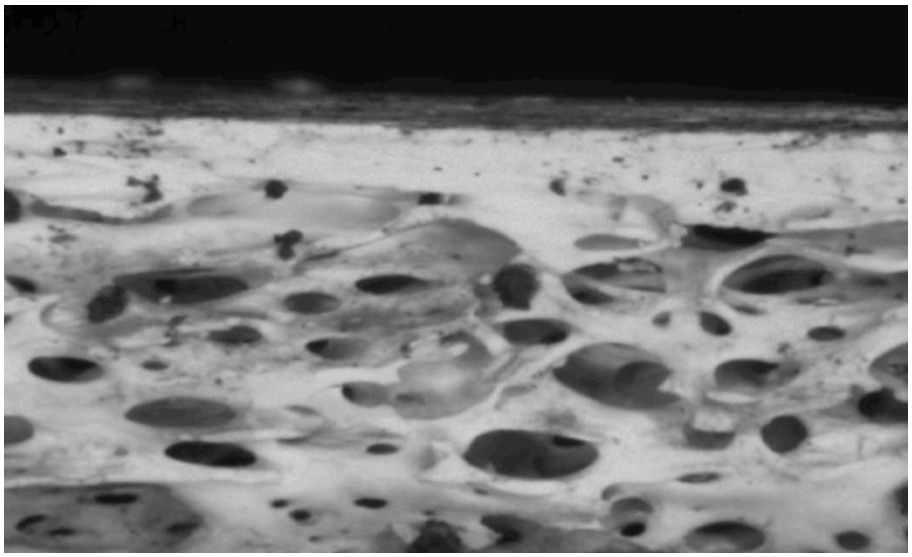

Figure 8.24: Microscopic surface examination of heat-induced fracture

These smooth features were derived from fast-propagating cracks of bone tissues undergoing substantial changes in moisture and organic contents. However, these criteria for distinguishing heat-induced fractures from traumatic fractures may not be as clear as the above situation indicates. Heat-induced fractures may develop as a slow propagation from a rapid expansion of medullary fluids while the bone is still intact. Pope and Smith (2004) advised using a microscopic examination

of fracture margin analysis to provide scientific evidence to discriminate heat-induced fractures from traumatic fractures. The reconstruction and macroscopic assessment of suspected fracture should be firstly conducted, Then selected fracture surfaces should be selected for additional examination by microscopic and SEM methods (Herrmann and Bennett, 1999; Pope and Smith, 2004).

8.2.3 Burned bones and their cut marks after environmental exposure

Examining burned bone is very complex and highly influential, with many variables having substantial impacts on how the bone responds to the depositional environment. Burning process can destruct remains and results in the reduction of the dead body to ashes with fire. Burned remains can also be subjected to size reductions and fragmentation by intentional cultures, natural processes, and recovery investigation (McKinley, 1993; Schmidt and Symes, 2015). Further, bone can be dispersed and modified by the influence of the depositional environment. The retention of diagnostic clues about the taphonomic effects on the cut marks is dependent on a suite of complex variables, such as a type of depositional environment, weather conditions, the duration of exposure, and micro-environmental conditions (Pankowská *et al.*, 2017; Fernández-Jalvo *et al.*, 2018). Knowledge about how weather conditions and the micro-environment affect burned bone and their traumatic lesions is an important aspect for scene recovery and trauma analysis (Fairgrieve, 2008; Waterhouse, 2013c). This study thusly focused on potential variability of sharp-inflicted lesions because of the decay effect of burned bones over time.

After surface environmental exposure, most of the cut marks on burned bone remained identifiable (Figure 8.9). This study found that the same amount of decline in morphologically identifiable bone occurred in both the spring and summer samples, since cut marks were present in 90% and 66% of the two-week and four-week surface-exposure samples, respectively. These were the result of similar weather conditions in both seasons, with low precipitation levels and wind speeds. However, the autumn and winter samples appeared to be significantly damaged after surface exposure to the outdoor environment. The winter samples showed more damaging cut marks in the first two weeks, with only 60% surviving, compared with 67% of the autumn samples. These findings might be due to freezing

temperature during the winter period. Freezing water within pore spaces has a potential to contribute to cause cracking and fragmentation. Waterhouse (2013c) explained that freezing temperature can accelerate burned bone fragmentation at 56 and 168 hours-exposure. Tersigni (2007) tested frozen human bones at 0°C for 21 days with SEM analysis and found that cracking originated from the Haversian systems, presumably he result of liquid expansion. Although burned bones in this study were dehydrated from burning process, they could uptake moisture with their porous and fracture surface (Pokines *et al.*, 2018). The formation of ice crystals within bone can cause fracturing and fragmentation from crystal expansion within an existing bone structure (Trueman *et al.,* 2004; Pokines *et al.*, 2016). During the freezing period, any moisture in and around the burned bone materials would have frozen and left micro-structural damage (Trueman *et al.,* 2004; Perkins, 2012). Microscopic damage can potentially progress to macroscopic damage if there is prolonged exposure.

When the autumn bones were recovered after the four-week surface exposure, 73% of the cut marks were unrecognisable (Figure 8.9). Higher rates of rainfall were observed during the period, which may have affected the burned bone structure. The moisture may have led to increased fragmentation as moisture accessed micro-fissures via the porous surface, resulting in cracking and weakening of the burned bone structure (Waterhouse, 2013c). Other factors in bone weathering such as the dissolution of some soluble minerals might also weaken the overall bone structure (White and Hannus, 1983; Pokines *et al.,* 2018). The traumatic effect of raindrop impact might be another factor, which could damage cut marks on fragile burned bones.

A consistent pattern of cut mark damage for every season was observed in the buried burned bone samples. In fact, the buried burned bones are protected from physical damage and environmental conditions fluctuations, including freeze-thaw cycle and wet-dry cycle (Rodriguez, 1997; Pokines *et al.*, 2018). Burned bones treated in the range of 400-1000°C and exposed to all pH levels is more susceptible to mechanical degradation than normal bone. In addition, acidic soil has an effect on unburned and burned bone degradation (Kalsbeek and Richter, 2006). Mild acidic

soil in this study might help the burned bones to have a higher potential for preservation than surface-exposure burned bones (Gilchrist and Mytum, 1986).

In general, various taphonomic variables have an influence on the level of burned bone preservation, and that the fate of a burned bone sample is site-dependent (Madgwick and Mulville, 2012). After the burning process, burned bones are more fragile than unburned bones, and therefore more susceptible to a change from diagenetic process. A gradual decrease in maximum length and width of most of the cut marks on the surface and buried burned bones was observed in this study. Therefore, the diagnostic metric features remain stable and resistant to the one-month environmental condition. Nevertheless, extreme caution should be used with kerf dimensional analysis because of heat-induced shrinkage.

Different patterns of dimensional change were present in the autumn and winter surface-exposure group, which showed an increase in kerf width (Figure 8.14). This characteristic was found with different slope of increase for slight slope for non-serrated blade, and steeper slope for coarse-serrated and fine-serrated blade knife. Therefore, dimensional changes of the cut mark inflicted by coarse-serrated and fine-serrated blade knife were more significant than the cut marks inflicted by the non-serrated blade. These changes were possibly explained by morphological erosion of the kerf margin. The morphological data of the kerf margins inflicted by coarse-serrated blades showed that 85.7% of the surface autumn group and 71.4% of the surface winter group had significant deteriorations after four weeks of exposure (Figure 8.25). Although some raised features of the kerf margin survived the burning process, their structures were weakened by heat exposure. These extremely fragile structures were then particularly sensitive to taphonomic factors and were unable to withstand the effects of environmental factors. After the four-week surface exposure, the cut marks carried out by coarse-serrated blades lost their kerf margin regularity, with an important loss of information on the used tool. Burial samples; by the way, showed less damage comparing with surface-deposited samples, with kerf margin showing less damage of four-week exposure in autumn and winter groups.

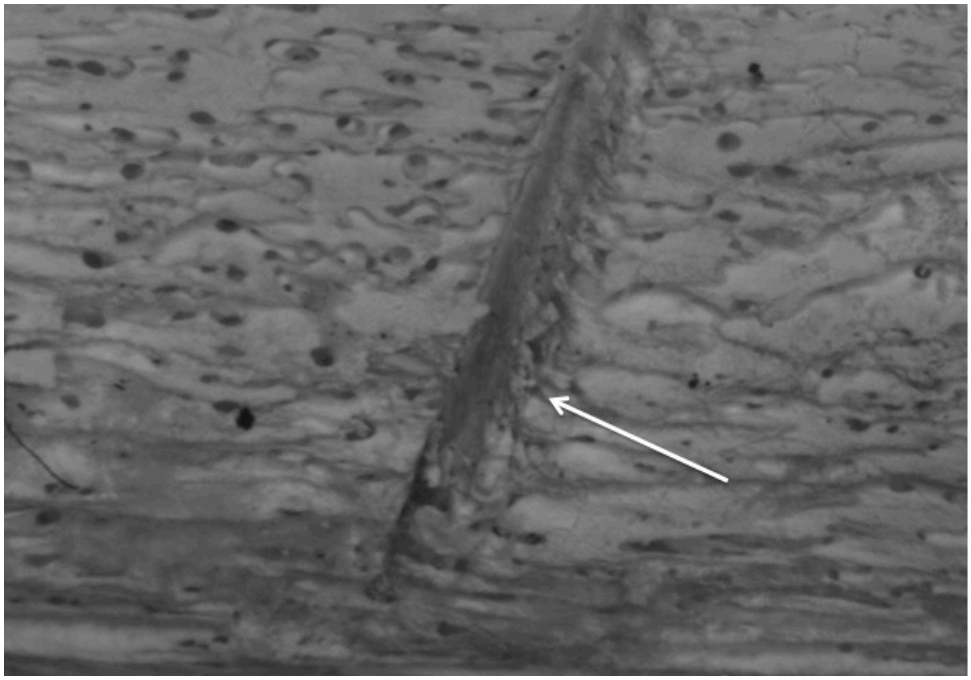

Figure 8.25: Kerf marginal erosion (the white arrow) of the cut mark inflicted by coarse-serrated blade knife after one-month environmental exposure

If the burned bones were exposed in the surface environment for a longer duration and if the rainfall was the same level as that in the autumn of this study, the finding of this study would be different. The ability to identify diagnostic characteristics of cut marks is increasingly difficult since exposure to the surface environment has the potential to destroy kerf shape and margin or make them less identifiable. These damages will affect a forensic anthropologist's ability to deduce cut mark morphology produced by a particular knife. However, the cut marks inflicted by non-serrated knife blade in this study could be identified as a few characteristics change after environmental exposure. It is expected that despite prolonged surface exposure, these cut marks exhibit a degree of preservation and their individual classification is identifiable.

In sum, there was a high degree of morphological complexity of the burned bones and their cut marks after environmental exposure. In particular, the survivability of the burned bones was dependent on weather conditions and the depositional environment. Greater damage of cut mark and fragmentation were observed in the autumn and winter group, while the buried groups had better survival than the surface-exposure groups. Some features that were observed

during the pre-exposure examination and described in detail in the report were no longer identifiable during the forensic analysis due to taphonomic factors.

8.2.4 Burned bone fragmentation

Heat exposure complicates trauma interpretation by the formation of fragmentation and fracturing. Burned bones usually display different degrees of fragmented forms, which is particularly problematic since it complicates trauma analysis and makes the trauma evidence harder to identify (Mayne Correira, 1997; de Gruchy and Rogers, 2002; Fairgrieve, 2008; Thompson, 2015). Reconstruction is the most suitable technique for analysis trauma evidence in post-burning fragmentation, as a correct and complete recovery and reconstruction of bone fragments becomes essential and necessary in a forensic setting (Grevin *et al.*, 1998; Ubelaker, 2009; Imaizumi, 2015). Analysis of perimortem trauma is able to recognise and identify fragmentary skeletal remains, and hence permit to re-associate and reconstruct of skeletal elements (Buikstra and Ubelaker, 1994). It has been demonstrated in this study that levels of fragmentation varies greatly for burned porcine bones exposed to different duration of exposure, different depositional environment, and different weather conditions. A careful interpretation of these findings can provide useful information relating to how some environmental factors have an effect on the fragmentation of burned bones.

The juvenile bones used in this study had an effect on the identified burned bone fragmentation. As discussed earlier, juvenile bones have a higher proportion of organic components and are less mineralised than adult bones. Therefore, burned juvenile bones undergo more heat-induced fractures due to greater organic content loss (Waterhouse, 2013b; Robbins *et al.,* 2015). In addition, samples with soft tissues clearly show a higher degree of fragile and fragmented bones. This phenomenon is possibly due to the shrinkage and traction of remaining soft tissues on the underlying bone (Grevin *et al.*, 1998; Ubelaker, 2009). However, samples used in this study were macerated to keep the least remaining soft tissues, therefore post-burning fragmentation in this study should not mainly happen from this effect.

8.2.4.1 Surface-deposited burned sample

The overall increase in burned bone fragmentation is expected when it is exposed to an outdoor environment (Fairgrieve, 2008; Waterhouse, 2013a). Some weather conditions, such as freezing or fluctuating temperatures, and wet conditions increase the degree of fragmentation (Waterhouse, 2013c). Burned bone fragmentation recovered after four-week surface-exposure in this study showed higher levels for the small category than the burned samples recovered after two-week surface-exposure. When surface-deposited burned samples recovery was delayed by one week, a gradual decrease in the proportional mass of large size category could be observed.

Reasonably, there is a clear trend of a continuous increase in the level of fragmentation over time, and this trend is expected to continue when burned bones are exposed to a variable environment, with differences in temperature, precipitation, and other environmental factors (Stiner *et al.,* 1995; Waterhouse, 2013a, 2013c). The brittle burned bones were unable to withstand these disturbing factors and started to progress toward fragmentation, either to flake off of a number of pieces or to fracture into smaller pieces. The highest level of fragmentation for the large category was observed in the autumn samples, with an elimination of most of the large category and high proportional masses of small and medium categories at the end of fourth week. The most noticeable weather condition in this season is heavy rainfall, which can increase levels of fragmentation (Waterhouse, 2013c). Apparently, large fragments (largest dimension more than 5 mm) were unable to withstand the effects of prolonged exposure to rainfall. This finding can also be observed during heavy rainfall of the first week of spring samples and the fourth week of spring and winter samples, leading to the widespread fragmentation of the large category during these periods. However, it is unclear how increased exposure to rainfall and moisture can increase the amount of fragmentation (Waterhouse, 2013c). Perhaps the mechanism behind this may relate to water penetrating micro-fissures and cracks in the burned bone, thereby weakening its structure. In addition, heavy raindrop can directly impact on fragile calcined bone and cause an increase in fragmentation. When wet burned bones start to dry, the loss of moisture leads to

alterations in the pressures and strains of the bone structure, leading to further fracture and fragmentation (Waterhouse, 2013c; Pokines *et al.,* 2018).

Low temperature in the winter affects fragmentation when the daily temperatures fluctuate above and below the freezing point of water. Waterhouse (2013b) and Pokines *et al.* (2016) suggested that freeze and thaw of water molecules within bone materials can contribute to fragmentation. Repeated cycles begin when water penetrates existing cracks and pores, and then absorbed when the water freezes. Freezing water within pore spaces and cracks will expand and introduce new tensile forces onto brittle burned bone material. Subsequent thaw allows for deeper penetration of water into the expandable crack before it re-freezes again and more expansion (Junod and Pokines, 2014; Pokines *et al.*, 2016). Therefore, the winter samples experienced greater dynamic temperature than the more static temperatures seen in the other seasons. The freeze-thaw cycle had a devastating effect on large and small categories, but not the medium category that was usually high level in the winter samples. A possible reason might be due to more complete structure of fragmented bones in this category. As was observed in the winter samples, the medium series was more significantly complete fragment bone than small and large series and its structure could resist the fragmenting effects of the freeze-thaw cycle. Large fragments usually had several heat-induced fractures and cracks, with these structural defects potentially being less able to withstand the effects of exposure to various environmental factors, resulting in more fragmentation.

High wind speed was noted during the autumn and winter season. However, its effect on fragmentation is not dominant as other environmental factors such as temperature and rainfall. It is possible to explain the low level of the small category in the winter sample. The lowest level of the small category in this group might be due to the blowing of the wind to the burned samples deposited in the grassland with dry short vegetation in the winter, whereas high vegetation growth was observed in the other seasons. The coverage by surface vegetation might affect the survivability of small burned bone category.

The trend of stability of summer samples compared with other seasonal samples was observed. The large category was able to withstand environmental

factors and remain relatively stable. A drop in a proportional mass of the medium and small categories also revealed a reduction in fragmentation of the large category. Concisely, hours of sunshine presented its highest level during summer. The indirect implication was that it is suitable for vegetation to grow and cover burned samples. These protective circumstances can prevent burned samples from physical damage such as rainfall impact and wind blowing, resulting in less fragmentation. Therefore, it is clear that non-fluctuated warm temperature and strong sunlight have a beneficial effect on burned bone preservation as a whole.

In sum, the level of fragmentation of burned bones is very complex and is dependent on many factors of depositional macro-habitat and microenvironment. This experimental data show that fragmentation is time specific and is powerfully influenced by specific environmental factors such as freeze-thaw cycles and rainfall. Burned bone fragments are more likely to disperse far beyond the main bone accumulation. Hence, Pankowská *et al.* (2017) advised exploring the area farther beyond recovery area.

8.2.4.2 Buried burned sample

The current study attempted to establish the relationship between buried environment and fragmentation rate and pattern. Typically, when burned bones recovery is delayed, there is a clear trend of increasing fragmentation and pattern alterations over time (Waterhouse, 2013a). After a delay of two weeks, proportional mass data showed a marked increase in fragmentation of the large category in spring and autumn comparing with the summer and winter group, which had a higher level of the large category and lower level of the small category. These patterns were also observed until the end of four weeks, with the higher level of fragmentation in the spring and autumn.

An increase in burned bone fragmentation was associated with high soil moisture content in the spring (24.9-25.1%) and autumn (24.9-25.2%), while the lowest fragmentation was seen in a low level of soil moisture content in the summer (21.4-21.7%). As discussed earlier, the dampening condition increase fragmentation as soil water content might penetrate into micro-fissures and micro-cracks in burned bone matrix, weakening its structure (Waterhouse, 2013c). Therefore, the brittle and

fragile burned bones are unable to withstand and progressively fragments by fracturing or flaking into small pieces. These findings lead to conclude that soil moisture content can be one of the major environmental factors governing burned bone fragmentation in the soil. Soil pH had no effect on buried burned bone fragmentation because the relationship between soil pH and fragmentation rate was not observed. While both acidic soil (pH 5.9) in autumn and more alkali soil (pH 6.45) in spring increase fragmentation rate, the summer samples in mildly acidic soil (pH 6.1); nevertheless, showed the lowest degree of fragmentation.

The fragmentation patterns suggest that the large category is breaking down in a similar manner to a smaller category. Considering the potential effect of burial contexts on burned bone fragmentation, it is noticeable that the high level of the medium category was observed in every seasonal group. As described in surface group discussion, medium-sized bone structure is more complete and can resist to surrounding taphonomic factors. Straightforwardly, buried burned samples were protected or at least buffered from direct effects of the environmental condition. It is clear that surface-exposure burned samples underwent more fragmentation when compared with buried burned group. And therefore by four weeks delay the larger bone category began to break and any delay in recovery process might result in significant further losses.

8.2.5 Changes in burned bone mass

After burning process, a reduction of bone weight is expected because of dehydration and decomposition stages of heat-induced transformation process (Mayne Correira, 1997; Hiller *et al.,* 2003; Thompson, 2003; Fairgrieve, 2008; Gonçalves *et al.,* 2013; Thompson *et al.,* 2017). Traditionally, an obvious advantage of measurement of bone mass loss is that it is not significantly affected by other heat-induced change such as shrinkage and fragmentation. Thus it can be used as an alternative method to analyse the completeness of burned bones from archaeological or forensic contexts (Goncalves *et al.*, 2013; Thompson *et al.*, 2017). In case the identification of burned bone materials are uncertain, bone mass may help to confirm that the remains are indeed burned (Thompson *et al.*, 2017).

According to previous literature, this weight loss can reach between 30-60% of its original weight depending upon factors associated with cremation such as temperature of combustion and pre-burned conditions of the bone material (Thompson, 2004; Gonçalves *et al.,* 2011; Gonçalves *et al.,* 2013; Hiller *et al.,* 2013; Thompson *et al.*, 2017). However, the effect of the burning process in this study on a sample of unburned bones presented higher than average reference values, with 71.1-77.7% of their original weight losing during the burning process. Limitations of skeletal weight analysis have been explored in this study. Reference samples were limited to whole body cremation of modern adult individuals (often quite old age) in a gas-fuelled furnace (McKinley, 1994; Goncalves *et al.*, 2013), so a comparison with other characteristics of samples such as non-human or juvenile remains may be problematic. Furthermore, differences in skeletal mass of separated pieces of bone have been reported. In conclusion, the selection of references is not straightforward and there is still no standard reference at this moment (Thompson *et al.*, 2017).

Outdoor environments have an effect on exposed burned bones weight and fragmentation. The total bone mass reduction may result from loss of too small bone fragments to be recovered or removal of bone pieces by physical disturbance such as blowing away by the strong wind (Fairgrieve, 2008; Waterhouse, 2013a, 2013c). In addition, this study found a clear and direct association between weather conditions of different seasons and burned bone mass. The results demonstrated that the autumn and winter samples were significantly lighter when compared with the spring and summer samples at both two and four weeks surface-exposure. A similar directional effect was found in accordance with fragmentation rate discussed in the last section, thus demonstrating that a decrease in burned bone mass was due to burned bone fragmentation. Moreover, it has been shown that loss of bone mass in the winter group was significantly observed at four-week surface exposure. This finding was corresponding with the lowest level of the small category of fragmentation and would be due to strong wind occurring at the third week of surface-exposure.

This study also found the relationship between bone mass change and fragmentation rate in the burial group. Further investigation demonstrated that the mean weight of the spring and autumn groups were significantly low at two-weeks

and four-weeks buried exposure. The loss of burned bone weight in burial condition would be due to recovery problem of very small fragments, as reflected the more fragments of bone associated with soil moisture content.

8.2.6 Summary

After the burning process, cut marks on ribs remained surprisingly identifiable and did not change significantly. A degree of preservation was dependent on the cutting property and the variable characteristics of knife blade itself, such as serration blade pattern and adjacent bone tissue injury. There were certain knife blade patterns that produced cut marks, which remained recognisable and identifiable in spite of the heat and environmental exposure. For instance, the cut marks of non-serrated blade knife were preserved after the burning process and four-week environmental exposure, while the cut marks inflicted by coarse-serrated blade knife changed significantly after the burning process and environmental exposure. Apparently, different bone structural changes occurring during the trauma event did have an effect on the survivability of the cut mark characteristics.

As the burning process can render bone tissues more susceptible to fracture and fragmentation, many fragile portions of the traumatic lesions of burned bone tend to be lost soon after environmental deposition. Trauma analysis is complicated by heat-induced fracture and fragmentation due to heat exposure and later environmental exposure, leading to the absence or misidentification of the diagnostic characteristics of trauma interpretation. Surface environmental exposure is capable of greatly reducing specific portions of cut mark to unrecognisable remnants and subsequently reduces the ability to recognise the cut marks themselves. Freezing in winter and heavy rainfall in autumn could accelerate the loss of burned bone fragments especially more vulnerable areas (Waterhouse, 2013c). Suspected features should be carefully examined and visually compared with the known postmortem damage and skeletal trauma surrounding the area of interest and overall bone surface (Pope and Smith, 2004; Schmidt and Symes, 2015).

The main cause of cut mark loss during environmental deposition may be due to fragmentation. The forensic investigator should be aware to recognise the

multiple features of perimortem injury and taphonomic modifications as supportive evidence during skeletal trauma analysis. Therefore, it is highly recommended to collect all bone fragments in such cases (Herrmann and Bennett, 1999; Fairgrieve, 2008; Robbins *et al.,* 2015). Careful recovery and reconstruction techniques of burned bone are essential to bring the diagnostic areas of cut marks into evidence (Schmidt and Symes, 2015). This study created a situation where some of the factors involved in criminal activity were known. The temperature to cremate bone materials, the presence of cut marks and heat-induced fractures, and the conditions of the outdoor environment were observed and documented. If a similar forensic case was found, the results of this study would be used as a standard to compare postmortem finding of bone materials and their trauma. Further study should focus on different weather and microenvironment with different weapon class or subclass on burned bone. The further assessment can also demonstrate the applicability of identifying the characteristics of skeletal trauma and enable its use in courtroom testimony by an expert witness.

Chapter 9: Conclusions

9.1 Skeletal trauma and taphonomic modifications

Skeletal trauma analysis is an important issue in forensic anthropology, both for what concerns the considerable importance of the identification of the inflicted weapon and for the difficulty of assessing factors involving in traumatic lesions. The main purpose of this study is to discern taphonomic alterations of skeletal traumatic evidence after exposure to an outdoor environment and cremation, and to apprehend if there is a statistical significance of morphological and dimensional evidence between pre-exposure and post-exposure samples.

In this study, perimortem blunt and sharp force traumatic lesions on ribs and femurs could be clearly identifiable even after 18 months of environmental exposure and most of their morphology did not seem to change significantly regardless of taphonomy. In contrast, this finding could not be said for sharp force trauma inflicted on burned bones, which appeared to be more modified by time and environmental variables, making it more difficult to identify accurately. The comparison between pre- and post-environmental exposure data conducted in this burning study emphasizes the difficulties in forensic anthropological works. In fact, taphonomic factors could not only modify perimortem fractures by the removal of important perimortem parameters, but also add new postmortem features such as warping, rounding and discolouration. Understanding the taphonomic factors and postmortem environment of each setting could assist in differentiating between environmental and criminal activity to human skeletal remains so that forensic anthropologists would make an accurate legal assessment.

The physical conditions of bone samples were also imperative. Some crucial information arose from this study. Pre-exposure conditions of the bone structure had a great influence on the rate and pattern of taphonomic modifications on skeletal traumatic lesions. Dynamic changes of perimortem traumatic lesions were observed especially in the fragile or more damaged areas of bone materials. With the erosion and environmental modifications, risky areas might undergo taphonomic change (Calce and Rogers, 2007). Extrinsic factors namely types of weapon used

in the trauma event influenced traumatic morphology and its taphonomic modifications. For example, the chop mark derived from a machete is not quite clear and survives well after environmental exposure when compares with those from a cleaver. Indeed, both implements have sharp and blunt mechanical properties, yet blunt characteristics of the machete weaken bone involved more significantly (Humphrey and Hutchinson, 2001; Capuani *et al.,* 2014). As the same reason, the cut marks made by different types of knife blade demonstrated dissimilar characteristics when they exposed to environmental factors. The blunt mechanism of the machete and the serrated blade knife is more destructive in rib and femoral marks.

This study demonstrated that taphonomic modifications of cut marks, chop marks and blunt injuries are dynamic and depend on types of depositional environment and exposure time. Long postmortem interval and depositional environment are also the important factors that provide taphonomic changes to a fragile area of skeletal remains. Fresh skeletal tissue is able to tolerate environmental stresses due to its high moisture content and organic components, leading to high elasticity and plasticity. This is the basic property of perimortem skeletal tissue unless some taphonomic variables are severely involved (Ubelaker and Adams, 1995; Ubelaker, 1997; Calce and Rogers, 2007; Wheatley, 2008; Wieberg and Wescott, 2008; Symes *et al.*, 2014; Zephro and Galloway, 2014). As the loss of organic matters and moisture, the bone elasticity decreases progressively. This “dry” bone; however, is characterised by little moisture content and organic matter with the more rigid and brittle property as well as the loss of elasticity (Moraitis *et al.*, 2008; Symes *et al.*, 2014). Therefore, this degraded bone can easily develop a fracture as well as other surface modifications as a result of fewer amounts of force or environmental stress. Furthermore, different taphonomic modifications of cut and chop marks in this study indicates the likely effect of factors other than time, such as temperature, soil chemistry, and climatic factors will have a great impact on the rate and pattern of taphonomic modification in a bone. These factors have been independently assessed and proven to have a substantial influence on the bone diagenetic process as well (Bell *et al.*, 1996; Nielsen-Marsh and Hedges, 2000; Nielsen-Marsh *et al.,* 2007).

The finding in this study further assisted in the clarification of alterations of blunt and sharp force lesions and provided an idea to standardise a method to refine a variety of weapon type. In addition, these dimensional and morphological studies had the potential to add such detailed information of scientific inquiry when presenting evidence in a court. To establish and predict the additional taphonomic damage to traumatic lesions is essential in forensic contexts. By and large, the current study discovered it is possible to use macroscopic, stereo-microscopic, and radiological examinations for making a reasonable comment for taphonomic perspectives of skeletal traumatic lesions. In general, the macroscopic examination can be mainly used to distinguish a perimortem fracture from postmortem damage (Schotsmans *et al.*, 2017). However, macroscopic characteristics of individual traumatic lesions alone provide insufficient evidence of weapon used in this study. Using a methodology that combines the macroscopic and microscopic examination of traumatic lesions with taphonomic reconstruction is more appropriate. Therefore, it is possible to identify the weapon used at the least of the common class characteristics. In addition, thanks to micro-CT imaging, the researcher could identify for the first time various chop mark modelling different from one hacking weapon to another as well as taphonomic modifications observed after the outdoor environment. These findings could also help forensic anthropologists link a chop mark to the specific weapon and environment. In addition, the researcher displayed some idea of biomechanical variability, particularly how the blade was applied and providing detailed information about the blow.

Heat-induced transformations in bone structure, colour, strength, dimension and morphology have been commonly regarded as the result of the loss of organic matters and recrystallization of the bone. All post-burned cut marks were identifiable, and they can be clearly differentiated from heat-induced fractures. Instead of no soft tissue coverage on any of the bones, heat-induced warping can be observed in 30% of burned samples. Dimensional changes were significantly observed in post-burned cut marks made from all types of the knife blade, but a small decrease was observed after one-month environmental exposure. Morphological changes were substantially noticed in cut marks made by coarse-serrated blade, especially fragile raised kerf margin. Autumn and winter season affected traumatic lesion with fluctuated temperature and rainfall, resulting in a

higher morphological change and fragmentation. Therefore, these can imply that there is a probability of a forensic anthropologist to encounter burned remains that have some significant heat-induced alterations on their traumatic lesions.

After the refinement of the current study, it is interesting to see how traumatic lesions change in an outdoor environment. This study demonstrated that the surface environment altered pre-existing traumatic lesions more rapidly and completely than buried environment so far. There are some contextual criteria used to argue against environmental factors as the main cause of alterations of traumatic lesions on bones. The inconsistent changes of lesions in each bone exposed to the same environment were observed, even though they exposed to the same macroenvironment. Microenvironment and intrinsic factors such as bone structural composition have an influence on the taphonomic rate of traumatic lesions. The current study has also emphasised the necessity of a multidisciplinary approach when analysing taphonomic phenomena. A careful consideration of biotaphonomic and geotaphonomic characteristics is recommended because depositional environment have an influence on the progression of taphonomic modification (Nawrocki, 1996).

This study communicates an idea of forensic anthropology and archaeology application in general. The most significant is that a perimortem traumatic lesion by blunt and sharp instruments is possible to modify after environmental exposure. In fact, it is considerably difficult to clarify if any taphonomic feature appears solely in a traumatic lesion. Therefore, it is advisable for forensic anthropologists and bio-archaeologists to make a statement regarding prolong-exposure blunt- or sharp-inflicted skeletal trauma with caution. Also, investigations into skeletal trauma are applicable to archaeological and bio-archaeological studies (Bromage and Boyde, 1984; Bello and Soligo, 2008; Boschin and Crezzini, 2012), which may be relevant to the examination of a traumatic injury made from metal instruments and edged stone weapons. The current study may help archaeologists to aware and reconstruct violent evidence if found on human bones as well as butchering practices on animal bones.

In sum, this PhD project has highlighted the importance of the higher complexity in the blunt and sharp force trauma analysis. This thesis also provided a

wealth of data relating to the interaction between bone materials and the surrounding environment. Particularly the current study drew careful attention to the chance that an original traumatic bone lesion can be modified by time and environmental variables, hence becoming perhaps recognisable but no longer identified as perimortem trauma. Results obtained in fact stressed the need to adopt great care with effects of environmental on skeletal trauma. Though simplistic, this type of study had never been performed previously. Therefore, taphonomy seems to be the main protagonist of many of the problems in skeletal trauma analysis.

9.2 Surface modification of skeletal tissues in South East England

There are very few techniques to determine post-mortem interval when all soft tissues have decomposed. Bone weathering patterns can be a valuable method in order to reconstruct the depositional environment and post-mortem events in forensic situations. The results of initial rates of bone weathering are comparable to other temperate climate taphonomic studies (Andrews and Cook, 1985; Andrews, 1995; Junod, 2013). All samples were categorised into stage 0 on the Behrensmeyer (1978) staging of weathering after 18 months of environmental exposure. On the contrary, significant differences are noticed when compared to tropical and savannah climate (Tappen, 1994; Ross and Cunningham, 2011). Type and shape of the affected bone are important for cortical bone erosion, as thick compact bones can resist environmental stresses better than thinner cortical bones, and different bone materials from the same bones or different areas of the same can present diverse taphonomic modifications. However, a longer experimental duration is required in order to glean more meaningful data into the advanced stages of bone weathering.

Different bone staining colours and patterns were observed depending on the depositional environment and seasonal period. These findings are valuable for a forensic investigation to reconstruct the original crime scene in which skeletal remains have been deposited and may link the bone to a certain circumstance surrounding the death of an individual (Ubelaker, 1997; Pollock *et al.,* 2018). Other taphonomic variables that were commonly observed in this study included soil and algae staining, sun bleaching, rodent gnawing and plant root etching. Plant and

vegetation have an important role in grassland microenvironment in this study. Sunlight shading over a bone from plant cover is expected during the spring and summer period, leading to slower bone surface modification (Behrensmeyer, 1978; Lyman and Fox, 1997). Understanding taphonomic modifications of skeletal materials can assist a forensic anthropologist and forensic pathologist to assess a more accurate postmortem interval and damage to resolve forensic investigations (Calce and Rogers, 2007; Symes *et al.,* 2012; Junod, 2013).

9.3 Limitations and implications for further research

This PhD project has provided several stepping-stones for future study in skeletal trauma analysis. Investigations in the current study have yet to determine fracture characteristics specific to perimortem trauma. In fact, it is extremely difficult to identify if any fracture characteristics appear solely in bone broken during the time of death due to taphonomic factors. However, limitations are found and further study is needed to allow a more reliable method to assess a forensic case, which usually involves in a serious legal consequence.

There are however limitations imposed by the design of this study. The first limitation includes the several factors influencing fracture dynamics. The researcher tried to include all types of traumatic infliction in this study. A variety of traumatisation event included manual cutting by knife, bending long bones, and mechanical chop mark by the drop-tower. However, none was the best method for trauma experiment. As the amount of force in the cut mark experiment was not standardised due to the limitation of instrument application, slight variation in force may lead to different resultant morphology. Another variation of angle of impact may not have a significant effect on the overall results, but it may affect certain observations such as an increase in the raised edge and chattering of a chop mark. Indeed, variations of force and angle of impact are parts of the actual forensic setting, demonstrating that any results regarding sharp force trauma may be independent of force and angle of impact. The relationship between taphonomic modifications of the traumatic lesion and the extrinsic factors involving in its origin such as the force and angle of the blow is still complex and unclear. Therefore, it is essential to investigate different factors such as force and direction, as well as try

an experiment in a differently controlled environment to compare between selected parameters. This would allow the standard formulas with sufficient reliability for application to forensic cases. Therefore, it appears evident the need to develop new models in the future study.

A second limitation of this study is the choice of weapon and specimen. It is imperative to memorize that these traumatic characteristics are tested with particular types of weapon. In order to guarantee that these characteristics are able to apply to all types of hacking weapon (such as hatchet, axe, katana, broadsword) and knife (carving knife, chef's knife, utility knife), this study should be repeated using different weapon class and subclass. It is also useful to investigate traumatic lesions left behind by other types of weapon (i.e. saw) or different mechanisms (i.e. crushing injury, gunshot injury). Moreover, trauma infliction event should be taken into consideration. The skeletal injuries in this study were made directly to bone materials without the coverage of soft tissue and periosteum as a buffer. The absence of soft tissue coverage in anatomical orientation also limits the fracture production because the biomechanical property does not accurately represent what should be observed in real forensic cases. As a result, the absence of these would have an effect on the dimension and morphology of traumatic lesions on the bone materials. Future study should be developed to accurately and precisely quantify many more features of traumatic lesion morphology.

The knives, cleavers and machetes used in the current study were newly purchased. In addition, they were used to inflict only 20 traumatic lesions in the bone samples before changing to a new one. However, this causes the limitations of the variability of wear-and-tear patterns on the weapon blades. Because this study conducted research focuses on a baseline study of skeletal trauma, a feasible alternative such as wear patterns on the knife blade mimicking striation should be excluded. Nevertheless, sharp-inflicted injury in the real-world scenario may not be newly purchased, so that it would have an effect on sharp force lesions and wear patterns should be considered. Wenham (1989) suggested that the same weapon could produce bone wounds of varying appearance, resulting in the conclusion that these traumatic lesions may only be characterised in general terms.

It is imperative to remember that this study was carried out on only ribs and femurs. Also, detailed research into variations of blunt and sharp force trauma on different bone types is necessary. It is essential to see if the traumatic lesions identified in the current study can be applicable to other types of bone that are common areas for skeletal trauma as well, i.e. vertebrae and skull. An investigation into traumatic injuries on different types of bone varying in their geometry and density would test whether the different types of fracture have an effect on taphonomic modifications. It is expected that different skeletal elements should react differently to taphonomic factors such as by showing different morphological changes. In addition, the differences in the taphonomic changes of the cut mark on the different positions of the same bone need to be explored. Therefore, a study of the variations in different skeletal elements and architecture exposing to the different environment should be beneficial.

The results of this study were limited by the fact that the decomposition and burning process was not exactly normal. Initially, the bones used in this study were relatively fresh and were free of periosteum and soft tissues surrounding traumatic areas in order that the pre-exposure examination could be carried out. However, in real scenario bone materials are protected and covered by soft tissues, resulting to increase in the time interval before the traumatic lesions expose to the environment or burning process. Even so, this experiment is still limited to bone deposited in surface and buried environment in the temperate climate of South-east England. It also suggests that all findings in this study could not be applied universally to all depositional environments. In this experiment where there were observed studies under surface and buried natural environments. There seems to have a mixture of environments to affect taphonomic changes. Therefore, it may be more useful to separate controlled microenvironment and study its individual reaction to bone degradation. Baseline variables of disparate depositional contexts should be established in order to investigate traumatic lesion changes. Though this may limit the widespread use of this result, it is not beyond the scope of a forensic anthropologist who has worked in a specific region to apply other very similar contexts with diminished, yet meaningful outcomes.

Although domestic pig bone has been determined to closely resemble human bones compared with other mammals, fundamental differences still convolute experimental results. The best choice is that skeletal samples from human cadavers should be tested for the same pattern of bone degradation. However, due to the strictly ethical implications of using human materials for scientific researches, the other choice may be a more suitable alternative animal for this purpose. In addition, the researcher has only conducted research with juvenile bones, the results could be adapted to mature bones. As adult skeletons are much harder and stronger than juvenile skeletons, a lesser effect of taphonomic modification should occur in this harder skeleton when it exposes to the same environmental condition. Detailed research focusing on a number of mature remains over a long-term basis should be carried out. Further study has to be carried out on this topic, using donated human skeletal materials or a different animal model with similar characteristics.

The use of a stereomicroscope in the examination of sharp force injury on bone may be satisfactory in most cases. Nonetheless, limitation to access other techniques such as histological examination and more advanced microscope such as SEM and epifluorescence microscope with the real biological samples is inevitable. SEM should be utilized to analyse cut mark characteristics. The direct examination with SEM is able to not only enhance the observation of traumatic bone characteristics but also confirm the presence of interesting characteristics, as many authors have described how advanced technology can help in trauma and taphonomic interpretation (Kooi and Fairgrieve, 2013; Capuani *et al.,* 2014). Future analytical methods can expand and enrich the findings presented here to compare other morphological variables such as bone surface or kerf wall surface topography; it is not possible with the data in this study but could be explored further. It is essential to set the fundamentals for possible solutions to these crucial problems, which need to be considered in the future with further scientific study.

Time limitation in this study is inevitable as it is outlined by three years of full-time PhD. As this study only demonstrated taphonomic changes of traumatic lesions during eighteen months, it begs the question of whether taphonomy can even give more variable to skeletal trauma morphology after longer exposure. In

fact, taphonomic contexts increase their complexity as the postmortem interval increases. An increase in exposure time may be more useful to prove the effect of outdoor environment on skeletal trauma characteristics. In addition, since the present study considered every six months of depositional samples at the site, it may be beneficial to add more frequently examined group (i.e. every three months) to further observe whether these may provide more insight into how the starting point of a taphonomic change.

Despite the requirement of further research, this preliminary project provides a reference to assess and understand the nature of taphonomic alterations of traumatic lesions. By utilizing the results and ideas developed in this study, researchers will have an appropriate tool to improve analysis of taphonomic modifications of skeletal trauma.

Reference cited

Aerssens, J., Boonen, S., Lowet, G., DeQueker, J. 1998. Interspecies differences in bone composition , density , and quality: potential implications for in vivo bone research, *Endocrinology*, 139(2): 663–670.

Allen, G., Audickas, L. 2018 *Knife Crime in England and Wales*. House of Commons Library London.

Alunni-Perret, V., Bolla-Muller, M., Laugier, J.P., Lupi-Pegurier, L., Bertrand, M.F., Staccini, P., Bolla, M., Quatrehomme, G. 2005. Scanning electron microscopy analysis of experimental bone hacking trauma, *Journal of Forensic Sciences*, 50(4): 796–801.

Ambade, V.N., Godbole, H.V. 2006. Comparison of wound patterns in homicide by sharp and blunt force, *Forensic Science International*, 156: 166–170.

Andrews, P. 1995. Experiments in taphonomy, *Journal of Archaeological Science*, 22: 147–153.

Andrews, P., Cook, J. 1985. Natural modifications to bones in a temperate setting, *Man, New Series*, 20(4): 675–691.

Andrews, P., Fernández-Jalvo, Y. 2012. How to approach perimortem injury and other modifications, In: Lynne, S.B. (ed.) *Forensic Microscopy for Skeletal Tissues: Methods and Protocols*. New York: Humana Press: 191–226.

Andrews, P., Whybrow, P. 2005. Taphonomic observation on a camel skeleton in a desert environment in Abu Dhabi, *Palaeontologia Electronica*, 8(1): 1–17.

Archer, M.S. 2004. Rainfall and temperature effects on the decomposition rate of exposed neonatal remains, *Sci Justice*, 44: 35–41.

Bai, R., Wan, L., Li, H., Zhang, Z., Ma, Z. 2007. Identifying the injury implements by SEM-EDX and ICP-AES. *Forensic Science International,* 166(1): 8-13.

Bailey, J.A., Wang, Y., Van de Goot, F.R.W., Gerretsen, R.R. 2011. Statistical

analysis of kerf mark measurements in bone, *Forensic Science, Medicine, and Pathology*, 7(1): 53–62.

Banasr, A., Lorin De La Grandmaison, G., Durigon, M. 2003. Frequency of bone/cartilage lesions in stab and incised wounds fatalities, *Forensic Science International*, 131(2–3): 131–133.

Bartelink, E., Wiersema, J., Demaree, R. 2001. Quantitative analysis of sharp-force trauma : An application of scanning electron microscopy in forensic anthropology, *Journal of Forensic Sciences*, 46(6): 1288–1293.

Bartelink, E.J. 2015. Blunt force trauma patterns in the human skull and thorax: a case study from Northern California, In: Passalacqua, N.V., Rainwater, C.W. (eds.) *Skeletal Trauma Analysis: Case Studies in Context*. Oxford, the UK: Wiley-Blackwell Publishing Ltd: 56-73.

Bass, W.M. 1997. Outdoor decomposition rates in Tennessee. In: Haglund, W.D., Sorg, M.H. (eds.) *Forensic Taphonomy: The Postmortem Fate of Human Remains*. Boca Raton, FL: CRC Press: 181–185.

Beary, M.O., Lyman, R.L. 2012. The use of taphonomy in forensic anthropology: past trends and future perspects. In: Dirkmaat, D.C. (ed.) *A Companion to Forensic Anthropology*. Chichester, West Sussex: Wiley-Blackwell Publishing Ltd: 499–527.

Behrensmeyer, A.K. 1978. Taphonomic and ecologic information from bone weathering, *Paleobiology*, 4(2): 150–162.

Behrensmeyer, A.K., Gordon, K.D., Yanagi, G.T. 1986. Trampling as a cause of bone surface damage and pseudo-cutmarks, *Nature*, 319: 768.

Bell, L.S., Skinnerb, M.F., Jones, S.J. 1996. The speed of post mortem change to the human skeleton and its taphonomic significance, *Forensic Science International*, 82: 129–140.

Bello, S.M., Thomann, A., Signoli, M., Dutour, O., Andrew, P. 2006. Age and sex bias in the reconstruction of past population structures, *American Journal of*

Physical Anthropology, 129: 24–38.

Bello, S.M., Parfitt, S.A., Stringer, C. 2009 Quantitative micromorphological analyses of cut marks produced by ancient and modern handaxes, *Journal of Archaeological Science*, 36(9): 1869–1880.

Bello, S.M., Soligo, C. 2008. A new method for the quantitative analysis of cutmark micromorphology, *Journal of Archaeological Science*, 35: 1542–1552.

Bennett, J.L. 1999. Thermal alteration of buried bone, *Journal of Archaeological Science*, 26: 1–8.

Berryman, H.E., Symes, S.A. 1998. Recognizing gunshot and blunt cranial trauma through fracture interpretation, In: Reichs, K.J. (ed.) *Forensic Osteology: Advances in the Identification of Human Remains*, Springfield, IL: Charles C Thomas: 333–352.

Berryman, H.E., Saul, T.B. 2015. Skeletal evidence of violent sexual assault in remains with excessive evidence of scavenging, In: Passalacqua, N.V., Rainwater, C.W. (eds.) *Skeletal Trauma Analysis: Case Studies in Context*. Oxford, the UK: Wiley-Blackwell Publishing Ltd: 118-129.

Blau, S. 2017. The effects of weathering on bone preservation, In: Schotsmans, E.M.J., Marquez-Grant, N., Forbes, S.L. (eds.) *Taphonomy of Human Remains: Forensic Analysis of the Dead and the Depositional Environment*. Chichester, West Sussex: Wiley-Blackwell Publishing Ltd: 201-211.

Boaks, A., Siwek, D., Mortazavi, F. 2014. The temporal degradation of bone collagen: A histochemical approach, *Forensic Science International*, 240: 104–110.

Bohnert, M., Rost, T., Faller-Marquardt, M., Ropohl, D., Pollak, S. 1997. Fractures of the base of the skull in charred bodies: post-mortem heat injuries or signs of mechanical traumatisation, *Forensic Science International*, 87: 55–62.

Bohnert, M., Schmidt, U., Perdekamp, M.G., Pollak, S. 2002. Diagnosis of a captive-bolt injury in a skull extremely destroyed by fire, *Forensic Science International*,

127(3): 192–197.

Bohnert, M., Rost, T., Pollak, S. 1998. The degree of destruction of human bodies in relation to the duration of the fire, *Forensic Science International*, 95: 11–21.

Bonte, W. 1975. Tool marks in bones and cartilage, *Journal of Forensic Sciences*, 20(2): 315–325.

Bontrager, A.B., Nawrocki, S.P. 2015. A taphonomic analysis of human cremains from the Fox Hollow farm serial homicide site, In: Schmidt, C.W., Symes, S.A. (eds.) *The Analysis of Burned Human Remains*. 2nd edition. London: Academic Press: 229-246.

Borchers, R.E., Gibson, L.J., Burchardt, H., Hayes, W.C. 1995. Effects of selected thermal variables on the mechanical properties, *Biomaterials*, 16: 545–551.

Boschin, F., Crezzini, J. 2012. Morphometrical analysis on cut marks using a 3D digital microscope, *International Journal of Osteoarchaeology*, 22(5): 549–562.

Boucherie, A., Marie, M.L., Smith, M. 2017. Wounded to the bone: digital microscopic analysis of traumas in a medieval mass grave assemblage (Sandbjerget, Denmark, AD 1300–1350), *International Journal of Paleopathology*, 19: 66–79.

Bouxsein, M.L., Boyd, S.K., Christiansen, B.A., Guldberg, R.E., Jepsen, K.J., Muller, R. 2010. Guidelines for assessment of bone microstructure in rodents using micro – computed tomography, *Journal of Bone and Mineral Research*, 25(7): 1468–1486.

Bradley, A.L., Swain, M.V., Waddell, J.N., Das, R., Athens, J., Kieser, J.A. 2014. A comparison between rib fracture patterns in peri- and post-mortem compressive injury in a piglet model, *Journal of the Mechanical Behavior of Biomedical Materials*, 33: 67–75.

Bradtmiller, B., Buikstra, J.E. 1984. Effects of burning on human bone microstructure: a preliminary study, *Journal of Forensic Sciences*, 29: 535–540.

Braidotti, P., Bemporad, E., D'Alession, T., Sciuto, S.A., Stagni, L. 2000. Tensile

experiments and SEM fractography on bovine subchondral bone, *Journal of Biomechanics*, 33: 1153–1157.

Braidotti, P., Brancal, F.P., Stagnil, L. 1997. Scanning electron microscopy of human bone failure surfaces, *Journal of Biomechanics*, 30(2): 155–162.

Brain, C.K. 1967. Bone weathering and the problem of bone pseudo-tool, *The South African Journal of Science*, 63(3): 97–99.

Brett, C.E., Baird, G.C. 1986. Comparative taphonomy: a key to paleoenvironmental interpretation based on fossil preservation, *PALAIOS*, 3(1): 207–227.

Brinckmann, P., Frobin, W., Leivseth, G. 2002. *Musculoskeletal Biomechanics*. New York: Thieme.

Bristow, J., Simms, Z., Randolph-Quinney, P. 2011. Taphonomy, In: Black, S., Ferguson, E. (eds.). *Forensic Anthropology 2000-2010*. Boca Raton, FL: CRC Press: 279-317.

British Standard ISO10390 2005. *Soil quality-determination of pH*. March 2005, London.

Bromage, T.G., Boyde, A. 1984. Microscopic criteria for the determination of directionality of cutmarks on bone, *American Journal of Physical Anthropology*, 65(4): 359–366.

Brouchoud, J.E. 2014. *The effects of thermal alteration on saw mark characteristics*. MSc Dissertation. Boston University.

Brown, R.B. 2003. *Soil Texture*. University of Florida. Available at: http://ufdcimages.uflib.ufl.edu/IR/00/00/31/07/00001/SS16900.pdf.

Buikstra, J.E., Ubelaker, D.H. 1994. *Standards for Data Collection from Human Skeletal Remains: Proceedings of a seminar at the field museum of natural history*.

Bunn, H.T. 1981. Archaeological evidence for meat-eating by Plio-Pleistocene hominids from Koobi Fora and Olduvai Gorge, *Nature*, 291: 574–577.

Byers, S.N. 2010. *Introduction to Forensic Anthropology*. 4th editions. Boston, MA: Pearson Education.

Calce, S.E., Rogers, T.L. 2007. Taphonomic changes to blunt force trauma : A preliminary study, *Journal of Forensic Sciences*, 52(3): 520–527.

Camaros, E., Sanchez-Hernandez, C., Rivals, F. 2016. Make it clear: molds, transparent casts and lightning techniques for stereomicroscopic analysis of taphonomic modifications on bone surfaces, *Journal of Anthropological Sciences*, 94: 223–230.

Cappella, A., Castoldi, E., Sforza, C., Cattaneo, C. 2014. An osteological revisitation of autopsies: Comparing anthropological findings on exhumed skeletons to their respective autopsy reports in seven cases, *Forensic Science International*, 244: 315.e1-315.e10.

Cappella, A. Amadasi, A., Castoldi, E., Mazzarelli, D., Gaudio, D., Cattaneo, C. 2014. The difficult task of assessing perimortem and postmortem fractures on the skeleton: A blind text on 210 fractures of known origin, *Journal of Forensic Sciences*, 59(6): 1598–1601.

Capuani, C., Telmon, N., Moscovici, J., Molinier, F., Aymeric, A., Delisle, M.B., Rouge, D., Guilbeau-Frugier, C. 2014. Modeling and determination of directionality of the kerf in epifluorescence sharp bone trauma analysis, *International Journal of Legal Medicine*, 128(6): 1059–1066.

Carter, D.O., Tibbett, M. 2008. Cadaver decomposition and soil: processes, In: Tibbett, M., Carter, D.O. (eds) *Soil Analysis in Forensic Taphonomy*. Boca Raton, FL: CRC Press: 29–52.

Carter, D.O., Metcalf, J.L., Bibat, A., Knight, R. 2015. Seasonal variation of postmortem microbial communities, *Forensic Science, Medicine, and Pathology*, 11: 202–207.

Carter, D.O., Yellowlees, D., Tibbett, M. 2007. Cadaver decomposition in terrestrial ecosystems, *Naturwissenschaften*, 94: 12–24.

Carter, D.O., Yellowlees, D., Tibbett, M. 2010. Moisture can be the dominant environmental parameter governing cadaver decomposition in soil, *Forensic Science International*, 200: 60–66.

Cassidy, M.T., Curtis, M. 2005. Victims of penetrating and incised wounds, In: Gilchrist, M.D. (ed.) *IUTAM Symposium on Impact Biomachnics: From Fundamental Insights to Applications*: 405–414.

Cattaneo, C., DiMartino, S., Scali, S., Craig, O.E., Grandi, M., Sokol, R.J. 1999. Determining the human origin of fragments of burnt bone : a comparative study of histological, immunological and DNA techniques, *Forensic Science International*, 102: 181–191.

Cattaneo, C., Cappella, A. 2017. Distinguishing between peri- and post-mortem trauma on bone, In: Schotsmans, E.M.J., Marquez-Grant, N., Forbes, S.L. *Taphonomy of Human Remains: Forensic Analysis of the Dead and the Depositional Environment*. Chichester, West Sussex: Wiley-Blackwell Publishing Ltd: 352-368.

Catts, E.P., Goff, M.L. 1992. Forensic entomology in criminal investigations, *Annual Review of Entomology*, 37(116): 253–272.

Cecchetto, G., Giraudo, C., Amagliani, A., Viel, G., Fais, P., Cavarzeren, F., Feltrin, G., Ferrara, S.D., Montisci, M. 2011. Estimation of firing distance through micro-CT analysis of gunshot wounds, *International Journal of Legal Medicine*, 125: 245–251.

Cecchetto, G., Amagliani, A., Giraudo, C., Fais, P., Cavarzeren, F., Montisci, M., Feltrin, G., Viel, G., Ferrara, S.D. 2012. Micro-CT detection of gunshot residue in fresh and decomposed firearm wounds, *International Journal of Legal Medicine*, 126: 377–383.

Cerutti, E., Magli, F., Porta, D., Gibelli, D., Cattaneo, C. 2014. Metrical assessment of cutmarks on bone : Is size important?, *Legal Medicine*, 16: 208–213.

Cerutti, E., Spagnoli, L., Araujo, N., Gibelli, D., Mazzarelli, D., Cattaneo, C. 2016 Analysis of cutmarks on bone: Can light microscopy be of any help?, *American Journal of Forensic Medicine and Pathology*, 37(4): 248–254.

Chadwick, E.K., Nicol, A.C., Lane, J.V., Gray, T.G. 1999. Biomechanics of knife stab attacks, *Forensic Science International*, 105: 35–44.

Chappard, D., Retailleau-Giborit, N., Legrand, E., Basle, M.F., Audran, M. 2005. Comparison insight bone measurements by histomorphometry and micro-CT, *Journal of Bone and Mineral Research*, 20(7): 1177–1184.

Christensen, A.M., Hefner, J.T., Smith, M.A., Webb, J.B., Bottrell, M.C., Fenton, T.W. 2018. Forensic fractography of bone: a new approach to skeletal trauma analysis, *Forensic Anthropology*, 1(1): 32–51.

Christensen, A.M., Passalacqua, N.V., Bartelink, E.J. 2014. *Forensic Anthropology: Current Methods and Practice*. London: Academic Press.

Collini, F., Amadasi, A., Mazzucchi, A., Porta, D., Regazzola, V.L., Garofalo, P., DiBlasio, A., Cattaneo, A. 2015. The erratic behavior of lesions in burnt bone, *Journal of Forensic Sciences*, 60(5): 1290–1294.

Collins, M.J., Nielsen-Marsh, C.M., Hiller, J., Smith, C.I., Roberts, J.P. 2002. The survival of organic matter in bone: a review, *Archaeometry*, 44(3): 383–394.

Corondan, G., Haworth, W.L. 1986. A fractographic study on human long bone, *Journal of Biomechanics*, 19: 207–218.

Coyle, H.M. 2004. *Forensic Botany: Principles and Applications to Criminal Casework*. Boca Raton, FL: CRC Press.

Crist, T.A.J., Washburn, A., Park, H., Hood, I., Hickey, M.A. 1997. Cranial bone displacement as a taphonomic process in potential child abuse cases, In: Haglund, W.D., Sorg, M.H. (eds.) *Forensic Taphonomy: The Postmortem Fate of Human Remains*. Boca Raton, FL: CRC Press: 319–336.

Crowder, C., Rainwater, C.W., Fridie, J.S. 2011. *Microscopic Analysis of Sharp Force Trauma in Bone and Cartilage: A Validation Study*. National Institute of Justice. The U.S. Department of Justice. New York.

Cunningham, S.L., Kirkland, S.A., Ross, A.H. 2011. Bone weathering of juvenile-

sized remains in the North Carolina Piedmont, In: Ross, A.H., Abel, S.M. (eds.) *The Juvenile Skeleton in Forensic Abuse Investigations*. New York: Humana Press: 179–196.

Currey, J.D. 2002. *Bones: Structure and Mechanics*. Oxfordshire: Princeton university press.

Damann, F.E. 2010. *Human decomposition ecology at the university of Tennessee Anthropology Research Facility*. Ph.D. Thesis. University of Tennessee.

Davidson, K., Davies, C., Randolph-Quinney, P. 2011. Skeletal trauma, In: Black, S., Ferguson, E. (eds.). *Forensic Anthropology 2000-2010*. Boca Raton, FL: CRC Press: 183-235.

DeHaan, J.D. 2015. Fire and bodies, In: Schmidt, C.W., Symes, S.A. (eds.) *The Analysis of Burned Human Remains*. 2nd edition. London: Academic Press: 1-15.

Dent, B.B., Forbes, S.L., Stuart, B.H. 2004. Review of human decomposition processes in soil, *Environmental Geology*, 45: 576–585.

Department of transport 2017. *Reports Road Casualties in Great Britain: Annual Report, 2017*. Available at: https://www.gov.uk/government/uploads /system/uploads/attachment_data/file/438040/reported-road-casualties-in-great-britain-annual-report-2017-release.pdf.

Devlin, J.B., Herrmann, N.P. 2015. Bone colour, In: Schmidt, C.W., Symes, S.A. (eds.) *The Analysis of Burned Human Remains*. 2nd edition. London: Academic Press: 119–138.

DiMaio, V.J., DiMaio, D. 2001. *Forensic Pathology: Practical Aspects of Criminal and Forensic Investigations*. Boca Raton, FL: CRC Press.

Dominguez-Rodrigo, M., de Juana, S., Galan, A.B., Rodriguez, M. 2009. A new protocol to differentiate trampling marks from butchery cut marks, *Journal of Archaeological Science*, 36: 2643–2654.

Donnellan, S.M.K., Chatzinikolaou, F., Kranioti, E. 2013. Morphological Analysis of

Sharp Force Trauma Using High Resolution Casts, *Proceedings of the 22rd Congress of the International Academy of Legal Medicine, Istanbul, Turkey 5-8 2012*: 107–114.

Dupras, T.L., Schultz, J.J. 2014. Taphonomic bone staining and colour changes in forensic contexts, In: Pokines, J.T., Symes, S.A. (eds.) *Manual of Forensic Taphonomy*. Boca Raton, FL: CRC Press: 315–340.

Eickhoff, S., Herrmann, B. 1985. Surface marks on bone from a neolithic collective grave (Odagsen, Lower Saxony)- A study on differential diagnosis, *Journal of Human Evolution*, 14: 163–174.

Ellingham, S.T.D., Thompson, T.J.U., Islam, M., Taylor, G. 2015. Esimating temperature exposure of burnt bone- A methodological review, *Science and Justice,* 55: 181-188.

European Commission 2005. *Soil Atlas of Europe*. European Soil Bureau Network.

von Endt, D.W., Ortner, D.J. 1984. Experimental effects of bone size and temperature on bone diagenesis, *Journal of Archaeological Science*, 11: 247–253.

Escoffery, C.T., Shirley, S.E. 1992. Traumatic deaths in Jamaica: a coroner's (medico-legal) autopsy study from the University Hospital of the West Indies, *Medicine, Science and the Law*, 42(3): 185–191.

Evans, J.G., Ward, H.C., Blake, J.R., Hewitt, E.J., Morrison, R., Fry, M., Ball, L.A., Doughty, L.C., Libre, J.W., Hitt, O., Rylett, D., Ellis, R., Warwick, A.C., Brooks, M., Parkes, M.S., Wright, G.M.H., Singer, A.C., Boorman, D.B., Jenkins, A. 2016. Soil water content in southern England derived from a cosmic-ray soil moisture observing system – COSMOS-UK, *Hydrological Processes*, 30(26): 4987–4999.

Fairgrieve, S.I. 2008. *Forensic Cremation: Recovery and Analysis*. Boca Raton: FL: CRC Press.

Fantner, G.E., Birkedal, H., Kindt, J.H., Hassenkam, T., Weaver, J.C., Cutroni, J.A., Bosma, B.L., Finch, M.M., Cidade, G.A., Morse, D.E., Stucky, G.D., Hansma, P.K.

2004 Influence of the degradation of the organic matrix on the microscopic fracture behavior of trabecular bone, *Bone*, 35: 1013–1022.

Fanton, L., Jdeed, K., Tilhet-Coartet, S., Malicier, D. (2006). Criminal burning, *Forensic Science International,* 158: 87-93.

Fenton, T.W., Birkby, W.H., Cornelison, J. 2003. A fast and safe non-bleaching method for forensic skeletal preparation, *Journal of Forensic Sciences*, 48(2): 274–276.

Ferllini, R. 2012. Macroscopic and microscopic analysis of knife stab wounds on fleshed and clothed ribs, *Journal of Forensic Sciences*, 57(3): 683–690.

Fernández-Jalvo, Y., Andrews, P., Pesquero, D., Smith, C., Marin-Monfort, M.D., Sanchez, B., Geigl, E., Alonso, A. 2010. Early bone diagenesis in temperate environments Part I: Surface features and histology, *Paleogeography, Paleoclimatology, Paleoecology*, 288: 62–81.

Fernández-Jalvo, Y., Tormo, L., Andrews, P., Marin-Monfort, M.D. 2018. Taphonomy of burnt bones from Wonderwerk Cave (South Africa), *Quaternary International*, 495: 19–29.

Fernández-Jalvo, Y., Andrews, P. 2016. *Atlas of Taphonomic Identifications*. New York: Springer.

Fernández-Jalvo, Y., Pesquero, M.D., Tormo, L. 2016. Now a bone , then calcite, *Palaeogeography, Palaeoclimatology, Palaeoecology*, 444: 60–70.

Fisher, J.W. 1995. Bone surface modifications in zooarchaeology, *Journal of Archaeological Method and Theory*, 2(1): 7–68.

Forbes, S.L., Dent, B.B., Stuart, B.H. 2005. The effect of soil type on adipocere formation, *Forensic Science International*, 154: 35–43.

Frayer, D.W., Bridgens, J.G. 1985. Stab wounds and personal identity determined from skeletal remains: a case from Kansas, *Journal of Forensic Sciences*, 30(1): 232–238.

Freas, L.E. 2010. Assessment of wear-related features of the kerf wall from saw marks in bone, *Journal of Forensic Sciences*, 55(6): 1561–1569.

Freivalds, A. 2011. *Biomechanics of the Upper Limbs: Mechanics, Modeling and Musculoskeletal injuries*. 2nd edition. Boca Raton, FL: CRC Press.

Galloway, A., Birkby, W.H., Jones, A.M., Henry, T.E., Parks, B.O. 1989. Decay rates of human remains in an arid environment, *Journal of Forensic Sciences*, 34(3): 607–616.

Galloway, A., Walsh-Haney, H., Byrd, J.H. 2001. Recovering buried bodies and surface scatter: The associated anthropological, botanical, and entomological evidence, In: Byrd, J.H., Castner, J.L. (eds.) *Forensic Entomology: The Utility of Arthropods in Legal Investigations*. Boca Raton, FL: CRC Press: 223–262.

Galloway, A., Zephro, L., Wedel, V.L. 2014. Diagnistic criteria for the determination of timing and fracture mechanism, In: Wedel, V.L., Galloway, A. (eds.). *Broken Bones: Anthropological Analysis of Blunt Force Trauma*. 2nd edition. Springfield, IL: Charles C Thomas: 47-58.

Galloway, A., Zephro, L., Wedel, V.L. 2014. Classification of fractures, In: Wedel, V.L., Galloway, A. (eds.). *Broken Bones: Anthropological Analysis of Blunt Force Trauma*. 2nd edition. Springfield, IL: Charles C Thomas: 59-72.

Le Garff, E., Mesli, V., Delannoy, Y., Colard, T., Demondion, X., Becart, A., Hedouin, V. 2017. Technical note : early post-mortem changes of human bone in taphonomy with µCT, International Journal of Legal Medicine, 131: 761–770.

Gaudio, D., Di Giancamilo, M., Gibelli, D., Galassi, A., Cerutti, E., Cattaneo, C. 2014. Does cone beam CT actually ameliorate stab wound analysis in bone?, *International Journal of Legal Medicine*, 128(1): 151–159.

Gerling, I., Meissner, C., Reiter, A., Oehmichen, M. 2001. Death from thermal effects and burns, *Forensic Science International*, 115: 33–41.

Gifford, D.P. 1981. Taphonomy and paleoecology: a critical review of archaeology's

sister disciplines, In: Schiffer, M.B. (ed.) *Advances in Archaeological Method and Theory vol.4*. New York: Academic Press: 365–438.

Gilchrist, R., Mytum, C. 1986. Experimental archaeology and burnt animal bone from archaeological sites, *Circaea*, 4: 29–38.

Gill-King, H. 1997. Chemical and ultrastructural aspects of decomposition, In: Haglund, W.D., Sorg, M.H. (eds.) *Forensic Taphonomy: The Postmortem Fate of Human Remains*. Boca Raton, FL: CRC Press.

Glassman, D.M., Crow, R.M. 1996. Standardization model for describing the extent of burn injury to human remains, *Journal of Forensic Sciences*, 41(1): 152–4.

Golden, G.S. 2011. Standards and practices for bite mark photography, *Journal of Forensic Odonto-Stomatology*, 29(2): 29–37.

Gonçalves, D., Cunha, E., Thompson, T.J.U. 2013. Weight references for burned human skeletal remains from Portuguese samples, *Journal of Forensic Sciences*, 58(5): 1134–1140.

Gonçalves, D., Thompson, T.J.U., Cunha, E. 2011. Implications of heat-induced changes in bone on the interpretation of funerary behaviour and practice, *Journal of Archaeological Science*, 38(6): 1308–1313.

Goodhew, P.J., Humphrey, J., Beanland, R. 2001. The scanning electron microscope, In: Goodhew, P.J., Humphrey, J., Beanland, R. (eds.) *Electron Microscopy and Analysis*. 3rd edition. London: Taylor and Francis Inc: 122–168.

Gordon, C.C., Buikstra, J.E. 1981. Soil pH, bone preservation, and sampling bias at mortuary sites, *American Antiquity*, 46(3): 566–571.

Gozna, E.R. 1982. Biomechanics of long bone injuries, In: Whiting, W.C., Zernicke, R.F. (eds.) *Biomechanics of Musculoskeletal Injury.* London: Human Kinetics: 1–24.

Grevin, G., Bailet, P., Quatrehomme, G., Ollier, A. 1998. Anatomical reconstruction of fragments of burned human bones : a necessary means for forensic identification, *Forensic Science International*, 96: 129–134.

de Gruchy, S., Rogers, T.L. 2002. Identifying chop marks on cremated bone: a preliminary study, *Journal of Forensic Sciences*, 47(5): 933–936.

Grupe, G., Hummel, S. 1991. Trace element studies on experimentally cremated bone I. Alteration of the chemical composition at high temperatures, *Journal of Archaeological Science,* 18: 177-186.

Gutierrez, M.A. 2001. Bone diagenesis and taphonomic history of the Paso Otero 1 bone bed, Pampas of Argentina, *Journal of Archaeological Science*, 28: 1277–1290.

Guy, H., Masset, C., Baud, C.A. 1997. Infant taphonomy, *International Journal of Osteoarchaeology*, 7: 221–229.

Haglund, W.D. 1997a. Dogs and coyotes: postmortem involvement with human remains, In: Haglund, W.D., Sorg, M.H. (eds.). *Forensic Taphonomy: The Postmortem Fate of Human Remains.* Boca Raton, FL: CRC Press: 365-382.

Haglund, W.D. 1997b. Rodents and human remains, In: Haglund, W.D., Sorg, M.H. (eds.). *Forensic Taphonomy: The Postmortem Fate of Human Remains.* Boca Raton, FL: CRC Press: 405-411.

Haglund, W.D., Sorg, M.H. 1997. Method and theory of forensic taphonomy research, In: Haglund, W.D., Sorg, M.H. (eds.). *Forensic Taphonomy: The Postmortem Fate of Human Remains.* Boca Raton, FL: CRC Press: 13-26.

Hainsworth, S.V., Delaney, R.J., Rutty, G.N. 2008. How sharp is sharp? Towards quantification of the sharpness and penetration ability of kitchen knives used in stabbing, *International Journal of Legal Medicine*, 122(4): 281–291.

Hall, D.W. 1997. Forensic botany, In: Haglund, W.D., Sorg, M.H. (eds.) *Forensic Taphonomy: The Postmortem Fate of Human Remains.* Boca Raton, FL: CRC Press: 353-366.

Hart, G. 2015. Man's best friend: a case study of ballistics trauma and animal scavenging, In: Passalacqua, N.V., Rainwater, C.W. (eds.) *Skeletal Trauma Analysis: Case Studies in Context*. Oxford, the UK: Wiley-Blackwell Publishing Ltd:

108-117.

Haynes, G. 1981. *Bone Modification and Skeletal Disturbances by Natural Agencies: Studies in North America*. The Catholic University of America.

Hedges, R.E.M. 2002. Bone Diagenesis: an overview of processes, *Archaeometry*, 44: 319–328.

Henderson, J.P., Morgan, S.E., Patel, M. Tiplady, F.E. 2005. Patterns of non-firearm homicide, *Journal of Clinical Forensic Medicine*, 12: 128–132.

Hentschel, K.C. 2014. *Postmortem fracture surface topography: an investigation into differentiating perimortem and postmortem long bone blunt force trauma fractures*. MSc Dissertation. Texas State University.

Hentschel, K., Wescott, D.J. 2015. Differentiating peri-mortem from post-mortem blunt force trauma by evaluating fracture tension surface topography using geographic information systems, In *Proceedings of the 67th annual meeting of the American Academy of Forensic Sciences; February 16–21*. Orlando, FL.

Herrmann, N.P., Bennett, J.L. 1999. The differentiation of traumatic and heat-related fractures in burned bone, *Journal of Forensic Sciences*, 44(3): 461–469.

Hiller, J.C., Thompson T.J.U., Evison, M.P., Chamberlain, A.T., Wess, T.J. 2003. Bone mineral change during experimental heating : an X-ray scattering investigation, *Biomaterials*, 24: 5091–5097.

Hiller, L.P., Stover, S.M., Gibson, V., Gibeling, J.C., Prater, C.S., Hazelwood, S.J., Yeh, O.C., Martin, R.B. 2003. Osteon pullout in the equine third metacarpal bone : effects of ex vivo fatigue, *Journal of Orthopaedic Research*, 21: 481–488.

Hillier, M.L., Bell, L.S. 2007. Differentiating human bone from animal bone: a review of histological methods, *Journal of Forensic Sciences*, 52(2): 249–263.

Holden, J.L., Phakey, P.P., Clementalb, J.G. 1995. Scanning electron microscope observations of heat-treated human bone, *Forensic Science International*, 74: 29–45.

Honeycutt, K.K. 2012. *Fracture patterns and taphonomic processes in a mass grave environment: a quantitative analysis*. MSc Dissetation. North Carolica State University.

Houck, M.H. 1998. Skeletal trauma and the individualization of knife marks in bones, In: Reichs, K.J. (ed.) *Forensic Osteology: Advances in the Identification of Human Remains*. Springfield, IL: Charles C Thomas: 410–424.

Huculak, M.A., Rogers, T.L. 2009. Reconstructing the Sequence of Events Surrounding Body Disposition Based on Color Staining of Bone, *Journal of Forensic Sciences*, 54(5): 979–984.

Human Tissue Authorities 2004. *Human Tissue Act*. Available at: http://www.hta.gov.uk/human-tissue-act-2004.

Humphrey, C., Kumaratilake, J., Henneberg, M. 2017. Characteristics of Bone Injuries Resulting from Knife Wounds Incised with Different Forces, *Journal of Forensic Sciences*, 62(6): 1445–1451.

Humphrey, J., Hutchinson, D.L. 2001. Macroscopic characteristics of hacking trauma, *Journal of Forensic Sciences*, 46(2): 228–233.

Hunt, A.C., Cowling, R.J. 1991. Murder by stabbing, *Forensic Science International*, 52: 107–112.

Hunter, J., Simpson, B., Colls, C.S. 2013. *Forensic approaches to buried remains*. Chichester, West Sussex: Wiley-Blackwell Publishing Ltd.

Hyde, E.R., Haarman, D.P., Lynne, A.M., Bucheli, S.R. 2013. The living dead: bacterial community structure of a cadaver at the onset and end of the bloat stage of decomposition, *PloS one*, 8(10): 1-10.

Imaizumi, K. 2015. Forensic investigation of burnt human remains, *Research and Reports in Forensic Medical Science*, Volume 5: 67.

Isa, M.I., Fenton, T.W., Deland, T., Haut, R.C. 2017. Assessing Impact Direction in 3-point Bending of Human Femora: Incomplete Butterfly Fractures and Fracture

Surfaces, *Journal of Forensic Sciences*, 63(1): 1–9.

Jaggers, K.A., Rogers, T.L. 2009. The effects of soil environment on postmortem interval: a macroscopic analysis, *Journal of Forensic Sciences*, 54(6): 1217–1222.

Janaway, R.C., Percival, S.L., Wilson, A.S. 2009. Decomposition of human remains, In: Percival, S.L. (ed.) *Microbiology and Aging.* New York: Springer: 313–334.

Janjua, M.A., Rogers, T.L. 2008. Bone weathering patterns of metatarsal vs. femur and the postmortem interval in Southern Ontario, *Forensic Science International*, 178(1); 16–23.

Johnson, E. 1985. Current developments in bone technology, In: Schiffer, M.B. (ed.) *Advances in Archaeological Method and Theory vol.8*. Orlando: Academic Press: 157–235.

Jones, S., Nokes, L., Leadbeatter, S. 1994. The mechanics of stab wounding, *Forensic Science International*, 67(1): 59–63.

de Juana, S., Galan, A.B., Dominguez-Rodrigo, M. 2010. Taphonomic identification of cut marks made with lithic handaxes: An experimental study, *Journal of Archaeological Science*, 37(8): 1841–1850.

Jung, H.J., Vangipuram, G., Fisher, M.B., Yang, G., Hsu, S., Bianchi, J., Ronholdt, C., Woo, S.L. 2011. The effects of multiple freeze-thaw cycles on the biomechanical properties of the human bone-patellar tendon-bone allograft, *J. Orthop. Res.*, 29: 1193–1198.

Junkins, E.A., Carter, D.O. 2017, relationships between human remains, gravesand the depositional environment. In: Schotsmans, E.M.J., Marquez-Grant, N., Forbes, S.L. (eds.) *Taphonomy of Human Remains: Forensic Analysis of The Dead and The Depositional Environment*. Chichester, West Sussex: Wiley-Blackwell Publishing Ltd: 145-154.

Junod, C.A. 2013. *Subaerial bone weathering and other taphonomic changes in a temperate climate*. MSc Dissertation. Boston University.

Junod, C.A., Pokines, J.T. 2014. Subaerial weathering, In: Pokines, J.T., Symes, S.A. (eds.) *Manual of Forensic Taphonomy*. Boca Raton, FL: CRC Press: 286–314.

Kalkwarf, H.J., Zemel, B.S., Gilsanz, V., Lappe, J.M., Horlick, M., Oberfield, S., Mahboubi, S., Fan, B., Frederick, M.M., Winer, K., Shepherd, J.A. 2007. The bone mineral density in childhood study: bone mineral content and density according to age, sex, and race, *J. Clin. Endocrinol. Metab.*, 92(6): 2087–2099.

Kalsbeek, N., Richter, J. 2006. Preservation of Burned Bones: An Investigation of the Effects of Temperature and pH on Hardness, *Studies in Conservation*, 51(2): 123–138.

Karch, D.L., Logan, J., Patel, N. 2011. Surveillance for violent deaths - National Violent Death Reporting System, 16 states, 2010, *Morbidity and mortality weekly report. Surveillance Summaries,* 63(1): 1–33.

Karr, L.P., Outram, A.K. 2012. Tracking changes in bone fracture morphology over time: environment , taphonomy , and the archaeological record, *Journal of Archaeological Science*, 39: 555–559.

Katterwe, H. 1996. Modern approaches for the examination of toolmarks and other surface marks, *Forensic Science Review*, 8(1): 46–72.

Kendall, C., Eriksen, A.M.H., Kontopoulos, I., Collins, M.J., Turner-Walker, G. 2018. Diagenesis of archaeological bone and tooth', *Palaeogeography, Palaeoclimatology, Palaeoecology*, 491, pp. 21–37.

Kimmerle, E.H., Baraybar, J.P. 2008. *Skeletal Trauma: Identification of Injuries resulting from Human Rights Abuse and Armed Conflict*. Boca Raton, FL: CRC Press.

Kimura, T., Ogawa, K., Kamiya, M. 1977. Fractography of Human Intact Long Bone by Bending, *Z.Rechtsmedizin*, 79: 301–310.

King, C., Birch, W. 2015. Assessment of maceration techniques used to remove soft tissue from bone in cut mark analysis, *Journal of Forensic Sciences*, 60(1): 124–

135.

van Klinken, G.J., Hedges, R.E.M. 1995. Experiments on collagen – humic interactions: speed of humic uptake, and effects of diverse chemical treatments, *Journal of Archaeological Science*, 22: 263–270.

Kominato Y, Shimada I, Hata N, Takizawa H.F.T. 1997. Homicide patterns in the Toyama Prefecture, Japan, *Med Sci Law*, 37(4): 316–320.

Komo, L., Grassberger, M. 2018. Experimental sharp force injuries to ribs: Multimodal morphological and geometric morphometric analyses using micro-CT, macro photography and SEM', *Forensic Science International*, 288: 189–200.

Kontopoulos, I., Nystrom, P., White, L. 2016. Experimental taphonomy: post-mortem microstructural modifications in Sus scrofa domesticus bone, *Forensic Science International*, 266: 320–328.

Kooi, R.J., Fairgrieve, S.I. 2013. SEM and stereomicroscopic analysis of cut marks in fresh and burned bone, *Journal of Forensic Sciences*, 58(2): 452–458.

Kottek, M., Jurgen, G., Beck, C., Rodolf, B., Rubel, F. 2006. World Map of the Köppen-Geiger climate classification updated, *Meteorologische Zeitschrift*, 15(3): 259–263.

Kroman, A.M. 2007. *Fracture biomechanics of the human skeleton*. Ph.D. Thesis. University of Tennessee.

Kroman, A.M., Symes, S.A. 2013. Investigation of skeletal trauma, In: DiGangi, E.A., Moore, M.K. (eds.) *Research Methods in Human Skeletal Biology*. Oxford: Elsevier: 219–240.

Krüsemann, H. 2001. SEMs and forensic science, *Problems of Forensic Sciences*, 47: 110–121.

Langley, N.R. 2017. Analysis of skeletal trauma, In: Langley, N.R., Tersigni-Tarrant, M.A. (eds.) *Forensic Anthropology: A Comprehensive Introduction.* 2nd edition. Boca Raton, FL: CRC Press: 231-254.

Lee, W., Jasiuk, I. 2014. Effects of freeze-thaw and micro-computed tomography irradiation on structure-property relations of porcine trabecular bone, *J. Biomech.*, 47: 1495–1498.

Lewis, J.E. 2008. Identifying sword marks on bone : criteria for distinguishing between cut marks made by different classes of bladed weapons, *Journal of Archaeological Science*, 35: 2001–2008.

Lewis, M.E. 2010. Life and death in a civitas capital: metabolic disease and trauma in the children from late Roman Dorchester, Dorset, *American Journal of Physical Anthropology*, 142(3): 405–416.

Liebschner, M.A.K. 2004. Biomechanical considerations of animal models used in tissue engineering of bone, *Biomaterials*, 25: 1697–1714.

Lininger, S.L. 2015. *The taphonomic factors on human remains inside Chullpas: Marcajirca, Peru*. MSc Dissertation. Western michigan University.

Littleton, J. 2000. Taphonomic effects of erosion on deliberately buried bodies', *Journal of Archaeological Science*, 27(1): 5–18.

Lyman, R.L. 1994. *Vertebrate Taphonomy*. Cambridge, UK: Cambridge university press.

Lyman, R.L. 2004. The concept of equifinality in Taphonomy, *Journal of Taphonomy,* 2(1): 15-26.

Lyman, R.L. 2005. Analyzing cut marks: lessons from artiodactyl remains in the northwestern United States, *Journal of Archaeological Science*, 32(12): 1722–1732.

Lyman, R.L. 2010. What taphonomy is, what it isn't, and why taphonomists should care about the difference, *Journal of Taphonomy,* 8(1): 1-16.

Lyman, R.L., Fox, G.L. 1997. A critical evaluation of bone weathering as an indication of bone assemblage formation, In: Haglund, W.D., Sorg, M.H. (eds.) *Forensic Taphonomy: The Postmortem Fate of Human Remains*. Boca Raton, FL: CRC Press: 223–247.

Lynn, K.S., Fairgrieve, S.I. 2009a. Macroscopic analysis of axe and hatchet trauma in fleshed and defleshed mammalian long bones, *Journal of Forensic Sciences*, 54(4), pp. 786–792.

Lynn, K.S., Fairgrieve, S.I. 2009b. Microscopic indicators of axe and hatchet trauma in fleshed and defleshed mammalian long bones, *Journal of Forensic Sciences*, 54(4): 793–797.

Macoveciuc, I., Marquez-Grant, N., Horsfall, I., Zioupos, P. 2017. Sharp and blunt force trauma concealment by thermal alteration in homicides : An in-vitro experiment for methodology and protocol development in forensic anthropological analysis of burnt bones, *Forensic Science International*, 275: 260–271.

Madgwick, R., Mulville, J. 2012. Investigating variation in the prevalence of weathering in faunal assemblages in the UK: A multivariate statistical approach, *International Journal of Osteoarchaeology*, 22(5): 509–522.

Manifold, B.M. 2012. Intrinsic and extrinsic factors involved in the preservation of non-adult skeletal remains in Archaeology and Forensic sciences, *Bull Int Assoc Paleodont*, 6(2): 51–69.

Mann, R.W., Bass, W.M., Meadows, L. 1990. Time since death and decomposition of the human body : variables and observations in case and experimental field studies, *Journal of Forensic Sciences*, 35(1): 103–111.

Maples, W.R., Gatliff, B.P., Ludena, H., Benfer, R., Goza,1989. The death and mortal remains of Francisco Pizarro, *Journal of Forensic Sciences*, 34(4): 1021–1036.

Marceau, C.M. 2007. *Bone weathering in a cold climate: forensic applications of a field experiment using animal models*. MSc Dissertation. University of Alberta.

Marciniak, S.M. 2009. A preliminary assessment of the identification of saw marks on burned bone, *Journal of Forensic Sciences*, 54(4): 779–785.

Martin, R.B., Burr, D.B., Sharkey, N.A. 1998. Skeletal biology, In: Martin, R.B., Burr,

D.B., Sharkey, N.A. (eds.) *Skeletal Tissue Mechanics*. New York: Springer: 29–78.

Maté-González, M.Á., Plomeque-Gonzalez, J.F., Yravedra, J., Gonzalez-Aguilera, D., Dominguez-Rodrigo, M. 2018. Micro-photogrammetric and morphometric differentiation of cut marks on bones using metal knives, quartzite, and flint flakes, *Archaeological and Anthropological Sciences*, 10(4): 805–816.

Mayne Correira, P. 1997. Fire modification of bone: a review of the literature, In: Haglund, W.D., Sorg, M.H. (eds.) *Forensic Taphonomy: The Postmortem Fate of Human Remains*. Boca Raton, FL: CRC Press: 275–293.

Mayne Correira, P. 1990. *The Identification of precremation trauma in cremated bone*. MSc Dissertation. University of Alberta.

McCardle, P., Lyons, T. 2015. Machete cut marks on bone : our current knowledge, *Forensic Res Criminol Int J*, 1(2): 2–4.

McCardle, P., Stojanovski, E. 2018. Identifying differences between cut marks made on bone by a machete and katana: a pilot study, *Journal of Forensic Sciences*, 63(6): 1813–1818.

McKinley, J. 2000. The analysis of cremated bone, In: Cox, M., Mays, S. (eds.) *Human Osteology in Archaeology and Forensic Science*. London: Greenwich Medical Media Ltd: 403–421.

McKinley, J.I. 1993. Bone fragment size and weights of bone from modern British cremations and the implications for the interpretation of archaeological cremations, *International Journal of Osteoarchaeology*, 3: 283–287.

McKinley, J.I. 1994. Bone fragment size in British cremation burials and its implications for pyre technology and ritual, *Journal of Archaeological Science*, 21: 339–342.

McKinley, J.I. 2004. Compiling a skeletal inventory: disarticulated and co-mingled remains, In: Brickley, M., McKinley, J.I. (eds.) *Guidelines to the Standards for Recording Human Remains*. Southampton: BABAO: 14–17.

Megyesi, M.S., Nawrocki, S.P., Haskell, N.H. 2005. Using Accumulated Degree-Days to estimate the postmortem Interval from decomposed human remains, *Journal of Forensic Sciences*, 50(3): 1–9.

Miller, J. 2017, Forensic Botany and stomach content analysis: established practice and innovation. In: Schotsmans, E.M.J., Marquez-Grant, N., Forbes, S.L. (eds.) *Taphonomy of Human Remains: Forensic Analysis of the Dead and the Depositional Environment*. Chichester, West Sussex: Wiley-Blackwell Publishing Ltd: 187-200.

Mills, K., Davis, J.R., Destefani, J.D., Dieterich, D.A., Frissell, H.J., Crankovic, G.M., Jenkins, D.M. 1987. Metals Handbook Volume 12 Fractography. Ohio: ASM International.

Moraitis, K., Eliopoulos, C., Spiliopoulou, C. 2008. Fracture Characteristics of Perimortem Trauma in Skeletal Material, *The Internet Journal of Biological Anthropology*, 3(2): 1–8.

Moraitis, K., Spiliopoulou, C. 2006. Identification and Differential Diagnosis of Perimortem Blunt Force Trauma in Tubular Long Bones, *Forensic Science International*, 2(4): 221–229.

Moretti, E., Arrighi, S., Boschin, F., Crezzini, J., Aureli, D., Ronchitelli, A. 2015. Using 3D microscopy to analyze Experimental cut marks on animal bones produced with different stone tools, *Ethnobiology Letters*, 6(2): 267–275.

Möser, M. 1987. Fractography with the SEM (Failure Analysis), In: Heydenreich, J., Bethge, H. (eds.) *Materials Science Monographs vol. 40: Electron Microscopy in Solid State Physics*. Elsevier Science: 366–385.

Mulhern, D.M., Ubelaker, D.H. 2001. Differences in osteon banding between human and nonhuman bone, *Journal of Forensic Sciences*, 46(2): 220–222.

Muller, R., van Campenhout, H., van Damme, B., van der Perre, G., Dequeker, J., Hildebrand, T., Ruegsegger, P. 1998. Morphometric analysis of human bone biopsies: a quantitative structural comparison of histological sections and micro-computed tomography, *Bone*, 23(1): 59–66.

Munsell 1992. *Munsell Soil Color Chart*. New York; USA.

Nalla, R.K., Kinney, J.H., Ritchie, R.O. 2003. Mechanistic fracture criteria for the failure of human cortical bone, *Nat Matters*, 2: 164–168.

Nawrocki, S.P. 1996. *An Outline of Forensic Taphonomy*, *University of Indianapolis Archaeology anf forensic laboratory*. Available at: http://archlab.uindy.edu/documents/ForensicTaph.pdf (Accessed: 20 July 2012).

Nawrocki, S.P. (2016) Forensic taphonomy, In: Blau, S., Ubelaker, D.H. (eds.) *Handbook of Forensic Anthropology and Archaeology*. 2nd edition. New York: Routledge: 373–390.

Neher, D.A., Barbercheck, M.E., El-Allaf, S.M., Anas, O. 2003. Effects of disturbance and ecosystem on decomposition, *Applied Soil Ecology*, 23: 165–179.

Neyt, J.G.V., Buckwalter, J.A., Carroll, N.C. 1998. Use of animal models in musculoskeletal research, *The Iowa Orthopardic Journal*, 18: 118–123.

Nicholson, R.A. 1996. Bone degradation, burial medium and species representation: debunking the myths, an experiment-based approach, *Journal of Archaeological science*, 23: 513–533.

Nielsen-Marsh, C.M., 2000. The chemical degradation of bone, In: Cox, M., Mays, M. (eds.) *Human Osteology in Archaeology and Forensic Science*. London: Greenwich Medical Media: 439–454.

Nielsen-marsh, C.M., Smith, C., Jans, M.M.E., Nord, A., Kars, H., Collins, M.J. 2007. Bone diagenesis in the European Holocene II : taphonomic and environmental considerations, *Journal of Archaeological Science*, 34: 1523–1531.

Nielsen-Marsh, C.M., Hedges, R.E. 2000. Patterns of diagenesis in bone I: the effects of site environments, *Journal of Archaeological Science*, 27(12): 1139–1150.

Norman, D.G., Watson, D.G., Burnett, B., Fenne, P.M., Williams, M.A. 2018. The cutting edge: Micro-CT for quantitative toolmark analysis of sharp force trauma to bone, *Forensic Science International*, 283: 156–172.

O'Callaghan, P.T., Jones, M.D., James, D.S., Leadbeatter, S., Holt, C.A., Nokes, L.D. 1999. Dynamics of stab wounds: force required for penetration of various cadaveric human tissues, *Forensic Science International*, 104: 173–178.

Office for National Statistics 2015. *Chapter 2: Violent Crime and Sexual Offences - Overview*. Available at: http://www.ons.gov.uk/ons/dcp171776_394478.pdf.

Olsen, S.L. 1988. Surface modification on bones: trampling versus butchery, *Journal of Archaeological Science*, 15: 535–553.

Olszta, M.J., Cheng, X., Jee, S.S., Kumar, R., Kim, Y., Kaufman, M.J., Douglas, E.P., Gower, L.B. 2007. Bone structure and formation: a new perspective, *Material Science and Engineering*, 58: 77–116.

Outram, A.K. 2001. A new approach to identifying bone marrow and grease exploitation: why the "indeterminate" fragments should not be ignored, *Journal of Archaeological Science*, 28: 401–410.

Owsley, D.W., Ubelaker, D.H., Houck, M.M., Sandness, K.L., Grant, W.E., Craig, E.A., Woltanski, T.J., Peerwani, N. 1995. The role of forensic anthropology in the recovery and analysis of Branch Davidian Compound victims: techniques of analysis, *Journal of Forensic Sciences*, 40(3): 341–348.

Pankowská, A., Spevackova, P., Kasparova, H., Sneberger, J. 2017. Taphonomy of burnt burials: Spatial analysis of bone fragments in their secondary deposition, *International Journal of Osteoarchaeology*, 27(2): 143–154.

Park, J., Son, H. 2018. Weapon use in Korean homicide: Differences between homicides involving sharp and blunt instruments, *Journal of Forensic Sciences*, 63(4): 1134–1137.

Pechal, J.L., Crippen, T.L., Tarone, A.M., Lewis, A.J., Tomberlin, J.K., Benbow, M.E. 2013. Microbial community functional change during vertebrate carrion decomposition, *PLoS ONE*, 8(11): 1–11.

Pechníková, M., Porta, D., Cattaneo, C. 2011. Distinguishing between perimortem

and postmortem fractures : are osteons of any help ?, *International Journal of Legal Medicine*, 125: 591–595.

Peden, M., McGee, K., Sharma, G. 2002. *The Injury Chart Book: A Graphical Overview of the Global Burden of Injuries*. Geneva.

Pelletti, G., Cecchetto, G., Viero, A., Fais, P., Weber, M., Miotto, D., Montisci, M., Viel, G., Giraudo, C. 2017. Accuracy, precision and inter-rater reliability of micro-CT analysis of false starts on bones. A preliminary validation study, *Legal Medicine*, 29: 38–43.

Pelletti, G., Viel, G., Fais, P., Viero, A., Visentin, S., Miotto, D., Montisci, M., Cecchetto, G., Giraudo, C. 2017. Micro-computed tomography of false starts produced on bone by different hand-saws, *Legal Medicine*, 26: 1–5.

Perkins, A. 2012. *An Evaluation of Embalmed Cadaveric Human Tissue in the Investigation of Multiple Freeze and Thaw Cycles on the Histological Morphology of Human Bone*. MSc Dissertation. University of Alberta.

Pinheiro, J. 2006. Decay process of a cadaver, In: Schmitt, A., Cunha, E., Pinheiro, J. (eds.) *Forensic Anthropology and Medicine*. New Jersey: Humana Press: 85–116.

Pinheiro, J., Cunha, E., Symes, S. 2015. Over-interpretation of bone injuries and implications for cause and manner of death, In: Passalacqua, N.V., Rainwater, C.W. 2015. *Skeletal Trauma Analysis: Case studies in context*. Oxford, the UK: Wiley-Blackwell Publishing Ltd: 27-41.

Pokines, J.T. 2009. Forensic recoveries of U.S. war dead and the effects of taphonomy and other site-altering processes, In: Steadman, D.W. (ed.) *Hard Evidence: Case Studies in Forensic Anthropology*. Upper Saddle River, NJ: Prentice Hall: 141–154.

Pokines, J.T., Baker, J.E. 2014. Effects of burial environment on osseous remains, In: Pokines, J.T., Symes, S.A. 2014. Manual of Forensic Taphonomy. Boca Raton, FL: CRC Press: 73-114.

Pokines, J.T. 2016. Taphonomic alterations to terrestrial surface-deposited human osseous Remains in a New England environment, *Journal of Forensic Identification*, 66(1): 59–78.

Pokines, J.T., King, R.E., Graham, D.D., Costello, A.K., Adams, D.M., Pendray, J.M., Rao, K., Siwek, D. 2016. The effects of experimental freeze-thaw cycles to bone as a component of subaerial weathering, *Journal of Archaeological Science: Reports*, 6, pp. 594–602.

Pokines, J.T. 2018. Differential diagnosis of the taphonomic histories of common types of forensic osseous remains, *Journal of Forensic Identification*, 68(1): 87–145.

Pokines, J.T., Faillace, K., Berger, J., Pirtle, D., Sharpe, D., Curtis, A., Lombardi, K., Admans, J. 2018. The effects of repeated wet-dry cycles as a component of bone weathering, *Journal of Archaeological Science: Reports*, 17: 433–441.

Pollock, C.R., Pokines, J.T., Bethard, J.D. 2018. Organic staining on bone from exposure to wood and other plant materials, *Forensic Science International*, 283: 200–210.

Pope, E.J. 2007. *The effects of fire on human remains: characteristics of taphonomy and trauma*. Ph.D. Thesis. University of Arkansas.

Pope, E.J., Smith, O.C. 2004. Identification of traumatic injury in burned cranial bone : an experimental approach, *Journal of Forensic Sciences*, 49(3): 1–10.

Poppa, P., Porta, D., Gibelli, D., Mazzucchi, A., Brandone, A., Grandi, M., Cattaneo, C. 2011. Detection of blunt, sharp Force and gunshot lesions on burnt remains: a cautionary note, *Am J Forensic Med Pathol*, 32(3): 275–279.

Potmesil, M. 2005. *Bone Dispersion , Weathering , and Scavenging of Cattle Bones*. University of Nebraska.

Potts, R., Shipman, P. 1981. Cutmarks made by stone tools on bones from Olduvai Gorge, Tanzania, *Nature*, 291: 577–580.

Pounder, D.J., Reeder, F.D. 2011. Striation patterns in serrated blade stabs to

cartilage, *Forensic Science International*, 208: 91–94.

Pounder, D.J., Sim, L.J. 2011. Virtual casting of stab wounds in cartilage using micro-computed tomography, *J Forensic Med. Pathol.*, 32: 97–99.

Pyle, J.A. 2016. *Using solar radiation as a means for understanding skeletal decomposition through physical changes caused by bone weathering*. MSc Dissertation. Texas State University.

Quatrehomme, G., Bolla, M., Muller, M., Rocca, J.P., Grevin, G., Bailet, P., Ollier, A. 1998. Experimental single controlled study of burned bone: contribution of scanning electron microscopy, *Journal of Forensic Sciences*, 43: 417–422.

Reber, S.L., Simmons, T. 2015. Interpreting Injury Mechanisms of Blunt Force Trauma from Butterfly Fracture Formation, *Journal of Forensic Sciences*, 60(6): 1401–1411.

Reeves, N.M. 2009. Taphonomic effects of vulture scavenging', *Journal of Forensic Sciences*, 54(3): 523–528.

Reinhard, K., Fink, T. 1994. Cremation in southwestern North America: Aspects of taphonomy that affect pathological analysis, *Journal of Archaeological Science*, 21: 597–605.

Rho, J., Kuhn-Spearing, L., Zioupos, P. 1998. Mechanical properties and the hierarchical structure of bone, *Medical Engineering and Physics*, 20: 92–102.

Richards, C.S., Simonsen, T.J., Abel, R.L., Hall, M.J., Schwayn, D.A., Wicklein, M. 2012. Virtual forensic entomology: improving estimates of minimum post-mortem interval with 3D micro-computed tomography, *Forensic Science International*, 220: 251–264.

Ritchie, R.O., Kinney, J.H., Kruzic, J.J., Nalla, R.K., 2005. A fracture mechanics and mechanistic approach to the failure of cortical bone, *Fatigue Fract Eng Mater Struct*, 28: 345–371.

Robbins, S., Fairgrieve, S.I., Oost, T.S. 2015. Interpreting the effects of burning on

pre-incineration saw marks in bone, *Journal of Forensic sciences*, 60(S1): S182–S187.

Rodriguez, W.C. 1997. Decomposition of buried and submerged bodies, In: Haglung, W.D., Sorg, M.H. *Forensic Taphonomy: The Postmortem Fate of Human Remains*. Boca Raton, FL: CRC Press: 457–467.

Rodriguez, W.C., Bass, W.M. 1985. Decomposition of buried bodies and methods that may aid in their location, *Journal of Forensic Sciences*, 30(3): 836–852.

Rogde, S., Hougen, H.P., Poulsen, K. 2000. Homicide by sharp force in two Scandinavian capitals, *Forensic Science International*, 109: 135–145.

Rogers, C.J. 2010. *Dating death: Forensic taphonomy and the postmortem interval*. Ph.D. Thesis. University of Wolverhampton.

Ross, A.H., Cunningham, S.L. 2011. Time-since-death and bone weathering in a tropical environment, *Forensic Science International*, 204: 126–133.

Rutty, G.N., Brough, A., Biggs, M.J., Robinson, C., Lawes, S.D., Hainsworth, S.V. 2013. The role of micro-computed tomography in forensic investigations, *Forensic Science International*, 225: 60–66.

Sahar, N.D., Hong, S.I., Kohn, D.H. 2005. Micro- and nano-structural analyses of damage in bone, *Micron*, 36: 617–629.

Sauer, N.J. 1998. The timing of injuries and manner of death: Distinguishing among antemortem, perimortem and postmortem trauma. In: Reichs, K.J. (ed.) *Forensic Osteology: Advances in the Identification of Human Remains*. Springfield, IL: Charles C Thomas: 321–332.

Saukko, P.J., Knight, B. 2015. *Knight's Forensic Pathology*. 4th edition. London: Taylor and Francis Ltd.

Saville, P.A., Hainsworth, S.V., Rutty, G.N. 2007. Cutting crime: the analysis of the "uniqueness" of saw marks on bone, *International Journal of Legal Medicine*, 121: 349–357.

Scheirs, S., Malgosa, A., Sanchez-Molina, D., Ortega-Sanchez, M., Velazquez-Ameijide, J., Arregui-Dalmases, C., Medallo-Muniz, J., Galtes, I. 2017. New insights in the analysis of blunt force trauma in human bones: Preliminary results, *International Journal of Legal Medicine*, 131: 867–875.

Schmidt, C.W., Uhlig, R. 2012. Light microscopy of microfractures in burned bone, In: Bell, L.S. (ed.) *Forensic Microscopy for Skeletal Tissues: Methods and Protocols*. New York: Humana Press:. 227–234.

Schmidt, U., Pollak, S. 2006. Sharp force injuries in clinical forensic medicine-Findings in victims and perpetrators, *Forensic Science International*, 159(2–3): 113–118.

Schmitt, K.U., Niederer, P.F., Cronin, D.S., Muser, M.H., Walz, F. 2014 *Trauma Biomechanics: An Introduction to Injury Biomechanics*. 4th edition. Berlin: Springer-Verlag.

Schnider, J., Thali, M.J., Ross, S., Oesterhelweg, L., Spendlove, D., Bolliger, S.A. 2009. Injuries due to sharp trauma detected by post-mortem multislice computed tomography (MSCT): A feasibility study, *Legal Medicine*, 11(1): 4–9.

Shaw, K.P., Chung, J.H., Chung, F.C., Tseng, B.Y., Pan, C.H., Yang, K.T., Yang, C.P. 2011. A method for studying knife tool marks on bone, *Journal of Forensic Sciences*, 56(4): 967–971.

Shipman, P. 1983. Early hominid lifestyle: hunting and gathering or foraging and scavenging?, *British Archaeological Report*, 163: 31–49.

Shipman, P., Foster, G., Schoeinger, M. 1984. Burnt bones and teeth: an experimental study of color, morphology, crystal structure and shrinkage, *Journal of Archaeological Science*, 11: 307–325.

Shipman, P., Rose, J. 1983. Early hominids hunting, butchering, and carcass-processing behaviours: approaches to the fossil record, *Journal of Anthropological Archaeology*, 2: 57–96.

Sidrim, J.J.C., Moreira Filho, R.E., Cordeiro, R.A., Rocha, M.F., Caetano, E.P., Monteiro, A.J., Brihante, R.S. 2010. Fungal microbiota dynamics as a postmortem investigation tool: Focus on Aspergillus, Penicillium and Candida species, *Journal of Applied Microbiology*, 108(5): 1751–1756.

Simmons, T. 2017. Post-mortem interval estimation: an overview of techniques, In: Schotsmans, E.M.J., Marquez-Grant, N., Forbes, S.L. (eds.) *Taphonomy of Human Remains: Forensic Analysis of the Dead and the Depositional Environment*. Chichester, West Sussex: Wiley-Blackwell Publishing Ltd: 134-142.

Sitiene, R., Zakaras, A., Pauliukevicius, A., Kisielius, G. 2007. Morphologic, experimental-comparative investigation as an identification of the injuring instrument method, *Forensic Science International*, 167(2–3): 255–260.

Smith, C. 2002. *Modelling diagenesis in archaeological bone*. MSc Dissertation. University of Newcastle-upon-Tyne.

Soil Science Society of America 1997. *Glossary of soil science terms*. Madison. Available at: http://www.soils.org/publications/soils-glossary (Access at 22/02/19).

Spatola, B.F. 2015. Atypical gunshot and blunt force injuries: wounds along the biomechanical continuum, In: Passalacqua, N.V., Rainwater, C.W. (eds.) *Skeletal Trauma Analysis: Case Studies in Context*. Oxford, the UK: Wiley-Blackwell Publishing Ltd: 7-26.

Spennemann, D.H.R., Colley, S.M. 1989. Fire in a Pit: the effects of burning on faunal remais, *Archaeozoologia*, 3(1, 2): 51–64.

Stiner, M.C., Kuhn, S.L., Weiner, S., Bar-Yosef, O. 1995. Differential burning, recrystallization, and fragmentation of archaeological bone, *Journal of Archaeological Science*, 22: 223–237.

Stock, S.R. 2008. *Micro-computed Tomography: Methodology and Application*. Boca Raton, FL: CRC Press.

Stodder, A.L.W. 2008. Taphonomy and the nature of archaeological assemblages,

In: Katzenberg, M.A., Saunders, S.R. (eds.) *Biological Anthropology of the Human Skeleton*. New Jersey: A John Wiley & Sons, Inc: 71–114.

Surabian, D. 2012. *Preservation of buried human remains in soil*. U.S. Department of Agriculture. Connecticut.

Symes, S.A. 1992. *Morphology of saw marks in human bones: identification of class characteristics*. Ph.D. Thesis. University of Tennessee.

Symes, S.A., Williams, J.A., Murray, E.A., Hoffman, J.L., Holland, T.D., Saul, J.M., Saul, F.P., Pope, E.J. 2002. Taphonomic context of sharp-force trauma in suspected cases of human mutilation and dismemberment, In: Haglund, W.D., Sorg, M.H. (eds.) *Advances in Forensic Taphonomy: Method, Theory, and Archaeological Perspectives*. Boca Raton: FL: CRC Press: 403–434.

Symes, S.A., Chapman, E.N., Rainwater, C.W., Cabo, L.L., Myster, S.M.T. 2010. *Knife and saw toolmark analysis in bone: a manual designed for the examination of criminal mutilationand dismemberment*. Available at: https://www.ncjrs.gov/pdffiles1/nij/grants/232227.pdf (Access at 22/05/17).

Symes, S.A., L'Abbé, E.N., Chapman, E.N., Wolff, I., Dirkmatt, D.C. 2012. Interpreting traumatic injury to bone in medicolegal investigations, In: Dirkmaat, D.C. (ed.) *A Companion to Forensic Anthropology*. West Sussex, UK: Wiley-Blackwell Publishing Ltd: 340–389.

Symes, S.A., Dirkmaat, D.C., *Ousley, S., Chapman, E.N., Cabo, L.* 2012. *Recovery and Interpretation of Burned Human Remains*. The U.S. Department of Justice. Available at http://www.ncjrs.gov/pdffiles1/nij/grants/232227.pdf (Access at 01/06/17).

Symes, S.A., L'Abbe, E.N., Stull, K.E., Lacroix, M., Pokines, J.T. 2014, In: Pokines, J.T., Symes, S.A. (eds.). Manual of Forensic Taphonomy. Boca Raton, FL: CRC Press: 341-366.

Symes, S.A., L'Abbe, E.N., Chapman, E.A., Pinheiro, J.E.S. Stull, K.E., Raymond, D. 2014. The Rorschach butterfly: The use of nomenclature in lieu of understanding

the effects and components of kinetic energy in bone trauma interpretations, *Proceedings of the 66th Annual Meeting of the American Academy of Forensic Sciences; February 17-22*. Seattle, WA.

Symes, S.A., Rainwater, C.W., Chapman, E.N., Gipson, D.R., Piper, A.L. 2015. Patterned thermal destruction in a forensic setting, In: Schmidt, C.W., Symes, S.A. (eds.) *The Analysis of Burned Human Remains*. 2nd edition. San Diego, CA: Academic Press: 18–59.

Tappen, M. 1994. Bone weathering in the tropical rain forest, *Journal of Archaeological Science*, 21: 667–673.

Tappen, N.C., Peske, G.R. 1970. Weathering cracks and split-line patterns in archaeological bone, *American Antiquity*, 35(3): 383–386.

Tegtmeyer, C.E. 2012. *A comparative analysis of serrated and non-serrated sharp force trauma to bone*. MSc Dissertation. Texas State University.

Telmon, N., Gaston, A., Chemia, P., Blanc, A., Joffre, F., Rouge, D. 2005. Application of the Suchey-Brooks method to three-dimensional imaging of the pubic symphysis, *Journal of Forensic Sciences*, 50: 507–512.

Tennick, C.J. 2012. *The identification and classification of sharp force trauma on bone using low power microscopy*. Ph.D. Thesis. University of Central Lancashire.

Tersigni, M.A. 2007. Frozen human bone: A microscopic investigation, *Journal of Forensic Sciences*, 52(1): 16–20.

Tersigni-Tarrant, M.A., Langley, N.R. 2017. Forensic anthropology in the United States past and present. In: Langley, N.R., Tersigni-Tarrant, M.A. (eds.) *Forensic Anthropology: A Comprehensive Introduction*. 2nd edition. Boca Raton, FL: CRC Press: 3-22.

Thali, M.J., Taubenreuther, U., Karolczak, M., Braun, M., Brueschweiler, W., Kalender, W.A., Dirnhofer, R. 2003. Forensic microradiology: micro-computed tomography (Micro-CT) and analysis of patterned injuries inside of bone, *Journal of*

Forensic Sciences, 48(6): 1336–1342.

Thali, M.J., Dirnhofer, R., Vock, P. 2009. *The Virtopsy Approach: 3D Optical and Radiological Scanning and Reconstruction in Forensic Medicine*. Boca Raton, FL: CRC Press.

Thompson, T.J.U. 2003. *An experimental study of the effects of heating and burning on the hard tissues of the human body, and its implications for anthropology and forensic science*. Ph.D. Thesis. University of Sheffield.

Thompson, T.J.U. 2004. Recent advances in the study of burned bone and their implications for forensic anthropology, *Forensic Science International*, 146S: 203–205.

Thompson, T.J.U. 2005. Heat-induced dimensional changes in bone and their consequences for forensic anthropology, *Journal of Forensic Sciences*, 50(5): 1–8.

Thompson, T.J.U., Gonçalves, D., Squires, K., Ulguim, P. 2017. Thermal alteration to the body, In: Schotsmans, E.M.J., Marquez-Grant, N., Forbes, S.L. (eds.) *Taphonomy of Human Remains: Forensic Analysis of the Dead and the Depositional Environment*. Oxford: Wiley-Blackwell Publishing Ltd: 318–334.

Thompson, T.J.U. and Inglis, J. (2009) Differentiation of serrated and non-serrated blades from stab marks in bone, *International Journal of Legal Medicine*, 123: 129–135.

Tibbett, M., Carter, D.O., Haslam, T., Major, R., Haslam, R. 2004. A laboratory incubation method for determining the rate of microbiological degradation of skeletal muscle tissue in soil, *Journal of Forensic Sciences*, 49(3): 1–6.

Trovillo, K.A. 2015. *Bone degradation under differing environments*. Ph.D. Thesis. University of Tennessee.

Trueman, C.N.G., Behrensmeyer, A.K., Tuross, N., Weiner, S. 2004. Mineralogical and compositional changes in bones exposed on soil surfaces in Amboseli National Park, Kenya: Diagenetic mechanisms and the role of sediment pore fluids, *Journal*

of Archaeological Science, 31(6): 721–739.

Tsokos, M., Schulz, F. 1999. Indoor postmortem animal interference by carnivores and rodents: report of two cases and review of the literature, *International Journal of Legal Medicine*, 112(2): 115–119.

Tucker, B.K., Hutchinson, D.L., Gilliland, M., Charles, T.M., Daniel, H.J., Wolfe, L.D. 2001. Microscopic characteristics of hacking trauma, *Journal of Forensic Sciences*, 46(2): 228–233.

Tumer, A.R., Karacaoglu, E., Namli, A., Keten, A., Farasat, S., Akcan, R., Sert, O., Odabasi, A.B. 2013. Effects of different types of soil on decomposition: An experimental study, *Legal Medicine*, 15: 149–156.

Turner-Walker, G. 2008. The chemical and microbial degradation of bone and teeth, In: Pinhasi, R., Mays, S. (eds.) *Advances in Human Paleopathology*. Chichester, West Sussex: John Wiley and Sons: 3–31.

Turner-Walker, G., Syversen, U. 2002. Quantifiying histological changes in archaeological bone using BSE-SEM image analysis, *Archaeometry*, 44(3): 461–468.

Turner, C., Burr, D.B. 1993. Basic biomechanical measurements of bone: a tutorial, *Bone*, 14: 595–608.

Tutken, T., Vennemann, T.W. 2011. Fossil bones and teeth: preservation or alteration of biogenic compositions ?, *Palaeogeography, Palaeoclimatology, Palaeoecology*, 310: 1–8.

Ubelaker, D.H. 1997. Taphonomuic applications in forensic anthropology, In: Haglund, W.D., Sorg, M.H. (eds.) *Forensic Taphonomy: The Postmortem Fate of Human Remains*. Boca Raton, FL: CRC Press: 77–87.

Ubelaker, D.H. 2009. The forensic evaluation of burned skeletal remains: A synthesis, *Forensic Science International*, 183: 1–5.

Ubelaker, D.H. 2015. Case applications of recent research on thermal effects on the

skeleton, In: Thompson, T. (ed.) *The Archaeology of Cremation*. Oxford: Oxbow books: 213–226.

Ubelaker, D.H., Adams, B.J. 1995. Differentiation of perimortem and postmortem trauma using taphonomic indicators, *Journal of Forensic Sciences*, 40(3): 509–512.

Ubelaker, D.H., Zarenko, K.M. 2011. Adipocere: what is known after over two centuries of research, *Forensic Science International*, 208(1–3): 167–172.

Vandervoorte, F.M. 2004. Age calculation using X-ray microfocus computed tomographic scanning of teeth: a pilot study, *Journal of Forensic Sciences*, 49: 787–790.

Vass, A.A., Bass, W.M., Wolt, J.D., Foss, J.E., Ammons, J.T. 1992. Time since death determinations of human cadavers using soil solution, *Journal of Forensic Sciences*, 37(5): 1236–1253.

Vassalini, M., Verzeletti, A., de Ferrari, F. 2014. Sharp force injury fatalities: a retrospective study (1982-2012) in Brescia (Italy), *Journal of Forensic Sciences*, 59(6): 1568–1574.

Vegh, E.I., Rando, C. 2019. Effects of heat as a taphonomic agent on kerf dimensions, *Archaeological and Environmental Forensic Science*, 2: 105–118.

Viguet-Carrin, S., Garnero, P., Delmas, P.D. 2006. The role of collagen in bone strength, *Osteoporosis International*, 17(3): 319–336.

Wakely, J. 1993. The uses of scanning electron microscopy in the interpretation of some examples of trauma in human skeletal remains, In: Grupe, G.G. (ed.) *The Histology of Ancient Human Bone*. Berlin: Springer-Verlag: 205–218.

Waldron, T. 1987. The relative survival of the human skeleton: implications for paleopathology, In: Boddington, A., Garland, A., Janaway, R. (eds.) *Death, Decay and Reconstruction: Approaches to Archaeology and Forensic Science*. Manchester: Manchester University press: 55–64.

Walker, P.L., Long, J.C. 1977. An experimental study of the morphological

characteristics of tool marks, *American Antiquity*, 4: 605–616.

Walsh-Haney, B.A. 1999. Sharp-force trauma analysis and the forensic anthropologist : techniques advocated by William R.Maples, Ph.D, *Journal of Forensic Sciences*, 44(4): 720–723.

Waltenberger, L., Schutkowski, H. 2017. Effects of heat on cut mark characteristics, *Forensic Science International*, 271: 49–58.

Wang, X., Mabrey, J.D., Agrawal, C.M. 1998. An interspecies comparison of bone fracture properties, *Bio-medical Materials and Engineering*, 8: 1–9.

Waterhouse, K. 2013a. Post-burning fragmentation of calcined bone: Implications for remains recovery from fatal fire scenes, *Journal of Forensic and Legal Medicine*, 20: 1112–1117.

Waterhouse, K. 2013b. The effect of victim age on burnt bone fragmentation : Implications for remains recovery, *Forensic Science International*, 231: 409.e1-409.e7.

Waterhouse, K. 2013c. The effect of weather conditions on burnt bone fragmentation, *Journal of Forensic and Legal Medicine*, 20: 489–495.

Webb, E., Wyatt, J.P., Henry, J., Busuttil, A. 1999. A comparison of fatal with non-fatal knife injuries in Edinburgh, *Forensic science international*, 99(3): 179–87.

Wenham, S.J. 1989. Anatomical interpretations of Anglo-Saxon weapon injuries, In: Chadwick, H.S. (ed.) *Weapons and welfare in Anglo-Saxon England. Oxford: Oxford Committee for Archaeology Monograph No.21*. Oxford: 123–139.

Wheatley, B.P. 2008. Perimortem or postmortem bone fractures? An experimental study of fracture patterns in deer femora, *Journal of Forensic Sciences*, 53(1): 69–72.

White, E.M., Hannus, A.L. 1983. Chemical weathering of bone in archaeological soils, *American Antiquity*, 48(1): 316–322.

White, T.D., Black, M.T., Folkens, P.A. 2012. *Human Osteology*. 3rd edition. London: Academic Press.

Whyte, T.R. 2001. Distinguishing remains of human cremations from burned animal bones, *Journal of Field Archaeology*, 28(3–4): 437–448.

Wieberg, D.A.M., Wescott, D.J. 2008. Estimating the timing of long bone fractures : correlation between the postmortem interval, bone moisture content, and blunt force trauma fracture characteristics, *Journal of Forensic Sciences*, 53(5): 1028–1034.

Willey, P., Galloway, A., Snyder, L. 1997. Human bone mineral densities and survival of bone elements: a contemporary sample, In: Haglund, W.D., Sorg, M.H. (eds.) *Forensic Taphonomy: The Postmortem Fate of Human Remains*. Boca Raton, FL: CRC Press: 295–318.

Willey, P., Heilman, A. 1987. Estimating time since death using plant roots and stems, *Journal of Forensic Sciences*, 32(5): 1264–1270.

Wise, L.M., Wang, Z., Grynpas, M.D. 2007. The use of fractography to supplement analysis of bone mechanical properties in different strains of mice, *Bone*, 41(4): 620–630.

Wright, C.S. 2009. *Perimortem and postmortem fracture patterns in deer femora*. MSc Dissertation. The University of Alabama.

Wynnyckyj, C., Wise-Milestone, L., Omelon, S., Wang, Z., Grynpas, M. 2011. Fracture surface analysis to understand the failure mechanisms of collagen degraded bone, *J Bone Miner Metab*, 29: 359–368.

Young, A. 2017. The effects of terrestrial mammalian scavenging and avian scavenging on the body, In: Schotsmans, E.M.J., Marquez-Grant, N., Forbes, S.L. (eds.). *Taphonomy of HumanRremains: Forensic Analysis of the Dead and the Depositional Environment*. Chichester, West Sussex: Wiley-Blackwell Publishing Ltd: 212-234.

Zephro, L., Galloway, A. 2014. The biomechanics of fracture production, In: Wedel,

V.L., Galloway, A. (eds.). *Broken Bones: Anthropological Analysis of Blunt Force Trauma*. 2nd edition. Springfield, IL: Charles C Thomas: 33-45.

Zephro, L., Galloway, A., Wedel, V.L. 2014. Theoretical considerations in designing experimental trauma Studies and implementing their results, In: Wedel, V.L., Galloway, A. (eds.) *Broken Bones: Anthropological Analysis of Blunt Force Trauma*. 2nd edition. Springfield, IL: Charles C Thomas: 73–89.

Zioupos, P., Currey, J.D., Casinos, A. 2000. Exploring the effects of hypermineralization in bone tissue by using an extreme biological example, *Connect. Tissue Res.*, 41: 229–248.

APPENDIX

APPENDIX 1: Sample reference

Sample number	Trauma type	Heat exposure	Depositional environment	Exposure time
Rib 6S-01	Sharp trauma	No	Surface	6 months
Rib 6S-02	Sharp trauma	No	Surface	6 months
Rib 6S-03	Sharp trauma	No	Surface	6 months
Rib 6S-04	Sharp trauma	No	Surface	6 months
Rib 6S-05	Sharp trauma	No	Surface	6 months
Rib 6S-06	Sharp trauma	No	Surface	6 months
Rib 6S-07	Sharp trauma	No	Surface	6 months
Rib 6S-08	Sharp trauma	No	Surface	6 months
Rib 6S-09	Sharp trauma	No	Surface	6 months
Rib 6S-10	Sharp trauma	No	Surface	6 months
Rib 6B-01	Sharp trauma	No	Burial	6 months
Rib 6B-02	Sharp trauma	No	Burial	6 months
Rib 6B-03	Sharp trauma	No	Burial	6 months
Rib 6B-04	Sharp trauma	No	Burial	6 months
Rib 6B-05	Sharp trauma	No	Burial	6 months
Rib 6B-06	Sharp trauma	No	Burial	6 months
Rib 6B-07	Sharp trauma	No	Burial	6 months
Rib 6B-08	Sharp trauma	No	Burial	6 months
Rib 6B-09	Sharp trauma	No	Burial	6 months
Rib 6B-10	Sharp trauma	No	Burial	6 months
Rib 12S-01	Sharp trauma	No	Surface	12 months
Rib 12S-02	Sharp trauma	No	Surface	12 months
Rib 12S-03	Sharp trauma	No	Surface	12 months
Rib 12S-04	Sharp trauma	No	Surface	12 months
Rib 12S-05	Sharp trauma	No	Surface	12 months
Rib 12S-06	Sharp trauma	No	Surface	12 months
Rib 12S-07	Sharp trauma	No	Surface	12 months
Rib 12S-08	Sharp trauma	No	Surface	12 months
Rib 12S-09	Sharp trauma	No	Surface	12 months
Rib 12S-10	Sharp trauma	No	Surface	12 months
Rib 12B-01	Sharp trauma	No	Burial	12 months

Sample number	Trauma type	Heat exposure	Depositional environment	Exposure time
Rib 12B-02	Sharp trauma	No	Burial	12 months
Rib 12B-03	Sharp trauma	No	Burial	12 months
Rib 12B-04	Sharp trauma	No	Burial	12 months
Rib 12B-05	Sharp trauma	No	Burial	12 months
Rib 12B-06	Sharp trauma	No	Burial	12 months
Rib 12B-07	Sharp trauma	No	Burial	12 months
Rib 12B-08	Sharp trauma	No	Burial	12 months
Rib 12B-09	Sharp trauma	No	Burial	12 months
Rib 12B-10	Sharp trauma	No	Burial	12 months
Rib 18S-01	Sharp trauma	No	Surface	18 months
Rib 18S-02	Sharp trauma	No	Surface	18 months
Rib 18S-03	Sharp trauma	No	Surface	18 months
Rib 18S-04	Sharp trauma	No	Surface	18 months
Rib 18S-05	Sharp trauma	No	Surface	18 months
Rib 18S-06	Sharp trauma	No	Surface	18 months
Rib 18S-07	Sharp trauma	No	Surface	18 months
Rib 18S-08	Sharp trauma	No	Surface	18 months
Rib 18S-09	Sharp trauma	No	Surface	18 months
Rib 18S-10	Sharp trauma	No	Surface	18 months
Rib 18B-01	Sharp trauma	No	Burial	18 months
Rib 18B-02	Sharp trauma	No	Burial	18 months
Rib 18B-03	Sharp trauma	No	Burial	18 months
Rib 18B-04	Sharp trauma	No	Burial	18 months
Rib 18B-05	Sharp trauma	No	Burial	18 months
Rib 18B-06	Sharp trauma	No	Burial	18 months
Rib 18B-07	Sharp trauma	No	Burial	18 months
Rib 18B-08	Sharp trauma	No	Burial	18 months
Rib 18B-09	Sharp trauma	No	Burial	18 months
Rib 18B-10	Sharp trauma	No	Burial	18 months
Femur 6S-1	Chopping trauma	No	Surface	6 months
Femur 6S-2	Chopping trauma	No	Surface	6 months
Femur 6S-3	Chopping trauma	No	Surface	6 months
Femur 6B-1	Chopping trauma	No	Burial	6 months
Femur 6B-2	Chopping trauma	No	Burial	6 months
Femur 6B-3	Chopping trauma	No	Burial	6 months

Sample number	Trauma type	Heat exposure	Depositional environment	Exposure time
Femur 12S-1	Chopping trauma	No	Surface	12 months
Femur 12S-2	Chopping trauma	No	Surface	12 months
Femur 12S-3	Chopping trauma	No	Surface	12 months
Femur 12B-1	Chopping trauma	No	Burial	12 months
Femur 12B-2	Chopping trauma	No	Burial	12 months
Femur 12B-3	Chopping trauma	No	Burial	12 months
Femur 18S-1	Chopping trauma	No	Surface	18 months
Femur 18S-2	Chopping trauma	No	Surface	18 months
Femur 18S-3	Chopping trauma	No	Surface	18 months
Femur 18B-1	Chopping trauma	No	Burial	18 months
Femur 18B-2	Chopping trauma	No	Burial	18 months
Femur 18B-3	Chopping trauma	No	Burial	18 months
Femur 6BC-1	Blunt trauma	No	Control	-
Femur 6BC-2	Blunt trauma	No	Control	-
Femur 6BC-3	Blunt trauma	No	Control	-
Femur 6BC-4	Blunt trauma	No	Control	-
Femur 6BC-5	Blunt trauma	No	Control	-
Femur 6BC-6	Blunt trauma	No	Control	-
Femur 6BS-1	Blunt trauma	No	Surface	6 months
Femur 6BS-2	Blunt trauma	No	Surface	6 months
Femur 6BS-3	Blunt trauma	No	Surface	6 months
Femur 6BS-4	Blunt trauma	No	Surface	6 months
Femur 6BS-5	Blunt trauma	No	Surface	6 months
Femur 6BS-6	Blunt trauma	No	Surface	6 months
Femur 6BB-1	Blunt trauma	No	Burial	6 months
Femur 6BB-2	Blunt trauma	No	Burial	6 months
Femur 6BB-3	Blunt trauma	No	Burial	6 months
Femur 6BB-4	Blunt trauma	No	Burial	6 months
Femur 6BB-5	Blunt trauma	No	Burial	6 months
Femur 6BB-6	Blunt trauma	No	Burial	6 months
Femur 12BS-1	Blunt trauma	No	Surface	12 months
Femur 12BS-2	Blunt trauma	No	Surface	12 months
Femur 12BS-3	Blunt trauma	No	Surface	12 months
Femur 12BS-4	Blunt trauma	No	Surface	12 months
Femur 12BS-5	Blunt trauma	No	Surface	12 months

Sample number	Trauma type	Heat exposure	Depositional environment	Exposure time
Femur 12BS-6	Blunt trauma	No	Surface	12 months
Femur 12BB-1	Blunt trauma	No	Burial	12 months
Femur 12BB-2	Blunt trauma	No	Burial	12 months
Femur 12BB-3	Blunt trauma	No	Burial	12 months
Femur 12BB-4	Blunt trauma	No	Burial	12 months
Femur 12BB-5	Blunt trauma	No	Burial	12 months
Femur 12BB-6	Blunt trauma	No	Burial	12 months
Femur 18BS-1	Blunt trauma	No	Surface	18 months
Femur 18BS-2	Blunt trauma	No	Surface	18 months
Femur 18BS-3	Blunt trauma	No	Surface	18 months
Femur 18BS-4	Blunt trauma	No	Surface	18 months
Femur 18BS-5	Blunt trauma	No	Surface	18 months
Femur 18BS-6	Blunt trauma	No	Surface	18 months
Femur 18BB-1	Blunt trauma	No	Burial	18 months
Femur 18BB-2	Blunt trauma	No	Burial	18 months
Femur 18BB-3	Blunt trauma	No	Burial	18 months
Femur 18BB-4	Blunt trauma	No	Burial	18 months
Femur 18BB-5	Blunt trauma	No	Burial	18 months
Femur 18BB-6	Blunt trauma	No	Burial	18 months
Rib 2wkS-01	Sharp trauma	Yes	Surface	2 weeks
Rib 2wkS-02	Sharp trauma	Yes	Surface	2 weeks
Rib 2wkS-03	Sharp trauma	Yes	Surface	2 weeks
Rib 2wkS-04	Sharp trauma	Yes	Surface	2 weeks
Rib 2wkS-05	Sharp trauma	Yes	Surface	2 weeks
Rib 2wkS-06	Sharp trauma	Yes	Surface	2 weeks
Rib 2wkS-07	Sharp trauma	Yes	Surface	2 weeks
Rib 2wkS-08	Sharp trauma	Yes	Surface	2 weeks
Rib 2wkS-09	Sharp trauma	Yes	Surface	2 weeks
Rib 2wkS-10	Sharp trauma	Yes	Surface	2 weeks
Rib 2wkB-01	Sharp trauma	Yes	Burial	2 weeks
Rib 2wkB-02	Sharp trauma	Yes	Burial	2 weeks
Rib 2wkB-03	Sharp trauma	Yes	Burial	2 weeks
Rib 2wkB-04	Sharp trauma	Yes	Burial	2 weeks
Rib 2wkB-05	Sharp trauma	Yes	Burial	2 weeks
Rib 2wkB-06	Sharp trauma	Yes	Burial	2 weeks

Sample number	Trauma type	Heat exposure	Depositional environment	Exposure time
Rib 2wkB-07	Sharp trauma	Yes	Burial	2 weeks
Rib 2wkB-08	Sharp trauma	Yes	Burial	2 weeks
Rib 2wkB-09	Sharp trauma	Yes	Burial	2 weeks
Rib 2wkB-10	Sharp trauma	Yes	Burial	2 weeks
Rib 4wkS-01	Sharp trauma	Yes	Surface	4 weeks
Rib 4wkS-02	Sharp trauma	Yes	Surface	4 weeks
Rib 4wkS-03	Sharp trauma	Yes	Surface	4 weeks
Rib 4wkS-04	Sharp trauma	Yes	Surface	4 weeks
Rib 4wkS-05	Sharp trauma	Yes	Surface	4 weeks
Rib 4wkS-06	Sharp trauma	Yes	Surface	4 weeks
Rib 4wkS-07	Sharp trauma	Yes	Surface	4 weeks
Rib 4wkS-08	Sharp trauma	Yes	Surface	4 weeks
Rib 4wkS-09	Sharp trauma	Yes	Surface	4 weeks
Rib 4wkS-10	Sharp trauma	Yes	Surface	4 weeks
Rib 4wkB-01	Sharp trauma	Yes	Burial	4 weeks
Rib 4wkB-02	Sharp trauma	Yes	Burial	4 weeks
Rib 4wkB-03	Sharp trauma	Yes	Burial	4 weeks
Rib 4wkB-04	Sharp trauma	Yes	Burial	4 weeks
Rib 4wkB-05	Sharp trauma	Yes	Burial	4 weeks
Rib 4wkB-06	Sharp trauma	Yes	Burial	4 weeks
Rib 4wkB-07	Sharp trauma	Yes	Burial	4 weeks
Rib 4wkB-08	Sharp trauma	Yes	Burial	4 weeks
Rib 4wkB-09	Sharp trauma	Yes	Burial	4 weeks
Rib 4wkB-10	Sharp trauma	Yes	Burial	4 weeks

APPENDIX 3

3.A ImageJ Program for length and surface area measurement

ImageJ is a free downloadable Java-based image processing and analysis software inspired by NIH image for the Macintosh (free download from http://imagej.en.softonic.com/mac). It can be used for area and pixel value calculation for an area-defined selection, as well as distance and angle (Kooi and Fairgrieve, 2013). This software can also be applied to forensic image processing such as histological age-at-death estimation (Kranioti, E., personal communication).

A common method using for kerf width measurement is explained step-by-step here.

1. Open the image by going to File> Open> Select image
2. Go to magnifying glass symbol and press to close up on the image (Figure 3.A.1)
3. Click on the straight line tool and draw a line over the reference scale on the image: click on Analyse> Set scale> Known distance> introduce the known distance (for example 1 mm) > then click OK (Figure 3.A.2)
4. Go to Straight, segmented and try to cover an interested area on the picture (Figure 3.A.3)
5. In case of area measurement, the freehand selection is selected to draw a line cover the interesting area (Figure 3.A.4).
6. Go to Analyse> Measure and see the results (Figure 3.A.5)

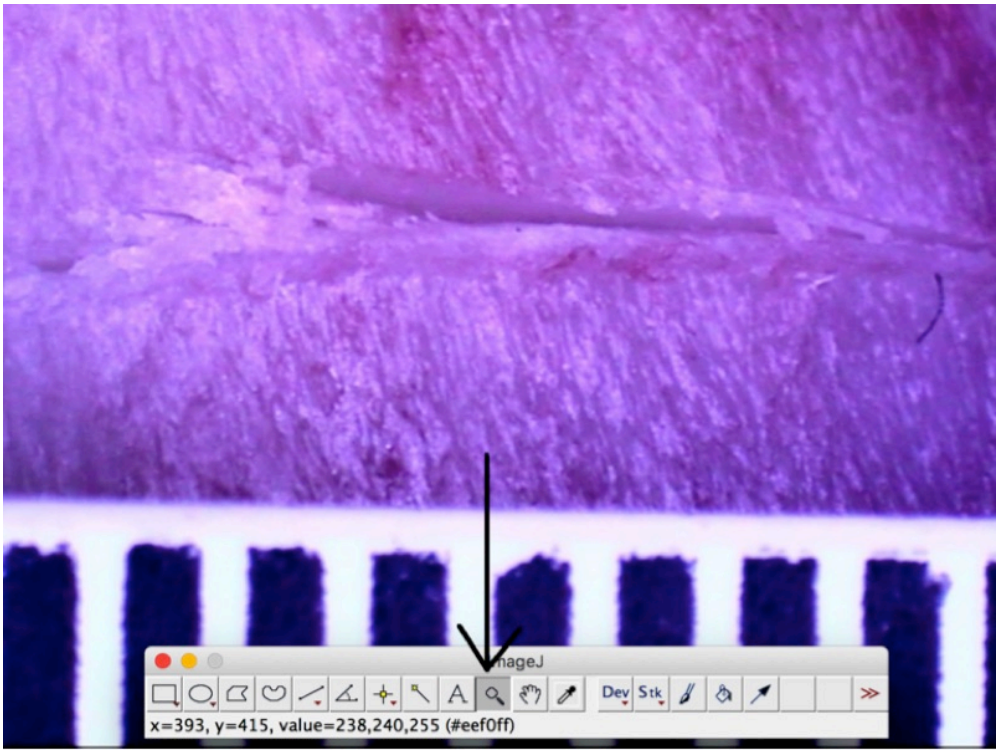

Figure 3.A.1: Illustration of picture after zoom-in; the black arrow points at magnifying glass symbol

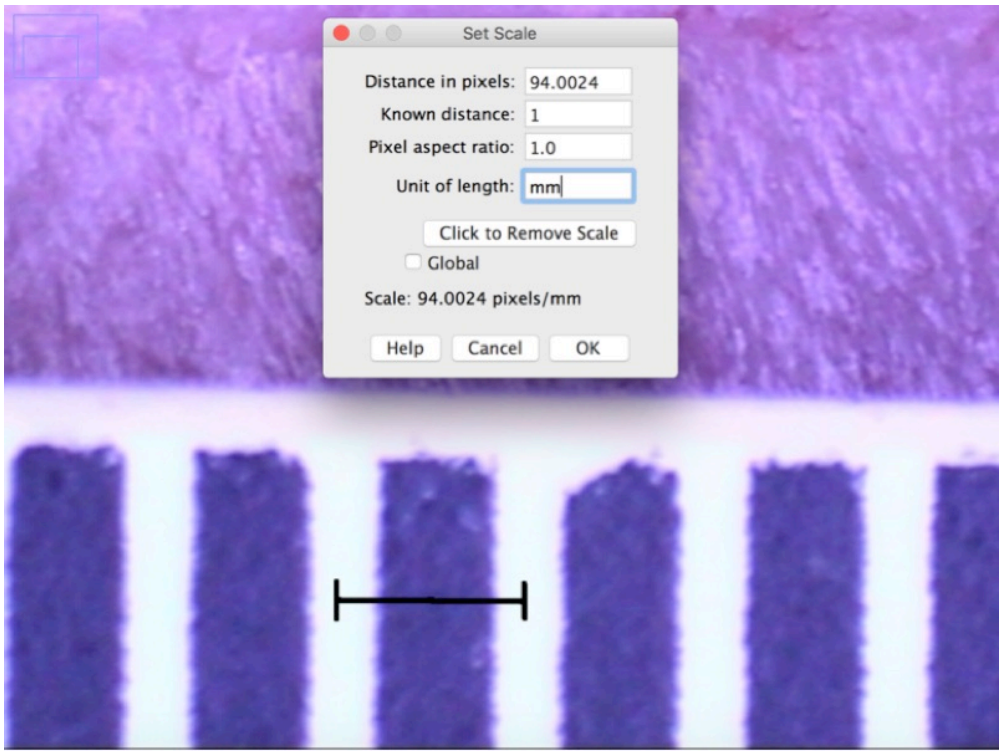

Figure 3.A.2: Illustration of length referencing method; a black line is a referencing line

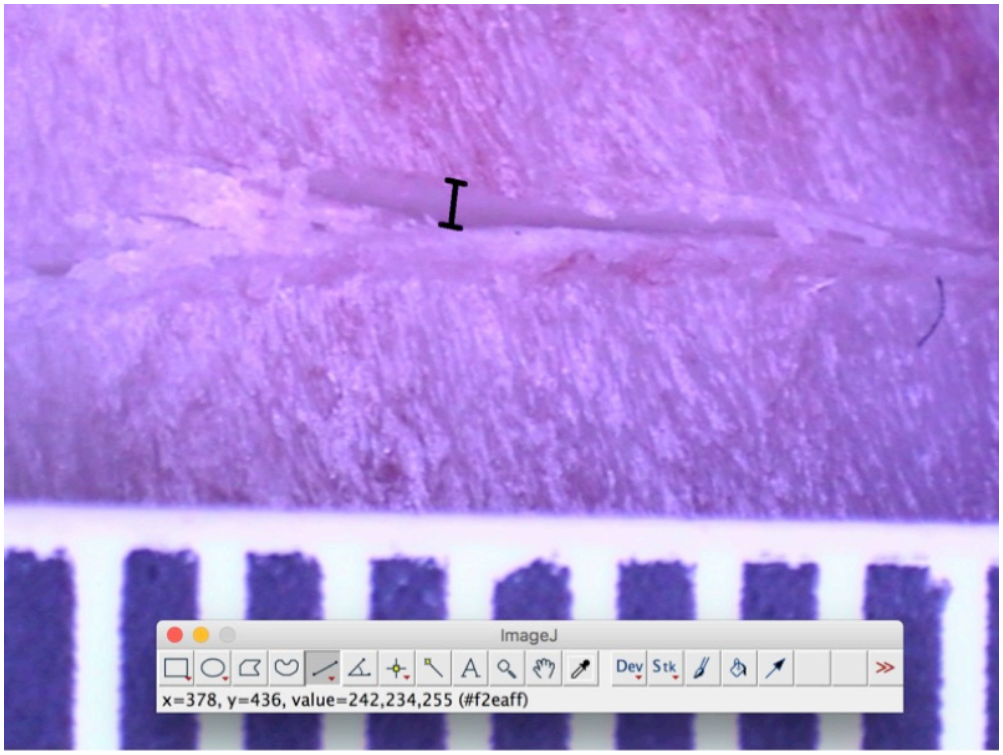

Figure 3.A.3: Illustration of drawing line at an interesting area; a black line is a drawing line between area

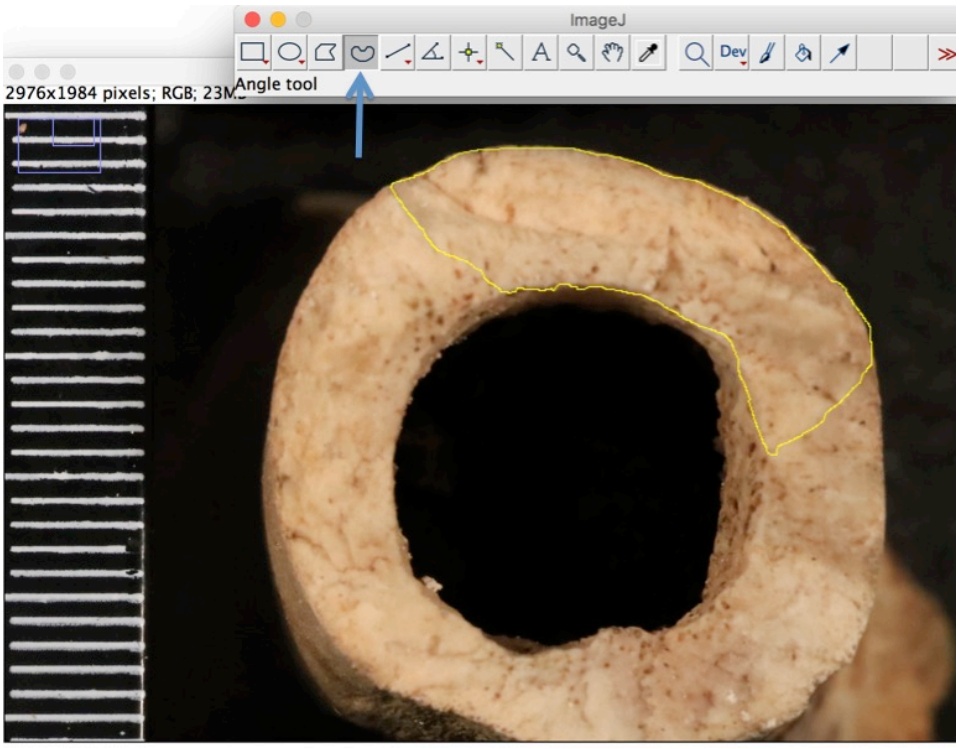

Figure 3.A.4: Illustration of drawing line at an interesting area; the black arrow points at the freehand selection

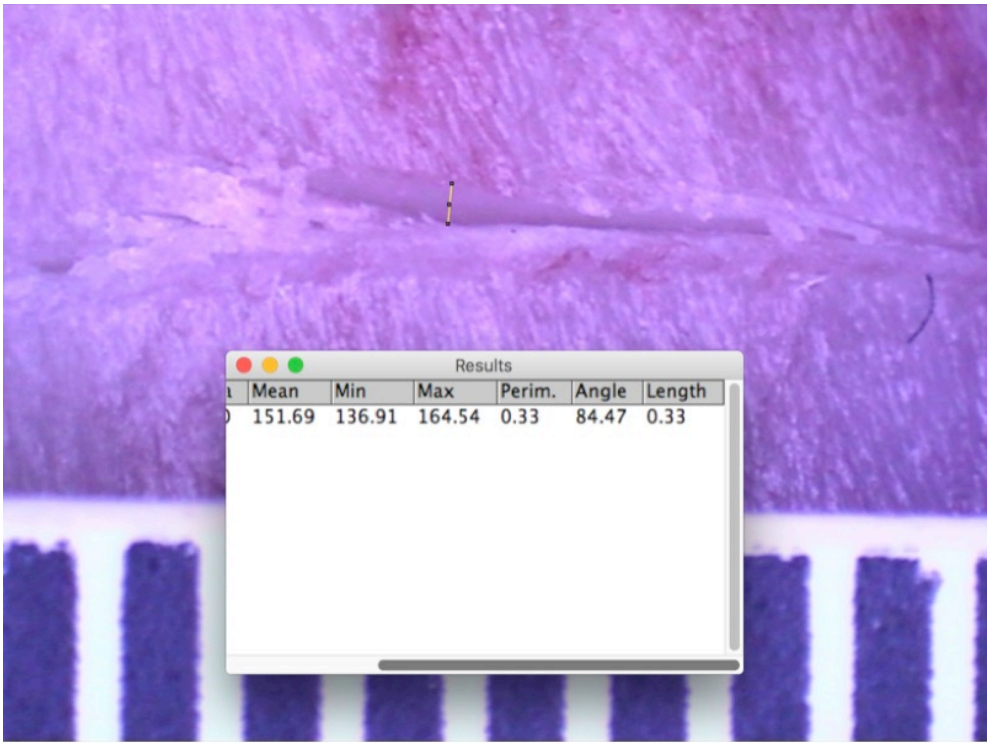

Figure 3.A.5: Result of the measurement

3.B VGStudio MAX 2.1 Micro-CT image processing

The objective of this chapter is to guide the reader through steps of micro-CT VGL image processing by VGStudio MAX 2.1. The observer used a series of micro-CT of femoral samples for analysis. Model-independent methods were chosen in order to make assumptions of underlying geometry. First, an 8-bit grayscale three-dimensional image was processed with noise reduction to a smoothened version of the 3D image. Then, the observer applied a threshold to binarize the image with the dark background. Afterwards, developmental parameters were used to collect experimental data. Processing steps were recorded with VGStudio MAX 2.1 software's commands.

Step 1: Launch the program and import the data into the program

Start VGStudio MAX 2.1 from the Windows start menu, then select File > Open file to upload data. The top, right, and front views as well as three-dimensional view of the micro-CT images were shown (Figure 3.B.1).

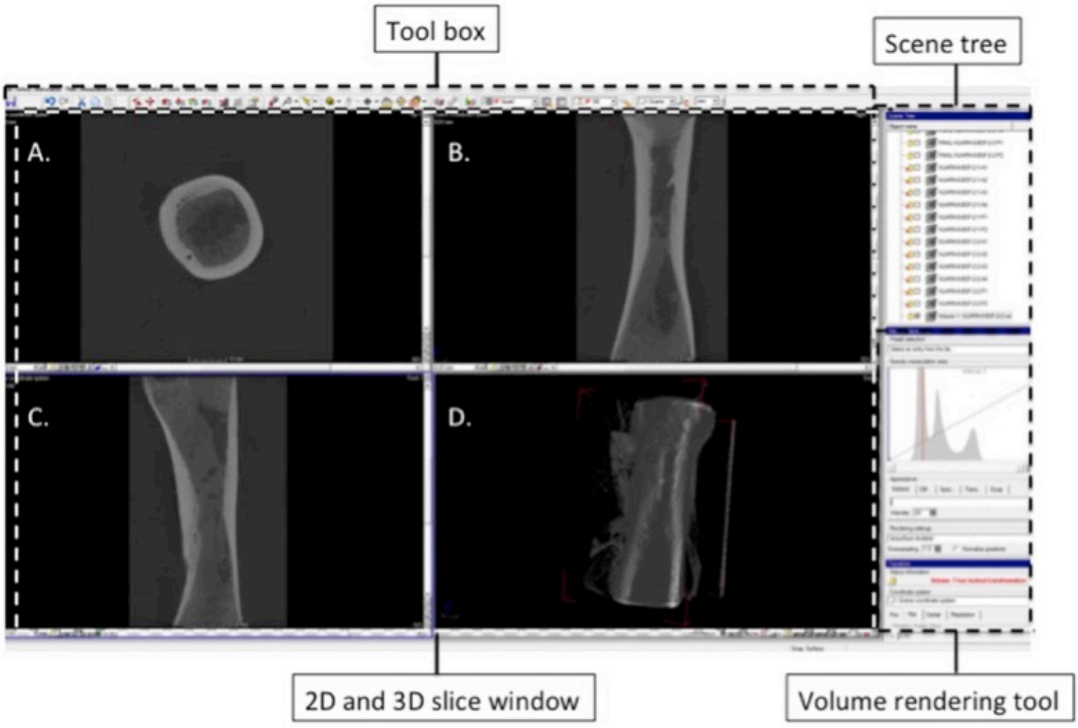

Figure 3.B.1: Overview of VGStudio MAX 2.1 screen; A, B, and C slice windows represent 2D window; D window represent 3D window

Step 2: Volume rendering setting

Select volume renderer (Phong) and adjust mage histogram in order to acquire the best exposure and contrast images (Figure 3.B.2).

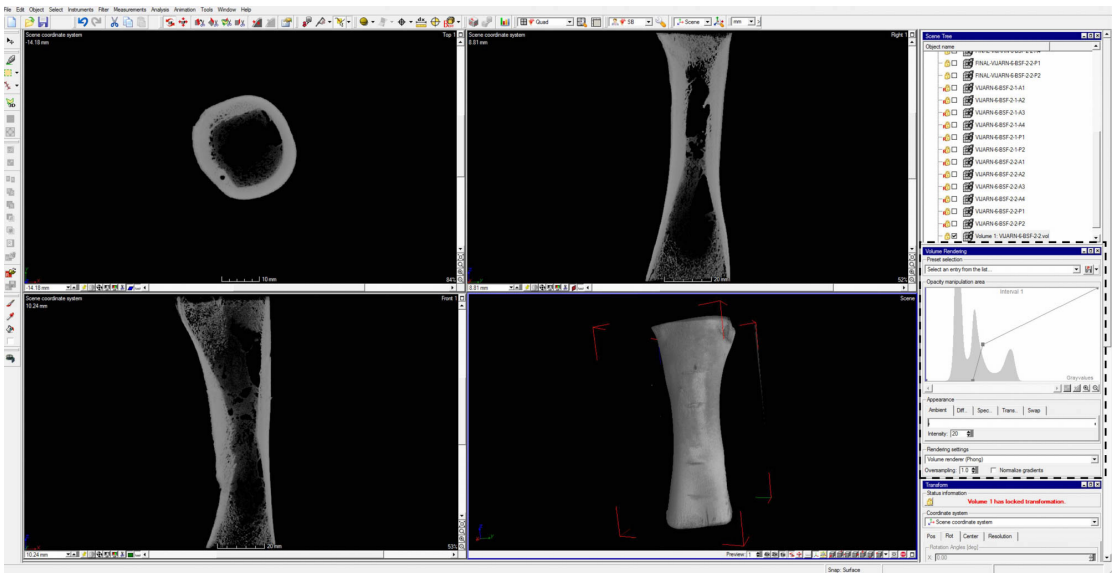

Figure 3.B.2: Volume rendering setting; dashed-line box demonstrating area for volume render settings tool

Step 3: Identify the interesting cut mark with navigation cursor activation

Step 4: Region of interest (ROI) setting

Activate the checkbox ROI (select > selection mode > ellipse), adjust ROI for a specified area of the interesting volume (due to long bone shape, elliptical area is the most suitable) (Figure 3.B.3).

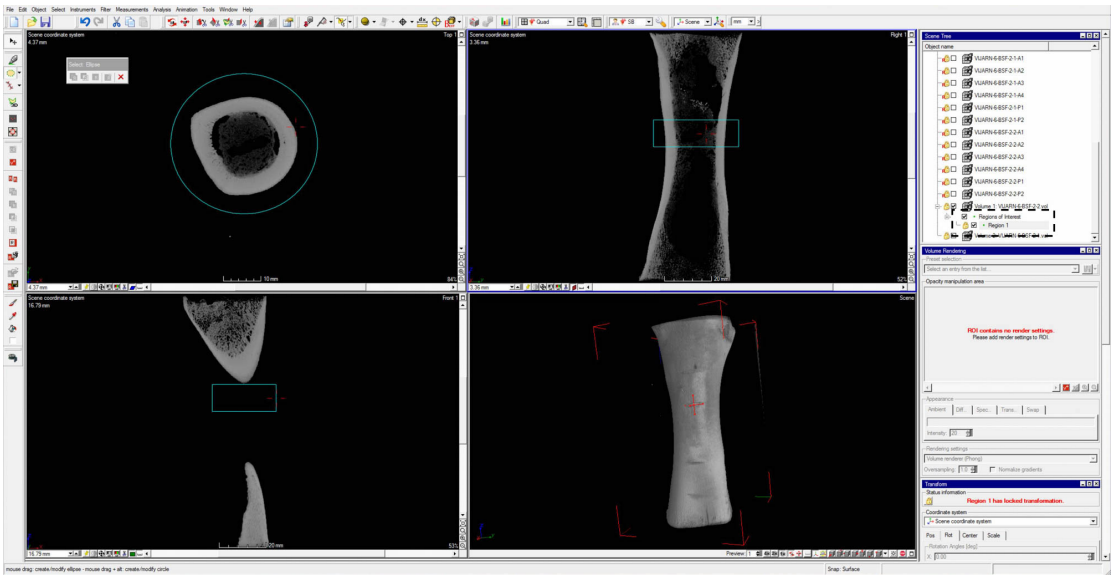

Figure 3.B.3: Region of interest showed with blue regions in top and right images; dashed-line box demonstrating adjustable ROI name

Step 5: ROI extraction, then do ROI determination again with corresponding image (in this case, both pre-exposure and post-exposure bone samples were prepared for image analysis).

Step 6: At this point, both pre-exposure and post-exposure images had to be adjusted to the same position. Each 3D-image surface was determined (click surface determination command) (Figure 3.B.4) in order to prepare 3D-images' surface for their dimensional fit.

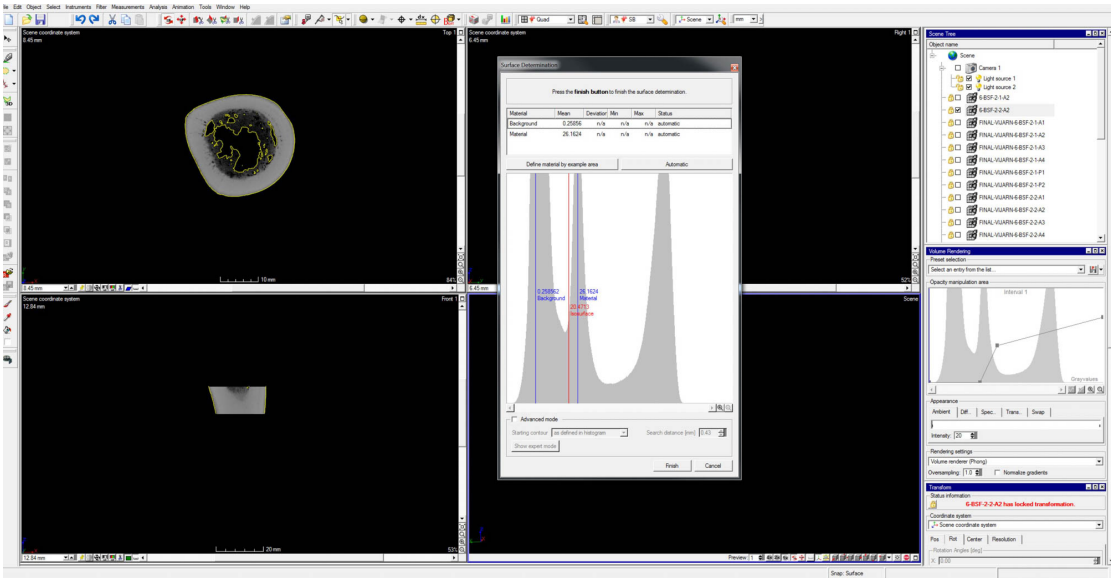

Figure 3.B.4: Surface determination process

Step 7: Once the surface determination process finished, the volume-rendering tool has to be updated.

Step 8: Reference 3D-object was adjusted its orientation and angle to appropriate position (click simple registration command) (Figure 3.B.5).

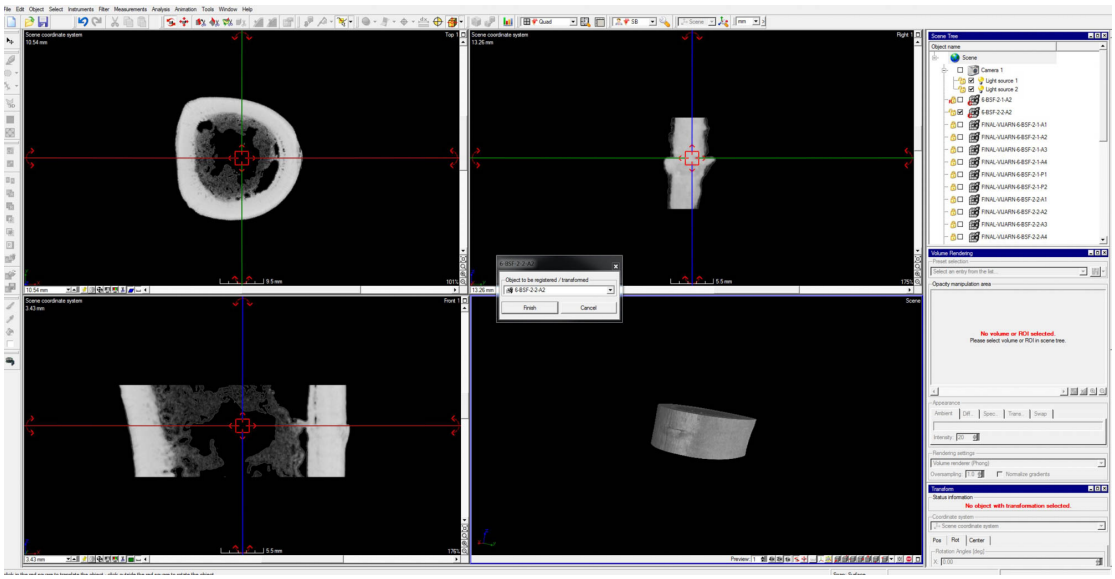

Figure 3.B.5: Image adjustment to suitable position

Step 9: 3D-datasets are compared their external and internal surface between two objects (click register object command > best fit with registered object from step 8) (Figure 3.B.6). This was result in a rough but quick alignment of the two objects.

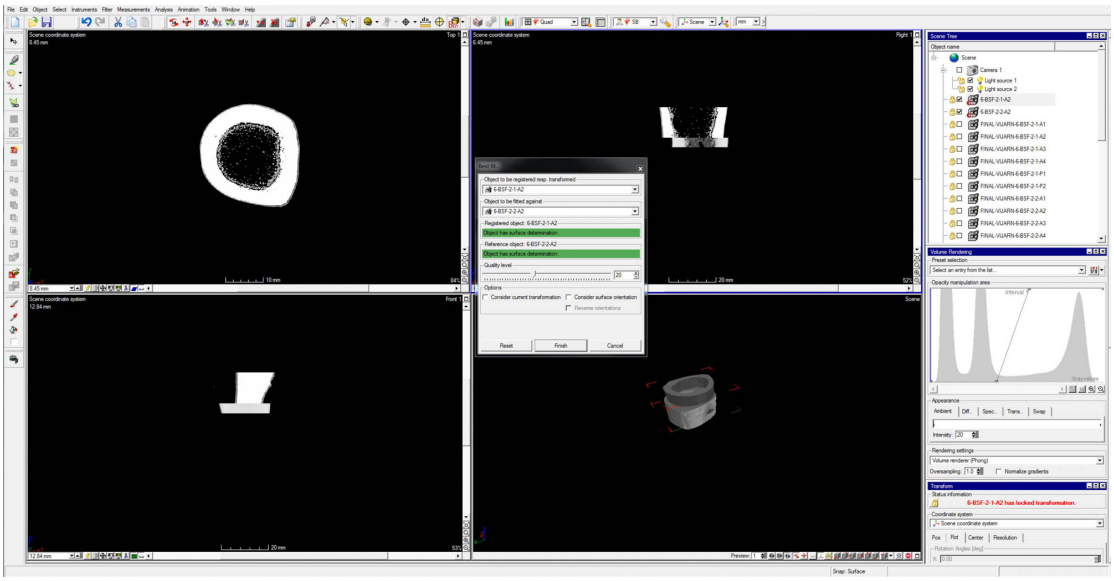

Figure 3.B.6: Best fit command

Step 10: Reselect register object > best fit, and choose consider surface orientation and move the quality level to the right. After finish this step, a high quality fit was completely prepared based on the reference position (Figure 3.B.7).

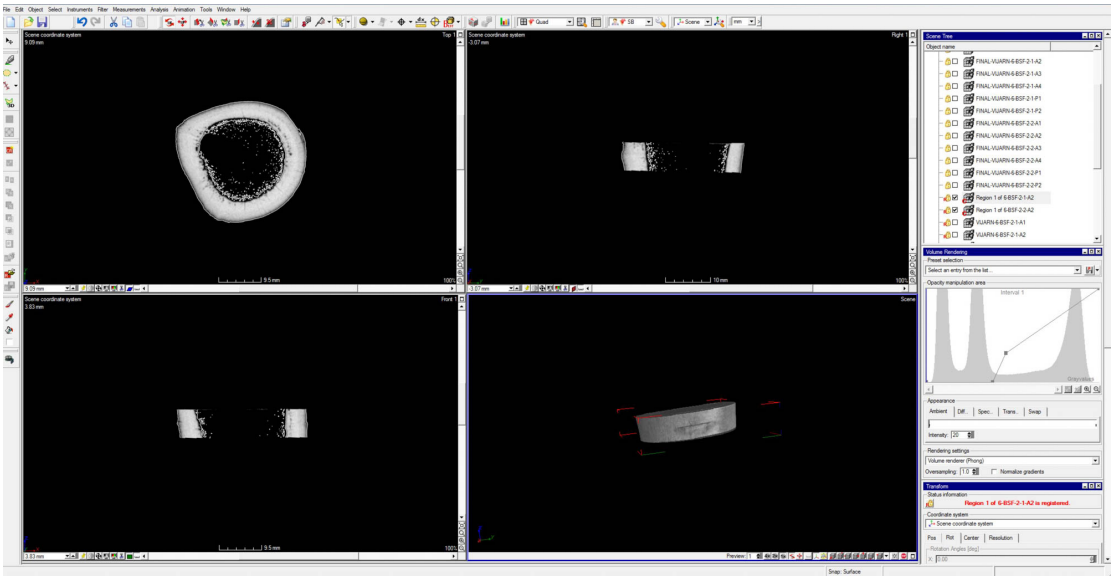

Figure 3.B.7: The high quality fit between two datasets

Step 11: The datasets were prepared for export. Surface determination was removed, and volume rendering was set up to volume renderer (Phong).

Step 12: The datasets were saved as a series of TIFF image (click File > save AVI/ image stack). 2D views were separately saved as top, right and front view. Image slice range start and end, as well as number of slice and distance in millimetre, were set up as appropriate (Figure 3.B.8).

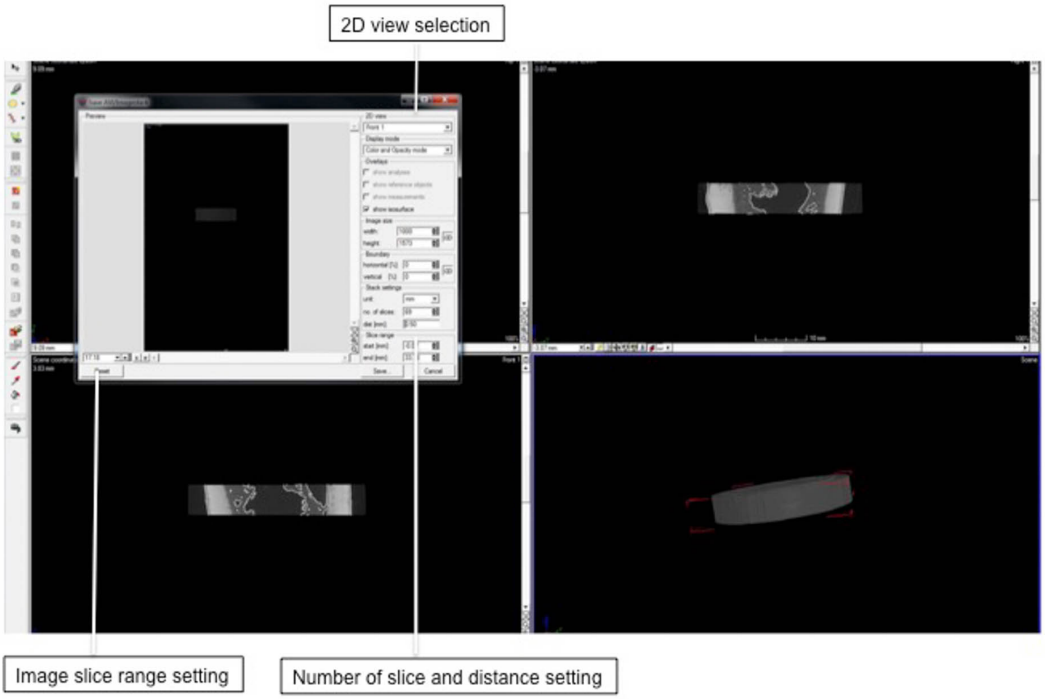

Figure 3.B.8: AVI export command

APPENDIX 4

Table 4.A: Average values of weather data during the experimental period at F3 taphonomic facility, Shrivenham campus of Cranfield University, Oxfordshire, United Kingdom

Month and year	Average temperature (°C)	Average precipitation (mm)	Average hours of sunshine (hr)	Average speed of wind (kn)
Sep'16	16.4	1.57	4.1	6
Oct'16	11.1	0.8	3.5	6
Nov'16	6.1	3.38	2.8	7
Dec'16	5.7	1.1	1.5	4
Jan'17	3.7	2.4	1.8	5
Feb'17	6.3	1.6	1.5	7
Mar'17	9.2	1.9	3.5	8
Apr'17	9.6	0.34	5.9	5
May'17	13.8	2.0	5.2	7
Jun'17	17.0	1.4	6.7	6
Jul'17	17.9	3.4	5.2	6
Aug'17	16.3	2.2	4.9	5
Sep'17	14.0	2.28	3.8	5
Oct'17	12.8	0.9	2.6	6
Nov'17	6.9	2.3	3.1	5
Dec'17	5.1	3.72	1.5	7
Jan'18	5.7	2.6	1.8	8
Feb'18	3.0	1.2	3.8	8
Mar'18	5.3	3.25	2.2	8
Apr'18	10.5	2.2	2.8	7
May'18	13.9	2.9	7.5	6
Jun'18	17.0	0.1	8.0	7
Jul'18	20.5	0.5	9.0	6
Aug'18	17.7	1.7	5.8	5

Table 4.B: General F3 soil property

Date and month	Soil pH	Soil moisture (%)
2nd Sep 2016	6.0	13.479
4th Nov 2016	5.9	15.624
3rd Jan 2017	5.9	19.559
14th Mar 2017	6.2	24.119
25th May 2017	6.4	25.539
7th Jul 2017	6.2	21.398
8th Sep 2017	6.0	23.398
20th Oct 2017	5.8	20.445
1st Dec 2017	5.9	24.376
25th Jan 2018	6.0	26.903
14th Mar 2018	6.1	24.823
20th May 2018	6.2	23.271
6th Jul 2018	6.0	14.696
30th Aug 2018	6.0	10.335

APPENDIX 5

5.1 Non-serrated knife

Table 5.A: Summary of kerf dimension of cut marks from non-serrated knife (in mm); Pre-E: Pre-exposure; Post-E: Post-environmental exposure; each n=10

Sample group	Size	6-months (n=12)		12-months (n=12)		18-months (n=12)	
		Pre-E	Post-E	Pre-E	Post-E	Pre-E	Post-E
Surface	Length	8.601±1	8.06±1.1	8.06±1.16	7.23±1.42	9.28±1.01	8.32±1.03
	Width	0.14±0.02	0.12±0.02	0.14±0.02	0.13±0.02	0.14±0.02	0.12±0.02
Burial	Length	9.48±1.04	8.95±0.89	7.88±1.51	7.36±1.41	8.46±0.98	7.82±1.01
	Width	0.14±0.02	0.14±0.02	0.14±0.02	0.13±0.01	0.15±0.03	0.13±0.02

Table 5.B: Summary of statistical significance of kerf dimension of cut marks from non-serrated knife between the pre-exposure and the post-exposure marks

Sample group	Dimension	6-months exposure	12-months exposure	18-months exposure
Surface	Length	t=-0.816, df=18, p=0.4382	t=-1.021, df=18, p=0.3373	t=-1.479, df=18, p=0.1774
	Width	t=-1.089, df=18, p=0.308	t=-0.822, df=18, p=0.4349	t=-1.633, df=18, p=0.1411
Burial	Length	t=-0.88, df=18, p=0.4047	t=-0.568, df=18, p=0.5854	t=-1.011, df=18, p=0.3415
	Width	t=-0.119, df=18, p=0.9081	t=-1.307, df=18, p=0.2277	t=-1.037, df=18, p=0.3303

Table 5.C: Statistical significance of cut marks morphology of the ribs from non-serrated knife between the pre-exposure and the post-exposure marks

	Kerf morphology	6-months exposure	12-months exposure	18-months exposure
Surface group	Kerf shape	Fisher's test: p=1	Fisher's test: p=0.4737	Fisher's test: p=0.2105
	Cross-sectional shape	Fisher's test: p=1	Fisher's test: p=0.6285	Fisher's test: p=0.3498
Buried group	Kerf shape	Fisher's test: p=1	Fisher's test: p=1	Fisher's test: p=0.4737
	Cross-sectional shape	Fisher's test: p=1	Fisher's test: p=1	Fisher's test: p=1

5.2 Coarse-serrated knife

Table 5.D: Summary of kerf dimension of cut marks from coarse-serrated knife (in mm); Pre-E: Pre-exposure; Post-E: Post-environmental exposure; each n=10

Sample group	Size	6-months (n=12)		12-months (n=12)		18-months (n=12)	
		Pre-E	Post-E	Pre-E	Post-E	Pre-E	Post-E
Surface	Length	8.52±1.01	8.06±1.1	8.79±1.63	7.9±1.35	8.47±0.95	7.41±0.88
	Width	0.38±0.04	0.35±0.04	0.43±0.05	0.39±0.04	0.4±0.03	0.37±0.02
Burial	Length	7.66±1.23	7.41±1.1	9.16±1.37	8.61±1.34	8.27±0.68	7.49±0.6
	Width	0.38±0.05	0.34±0.06	0.41±0.03	0.39±0.04	0.4±0.04	0.37±0.03

Table 5.E: Summary of statistical significance of kerf dimension of cut marks from coarse-serrated knife between the pre-exposure and the post-exposure marks

Sample group	Dimension	6-months exposure	12-months exposure	18-months exposure
Surface	Length	t=-0.856 df=18, p=0.4169	t=-0.942, df=18, p=0.3738	t=-1.82, df=18, p=0.1063
	Width	t=-1.157, df=18, p=0.2805	t=-1.233, df=18, p=0.2526	t=-1.612, df=18, p=0.1456
Burial	Length	t=-0.355, df=18, p=0.732	t=-0.638, df=18, p=0.5415	t=-1.96, df=18, p=0.08562
	Width	t=-0.955, df=18, p=0.3674	t=-1.29, df=18, p=0.233	t=-1.359, df=18, p=0.2112

Table 5.F: Statistical significance of cut marks morphology of the ribs from coarse-serrated knife between the pre-exposure and the post-exposure marks

	Kerf morphology	6-months exposure	12-months exposure	18-months exposure
Surface group	Kerf shape	Fisher's test: p=1	Fisher's test: p=0.517	Fisher's test: p=0.357
	Cross-section	Fisher's test: p=1	Fisher's test: p=1	Fisher's test: p=1
	Kerf margin	Fisher's test: p=1	Fisher's test: p=1	Fisher's test: p=0.6499
	Striations	Fisher's test: p=1	Fisher's test: p=0.6499	Fisher's test: p=0.6563
Buried group	Kerf shape	Fisher's test: p=1	Fisher's test: p=1	Fisher's test: p=0.6285
	Cross-section	Fisher's test: p=1	Fisher's test: p=1	Fisher's test: p=1
	Kerf margin	Fisher's test: p=1	Fisher's test: p=1	Fisher's test: p=1
	Striations	Fisher's test: p=1	Fisher's test: p=1	Fisher's test: p=1

5.3 Fine-serrated knife

Table 5.G: Summary of kerf dimension of cut marks from fine-serrated knife (in mm) Pre-E: Pre-exposure; Post-E: Post-environmental exposure; each n=10

Sample group	Size	6-months (n=12)		12-months (n=12)		18-months (n=12)	
		Pre-E	Post-E	Pre-E	Post-E	Pre-E	Post-E
Surface	Length	8.56±0.97	8.12±0.89	8.37±0.65	7.51±0.7	8.57±1.06	7.81±1.02
	Width	0.35±0.04	0.32±0.04	0.35±0.04	0.32±0.03	0.35±0.05	0.31±0.04
Burial	Length	8.07±1.23	7.82±1.28	8.67±1.27	7.96±1.12	8.81±0.91	8.33±0.86
	Width	0.35±0.02	0.33±0.02	0.35±0.02	0.33±0.02	0.34±0.04	0.3±0.03

Table 5.H: Summary of statistical significance of kerf dimension of cut marks from fine-serrated knife between the pre-exposure and the post-exposure marks

Sample group	Dimension	6-months exposure	12-months exposure	18-months exposure
Surface	Length	t=-0.736, df=18, p=0.4827	t=-2.011, df=18, p=0.07918	t=-1.025, df=18, p=0.3354
	Width	t=-1.15, df=18, p=0.2833	t=-1.212, df=18, p=0.2602	t=-1.457, df=18, p=0.1832
Burial	Length	t=-0.314, df=18, p=0.7618	t=-0.944, df=18, p=0.3729	t=-0.855, df=18, p=0.4173
	Width	t=-1.187, df=18, p=0.2693	t=-1.407, df=18, p=0.197	t=-1.401, df=18, p=0.1989

Table 5.I: Statistical significance of cut marks morphology of the ribs from fine-serrated knife between the pre-exposure and the post-exposure marks

	Kerf morphology	6-months exposure	12-months exposure	18-months exposure
Surface group	Kerf shape	Fisher's test: p=1	Fisher's test: p=0.7214	Fisher's test: p=0.1734
	Cross-sectional shape	Fisher's test: p=1	Fisher's test: p=0.582	Fisher's test: p=0.2105
	Kerf margin	Fisher's test: p=1	Fisher's test: p=1	Fisher's test: p=1
	Striations	Fisher's test: p=1	Fisher's test: p=1	Fisher's test: p=1
Buried group	Kerf shape	Fisher's test: p=1	Fisher's test: p=0.7214	Fisher's test: p=0.4427
	Cross-sectional shape	Fisher's test: p=1	Fisher's test: p=1	Fisher's test: p=1
	Kerf margin	Fisher's test: p=1	Fisher's test: p=1	Fisher's test: p=1
	Striations	Fisher's test: p=1	Fisher's test: p=1	Fisher's test: p=0.6285

5.4 Raw data

Table 5.J: Raw data of pre-exposure ribs; 6-month group

Number	Non-serrated blade						Coarse-serrated blade						Fine-serrated blade					
	L	W	KS	CS	KM	KSt	L	W	KS	CS	KM	KSt	L	W	KS	CS	KM	KSt
6S-01	7.177	0.15	Linear	Narr.	Smo.	Abs.	7.36	0.43	Ellip.	U	Raise	Pre.	7.18	0.33	Ellip.	V	Smo.	Pre.
6S-02	8.31	0.12	Linear	Narr.	Smo.	Abs.	8.42	0.37	Ellip.	V	Smo.	Pre.	9.11	0.38	Ellip.	V	Smo.	Abs.
6S-03	9.672	0.17	Linear	Narr.	Smo.	Abs.	7.99	0.36	Ellip.	V	Smo.	Abs.	8.73	0.4	Ellip.	V	Raise	Pre.
6S-04	8.092	0.13	Linear	V	Smo.	Abs.	8.31	0.32	Rect.	V	Raise	Pre.	8.46	0.29	Irreg.	V	Smo.	Abs.
6S-05	9.355	0.11	Linear	Narr.	Smo.	Abs.	8.79	0.4	Rect.	U	Smo.	Pre.	9.69	0.35	Ellip.	V	Smo.	Pre.
6S-06	9.112	0.1	Linear	Narr.	Smo.	Abs.	9.49	0.35	Ellip.	V	Raise	Abs.	8.42	0.34	Ellip.	V	Smo.	Pre.
6S-07	8.77	0.11	Linear	Narr.	Smo.	Abs.	8.61	0.42	Ellip.	V	Raise	Abs.	8.79	0.37	Ellip.	U	Raise	Pre.
6S-08	8.51	0.09	Linear	Narr.	Smo.	Abs.	9.55	0.38	Ellip.	U	Raise	Abs.	8.95	0.35	Ellip.	V	Raise	Pre.
6S-09	8.91	0.12	Linear	V	Smo.	Abs.	7.8	0.32	Ellip.	U	Raise	Pre.	8.44	0.35	Ellip.	V	Smo.	Abs.
6S-10	8.102	0.1	Linear	Narr.	Smo.	Abs.	8.88	0.45	Ellip.	U	Raise	Abs.	7.83	0.34	Ellip.	V	Smo.	Pre.
6B-01	8.05	0.13	Linear	Narr.	Smo.	Abs.	7.61	0.3	Ellip.	V	Raise	Pre.	6.48	0.32	Irreg.	V	Smo.	Pre.
6B-02	10.82	0.12	Linear	Narr.	Smo.	Abs.	8.59	0.38	Ellip.	U	Raise	Pre.	8.39	0.38	Ellip.	U	Smo.	Abs.
6B-03	9.98	0.16	Linear	V	Smo.	Abs.	9.12	0.41	Ellip.	U	Raise	Abs.	9.03	0.36	Ellip.	V	Smo.	Pre.
6B-04	9.59	0.15	Linear	Narr.	Smo.	Abs.	6.08	0.43	Ellip.	V	Smo.	Pre.	7.13	0.33	Ellip.	U	Smo.	Pre.
6B-05	9	0.15	Linear	V	Smo.	Abs.	6.93	0.36	Ellip.	V	Raise	Abs.	9.33	0.34	Ellip.	V	Smo.	Pre.
6B-06	8.85	0.13	Linear	Narr.	Smo.	Abs.	7.13	0.45	Rect.	V	Raise	Pre.	7.53	0.42	Ellip.	V	Raise	Abs.
6B-07	9.44	0.15	Linear	Narr.	Smo.	Abs.	8.47	0.34	Irreg.	V	Raise	Pre.	8.44	0.33	Irreg.	V	Smo.	Pre.
6B-08	8.69	0.12	Linear	Narr.	Smo.	Abs.	8.06	0.38	Ellip.	U	Smo.	Pre.	7.79	0.36	Ellip.	V	Raise	Abs.
6B-09	10.16	0.14	Linear	Narr.	Smo.	Abs.	7.55	0.41	Ellip.	V	Raise	Pre.	8.49	0.3	Ellip.	V	Smo.	Abs.
6B-10	10.22	0.15	Linear	Narr.	Smo.	Abs.	7.06	0.34	Ellip.	U	Raise	Abs.	8.09	0.36	Ellip.	V	Smo.	Abs.

(Narr.: Narrow; Smo.: Smooth; Abs.: Absent; Ellip.: Ellipse; Rect.: Rectangle; Irreg.: Irregular; Pre.: Present)

Table 5.K: Raw data of post-exposure ribs; 6-month group

Number	Non-serrated blade						Coarse-serrated blade						Fine-serrated blade					
	L	W	KS	CS	KM	KSt	L	W	KS	CS	KM	KSt	L	W	KS	CS	KM	KSt
6S-01	7.56	0.13	Linear	Narr.	Smo.	Abs.	7.85	0.39	Ellip.	U	Smo.	Pre.	7.52	0.36	Ellip.	V	Smo.	Pre.
6S-02	7.88	0.14	Linear	Narr.	Smo.	Abs.	7.96	0.34	Ellip.	V	Smo.	Pre.	8.42	0.34	Ellip.	V	Smo.	Abs.
6S-03	8.11	0.16	Linear	Narr.	Smo.	Abs.	8.55	0.32	Ellip.	V	Smo.	Abs.	8.19	0.35	Ellip.	V	Raise	Pre.
6S-04	9.56	0.11	Linear	V	Smo.	Abs.	7.04	0.3	Rect.	V	Raise	Pre.	8.05	0.27	Irreg.	V	Smo.	Abs.
6S-05	8.65	0.1	Linear	Narr.	Smo.	Abs.	8.21	0.35	Rect.	U	Smo.	Pre.	9.21	0.3	Ellip.	V	Smo.	Pre.
6S-06	8.31	0.13	Linear	Narr.	Smo.	Abs.	8.92	0.41	Ellip.	V	Raise	Abs.	7.45	0.3	Ellip.	V	Smo.	Pre.
6S-07	8.96	0.1	Linear	Narr.	Smo.	Abs.	7.97	0.36	Irreg.	V	Raise	Abs.	8.04	0.33	Ellip.	U	Raise	Pre.
6S-08	7.3	0.13	Linear	Narr.	Smo.	Abs.	8.55	0.37	Ellip.	U	Raise	Abs.	7.82	0.31	Ellip.	V	Raise	Pre.
6S-09	7.17	0.11	Linear	V	Smo.	Abs.	8.11	0.28	Ellip.	U	Raise	Pre.	8.5	0.33	Ellip.	V	Smo.	Abs.
6S-10	7.1	0.09	Linear	Narr.	Smo.	Abs.	7.44	0.38	Ellip.	U	Raise	Abs.	8.03	0.31	Ellip.	V	Smo.	Pre.
6B-01	8.66	0.15	Linear	Narr.	Smo.	Abs.	8.22	0.34	Ellip.	V	Raise	Pre.	7.15	0.3	Irreg.	V	Smo.	Pre.
6B-02	10.08	0.13	Linear	Narr.	Smo.	Abs.	8.04	0.36	Ellip.	U	Raise	Pre.	7.93	0.35	Ellip.	U	Smo.	Abs.
6B-03	9.25	0.14	Linear	V	Smo.	Abs.	8.56	0.37	Ellip.	U	Raise	Abs.	8.47	0.33	Ellip.	V	Smo.	Pre.
6B-04	8.79	0.12	Linear	Narr.	Smo.	Abs.	6.41	0.38	Ellip.	V	Smo.	Pre.	7.78	0.29	Ellip.	U	Smo.	Pre.
6B-05	9.62	0.13	Linear	V	Smo.	Abs.	6.36	0.32	Ellip.	V	Raise	Abs.	8.71	0.36	Ellip.	V	Smo.	Pre.
6B-06	9.54	0.16	Linear	Narr.	Smo.	Abs.	6.78	0.32	Rect.	V	Raise	Pre.	7.19	0.35	Ellip.	V	Raise	Abs.
6B-07	9.06	0.14	Linear	Narr.	Smo.	Abs.	7.52	0.34	Irreg.	V	Raise	Pre.	7.03	0.28	Irreg.	V	Smo.	Pre.
6B-08	10.05	0.16	Linear	Narr.	Smo.	Abs.	8.3	0.33	Ellip.	U	Smo.	Pre.	8.06	0.31	Ellip.	V	Raise	Abs.
6B-09	9.62	0.13	Linear	Narr.	Smo.	Abs.	7.11	0.36	Ellip.	V	Raise	Pre.	7.56	0.32	Ellip.	V	Smo.	Abs.
6B-10	10.13	0.14	Linear	Narr.	Smo.	Abs.	6.8	0.37	Ellip.	U	Raise	Abs.	8.32	0.31	Ellip.	V	Smo.	Abs.

(Narr.: Narrow; Smo.: Smooth; Abs.: Absent; Ellip.: Ellipse; Rect.: Rectangle; Irreg.: Irregular; Pre.: Present)

Table 5.L: Raw data of pre-exposure ribs; 12-month group

Number	Non-serrated blade						Coarse-serrated blade						Fine-serrated blade					
	L	W	KS	CS	KM	KSt	L	W	KS	CS	KM	KSt	L	W	KS	CS	KM	KSt
12S-01	7.57	0.14	Linear	Narr.	Smo.	Abs.	7.45	0.43	Ellip.	V	Smo.	Abs.	8.75	0.35	Ellip.	U	Smo.	Pre.
12S-02	6.57	0.13	Linear	Narr.	Smo.	Abs.	7.02	0.37	Rect.	V	Smo.	Abs.	7.64	0.33	Ellip.	V	Raise	Pre.
12S-03	7.89	0.1	Linear	Narr.	Smo.	Abs.	8.75	0.36	Ellip.	U	Raise	Pre.	7.99	0.37	Ellip.	V	Smo.	Pre.
12S-04	8.61	0.14	Linear	Narr.	Smo.	Abs.	9.75	0.32	Ellip.	V	Raise	Abs.	9.29	0.4	Ellip.	V	Raise	Abs.
12S-05	9.67	0.2	Linear	V	Smo.	Abs.	10.9	0.4	Ellip.	V	Raise	Pre.	8.18	0.3	Ellip.	V	Raise	Pre.
12S-06	9.22	0.09	Linear	Narr.	Smo.	Abs.	9.12	0.45	Rect.	U	Smo.	Pre.	8.82	0.42	Ellip.	V	Smo.	Abs.
12S-07	8.78	0.11	Linear	V	Smo.	Abs.	8.59	0.51	Ellip.	U	Raise	Pre.	7.15	0.32	Ellip.	V	Smo.	Pre.
12S-08	9.95	0.11	Linear	Narr.	Smo.	Abs.	8.77	0.48	Ellip.	V	Raise	Pre.	9.42	0.36	Irreg.	V	Smo.	Abs.
12S-09	9.24	0.08	Linear	Narr.	Smo.	Abs.	9.35	0.54	Ellip.	U	Raise	Pre.	8.1	0.35	Ellip.	V	Smo.	Abs.
12S-10	8.51	0.1	Linear	Narr.	Smo.	Abs.	8.2	0.44	Ellip.	U	Raise	Pre.	8.36	0.3	Ellip.	V	Smo.	Abs.
12B-01	7.81	0.14	Linear	V	Smo.	Abs.	9.45	0.3	Ellip.	V	Smo.	Abs.	8.29	0.32	Ellip.	V	Smo.	Pre.
12B-02	10.82	0.15	Linear	Narr.	Smo.	Abs.	10.1	0.38	Rect.	V	Raise	Pre.	9.29	0.38	Ellip.	V	Raise	Abs.
12B-03	10.23	0.11	Linear	Narr.	Smo.	Abs.	10.6	0.41	Ellip.	U	Raise	Pre.	10.5	0.36	Ellip.	V	Smo.	Pre.
12B-04	8.67	0.13	Linear	Narr.	Smo.	Abs.	8.59	0.43	Ellip.	V	Smo.	Abs.	7.83	0.33	Ellip.	V	Raise	Abs.
12B-05	7.88	0.16	Linear	Narr.	Smo.	Abs.	7.11	0.36	Ellip.	V	Raise	Pre.	8.45	0.34	Ellip.	V	Smo.	Pre.
12B-06	6.55	0.12	Linear	Narr.	Smo.	Abs.	9.12	0.51	Irreg.	U	Raise	Pre.	8.44	0.41	Ellip.	V	Raise	Pre.
12B-07	6.49	0.16	Linear	Narr.	Smo.	Abs.	8.69	0.46	Rect.	V	Raise	Abs.	9.65	0.34	Ellip.	V	Raise	Pre.
12B-08	7.31	0.14	Linear	V	Smo.	Abs.	9.55	0.41	Ellip.	U	Smo.	Pre.	7.58	0.37	Ellip.	V	Smo.	Abs.
12B-09	6.99	0.15	Linear	Narr.	Smo.	Abs.	9.26	0.49	Ellip.	U	Raise	Pre.	8.08	0.32	Irreg.	U	Smo.	Abs.
12B-10	6.05	0.14	Linear	Narr.	Smo.	Abs.	9.13	0.35	Ellip.	U	Raise	Pre.	8.59	0.33	Ellip.	V	Smo.	Pre.

(Narr.: Narrow; Smo.: Smooth; Abs.: Absent; Ellip.: Ellipse; Rect.: Rectangle; Irreg.: Irregular; Pre.: Present)

Table 5.M: Raw data of post-exposure ribs; 12-month group

Number	Non-serrated blade						Coarse-serrated blade						Fine-serrated blade					
	L	W	KS	CS	KM	KSt	L	W	KS	CS	KM	KSt	L	W	KS	CS	KM	KSt
12S-01	6.75	0.13	Linear	Narr.	Smo.	Abs.	6.96	0.37	Ellip.	V	Smo.	Abs.	7.94	0.31	Ellip.	U	Smo.	Pre.
12S-02	6.07	0.12	Linear	V	Smo.	Abs.	6.37	0.37	Rect.	U	Smo.	Abs.	7.02	0.28	Rect.	V	Raise	Pre.
12S-03	6.61	0.13	Linear	Narr.	Smo.	Abs.	8.21	0.34	Ellip.	U	Raise	Pre.	7.45	0.34	Ellip.	V	Smo.	Pre.
12S-04	7.21	0.13	Linear	Narr.	Smo.	Abs.	8.69	0.3	Ellip.	V	Smo.	Abs.	8.48	0.34	Rect.	V	Raise	Abs.
12S-05	8.07	0.17	Ellip.	V	Smo.	Abs.	9.46	0.4	Ellip.	V	Raise	Pre.	7.53	0.28	Ellip.	V	Raise	Pre.
12S-06	8.22	0.09	Linear	V	Smo.	Abs.	8.45	0.4	Rect.	U	Smo.	Pre.	8.01	0.37	Ellip.	U	Smo.	Abs.
12S-07	6.8	0.1	Ellip.	V	Smo.	Abs.	7.73	0.45	Rect.	U	Raise	Abs.	6.65	0.32	Ellip.	V	Smo.	Pre.
12S-08	8.26	0.1	Linear	Narr.	Smo.	Abs.	8.04	0.43	Ellip.	V	Raise	Abs.	8.02	0.33	Irreg.	V	Smo.	Abs.
12S-09	7.68	0.13	Linear	Narr.	Smo.	Abs.	8.52	0.46	Ellip.	U	Smo.	Pre.	6.92	0.35	Ellip.	V	Smo.	Abs.
12S-10	7.13	0.09	Linear	Narr.	Smo.	Abs.	6.74	0.38	Rect.	U	Raise	Pre.	7.08	0.29	Ellip.	V	Smo.	Abs.
12B-01	7.11	0.12	Ellip.	V	Smo.	Abs.	8.76	0.38	Ellip.	V	Smo.	Abs.	7.44	0.29	Rect.	V	Smo.	Pre.
12B-02	10.08	0.13	Linear	Narr.	Smo.	Abs.	9.22	0.34	Rect.	V	Raise	Pre.	8.42	0.34	Ellip.	V	Raise	Abs.
12B-03	9.34	0.13	Linear	Narr.	Smo.	Abs.	9.67	0.38	Ellip.	U	Raise	Pre.	9.04	0.35	Ellip.	V	Smo.	Pre.
12B-04	8.02	0.13	Linear	Narr.	Smo.	Abs.	8.12	0.4	Ellip.	V	Smo.	Abs.	7.13	0.3	Rect.	U	Raise	Abs.
12B-05	7.01	0.14	Linear	Narr.	Smo.	Abs.	7.75	0.36	Ellip.	V	Raise	Pre.	7.36	0.31	Ellip.	V	Smo.	Pre.
12B-06	6.81	0.14	Linear	Narr.	Smo.	Abs.	8.68	0.46	Irreg.	U	Raise	Pre.	8.78	0.37	Ellip.	V	Raise	Pre.
12B-07	5.66	0.13	Linear	Narr.	Smo.	Abs.	8.94	0.39	Rect.	V	Raise	Abs.	8.65	0.37	Ellip.	V	Raise	Pre.
12B-08	6.63	0.11	Linear	V	Smo.	Abs.	8.51	0.39	Ellip.	U	Smo.	Pre.	7.79	0.32	Ellip.	V	Smo.	Abs.
12B-09	6.36	0.13	Linear	Narr.	Smo.	Abs.	8.2	0.45	Ellip.	U	Raise	Pre.	7.44	0.36	Irreg.	U	Smo.	Abs.
12B-10	6.57	0.14	Linear	Narr.	Smo.	Abs.	8.25	0.35	Ellip.	U	Raise	Pre.	7.55	0.29	Ellip.	V	Smo.	Pre.

(Narr.: Narrow; Smo.: Smooth; Abs.: Absent; Ellip.: Ellipse; Rect.: Rectangle; Irreg.: Irregular; Pre.: Present)

Table 5.N: Raw data of pre-exposure ribs; 18-month group

Number	Non-serrated blade						Coarse-serrated blade						Fine-serrated blade					
	L	W	KS	CS	KM	KSt	L	W	KS	CS	KM	KSt	L	W	KS	CS	KM	KSt
18S-01	9.78	0.14	Linear	Narr.	Smo.	Abs.	7.04	0.4	Irreg.	U	Smo.	Abs.	7.12	0.36	Ellip.	V	Smo.	Pre.
18S-02	7.78	0.11	Linear	V	Smo.	Abs.	8.35	0.43	Rect.	U	Raise	Pre.	8.62	0.28	Ellip.	V	Smo.	Pre.
18S-03	8.97	0.15	Linear	Narr.	Smo.	Abs.	8.94	0.44	Rect.	V	Raise	Pre.	8.02	0.4	Ellip.	V	Smo.	Pre.
18S-04	9.05	0.17	Linear	Narr.	Smo.	Abs.	9.61	0.36	Ellip.	V	Smo.	Pre.	9.86	0.38	Ellip.	V	Raise	Pre.
18S-05	10.5	0.13	Linear	Narr.	Smo.	Abs.	8.39	0.38	Ellip.	V	Smo.	Abs.	9.25	0.34	Irreg.	V	Smo.	Abs.
18S-06	8.11	0.13	Linear	Narr.	Smo.	Abs.	8.22	0.42	Ellip.	U	Raise	Abs.	8.46	0.33	Ellip.	V	Smo.	Abs.
18S-07	9.58	0.14	Linear	Narr.	Smo.	Abs.	9.06	0.35	Ellip.	V	Raise	Pre.	8.95	0.36	Ellip.	V	Raise	Pre.
18S-08	9.66	0.15	Linear	Narr.	Smo.	Abs.	8.63	0.45	Ellip.	V	Raise	Pre.	7.57	0.37	Ellip.	V	Raise	Pre.
18S-09	10.1	0.14	Linear	Narr.	Smo.	Abs.	8.94	0.38	Ellip.	V	Raise	Pre.	8.63	0.3	Ellip.	V	Smo.	Abs.
18S-10	9.27	0.14	Linear	V	Smo.	Abs.	7.52	0.39	Ellip.	U	Smo.	Abs.	9.22	0.38	Ellip.	V	Raise	Pre.
18B-01	11.6	0.11	Linear	Narr.	Smo.	Abs.	9.29	0.44	Rect.	U	Smo.	Abs.	10.2	0.32	Irreg.	U	Smo.	Pre.
18B-02	9.85	0.18	Linear	Narr.	Smo.	Abs.	8.42	0.4	Ellip.	V	Raise	Pre.	9.16	0.36	Ellip.	V	Raise	Pre.
18B-03	7.29	0.13	Linear	V	Smo.	Abs.	7.97	0.46	Ellip.	V	Smo.	Pre.	8.62	0.34	Irreg.	V	Smo.	Pre.
18B-04	8.57	0.15	Linear	Narr.	Smo.	Abs.	7.46	0.35	Ellip.	V	Raise	Abs.	8.18	0.38	Ellip.	V	Raise	Abs.
18B-05	7.21	0.16	Linear	Narr.	Smo.	Abs.	8.23	0.37	Ellip.	V	Smo.	Abs.	7.89	0.28	Ellip.	V	Smo.	Abs.
18B-06	7.95	0.13	Linear	V	Smo.	Abs.	8.33	0.44	Rect.	U	Raise	Pre.	9.62	0.41	Ellip.	V	Smo.	Pre.
18B-07	9.05	0.12	Linear	Narr.	Smo.	Abs.	7.69	0.45	Rect.	V	Raise	Pre.	8.7	0.37	Ellip.	V	Smo.	Pre.
18B-08	8.37	0.1	Linear	Narr.	Smo.	Abs.	8.65	0.39	Ellip.	V	Raise	Pre.	9.47	0.36	Ellip.	V	Raise	Pre.
18B-09	6.82	0.13	Linear	Narr.	Smo.	Abs.	8.57	0.32	Ellip.	U	Raise	Pre.	8.02	0.3	Ellip.	V	Smo.	Pre.
18B-10	7.89	0.09	Linear	Narr.	Smo.	Abs.	8.09	0.38	Ellip.	U	Raise	Abs.	8.24	0.28	Ellip.	V	Raise	Pre.

(Narr.: Narrow; Smo.: Smooth; Abs.: Absent; Ellip.: Ellipse; Rect.: Rectangle; Irreg.: Irregular; Pre.: Present)

Table 5.O: Raw data of post-exposure ribs; 18-month group

Number	Non-serrated blade						Coarse-serrated blade						Fine-serrated blade					
	L	W	KS	CS	KM	KSt	L	W	KS	CS	KM	KSt	L	W	KS	CS	KM	KSt
18S-01	8.55	0.13	Ellip.	V	Smo.	Abs.	6.26	0.35	Irreg.	U	Smo.	Abs.	6.49	0.32	Rect.	V	Smo.	Abs.
18S-02	6.68	0.09	Linear	V	Smo.	Abs.	7.34	0.41	Rect.	U	Smo.	Abs.	8.06	0.25	Ellip.	V	Smo.	Pre.
18S-03	8.05	0.13	Linear	Narr.	Smo.	Abs.	8.15	0.4	Rect.	V	Raise	Pre.	7.51	0.35	Irreg.	V	Smo.	Pre.
18S-04	8.43	0.14	Rect.	V	Smo.	Abs.	8.79	0.33	Irreg.	U	Smo.	Pre.	8.83	0.32	Ellip.	V	Raise	Pre.
18S-05	9.62	0.11	Linear	Narr.	Smo.	Abs.	7.57	0.34	Ellip.	V	Smo.	Abs.	8.57	0.29	Irreg.	U	Smo.	Abs.
18S-06	7.42	0.12	Linear	Narr.	Smo.	Abs.	7.13	0.36	Ellip.	U	Raise	Abs.	7.57	0.29	Ellip.	U	Smo.	Abs.
18S-07	8.87	0.12	Linear	V	Smo.	Abs.	7.58	0.3	Irreg.	V	Smo.	Pre.	7.99	0.32	Ellip.	V	Raise	Pre.
18S-08	8.9	0.12	Linear	Narr.	Smo.	Abs.	7.56	0.41	Ellip.	V	Raise	Pre.	7.05	0.35	Rect.	V	Raise	Pre.
18S-09	9.26	0.13	Irreg.	V	Smo.	Abs.	7.81	0.38	Irreg.	U	Raise	Abs.	7.89	0.27	Irreg.	V	Smo.	Abs.
18S-10	7.42	0.13	Linear	Narr.	Smo.	Abs.	5.91	0.35	Ellip.	U	Smo.	Abs.	8.14	0.34	Ellip.	V	Smo.	Pre.
18B-01	10.6	0.1	Linear	Narr.	Smo.	Abs.	8.38	0.4	Rect.	U	Smo.	Abs.	9.59	0.28	Rect.	U	Smo.	Pre.
18B-02	8.99	0.17	Linear	Narr.	Smo.	Abs.	7.31	0.37	Ellip.	V	Raise	Pre.	8.32	0.31	Ellip.	V	Raise	Pre.
18B-03	6.86	0.13	Linear	V	Smo.	Abs.	6.73	0.41	Irreg.	V	Smo.	Pre.	8.04	0.31	Irreg.	V	Smo.	Pre.
18B-04	7.92	0.14	Linear	Narr.	Smo.	Abs.	6.45	0.31	Ellip.	U	Raise	Abs.	7.93	0.33	Ellip.	V	Smo.	Abs.
18B-05	6.77	0.15	Linear	Narr.	Smo.	Abs.	7.59	0.37	Ellip.	V	Smo.	Abs.	7.43	0.26	Ellip.	V	Smo.	Abs.
18B-06	7.43	0.13	Ellip.	V	Smo.	Abs.	7.34	0.37	Rect.	U	Raise	Abs.	9.24	0.36	Ellip.	V	Smo.	Pre.
18B-07	8.44	0.11	Ellip.	V	Smo.	Abs.	6.92	0.36	Irreg.	V	Raise	Pre.	8.23	0.32	Rect.	U	Smo.	Pre.
18B-08	7.64	0.09	Linear	Narr.	Smo.	Abs.	8.11	0.32	Ellip.	V	Smo.	Pre.	8.75	0.31	Irreg.	V	Raise	Abs.
18B-09	6.32	0.12	Linear	Narr.	Smo.	Abs.	7.93	0.25	Ellip.	U	Raise	Pre.	7.55	0.27	Ellip.	V	Smo.	Abs.
18B-10	7.26	0.08	Linear	Narr.	Smo.	Abs.	7.64	0.33	Ellip.	U	Raise	Abs.	7.67	0.25	Ellip.	V	Raise	Pre.

(Narr.: Narrow; Smo.: Smooth; Abs.: Absent; Ellip.: Ellipse; Rect.: Rectangle; Irreg.: Irregular; Pre.: Present)

APPENDIX 6

6.1 Cleaver-inflicted chop mark data

Table 6.A: Summary of kerf dimension of cleaver-inflicted marks (in mm)

Sample group	Size	6-months (n=12)		12-months (n=12)		18-months (n=12)	
		Pre-	Post-	Pre-	Post-	Pre-	Post-
Surface	Length	10.47±0.6	10.16±0.5	9.78±0.43	9.58±0.5	9.82±1.18	9.14±0.8
	Width	1.37±0.08	1.32±0.08	1.34±0.05	1.32±0.03	1.34±0.04	1.31±0.05
Burial	Length	9.969±0.9	9.393±0.8	9.17±0.86	8.81±0.95	8.99±1.13	8.32±1.03
	Width	1.38±0.09	1.36±0.07	1.37±0.07	1.32±0.06	1.37±0.05	1.32±0.05

Table 6.B: Summary of statistical significance of kerf dimension of cleaver-inflicted samples between the pre-exposure and the post-exposure marks

Sample group	Dimension	6-months exposure	12-months exposure	18-months exposure
Surface	Length	t=-1.153, df=22, p=0.266	t=-0.935, df=22, p=0.364	t=-1.423, df=22, p=0.174
	Width	t=-1.23, df=22, p=0.236	t=-1.384, df=22, p=0.185	t=-1.71, df=22, p=0.107
Burial	Length	t=-1.427, df=22, p=0.171	t=-0.826, df=22, p=0.421	t=-1.377, df=22, p=0.185
	Width	t=-0.486, df=22, p=0.633	t=-1.629, df=22, p=0.123	t=-0.626, df=22, p=0.093

Table 6.C: Statistical significance of kerf morphology of cleaver-inflicted samples between the pre-exposure and the post-exposure marks

	Kerf morphology	6-months exposure	12-months exposure	18-months exposure
Surface group	Kerf shape	Fisher test; p=1	Fisher test; p=0.4101	Fisher test; p=0.1787
	Cross-section shape	Fisher test; p=0.6922	Fisher test; p=0.2407	Fisher test; p=0.2407
	Kerf margin	Fisher test; p=1	Fisher test; p=0.4922	X^2 =1.0358, p=0.3088
Buried group	Kerf shape	Fisher test; p=0.712	Fisher test; p=0.7242	Fisher test; p=0.2392
	Cross-section shape	Fisher test; p=0.4304	Fisher test; p=0.6947	Fisher test; p=0.6312
	Kerf margin	Fisher test; p=1	Fisher test; p=0.875	X^2 =1.0358, p=1

Table 6.D: Average and standard deviations of micro-CT parameter of cleaver-inflicted marks (in mm); L: Length; W: Width; D: Depth; PSH: Proximal Shoulder Height; DSH: Distal Shoulder Height; PSA: Proximal Slope Angle; DSA: Distal Slope Angle; OA: Opening Angle

Group		6-months (n=12)		12-months (n=12)		18-months (n=12)	
		Pre-	Post-	Pre-	Post-	Pre-	Post-
Surface	L	10.1±1.1	9.69±0.9	9.81±1.2	9.63±1.06	9.64±1.17	8.76±1.1
	W	1.4±0.1	1.35±0.1	1.38±0.1	1.34±0.05	1.36±0.09	1.31±0.06
	D	2.76±0.1	2.75±0.1	2.74±0.17	2.68±0.15	2.75±0.09	2.69±0.1
	PSH	1.11±0.2	1.06±0.2	1.2±0.15	1.03±0.14	1.11±0.24	1±0.16
	DSH	1.21±0.2	1.13±0.2	1.17±0.14	1.08±0.11	1.16±0.17	1.069±0.1
	PSA	91.54±7.1	89.07±7.9	91.95±6.7	90.33±6	91.8±11.4	89.31±6.6
	DSA	107.6±11	100.3±6.6	94.1±15.3	97.21±6.6	102.6±9.9	101.5±8.1
	OA	15.68±2.9	15.8±2.1	19±4.21	15.77±1.9	16.7±3.7	16.29±1.9
Burial	L	9.31±0.84	8.85±0.59	9.06±0.96	8.57±0.88	8.46±1.22	8.13±1.21
	W	1.39±0.09	1.34±0.07	1.39±0.06	1.35±0.04	1.37±0.06	1.34±0.06
	D	2.68±0.07	2.66±0.05	2.73±0.13	2.65±0.11	2.72±0.06	2.65±0.07
	PSH	1.05±0.2	0.98±0.2	1.01±0.22	0.94±0.22	1.08±0.21	0.99±0.19
	DSH	1.15±0.08	1.09±0.08	1.17±0.18	1.08±0.17	1.18±0.21	1.09±0.19
	PSA	101.6±7.3	103.1±6.9	101.7±14	99.66±12	98.5±13.7	98.9±11.2
	DSA	104.2±12	101.9±8.1	104.4±15	102±10.9	106±11.1	104.7±8.9
	OA	19.59±6.3	18.08±5.2	17.34±6.5	17.37±6.2	23.22±7.5	18.5±4.9

Table 6.E: Statistical differences of micro-CT data of cleaver-inflicted marks (*** statistical significance of the same sample between pre-exposure and post-exposure values)

Sample group	Parameter	6-months exposure	12-months exposure	18-months exposure
Surface group	Length	t=-0.871, df=22, p=0.396	t=-0.337, df=22, p=0.7405	t=-1.628, df=22, p=0.1231
	Width	t=-0.985, df=22, p=0.3394	t=-1.686, df=22, p=0.1112	t=-1.464, df=22, p=0.1625
	Depth	t=-0.388, df=22, p=0.7031	t=-0.881, df=22, p=0.3914	t=-1.474, df=22, p=0.16
	Proximal shoulder height	t=-0.533, df=22, p=0.6011	t=-1.597, df=22, p=0.237	t=-1.161, df=22, p=0.2625
	Distal shoulder height	t=-1.043, df=22, p=0.3123	t=-1.611, df=22, p=0.1267	t=-1.26, df=22, p=0.2259
	Proximal slope angle	t=-0.09, df=22, p=0.9291	t=-0.68, df=22, p=0.5065	t=-0.408, df=22, p=0.6886
	Distal slope angle	t=-1.74, df=22, p=0.1011	t=0.55, df=22, p=0.5899	t=-0.269, df=22, p=0.791
	Opening angle	t=-0.138, df=22, p=0.8921	t=-1.031, df=22, p=0.31	t=-0.299, df=22, p=0.769
Buried group	Length	t=-1.353, df=22, p=0.1948	t=-1.137, df=22, p=0.2722	t=-0.58, df=22, p=0.5703
	Width	t=-1.256, df=22, p=0.2273	t=-1.558, df=22, p=0.1389	t=-1.14, df=22, p=0.2712
	Depth	t=-0.776, df=22, p=0.4488	t=-1.45, df=22, p=0.1663	t=-1.914, df=22, p=0.07362
	Proximal shoulder height	t=-0.689, df=22, p=0.5005	t=-0.622, df=22, p=0.5429	t=-0.976, df=22, p=0.3435
	Distal shoulder height	t=-0.806, df=22, p=0.4978	t=-1.051, df=22, p=0.3089	t=-0.918, df=22, p=0.3723
	Proximal slope angle	t=-0.57, df=22, p=0.5769	t=-0.52, df=22, p=0.61	t=-0.641, df=22, p=0.5305
	Distal slope angle	t=-0.482, df=22, p=0.636	t=-0.453, df=22, p=0.6565	t=-0.214, df=22, p=0.8332
	Opening angle	t=-0.559, df=22, p=0.5842	t=0.045, df=22, p=0.9646	t=-1.575, df=22, p=0.1348

6.2 Machete-inflicted chop mark data

Table 6.F: Summary of kerf dimension of machete-inflicted marks (in mm)

Sample group	Size	6-months (n=12)		12-months (n=12)		18-months (n=12)	
		Pre-E	Post-E	Pre-E	Post-E	Pre-E	Post-E
Surface	Length	10.36±0.6	10.05±0.6	9.467±0.9	9.114±0.85	9.83±0.83	9.217±0.8
	Width	2.47±0.08	2.46±0.04	2.47±0.07	2.53±0.05	2.44±0.05	2.54±0.05
Burial	Length	10.6±1.21	10.02±1.29	9.62±0.84	9.134±0.88	9.8±1.01	9.09±0.96
	Width	2.51±0.08	2.45±0.06	2.49±0.11	2.42±0.09	2.48±0.05	2.5±0.05

Table 6.G: Summary of statistical significance of kerf dimension of machete-inflicted samples between the pre-exposure and the post-exposure marks (*** statistical significance of the same sample between pre-exposure and post-exposure values)

Sample group	Dimension	6-months exposure	12-months exposure	18-months exposure
Surface	Length	t=-1.004, df=22, p=0.3289	t=-0.536, df=22, p=0.5975	t=-1.593, df=22, p=0.1307
	Width	t=-0.43, df=22, p=0.672	t=2.394, df=22, p=0.0256***	t=4.436, df=22, p=0.00415***
Burial	Length	t=-1.027, df=22, p=0.3182	t=-1.262, df=22, p=0.223	t=-1.634, df=22, p=0.1197
	Width	t=-1.01, df=22, p=0.2971	t=-1.512, df=22, p=0.148	t=0.912, df=22, p=0.374

Table 6.H: Statistical significance of kerf morphology of machete-inflicted samples between the pre-exposure and the post-exposure marks (*** statistical significance of the same sample between pre-exposure and post-exposure values)

	Kerf morphology	6-months exposure	12-months exposure	18-months exposure
Surface group	Kerf shape	Fisher test; p=1	Fisher test; p=0.7354	Fisher test; p=0.2706
	Cross-sectional shape	Fisher test; p=1	Fisher test; p=0.4619	Fisher test; p=0.1392
	Kerf margin	Fisher test; p=0.3126	Fisher test; p=0.4136	Fisher test; p=0.03607***
	Striation	Fisher test; p=1	Fisher test; p=0.6404	Fisher test; p=0.193
	Chattering	Fisher test; p=1	Fisher test; p=1	Fisher test; p=0.6668
Buried group	Kerf shape	Fisher's test: p=0.7464	Fisher's test: p=0.2554	Fisher's test: p=0.466
	Cross-sectional shape	Fisher's test: p=0.4686	Fisher's test: p=0.6184	Fisher's test: p=0.574
	Kerf margin	Fisher's test: p=0.7406	Fisher's test: p=0.653	Fisher's test: p=0.3408
	Striation	Fisher's test: p=0.7305	Fisher's test: p=0.325	Fisher's test: p=0.325
	Chattering	Fisher's test: p=0.5048	Fisher's test: p=0,5048	Fisher's test: p=0.7434

Table 6.I: Average and standard deviations of micro-CT parameter of machete-inflicted marks (in mm); L: Length; W: Width; D: Depth; PSH: Proximal Shoulder Height; DSH: Distal Shoulder Height; PSA: Proximal Slope Angle; DSA: Distal Slope Angle; OA: Opening Angle

Group		6-months (n=12)		12-months (n=12)		18-months (n=12)	
		Pre-	Post-	Pre-	Post-	Pre-	Post-
Surface	L	9.33±0.98	8.89±0.93	9.01±0.99	8.63±0.94	9.16±0.71	8.43±0.83
	W	2.46±0.09	2.4±0.08	2.44±0.08	2.51±0.08	2.45±0.04	2.56±0.06
	D	3.855±0.2	3.78±0.15	3.77±0.12	3.73±0.09	3.794±0.1	3.714±0.1
	PSH	1.216±0.1	1.12±0.08	1.167±0.1	1.08±0.09	1.24±0.15	1.071±0.1
	DSH	0.951±0.1	0.91±0.08	0.99±0.08	0.9±0.08	0.99±0.11	0.879±0.1
	PSA	105.8±15	105.3±6.9	107.2±9.2	104.7±5.9	106.2±9.7	104.3±9.6
	DSA	109.9±9.9	105.1±7.5	105±10.4	102.5±6.7	108.4±9.9	105.1±5.3
	OA	25.71±8.3	24.8±3.98	24.84±7.4	23.31±2.6	24.3±9.19	23.39±2.7
Burial	L	9.379±1.9	9.117±1.9	9.083±0.8	9.021±1	9.697±0.8	9.156±0.8
	W	2.5±0.08	2.46±0.06	2.498±0.1	2.45±0.05	2.439±0.1	2.45±0.06
	D	3.67±0.08	3.63±0.08	3.711±0.2	3.65±0.19	3.68±0.07	3.616±0.1
	PSH	1.07±0.24	1.01±0.22	1.07±0.21	1±0.203	1.11±0.18	1.02±0.18
	DSH	0.87±0.11	0.811±0.1	0.92±0.22	0.84±0.21	0.92±0.21	0.84±0.19
	PSA	106.4±4.4	105.2±4.4	108±12.2	106±6.8	106±13.7	102±10.4
	DSA	113.6±6.1	113.8±5.5	103.4±10	105.9±8.3	111.3±14	109.2±10
	OA	27.94±5.4	26.33±4.9	27.24±6.5	27.37±6.2	25.69±7.9	24.76±3.9

Table 6.J: Statistical differences of micro-CT data of machete-inflicted marks (*** statistical significance of the same sample between pre-exposure and post-exposure values)

Sample group	Parameter	6-months exposure	12-months exposure	18-months exposure
Surface group	Length	t=-0.927, df=22, p=0.3697	t=-0.923, df=22, p=0.3671	t=-2.001, df=22, p=0.06268
	Width	t=-1.438, df=22, p=0.1724	t=2.216, df=22, p=0.03842***	t=5.027, df=22, p=0.000124***
	Depth	t=-0.879, df=22, p=0.3942	t=-0.928, df=22, p=0.3643	t=-1.752, df=22, p=0.09883
	Proximal shoulder height	t=-1.768, df=22, p=0.0925	t=-2.019 df=22, p=0.04713***	t=-2.74, df=22, p=0.01453***
	Distal shoulder height	t=-0.823, df=22, p=0.4246	t=-2.14, df=22, p=0.04414***	t=-2.291, df=22, p=0.03588***
	Proximal slope angle	t=-0.659, df=22, p=0.5207	t=-0.596, df=22, p=0.558	t=-0.557, df=22, p=0.5853
	Distal slope angle	t=-1.087, df=22, p=0.2956	t=0.583, df=22, p=0.5831	t=-0.881, df=22, p=0.3914
	Opening angle	t=-0.296, df=22, p=0.7718	t=-0.655, df=22, p=0.5202	t=-0.402, df=22, p=0.6929
Buried group	Length	t=-0.283, df=22, p=0.7808	t=-0.145, df=22, p=0.8868	t=-1.408, df=22, p=0.1782
	Width	t=-1.351, df=22, p=0.1954	t=-1.374, df=22, p=0.1883	t=0.378, df=22, p=0.7106
	Depth	t=-1.008, df=22, p=0.3286	t=-0.644, df=22, p=0.5287	t=-1.464, df=22, p=0.1625
	Proximal shoulder height	t=-0.629 df=22, p=0.5382	t=-0.749 df=22, p=0.4645	t=-1.053, df=22, p=0.3078
	Distal shoulder height	t=0.673, df=22, p=0.4258	t=-0.777, df=22, p=0.4484	t=-0.769, df=22, p=0.4531
	Proximal slope angle	t=0.435, df=22, p=0.6691	t=-0.333, df=22, p=0.7438	t=0.089, df=22, p=0.9301
	Distal slope angle	t=0.063, df=22, p=0.9507	t=0.566, df=22, p=0.5792	t=-0.35, df=22, p=0.731
	Opening angle	t=-0.663, df=22, p=0.5168	t=-0.113, df=22, p=0.9112	t=-0.315, df=22, p=0.7569

6.3 Raw data

Table 6.K: Raw data of pre-exposure femurs; 6-month group

Number	Cleaver							Machete						
	L	W	KS	CS	KM	KSt	Ch	L	W	KS	CS	KM	KSt	Ch
6S-1-1	10.15	1.49	Ellipse	V	Smooth	Absent	Absent	10.49	2.53	Ellipse	V	Raised	Present	Present
6S-1-2	9.55	1.29	Ellipse	V	Smooth	Absent	Absent	10.41	2.46	Ellipse	V	Smooth	Absent	Present
6S-1-3	10.16	1.3	Ellipse	V	Smooth	Absent	Absent	9.96	2.36	Ellipse	V	Raised	Present	Absent
6S-1-4	10.88	1.28	Rectangle	U	Raised	Absent	Absent	10.68	2.48	Ellipse	U	Smooth	Present	Absent
6S-2-1	10.3	1.25	Ellipse	V	Smooth	Absent	Absent	9	2.34	Ellipse	V	Raised	Present	Absent
6S-2-2	10.04	1.34	Ellipse	V	Raised	Absent	Absent	9.73	2.56	Ellipse	V	Raised	Present	Present
6S-2-3	11.37	1.47	Ellipse	V	Smooth	Absent	Absent	11.22	2.49	Irregular	V	Raised	Absent	Absent
6S-2-4	9.53	1.26	Ellipse	U	Smooth	Absent	Absent	10.18	2.46	Rectangle	U	Smooth	Present	Present
6S-3-1	10.78	1.45	Ellipse	V	Smooth	Absent	Absent	10.07	2.53	Irregular	V	Smooth	Present	Absent
6S-3-2	10.56	1.38	Ellipse	V	Smooth	Absent	Absent	10.97	2.51	Ellipse	V	Smooth	Absent	Absent
6S-3-3	11.28	1.38	Rectangle	U	Smooth	Absent	Absent	10.88	2.52	Ellipse	V	Raised	Present	Absent
6S-3-4	11.01	1.52	Ellipse	V	Smooth	Absent	Absent	10.75	2.41	Irregular	U	Raised	Present	Absent
6B-1-1	10.47	1.24	Ellipse	U	Smooth	Absent	Absent	11.15	2.46	Ellipse	V	Raised	Present	Present
6B-1-2	11.13	1.3	Ellipse	V	Smooth	Absent	Absent	12.38	2.59	Rectangle	V	Smooth	Absent	Present
6B-1-3	9.03	1.53	Ellipse	V	Smooth	Absent	Absent	9.38	2.44	Ellipse	V	Smooth	Present	Absent
6B-1-4	10.22	1.44	Rectangle	U	Smooth	Absent	Absent	10.51	2.55	Irregular	U	Smooth	Present	Absent
6B-2-1	10.21	1.38	Ellipse	V	Smooth	Absent	Absent	9.7	2.61	Ellipse	V	Smooth	Absent	Absent
6B-2-2	9.43	1.47	Ellipse	V	Smooth	Absent	Absent	9.45	2.57	Irregular	V	Raised	Present	Present
6B-2-3	11.57	1.42	Ellipse	V	Smooth	Absent	Absent	11.4	2.42	Ellipse	V	Smooth	Present	Absent
6B-2-4	10.58	1.32	Rectangle	U	Raised	Absent	Absent	10.36	2.59	Ellipse	V	Raised	Present	Absent
6B-3-1	8.42	1.32	Ellipse	V	Smooth	Absent	Absent	10.31	2.5	Ellipse	U	Raised	Present	Present
6B-3-2	9.33	1.31	Ellipse	V	Smooth	Absent	Absent	12.54	2.53	Irregular	V	Smooth	Absent	Absent
6B-3-3	10.24	1.33	Ellipse	V	Smooth	Absent	Absent	9.33	2.38	Ellipse	V	Raised	Absent	Present
6B-3-4	9.01	1.49	Ellipse	V	Smooth	Absent	Absent	10.65	2.49	Ellipse	V	Raised	Present	Absent

Table 6.L: Raw data of post-exposure femurs; 6-month group

Number	Cleaver							Machete						
	L	W	KS	CS	KM	KSt	Ch	L	W	KS	CS	KM	KSt	Ch
6S-1-1	9.52	1.42	Ellipse	V	Smooth	Absent	Absent	10.02	2.5	Ellipse	V	Raised	Present	Present
6S-1-2	10.01	1.22	Ellipse	V	Smooth	Absent	Absent	10.68	2.5	Ellipse	V	Smooth	Absent	Present
6S-1-3	9.63	1.35	Ellipse	V	Smooth	Absent	Absent	9.39	2.41	Ellipse	V	Raised	Present	Absent
6S-1-4	10.38	1.22	Rectangle	U	Raised	Absent	Absent	9.91	2.43	Ellipse	U	Smooth	Present	Absent
6S-2-1	10.51	1.3	Ellipse	V	Smooth	Absent	Absent	9.47	2.39	Ellipse	V	Smooth	Present	Absent
6S-2-2	9.45	1.29	Ellipse	V	Raised	Absent	Absent	9.02	2.5	Ellipse	V	Raised	Present	Present
6S-2-3	10.94	1.4	Ellipse	V	Smooth	Absent	Absent	10.63	2.44	Irregular	V	Raised	Absent	Absent
6S-2-4	10.02	1.19	Ellipse	U	Smooth	Absent	Absent	9.54	2.46	Rectangle	U	Smooth	Present	Present
6S-3-1	10.29	1.45	Ellipse	V	Smooth	Absent	Absent	10.41	2.48	Irregular	V	Smooth	Present	Absent
6S-3-2	9.94	1.33	Ellipse	V	Smooth	Absent	Absent	10.35	2.48	Ellipse	V	Smooth	Absent	Absent
6S-3-3	10.67	1.32	Rectangle	U	Smooth	Absent	Absent	10.22	2.47	Ellipse	V	Raised	Present	Absent
6S-3-4	10.58	1.41	Ellipse	V	Smooth	Absent	Absent	10.98	2.46	Irregular	U	Raised	Present	Absent
6B-1-1	9.67	1.28	Ellipse	U	Smooth	Absent	Absent	10.36	2.4	Ellipse	V	Raised	Present	Present
6B-1-2	10.39	1.3	Ellipse	V	Smooth	Absent	Absent	11.6	2.52	Rectangle	V	Smooth	Absent	Present
6B-1-3	8.33	1.48	Ellipse	V	Smooth	Absent	Absent	8.79	2.47	Ellipse	V	Smooth	Present	Absent
6B-1-4	9.57	1.39	Rectangle	U	Smooth	Absent	Absent	9.83	2.48	Irregular	U	Smooth	Present	Absent
6B-2-1	9.47	1.35	Ellipse	V	Smooth	Absent	Absent	10.05	2.54	Ellipse	V	Smooth	Absent	Absent
6B-2-2	9.62	1.43	Ellipse	V	Smooth	Absent	Absent	8.66	2.5	Irregular	V	Raised	Present	Present
6B-2-3	10.75	1.38	Ellipse	V	Smooth	Absent	Absent	10.52	2.45	Ellipse	V	Smooth	Present	Absent
6B-2-4	9.71	1.37	Rectangle	U	Raised	Absent	Absent	9.56	2.52	Ellipse	V	Raised	Present	Absent
6B-3-1	8.73	1.28	Ellipse	V	Smooth	Absent	Absent	10.68	2.5	Ellipse	U	Raised	Present	Present
6B-3-2	8.66	1.27	Ellipse	V	Smooth	Absent	Absent	11.76	2.45	Irregular	V	Smooth	Absent	Absent
6B-3-3	9.57	1.3	Ellipse	V	Smooth	Absent	Absent	8.54	2.32	Ellipse	V	Raised	Absent	Present
6B-3-4	8.42	1.44	Ellipse	V	Smooth	Absent	Absent	9.85	2.42	Ellipse	V	Raised	Present	Absent

Table 6.M: Raw data of pre-exposure femurs; 12-month group

Number	Cleaver							Machete						
	L	W	KS	CS	KM	KSt	Ch	L	W	KS	CS	KM	KSt	Ch
12S-1-1	9.41	1.36	Ellipse	V	Smooth	Absent	Absent	8.48	2.44	Ellipse	V	Raised	Present	Present
12S-1-2	10.12	1.3	Ellipse	V	Smooth	Absent	Absent	8.9	2.56	Ellipse	V	Raised	Present	Absent
12S-1-3	9.44	1.34	Ellipse	V	Smooth	Absent	Absent	10.33	2.49	Ellipse	V	Raised	Present	Present
12S-1-4	9.67	1.29	Ellipse	U	Smooth	Absent	Absent	9.12	2.54	Irregular	V	Smooth	Absent	Absent
12S-2-1	9.91	1.43	Ellipse	V	Smooth	Absent	Absent	9.94	2.41	Ellipse	V	Smooth	Present	Absent
12S-2-2	9.64	1.33	Ellipse	V	Smooth	Absent	Absent	10.93	2.44	Ellipse	V	Raised	Present	Present
12S-2-3	9.88	1.41	Ellipse	V	Smooth	Absent	Absent	10.02	2.41	Ellipse	V	Smooth	Present	Absent
12S-2-4	9.05	1.24	Rectangle	U	Raised	Absent	Absent	10.37	2.36	Irregular	V	Raised	Present	Present
12S-3-1	10.31	1.27	Ellipse	V	Smooth	Absent	Absent	8.03	2.57	Irregular	U	Raised	Present	Absent
12S-3-2	9.04	1.36	Ellipse	V	Smooth	Absent	Absent	8.68	2.53	Ellipse	U	Smooth	Present	Absent
12S-3-3	10.35	1.29	Ellipse	V	Smooth	Absent	Absent	8.91	2.42	Ellipse	V	Raised	Absent	Absent
12S-3-4	10.52	1.45	Ellipse	U	Raised	Absent	Absent	9.89	2.49	Rectangle	V	Raised	Present	Present
12B-1-1	8.76	1.27	Ellipse	V	Smooth	Absent	Absent	9.82	2.31	Ellipse	V	Smooth	Present	Present
12B-1-2	8.67	1.36	Ellipse	V	Raised	Absent	Absent	10.24	2.63	Rectangle	V	Raised	Present	Absent
12B-1-3	10.31	1.38	Ellipse	V	Smooth	Absent	Absent	9.72	2.48	Irregular	V	Smooth	Absent	Absent
12B-1-4	9.02	1.32	Ellipse	U	Smooth	Absent	Absent	9.71	2.53	Ellipse	U	Raised	Present	Absent
12B-2-1	9.49	1.4	Ellipse	V	Smooth	Absent	Absent	8.81	2.55	Ellipse	V	Raised	Present	Absent
12B-2-2	8.65	1.31	Rectangle	U	Smooth	Absent	Absent	9.07	2.62	Irregular	V	Raised	Absent	Present
12B-2-3	10.37	1.49	Ellipse	V	Raised	Absent	Absent	9.8	2.49	Ellipse	V	Smooth	Absent	Present
12B-2-4	8.66	1.29	Ellipse	V	Smooth	Absent	Absent	8.07	2.57	Irregular	V	Smooth	Present	Absent
12B-3-1	7.65	1.46	Ellipse	V	Smooth	Absent	Absent	9.32	2.31	Ellipse	V	Raised	Absent	Absent
12B-3-2	9.17	1.33	Ellipse	V	Smooth	Absent	Absent	10.39	2.46	Irregular	V	Raised	Present	Present
12B-3-3	9.43	1.36	Rectangle	U	Smooth	Absent	Absent	10.95	2.47	Ellipse	U	Smooth	Present	Present
12B-3-4	9.21	1.45	Ellipse	V	Smooth	Absent	Absent	9.55	2.43	Ellipse	V	Raised	Absent	Absent

Table 6.N: Raw data of post-exposure femurs; 12-month group

Number	Cleaver							Machete						
	L	W	KS	CS	KM	KSt	Ch	L	W	KS	CS	KM	KSt	Ch
12S-1-1	9.15	1.32	Ellipse	V	Smooth	Absent	Absent	8.05	2.5	Ellipse	V	Smooth	Absent	Absent
12S-1-2	9.73	1.26	Ellipse	V	Smooth	Absent	Absent	8.46	2.51	Ellipse	V	Smooth	Present	Absent
12S-1-3	9.09	1.3	Rectangle	U	Smooth	Absent	Absent	9.83	2.44	Ellipse	U	Raised	Present	Present
12S-1-4	9.82	1.25	Ellipse	U	Smooth	Absent	Absent	8.67	2.5	Irregular	V	Smooth	Absent	Absent
12S-2-1	9.58	1.38	Ellipse	V	Smooth	Absent	Absent	9.54	2.47	Ellipse	V	Smooth	Present	Absent
12S-2-2	9.33	1.28	Ellipse	V	Smooth	Absent	Absent	10.55	2.49	Ellipse	V	Raised	Absent	Present
12S-2-3	9.61	1.37	Ellipse	V	Smooth	Absent	Absent	9.51	2.47	Ellipse	U	Smooth	Present	Absent
12S-2-4	8.86	1.2	Rectangle	U	Raised	Absent	Absent	9.96	2.43	Irregular	V	Raised	Present	Present
12S-3-1	9.98	1.3	Ellipse	V	Smooth	Absent	Absent	8.56	2.53	Irregular	U	Raised	Present	Absent
12S-3-2	8.79	1.31	Ellipse	V	Smooth	Absent	Absent	8.32	2.59	Ellipse	U	Smooth	Present	Absent
12S-3-3	10.07	1.26	Ellipse	V	Smooth	Absent	Absent	8.47	2.48	Ellipse	V	Smooth	Absent	Absent
12S-3-4	10.22	1.41	Ellipse	U	Raised	Absent	Absent	9.45	2.56	Rectangle	V	Raised	Present	Present
12B-1-1	8.33	1.32	Ellipse	V	Smooth	Absent	Absent	9.34	2.35	Ellipse	U	Smooth	Present	Present
12B-1-2	8.38	1.32	Ellipse	V	Raised	Absent	Absent	9.62	2.54	Rectangle	V	Raised	Present	Absent
12B-1-3	9.85	1.34	Ellipse	V	Smooth	Absent	Absent	9.23	2.4	Irregular	V	Smooth	Absent	Absent
12B-1-4	8.76	1.27	Ellipse	U	Smooth	Absent	Absent	9.16	2.44	Ellipse	U	Smooth	Present	Absent
12B-2-1	9.02	1.34	Ellipse	V	Smooth	Absent	Absent	8.37	2.5	Ellipse	V	Raised	Present	Absent
12B-2-2	9.09	1.24	Rectangle	U	Smooth	Absent	Absent	9.33	2.53	Irregular	V	Raised	Absent	Present
12B-2-3	9.98	1.42	Ellipse	V	Raised	Absent	Absent	9.38	2.52	Ellipse	V	Smooth	Present	Present
12B-2-4	8.25	1.24	Ellipse	V	Smooth	Absent	Absent	7.57	2.49	Irregular	V	Smooth	Present	Absent
12B-3-1	7.36	1.39	Ellipse	V	Smooth	Absent	Absent	8.72	2.35	Ellipse	V	Raised	Absent	Absent
12B-3-2	8.76	1.33	Ellipse	V	Smooth	Absent	Absent	9.76	2.5	Irregular	V	Raised	Present	Present
12B-3-3	9.12	1.3	Rectangle	U	Smooth	Absent	Absent	10.2	2.4	Ellipse	U	Smooth	Present	Present
12B-3-4	8.8	1.39	Ellipse	V	Smooth	Absent	Absent	8.84	2.35	Ellipse	V	Raised	Absent	Absent

Table 6.O: Raw data of pre-exposure femurs; 18-month group

Number	Cleaver							Machete						
	L	W	KS	CS	KM	KSt	Ch	L	W	KS	CS	KM	KSt	Ch
18S-1-1	10.37	1.36	Ellipse	V	Raised	Absent	Absent	9.65	2.42	Irregular	U	Smooth	Present	Absent
18S-1-2	8.51	1.32	Ellipse	V	Smooth	Absent	Absent	11.02	2.43	Ellipse	V	Raised	Present	Present
18S-1-3	10.17	1.41	Ellipse	V	Smooth	Absent	Absent	8.31	2.4	Ellipse	V	Smooth	Present	Present
18S-1-4	9.67	1.36	Ellipse	V	Smooth	Absent	Absent	9.66	2.48	Ellipse	V	Raised	Present	Absent
18S-2-1	11.76	1.31	Ellipse	V	Smooth	Absent	Absent	10.34	2.37	Irregular	V	Raised	Absent	Absent
18S-2-2	10.07	1.36	Ellipse	U	Raised	Absent	Absent	10.7	2.43	Ellipse	U	Raised	Present	Absent
18S-2-3	9.06	1.34	Ellipse	V	Smooth	Absent	Absent	9.45	2.48	Rectangle	V	Smooth	Present	Absent
18S-2-4	9.6	1.29	Ellipse	V	Smooth	Absent	Absent	10.16	2.37	Irregular	V	Raised	Absent	Present
18S-3-1	8.69	1.38	Ellipse	V	Smooth	Absent	Absent	10.12	2.4	Ellipse	V	Raised	Present	Absent
18S-3-2	8.61	1.33	Ellipse	V	Smooth	Absent	Absent	9.83	2.5	Ellipse	V	Raised	Present	Absent
18S-3-3	11.16	1.29	Ellipse	V	Smooth	Absent	Absent	9.09	2.38	Ellipse	V	Smooth	Present	Present
18S-3-4	10.14	1.34	Rectangle	U	Smooth	Absent	Absent	9.62	2.6	Ellipse	U	Raised	Present	Present
18B-1-1	6.94	1.25	Rectangle	V	Smooth	Absent	Absent	10.46	2.51	Ellipse	U	Raised	Present	Absent
18B-1-2	7.8	1.37	Ellipse	V	Smooth	Absent	Absent	8.67	2.52	Ellipse	V	Raised	Absent	Absent
18B-1-3	10.5	1.29	Ellipse	V	Smooth	Absent	Absent	11.39	2.45	Rectangle	V	Smooth	Present	Present
18B-1-4	9.52	1.44	Ellipse	U	Smooth	Absent	Absent	9.13	2.55	Irregular	V	Raised	Present	Present
18B-2-1	9.69	1.28	Ellipse	U	Smooth	Absent	Absent	9.98	2.44	Rectangle	V	Raised	Present	Absent
18B-2-2	8.49	1.4	Ellipse	V	Raised	Absent	Absent	8.26	2.39	Irregular	V	Smooth	Present	Absent
18B-2-3	10.15	1.29	Ellipse	V	Smooth	Absent	Absent	10.91	2.43	Ellipse	V	Raised	Absent	Absent
18B-2-4	8.48	1.59	Ellipse	V	Smooth	Absent	Absent	9.69	2.47	Ellipse	V	Smooth	Present	Absent
18B-3-1	8.39	1.4	Ellipse	V	Smooth	Absent	Absent	10.36	2.53	Irregular	V	Raised	Present	Present
18B-3-2	8.86	1.35	Rectangle	V	Raised	Absent	Absent	9.79	2.48	Ellipse	V	Raised	Absent	Present
18B-3-3	9.07	1.38	Ellipse	V	Smooth	Absent	Absent	9.09	2.47	Ellipse	V	Smooth	Absent	Absent
18B-3-4	10.04	1.32	Ellipse	U	Smooth	Absent	Absent	9.91	2.52	Ellipse	V	Raised	Present	Present

Table 6.P: Raw data of post-exposure femurs; 18-month group

Number	Cleaver							Machete						
	L	W	KS	CS	KM	KSt	Ch	L	W	KS	CS	KM	KSt	Ch
18S-1-1	9.67	1.33	Ellipse	V	Raised	Absent	Absent	8.97	2.56	Irregular	U	Smooth	Present	Absent
18S-1-2	7.79	1.29	Ellipse	V	Smooth	Absent	Absent	10.45	2.38	Rectangle	V	Smooth	Absent	Absent
18S-1-3	9.42	1.38	Ellipse	U	Smooth	Absent	Absent	7.67	2.52	Ellipse	U	Smooth	Absent	Present
18S-1-4	8.85	1.31	Ellipse	V	Smooth	Absent	Absent	9.17	2.59	Irregular	V	Raised	Present	Absent
18S-2-1	10.93	1.27	Ellipse	V	Smooth	Absent	Absent	9.73	2.49	Irregular	V	Smooth	Absent	Absent
18S-2-2	9.41	1.33	Ellipse	U	Raised	Absent	Absent	10.07	2.55	Ellipse	U	Smooth	Present	Absent
18S-2-3	8.36	1.32	Rectangle	V	Smooth	Absent	Absent	8.88	2.59	Rectangle	V	Smooth	Absent	Absent
18S-2-4	8.92	1.26	Rectangle	V	Smooth	Absent	Absent	9.55	2.32	Irregular	U	Smooth	Absent	Present
18S-3-1	8.12	1.33	Ellipse	U	Smooth	Absent	Absent	9.63	2.36	Ellipse	U	Smooth	Present	Absent
18S-3-2	8.07	1.3	Ellipse	V	Smooth	Absent	Absent	9.11	2.61	Ellipse	V	Raised	Absent	Absent
18S-3-3	10.52	1.25	Ellipse	V	Smooth	Absent	Absent	8.34	2.48	Irregular	V	Smooth	Present	Present
18S-3-4	9.66	1.29	Rectangle	U	Smooth	Absent	Absent	9.03	2.68	Ellipse	U	Smooth	Present	Absent
18B-1-1	6.31	1.21	Rectangle	U	Smooth	Absent	Absent	9.77	2.46	Ellipse	U	Smooth	Present	Absent
18B-1-2	7.14	1.31	Ellipse	V	Smooth	Absent	Absent	7.9	2.57	Irregular	V	Raised	Absent	Absent
18B-1-3	9.86	1.24	Ellipse	V	Smooth	Absent	Absent	10.63	2.51	Rectangle	V	Smooth	Present	Present
18B-1-4	8.94	1.4	Ellipse	U	Smooth	Absent	Absent	8.51	2.61	Irregular	V	Raised	Absent	Absent
18B-2-1	9.03	1.23	Ellipse	U	Smooth	Absent	Absent	9.22	2.49	Rectangle	U	Raised	Absent	Absent
18B-2-2	7.74	1.35	Rectangle	V	Raised	Absent	Absent	7.53	2.45	Irregular	V	Smooth	Present	Absent
18B-2-3	9.51	1.24	Ellipse	V	Smooth	Absent	Absent	10.13	2.4	Ellipse	U	Raised	Absent	Absent
18B-2-4	7.8	1.54	Ellipse	V	Smooth	Absent	Absent	9.05	2.42	Ellipse	V	Smooth	Present	Absent
18B-3-1	7.69	1.36	Ellipse	V	Smooth	Absent	Absent	9.68	2.48	Irregular	V	Raised	Present	Present
18B-3-2	8.01	1.29	Rectangle	V	Raised	Absent	Absent	9.13	2.55	Ellipse	V	Smooth	Absent	Present
18B-3-3	8.36	1.33	Ellipse	V	Smooth	Absent	Absent	8.33	2.53	Ellipse	V	Smooth	Absent	Absent
18B-3-4	9.45	1.32	Ellipse	U	Smooth	Absent	Absent	9.14	2.47	Ellipse	V	Raised	Present	Present

APPENDIX 7

Table 7.A: Statistical significance of macroscopic assessments of blunt-inflicted fracture between pre-exposure and post-exposure

Parameters	6-months exposure	12-months exposure	18-months exposure
Maximum length	t=-0.166, df=22, p=0.868	t=-0.314, df=22, p=0.761	t=-0.922, df=22, p=0.425
Maximum circumference	t=-0.132, df=22, p=0.898	t=-0.288, df=22, p=0.764	t=-0.64, df=22, p=0.546
Maximum cortical thickness	t=-0.121, df=22, p=0.907	t=-0.313, df=22, p=0.75	t=-0.804, df=22, p=0.468
Minimum cortical thickness	t=-0.236, df=22, p=0.834	t=-0.656, df=22, p=0.557	t=-0.954, df=22, p=0.371
Tensile area	t=0.357, df=22, p=0.733	t=-0.65, df=22, p=0.537	t=-0.935, df=22, p=0.37
Compressive area	t=-0.446, df=22, p=0.658	t=-0.711, df=22, p=0.506	t=-0.96, df=22, p=0.355
Length of slope	t=0.215, df=22, p=0.847	t=-0.551, df=22, p=0.592	t=-0.933, df=22, p=0.379
Length of fracture surface	t=0.204, df=22, p=0.858	t=-0.66, df=22, p=0.554	t=-0.844, df=22, p=0.425
Fracture surface angle	t=-0.336, df=22, p=0.779	t=-0.557, df=22, p=0.579	t=-1.01, df=22, p=0.323
Maximum length of radiating fracture	t=-0.417, df=22, p=0.668	t=-0.651, df=22, p=0.563	t=-1.02, df=22, p=0.335

Table 7.B: Statistical significance of rough and smooth area of tension (Ten) and compression (Com) of blunt-inflicted fracture surface between the pre-exposure (Pre-E) and post-exposure groups; *** statistical significance

Sample type			Pre-E and 6-months exposure	Pre-E and 12-months exposure	Pre-E and 18-months exposure
Surface	Ten	Rough	t=0.823, df=22, p=0.434	t=1.455, df=22, p=0.1882	t=2.256, df=22, p=0.04024***
		Smooth	t=-0.935, df=22, p=0.4025	t=-1.503, df=22, p=0.1632	t=2.31, df=22, p=0.03967***
	Com	Rough	t=0.644, df=22, p=0.533	t=1.446, df=22, p=0.1905	t=2.097, df=22, p=0.0457***
		Smooth	t=-0.768, df=22, p=0.463	t=-1.52, df=22, p=0.166	t=-2.012, df=22, p=0.048***
Burial	Ten	Rough	t=0.386, df=22, p=0.734	t=0.504, df=22, p=0.613	t=0.811, df=22, p=0.4457
		Smooth	t=-0.401, df=22, p=0.686	t=-0.522, df=22, p=0.604	t=-0.82, df=22, p=0.439
	Com	Rough	t=0.392, df=22, p=0.729	t=0.479, df=22, p=0.625	t=0.837, df=22, p=0.4341
		Smooth	t=-0.408, df=22, p=0.683	t=-0.524, df=22, p=0.607	t=-0.865, df=22, p=0.426

Table 7.C: Statistical significance between rough and smooth area of tension (Ten) and compression (Com) of blunt-inflicted fracture surface; *** statistical significance

Sample type		Pre-exposure	6-months exposure	12-months exposure	18-months exposure
Surface	Ten	t=0.275, df=70, p=0.7821	t=0.575, df=22, p=0.583	t=1.411, df=22, p=0.178	t=2.12, df=22, p=0.046***
	Com	t=1.755, df=70, p=0.093	t=0.296, df=22, p=0.761	t=0.273, df=22, p=0.775	t=2.011, df=22, p=0.049***
Burial	Ten	t=0.271, df=70, p=0.07826	t=0.194, df=22, p=0.8552	t=0.307, df=22, p=0.743	t=1.994, df=22, p=0.0611
	Com	t=1.759, df=70, p=0.092	t=1.48, df=22, p=0.166	t=0.313, df=22, p=0.74	t=0.182, df=22, p=0.864

APPENDIX 8

Table 8.A: Average value of weather parameter during experimental period

Exposure period		Temperature (°C)	Precipitation (mm)	Hours of sunshine	Wind speed (knot)
Spring (May '17)	1st week	10.8	2.8	2.7	8
	2nd week	11	0.5	5.6	7
	3rd week	14.1	1.4	2.6	6
	4th week	15	4.5	6.1	4
Summer (August '17)	1st week	18.8	1.1	5.6	5
	2nd week	18.5	1.4	4.7	7
	3rd week	16.5	2.2	3.6	6
	4th week	16.1	2.9	3.3	7
Autumn (November '17)	1st week	6.9	3.2	3.4	12
	2nd week	6.1	2.9	2	14
	3rd week	8.1	4.6	2.4	7
	4th week	4	6.9	2.9	7
Winter (February '18)	1st week	0.9	1.4	3.1	6
	2nd week	0.3	1.6	5	9
	3rd week	0.5	2.2	1.7	11
	4th week	1.1	5.2	2.7	6

Table 8.B: Summary of kerf length of cut marks from pre-burned (PrB), post-burned (PoB), two-week surface exposure (2wkE), and four-week surface exposure (4wkE) groups; (NS: Non-serrated; CS: Coarse-serrated; FS: Fine-serrated: -: number of sample is too few to analyse)

Blade type and sample condition		Spring		Summer		Autumn		Winter	
		Mean	SD	Mean	SD	Mean	SD	Mean	SD
NS	PrB	9.776	1.58	9.171	1.42	8.425	1.28	8.171	1.12
	PoB	8.884	1.13	8.296	1.29	7.734	0.95	7.891	1.29
	2wkE	8.66	1.04	7.92	1.07	7.264	1.33	7.54	1.12
	4wkE	8.337	1.26	7.742	1.15	-	-	7.082	1.27
CS	PrB	9.92	1.28	9.288	1.14	8.891	1.49	8.565	0.97
	PoB	9.204	1.36	8.31	0.87	7.892	1.22	7.663	1.26
	2wkE	9.114	0.91	7.806	1.01	7.322	1.06	7.178	0.93
	4wkE	-	-	7.768	1.24	-	-	-	-
FS	PrB	9.842	1.05	9.443	1.27	8.942	1.28	8.63	1.25
	PoB	9.045	0.98	8.624	0.92	8.129	0.69	8.051	0.88
	2wkE	8.618	1.13	8.032	0.83	7.628	0.73	7.494	0.83
	4wkE	8.46	0.8	7.606	0..92	-	-	7.102	0.86

Table 8.C: Summary of kerf length of cut marks from pre-burned (PrB), post-burned (PoB), two-week burial exposure (2wkE), and four-week burial exposure (4wkE) groups; (NS: Non-serrated; CS: Coarse-serrated; FS: Fine-serrated: -: number of sample is too few to analyse)

Blade type and sample condition		Spring		Summer		Autumn		Winter	
		Mean	SD	Mean	SD	Mean	SD	Mean	SD
NS	PrB	8.868	1.35	8.654	1.14	8.578	1.05	8.903	1.04
	PoB	8.428	1.07	8.097	0.89	7.859	0.82	7.922	0.79
	2wkE	8.238	0.97	7.886	0.93	7.432	0.83	7.562	1.01
	4wkE	7.818	1.03	7.584	0.8	6.818	1.01	7.062	0.68
CS	PrB	9.929	1.33	8.815	1.13	9.403	1.38	8.919	1.05
	PoB	9.131	1.36	7.92	0.65	8.636	0.83	7.912	0.93
	2wkE	8.524	0.96	7.35	0.94	7.99	0.68	7.23	0.96
	4wkE	8.228	0.72	7.192	0.72	-	-	6.64	1.04
FS	PrB	9.472	1.29	8.712	1.06	8.315	1.28	8.946	1.12
	PoB	8.473	0.98	7.921	0.99	7.611	0.84	7.857	0.7
	2wkE	8.108	0.82	7.348	0.88	7.132	0.79	7.242	0.68
	4wkE	7.815	0.91	7.148	0.8	-	-	7.006	0.79

Table 8.D: Summary of kerf width of cut marks from pre-burned (PrB), post-burned (PoB), two-week surface exposure (2wkE), and four-week surface exposure (4wkE) groups; (NS: Non-serrated; CS: Coarse-serrated; FS: Fine-serrated: -: number of sample is too few to analyse)

Blade type and sample condition		Spring		Summer		Autumn		Winter	
		Mean	SD	Mean	SD	Mean	SD	Mean	SD
NS	PrB	0.139	0.03	0.136	0.05	0.139	0.04	0.135	0.04
	PoB	0.105	0.02	0.097	0.01	0.096	0.02	0.101	0.02
	2wkE	0.101	0.02	0.09	0.01	0.084	0.02	0.096	0.01
	4wkE	0.096	0.01	0.084	0.03	-	-	0.09	0.01
CS	PrB	0.353	0.08	0.416	0.06	0.388	0.07	0.372	0.06
	PoB	0.212	0.03	0.241	0.05	0.232	0.04	0.21	0.05
	2wkE	0.198	0.03	0.218	0.06	0.225	0.05	0.195	0.04
	4wkE	-	-	0.198	0.05	-	-	-	-
FS	PrB	0.293	0.06	0.329	0.05	0.335	0.05	0.309	0.05
	PoB	0.233	0.04	0.257	0.06	0.261	0.04	0.242	0.04
	2wkE	0.22	0.05	0.232	0.05	0.248	0.04	0.23	0.04
	4wkE	0.205	0.04	0.22	0.03	-	-	0.214	0.03

Table 8.E: Summary of kerf width of cut marks from pre-burned (PrB), post-burned (PoB), two-week burial exposure (2wkE), and four-week burial exposure (4wkE) groups; (NS: Non-serrated; CS: Coarse-serrated; FS: Fine-serrated: -: number of sample is too few to analyse)

Blade type and sample condition		Spring		Summer		Autumn		Winter	
		Mean	SD	Mean	SD	Mean	SD	Mean	SD
NS	PrB	0.128	0.02	0.141	0.04	0.142	0.03	0.134	0.03
	PoB	0.107	0.01	0.109	0.02	0.101	0.01	0.104	0.02
	2wkE	0.102	0.02	0.103	0.02	0.082	0.02	0.089	0.03
	4wkE	0.092	0.01	0.095	0.01	0.07	0.02	0.082	0.01
CS	PrB	0.389	0.12	0.424	0.1	0.367	0.09	0.395	0.08
	PoB	0.22	0.07	0.233	0.08	0.236	0.05	0.25	0.05
	2wkE	0.207	0.05	0.211	0.06	0.195	0.05	0.221	0.05
	4wkE	0.173	0.03	0.199	0.03	-	-	0.188	0.03
FS	PrB	0.319	0.06	0.311	0.06	0.321	0.08	0.322	0.07
	PoB	0.234	0.06	0.248	0.06	0.255	0.05	0.258	0.05
	2wkE	0.226	0.04	0.232	0.06	0.239	0.04	0.247	0.05
	4wkE	0.217	0.02	0.228	0.04	-	-	0.233	0.03

Table 8.F: Statistical significance of kerf length of cut marks between the pre-burned, post-burned (PB) and the post-exposure marks (E) (NS: Non-serrated; CS: Coarse-serrated; FS: Fine-serrated: -: number of sample is too few to analyse)

			Spring	Summer	Autumn	Winter
Surface	NS	PB and 2wk-E	t=-0.583, df=18, p=0.576	t=-0.548, df=18, p=0.5985	t=-1.09, df=16, p=0.3074	t=-1.031, df=18, p=0.3329
		PB and 4wk-E	t=-1.177, df=18, p=0.273	t=-1.776, df=18, p=0.1136	-	t=-1.495, df=16, p=0.1733
	CS	PB and 2wk-E	t=-0.824, df=18, p=0.4336	t=-0.747, df=18, p=0.4765	t=-0.934, df=15, p=0.3778	t=-1.079, df=16, p=0.3121
		PB and 4wk-E	-	t=-1.643, df=18, p=0.139	-	-
	FS	PB and 2wk-E	t=-0.507, df=18, p=0.6258	t=-0.758, df=18, p=0.47	t=-0.894, df=15, p=0.3972	t=-0.974, df=18, p=0.3585
		PB and 4wk-E	t=-0.417, df=18, p=0.5874	t=-1.58, df=16, p=0.1528	-	-
Burial	NS	PB and 2wk-E	t=-0.573, df=18, p=0.5823	t=-0.762, df=18, p=0.4681	t=-0.972, df=18, p=0.3594	t=-0.679, df=18, p=0.5165
		PB and 4wk-E	t=-1.07, df=18, p=0.3157	t=-1.416, df=18, p=0.1945	t=-1.416, df=16, p=0.1946	t=-1.903, df=16, p=0.09354
	CS	PB and 2wk-E	t=-1.122, df=18, p=0.2944	t=-1.167, df=18, p=0.2768	t=-1.691, df=14, p=0.1293	t=-0.895, df=18, p=0.3967
		PB and 4wk-E	t=-1.328, df=18, p=0.2208	t=-1.808, df=18, p=0.1083	-	t=-1.59, df=14, p=0.1506
	FS	PB and 2wk-E	t=-0.791, df=18, p=0.4515	t=-0.616, df=18, p=0.5548	t=-1.013, df=18, p=0.3407	t=-0.85, df=18, p=0.4201
		PB and 4wk-E	t=-0.969, df=18, p=0.3611	t=-1.675, df=18, p=0.1325	-	t=-1.767, df=16, p=0.1152

Table 8.G: Statistical significance of kerf width of cut marks between the pre-burned, post-burned (PB) and the post-exposure marks (E) (NS: Non-serrated; CS: Coarse-serrated; FS: Fine-serrated: -: number of sample is too few to analyse)

			Spring	Summer	Autumn	Winter
Surface	NS	PB and 2wk-E	t=-0.673, df=18, p=0.46	t=-0.849, df=18, p=0.3854	t=-0.69, df=16, p=0.447	t=-1.01, df=18, p=0.2911
		PB and 4wk-E	t=-1.21, df=18, p=0.253	t=-1.66, df=18, p=0.1235	-	t=-1.325, df=16, p=0.137
	CS	PB and 2wk-E	t=-0.941, df=18, p=0.3736	t=-0.618, df=18, p=0.5292	t=-0.824, df=15, p=0.468	t=-0.735, df=16, p=0.471
		PB and 4wk-E	-	t=-1.77, df=18, p=0.1105	-	-
	FS	PB and 2wk-E	t=-0.733, df=18, p=0.488	t=-0.644, df=18, p=0.492	t=-0.993, df=15, p=0.3626	t=-0.945, df=18, p=0.3854
		PB and 4wk-E	t=-0.994, df=18, p=0.377	t=-1.057, df=16, p=0.282	-	-
Burial	NS	PB and 2wk-E	t=-0.533, df=18, p=0.5634	t=-0.663, df=18, p=0.5173	t=-0.874, df=18, p=0.398	t=-0.519, df=18, p=0.565
		PB and 4wk-E	t=-0.832, df=18, p=0.4036	t=-0.835, df=18, p=0.402	t=-1.194, df=16, p=0.262	t=-0.941, df=16, p=0.364
	CS	PB and 2wk-E	t=-0.923, df=18, p=0.384	t=-0.985, df=18, p=0.3954	t=-1.09, df=14, p=0.285	t=-0.945, df=18, p=0.366
		PB and 4wk-E	t=-1.235, df=18, p=0.2398	t=-1.306, df=18, p=0.2183	-	t=-1.668, df=14, p=0.1206
	FS	PB and 2wk-E	t=-0.661, df=18, p=0.4995	t=-0.86, df=18, p=0.453	t=-1.18, df=18, p=0.3205	t=-1.015, df=18, p=0.3402
		PB and 4wk-E	t=-0.996, df=18, p=0.3546	t=-1.537, df=18, p=0.1508	-	t=-1.63, df=16, p=0.149

Table 8.H: Summary of statistical significant p-value comparing between post-burned and two-week exposure samples

Sample group	Blade type and Kerf dimensions		Spring	Summer	Autumn	Winter
Surface	NS	Kerf shape	1.0	1.0	1.0	1.0
		Cross-section	1.0	1.0	1.0	1.0
		Kerf margin	1.0	1.0	1.0	1.0
		Striations	1.0	1.0	1.0	1.0
	CS	Kerf shape	1.0	1.0	0.4749	0.517
		Cross-section	1.0	1.0	1.0	1.0
		Kerf margin	1.0	1.0	0.3698	0.6563
		Striations	1.0	1.0	0.6499	0.8012
	FS	Kerf shape	0.977	1.0	0.7771	0.931
		Cross-section	1.0	1.0	0.582	0.582
		Kerf margin	1.0	1.0	1.0	0.6285
		Striations	1.0	1.0	1.0	0.6499
Burial	NS	Kerf shape	1.0	1.0	1.0	1.0
		Cross-section	1.0	1.0	1.0	1.0
		Kerf margin	1.0	1.0	1.0	1.0
		Striations	1.0	1.0	1.0	1.0
	CS	Kerf shape	1.0	1.0	1.0	1.0
		Cross-section	1.0	1.0	1.0	1.0
		Kerf margin	1.0	1.0	0.6563	1.0
		Striations	1.0	1.0	1.0	1.0
	FS	Kerf shape	1.0	1.0	1.0	1.0
		Cross-section	1.0	1.0	1.0	1.0
		Kerf margin	1.0	1.0	1.0	1.0
		Striations	1.0	1.0	1.0	1.0

Table 8.I: Summary of statistical significant p-value comparing between post-burned and four-week exposure samples (*** statistical significance comparing between the same samples before and after exposure)

Sample group	Blade type and Kerf dimensions		Spring	Summer	Autumn	Winter
Surface	NS	Kerf shape	1.0	1.0	1.0	0.6285
		Cross-section	1.0	1.0	1.0	1.0
		Kerf margin	1.0	1.0	1.0	1.0
		Striations	1.0	1.0	1.0	1.0
	CS	Kerf shape	0.7771	0.8368	0.006289***	0.1537
		Cross-section	1.0	1.0	0.6563	0.6563
		Kerf margin	0.6563	0.6563	0.01977***	0.04978***
		Striations	1.0	0.6499	0.3698	0.6563
	FS	Kerf shape	0.6285	0.582	0.3034	0.4427
		Cross-section	1.0	1.0	0.6285	0.3498
		Kerf margin	1.0	1.0	0.3034	0.582
		Striations	1.0	0.6499	0.3698	0.6563
Burial	NS	Kerf shape	1.0	1.0	0.7458	0.8355
		Cross-section	1.0	1.0	1.0	1.0
		Kerf margin	1.0	1.0	1.0	1.0
		Striations	1.0	1.0	1.0	1.0
	CS	Kerf shape	0.6999	0.8	0.4749	0.7771
		Cross-section	1.0	1.0	1.0	1.0
		Kerf margin	0.6563	1.0	0.3698	0.6499
		Striations	1.0	1.0	0.6563	0.6563
	FS	Kerf shape	0.6285	1.0	0.4427	0.2105
		Cross-section	0.6285	0.6285	0.3498	0.3034
		Kerf margin	1.0	1.0	0.582	0.582
		Striations	1.0	1.0	0.6499	0.6563

Table 8.J: Raw data of pre-exposure surface-deposited burned ribs; spring group

Number	Non-serrated blade						Coarse-serrated blade						Fine-serrated blade					
	L	W	KS	CS	KM	KSt	L	W	KS	CS	KM	KSt	L	W	KS	CS	KM	KSt
2wkS-01	7.47	0.12	Linear	Narr.	Smo.	Abs.	8.12	0.24	Ellip.	U	Smo.	Pre.	7.94	0.23	Ellip.	V	Smo.	Pre.
2wkS-02	8.56	0.09	Linear	Narr.	Smo.	Abs.	9.23	0.21	Rect.	V	Smo.	Abs.	9.8	0.27	Ellip.	V	Raise	Pre.
2wkS-03	9.91	0.13	Linear	Narr.	Smo.	Abs.	8.71	0.21	Ellip.	V	Raise	Pre.	9.51	0.26	Ellip.	U	Smo.	Abs.
2wkS-04	8.38	0.1	Linear	V	Smo.	Abs.	9.04	0.16	Irreg.	V	Raise	Pre.	9.14	0.2	Rect.	V	Smo.	Abs.
2wkS-05	9.73	0.11	Ellip.	Narr.	Smo.	Abs.	9.36	0.23	Rect.	V	Smo.	Pre.	10.2	0.25	Ellip.	U	Raise	Pre.
2wkS-06	9.51	0.09	Linear	Narr.	Smo.	Abs.	10.1	0.21	Ellip.	U	Raise	Abs.	9.32	0.21	Irreg.	V	Smo.	Abs.
2wkS-07	9.04	0.11	Linear	V	Smo.	Abs.	9.31	0.25	Ellip.	V	Raise	Pre.	9.46	0.26	Ellip.	V	Raise	Pre.
2wkS-08	8.81	0.09	Linear	Narr.	Smo.	Abs.	10.3	0.23	Ellip.	U	Smo.	Abs.	9.61	0.23	Ellip.	V	Smo.	Pre.
2wkS-09	9.12	0.11	Ellip.	Narr.	Smo.	Abs.	8.57	0.19	Ellip.	V	Raise	Pre.	9.05	0.22	Ellip.	V	Smo.	Abs.
2wkS-10	8.33	0.1	Linear	Narr.	Smo.	Abs.	9.48	0.28	Ellip.	U	Raise	Pre.	8.52	0.24	Ellip.	V	Raise	Pre.
4wkS-01	7.45	0.1	Ellip.	Narr.	Smo.	Abs.	9.3	0.17	Ellip.	V	Raise	Pre.	7.36	0.24	Ellip.	V	Smo.	Pre.
4wkS-02	10.38	0.11	Linear	Narr.	Smo.	Abs.	9.52	0.23	Rect.	V	Smo.	Pre.	9.27	0.27	Irreg.	V	Smo.	Abs.
4wkS-03	9.4	0.12	Linear	V	Smo.	Abs.	10.5	0.25	Ellip.	U	Raise	Pre.	9.78	0.25	Ellip.	V	Raise	Abs.
4wkS-04	8.96	0.12	Linear	Narr.	Smo.	Abs.	7.61	0.25	Ellip.	V	Smo.	Pre.	7.92	0.2	Ellip.	V	Raise	Pre.
4wkS-05	8.38	0.11	Linear	Narr.	Smo.	Abs.	8.52	0.22	Ellip.	U	Raise	Abs.	9.95	0.21	Ellip.	U	Smo.	Pre.
4wkS-06	8.37	0.11	Ellip.	V	Smo.	Abs.	8.78	0.27	Ellip.	V	Raise	Pre.	8.28	0.28	Ellip.	V	Smo.	Abs.
4wkS-07	8.73	0.13	Linear	Narr.	Smo.	Abs.	10.2	0.22	Irreg.	V	Smo.	Abs.	9.21	0.2	Ellip.	V	Smo.	Pre.
4wkS-08	8.24	0.08	Linear	Narr.	Smo.	Abs.	9.45	0.22	Ellip.	U	Smo.	Abs.	8.56	0.23	Irreg.	V	Raise	Pre.
4wkS-09	9.45	0.11	Linear	Narr.	Smo.	Abs.	9.07	0.24	Ellip.	U	Raise	Pre.	9.13	0.18	Ellip.	V	Smo.	Pre.
4wkS-10	9.58	0.12	Linear	Narr.	Smo.	Abs.	8.85	0.18	Ellip.	U	Raise	Abs.	8.88	0.24	Ellip.	V	Smo.	Abs.

(Narr.: Narrow; Smo.: Smooth; Abs.: Absent; Ellip.: Ellipse; Rect.: Rectangle; Irreg.: Irregular; Pre.: Present)

Table 8.K: Raw data of post-exposure surface-deposited burned ribs; spring group

Number	Non-serrated blade						Coarse-serrated blade						Fine-serrated blade					
	L	W	KS	CS	KM	KSt	L	W	KS	CS	KM	KSt	L	W	KS	CS	KM	KSt
2wkS-01	7.25	0.12	Linear	Narr.	Smo.	Abs.	7.92	0.21	Ellip.	U	Smo.	Pre.	7.24	0.24	Ellip.	U	Smo.	Pre.
2wkS-02	8.36	0.09	Linear	V	Smo.	Abs.	9.16	0.2	Rect.	U	Smo.	Abs.	9.2	0.25	Irreg.	V	Raise	Pre.
2wkS-03	9.75	0.11	Linear	Narr.	Smo.	Abs.	8.58	0.18	Ellip.	V	Raise	Pre.	8.92	0.24	Ellip.	U	Smo.	Abs.
2wkS-04	8.15	0.1	Linear	V	Smo.	Abs.	8.95	0.16	Irreg.	V	Raise	Abs.	8.43	0.19	Rect.	V	Smo.	Abs.
2wkS-05	9.42	0.11	Linear	Narr.	Smo.	Abs.	9.32	0.23	Rect.	V	Smo.	Pre.	9.56	0.23	Ellip.	U	Raise	Pre.
2wkS-06	9.17	0.09	Linear	Narr.	Smo.	Abs.	9.94	0.2	Ellip.	U	Smo.	Abs.	8.72	0.21	Irreg.	V	Smo.	Abs.
2wkS-07	8.81	0.11	Linear	V	Smo.	Abs.	9.11	0.23	Ellip.	V	Raise	Pre.	8.81	0.24	Ellip.	V	Raise	Pre.
2wkS-08	8.58	0.09	Linear	Narr.	Smo.	Abs.	9.91	0.23	Ellip.	U	Smo.	Abs.	9.01	0.22	Ellip.	V	Smo.	Pre.
2wkS-09	8.95	0.11	Ellip.	Narr.	Smo.	Abs.	8.72	0.17	Irreg.	V	Raise	Pre.	8.44	0.21	Ellip.	V	Smo.	Abs.
2wkS-10	8.16	0.08	Linear	Narr.	Smo.	Abs.	9.54	0.26	Ellip.	U	Raise	Pre.	7.85	0.23	Ellip.	V	Smo.	Pre.
4wkS-01	6.95	0.1	Ellip.	Narr.	Smo.	Abs.	8.52	0.16	Irreg.	V	Smo.	Pre.	7.02	0.22	Irreg.	V	Smo.	Pre.
4wkS-02	9.67	0.11	Linear	Narr.	Smo.	Abs.	-	0.17	Rect.	V	Smo.	Pre.	8.92	0.25	Irreg.	U	Smo.	Abs.
4wkS-03	8.82	0.1	Linear	V	Smo.	Abs.	-	0.2	Ellip.	U	Raise	Abs.	9.35	0.24	Ellip.	V	Raise	Abs.
4wkS-04	8.44	0.09	Linear	Narr.	Smo.	Abs.	7.05	0.15	Ellip.	V	Smo.	Pre.	7.52	0.19	Ellip.	V	Smo.	Pre.
4wkS-05	7.87	0.09	Linear	Narr.	Smo.	Abs.	-	0.19	Ellip.	U	Raise	Abs.	9.57	0.2	Irreg.	U	Smo.	Abs.
4wkS-06	7.69	0.11	Ellip.	V	Smo.	Abs.	-	0.2	Ellip.	V	Smo.	Pre.	7.92	0.26	Ellip.	V	Smo.	Abs.
4wkS-07	8.26	0.1	Linear	Narr.	Smo.	Abs.	9.47	0.18	Irreg.	V	Smo.	Abs.	8.82	0.19	Ellip.	V	Smo.	Pre.
4wkS-08	7.55	0.08	Linear	Narr.	Smo.	Abs.	-	0.16	Irreg.	U	Smo.	Abs.	8.2	0.22	Irreg.	V	Raise	Pre.
4wkS-09	9.02	0.08	Linear	Narr.	Smo.	Abs.	8.36	0.17	Ellip.	U	Raise	Pre.	8.73	0.17	Ellip.	V	Smo.	Pre.
4wkS-10	9.13	0.1	Linear	Narr.	Smo.	Abs.	-	0.15	Ellip.	U	Raise	Abs.	8.55	0.23	Ellip.	V	Smo.	Abs.

(Narr.: Narrow; Smo.: Smooth; Abs.: Absent; Ellip.: Ellipse; Rect.: Rectangle; Irreg.: Irregular; Pre.: Present)

Table 8.L: Raw data of pre-exposure buried burned ribs; spring group

Number	Non-serrated blade						Coarse-serrated blade						Fine-serrated blade					
	L	W	KS	CS	KM	KSt	L	W	KS	CS	KM	KSt	L	W	KS	CS	KM	KSt
2wkB-01	6.65	0.12	Linear	Narr.	Smo.	Abs.	8.44	0.27	Ellip.	U	Raise	Pre.	7.29	0.21	Ellip.	V	Smo.	Pre.
2wkB-02	7.75	0.1	Linear	V	Smo.	Abs.	9.32	0.22	Ellip.	U	Raise	Pre.	9.28	0.26	Ellip.	V	Smo.	Pre.
2wkB-03	9.06	0.13	Linear	Narr.	Smo.	Abs.	9.05	0.2	Ellip.	V	Smo.	Pre.	8.86	0.28	Rect.	V	Smo.	Abs.
2wkB-04	7.35	0.11	Linear	V	Smo.	Abs.	9.42	0.17	Rect.	V	Raise	Pre.	8.59	0.19	Ellip.	V	Smo.	Pre.
2wkB-05	8.75	0.08	Linear	Narr.	Smo.	Abs.	9.85	0.24	Irreg.	U	Raise	Pre.	9.88	0.23	Ellip.	V	Raise	Abs.
2wkB-06	8.57	0.07	Linear	Narr.	Smo.	Abs.	10.5	0.19	Ellip.	V	Raise	Abs.	8.63	0.22	Ellip.	V	Smo.	Pre.
2wkB-07	8.15	0.09	Linear	V	Smo.	Abs.	9.73	0.26	Ellip.	V	Smo.	Abs.	8.96	0.25	Ellip.	U	Smo.	Pre.
2wkB-08	7.97	0.09	Linear	Narr.	Smo.	Abs.	10.5	0.22	Ellip.	V	Raise	Abs.	9.09	0.23	Ellip.	V	Raise	Abs.
2wkB-09	8.36	0.1	Ellip.	Narr.	Smo.	Abs.	8.85	0.17	Rect.	U	Raise	Pre.	8.62	0.24	Ellip.	V	Smo.	Abs.
2wkB-10	7.55	0.09	Linear	Narr.	Smo.	Abs.	9.82	0.28	Ellip.	U	Smo.	Abs.	7.98	0.24	Ellip.	V	Raise	Pre.
4wkB-01	7.35	0.11	Linear	Narr.	Smo.	Abs.	8.64	0.15	Irreg.	V	Smo.	Pre.	6.66	0.22	Ellip.	V	Smo.	Pre.
4wkB-02	10.25	0.1	Linear	Narr.	Smo.	Abs.	9.67	0.23	Ellip.	U	Raise	Pre.	8.51	0.26	Irreg.	V	Smo.	Pre.
4wkB-03	9.36	0.12	Linear	V	Smo.	Abs.	10.2	0.25	Ellip.	U	Raise	Pre.	9.18	0.24	Ellip.	U	Raise	Abs.
4wkB-04	8.85	0.12	Linear	Narr.	Smo.	Abs.	7.13	0.27	Ellip.	V	Smo.	Pre.	7.33	0.21	Ellip.	V	Smo.	Abs.
4wkB-05	8.48	0.12	Ellip.	V	Smo.	Abs.	7.98	0.2	Ellip.	U	Raise	Abs.	9.44	0.22	Ellip.	V	Smo.	Pre.
4wkB-06	8.23	0.11	Linear	Narr.	Smo.	Abs.	8.08	0.28	Rect.	V	Raise	Abs.	7.68	0.22	Ellip.	V	Smo.	Abs.
4wkB-07	8.83	0.12	Ellip.	Narr.	Smo.	Abs.	9.53	0.18	Irreg.	V	Raise	Abs.	8.58	0.21	Ellip.	U	Raise	Pre.
4wkB-08	8.05	0.11	Linear	V	Smo.	Abs.	9.06	0.21	Ellip.	U	Smo.	Pre.	7.96	0.24	Irreg.	V	Raise	Abs.
4wkB-09	9.53	0.13	Linear	Narr.	Smo.	Abs.	8.63	0.25	Ellip.	V	Raise	Pre.	8.68	0.19	Ellip.	V	Smo.	Pre.
4wkB-10	9.44	0.12	Linear	Narr.	Smo.	Abs.	8.11	0.18	Ellip.	U	Smo.	Pre.	8.26	0.24	Ellip.	V	Smo.	Pre.

(Narr.: Narrow; Smo.: Smooth; Abs.: Absent; Ellip.: Ellipse; Rect.: Rectangle; Irreg.: Irregular; Pre.: Present)

Table 8.M: Raw data of post-exposure buried burned ribs; spring group

Number	Non-serrated blade						Coarse-serrated blade						Fine-serrated blade					
	L	W	KS	CS	KM	KSt	L	W	KS	CS	KM	KSt	L	W	KS	CS	KM	KSt
2wkB-01	6.75	0.12	Linear	Narr.	Smo.	Abs.	7.41	0.24	Ellip.	U	Smo.	Pre.	6.68	0.2	Ellip.	V	Smo.	Pre.
2wkB-02	7.94	0.1	Linear	Narr.	Smo.	Abs.	8.27	0.21	Ellip.	U	Raise	Pre.	8.67	0.25	Ellip.	V	Smo.	Pre.
2wkB-03	9.22	0.11	Linear	Narr.	Smo.	Abs.	8.16	0.18	Ellip.	V	Smo.	Pre.	8.25	0.27	Rect.	U	Smo.	Abs.
2wkB-04	7.65	0.11	Linear	V	Smo.	Abs.	8.41	0.17	Rect.	V	Raise	Pre.	7.98	0.18	Ellip.	V	Smo.	Pre.
2wkB-05	9.11	0.1	Linear	Narr.	Smo.	Abs.	8.83	0.22	Irreg.	U	Raise	Pre.	9.27	0.22	Ellip.	V	Raise	Abs.
2wkB-06	8.76	0.09	Linear	Narr.	Smo.	Abs.	9.46	0.18	Ellip.	V	Raise	Abs.	8.01	0.21	Irreg.	V	Smo.	Pre.
2wkB-07	8.34	0.11	Linear	Narr.	Smo.	Abs.	8.65	0.24	Ellip.	V	Smo.	Abs.	8.35	0.24	Ellip.	U	Smo.	Pre.
2wkB-08	8.12	0.09	Linear	Narr.	Smo.	Abs.	9.46	0.21	Ellip.	V	Raise	Abs.	8.48	0.22	Ellip.	V	Raise	Abs.
2wkB-09	8.6	0.1	Linear	V	Smo.	Abs.	7.86	0.16	Rect.	U	Raise	Pre.	8.02	0.24	Ellip.	V	Smo.	Abs.
2wkB-10	7.89	0.09	Linear	Narr.	Smo.	Abs.	8.73	0.26	Ellip.	U	Smo.	Abs.	7.37	0.23	Ellip.	V	Raise	Pre.
4wkB-01	6.34	0.09	Linear	Narr.	Smo.	Abs.	8.16	0.15	Irreg.	V	Smo.	Pre.	6.24	0.21	Ellip.	U	Smo.	Pre.
4wkB-02	9.23	0.08	Linear	Narr.	Smo.	Abs.	9.12	0.18	Rect.	U	Smo.	Pre.	8.12	0.25	Irreg.	V	Smo.	Pre.
4wkB-03	8.25	0.09	Linear	V	Smo.	Abs.	9.84	0.19	Irreg.	U	Raise	Pre.	8.75	0.23	Ellip.	U	Raise	Abs.
4wkB-04	7.85	0.09	Linear	Narr.	Smo.	Abs.	6.62	0.2	Ellip.	V	Smo.	Pre.	6.96	0.2	Irreg.	V	Smo.	Abs.
4wkB-05	7.42	0.09	Ellip.	V	Smo.	Abs.	7.57	0.16	Ellip.	U	Raise	Abs.	9.02	0.22	Irreg.	V	Smo.	Pre.
4wkB-06	7.21	0.09	Linear	Narr.	Smo.	Abs.	7.57	0.21	Rect.	V	Smo.	Abs.	7.24	0.21	Ellip.	V	Smo.	Abs.
4wkB-07	7.76	0.11	Ellip.	Narr.	Smo.	Abs.	9.11	0.16	Irreg.	V	Raise	Abs.	8.16	0.2	Ellip.	U	Raise	Pre.
4wkB-08	7.07	0.08	Linear	V	Smo.	Abs.	8.48	0.16	Ellip.	U	Smo.	Pre.	7.55	0.23	Irreg.	U	Smo.	Abs.
4wkB-09	8.43	0.1	Linear	Narr.	Smo.	Abs.	8.14	0.18	Ellip.	V	Raise	Pre.	8.26	0.19	Ellip.	V	Smo.	Pre.
4wkB-10	8.62	0.1	Linear	Narr.	Smo.	Abs.	7.67	0.14	Ellip.	U	Smo.	Pre.	7.85	0.23	Ellip.	V	Smo.	Abs.

(Narr.: Narrow; Smo.: Smooth; Abs.: Absent; Ellip.: Ellipse; Rect.: Rectangle; Irreg.: Irregular; Pre.: Present)

Table 8.N: Raw data of pre-exposure surface-deposited burned ribs; summer group

Number	Non-serrated blade						Coarse-serrated blade						Fine-serrated blade					
	L	W	KS	CS	KM	KSt	L	W	KS	CS	KM	KSt	L	W	KS	CS	KM	KSt
2wkS-01	7.47	0.12	Ellip.	Narr.	Smo.	Abs.	7.06	0.29	Ellip.	V	Raise	Pre.	7.48	0.24	Ellip.	U	Smo.	Pre.
2wkS-02	8.62	0.09	Linear	Narr.	Smo.	Abs.	8.22	0.23	Ellip.	V	Raise	Abs.	9.44	0.29	Ellip.	V	Raise	Pre.
2wkS-03	8.32	0.12	Linear	Narr.	Smo.	Abs.	7.75	0.22	Ellip.	U	Smo.	Abs.	9.12	0.31	Ellip.	V	Smo.	Abs.
2wkS-04	8.3	0.1	Linear	V	Smo.	Abs.	7.92	0.18	Irreg.	V	Raise	Pre.	8.76	0.22	Ellip.	V	Smo.	Abs.
2wkS-05	8.93	0.12	Linear	Narr.	Smo.	Abs.	8.46	0.26	Rect.	U	Raise	Pre.	9.98	0.26	Ellip.	V	Raise	Pre.
2wkS-06	9.62	0.07	Ellip.	V	Smo.	Abs.	9.21	0.21	Ellip.	U	Smo.	Abs.	8.72	0.25	Ellip.	U	Smo.	Pre.
2wkS-07	8.62	0.08	Linear	Narr.	Smo.	Abs.	8.31	0.28	Ellip.	V	Raise	Pre.	9.04	0.26	Ellip.	V	Smo.	Pre.
2wkS-08	9.57	0.1	Linear	Narr.	Smo.	Abs.	9.32	0.24	Irreg.	U	Raise	Abs.	9.26	0.26	Irreg.	V	Raise	Pre.
2wkS-09	8.14	0.09	Linear	Narr.	Smo.	Abs.	7.66	0.25	Ellip.	V	Raise	Pre.	8.74	0.25	Ellip.	V	Smo.	Abs.
2wkS-10	9.02	0.11	Linear	Narr.	Smo.	Abs.	8.55	0.3	Ellip.	U	Smo.	Pre.	8.17	0.23	Ellip.	V	Smo.	Pre.
4wkS-01	7.91	0.1	Linear	Narr.	Smo.	Abs.	8.44	0.16	Rect.	V	Smo.	Abs.	6.78	0.23	Ellip.	V	Smo.	Pre.
4wkS-02	8.74	0.09	Linear	Narr.	Smo.	Abs.	8.65	0.24	Ellip.	V	Raise	Pre.	8.69	0.25	Ellip.	V	Raise	Pre.
4wkS-03	9.14	0.08	Linear	V	Smo.	Abs.	9.7	0.25	Ellip.	U	Raise	Pre.	9.33	0.27	Ellip.	V	Smo.	Abs.
4wkS-04	6.24	0.11	Linear	Narr.	Smo.	Abs.	6.91	0.27	Irreg.	U	Smo.	Pre.	7.43	0.26	Ellip.	V	Raise	Pre.
4wkS-05	7.12	0.12	Linear	Narr.	Smo.	Abs.	7.54	0.22	Ellip.	V	Smo.	Pre.	9.66	0.25	Ellip.	U	Smo.	Pre.
4wkS-06	8.28	0.1	Linear	Narr.	Smo.	Abs.	7.88	0.31	Rect.	V	Raise	Pre.	7.83	0.33	Ellip.	V	Smo.	Pre.
4wkS-07	8.7	0.07	Ellip.	Narr.	Smo.	Abs.	9.39	0.2	Irreg.	V	Raise	Abs.	8.74	0.24	Irreg.	V	Raise	Pre.
4wkS-08	8.33	0.09	Linear	V	Smo.	Abs.	8.81	0.24	Ellip.	V	Smo.	Pre.	8.1	0.27	Ellip.	U	Raise	Abs.
4wkS-09	7.54	0.07	Linear	Narr.	Smo.	Abs.	8.35	0.27	Ellip.	U	Raise	Pre.	8.79	0.21	Ellip.	V	Smo.	Pre.
4wkS-10	7.31	0.11	Linear	Narr.	Smo.	Abs.	7.79	0.2	Ellip.	U	Raise	Abs.	8.42	0.26	Ellip.	V	Smo.	Abs.

(Narr.: Narrow; Smo.: Smooth; Abs.: Absent; Ellip.: Ellipse; Rect.: Rectangle; Irreg.: Irregular; Pre.: Present)

Table 8.O: Raw data of post-exposure surface-deposited burned ribs; summer group

Number	Non-serrated blade						Coarse-serrated blade						Fine-serrated blade					
	L	W	KS	CS	KM	KSt	L	W	KS	CS	KM	KSt	L	W	KS	CS	KM	KSt
2wkS-01	6.76	0.11	Linear	Narr.	Smo.	Abs.	6.74	0.26	Irreg.	V	Smo.	Pre.	6.61	0.21	Ellip.	U	Smo.	Pre.
2wkS-02	7.88	0.08	Linear	Narr.	Smo.	Abs.	7.89	0.2	Ellip.	V	Raise	Abs.	8.29	0.27	Ellip.	V	Raise	Pre.
2wkS-03	7.58	0.11	Linear	Narr.	Smo.	Abs.	7.43	0.2	Ellip.	U	Smo.	Abs.	8.5	0.28	Irreg.	U	Smo.	Abs.
2wkS-04	7.66	0.09	Linear	V	Smo.	Abs.	7.6	0.15	Irreg.	V	Raise	Pre.	8.16	0.2	Ellip.	V	Smo.	Abs.
2wkS-05	8.19	0.11	Linear	Narr.	Smo.	Abs.	8.13	0.23	Rect.	U	Raise	Pre.	9.14	0.24	Ellip.	V	Raise	Pre.
2wkS-06	8.88	0.06	Linear	Narr.	Smo.	Abs.	8.88	0.18	Ellip.	U	Smo.	Abs.	8.05	0.23	Ellip.	U	Smo.	Abs.
2wkS-07	7.86	0.07	Linear	Narr.	Smo.	Abs.	7.98	0.25	Ellip.	V	Raise	Pre.	8.24	0.23	Ellip.	V	Smo.	Pre.
2wkS-08	8.72	0.09	Linear	Narr.	Smo.	Abs.	9.01	0.22	Irreg.	U	Raise	Abs.	8.42	0.24	Irreg.	V	Raise	Pre.
2wkS-09	7.43	0.08	Linear	V	Smo.	Abs.	7.33	0.22	Ellip.	V	Raise	Pre.	7.59	0.23	Ellip.	V	Smo.	Abs.
2wkS-10	8.24	0.1	Linear	Narr.	Smo.	Abs.	8.23	0.27	Ellip.	U	Smo.	Pre.	7.32	0.21	Ellip.	V	Smo.	Pre.
4wkS-01	7.51	0.09	Linear	Narr.	Smo.	Abs.	7.82	0.13	Rect.	U	Smo.	Abs.	6.02	0.2	Ellip.	V	Smo.	Abs.
4wkS-02	8.06	0.08	Linear	Narr.	Smo.	Abs.	8.03	0.2	Irreg.	V	Smo.	Pre.	7.9	0.21	Ellip.	V	Raise	Pre.
4wkS-03	9.23	0.07	Linear	V	Smo.	Abs.	9.11	0.21	Ellip.	U	Raise	Abs.	8.37	0.23	Ellip.	V	Smo.	Abs.
4wkS-04	6.64	0.1	Linear	Narr.	Smo.	Abs.	6.35	0.23	Irreg.	U	Smo.	Abs.	6.74	0.22	Irreg.	V	Raise	Abs.
4wkS-05	7.72	0.11	Linear	Narr.	Smo.	Abs.	6.94	0.19	Ellip.	V	Smo.	Pre.	8.81	0.22	Ellip.	U	Smo.	Pre.
4wkS-06	8.28	0.09	Linear	Narr.	Smo.	Abs.	7.27	0.25	Rect.	V	Smo.	Pre.	7.03	0.3	Ellip.	V	Smo.	Pre.
4wkS-07	8.3	0.06	Ellip.	Narr.	Smo.	Abs.	8.78	0.17	Irreg.	V	Raise	Abs.	7.98	0.2	Irreg.	V	Raise	Pre.
4wkS-08	7.83	0.08	Linear	V	Smo.	Abs.	8.2	0.2	Irreg.	V	Smo.	Pre.	7.45	0.23	Irreg.	U	Smo.	Abs.
4wkS-09	7.04	0.06	Linear	Narr.	Smo.	Abs.	7.74	0.23	Ellip.	U	Raise	Pre.	8.05	0.18	Ellip.	V	Smo.	Pre.
4wkS-10	6.81	0.1	Linear	Narr.	Smo.	Abs.	7.18	0.17	Ellip.	U	Raise	Abs.	7.71	0.22	Ellip.	V	Smo.	Abs.

(Narr.: Narrow; Smo.: Smooth; Abs.: Absent; Ellip.: Ellipse; Rect.: Rectangle; Irreg.: Irregular; Pre.: Present)

Table 8.P: Raw data of pre-exposure buried burned ribs; summer group

Number	Non-serrated blade						Coarse-serrated blade						Fine-serrated blade					
	L	W	KS	CS	KM	KSt	L	W	KS	CS	KM	KSt	L	W	KS	CS	KM	KSt
2wkB-01	8.54	0.13	Linear	Narr.	Smo.	Abs.	7.39	0.25	Ellip.	U	Raise	Pre.	6.78	0.23	Ellip.	V	Smo.	Pre.
2wkB-02	7.45	0.14	Linear	Narr.	Smo.	Abs.	8.25	0.26	Ellip.	V	Raise	Pre.	7.12	0.28	Ellip.	V	Smo.	Pre.
2wkB-03	8.5	0.14	Linear	Narr.	Smo.	Abs.	8.01	0.22	Ellip.	U	Smo.	Abs.	8.33	0.29	Ellip.	U	Raise	Abs.
2wkB-04	7.13	0.11	Ellip.	Narr.	Smo.	Abs.	8.34	0.29	Ellip.	V	Raise	Pre.	8.22	0.19	Ellip.	V	Smo.	Abs.
2wkB-05	8.39	0.09	Linear	V	Smo.	Abs.	8.5	0.26	Rect.	U	Raise	Abs.	6.77	0.24	Ellip.	V	Smo.	Pre.
2wkB-06	8.23	0.1	Linear	Narr.	Smo.	Abs.	9.32	0.21	Ellip.	V	Smo.	Abs.	8.51	0.24	Irreg.	U	Smo.	Pre.
2wkB-07	7.75	0.09	Linear	Narr.	Smo.	Abs.	8.44	0.23	Ellip.	V	Raise	Abs.	8.37	0.28	Ellip.	U	Raise	Pre.
2wkB-08	7.52	0.13	Linear	Narr.	Smo.	Abs.	9.08	0.24	Ellip.	V	Raise	Pre.	8.52	0.25	Ellip.	V	Smo.	Abs.
2wkB-09	9.04	0.13	Ellip.	V	Smo.	Abs.	7.53	0.19	Irreg.	U	Raise	Pre.	8.03	0.25	Ellip.	V	Raise	Pre.
2wkB-10	9.36	0.08	Linear	Narr.	Smo.	Abs.	8.78	0.31	Ellip.	U	Smo.	Pre.	7.42	0.24	Irreg.	V	Smo.	Pre.
4wkB-01	7.15	0.11	Linear	Narr.	Smo.	Abs.	7.44	0.18	Ellip.	V	Smo.	Pre.	6.56	0.21	Ellip.	V	Raise	Pre.
4wkB-02	9.73	0.1	Linear	Narr.	Smo.	Abs.	8.42	0.25	Irreg.	U	Raise	Pre.	7.97	0.28	Ellip.	V	Smo.	Abs.
4wkB-03	8.03	0.08	Linear	V	Smo.	Abs.	8.94	0.22	Ellip.	U	Raise	Pre.	8.62	0.26	Ellip.	V	Raise	Pre.
4wkB-04	8.63	0.11	Ellip.	Narr.	Smo.	Abs.	5.9	0.25	Ellip.	V	Smo.	Pre.	9.25	0.23	Ellip.	U	Smo.	Pre.
4wkB-05	8.08	0.07	Linear	Narr.	Smo.	Abs.	6.76	0.21	Ellip.	V	Raise	Abs.	8.96	0.24	Ellip.	V	Smo.	Abs.
4wkB-06	7.93	0.11	Linear	Narr.	Smo.	Abs.	6.96	0.2	Rect.	U	Raise	Abs.	8.79	0.29	Ellip.	V	Raise	Pre.
4wkB-07	6.26	0.13	Linear	Narr.	Smo.	Abs.	8.19	0.19	Irreg.	V	Smo.	Pre.	8.04	0.23	Irreg.	U	Smo.	Pre.
4wkB-08	7.77	0.1	Linear	Narr.	Smo.	Abs.	7.88	0.24	Ellip.	U	Smo.	Pre.	7.39	0.26	Ellip.	V	Raise	Abs.
4wkB-09	9.23	0.12	Linear	Narr.	Smo.	Abs.	7.38	0.26	Ellip.	V	Raise	Pre.	8.09	0.21	Ellip.	V	Smo.	Pre.
4wkB-10	7.22	0.1	Linear	Narr.	Smo.	Abs.	6.89	0.2	Ellip.	U	Raise	Abs.	6.68	0.26	Ellip.	V	Smo.	Pre.

(Narr.: Narrow; Smo.: Smooth; Abs.: Absent; Ellip.: Ellipse; Rect.: Rectangle; Irreg.: Irregular; Pre.: Present)

Table 8.Q: Raw data of post-exposure buried burned ribs; summer group

Number	Non-serrated blade						Coarse-serrated blade						Fine-serrated blade					
	L	W	KS	CS	KM	KSt	L	W	KS	CS	KM	KSt	L	W	KS	CS	KM	KSt
2wkB-01	8.24	0.12	Linear	Narr.	Smo.	Abs.	6.39	0.21	Ellip.	U	Smo.	Pre.	6.32	0.22	Ellip.	V	Smo.	Pre.
2wkB-02	7.15	0.13	Linear	Narr.	Smo.	Abs.	7.25	0.23	Ellip.	V	Raise	Pre.	6.67	0.26	Ellip.	V	Smo.	Pre.
2wkB-03	8.19	0.12	Linear	Narr.	Smo.	Abs.	7.12	0.19	Ellip.	U	Smo.	Abs.	7.86	0.27	Ellip.	U	Raise	Abs.
2wkB-04	6.82	0.1	Ellip.	Narr.	Smo.	Abs.	7.3	0.25	Ellip.	V	Raise	Pre.	7.76	0.18	Ellip.	V	Smo.	Abs.
2wkB-05	8.06	0.08	Linear	V	Smo.	Abs.	7.43	0.22	Rect.	U	Raise	Abs.	6.31	0.22	Ellip.	V	Smo.	Pre.
2wkB-06	7.91	0.09	Linear	Narr.	Smo.	Abs.	8.35	0.18	Ellip.	V	Smo.	Abs.	8.06	0.23	Irreg.	U	Smo.	Pre.
2wkB-07	7.45	0.08	Linear	Narr.	Smo.	Abs.	7.4	0.2	Ellip.	V	Raise	Abs.	7.91	0.26	Ellip.	U	Raise	Pre.
2wkB-08	7.26	0.12	Linear	Narr.	Smo.	Abs.	8.04	0.21	Ellip.	V	Raise	Pre.	8.06	0.23	Ellip.	V	Smo.	Abs.
2wkB-09	8.72	0.12	Ellip.	V	Smo.	Abs.	6.43	0.17	Irreg.	U	Raise	Pre.	7.57	0.23	Ellip.	V	Raise	Pre.
2wkB-10	9.06	0.07	Linear	Narr.	Smo.	Abs.	7.79	0.25	Ellip.	U	Smo.	Pre.	6.96	0.22	Irreg.	V	Smo.	Pre.
4wkB-01	6.72	0.1	Linear	Narr.	Smo.	Abs.	7.14	0.16	Irreg.	V	Smo.	Pre.	5.69	0.19	Ellip.	V	Raise	Abs.
4wkB-02	9.33	0.09	Linear	Narr.	Smo.	Abs.	8.18	0.23	Irreg.	U	Smo.	Pre.	7.09	0.26	Ellip.	U	Smo.	Abs.
4wkB-03	7.63	0.08	Linear	V	Smo.	Abs.	8.62	0.2	Ellip.	U	Raise	Pre.	7.75	0.24	Ellip.	V	Raise	Pre.
4wkB-04	8.23	0.1	Ellip.	Narr.	Smo.	Abs.	5.72	0.23	Irreg.	V	Smo.	Pre.	8.31	0.21	Irreg.	U	Smo.	Pre.
4wkB-05	7.62	0.06	Linear	Narr.	Smo.	Abs.	6.46	0.19	Ellip.	V	Raise	Abs.	8.02	0.22	Ellip.	V	Smo.	Abs.
4wkB-06	7.53	0.1	Linear	Narr.	Smo.	Abs.	6.68	0.18	Rect.	U	Raise	Abs.	7.95	0.27	Ellip.	V	Raise	Pre.
4wkB-07	5.82	0.12	Linear	Narr.	Smo.	Abs.	7.84	0.17	Irreg.	V	Smo.	Pre.	7.14	0.21	Irreg.	U	Smo.	Pre.
4wkB-08	7.34	0.1	Linear	Narr.	Smo.	Abs.	7.58	0.21	Ellip.	U	Smo.	Pre.	6.51	0.24	Ellip.	U	Smo.	Abs.
4wkB-09	8.8	0.11	Linear	Narr.	Smo.	Abs.	7.18	0.23	Ellip.	V	Raise	Pre.	7.22	0.2	Ellip.	V	Smo.	Pre.
4wkB-10	6.82	0.09	Linear	Narr.	Smo.	Abs.	6.52	0.19	Ellip.	U	Raise	Abs.	5.8	0.24	Ellip.	V	Smo.	Pre.

(Narr.: Narrow; Smo.: Smooth; Abs.: Absent; Ellip.: Ellipse; Rect.: Rectangle; Irreg.: Irregular; Pre.: Present)

Table 8.R: Raw data of pre-exposure surface-deposited burned ribs; autumn group

Number	Non-serrated blade						Coarse-serrated blade						Fine-serrated blade					
	L	W	KS	CS	KM	KSt	L	W	KS	CS	KM	KSt	L	W	KS	CS	KM	KSt
2wkS-01	8.66	0.12	Linear	Narr.	Smo.	Abs.	7.18	0.28	Ellip.	V	Raise	Pre.	7.01	0.24	Ellip.	V	Smo.	Pre.
2wkS-02	7.15	0.09	Linear	Narr.	Smo.	Abs.	8.24	0.23	Irreg.	U	Raise	Pre.	8.93	0.29	Ellip.	V	Smo.	Pre.
2wkS-03	8.27	0.14	Linear	Narr.	Smo.	Abs.	7.78	0.21	Ellip.	V	Smo.	Pre.	8.54	0.31	Rect.	V	Smo.	Abs.
2wkS-04	7.71	0.1	Ellip.	V	Smo.	Abs.	8.1	0.3	Rect.	V	Raise	Abs.	8.27	0.22	Irreg.	U	Smo.	Abs.
2wkS-05	8.85	0.09	Linear	Narr.	Smo.	Abs.	8.56	0.25	Ellip.	U	Smo.	Pre.	9.5	0.26	Ellip.	V	Smo.	Pre.
2wkS-06	7.82	0.09	Linear	Narr.	Smo.	Abs.	9.27	0.26	Irreg.	U	Raise	Pre.	8.24	0.25	Ellip.	V	Raise	Pre.
2wkS-07	7.45	0.1	Linear	Narr.	Smo.	Abs.	8.4	0.27	Ellip.	V	Smo.	Abs.	8.59	0.28	Ellip.	V	Raise	Abs.
2wkS-08	7.32	0.08	Linear	Narr.	Smo.	Abs.	9.34	0.23	Ellip.	U	Raise	Pre.	8.76	0.26	Ellip.	V	Smo.	Pre.
2wkS-09	7.65	0.09	Linear	V	Smo.	Abs.	7.61	0.18	Ellip.	U	Smo.	Pre.	8.25	0.25	Ellip.	V	Raise	Abs.
2wkS-10	6.78	0.08	Ellip.	Narr.	Smo.	Abs.	8.66	0.3	Ellip.	V	Raise	Pre.	7.64	0.25	Ellip.	V	Smo.	Pre.
4wkS-01	6.73	0.11	Linear	Narr.	Smo.	Abs.	7.46	0.17	Ellip.	V	Smo.	Pre.	6.31	0.23	Ellip.	V	Smo.	Pre.
4wkS-02	9.6	0.09	Linear	Narr.	Smo.	Abs.	8.36	0.22	Ellip.	U	Smo.	Pre.	8.2	0.29	Ellip.	V	Raise	Pre.
4wkS-03	5.82	0.12	Linear	V	Smo.	Abs.	8.93	0.26	Ellip.	V	Raise	Abs.	8.84	0.27	Ellip.	U	Smo.	Abs.
4wkS-04	8.29	0.12	Ellip.	Narr.	Smo.	Abs.	5.97	0.27	Ellip.	V	Smo.	Pre.	6.95	0.24	Ellip.	U	Raise	Pre.
4wkS-05	6.61	0.12	Linear	V	Smo.	Abs.	6.73	0.21	Ellip.	U	Raise	Pre.	9.13	0.25	Ellip.	V	Smo.	Pre.
4wkS-06	7.58	0.1	Linear	Narr.	Smo.	Abs.	6.94	0.18	Rect.	V	Raise	Abs.	7.34	0.33	Irreg.	V	Smo.	Abs.
4wkS-07	8.13	0.12	Ellip.	Narr.	Smo.	Abs.	8.27	0.19	Ellip.	V	Raise	Pre.	8.26	0.24	Ellip.	V	Raise	Pre.
4wkS-08	7.38	0.09	Linear	Narr.	Smo.	Abs.	7.83	0.23	Rec.	U	Raise	Pre.	7.6	0.27	Ellip.	V	Raise	Pre.
4wkS-09	7.95	0.11	Linear	Narr.	Smo.	Abs.	7.35	0.2	Ellip.	V	Raise	Pre.	8.31	0.22	Ellip.	V	Smo.	Pre.
4wkS-10	8.93	0.12	Linear	Narr.	Smo.	Abs.	6.86	0.2	Ellip.	U	Raise	Abs.	7.91	0.27	Ellip.	V	Smo.	Abs.

(Narr.: Narrow; Smo.: Smooth; Abs.: Absent; Ellip.: Ellipse; Rect.: Rectangle; Irreg.: Irregular; Pre.: Present)

Table 8.S: Raw data of post-exposure surface-deposited burned ribs; autumn group

Number	Non-serrated blade						Coarse-serrated blade						Fine-serrated blade					
	L	W	KS	CS	KM	KSt	L	W	KS	CS	KM	KSt	L	W	KS	CS	KM	KSt
2wkS-01	8.16	0.1	Linear	Narr.	Smo.	Abs.	6.23	0.25	Ellip.	V	Smo.	Pre.	6.32	0.23	Ellip.	V	Smo.	Pre.
2wkS-02	6.63	0.08	Linear	Narr.	Smo.	Abs.	7.26	0.21	Irreg.	U	Raise	Abs.	8.23	0.27	Ellip.	V	Smo.	Pre.
2wkS-03	7.77	0.11	Linear	Narr.	Smo.	Abs.	6.79	0.19	Ellip.	V	Smo.	Pre.	7.83	0.3	Rect.	V	Smo.	Abs.
2wkS-04	7.23	0.09	Linear	V	Smo.	Abs.	7.15	0.27	Rect.	V	Raise	Abs.	7.55	0.21	Irreg.	U	Smo.	Abs.
2wkS-05	8.35	0.08	Linear	Narr.	Smo.	Abs.	7.46	0.22	Irreg.	U	Smo.	Pre.	8.53	0.26	Ellip.	V	Smo.	Pre.
2wkS-06	7.33	0.08	Linear	Narr.	Smo.	Abs.	8.29	0.24	Irreg.	U	Smo.	Abs.	7.57	0.24	Irreg.	U	Raise	Pre.
2wkS-07	6.92	0.08	Linear	Narr.	Smo.	Abs.	7.43	0.25	Ellip.	V	Smo.	Abs.	7.88	0.26	Ellip.	V	Smo.	Abs.
2wkS-08	6.86	0.07	Linear	Narr.	Smo.	Abs.	8.4	0.21	Irreg.	U	Raise	Pre.	8.06	0.25	Ellip.	V	Smo.	Pre.
2wkS-09	7.15	0.08	Linear	V	Smo.	Abs.	6.56	0.16	Ellip.	U	Smo.	Pre.	7.39	0.24	Irreg.	U	Raise	Abs.
2wkS-10	6.24	0.07	Linear	Narr.	Smo.	Abs.	7.65	0.25	Irreg.	V	Smo.	Abs.	6.92	0.24	Ellip.	V	Smo.	Abs.
4wkS-01	5.93	0.09	Ellip.	Narr.	Smo.	Abs.	6.36	0.14	Irreg.	V	Smo.	Abs.	-	-	Ellip.	V	Smo.	Abs.
4wkS-02	-	-	Linear	Narr.	Smo.	Abs.	-	-	Ellip.	U	Smo.	Pre.	7.03	0.25	Irreg.	V	Smo.	Pre.
4wkS-03	5.11	0.1	Linear	V	Smo.	Abs.	-	-	Irreg.	U	Smo.	Abs.	-	-	Ellip.	U	Smo.	Abs.
4wkS-04	-	-	Ellip.	Narr.	Smo.	Abs.	-	-	Irreg.	V	Smo.	Abs.	-	-	Irreg.	U	Raise	Abs.
4wkS-05	6.01	0.08	Linear	V	Smo.	Abs.	6.53	0.17	Ellip.	U	Raise	Pre.	8.33	0.22	Ellip.	V	Smo.	Pre.
4wkS-06	-	-	Linear	Narr.	Smo.	Abs.	-	-	Irreg.	V	Smo.	Abs.	-	-	Irreg.	U	Smo.	Abs.
4wkS-07	7.22	0.1	Ellip.	Narr.	Smo.	Abs.	7.17	0.16	Ellip.	U	Smo.	Abs.	7.25	0.21	Ellip.	V	Smo.	Abs.
4wkS-08	-	-	Linear	Narr.	Smo.	Abs.	7.03	0.2	Rect.	U	Smo.	Pre.	6.53	0.24	Irreg.	V	Smo.	Abs.
4wkS-09	-	-	Linear	Narr.	Smo.	Abs.	-	-	Irreg.	V	Smo.	Pre.	-	-	Ellip.	V	Smo.	Pre.
4wkS-10	-	-	Linear	Narr.	Smo.	Abs.	-	-	Irreg.	U	Smo.	Abs.	-	-	Ellip.	U	Smo.	Abs.

(Narr.: Narrow; Smo.: Smooth; Abs.: Absent; Ellip.: Ellipse; Rect.: Rectangle; Irreg.: Irregular; Pre.: Present)

Table 8.T: Raw data of pre-exposure buried burned ribs; autumn group

Number	Non-serrated blade						Coarse-serrated blade						Fine-serrated blade					
	L	W	KS	CS	KM	KSt	L	W	KS	CS	KM	KSt	L	W	KS	CS	KM	KSt
2wkB-01	8.25	0.12	Linear	Narr.	Smo.	Abs.	7.91	0.27	Ellip.	V	Smo.	Pre.	6.58	0.24	Ellip.	V	Smo.	Pre.
2wkB-02	7.14	0.1	Linear	Narr.	Smo.	Abs.	8.97	0.23	Ellip.	V	Raise	Pre.	8.39	0.28	Ellip.	V	Raise	Abs.
2wkB-03	8.48	0.13	Ellip.	Narr.	Smo.	Abs.	8.54	0.22	Ellip.	U	Smo.	Pre.	8.02	0.31	Ellip.	U	Smo.	Pre.
2wkB-04	9.03	0.1	Linear	V	Smo.	Abs.	8.85	0.18	Ellip.	V	Raise	Abs.	7.75	0.2	Rect.	V	Smo.	Abs.
2wkB-05	8.17	0.09	Linear	Narr.	Smo.	Abs.	9.34	0.23	Rect.	U	Raise	Pre.	8.96	0.26	Ellip.	V	Raise	Pre.
2wkB-06	7.93	0.08	Ellip.	Narr.	Smo.	Abs.	9.9	0.21	Ellip.	U	Smo.	Pre.	7.78	0.25	Ellip.	V	Smo.	Abs.
2wkB-07	7.6	0.08	Linear	Narr.	Smo.	Abs.	9.16	0.28	Ellip.	V	Raise	Abs.	8.05	0.27	Irreg.	V	Smo.	Pre.
2wkB-08	7.33	0.07	Ellip.	Narr.	Smo.	Abs.	9.98	0.24	Irreg.	U	Smo.	Abs.	8.22	0.26	Ellip.	U	Raise	Pre.
2wkB-09	7.72	0.09	Linear	V	Smo.	Abs.	8.54	0.18	Ellip.	V	Raise	Pre.	7.72	0.26	Ellip.	V	Smo.	Pre.
2wkB-10	6.95	0.07	Linear	Narr.	Smo.	Abs.	9.43	0.31	Ellip.	U	Raise	Abs.	7.11	0.25	Ellip.	V	Smo.	Pre.
4wkB-01	6.85	0.1	Linear	Narr.	Smo.	Abs.	8.16	0.17	Irreg.	V	Smo.	Pre.	5.75	0.22	Ellip.	V	Raise	Pre.
4wkB-02	9.64	0.09	Ellip.	Narr.	Smo.	Abs.	9.15	0.24	Ellip.	U	Raise	Pre.	7.68	0.27	Rect.	V	Smo.	Pre.
4wkB-03	8.78	0.13	Linear	Narr.	Smo.	Abs.	9.67	0.26	Ellip.	U	Raise	Pre.	8.33	0.27	Ellip.	U	Raise	Pre.
4wkB-04	8.41	0.11	Ellip.	Narr.	Smo.	Abs.	6.62	0.27	Ellip.	V	Raise	Pre.	6.42	0.24	Ellip.	V	Smo.	Abs.
4wkB-05	7.81	0.12	Linear	V	Smo.	Abs.	7.47	0.22	Irreg.	U	Raise	Abs.	8.66	0.25	Ellip.	V	Smo.	Pre.
4wkB-06	7.66	0.1	Linear	Narr.	Smo.	Abs.	7.68	0.3	Rect.	V	Smo.	Abs.	6.91	0.32	Ellip.	U	Smo.	Abs.
4wkB-07	6.07	0.12	Linear	Narr.	Smo.	Abs.	9.04	0.2	Ellip.	V	Raise	Abs.	7.74	0.23	Ellip.	V	Smo.	Pre.
4wkB-08	7.51	0.09	Linear	Narr.	Smo.	Abs.	8.62	0.24	Ellip.	U	Smo.	Pre.	7.07	0.26	Irreg.	V	Raise	Abs.
4wkB-09	8.94	0.11	Ellip.	V	Smo.	Abs.	8.09	0.27	Ellip.	V	Raise	Pre.	7.76	0.21	Ellip.	V	Smo.	Pre.
4wkB-10	6.91	0.12	Linear	Narr.	Smo.	Abs.	7.6	0.2	Ellip.	V	Raise	Abs.	7.32	0.26	Ellip.	V	Smo.	Pre.

(Narr.: Narrow; Smo.: Smooth; Abs.: Absent; Ellip.: Ellipse; Rect.: Rectangle; Irreg.: Irregular; Pre.: Present)

Table 8.U: Raw data of post-exposure buried burned ribs; autumn group

Number	Non-serrated blade						Coarse-serrated blade						Fine-serrated blade					
	L	W	KS	CS	KM	KSt	L	W	KS	CS	KM	KSt	L	W	KS	CS	KM	KSt
2wkB-01	7.82	0.1	Linear	Narr.	Smo.	Abs.	6.82	0.23	Ellip.	V	Smo.	Abs.	5.88	0.22	Ellip.	U	Smo.	Pre.
2wkB-02	6.71	0.09	Linear	Narr.	Smo.	Abs.	7.88	0.19	Irreg.	V	Raise	Pre.	7.54	0.26	Ellip.	V	Raise	Abs.
2wkB-03	8.05	0.12	Ellip.	Narr.	Smo.	Abs.	7.47	0.18	Ellip.	U	Smo.	Pre.	7.3	0.29	Ellip.	U	Smo.	Abs.
2wkB-04	8.6	0.09	Linear	V	Smo.	Abs.	7.76	0.15	Ellip.	V	Smo.	Abs.	7.03	0.2	Rect.	V	Smo.	Abs.
2wkB-05	7.74	0.08	Linear	Narr.	Smo.	Abs.	8.27	0.19	Rect.	U	Raise	Pre.	8.24	0.23	Ellip.	V	Raise	Pre.
2wkB-06	7.49	0.07	Ellip.	Narr.	Smo.	Abs.	8.82	0.17	Ellip.	U	Smo.	Pre.	7.01	0.23	Ellip.	V	Smo.	Abs.
2wkB-07	7.16	0.07	Linear	Narr.	Smo.	Abs.	8.08	0.24	Ellip.	V	Raise	Abs.	7.33	0.25	Irreg.	V	Smo.	Pre.
2wkB-08	6.89	0.06	Ellip.	Narr.	Smo.	Abs.	8.99	0.2	Irreg.	U	Smo.	Abs.	7.51	0.24	Ellip.	U	Raise	Pre.
2wkB-09	7.35	0.08	Linear	V	Smo.	Abs.	7.46	0.15	Ellip.	V	Raise	Pre.	7.02	0.24	Irreg.	V	Smo.	Pre.
2wkB-10	6.51	0.06	Linear	Narr.	Smo.	Abs.	8.35	0.25	Ellip.	U	Smo.	Abs.	6.46	0.23	Ellip.	V	Smo.	Pre.
4wkB-01	5.82	0.07	Linear	Narr.	Smo.	Abs.	7.34	0.14	Irreg.	V	Smo.	Pre.	-	-	Ellip.	V	Smo.	Pre.
4wkB-02	8.6	0.06	Ellip.	Narr.	Smo.	Abs.	-	-	Irreg.	U	Raise	Abs.	6.78	0.22	Rect.	V	Smo.	Abs.
4wkB-03	7.73	0.07	Linear	Narr.	Smo.	Abs.	-	-	Ellip.	U	Smo.	Abs.	-	-	Irreg.	U	Raise	Pre.
4wkB-04	7.35	0.08	Ellip.	Narr.	Smo.	Abs.	5.82	0.21	Ellip.	V	Smo.	Pre.	-	-	Ellip.	V	Smo.	Abs.
4wkB-05	6.75	0.07	Linear	V	Smo.	Abs.	-	-	Irreg.	U	Raise	Abs.	7.64	0.2	Irreg.	V	Smo.	Pre.
4wkB-06	6.62	0.07	Linear	Narr.	Smo.	Abs.	6.98	0.22	Rect.	U	Smo.	Abs.	-	-	Irreg.	U	Smo.	Abs.
4wkB-07	5.04	0.08	Linear	Narr.	Smo.	Abs.	-	-	Irreg.	V	Raise	Abs.	7.02	0.17	Ellip.	U	Smo.	Pre.
4wkB-08	6.48	0.06	Linear	Narr.	Smo.	Abs.	-	-	Irreg.	U	Smo.	Pre.	-	-	Irreg.	U	Smo.	Abs.
4wkB-09	7.93	0.07	Ellip.	V	Smo.	Abs.	-	-	Ellip.	V	Smo.	Pre.	-	-	Ellip.	V	Smo.	Abs.
4wkB-10	5.86	0.07	Linear	Narr.	Smo.	Abs.	6.77	0.16	Ellip.	V	Raise	Abs.	6.77	0.19	Ellip.	U	Smo.	Pre.

(Narr.: Narrow; Smo.: Smooth; Abs.: Absent; Ellip.: Ellipse; Rect.: Rectangle; Irreg.: Irregular; Pre.: Present)

Table 8.V: Raw data of pre-exposure surface-deposited burned ribs; winter group

Number	Non-serrated blade						Coarse-serrated blade						Fine-serrated blade					
	L	W	KS	CS	KM	KSt	L	W	KS	CS	KM	KSt	L	W	KS	CS	KM	KSt
2wkS-01	9.66	0.12	Ellip.	V	Smo.	Abs.	6.94	0.26	Ellip.	U	Raise	Pre.	6.92	0.23	Ellip.	V	Raise	Pre.
2wkS-02	9.07	0.09	Linear	Narr.	Smo.	Abs.	7.99	0.24	Ellip.	V	Smo.	Pre.	8.85	0.28	Ellip.	V	Smo.	Pre.
2wkS-03	8.52	0.13	Linear	Narr.	Smo.	Abs.	7.55	0.28	Ellip.	U	Raise	Pre.	8.47	0.28	Ellip.	U	Raise	Pre.
2wkS-04	6.93	0.1	Linear	Narr.	Smo.	Abs.	7.88	0.24	Rect.	V	Raise	Pre.	8.2	0.19	Ellip.	V	Smo.	Pre.
2wkS-05	8.23	0.08	Linear	Narr.	Smo.	Abs.	8.36	0.23	Rect.	V	Smo.	Pre.	9.42	0.25	Ellip.	V	Smo.	Abs.
2wkS-06	7.97	0.13	Linear	Narr.	Smo.	Abs.	9.05	0.19	Ellip.	U	Smo.	Abs.	8.15	0.24	Ellip.	V	Smo.	Abs.
2wkS-07	7.62	0.08	Linear	Narr.	Smo.	Abs.	8.17	0.23	Ellip.	V	Raise	Pre.	8.53	0.26	Ellip.	V	Raise	Pre.
2wkS-08	7.36	0.12	Linear	Narr.	Smo.	Abs.	9.12	0.21	Ellip.	U	Raise	Abs.	8.69	0.25	Ellip.	V	Smo.	Pre.
2wkS-09	7.76	0.09	Ellip.	V	Smo.	Abs.	7.36	0.16	Ellip.	U	Smo.	Pre.	8.18	0.24	Irreg.	V	Smo.	Abs.
2wkS-10	6.96	0.12	Linear	Narr.	Smo.	Abs.	8.44	0.26	Ellip.	V	Raise	Abs.	7.57	0.24	Ellip.	V	Raise	Pre.
4wkS-01	6.9	0.1	Linear	Narr.	Smo.	Abs.	7.16	0.15	Ellip.	V	Smo.	Abs.	6.22	0.22	Ellip.	V	Smo.	Pre.
4wkS-02	6.03	0.09	Linear	Narr.	Smo.	Abs.	8.15	0.21	Rect.	U	Raise	Pre.	8.13	0.25	Irreg.	U	Smo.	Abs.
4wkS-03	8.82	0.12	Ellip.	V	Smo.	Abs.	8.69	0.16	Ellip.	V	Raise	Abs.	8.78	0.26	Ellip.	V	Smo.	Abs.
4wkS-04	8.44	0.07	Linear	Narr.	Smo.	Abs.	5.65	0.24	Ellip.	V	Smo.	Pre.	6.87	0.23	Ellip.	U	Smo.	Pre.
4wkS-05	7.85	0.09	Ellip.	Narr.	Smo.	Abs.	6.54	0.19	Irreg.	U	Smo.	Abs.	9.03	0.24	Ellip.	V	Smo.	Pre.
4wkS-06	7.7	0.1	Linear	Narr.	Smo.	Abs.	6.69	0.19	Rect.	V	Raise	Pre.	7.26	0.27	Ellip.	V	Raise	Abs.
4wkS-07	8.29	0.12	Linear	V	Smo.	Abs.	8.09	0.17	Ellip.	V	Raise	Pre.	8.18	0.23	Ellip.	V	Smo.	Pre.
4wkS-08	7.54	0.09	Linear	Narr.	Smo.	Abs.	7.62	0.21	Ellip.	U	Raise	Pre.	7.51	0.24	Rect.	V	Raise	Abs.
4wkS-09	9.01	0.11	Linear	Narr.	Smo.	Abs.	7.18	0.2	Ellip.	V	Raise	Pre.	8.23	0.2	Ellip.	V	Smo.	Pre.
4wkS-10	7.16	0.07	Linear	Narr.	Smo.	Abs.	6.63	0.18	Ellip.	U	Raise	Abs.	7.83	0.24	Ellip.	V	Smo.	Pre.

(Narr.: Narrow; Smo.: Smooth; Abs.: Absent; Ellip.: Ellipse; Rect.: Rectangle; Irreg.: Irregular; Pre.: Present)

Table 8.W: Raw data of post-exposure surface-deposited burned ribs; winter group

Number	Non-serrated blade						Coarse-serrated blade						Fine-serrated blade					
	L	W	KS	CS	KM	KSt	L	W	KS	CS	KM	KSt	L	W	KS	CS	KM	KSt
2wkS-01	9.19	0.11	Linear	Narr.	Smo.	Abs.	6.02	0.22	Ellip.	U	Raise	Abs.	6.12	0.22	Ellip.	U	Smo.	Pre.
2wkS-02	8.6	0.08	Linear	Narr.	Smo.	Abs.	7.08	0.2	Ellip.	V	Smo.	Pre.	8.04	0.25	Ellip.	V	Smo.	Abs.
2wkS-03	8.05	0.11	Linear	Narr.	Smo.	Abs.	6.64	0.23	Irreg.	U	Raise	Pre.	7.64	0.25	Ellip.	U	Raise	Pre.
2wkS-04	6.46	0.09	Linear	V	Smo.	Abs.	6.94	0.2	Rect.	V	Raise	Pre.	7.43	0.18	Irreg.	V	Smo.	Abs.
2wkS-05	7.76	0.08	Linear	Narr.	Smo.	Abs.	7.45	0.2	Rect.	V	Smo.	Pre.	8.64	0.24	Ellip.	V	Smo.	Abs.
2wkS-06	7.5	0.12	Linear	Narr.	Smo.	Abs.	8.13	0.17	Ellip.	U	Smo.	Abs.	7.36	0.23	Ellip.	V	Smo.	Abs.
2wkS-07	7.15	0.07	Linear	Narr.	Smo.	Abs.	7.25	0.2	Ellip.	V	Smo.	Pre.	7.78	0.25	Ellip.	U	Raise	Pre.
2wkS-08	6.91	0.11	Linear	Narr.	Smo.	Abs.	8.23	0.17	Ellip.	U	Raise	Abs.	7.84	0.23	Ellip.	V	Smo.	Pre.
2wkS-09	7.29	0.08	Linear	V	Smo.	Abs.	6.48	0.14	Irreg.	U	Smo.	Pre.	7.33	0.22	Irreg.	V	Smo.	Abs.
2wkS-10	6.49	0.11	Linear	Narr.	Smo.	Abs.	7.55	0.22	Ellip.	V	Smo.	Abs.	6.76	0.23	Ellip.	V	Smo.	Pre.
4wkS-01	6.2	0.09	Linear	Narr.	Smo.	Abs.	6.34	0.13	Ellip.	U	Smo.	Abs.	5.57	0.2	Irreg.	V	Smo.	Abs.
4wkS-02	5.33	0.08	Linear	Narr.	Smo.	Abs.	-	-	Rect.	U	Smo.	Abs.	7.42	0.23	Irreg.	U	Smo.	Abs.
4wkS-03	8.12	0.11	Ellip.	V	Smo.	Abs.	7.62	0.14	Ellip.	V	Smo.	Abs.	8.06	0.22	Ellip.	V	Smo.	Abs.
4wkS-04	7.73	0.07	Linear	Narr.	Smo.	Abs.	-	-	Ellip.	V	Smo.	Pre.	6.15	0.21	Irreg.	U	Smo.	Pre.
4wkS-05	7.15	0.09	Ellip.	Narr.	Smo.	Abs.	-	-	Irreg.	U	Smo.	Abs.	8.32	0.22	Ellip.	V	Smo.	Pre.
4wkS-06	7.11	0.09	Linear	Narr.	Smo.	Abs.	-	-	Rect.	U	Smo.	Pre.	6.56	0.23	Irreg.	V	Raise	Abs.
4wkS-07	7.58	0.11	Ellip.	V	Smo.	Abs.	7.29	0.15	Ellip.	V	Raise	Abs.	7.47	0.21	Ellip.	V	Smo.	Pre.
4wkS-08	6.83	0.09	Linear	Narr.	Smo.	Abs.	-	-	Ellip.	U	Smo.	Pre.	6.8	0.22	Rect.	V	Raise	Abs.
4wkS-09	8.32	0.1	Ellip.	Narr.	Smo.	Abs.	6.33	0.16	Ellip.	V	Smo.	Pre.	7.54	0.19	Ellip.	V	Smo.	Abs.
4wkS-10	6.45	0.07	Linear	Narr.	Smo.	Abs.	-	-	Ellip.	U	Raise	Abs.	7.13	0.21	Ellip.	V	Smo.	Pre.

(Narr.: Narrow; Smo.: Smooth; Abs.: Absent; Ellip.: Ellipse; Rect.: Rectangle; Irreg.: Irregular; Pre.: Present)

Table 8.X: Raw data of pre-exposure buried burned ribs; winter group

Number	Non-serrated blade						Coarse-serrated blade						Fine-serrated blade					
	L	W	KS	CS	KM	KSt	L	W	KS	CS	KM	KSt	L	W	KS	CS	KM	KSt
2wkB-01	9.16	0.12	Ellip.	V	Smo.	Abs.	7.18	0.3	Ellip.	V	Raise	Pre.	6.72	0.24	Ellip.	V	Smo.	Pre.
2wkB-02	7.19	0.1	Linear	Narr.	Smo.	Abs.	8.24	0.24	Ellip.	V	Raise	Pre.	8.65	0.29	Irreg.	U	Smo.	Pre.
2wkB-03	8.55	0.12	Linear	Narr.	Smo.	Abs.	7.81	0.23	Irreg.	V	Smo.	Pre.	8.28	0.31	Ellip.	V	Smo.	Pre.
2wkB-04	9.75	0.11	Linear	Narr.	Smo.	Abs.	8.13	0.19	Rect.	V	Raise	Pre.	8.01	0.2	Ellip.	V	Raise	Abs.
2wkB-05	8.23	0.09	Linear	V	Smo.	Abs.	8.61	0.27	Irreg.	U	Smo.	Pre.	9.23	0.26	Rect.	V	Raise	Abs.
2wkB-06	8.01	0.12	Ellip.	Narr.	Smo.	Abs.	9.31	0.22	Ellip.	V	Raise	Abs.	7.98	0.25	Ellip.	V	Raise	Pre.
2wkB-07	7.65	0.09	Linear	Narr.	Smo.	Abs.	8.43	0.29	Ellip.	U	Smo.	Pre.	8.33	0.28	Ellip.	V	Smo.	Pre.
2wkB-08	7.38	0.07	Ellip.	Narr.	Smo.	Abs.	9.37	0.25	Ellip.	V	Smo.	Abs.	8.49	0.26	Ellip.	V	Raise	Pre.
2wkB-09	7.79	0.1	Linear	V	Smo.	Abs.	7.62	0.19	Rect.	U	Raise	Pre.	7.98	0.26	Ellip.	V	Smo.	Abs.
2wkB-10	6.95	0.08	Linear	Narr.	Smo.	Abs.	8.7	0.31	Ellip.	U	Raise	Abs.	7.37	0.25	Ellip.	V	Smo.	Abs.
4wkB-01	6.93	0.1	Linear	Narr.	Smo.	Abs.	7.43	0.18	Ellip.	V	Smo.	Pre.	6.26	0.23	Ellip.	V	Smo.	Abs.
4wkB-02	6.95	0.1	Ellip.	Narr.	Smo.	Abs.	8.41	0.25	Ellip.	U	Raise	Pre.	7.93	0.27	Ellip.	V	Smo.	Pre.
4wkB-03	8.85	0.12	Linear	V	Smo.	Abs.	8.94	0.28	Ellip.	U	Raise	Pre.	8.57	0.27	Rect.	V	Raise	Pre.
4wkB-04	8.46	0.11	Linear	Narr.	Smo.	Abs.	5.95	0.3	Ellip.	V	Smo.	Pre.	6.47	0.24	Ellip.	V	Smo.	Abs.
4wkB-05	7.84	0.13	Linear	V	Smo.	Abs.	6.75	0.23	Ellip.	V	Raise	Abs.	8.86	0.24	Ellip.	V	Raise	Pre.
4wkB-06	7.73	0.11	Ellip.	Narr.	Smo.	Abs.	6.94	0.32	Ellip.	V	Raise	Pre.	7.07	0.33	Ellip.	U	Smo.	Pre.
4wkB-07	8.36	0.12	Linear	Narr.	Smo.	Abs.	8.29	0.21	Rect.	V	Raise	Abs.	7.96	0.24	Ellip.	V	Smo.	Pre.
4wkB-08	7.56	0.1	Linear	V	Smo.	Abs.	7.88	0.25	Ellip.	U	Smo.	Abs.	7.33	0.27	Ellip.	V	Raise	Abs.
4wkB-09	9.04	0.08	Linear	Narr.	Smo.	Abs.	7.37	0.28	Ellip.	V	Raise	Pre.	8.03	0.21	Ellip.	V	Smo.	Abs.
4wkB-10	6.06	0.11	Linear	Narr.	Smo.	Abs.	6.88	0.21	Ellip.	U	Raise	Abs.	7.62	0.26	Ellip.	V	Smo.	Pre.

(Narr.: Narrow; Smo.: Smooth; Abs.: Absent; Ellip.: Ellipse; Rect.: Rectangle; Irreg.: Irregular; Pre.: Present)

Table 8.Y: Raw data of post-exposure buried burned ribs; winter group

Number	Non-serrated blade						Coarse-serrated blade						Fine-serrated blade					
	L	W	KS	CS	KM	KSt	L	W	KS	CS	KM	KSt	L	W	KS	CS	KM	KSt
2wkB-01	8.64	0.1	Ellip.	V	Smo.	Abs.	6.08	0.27	Ellip.	V	Smo.	Pre.	5.86	0.23	Ellip.	V	Smo.	Pre.
2wkB-02	6.68	0.09	Linear	Narr.	Smo.	Abs.	7.13	0.22	Ellip.	V	Raise	Abs.	7.81	0.27	Irreg.	U	Smo.	Pre.
2wkB-03	8.05	0.11	Linear	Narr.	Smo.	Abs.	6.7	0.22	Irreg.	U	Smo.	Pre.	7.42	0.29	Ellip.	V	Smo.	Pre.
2wkB-04	9.24	0.1	Linear	Narr.	Smo.	Abs.	7.02	0.18	Rect.	V	Raise	Pre.	7.15	0.19	Ellip.	V	Raise	Abs.
2wkB-05	7.71	0.08	Linear	V	Smo.	Abs.	7.5	0.23	Irreg.	U	Smo.	Pre.	8.32	0.25	Rect.	U	Smo.	Abs.
2wkB-06	7.53	0.11	Ellip.	Narr.	Smo.	Abs.	8.19	0.2	Ellip.	V	Raise	Abs.	7.12	0.24	Ellip.	V	Raise	Pre.
2wkB-07	7.15	0.08	Linear	Narr.	Smo.	Abs.	7.32	0.25	Ellip.	U	Smo.	Pre.	7.53	0.26	Ellip.	V	Smo.	Pre.
2wkB-08	6.89	0.06	Ellip.	Narr.	Smo.	Abs.	8.26	0.21	Ellip.	V	Smo.	Abs.	7.58	0.25	Ellip.	V	Raise	Pre.
2wkB-09	7.29	0.09	Linear	V	Smo.	Abs.	6.52	0.18	Rect.	U	Raise	Pre.	7.12	0.25	Ellip.	V	Smo.	Abs.
2wkB-10	6.44	0.07	Linear	Narr.	Smo.	Abs.	7.58	0.25	Ellip.	U	Raise	Abs.	6.51	0.24	Ellip.	V	Smo.	Abs.
4wkB-01	6.22	0.08	Linear	Narr.	Smo.	Abs.	6.58	0.15	Irreg.	V	Smo.	Abs.	5.66	0.21	Irreg.	V	Smo.	Abs.
4wkB-02	6.21	0.06	Ellip.	Narr.	Smo.	Abs.	7.6	0.19	Ellip.	U	Raise	Pre.	7.33	0.24	Ellip.	V	Smo.	Abs.
4wkB-03	8.14	0.09	Linear	V	Smo.	Abs.	8.03	0.2	Ellip.	U	Smo.	Pre.	7.97	0.25	Rect.	U	Raise	Pre.
4wkB-04	7.75	0.09	Linear	Narr.	Smo.	Abs.	5.11	0.2	Irreg.	V	Smo.	Pre.	5.85	0.21	Ellip.	U	Smo.	Abs.
4wkB-05	7.13	0.1	Linear	V	Smo.	Abs.	5.94	0.18	Ellip.	U	Raise	Abs.	8.23	0.22	Irreg.	V	Smo.	Pre.
4wkB-06	7.02	0.07	Ellip.	Narr.	Smo.	Abs.	6.1	0.21	Ellip.	V	Raise	Pre.	6.45	0.3	Ellip.	U	Smo.	Pre.
4wkB-07	7.63	0.1	Linear	Narr.	Smo.	Abs.	7.45	0.17	Rect.	V	Raise	Abs.	7.36	0.22	Ellip.	V	Smo.	Pre.
4wkB-08	6.85	0.08	Linear	V	Smo.	Abs.	7.03	0.2	Ellip.	U	Smo.	Abs.	6.72	0.24	Ellip.	V	Smo.	Abs.
4wkB-09	8.31	0.06	Linear	Narr.	Smo.	Abs.	6.53	0.21	Ellip.	V	Smo.	Abs.	7.43	0.2	Irreg.	U	Smo.	Abs.
4wkB-10	5.36	0.09	Linear	Narr.	Smo.	Abs.	6.03	0.17	Ellip.	U	Raise	Abs.	7.06	0.24	Ellip.	V	Smo.	Abs.

(Narr.: Narrow; Smo.: Smooth; Abs.: Absent; Ellip.: Ellipse; Rect.: Rectangle; Irreg.: Irregular; Pre.: Present)